IAEA-TECDOC-827

Application of uranium exploration data and techniques in environmental studies

Proceedings of a Technical Committee meeting held in Vienna, 9–12 November 1993

INTERNATIONAL ATOMIC ENERGY AGENCY IAEA

The IAEA does not normally maintain stocks of reports in this series.
However, copies of these reports on microfiche or in electronic form can be obtained from

INIS Clearinghouse
International Atomic Energy Agency
Wagramer Strasse 5
P.O. Box 100
A-1400 Vienna, Austria
E-mail: CHOUSE@IAEA.ORG
URL: http://www.iaea.org/programmes/inis/inis.htm

Orders should be accompanied by prepayment of Austrian Schillings 100,–
in the form of a cheque or in the form of IAEA microfiche service coupons
which may be ordered separately from the INIS Clearinghouse.

The originating Section of this publication in the IAEA was:

Nuclear Materials and Fuel Cycle Technology Section
International Atomic Energy Agency
Wagramerstrasse 5
P.O. Box 100
A-1400 Vienna, Austria

APPLICATION OF URANIUM EXPLORATION DATA AND TECHNIQUES IN ENVIRONMENTAL STUDIES

IAEA, VIENNA, 1995
IAEA-TECDOC-827
ISSN 1011–4289

Printed by the IAEA in Austria
October 1995

FOREWORD

During recent years, the degradation of the environment has become the subject of daily conversation, as well as popular and scientific articles. Usually the concern is man's destruction or alteration of the perceived natural environment. More often than not there is little understanding that the earth's natural environment is largely determined by the underlying geology, and its derivatives, modified by the local biosphere and climatic conditions. Without reliable baseline information, studies and monitoring of the environment may be distorted.

Exploration for mineral commodities, uranium included, normally utilizes extensive, systematic geophysical and geochemical surveys covering very large areas, often entire countries. This information represents a great wealth of data that could be used to produce baseline information for environmental studies and monitoring. It is with this appreciation that IAEA convened a Technical Committee meeting with the purpose of bringing together experts in uranium exploration, geophysics and geochemistry to discuss and exchange information on the benefits of past exploration data and commonly applied techniques in environmental studies.

The Technical Committee Meeting on the Use of Uranium Exploration Data and Techniques in Environmental Studies was held in Vienna from 9 to 12 November 1993 and was attended by 44 participants from 23 countries and one international organization. Thirty-two papers covering case histories on the use of old uranium exploration data to prepare exposure dose rate and radon potential maps, the use of airborne gamma ray spectrometric systems to monitor nuclear power plants and nuclear fuel cycle facilities, and the use of similar systems in response to emergency measures in the case of accidental releases were presented.

The IAEA is grateful to those participants who contributed papers and took part in the discussion. Special thanks are extended to F. Barthel (Germany), A.G. Darnley (Canada), J.K. Otton (USA) and M. Matolin (Czech Republic), who chaired the sessions.

The IAEA staff member responsible for the organization and implementation of the meeting was M. Tauchid of the Division of Nuclear Fuel Cycle and Waste Management.

EDITORIAL NOTE

In preparing this publication for press, staff of the IAEA have made up the pages from the original manuscripts as submitted by the authors. The views expressed do not necessarily reflect those of the governments of the nominating Member States or of the nominating organizations.

Throughout the text names of Member States are retained as they were when the text was compiled.

The use of particular designations of countries or territories does not imply any judgement by the publisher, the IAEA, as to the legal status of such countries or territories, of their authorities and institutions or of the delimitation of their boundaries.

The mention of names of specific companies or products (whether or not indicated as registered) does not imply any intention to infringe proprietary rights, nor should it be construed as an endorsement or recommendation on the part of the IAEA.

The authors are responsible for having obtained the necessary permission for the IAEA to reproduce, translate or use material from sources already protected by copyrights.

CONTENTS

SUMMARY OF THE TECHNICAL COMMITTEE MEETING

It is not uncommon that a technique developed for a certain purpose might find an application in a completely different field. A notable example is the use of airborne gamma ray spectrometer techniques, developed primarily for uranium exploration, for locating and mapping debris of the fallen Russian satellite, COSMOS-954, in northern Canada in 1978; finding lost cobalt sources in the USA; and more recently, rapidly mapping fallout from Chernobyl. Similarly, information collected for the assessment of uranium resources has also been the base for the preparation of natural radioactivity or exposure dose rate and radon potential maps in a number of countries. It is for this reason that a Technical Committee Meeting on the Use of Uranium Exploration Data and Techniques in Environmental Studies was organized by the International Atomic Energy Agency. The meeting was held in Vienna from 9 to 12 November 1993 and attracted a large number of prominent workers in this field.

The technical papers presented represent a collection of important contributions by earth scientists (geologists, geophysicists and geochemists) to the understanding of the earth's environment and the use of environment monitoring techniques. These papers can be divided into the following groupings:

(a) the use of old uranium exploration data, airborne and vehicle-borne (car-borne) radiometric surveys in particular, to produce exposure dose rate and radon potential maps;

(b) new developments in the use of widely spaced ground gamma ray spectrometer surveys to assess the natural radioactivity level of the country;

(c) experiences in the use of airborne gamma ray spectrometer systems for environmental monitoring over nuclear power plants, nuclear fuel cycle facilities and large industrial complexes;

(d) the use of vehicle-borne gamma ray spectrometer systems in emergency response situation;

(e) and other uses of uranium exploration data and techniques.

Almost without exception, all the papers presented recognized the importance and the need for a correlatable baseline information on the earth's environment. Darnley's first paper addresses the existing problem of the inconsistency and incompleteness of available information/database on the distribution of chemical elements, radioactive elements included, in the earth's surface materials. The first two groups of papers presented at the meeting addressed this particular problem. Descriptions of methodology developed and presented at the meeting offer useful guides to other countries wishing to carry out similar programmes, even those with very limited resources.

Excellent case studies on how 20 to over 30 years old ground and airborne radiometric data for uranium exploration can be successfully used in the preparation of the natural radioactivity level and radon potential maps of the country were presented in the papers by Grasty et al.; Suárez Mahou and Fernández Amigot; Torres and Grasty; Otton et al.; Barnet; and Åkerblom.

As noted in a map showing the extent of gamma ray survey coverage in the world (Grasty et al.), a large part of the earth's surface has not been and most likely will never be covered by such surveys. Regardless, there are still a number of areas in the world where this valuable information has been collected but not used for production of maps showing the natural radiation of the earth's surface. On the radon problem, all speakers commented that uranium exploration data (radiometric) are of obvious benefit in identifying areas with high level radon concentration. This information alone, however, is not sufficient to estimate the risk that might be caused by it. It needs to be combined with other relevant information.

It is well known that airborne survey is costly and beyond the capability of many countries. The development of a large spacing ground spectrometer survey for the production of radioelement and natural radioactivity level maps, and possible anthropogenic pollution were successfully demonstrated in Poland (Strzelecki et al.) and in Slovenia (Andjelov et al.). This approach offers a practical alternative that is within the means of most government survey organizations.

For the past five years, there has been an increasing number of airborne gamma ray spectrometer systems used to monitor nuclear power plants, nuclear fuel cycle facilities, nuclear research institutes and large industrial complexes. Good examples of these works are noted in the papers by Schwarz et al.; Grasty and that of Sanderson et al. Parallel to this, are the establishment of similar systems that are dedicated to respond in the case of an emergency (the second paper of Sanderson et al. and Mellander).

In summary, the meeting was successful in bringing together important workers in this field. The various papers presented demonstrated the side benefit that can be drawn from past uranium exploration activities and the technology developed for this purpose. Since the environment does not recognize political boundaries, the meeting indicated the need for better co-ordination/collaboration among these workers in their studies of the earth's environment. The various activities presented at the meeting represent a step towards the improved assessment of the level of natural radioactivity of the earth's surface, a basic information often neglected in discussing our environment.

URANIUM EXPLORATION DATA, INTERNATIONAL GEOCHEMICAL MAPPING AND THE ENVIRONMENT

A.G. DARNLEY
Geological Survey of Canada, Ottawa, Ontario, Canada

Abstract

Public concern about environmental problems, about the possibility of irreversible changes affecting climate, sea level, vegetation patterns etc., and thus the capacity of the earth to support human life, has highlighted the need to obtain a much more complete description of present conditions. One field of knowledge where current information is inconsistent and incomplete concerns the distribution of chemical elements in the earth's surface materials. The International Geochemical Mapping (IGM) project, which was launched in 1987 to address this problem, was an outgrowth of earlier IAEA-sponsored activities directed towards methods of uranium exploration. The IGM project is organized under the International Geological Correlation Program, sponsored by UNESCO and IUGS. The IAEA has supported that part of the IGM project which relates to radioactive elements. These elements, both natural and man-made, are part of the geochemical environment and subject to the same chemical and physical processes as non-radioactive elements. For many reasons information about their spatial distribution and the processes which control them should be compatible and available from a common database. A series of recommendations have been prepared as part of the IGM project, to extend many of the concepts developed under IAEA auspices to assist uranium exploration, into the field of non-radioactive elements. Recommendations are concerned with acquisition and adoption of standard reference materials, standardization of methods, emphasis on sensitivity and quality control, international compatibility of data, and the establishment of a global geochemical database. The recommendations will be published by the International Council of Scientific Unions. The objectives of the IGM project cannot be attained without the participation of leading national laboratories. In many countries the national atomic energy agency often possesses the best trained analytical staff, the best equipped laboratories, and in some countries an extensive earth science database relating to radioactive minerals. It is suggested that it would materially benefit the countries involved, and facilitate the establishment of a comprehensive global geochemical database if national atomic energy organizations could participate in meeting the objectives of the IGM project. The end products will have both economic and environmental applications.

1. INTRODUCTION

There is steadily increasing public concern over the condition of the global environment. The past and present work of the IAEA in the field of uranium exploration has considerable relevance to an important sector of environmental knowledge, namely, the chemical composition of the Earth's surface. Considering the world as a whole, this topic has been relatively neglected, resulting in a scattered patchwork of incomplete and inconsistent information. Current literature describing pollution studies (e.g., Heavy Metals in the Environment, Conference Proceedings, 1993) often omits to mention the elemental composition of the natural surface environment, seemingly implying that it is known, is relatively constant, and can be ignored. In fact, the natural variations in surface geochemistry have important environmental and economic implications.

A systematic database is a necessary starting point for any scientific study. Over the past 25 years the efforts of the IAEA to increase knowledge concerning the world's uranium resources have simultaneously, as a by-product, contributed to increasing knowledge concerning the geochemistry of the earth's surface. Both radioactive and non-radioactive minerals occur side-by side within the natural environment and are subject to identical external processes. IAEA-sponsored activities have encouraged the development of an approach which is equally applicable to radioactive and non-radioactive elements. Geochemical mapping, using a variety of methods, is an essential component of uranium exploration (IAEA, 1988). It is not possible to search for one element without simultaneously gathering information about the distribution of others in the same region, and it is always advantageous to do this.

The task of trying to assemble an international (or national) database containing information on the natural distribution of a metal (there is much less information on non-metals) quickly identifies the deficiences, incompleteness and heterogeneity of existing geochemical datasets. Work specifically relating to uranium, coordinated through the IAEA, has demonstrated the need for international reference materials, standardised methodologies, reporting methods, improved detection limits, and better quality control. It has also demonstrated the need for coordination in the provision of technical advice and training, and the benefits flowing from international standardization of geoscientific information. Much of the experience which has been gained in working towards a global database for uranium could and should be applied to the task of building a comprehensive database for *all* the elements in the natural surface environment. This paper explains why and how.

2. THE IMPORTANCE OF GEOCHEMICAL MAPPING

Multielement geochemical mapping, showing the spatial distribution of the elements at the surface of the lithosphere, is directly relevant to economic and environmental problems involving minerals, agriculture, forestry, animal and human health and land-use planning. Mapping is necessary for the establishment of valid baselines for the regulation of industrial pollution and should be conducted so as to provide data against which any subsequent change can be measured. Geochemical mapping has resulted in the discovery of many mineral deposits over the past four decades (Thornton and Howarth, 1986); a variety of biochemical phenomena have been discovered through the recognition of empirical associations between trace element and morbidity patterns (Thornton, 1983). Thus, a geochemical database and its representation in map form is directly pertinent to human occupation and exploitation of the earth's surface. The need for an adequate geochemical database increases in step with population. World population is now in excess of 5.5 billion and it is increasing at the rate of 90 million per year. All projections of population growth, based on a variety of assumptions, show that within 50 years, unless there is some unforeseen catastrophe, world population will grow to 8 billion, approximately a 50 per cent increase on present numbers (Arizpe et al., in ICSU 1992). If present growth rates continue, this will happen by 2015; if growth slows down, it will happen by 2040. Within 50 years world population could considerably exceed 8 billion. Population expansion will inevitably cause more intensive exploitation of minerals, agricultural land, forests, water and living space and because most people aspire to a higher standard of living than they currently have, there will be additional pressure upon these resources. Greater efforts will have to be made to keep the planet habitable and recycle the resources now in use. Much more energy will be required, even assuming that usage becomes more efficient. This could increase the use of nuclear energy and increase the consumption of uranium. To anticipate all these demands and react in an intelligent way it will be essential to establish a comprehensive database concerning all types of resources and all aspects of the environment. Geochemical information is an essential part of this database.

Public interest in matters relating to sustainable development and the maintenance of the environment has been reflected in and stimulated by the work of the World Commission on Environment and Development (published in the Brundtland Report of 1987), and the ASCEND 21 and Rio de Janeiro UNCED Conferences of 1991/1992 (ICSU,1992). The need for a comprehensive database describing the principal features of the global environment is amongst the many issues identified at these meetings. Such a database is an essential foundation for the many studies required to understand complex natural processes. Public concern is focussed around the possibility of ill-defined "global change". The fact that change cannot be detected or measured if there is an incomplete description of present conditions is often overlooked; furthermore, the real consequences of changing conditions cannot be anticipated if all the variables have not been recognised.

The earth's surface layer is the source of all the chemical elements involved in biological processes and all the elements exploited by man (Fig. 1). Life on earth has evolved in the presence of all the elements, and possibly every element has some function in the biosphere. Recognition of

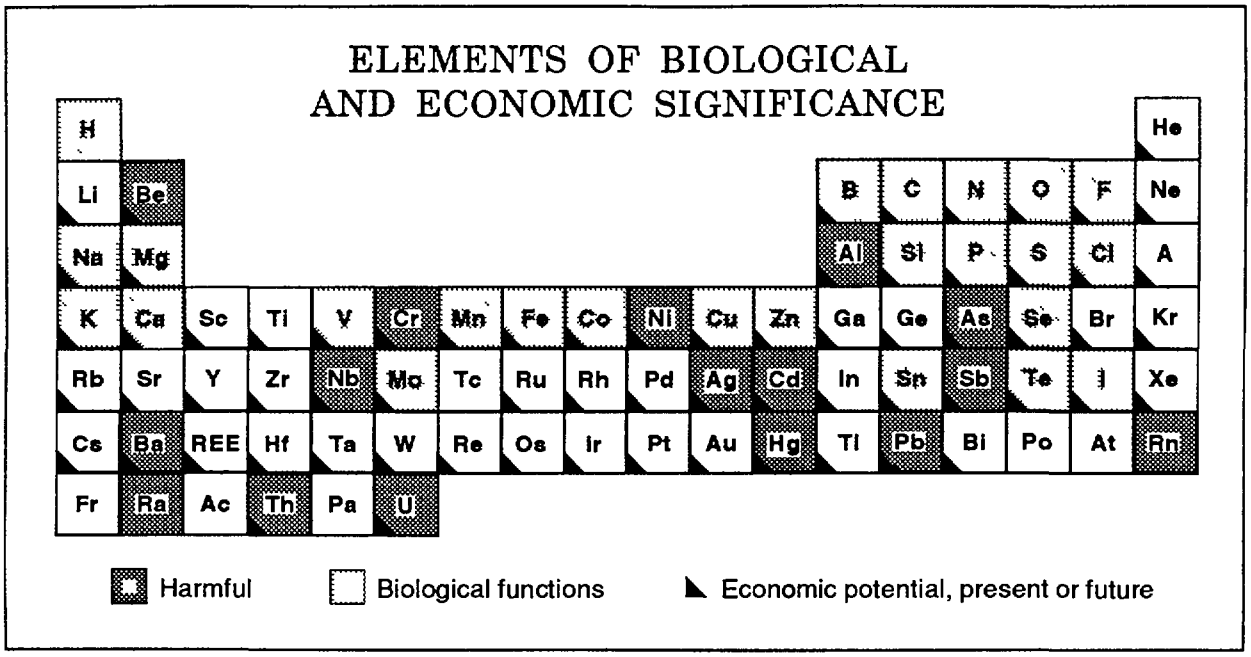

FIG. 1. Periodic table, showing elements which have known biological effects (beneficial and/or harmful) and elements with existing or potential economic importance. From various sources.

the part played by trace elements in biological processes has only been recognised as analytical procedures have advanced. The importance of Fe in blood was first suspected about 300 years ago, but only during the past 50 years has the importance of, for example, Co, Mo, Cr, Se, F, Sn, V, been established (Koros in Pais, 1989). With each passing decade additional "bioactive" elements, have been identified as having some specific biological role. It appears that for many (possibly most) organisms there is an optimum range of concentration for a particular element, specific to the organism. Outside this range harmful or toxic effects may be observed. In the case of homo sapiens, for example, optimum concentration ranges apply to Na, K, Mg, Fe, F, Cl, I, P, Co, Se and other elements. The processes involved are complex and in general poorly understood.

Because of the influence of surface geochemistry upon the biosphere it is important to know where and how the elements are distributed in their natural state and where they may have been redistributed by man. On theoretical grounds it is desirable to have data about the distribution of all the elements. The natural abundance of elements can vary by 2 to 3 orders of magnitude, depending upon geological, geographical and environmental factors. Fig. 2 illustrates the distribution of U in lake sediments in Labrador, Canada, an undeveloped region where a 10^3 range in concentration occurs. Distribution patterns of trace elements are seldom obvious, hence the need for mapping.

3. THE CURRENT STATUS OF GEOCHEMICAL MAPPING

Work to produce a *geological map* of the world began about 50 years ago. A first edition was published in 1989 by an IUGS Commission established for the purpose. The Geological Survey of Canada has recently assembled a digital database for a world map. Any study of global or continental scale processes requires systematic data for the parameters of interest. The compilation of any large scale map forces the issue of establishing the comparability and compatibility of data between and across continents. Such compilations may provide the key to otherwise seemingly unconnected phenomena. They provide a framework within which detailed investigations can be correlated and compared.

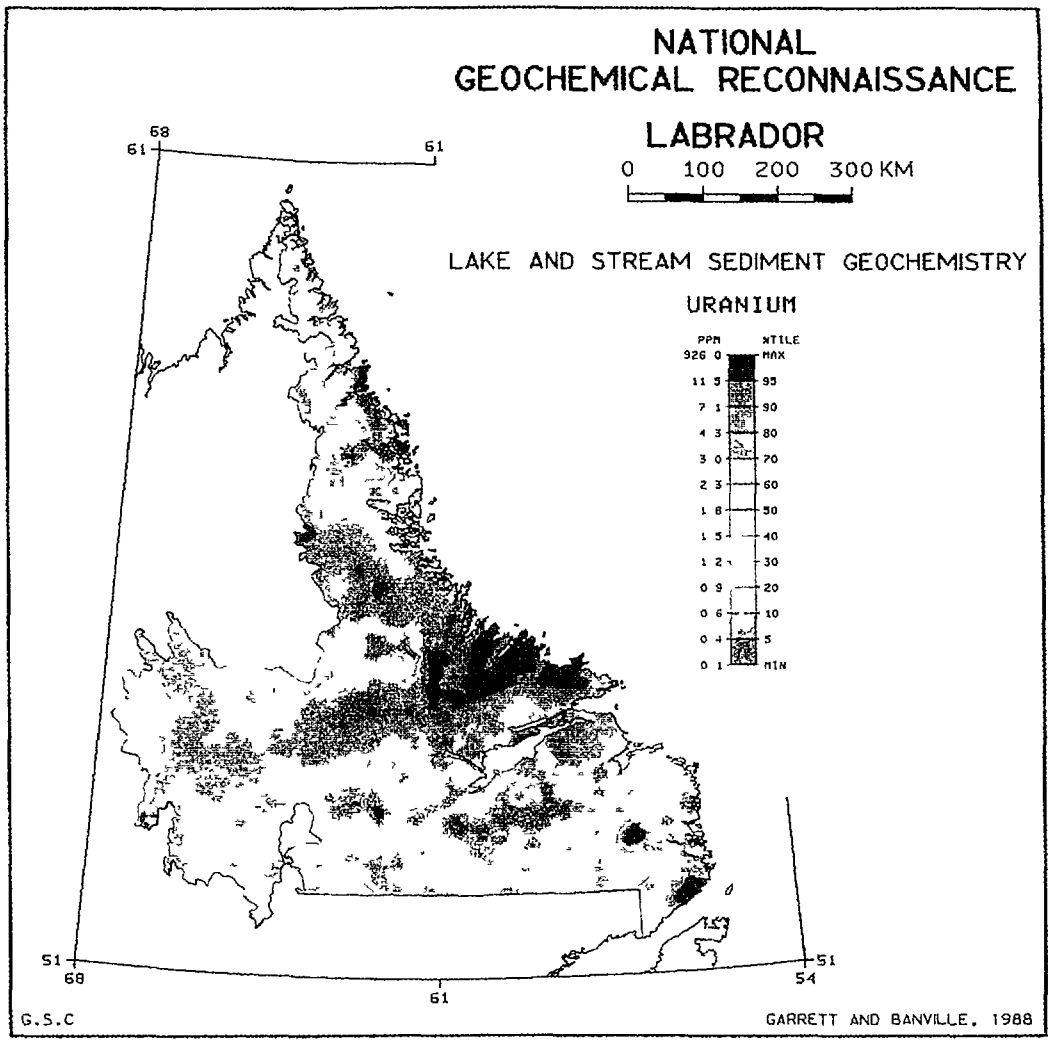

FIG 2. Natural distribution of an element in an undeveloped region, Labrador, Canada. U in lake sediments; range from 0.1 to 1000 ppm. From Garrett et al. 1990.

A geological map is not a substitute for a geochemical map. Lithological information on a geological map generally indicates the probable distribution of major elements but inferences concerning minor and (especially) trace elements may be erroneous or unknown, with important consequences. This is illustrated by the pattern of Se distribution in China, which shows a NE-SW belt of low Se values, about 2500 km long (Fig. 3). This does not correlate with any obvious feature on a geological map of China at the same scale, but it would be large enough to stand out on a Se map of Asia if such existed. The zone of low Se values corresponds with the occurrence of two serious, sometimes fatal diseases, Keshan (cardiomyopathy) and Kaschin-Beck (osteoarthropathy). Differences in Se values between deficient and normal areas do not exceed 2 or 3 parts per million.

As of 1993 there is no geochemical map of the world because the necessary data do not exist. Geochemical mapping began to develop in the early 1950s, with the introduction of rapid colorimetric methods of analysis which could be used in prospecting for base-metals. Most of the early work entailed the collection and analysis of soil samples. By the late 1950s stream sediment sampling had become the most common method wherever suitable drainage patterns existed. Initially attention was

limited to a few elements of immediate economic interest, such as Cu, Ni, Pb and Zn. Uranium began to be a target for some geochemical surveys during the 1960s. In recent years, as a result of major developments in analytical techniques, as many as 50 elements have been included in the analytical list for some national surveys. Geochemical mapping methodologies have now evolved to the point where it is possible to obtain reproducible quantitative information about the chemical composition of the surface environment with whatever spatial resolution is required.

The use of radioactivity surveys, initially employing Geiger counters, to find uranium mineralization began in the late 1940s, before geochemical exploration methods became established. Initially radiometric surveys only provided a method of measuring total radioactivity, caused by some combination of U, Th, and K, possibly with some contribution from radioactive fallout. These early radiometric surveys cannot be considered as geochemical surveys. It was not until the development of high-sensitivity gamma ray spectrometry in the late 60s, which made it possible to produce quantitative radioelement maps for K, U and Th (plus specific fallout products), that radiometric surveys became a geochemical mapping method for these elements. Because K, U and Th are large-ion lithophile elements with distinctive properties they happen to be sensitive indicators of a variety of economically significant geological and geochemical processes. For these and other reasons described in a companion paper, airborne gamma ray spectrometry provides a valuable complement to conventional geochemical surface sampling.

Although scattered geochemical mapping programs had been started by government agencies in a few countries prior to 1970, the oil embargo of 1973 resulted in funds being made available to start national geochemical mapping programs in Canada, the USA and elsewhere. It provided an opportunity to apply recently developed methods. Nuclear energy was seen as a way of reducing dependance upon imported oil, so more uranium would be needed, and this could be found through radiometric and geochemical exploration. Although uranium was the prime target, work was planned so as to gather data for other elements simultaneously. In Canada and the USA a broadly similar approach was taken. It involved two components: systematic airborne gamma ray spectrometry to map eU, eTh and K; and surface sampling of stream sediment and (in Canada) lake sediment, to obtain multielement data (initially 12 to 15 elements in Canada, 30+ in the USA). Both the US and Canadian programs operated principally through private contractors, according to predefined specifications. The Canadian programme required the use of approved equipment, standardised techniques, reference materials for geochemical analysis, and calibration facilities for radiometric instruments (Darnley et al. 1975). The US programme allowed its larger number of contractors more flexibility in execution.

The concept of internationally approved methodology and standards for geochemical mapping evolved from the need to introduce order into gamma ray spectrometry measurements. The problem was identified at an IAEA panel meeting in Vienna in 1972 (IAEA, 1973). This led to a series of IAEA Consultants' meetings in 1973/74. An IAEA technical report with recommendations was published in 1976 (IAEA, 1976). Those recommendations, with subsequent revisions and additions, have provided the international standards for ground and airborne gamma ray surveys from that time forward (IAEA 1979, IAEA 1991). As a parallel step, during the 70s the IAEA was responsible for preparing laboratory reference materials for radiometric and chemical analyses. These activities were influential because of the IAEA 's mandate, arising from its UN charter, for all matters relating to nuclear energy, including radioactive minerals. The agency can thus act as international coordinator and facilitator for a wide range of technical activities in its field. A number of large airborne gamma ray surveys undertaken over the last 15 years, for example in Thailand, have a degree of conformity and standardization because of IAEA influence. Regrettably, neither the IAEA nor any other international agency has a mandate for sponsoring standardization for data relating to non-nuclear elements in the environment. There has been no institutional support to facilitate systematic data collection pertaining to the remainder of the periodic table, dispersed alongside radioactive elements in soil, rocks and natural waters. Consequently, on an international basis, there has been no coordination of methodology or data with respect to geochemical surveys. In general, data from neighbouring countries can only be correlated in a qualitative manner, if at all.

3.1. THE DEFICIENCIES OF EXISTING MULTIELEMENT DATASETS

Although a few countries have produced geochemical atlases, beginning in the 1970s, no country, or region within any country, has geochemical maps for more than a sometimes rather arbitrary mix of elements. The selection has commonly been determined by the limitations of the responsible institution's analytical facilities or analytical budget. As a result of an ambitious program throughout the past decade a large part of China has been covered with detailed systematic geochemical mapping (Xie and Ren, 1991). Recently published national geochemical atlases from Germany, Austria and Finland are of high quality, but, as elsewhere, they are stand-alone items with respect to their neighbours (see references). Each country or organization has developed its own code of practice and style of presenting data. This can be readily appreciated by comparing the products. Geochemical databases vary from country to country and many countries do not have any. Those which exist are incomplete, inconsistent across (often within) national boundaries, and often lack information on quality control. Different sample media, methods of sample collection and preparation, extraction and analytical techniques have been used. As a result, numerical values can only be compared within areas where consistent methods and standards have been applied.

Table I lists countries where *some* geochemical mapping is known to have taken place, and shows the percentage of their area which has been covered. It is important to recognise that this indicates nothing about the number of elements analysed, or the quality or consistency of data. Table II indicates one of the inconsistencies which exist in a selection of the available large-area datasets from different parts of the world. This table shows how few elements are included in the majority of published regional map sets. Of 18 regions considered on 6 different continents, only 3 elements (Cr, Cu and Zn) are included in all the map sets. Analytical suites have normally been decided primarily according to short term mineral exploration priorities, coupled with a need to minimize costs. In some survey programs there has been what can be termed as "analytical fallout", that is to say, elements for which analytical data have been obtained, for little or no extra cost, as a by-product of the methods selected for the elements of immediate economic interest.

The dimensions of geochemical phenomena are an important consideration with respect to the amount of on-the-ground-data, i.e. sampling density, required to recognise them and the scale at which useful geochemical information can be conveyed. There are patterns in nature, that is to say, non-random arrangements of like-objects, at all scales, from the atomic to the galactic. Patterns are recognisable at all scales in geology, for example, ranging from rhythmic sedimentation to the structure of orogenic belts. Similarly there are patterns at all scales in geochemistry (for a recent discussion see Bolviken at al, 1992). It has been known for a century that the major element composition of the continents is different from the major element composition of the ocean floor. However, it is only within the last decade that data have been compiled over sufficiently large continental areas to demonstrate that trace element distribution exhibits large as well as small-dimension patterns. There are examples from China (Xie and Yin, 1993), Fennoscandia (Gustavsson et al, in press) and USA. Compilations for the latter are based on airborne gamma ray spectrometry, showing K, eU, and eTh (Duval,1991), and conventional ground sampling for multielement analysis (Shacklette et al 1981). Both the airborne and ground data measure the composition of the regolith. The latest geochemical atlas published by the Geological Survey of Finland is based on the analysis of till samples collected at a density of 1 per 300 km^2. This volume displays much interesting information relating to varying levels of element abundance, showing the existence of large and in some cases unexpected and difficult-to-explain features. Over most of the world there is a serious data-deficiency, with, at best, patchy coverage for a few elements. In many countries data are limited to scattered small areas which are insufficient to permit continuity of large features to be traced.

4. THE INTERNATIONAL GEOCHEMICAL MAPPING PROJECT

The International Geochemical Mapping project grew out of the Joint IAEA/NEA R&D Group on Uranium Exploration Methods, which was active from 1976-1984. This group disbanded because

uranium demand was declining and known resources were considered to be adequate. At its final meeting, held in Lulea, Sweden, in September 1984, concern was expressed that large quantities of uranium exploration data, which had been acquired at considerable cost during the previous decade, were in danger of disappearing as commercial and government organizations closed offices. The group agreed that an effort should be made to preserve the larger blocks of data, with a view to future compilation. Unfortunately, it was simple to recognise the problem but difficult to find any solution. The IAEA was willing to encourage the assembly of uranium resource data, but not data relating to other elements. National institutions, to the extent that they were interested in collecting data, were more concerned about other elements. It was 2 years before the situation first discussed in Lulea resulted in the drafting of a proposal for an International Geochemical Mapping project, and it was 1988 when it was formally accepted by the International Geological Correlation Programme.

The International Geological Correlation Programme is sponsored jointly by UNESCO and the International Union of Geological Sciences. Acceptance of a project indicates a "seal of approval" for the concept involved; it is intended to encourage international participation; a small amount of money is provided to assist project participants to meet together. There is no funding for scientific data collection, processing, research, or publication, which it is assumed will be supported by the employers of participants from interested countries as part of their work. This limits what can be accomplished.

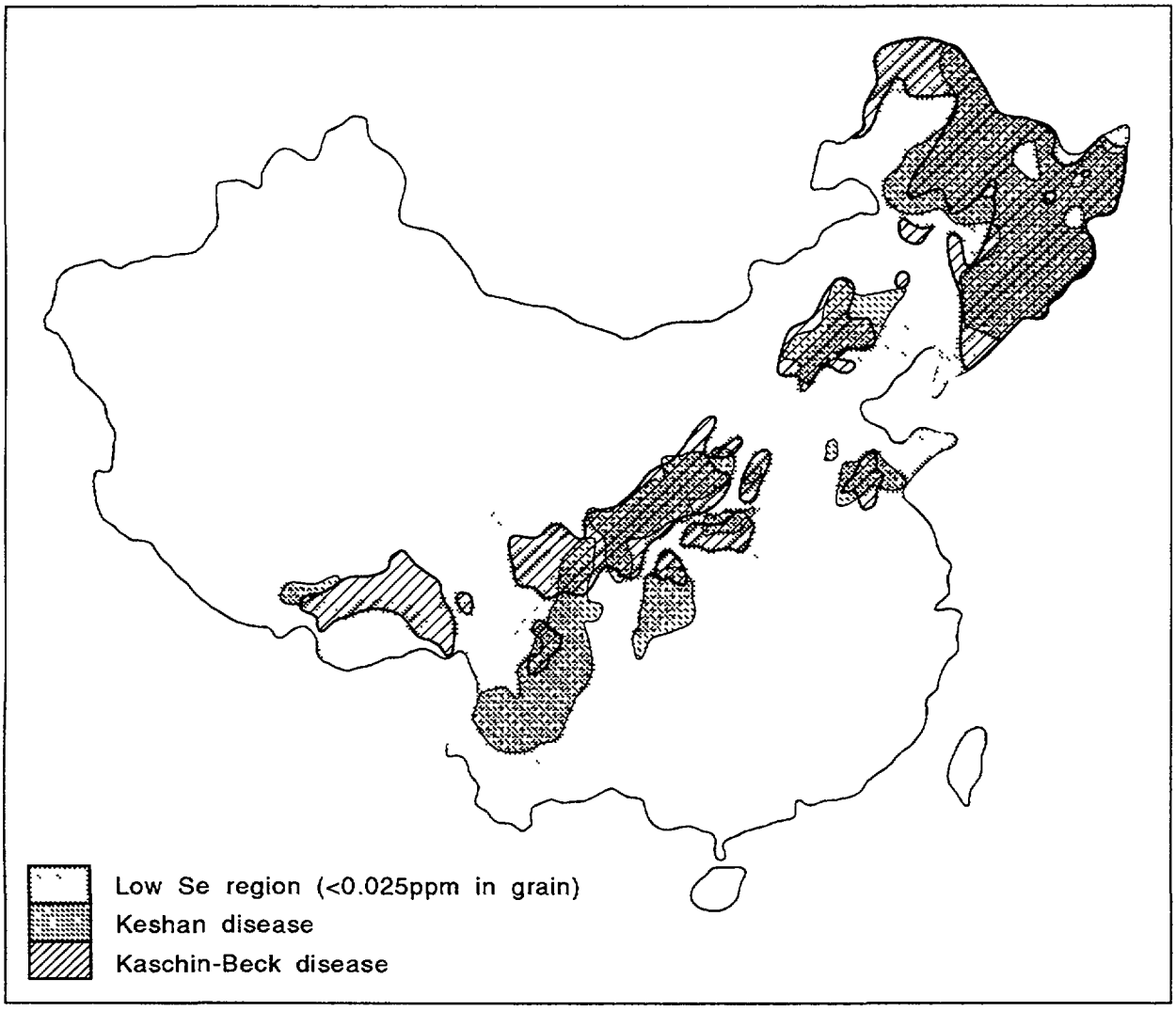

FIG. 3. Region of low Se content in China and associated disease patterns. From Atlas of endemic diseases and their environments in the Peoples Republic of China, 1989.

It has taken time for the deficiencies of the existing scattered, locally oriented, geochemical databases to become recognised outside the geochemical profession. However, during the 6 years since the International Geochemical Mapping project began, it has become apparent to a growing number of scientists concerned with the environment that standardised geochemical data are a necessary component of the public scientific infrastructure.

The objective for Phase 1 of the International Geochemical Mapping project, which was completed in 1992, was to take steps which would promote the greater standardisation of regional surficial geochemical surveys. This was done by:

1) making an inventory of existing data and methods;
2) conducting research to overcome recognised problems;
3) compiling demonstration products from different regions of the world;
4) developing recommendations that can be applied to future systematic geochemical mapping.

Recommendations will be published in full by the International Council of Scientific Unions in 1994 as part of a report prepared by members of the project's five Technical Committees, to which more than 20 people have contributed. Leading contributors from China, Europe, North America and Russia, are named in the acknowledgments section of this report.

4.1. RECOMMENDATIONS FOR PHASE 2 OF THE IGM PROJECT

The recommendations for the implementation of Phase 2 of the International Geochemical Mapping project are focussed around the establishment of Global Geochemical Baselines. The following is a summary of salient points.

The area of the world's land surface is approximately 140 million km^2. Even if it could be afforded, it would be impracticable to initiate a one-stage operation to collect 1 sample/km^2 over the Earth's land surface and ensure adequate quality control at each stage of the work. Such an approach is possible for measurements that can be made from satellite platforms, but no technique exists which is applicable to multielement geochemical mapping of the surface. International geochemical mapping can only be accomplished in stages on, or in the case of the radioactive elements, close to the ground.

Geochemical mapping should be regarded as a continuum of activities, extending from a multipurpose planetary overview at one extremity to a wide variety of specialized and detailed investigations (possibly confined to small areas) at the other. To the greatest extent possible, data at all scales should be interlinked. Conceptually, national and international surveys can be linked by means of a hierarchial sampling pattern based on a 10 × 10 km cell. National surveys can subdivide this cell, for example into 5, 2 or 1 km units to provide better definition of local geochemical patterns in economically important and populated areas. For international correlation and initial reconnaissance of large areas (and also for the preparation of a world atlas) a larger cell is advocated, for example 20, 40 or 80 km. But, as a first step, to tie all regions and continents together, a global collection of standard reference materials is recommended based on a 160 × 160 km cell. This is the equivalent of a geodetic network in topographic surveys.

Sample spacing and sample media are interrelated issues in any type of geochemical mapping. For area mapping, samples should be representative of as large an area as possible. There are 2 ways of obtaining representative large area samples, either by using a natural composite, such as flood plain sediment derived from a very large area, or devising a statistically valid sampling pattern for materials with a more restricted derivation. Either way, wide-spaced sampling is crucial to the initiation of international geochemical mapping because it provides the only practical method of obtaining a relatively rapid and consistent overview of global geochemistry. It can be organized and undertaken by a relatively small number of people in each region of the world. This is a key factor in obtaining consistency. Valuable demonstrations of the effectiveness of wide-spaced sampling are available from

China (Xie and Yin 1993) Canada (Garrett 1993), Fennoscandia (Koljonen et al. 1992) and USA (Shacklette and Boerngen 1984).

The earth's land surface can be covered by approximately five thousand 160 × 160 km cells. Ideally, the sampling pattern should be more-or-less evenly distributed, with a site in each quarter of the 160 km grid cell. This is easy to carry out over large populated regions with a good road network, such as the North American prairies, the North European plain, etc. Where equi-spaced two-dimensional sampling is difficult to execute, it is recommended that as an alternative measure a database can be obtained from reference materials collected along corridors, for example by following suitably located transportation routes, spaced not more than 160 km apart. Where possible, routes should be chosen which are normal to the regional strike. Airborne gamma ray spectrometry, which has a complementary role in the acquisition of geochemical baseline data, collects data in continuous traverses, and these can be laid-out to coincide with ground corridors. This is the subject of a separate paper. The work of Shacklette in the USA, demonstrated that sampling the regolith at about 80 km intervals, adjacent to the national interstate highway system, was capable of providing a coherent national geochemical overview, based on 1318 sites (Shacklette et Boerngen 1984).

In remote areas where there is no convenient surface access, it will be necessary to use aircraft to reach sample collection sites. Whatever the mode of access, whether the sampling pattern is equidimensional, or linear along a corridor, a minimum of 5 sites should be sampled within each global reference cell, 2 of these sites being close together in order to check site reproducibility. A detailed sampling protocol is contained in the recommendations (Darnley et al. 1994).

With respect to the types of sample to be collected, mineral exploration geochemists, wherever the landscape permits, have adopted stream sediments as the preferred sampling medium for regional geochemical surveys. Therefore, wherever possible this type of sample should be taken. However, for environmental scientists, soil and the surfaces on which people live are of greater interest. Hence emphasis must be placed upon the upper regolith, which may consist of residual or transported soils, flood plain sediments, raised beaches, etc. Because there is public concern in many countries about radioactivity, radioactive dose-rates and in situ radioelement concentration should be measured at each reference site, using a calibrated field gamma ray spectrometer. Geologists seek information about bedrock if they can obtain it, therefore a "C" horizon sample should be collected wherever the weathering profile permits. Water, for obvious reasons, is of great environmental concern, and the inorganic composition of water samples must form part of a global dataset. Similarly humus should be collected wherever it is present, to provide a link with more specialized biogeochemical surveys.

It is important to stress that in order to obtain sufficient baseline data to produce atlas-scale maps, the primary 160 km grid must be subdivided and sampled (either at the time the reference samples are collected, or subsequently) in smaller cells, 80 × 80 km, 40 × 40 km etc., according to the spatial definition that can be afforded. The latter, or closer spacing, is recommended for the purpose of establishing national baseline data in a small country. Note that planning documents prepared in connection with the International Global Change Programme often refer to a hierarchy of investigative sites for different types of monitoring and research, so we are advocating a similar approach in the International Geochemical Mapping project.

5. IMPLEMENTATION OF THE IGM PROJECT

It is expected that Phase 2 of the IGM project, IGCP 360 Global Geochemical Baselines, will commence in 1994, beginning with the collection and analysis of wide-spaced reference materials. These will be for ongoing use by both national and international institutions. However, before this work can proceed very far some important decisions must be taken. Currently the only scientific data collection and research work taking place which is relevant to the IGM project is being accomplished

in countries where there are geochemical mapping projects with activities which closely resemble the requirements of the international project. In these situations progress is largely dependant upon the interest and persistence of the individual project scientists, and upon their persuasiveness with respect to local funding agencies. This is an unsatisfactory foundation on which to build a permanent international database. For substantial progress to be made it is necessary for the project to be adopted by responsible national institutions, which could include geological surveys, environmental and nuclear energy organizations. They are in a position to implement the recommendations relating to standards, methods and quality control, to a nation's advantage. In many countries excellent analytical and computing laboratories are to be found in nuclear energy institutes and, especially where other facilities are lacking, consideration should be given to utilising these for geochemical purposes.

To make it possible for national organizations to collaborate in an international project and follow common specifications, there is a need for an international coordinating agency with expertise in the relevant field of activity. The IAEA has performed this function for matters relating to uranium. In order to obtain a *global* multielement geochemical database the following practical considerations need to be addressed:

- data acquisition will require a minimum of a decade, it could be much longer;
- the quality and consistency of data must be controlled throughout the acquisition period;
- standard reference materials must be provided and renewed as necessary;
- there should be a mechanism for assessing and introducing new techniques as they become available;
- there should be a central record of work undertaken;
- global and regional data must be accessible to be useful;
- a single world geochemical data centre is required to facilitate links to other global-scale phenomena, including population, environmental, natural resource and global change datasets.

Because the scientific and technical requirements of systematic geochemical mapping have practical significance for all countries:

- all countries should be encouraged to participate in every stage of the work;
- appropriate training and technical assistance should be offered where required.

These various considerations lead to the conclusion that:

- management continuity and assured funding will be necessary;
- global co-operation must be encouraged and assisted by a small technical secretariat, funded and administered through a permanent international agency.

The work of the IAEA over the past 25 years in providing a scientific infrastructure relating to uranium geochemistry provides a model of what is required to establish baseline data concerning the whole periodic table. Given the importance of the task, it is to be hoped that, if the IAEA is unable to include it within its own mandate, then it will encourage and assist the creation of appropriate arrangements elsewhere.

TABLE I. GEOCHEMICAL MAP COVERAGE, BY COUNTRY (EXCLUDING RADIOMETRIC MAPPING)

Country	Coverage	Area	Percent
Albania	6 000	28 748	21
Argentina	200 000	2 766 889	7
Australia	566 000	7 686 848	7
Austria	42 000	83 835	50
Belgium	12 000	30 513	39
Bolivia	130 000	1 098 581	11
Brazil	2 428 343	8 511 965	29
Burma	9 430	676 552	1
Canada	2 084 000	9 976 139	21
China	9 500 000	9 596 968	95
Czech+Slovak Republics	91 000	127 870	71
Ecuador	6 000	283 561	2
Egypt	110 000	1 001 449	11
Ethiopia	96 000	1 207 808	8
Finland	337 030	337 030	100
France	90 000	547 026	16
Gabon	50 000	267 667	19
Germany	264 000	356 910	74
Greenland	190 000	383 600*	50
Hungary	37 000	93 030	40
Indonesia	190 000	1 919 440	10
Iran	349 500	1 648 000	21
Israel	15 000	20 770	71
Italy	10 000	301 230	3
Japan	79 000	377 835	21
Jordan	ns	91 880	
Kenya	50 000	582 646	9
Malaysia	31 000	329 750	9
Mozambique	306 100	801 590	38
Norway	324 219	324 219	100
Pakistan	6 000	803 943	1
Peru	6 300	1 285 216	1
Poland	100 000	312 680	32
Russia	1 000 000	22 402 200	4
Saudi Arabia	10 500	2 149 690	1
Sierra Leone	40 250	71 740	56
Solomon Is.	8 600	28 450	30
Somalia	ns	637 657	
South Africa	200 000	1 221 037	16
Spain	ns	504 750	
Sweden	190 000	449 964	42
Syria	21 000	185 180	11
Tanzania	643 000	945 090	68
Thailand	12 000	506 880	2
Uganda	230 000	236 040	97
UK	244 820	244 820	100
USA	4 959 539	9 235 699	54
Venezuela	400 000	912 050	44
Zambia	207 000	752 614	27
Zimbabwe	13 200	390 580	3

Country	Coverage	Area	Percent
TOTAL (51 countries with listed data)	25 894 540	94 740 685	27
TOTAL (WORLD LAND SURFACE *excluding icecaps)	25 894 540	136 000 000	19

(N.B. This list is compiled solely to indicate that *some* geochemical map data exist over the areas shown for the various countries. There is a great diversity in methods used and elements for which there is analytical information. Data are unstandardized between countries and commonly also within countries)

TABLE II. ELEMENTS MAPPED IN 18 REGIONAL GEOCHEMICAL SURVEYS FROM AMERICA, EUROPE, AFRICA, ASIA

Bioactive elements in italics[1]

No. of regions in which the following elements have been mapped[2]

18	*Cr Cu Zn*
17	*Co Pb*
16	*Ni*
15	*Mn Fe* Ba
14	*V*
13	*Sn*
12	*Sr W*
11	*As Mo*
10	*K* Zr *U*
9	*Al Ca Ti* Ag
8	Sc Y La
7	*Be Mg Rb Nb* Ce Au *Th*
6	*Na P Sb*
5	*Cd* RE Ta
4	*Li B Si Ga Br Cs* Hf
3	*pH F Se* Bi
2	*C*(LOI), *Cl Hg*
1	Te *I* Re Os Ir *Pt*
0	He *N O* Ne *S* Ar *Ge* Kr Tc Ru Rh Pd In Xe *Tl* Po At Fr Ac Pa

Table II, Notes

1) The bioactive elements, i.e. elements for which there is evidence that they are necessary and/or harmful to life (varying with organism, circumstances, chemical form and concentration) are identified from papers in "The Biogeochemical Cycle of Elements in Nature", Ed. I. Pais, Hungarian Academy of Sciences, Budapest, 1989, 240pp.

2) The list of elements determined in any given survey is primarily dependent upon the analytical facilities available to the various institutions responsible. Different techniques (e.g. optical emission spectroscopy, atomic absorption, XRF, INAA, etc) are effective for different groups of elements. Thus, surveys undertaken by different institutions commonly produce data for different combinations of elements.

General Notes:

Note that many elements of environmental importance have often not been determined in past survey work. For example, fewer than half the surveys have provided data on such important elements as Cd, Se, Hg, Tl and halides.

The position of elements in this compilation is no guarantee that the quality of analytical data is satisfactory by present day standards. This list has been prepared to illustrate only one of many reasons why there is a need for a systematic, global geochemical data base.

Rn Ra, measured radiometrically, are not included in this compilation.

The elements Po et seq are shown in italics because they are present in ultra trace amounts as part of the uranium and thorium radioactive decay series.

Regions and sources of data (which cover from 5000 to 2 500 000 km^2): [For full references see Darnley et al 1994]

Alaska (NURE Atlas, Los Alamos National Laboratory)
Canada (NGR Open File Maps, Geological Survey of Canada)
Costa Rica (Los Alamos National Lab.)
Venezuela (University of Caracas)
Brazil (CPRM, Recife)
Bolivia (GEOBOL & British Geological Survey)
Northern Fennoscandia (Nordkalott Cooperative Project)
Germany (Atlas of W. Germany, BGR, Hanover)
Northern Scotland (British Geological Survey, Keyworth)
Northern Ireland (Webb Atlas, Imperial College, London)
England & Wales (Wolfson Atlas, Imperial College, London)
Austria (Geologische Bundesanstalt, Vienna)
Egypt (Geological Survey, Cairo)
Gabon (BRGM, Paris)
South Africa (Geological Survey, Pretoria)
Iran (Geological Survey, Tehran)
China (Inst.Geophysics & Geochem. Beijing)
Japan (Geological Survey, Tokyo)

BIBLIOGRAPHY

ATLASES

Atlas of endemic diseases and their environments in the People's Republic of China, Science Press, Beijing (1989).

Geochemischer Atlas, Bundesrepublik Deutschland, Verteilung von Schwermetall in Wassern und Bachsedimenten, H.Fauth, R.Hindel, U.Sievers, and J.Zinner, Bundeanstalt für Geowissenschaften und Rohstoffe, Hannover (1985) 79pp.

Geochemical Atlas of Finland, Part 2, Till., T.Koljonen, (ed). Geological Survey of Finland (1992) 218pp.

Geochemical Atlas of the Republic of Austria, 1:1 000 000, Bohemian Massif and Central Zone of the Eastern Alps (Stream Sediments <80 mesh), F. Thalmann, O. Schermann, E. Schroll and G. Hausberger, Geological Survey of Austria, Vienna. (in 2 volumes, maps and text) (1989).

GENERAL

CEP Consultants Ltd., Heavy Metals in the Environment, Proceedings of an International Conference, Toronto, September 1993. CEP Consultants Ltd, Albany Street, Edinburgh (1993) 750pp.

DARNLEY, A.G., CAMERON, E.M. and RICHARDSON, K.A., The Federal-Provincial Uranium Reconnaissance Program. in Uranium Exploration '75, Geological survey of Canada Paper 75-26 (1975) 49-71.

DARNLEY, A.G., BJORKLUND, A.J., BOLVIKEN, B., GUSTAVSSON, N., KOVAL, P., PLANT, J.A., STEENFELT, A., TAUCHID, M., and XIE XUEJING, A global geochemical database: recommendations for international geochemical mapping. Final report for IGCP project 259. ICSU Paris (1994) (in preparation).

DUVAL, J.S., Potassium, uranium and thorium geochemical maps of the conterminous U.S.A. Transactions Institution of Mining and Metallurgy (Sect.B: Applied earth science) (1991) p.B66-B73.

GARRETT, R.G., Ultra-low density geochemical mapping on the Canadian prairie. Abstracts, 16th International Geochemical Mapping Symposium, 1-6 September 1993, Beijing, China (1993) p.50.

GARRETT, R.G., BANVILLE, R.M.P., and ADCOCK, S.W., Regional data compilation and map preparation, Labrador, Canada. Journal of Geochemical Exploration, 39 (1990) 91-116.

GUSTAVSSON, N., LAMPIO, E., NILSSON, B., NORBLAD, G., ROS, F. and SALMINEN, R., Geochemical Maps of Finland and Sweden. Journal of Geochemical Exploration (1994) (in press).

INTERNATIONAL ATOMIC ENERGY AGENCY, Geochemical exploration for uranium, Technical Report Series No. 284, IAEA, Vienna (1988) 96pp.

INTERNATIONAL ATOMIC ENERGY AGENCY, Uranium Exploration Methods, Proceedings of a Panel, IAEA, Vienna (1973) 320 pp.

INTERNATIONAL ATOMIC ENERGY AGENCY, Radiometric Reporting Methods and Calibration in Uranium Exploration, Technical Report Series No. 174, IAEA, Vienna (1976) 57 pp.

INTERNATIONAL ATOMIC ENERGY AGENCY, Gamma ray surveys in uranium exploration, Technical Report Series No. 186, IAEA, Vienna (1979) 90 pp.

INTERNATIONAL ATOMIC ENERGY AGENCY, Airborne gamma ray spectrometer surveying, Technical Report Series No. 323, IAEA, Vienna (1991) 97 pp.

ICSU, International conference on an agenda of science for environment and development into the 21st Century. Compiled by M. Brennan. Cambridge University Press (1992) 331pp.

PAIS, I. Ed., The Biogeochemical Cycle of Elements in Nature, Proceedings of a conference, Hungarian Academy of Sciences, Budapest (1989) 240pp.

THORNTON, I. Ed., Applied Environmental Geochemistry. Academic Press, London (1983) 501pp.

THORNTON, I. and HOWARTH, R.J. Eds., Applied Geochemistry in the 1980s Graham & Trotman, London (1986) 347pp.

XIE, X. and REN, T., A decade of regional geochemistry in China — the national reconnaissance project. Transactions Institution of Mining and Metallurgy (Sect.B: Applied earth science) (1991) p.B57-B65.

XIE, X. and YIN, B., Geochemical patterns from local to global. Journal of Geochemical Exploration, 47 (1993) p 109-129.

Next page(s) left blank

DEVELOPMENT AND CALIBRATION OF AN AIRBORNE RADIOMETRIC MEASURING SYSTEM

G.F. SCHWARZ, L. RYBACH, C.K. BÄRLOCHER, E.E. KLINGELÉ
Institut für Geophysik, Eidgenössische Technische Hochschule, Zurich, Switzerland

Abstract

Airborne radiometric measurements are the most efficient tool to delimit surface contaminations and to locate lost radioactive sources. To increase the efficiency of airborne radiometric system in emergency situations an existing equipment has completely been renewed.

The new system is to its main part self-developed and is based on a modern airborne spectrometer with automatic gain control. It covers the gamma ray energy range of 40 keV to 3000 keV with 256 channels. The detector used for the survey consists of a package of four 4" × 4" × 16" prismatic, thallium-doped, sodium iodide crystals (total volume 16.8 liters). A PC-based data acquisition system equipped with rack keyboard and 9"-monitor synchronizes and controls the measurements. Positioning is done with the satellite navigation system GPS. The positions and the raw data are displayed to the operator for navigation and stored together with the spectrum data.

The calibration of an airborne radiometric system is ideally performed on concrete calibration pads with a precisely known radioisotope content. Unfortunately there are no full sized calibration pads available in central Europe. The calibration factors where therefore determined using radioactive point sources and mathematically corrected for the different source geometry. The results of this calibration procedure were controlled by high precision in-situ gamma spectrometric measurements together with laboratory measurements on rock samples and show good correlation between airborne and ground measurements.

The detection limit of the airborne radiometric system lies between 0.4 GBq (10 mCi) and 1.9 GBq (50 mCi) depending on vegetation cover, background and topography.

1. INTRODUCTION

The continuous observation of artificial radioactivity in Switzerland is mainly based on three monitoring networks. The NADAM system (Net for Automatic Dose Alert and Measurement), 51 stationary dose measuring installations with remote data transfer that records the radioactivity level on a nation wide scale. The radioactivity of the air and the environs of the nuclear power stations are surveyed in more detail with two additional networks (RADAIR and MADUK).

Besides these punctual routine measurements spot checks and measurement series on samples of air, rain, food and so on are carried out. In case of accidents with radioactive material (transport and industry accidents) or contamination with debris of nuclear-powered satellites airborne measurements will be used to locate the radioactive sources or to get an overview of the contamination situation.

Airborne radiometric measurements are the most efficient tool to delimit surface contaminations and to locate lost radioactive sources. Because of the larger ground clearance and the higher speed, the coverage per unit time of an airborne system is about 2500 times larger than of a comparable ground system, which is of key importance in radiological accidents. The emergency measurements will be done by military helicopters under the control of the Swiss National Emergency Operation Center (NAZ). Training flights are made each year in order to deploy the measuring system optimally.

To increase the efficiency of the airborne radiometric system in emergency situations an existing equipment from EG&G Geometrics has completely been renewed. The configuration and the calibration of the new system will be described in this paper.

2. MEASURING EQUIPMENT

The measuring system consists of a helicopter-borne gamma ray spectrometer with data control and storage and flight positioning instrumentation. The intention in the development of the measuring equipment was to construct a system with high data quality and security that is easy to operate and to maintain. This aim was achieved by using a spectrometer with automatic gain control and a PC-based data acquisition system.

The gain control in older systems was accomplished by using temperature stabilization methods. The new system monitors each of the input detectors during operation and uses the peak of the natural potassium isotope K^{40} as stabilization peak for the gain control. The automatic gain control eliminates the need of heating systems to keep the detector temperature constant, which reduces logistic problems significantly. Furthermore the drift is reduced and there is no more need of manually calibrating the spectrometer.

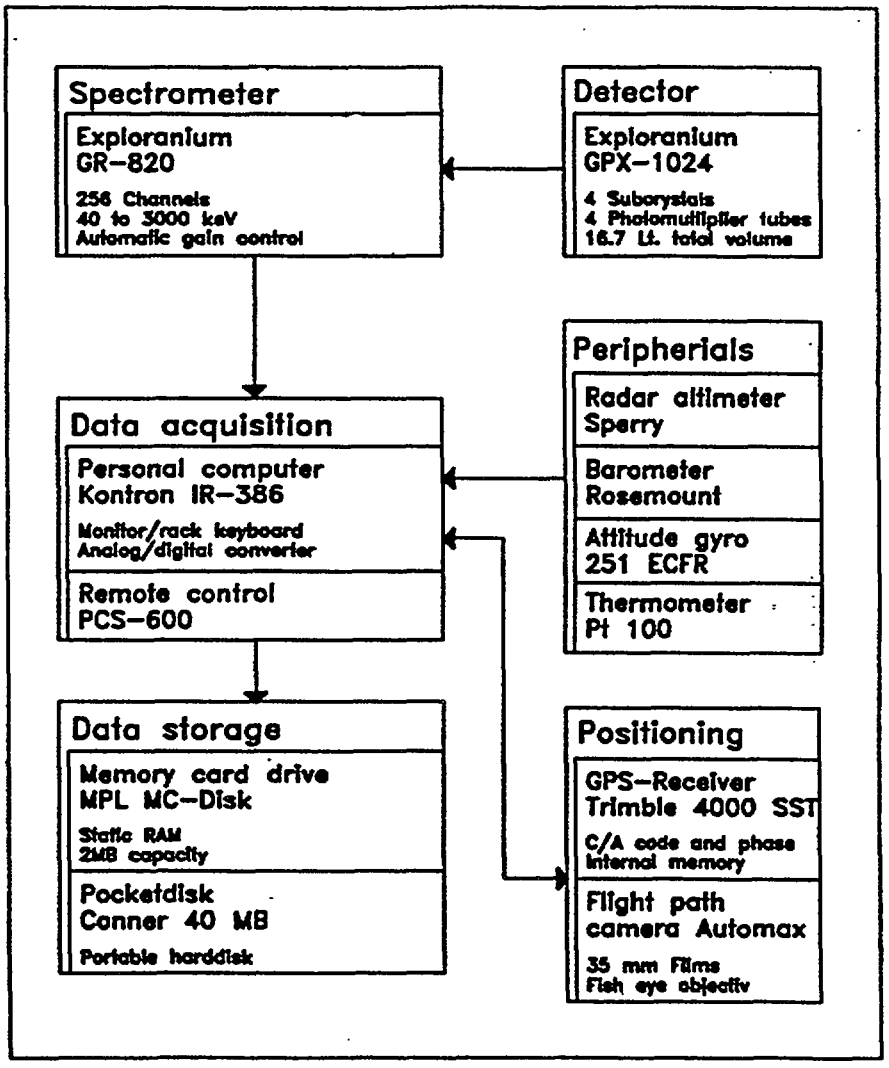

FIG. 1. Block diagram of the measuring system.

The use of a powerful personal computer as data acquisition system has several advantages. The maintenance is simplified since reserve components are generally available. Because the source code of the control program is at hand, changes and extensions to the system can be realized easily.

Fig. 1 shows the block diagram of the complete system. The system is presented in more detail below. The equipment consists of the following components:

- A detector package (Exploranium GPX-1024) consisting of four 4" × 4" × 16" sized prismatic thallium doped sodium iodide crystals. Each crystal is equipped with its own photomultiplier tube (PMT). The whole package is heat and shock isolated and includes the high voltage power supplies and controls for the PMT's.

- A Multi channel spectrometer (GR-820) from Exploranium, a modern airborne spectrometer originally designed for uranium exploration. It covers the gamma ray energy range of 40 keV to 3000 keV with 255 channels. An additional channel is used for the registration of high energy cosmic radiation. The main advantage of the spectrometer is the automatic gain control. During operation the system monitors each of the crystals and a separate spectrum is accumulated for every crystal. Based on the K^{40} peak the gains of each spectrum are determined. The aligned spectra are stacked together afterwards. The spectrometer is equipped with a small graphic display to show the raw data and can be controlled with an integrated keyboard.

- A data acquisition system based on an industrial PC equipped with rack keyboard and 9"-monitor. It synchronizes and controls the measurements. The spectrometer data are collected together with time, fiducial, and flight number. Additional peripheral devices can be added to the system using one of the eight available analog/digital converters. The measured data are stored on JEIDA memory cards with a storage capacity of 2 Mb. This new

  storage medium in credit card size works without moving mechanical parts and is therefore insensitive against vibrations, humidity and temperature changes. During operation the system is controlled by a remote control console.

- Additionally radar altitude (Sperry AA-200), barometric pressure (Rosemount 1241), outside air temperature (Pt 100) and attitude angles of the helicopter (AIM 251 CFR) are registered continuously. The signals are recorded with a commercial ADC board.

- Positioning is done with the satellite navigation system GPS (Trimble TN4000 SST). The acquired positions are displayed to the operator for navigation and stored together with the spectrum data. If no satellite signal is available a vertically mounted camera is used for flight path recovery.

All electronic components are combined in a 19" rack. Fig. 2 shows the front view and a schematic rear view of the Rack. The spectrometer is installed at the top position. It is succeeded by the computer and the accompanying keyboard. The following assembly unit contains the control electronics for the attitude gyro and the barometric altimeter, followed by the attitude gyro display. Beneath are the systems circuit breakers and the transceiver of the radar altimeter.

The equipment can be installed into three different kinds of helicopters. Normally an AS350B1 Ecureuil helicopter of Heliswiss AG (Belp/BE) is used for routine surveys. Emergency flights are performed with Swiss army Alouette-III or Super Puma helicopters. The detector and the rack are mounted behind the two front seats, in place of the passenger's seats. For the installation of the equipment no modifications to the helicopter are needed. The whole equipment can be fixed to standard attach points in the cabin and installed within an hour.

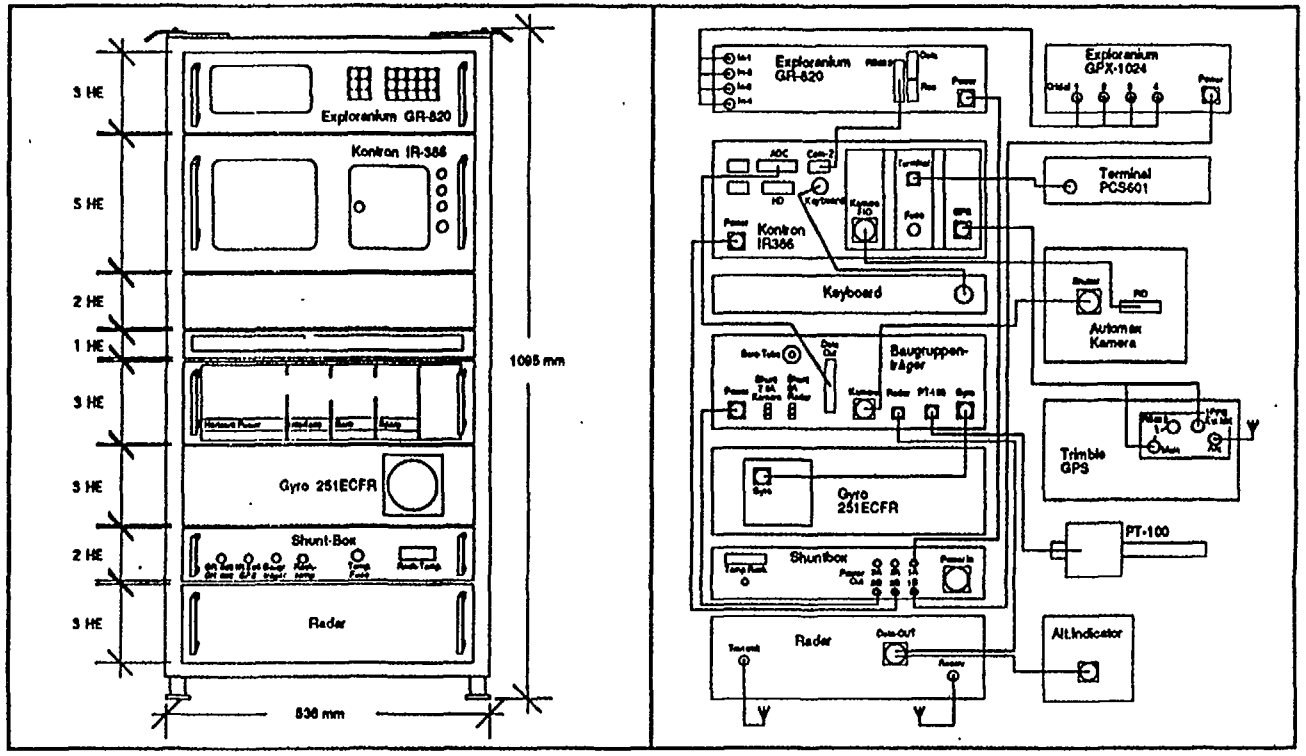

FIG. 2. Front and rear view of the rack containing the spectrometer (first), the computer (second) the rack keyboard (third), the assembly unit with the control electronics for the attitude gyro and the barometric altimeter (fourth), the attitude gyro display (fifth), the shunt box (sixth) and the transceiver of the radar altimeter (last).

3. DATA ACQUISITION

In order to achieve uniform coverage of the surveyed area the flights are carried out on a regular grid of flight lines. The flight line spacing depends on the flight altitude and on the desired ground coverage. It is desirable to fly as low as possible because of the absorption of gamma-rays by the air. For safety reasons (flight obstacles, flight limitations) the flight altitude can not be lower than 92 m (300 ft) in flat terrain resp. 122 m (400 ft) in mountainous areas. For overview surveys usually a flight line spacing of 500 m is used which corresponds roughly to a ground coverage of 75% at 122 m ground clearance. Detailed surveys are flown with 250 m line spacing and 90 m ground clearance. The ground speed is only of minor importance if the measurements are carried out with helicopters which always fly relatively slow.

Positioning is done with the satellite navigation system GPS with a precision of ± 5 m. If no satellite signal is available a vertically mounted camera is used for flight path recovery. An example of the positioning can be seen in Fig. 3. Unfortunately the high positioning precision is only available after post processing the GPS data using a reference station. The on-line positions available during the flights are intentionally disturbed by the U.S. Department of Defense up to ± 100 m for civil users (selective availability).

Navigation is therefore done visually using flight maps of 1:25'000 scale. It is clear that following the planned flight path at very low ground clearance (less than 120 m), makes high demands to the pilot, the navigator and the helicopter, especially in mountainous regions with many flight obstacles. The deviation from the planned flight lines are generally less than 50 m using visual navigation.

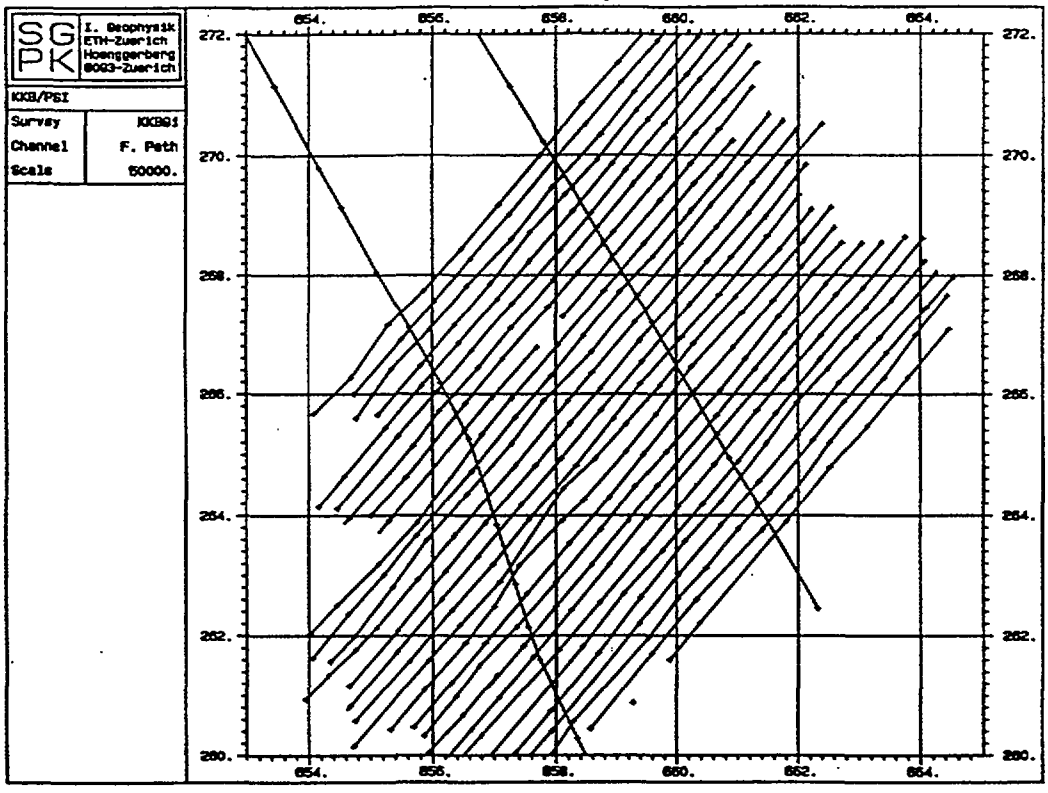

FIG. 3. Flight path in the environs of the nuclear research facility Paul Scherrer Institut (PSI) derived from GPS-data.

During the measurements the incoming gamma rays are accumulated during one second by the spectrometer. The resulting spectrum is written together with the fiducial number, the outside air temperature, the radar altitude, the barometric pressure, the actual time and the GPS position to the memory card.

Totally 512 Bytes of information are stored every second. The characteristic data of each flight line (fiducial of line start and line end, heading and time) are noted on a flight protocol for control purposes.

To check the function of the measuring system a test is carried out at the beginning and the end of every flight. For this the system is run for about 30 s at ground. The second test, a flight line always flown at the same place, provides information about the actual radon concentration. Measurements that vary heavily from the average of all other test lines indicate an increase of radon concentration.

At a base station barometric pressure, temperature, humidity and the GPS reference position are recorded simultaneously with the flights.

The quality check takes place directly after landing. For this purpose the complete processing software including the modules for corrections and map outputs has been implemented on a transportable personal computer. This enables not only the quality control of the acquired raw data, but also the complete processing directly in the field, a facility of great importance in the event of a radiological accident.

4. CALIBRATION

The spectral stripping factors, the attenuation coefficient of air and the detector efficiency and sensitivity are determined ideally on large concrete calibration pads with a precisely known radioisotope content [1]. Unfortunately there are no such calibration pads available in central Europe.

The stripping factors where determined using radioactive point sources with small activities around 37 kBq. The precise activity of the calibration sources must not be known, since only ratios are used in the calculations. For each energy window a corresponding calibration source is needed. The factors determined with point sources have been corrected mathematically to account for the different geometry of the pads [2, 3].

The determination of the detector sensitivity is based on the detector efficiency and model calculation of the gamma ray flux. For detector efficiency determination a Cs137 and a Co60 source (each of 1.9 GBq) were used. The measurements were carried out with the helicopter at different source distances. The measured count rate of the point source leads to the detector efficiency and the attenuation coefficient of the air at the corresponding gamma energies. The detector efficiency at other energies can be derived by extrapolation using an approximation of the efficiency curve of sodium iodide detectors [2]. In a last step the detector sensitivity at flight altitude is calculated from the detector efficiency and gamma ray flux calculations [3, 4].

The results of this calibration procedure were controlled by high precision in-situ gamma spectrometric measurements [5, 6] together with gamma spectrometric measurements of natural isotopes on rock samples [7, 8]. The corrected count rates measured with the airborne system are plotted against the determinations of ground activity in Fig. 4. As can be seen from Fig. 4 the data show a reasonably good correlation between the airborne and the ground measurements.

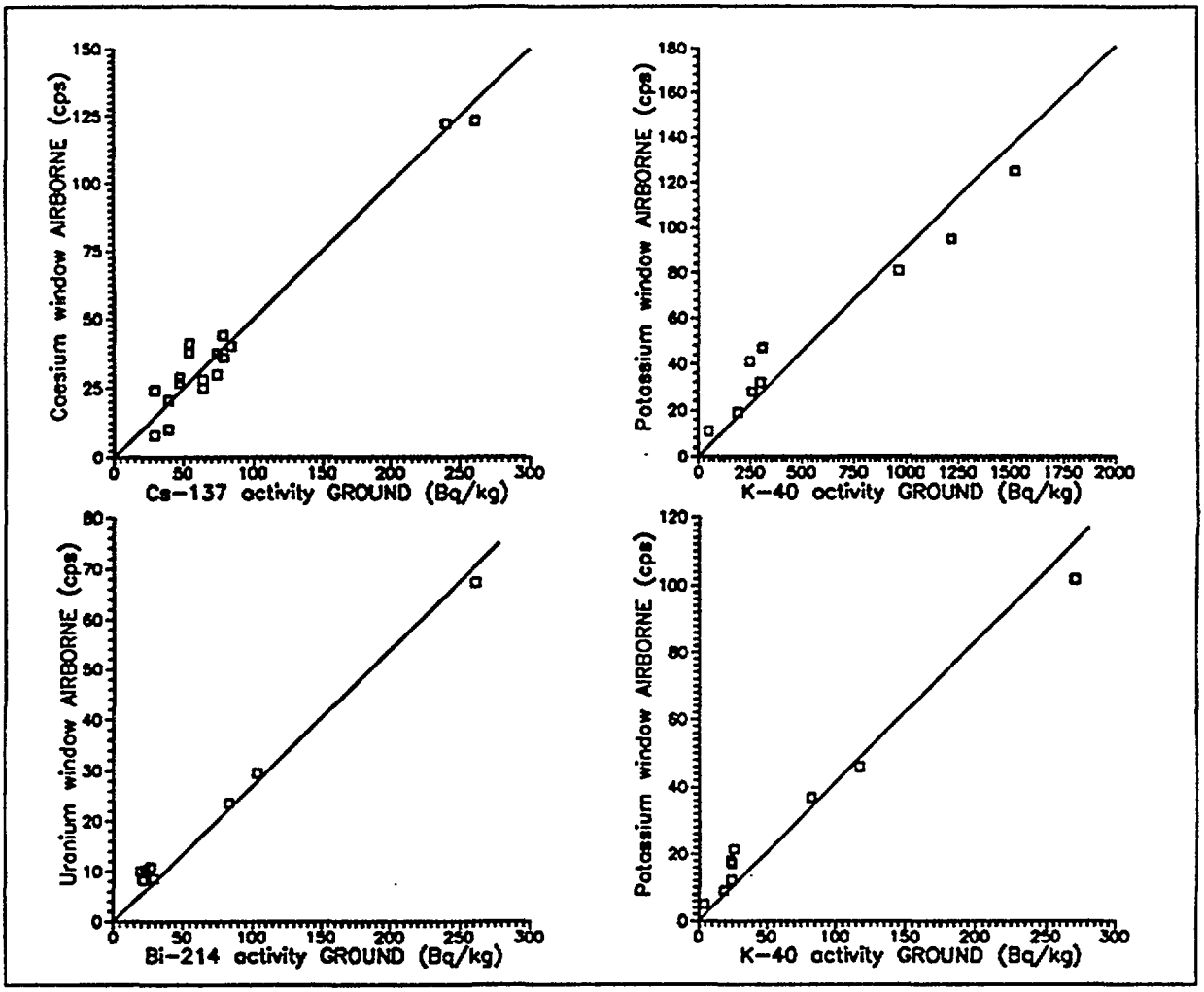

FIG. 4. Experimentally determined detector sensitivities.

TABLE I. SUMMARY OF THE DETECTOR SENSITIVITY DETERMINATIONS (100 M ABOVE GROUND).

Window	Radio nuclide	Activity [Bq/kg]	Z_{ETH} Model [cps]	Z_{ETH} Exp. [cps]	Dose rate [nSv/h]
Cesium	Cs^{137}	100	50	-	17
Potassium	K^{40}	100	9	7	5
Uranium	Bi^{214}	100	27	27	52
Thorium	Tl^{208}	100	41	42	73

The ratio count rate/ground activity allows to determine the detector sensitivity for the specific flight altitude (100 m in this case) for each energy window. As can be seen from Table I the experimentally found values are in good agreement with the values derived from point sources. The advantage of the calibration using point sources is that it is not limited to isotopes abundant in the natural environment.

5. DETECTION LIMITS

Airborne radiometric measurements are the most efficient tool to delimit surface contaminations and to locate lost radioactive sources. Extended contamination can be detected and mapped easily even with a relative simple measuring system. The precise localization of lost radioactive point sources from transport accidents or debris from nuclear-powered satellites is much more difficult, since the radiation intensity of a point source decreases very fast with increasing distance.

Due to the limited precision of navigation the smallest attainable flight line spacing is about 200 m. The minimal flight altitude lies between 60 m and 120 m depending on topography and flight obstacles. To determine the minimal detectable source strength at these flight parameters one must keep in mind that a radioactive source can only be detected if its count rate (IQ) exceeds the confidence interval of the background count rate (IB, normally around 100 cps). This is satisfied if

$$I_Q = 2.\sqrt{I_B} \quad (\textit{confidence interval} = \pm 1\sigma)$$

The detector efficiency is known from the calibration measurements (see chapter 4). Using these data and the preceding relation, a cesium source with a minimal activity of 0.4 GBq (10 mCi) should be detectable at a flight altitude of 90 m and a flight line spacing of 250 m with our system.

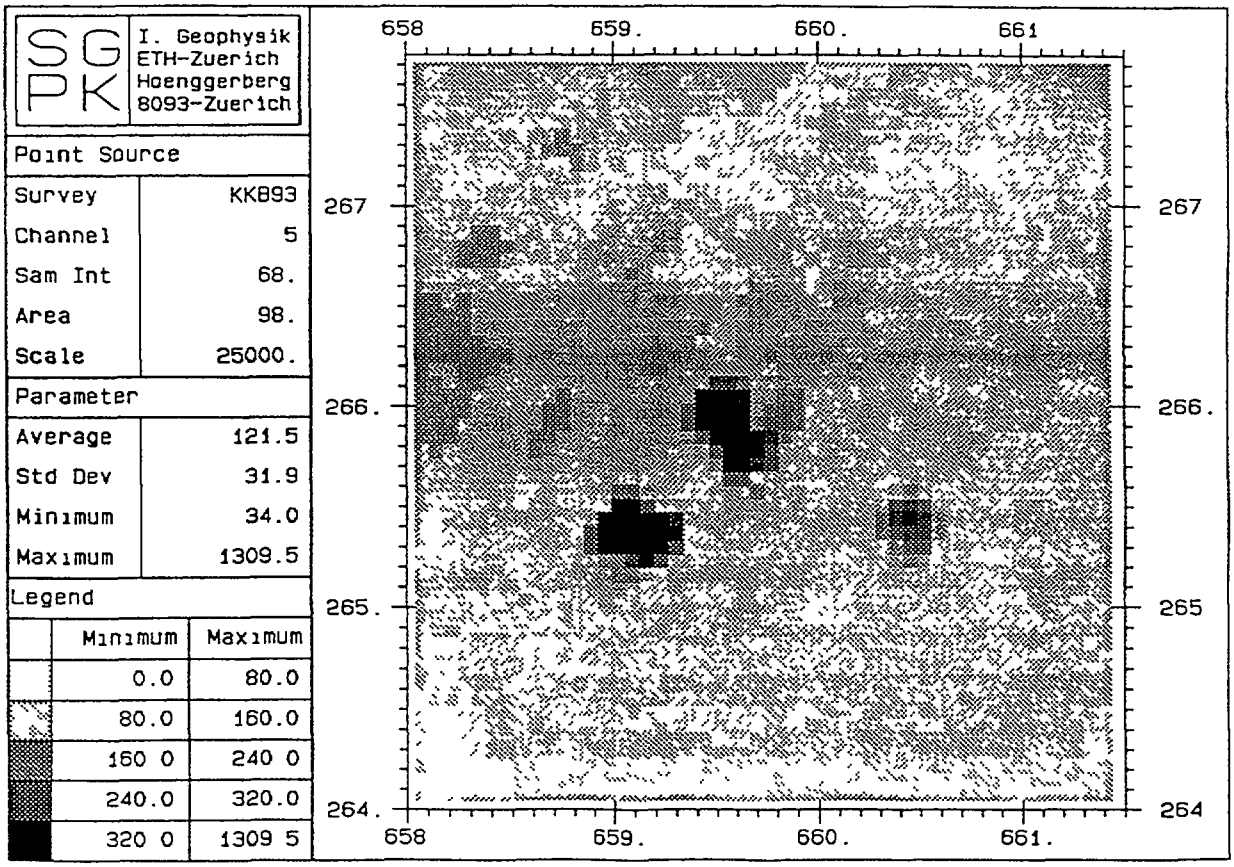

FIG. 5. Map of the raw count rate in the cesium window acquired during a test flight in the environs of the research facility Paul Scherrer Institut (PSI). The black spot to the right is caused by a Cs^{137} source (activity = 2.6 GBq) on the ground. The other two anomalies are caused by the direct radiation of the storage areas for radioactive components and waste of the PSI.

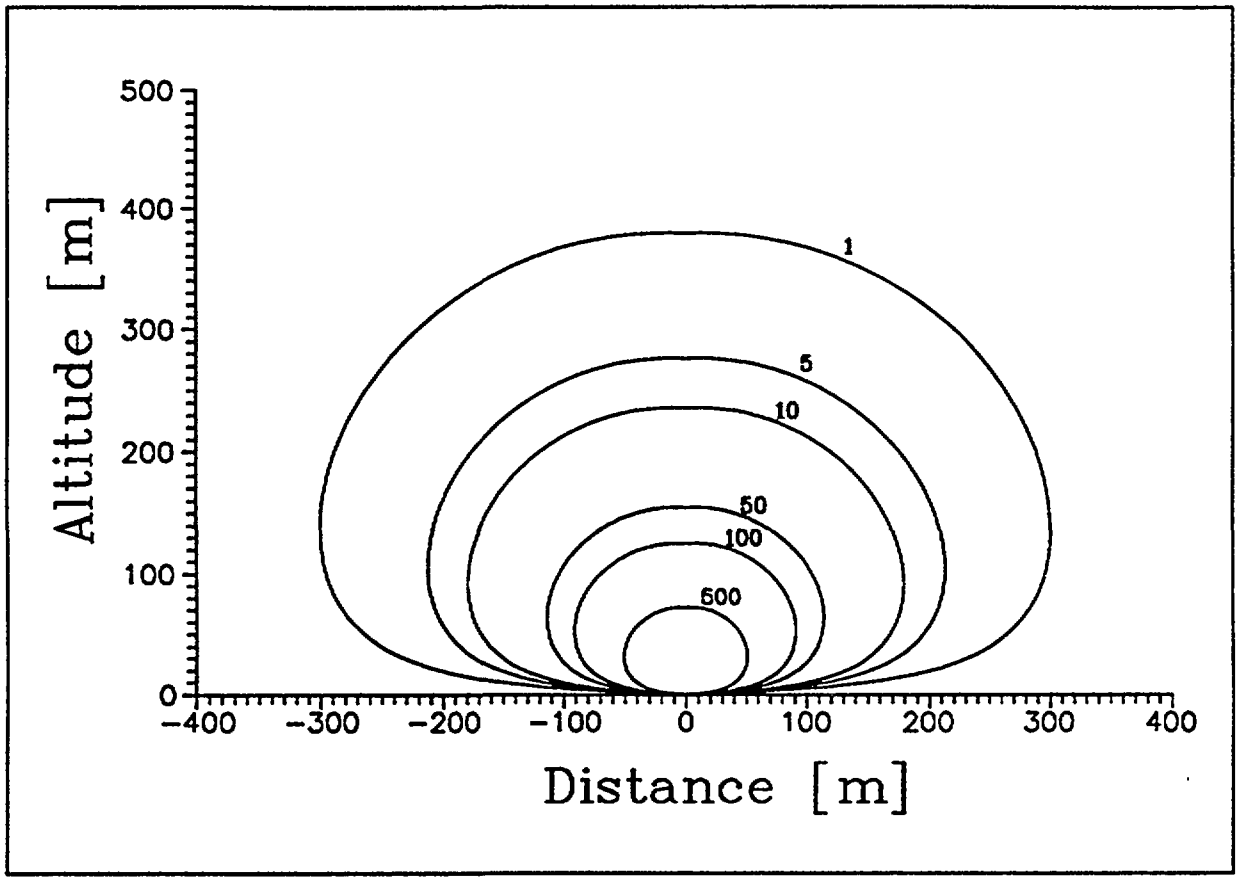

FIG. 6. Modelled count rate (1, 5, 10, 50, 100, 500 cps isolines) of a of a 1.9 GBq (50 mCi) Cs^{137} source buried at a depth of 1 cm using the experimentally determined detector efficiency.

To confirm this detection limit several search flights for point sources were carried out under realistic conditions. Fig. 5 shows the map of such a search flight. The Cs^{137} source placed on the ground had an activity of 2.6 GBq (70 mCi). It can be identified clearly on the map as the black spot on the right. The other two anomalies are caused by the direct radiation of storage areas for radioactive components and waste of the research facility Paul Scherrer Institut (PSI). The precision of the localization was around ± 30 m.

The processing of the search flights showed that the theoretical detection limit of 0.4 GBq Cs^{137} can not be achieved under realistic conditions for two reasons. First the "natural" Cs^{137} background is not constant. It varies depending on soil humidity, vegetation cover and penetration depth of the contamination. This makes it difficult to distinguish the a small increase caused by the source from other variations. The effects of humidity and vegetation can be reduced with the aid of ratios, which is not possible for the effects of different penetration.

A second effect is that the radiation of the point source is additionally damped by ground roughness and trees especially at low view angles. The field experiments showed that these effects can be approximated by a model of the source buried at 1 cm depth.

The modelled count rate of such a buried source of 1.9 GBq activity using the experimentally determined detector efficiency is shown in Fig. 6. The detection limit lies between 10 cps and 50 cps depending on the background count rate. As can be seen from Fig. 6 the source can be detected using a flight line spacing of 250 m and a ground clearance of 90 m.

The detection limit of the airborne radiometric system lies between 0.4 GBq (10 mCi) and 1.9 GBq (50 mCi) depending on vegetation cover, background and topography.

REFERENCES

[1] PURVANCE, D., NOVAK, E., General procedure for calibration and reduction of aerial gamma-ray measurements: Specification BFEC 1250-B, U.S. Department of Energy, Rep. GJBX-16(83) DE84004974 (1983).

[2] GRASTY, R.L., Uranium measurements by airborne gamma-ray spectrometry, Geophysics 40 (1975) 503-519.

[3] SCHWARZ, G.F., Methodische Entwicklungen zur Aerogammaspektrometrie, Beiträge zur Geologie der Schweiz, Geophysik Nr.23, Schweizerische Geophysikalische Kommission (1991).

[4] LØVBORG, L., BØTTER-JENSEN, L., CHRISTIANSEN, Gamma-ray measurements in an area of high natural radioactivity, Proc. of the third international symposium on the natural radiation environment, Houston (Texas), CONF-780422, US DOE Technique Information Center (1975).

[5] LEUPIN, A., Vergleich aeroradiometrischer Messungen in der Umgebung von KKB/PSI mit In-Situ-Gamma-Spektrometrie-Messungen am Boden, Interner HSK-Bericht, Bundesamt für Energiewirtschaft (1990).

[6] MURITH, C., VOELKLE, H.R., SURBECK, H., PILLER, G., BAERISWIL, L., BEURET, P., FERRERI, G., GOBET, M., GURTNER, A., RIBODRY, L., Mesures in situ mesures aéroradiométrie dans le voisinage du PSI, Interner SUeR-Bericht, Bundesamt für Gesundheitswesen; Abteilung Strahlenschutz (1990).

[7] KISSLING, E., Radiometrische Untersuchungen im Rotondogranit, Diplomarbeit, Institut für Geophysik ETHZ, Zürich (1976).

[8] LABHART, T.P., RYBACH, L., Abundance and distribution of uranium and thorium in the syenite of Piz Giuv (Aar-Massif, Switzerland). Chemical Geology 7 (1971) 237-251.

STANDARDIZATION OF OLD GAMMA RAY SURVEY DATA

R.L. GRASTY
Geological Survey of Canada, Ottawa, Canada

M. TAUCHID
International Atomic Energy Agency, Vienna, Austria

L.M. de M. TORRES
Instituto Geologico e Mineiro, Lisbon, Portugal

Abstract

A large part of the world has been covered by ground and airborne gamma ray surveys, many of which have not been standardized. In 1990, the IAEA supported a mission to Malaysia to produce background radiation maps from a large airborne gamma ray survey flown in 1981. The airborne count rate data were successfully converted to ground concentrations of potassium, uranium and thorium by comparing the airborne measurements with those made with a calibrated portable gamma ray spectrometer along an aircraft flight line. The resulting ground concentrations of potassium, uranium and thorium were then used to produce a background exposure rate map. A similar programme of back-calibration of old gamma ray survey data was recently initiated by the Portuguese government through an IAEA sponsored programme. However, in this case, the gamma ray measurements were made using three different types of equipment — ground and car-borne total count gamma ray scintillometers as well as airborne gamma ray spectrometry. This paper describes how three different modes of gamma ray measurements can be standardized to produce maps showing the potassium, uranium and thorium concentration of the ground as well as the exposure rate at ground level.

1. INTRODUCTION

In the last few years there has been increasing public concern regarding the safe use of nuclear energy, particularly since the nuclear reactor accident at Chernobyl. This concern has led to an increased interest in natural background radiation levels. Unless these levels are known, it is difficult to assess the effect on man of the increased radiation caused by man-made radiation.

A large part of the world's land area has been covered by ground and airborne gamma ray measurements. This vast source of gamma ray data is potentially valuable for assessing background radiation levels throughout the world. The extent of world-wide coverage is shown in Fig. 1., based on an International Atomic Energy Agency (IAEA) questionnaire to member states and published information. Many additional survey areas may have been covered through private contracts to survey companies.

Ground gamma ray surveys commenced in the late 1950s and early 1960s due to the interest for uranium, and were mostly made with small hand-held NaI (Tl) total count scintillometers. Airborne gamma ray spectrometry started around the mid-1960's following the development of much larger scintillator detectors.

Procedures for standardizing airborne and ground gamma ray measurements were developed in the late 1970's as a result of large government uranium exploration programmes such as those carried out in the United States and Canada [1,2]. These procedures were developed because many systems with different detector volumes were involved in these national programmes. However, the results for these national programmes were not presented in units of general interest to the health

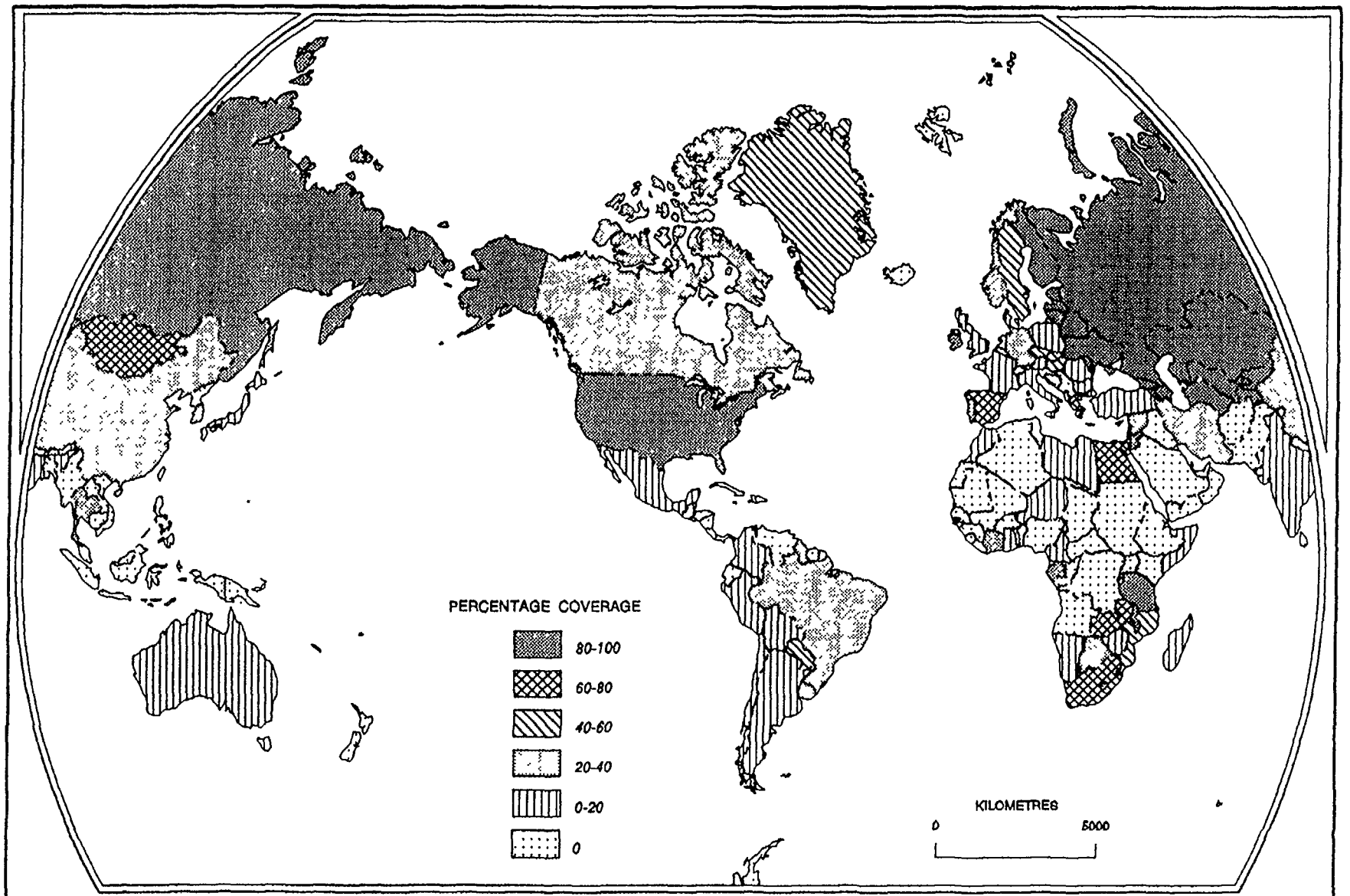

FIG. 1. A map showing the extent of world gamma ray survey coverage.

physicist, normally being presented as ground concentrations of potassium (in percent) and parts per million (ppm) of uranium and thorium.

In spite of the existence of standardized procedures, it is still common for airborne survey companies to present data to their clients, normally exploration companies, as corrected counts per second in the potassium, uranium and thorium windows. This is mainly because the explorationist is concerned with the relative concentrations of the radioactive elements, not in their absolute concentrations.

The International Atomic Energy Agency (IAEA) has directed much attention to the problems of standardization of gamma ray measurements through various consultant reports on the construction of calibration facilities for ground and airborne gamma ray spectrometers [3,4]. The preparation of laboratory gamma ray counting standards for potassium, uranium and thorium was also initiated by the IAEA [5].

Recently, the IAEA investigated the possibility of standardizing old gamma ray data. In 1990, the IAEA sponsored a mission to Malaysia to assess the quality of a large airborne gamma ray survey previously flown in 1980. Data from this survey were successfully converted from count rates to concentrations of the respective radioelements which were then used to calculate ground level exposure rates [6]. A similar programme of back-calibration of old gamma ray survey data was recently initiated by the Portuguese government through an IAEA sponsored programme. However, in this case, the gamma ray measurements were made using three different types of equipment, ground and truck total count gamma ray instruments, as well as airborne gamma ray spectrometer measurements.

This paper describes how gamma ray data from the surveys in Malaysia and Portugal were standardized and used to produce background radiation maps for large areas of these countries.

2. MALAYSIA

2.1. INTRODUCTION

In 1980 the Government of Malaysia funded an airborne magnetic and spectrometric survey over a large area of Peninsular Malaysia. The main outputs from the survey were maps and profiles of total count and the potassium, uranium and thorium window count rates.

In 1990 an IAEA consultant assessed the quality of the airborne gamma-ray data and identified levelling problems in the uranium channel. These level changes between adjacent flight lines were believed to be due to atmospheric background variations. The thorium map, however, exhibited none of these problems and showed good correlation with the known geology. In view of the quality of the original data and the cost of the survey, it was recommended that the digital data be reprocessed. Back-calibration of the airborne data was also recommended for conversion of the airborne data to ground concentrations of potassium, uranium and thorium. This conversion was a necessary requirement for the production of a background exposure rate map.

2.2. BACKGROUND AND STRIPPING CORRECTIONS

In the original processing of the airborne data, background determinations were made approximately 750 m above the ground where ground radiation is reduced substantially. However, only one value, the lowest, was used as a background for the entire survey. Analysis of these background measurements showed that there were considerable daily variations in the uranium

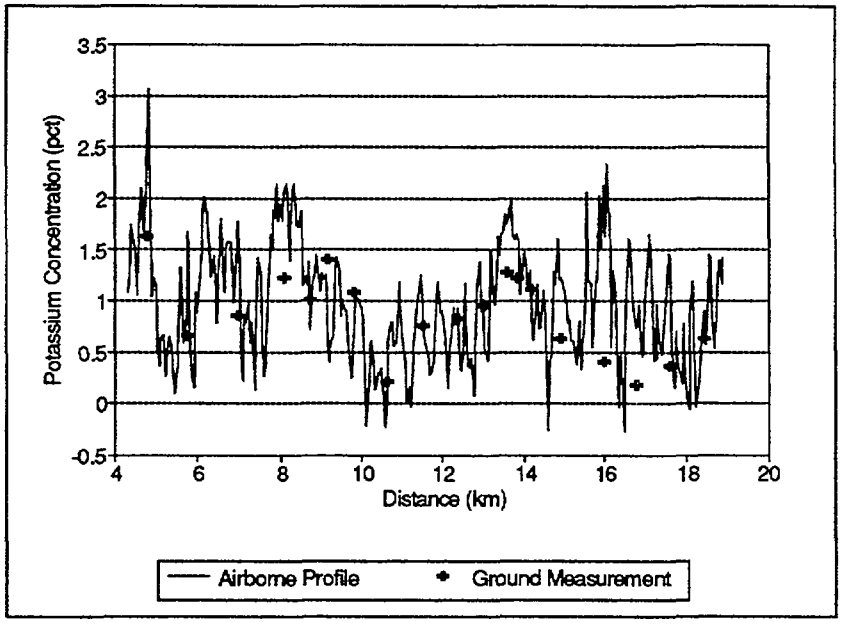

FIG. 2. The relationship between the potassium ground concentration and the calibrated airborne measurements in Malaysia.

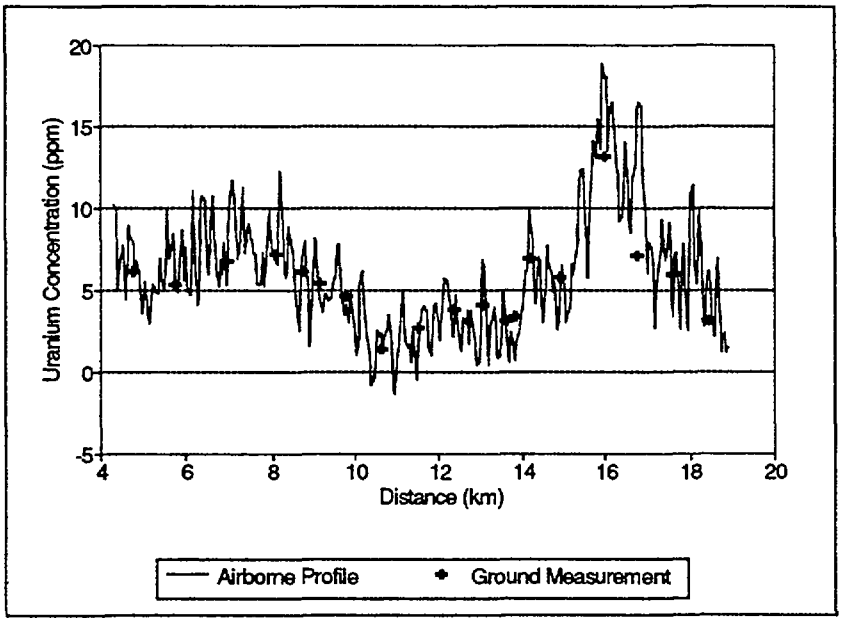

FIG. 3. The relationship between the uranium ground concentration and the calibrated airborne measurements in Malaysia.

channel. This was attributed to fluctuations in the bismuth-214 concentration in the air. These measurements at 750 m were used as initial backgrounds for each channel and improved the uranium map considerably. Final levelling was achieved by filtering the gridded data.

In the initial processing, the stripping ratios used to remove the interfering effects between the potassium, uranium and thorium windows were based on measurements with small sources of uranium and thorium. These small source measurements do not include any component due to Compton scattering in the ground. By comparing measurements with a small source to those from calibration pads the increases in the stripping ratios can be determined [7]. The stripping ratios also increase with altitude due to Compton scattering in the air. These stripping ratio increases were used in the reprocessing of the original data, following the procedures described by the IAEA [4].

2.3. BACK CALIBRATION

The standard procedure for converting airborne gamma ray measurements to ground concentrations of potassium, uranium and thorium is to fly over a test strip with known concentrations of the three radioactive elements [4]. For the Malaysia survey, no test strip was flown and therefore an alternative calibration procedure was required.

Ideally, a calibration line would be a flat and radioactively uniform area with easy road access. In most of the surveyed area there are very few roads, vegetation is dense and there is considerable topographic relief. However, in the north-east of the survey area, close to Kota Baru and the Thailand border, there were a few areas with roads and tracks where ground measurements could be made relatively easily.

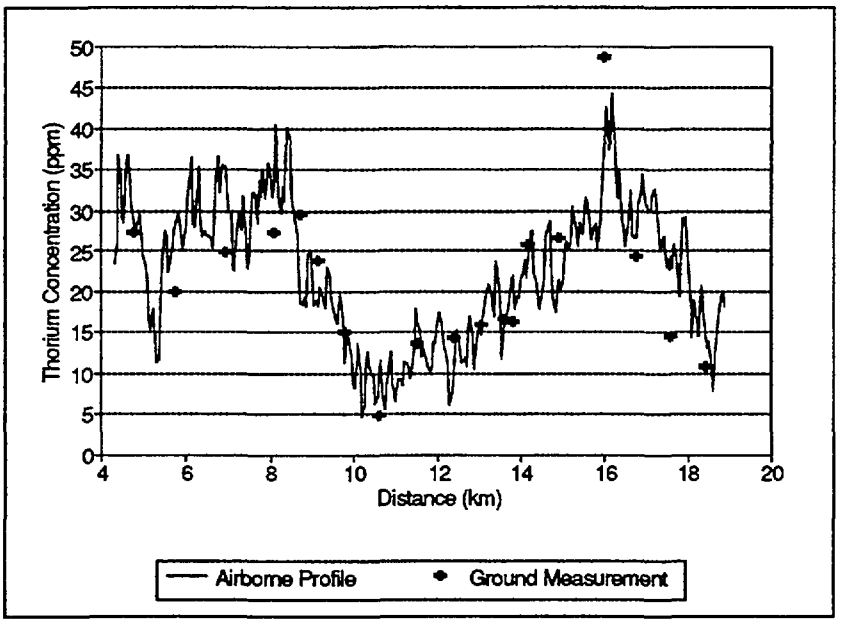

FIG. 4. The relationship between the thorium ground concentration and the calibrated airborne measurements in Malaysia.

A 10 km section of a flight line was selected as a calibration line for comparing ground and airborne measurements. 19 ground measurement sites were selected on this line at the intersection of roads or tracks with the aircraft flight track, approximately every 500 m. These sites were readily identifiable on the topographic map showing the aircraft flight line. At each site, 4 ground measurements were made, two on either side of the road and typically 10 to 20 m apart. The four measurements were used to estimate the errors associated with the ground measurements.

The reprocessed channel count rate profiles along the calibration line showed considerable variations in radioactivity. The airborne and ground measurements were therefore compared separately at each measurement site to derive 19 separate sensitivities. The errors in these sensitivities were computed from the error on the mean value of the airborne count rates and the four ground measurements as shown in Table I. The potassium, uranium and thorium sensitivities and their associated error were then calculated from the 19 individual sensitivities at each site taking into consideration the associated errors.

TABLE I. AN EXAMPLE OF THE AIRBORNE CALIBRATION PROCEDURE FOR URANIUM

Site number	Ground concentration Uranium (ppm)	Airborne Uranium (cps)	Sensitivity (cps/ppmU)
1	6.1±0.5	13.6±4.5	2.2±0.8
2	5.4±0.3	14.1±3.8	2.6±0.7
-	-	-	-
-	-	-	-
19	3.2±0.4	11.2±6.6	3.5±2.1

Using the calculated system sensitivities, the airborne count rates for the calibration line were converted to concentrations and compared to the 19 ground measurements. These results in Figures 2, 3 and 4 show the excellent agreement between the ground and airborne measurements. Finally the exposure rate was calculated from the ground concentrations of potassium, uranium and thorium using the following relationships [8]:

$$1 \text{ percent K} = 1.505\ \mu\text{R/hr} \quad (1)$$

$$1 \text{ ppm eU} = 0.625\ \mu\text{R/hr} \quad (2)$$

$$1 \text{ ppm eTh} = 0.31\ \mu\text{R/hr} \quad (3)$$

3. PORTUGAL

3.1. INTRODUCTION

A large part of Portugal has been surveyed by ground and truck total count scintillometer measurements. These measurements commenced in the late 1950's in the search for uranium. In addition three areas have been covered by airborne gamma ray spectrometry including a large area of southern Portugal flown recently in 1991.

The airborne maps were originally presented in counts per second in the total count, potassium, uranium and thorium windows. Following the Malaysian procedure, back calibration of the airborne data was carried out to convert the airborne count rate data to ground concentrations of

potassium, uranium and thorium. Comparisons of the calibrated airborne data with the ground measurements are shown in Figs 5 to 7 for one of the airborne surveys.

Many tens of thousands of spot total count measurements have been carried out with hand-held scintillometers. Almost all these measurements were made with the SPP-2 total count scintillometer with a 3.7 × 2.5 cm (1.5 inch diameter and 1 inch thick) NaI(T1) detector manufactured by the French company Societé de Recherches et D'Applications Techniques. The total count readings and their coordinates were plotted on 1:25,000 maps.

In the late 1950s two truck systems commenced measurements along roads, mainly concentrating in the northern areas of Portugal. The equipment was manufactured by the Atomic Energy Research Establishment in Harwell, UK and has been used for uranium exploration in many places throughout the world. The systems also used total count scintillometers with the same detector size as the SPP-2. Approximately 50,000 line km of truck measurement were made between 1957 and 1962. The measurements were recorded on chart records which could be accurately tied into reference points marked on detailed 1:25,000 maps.

There are approximately 240 1:25,000 maps with ground and truck data which, after standardization, could be used to produce a radioactivity map for a large area of Portugal. In 1991 and 1992, the IAEA supported two missions to Portugal to investigate standardizing these total count measurements. In the following section we describe how the ground and truck measurements were converted to exposure rate. The procedures used to produce the radioactivity map is described in another paper by Torres and Grasty in this publication [9].

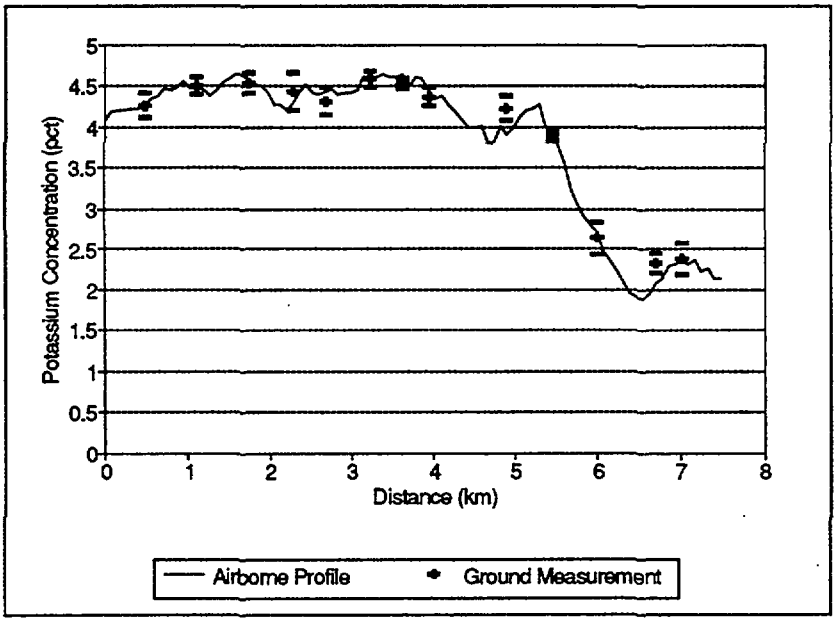

FIG. 5. The relationship between the potassium ground concentration and the calibrated airborne measurements in Portugal.

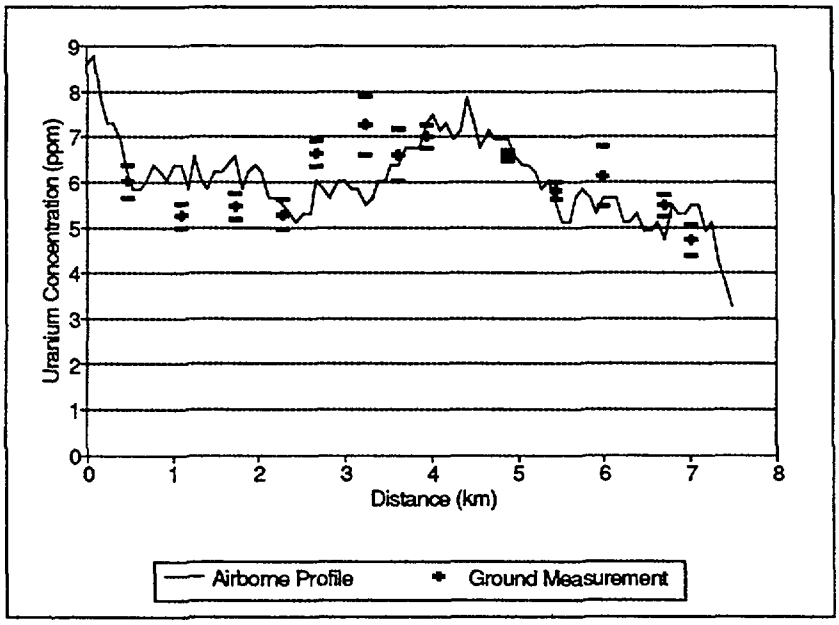

FIG. 6. The relationship between the uranium ground concentration and the calibrated airborne measurements in Portugal.

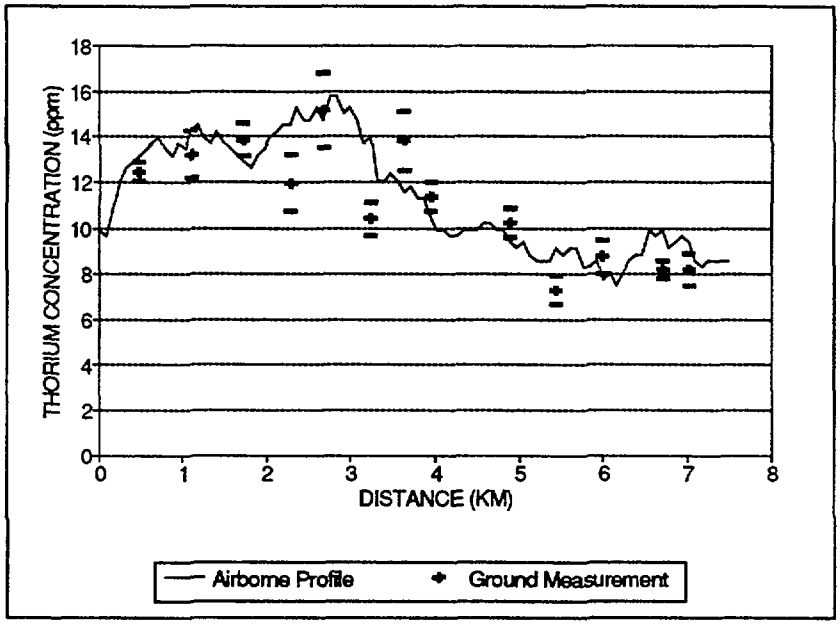

FIG. 7. The relationship between the thorium ground concentration and the calibrated airborne measurements in Portugal.

3.2. CALIBRATION OF SPP-2 TOTAL COUNT SCINTILLOMETERS

The relationship between total count and exposure rate depends both on the size of the detector and its lower energy threshold [3]. In addition, because of the different energy distributions of gamma-radiation from potassium, uranium and thorium, this relationship may vary with the potassium, uranium and thorium concentration of the ground.

A total count scintillometer receives primary unscattered radiation, radiation scattered in the ground as well as a significant fraction of "Skyshine" radiation. This Skyshine component is downward scattered radiation from the air above the detector and is predominantly of low energy. It can originate from sources several hundred meters from the measurement location. In the case of a portable spectrometer, the high energy gamma rays used for monitoring potassium, uranium and thorium gamma-radiation in the ground originate from sources within a few meters of the measurement location. Therefore, in comparing the SPP-2 measurements with those from a portable spectrometer, the ground should be relatively uniform over a large area.

During the first IAEA mission, 14 sites with varying concentrations of potassium, uranium and thorium were investigated as possible calibration sites for the SPP-2 scintillometers. At each of the sites, three measurements several tens of meters apart were made with two SPP-2 scintillometers. The potassium, uranium and thorium concentrations were also determined at these sites using an Exploranium GR-256 portable gamma ray spectrometer calibrated on transportable pads in Canada [6]. 11 of the sites were found to be sufficiently uniform in their radioactivity to be suitable as calibration site sites.

For each site, the calculated exposure rate from the three GR-256 measurements of the potassium, uranium and thorium concentrations (equations (1) to (3)) were compared to the average of the two SPP-2 scintillometer readings. The calibration line shown in Fig. 8. was obtained by linear regression and indicates a non-zero intercept on the horizontal axis. This intercept corresponds to the background count rate of the SPP-2 instruments and is due to cosmic radiation, the radioactivity of the instrument and any radioactivity due to radon decay products in the air. Similar values were found from measurements over water where the contribution from potassium, uranium and thorium was assumed to be negligible.

The good linear relationship between the SPP-2 readings and exposure rate was initially somewhat surprising because of the different relationship between total count and exposure rate for sources of potassium, uranium and thorium. In practice, however, it is unusual to have rocks or soils containing relatively pure sources of potassium, uranium and thorium. Also if the radioactivity of a rock or soil increases, the concentrations of all three radio-elements tend to increase. In addition, it has been shown that for a 7.6 × 7.6 cm. (3 × 3 in.) detector with a threshold of 0.37 MeV, the relationship between total count and exposure rate is independent of the concentration of potassium, uranium or thorium [10]. These results have therefore demonstrated that provided measurements are made on typical soils, a total count instrument can be calibrated to estimate the exposure rate (or dose rate) due to gamma-radiation from potassium, uranium and thorium.

3.3. CALIBRATION OF TRUCK SYSTEM

The calibration of the truck system was achieved by comparing the truck measurements with the exposure rate also calculated from measurements with an Exploranium GR-256 portable gamma ray spectrometer. However, in this case the portable spectrometer was calibrated in Portugal on transportable pads provided by the IAEA.

In calibrating the truck measurements, there are several factors to consider. These include such things as the distance travelled during the sampling period, the field of view of the detector,as

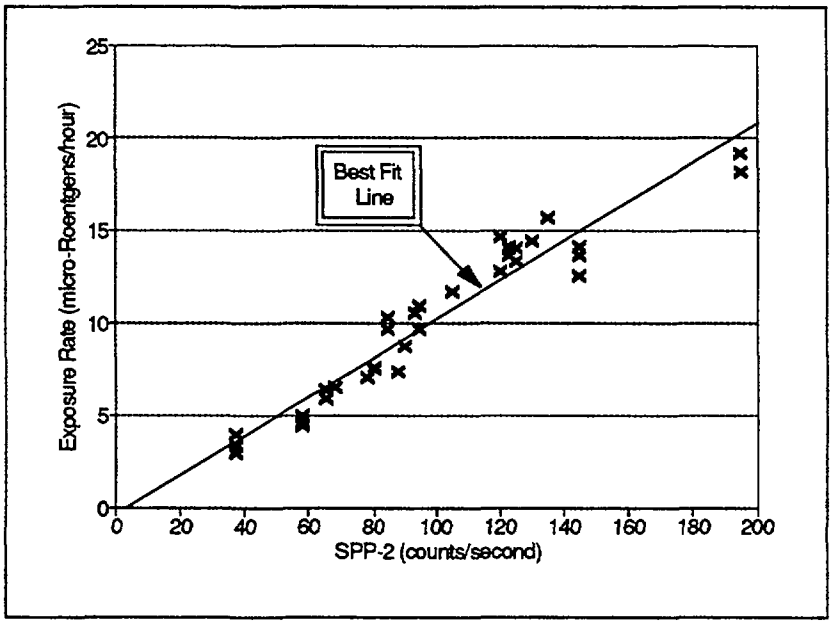

FIG. 8. The relationship between the SPP-2 total count rate and the exposure rate calculated from the ground concentrations of potassium, uranium and thorium.

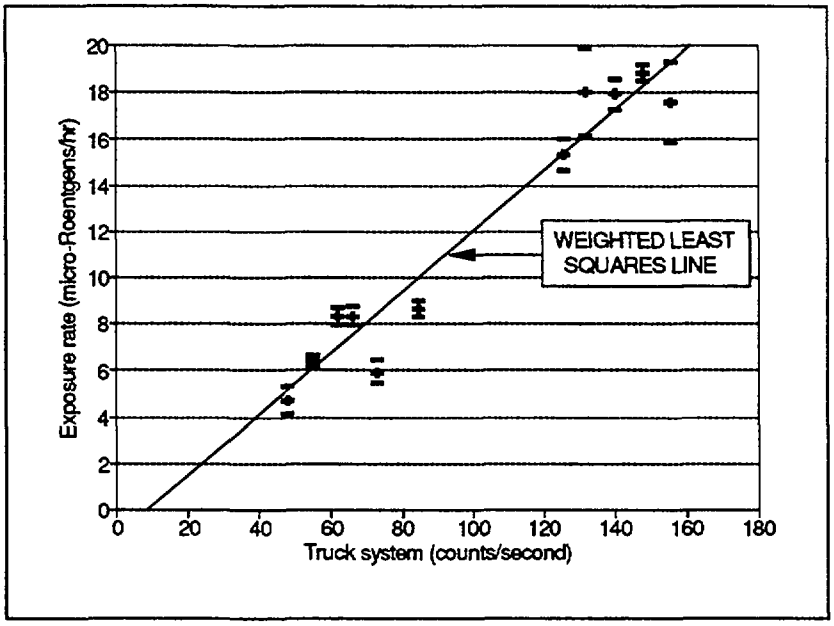

FIG. 9. The relationship between the truck system total count rate and the exposure rate calculated from the ground concentrations of potassium, uranium and thorium.

well as possible differences in the road surface or surrounding ground from the time the measurements were taken, 30 to 35 years previously.

Based on the sampling speed and time constant of the equipment as well as on the estimated speed of the vehicle, it was determined that each measurement on the chart record would correspond to a distance of approximately 50 m along the road. The sites for calibration of the truck system were selected to cover a wide range of radioactivity as indicated by the analog total count traces. All the measurement sites could be clearly identified on the 1:25,000 maps showing the tracks of the truck surveys. These sites were typically road intersections, but also included the boundaries of fields, gates etc.

Three measurements were made with the GR-256 portable gamma ray spectrometer on the road surface at each selected site. One measurements was made at the location indicated on the map of the vehicle routes, with two additional measurements being taken 25 m either side of the first measurement. These 3 measurements took into consideration the distance travelled by the vehicle and permitted an estimate of the errors in the measurements at each site.

Approximately 50 sites were visited as possible calibration sites. However, only 19 were found to be suitable. Sites were rejected if they were close to man-made features such as a building, or if the road was surfaced with asphalt or material that may have originated from another location. At several locations, the road was narrow with high stone walls. These sites were rejected on the basis of the different geometries of the truck system and the portable spectrometer which was calibrated for use at ground level. In the truck system, the detector which was mounted near the roof of the vehicle, could 'see' over the stone walls. Because of the proximity of the walls, the walls could have a significant effect on the ground spectrometer measurements.

At each selected calibration site, the potassium, uranium and thorium concentrations were calculated from the portable gamma ray spectrometer measurements. These measurements were then used to calculate the exposure rate using equation (1) to (3) which was then compared to the count rates digitized from the old truck records.

Fig. 9. shows the comparison between the calculated exposure rates and the count rates from the truck systems. The data presented is the mean value of the exposure rate for all truck measurements with the same value. By sorting the data in this manner all the errors (indicated in the figure) are associated with the exposure rate axis. It is then justified to compute a calibration line by weighted least squares regression. This calibration line as shown in the figure was used to convert all the truck measurements to exposure rate.

ACKNOWLEDGMENTS

We would like to thank Mr Mohd Zaidi and Mr Dzazali of the Geological Survey of Malaysia and Mr Leote from the Geological Survey of Portugal for co-ordinating the field work during the IAEA missions to Malaysia and Portugal. Without their valuable assistance, back-calibration of the gamma ray measurements would not have been so successful.

REFERENCES

[1] DUVAL, J.S., Potassium, uranium and thorium geochemical maps of the conterminous U.S.A.; Transactions of the Institution of Mining and Metallurgy (Section B; Applied earth science), 100 (1991) 66-73.

[2] DARNLEY A.G., CAMERON E.M. RICHARDSON K.A. 1975. The Federal-Provincial

Uranium Reconnaissance Program, Geological Survey of Canada Paper 75-26, Uranium Exploration '75 (1975) 49-63.

[3] INTERNATIONAL ATOMIC ENERGY AGENCY, Construction and use of calibration facilities for radiometric field equipment, IAEA Technical Report Series-309, Vienna (1989).

[4] INTERNATIONAL ATOMIC ENERGY AGENCY, Airborne gamma ray spectrometer surveying, IAEA Technical Reports Series-323, Vienna (1991).

[5] INTERNATIONAL ATOMIC ENERGY AGENCY, Preparation and certification of IAEA gamma ray spectrometry reference materials RGU-1, RGTh-1 and RGK-1, IAEA Technical Report IAEA/RL/148, Vienna (1987). p.

[6] GRASTY R.L. WHITTON R.M. and DUFFY A, Back calibration and reprocessing an airborne gamma ray survey, Malaysia. Expanded abstracts, Society of Exploration Geophysicists annual meeting, New Orleans (1992) 550-551.

[7] GRASTY R.L., Holman P.B. and Blanchard, Y. 1991: Transportable calibration pads for ground and airborne gamma ray spectrometers, Geol. Surv. Canada pap. 90-23 (1991).

[8] GRASTY R.L., CARSON J.M., CHARBONNEAU B.W. and HOLMAN P.B., Natural background radiation in Canada. Geol. Surv. Canada, Bull. 360, (1984).

[9] TORRES L.M. and GRASTY R.L., The natural radioactivity map of Portugal: Baseline information on natural radioactivity background, Proceedings IAEA technical meeting on the Use of Uranium Exploration Data and Techniques in Environmental Studies, IAEA-TECDOC (This publication).

[10] LØVBORG L., and KIRKEGAARD P., Response of 3" × 3" NaI(Tl) detectors to terrestrial gamma radiation; Nucl. Instr. and Meth. 121, (1974), 239-251.

THE RELEVANCE OF AIRBORNE AND GROUND GAMMA RAY SPECTROMETRY TO GLOBAL GEOCHEMICAL BASELINES

A.G. DARNLEY
Geological Survey of Canada, Ottawa, Ontario, Canada

Abstract

The International Geochemical Mapping (IGM) project is a response to the fact that information about the distribution of radioactive and non-radioactive elements in the earth's surface materials is inconsistent and incomplete. The IGM project is organized under the International Geological Correlation Program, sponsored by UNESCO and IUGS. The IAEA has provided support for that part of the project which relates to radioactive elements. These elements, both natural and man-made, are part of the geochemical environment and subject to the same chemical and physical processes as non-radioactive elements. For many reasons their spatial distribution should be studied and recorded as part of a common database. Phase 1 of the IGM project has been concerned with the establishment of recommendations for the conduct of future work. Phase 2 of the project will be concerned with establishing global geochemical baselines for all elements. Gamma ray spectrometry is an efficient method of identifying and quantifying radioactive elements, either by in situ measurements at fixed sites, or from a moving vehicle or aircraft. All modes of measurement are required to establish reliable global baselines. However, airborne gamma ray spectrometry (AGRS) has a unique advantage because it provides a continuous profile over any land surface, independent of surface terrain. With calibrated systems, quantitative correlation of airborne and ground data can be assured within definable limits. The IGM project involves the acquisition of new data and, where quality is acceptable, incorporation of old. There are many pattern and level discrepancies between neighbouring blocks of conventional geochemical data collected in different regions of the world due to diverse methods and lack of standardization. Are these discrepancies real or apparent? Thorium and K surface abundance profiles, derived from widely spaced gamma ray transects, can provide an independent reference level against which discontinuities in other datasets can be assessed. The abundance of man-made radioisotopes can be measured simultaneously. These transects will contribute to more reliable and comprehensive baseline data for all elements.

1. INTRODUCTION

Radioactive elements (radioelements or radionuclides) form part of the natural global environment. Their distribution and mode of occurrence are subject to the same natural laws as non-radioactive elements, many of which can also be harmful under some circumstances. Despite their ubiquity and the fact that K,U,Th and their decay products have always formed part of the environment, many members of the public are apprehensive about any source of radioactivity or any possible exposure to radiation. This is an important reason why data concerning the spatial distribution of the naturally occurring radioactive elements should be familiar to the public through information and education facilities. The same databank should also contain information about long half-life products of nuclear weapon tests and reactor accidents, such as ^{137}Cs, which have accumulated in the environment.

The rationale for the International Geochemical Mapping project, its relevance to many environmental and economic issues, and its connection to IAEA activities in the field of uranium exploration, have been described in an accompanying paper [5]. Phase 1 of the International Geochemical Mapping project commenced in 1988 to discuss methods of obtaining globally consistent, comprehensive, multielement base-line data. Phase 2, with the subtitle of Global Geochemical Baselines, will implement plans generated in Phase 1. It is proposed that this will start with the collection of very wide-spaced drainage, regolith, and water samples based on a 160 × 160 km grid, involving approximately 5000 site-clusters worldwide [4]. It is recommended that gamma ray measurements be taken at each of these sites, which can be linked by car-borne gamma ray profiles, and which should be overflown by wide-spaced airborne profiles. It is desirable that radioelement and

non-radioactive element baseline data should be held in a common databank,The Global Geochemical Baselines project is intended to establish a network of reference measurements and materials, analogous to the geodetic network used as a base for topographic surveys. The sample points established for this geochemical network can be used for subsequent periodic monitoring of the environment. Data from the reference collection will be also be used for the secondary purpose of compiling a map of the large-dimension geochemical variations of the earth's surface.

2. RADIONUCLIDES IN THE NATURAL ENVIRONMENT

Although K, U and Th constitute a small fraction of the total natural geochemical environment, it is sensible to map their distribution for reasons which are quite separate from any need to discover uranium resources. In brief, they constitute convenient markers, because of their radioactivity. They are present almost everywhere on the land surface, in measurable amounts. Their characteristic gamma emissions permit in situ field determination and remote measurement from a vehicle or low-flying aircraft. The practical significance of field and airborne gamma ray spectrometry hinges on the fact that the detection limits for K, U and Th, with these methods, are below their normal ranges of abundance. This makes it possible to map quantitatively the distribution of the radioelements almost everywhere, in situations where some other non-radioactive elements are undetectable because the commonly used methods lack sensitivity. As large-ion lithophile elements, K, U and Th possess distinctive geochemical properties, with the result that their relative distribution patterns can point to scientifically interesting and economically important geological processes. This is discussed in [7] and [3].

In the context of comprehensive baselines, this paper is concerned with ground (field portable and car-borne) and airborne gamma ray measurements. A field portable spectometer can be used for in situ spot measurements or whilst in motion on a traverse. A portable gamma ray spectrometer is relatively compact and lightweight (the NaI detector crystal is the heaviest item), reliable and simple to use. Properly calibrated according to the method recommended by the IAEA [19] they can provide detection limits/sensitivities of 0.25% K, 0.5 ppm eU, 1 ppm eTh, with repeatability within statistical limits which are set by concentration levels and counting time. To ensure meaningful measurements the geometric relationship between detector and ground must duplicate the calibration geometry, i.e., a fixed distance above an effectively infinite flat source area, or resting on the surface of a smaller (minimum 1.5 m diameter) source. Ground measurements (of K, eU, eTh, also ^{137}Cs if present) with a portable gamma ray spectrometer are needed to correlate with:

a) conventional geochemical analysis of the upper regolith or "A" soil horizon (which will provide multielement data including K, Cs, U, and Th measurements).

b) airborne gamma ray spectrometer overflights (providing K, eU, eTh and ^{137}Cs if present).

At least 90 per cent of natural gamma radiation emerging from the ground originates from within the upper 25 cm. (Gregory and Horwood 1961). In a uniform field a gamma ray detector carried at shoulder height is dominated by radiation received from a 10 m radius. A gamma ray spectrometer in a vehicle can move relatively rapidly in open prairie or open savannah woodland and can be effective on narrow or unsurfaced roads (but not wide highways made of exotic materials). If the detector is mounted on a mast 3 m high, in flat country most of the gamma signal will be received from a 25 m swath. In rough country a car-borne survey is restricted to the available tracks and roads; in the same situation a foot-borne traverse may be obstructed by thick vegetation, fallen trees, swamp, water courses, steep slopes etc., with the result that ground coverage will be very uneven. For these reasons, the most effective way to obtain a representative overview of ground level radioelement content and radioactivity is by means of an airborne gamma ray spectrometer (AGRS) survey, using high sensitivity equipment. In terrain with low topographic gradients fixed wing aircraft can be used, elsewhere helicopters are necessary. Equipment in an aircraft can overlook surface

access problems, can be carried in a straight line, responds to a broad swath (with 125 m terrain clearance a 250 m swath is covered), and collects data rapidly. The principles, development, and technical requirements for high sensitivity quantitative AGRS have been fully described in various publications [21]. Airborne gamma ray spectrometry is a major component of the International Geochemical Mapping project because it can provide:

a) continuous profiles measuring the variations in the concentration of natural and man-made radionuclides on and in the surface layer of the earth;

b) a method of making radioelement maps for geoscience and environmental purposes;

c) a method of comparing and linking regions, countries and continents by providing eTh and/or K reference profiles across any land surface.

The importance of the latter function is discussed in the following two sections.

3. THE BASELINE PROBLEM IN GEOCHEMICAL DATA

The concept of international geochemical mapping requires that numerical values for the abundance of elements in, for example, the regolith are equally valid and related to the same scale of absolute values wherever regolith samples are taken. Unfortunately geochemical mapping as practiced during the past 40 years has had many variations. Different sample media have been used in different geographic regions; e.g. soils, laterites, and desert wash; stream and lake sediments; heavy minerals; glacial till. Bolviken et al.(1986) illustrate the effects of different sample media and different analytical treatments upon spatial patterns and quantitative values. Even within regions where a single sample medium and a nominally similar sample preparation and analytical approach have been used, level discrepancies between adjacent data blocks are often apparent, due to work being carried out at different times [see Geochemical Atlas of Alaska, 1989] or by different organizations using non-identical procedures [12]. Inconsistencies become obvious when compilations are attempted using existing data. Major discontinuities are present where changes in methodology have taken place, commonly, but not exclusively, at administrative boundaries. An extreme example of artificial discontinuities, due to the averaging of data within political units, is provided by the Radiation Atlas for Europe [15]. Plant and Ridgway [23] have listed the heterogeneities of geochemical data within Western Europe.

A method of normalizing broadly similar adjoining or overlapping sets of lake sediment data has been demonstrated by Garrett et al. [12]. The problems of relating overlapping lake and stream sediment data have been discussed by Davenport [9] and Garrett et al. [11]. In these examples the datasets under consideration have involved relatively close-spaced sampling. The problems increase as sample density decreases. The levelling of scattered "islands" of dissimilar data presents additional difficulties.

In order to compile a world geochemical map or establish reliable baselines, there is clearly a need for a worldwide geochemical reference datum (a geochemical "mean sea-level") against which all surveys can be compared. Ideally this would be a datum for all elements, all types of media and all analytical methods. Wide-spaced sampling which is the starting point for multi-element baselines can only go part way towards meeting the levelling requirement. It provides a series of geochemical control points or "spot-heights". Wide-spaced drainage samples are selected to be representative of large areas, but they are necessarily few in number. This is in order to restrict the number of samples to a quantity that can be processed by a small number of internationally recognised laboratories, to ensure consistent quality. The resulting coverage is therefore discontinuous and it cannot show the exact position of boundaries or easily distinguish anthropogenic from geological effects.

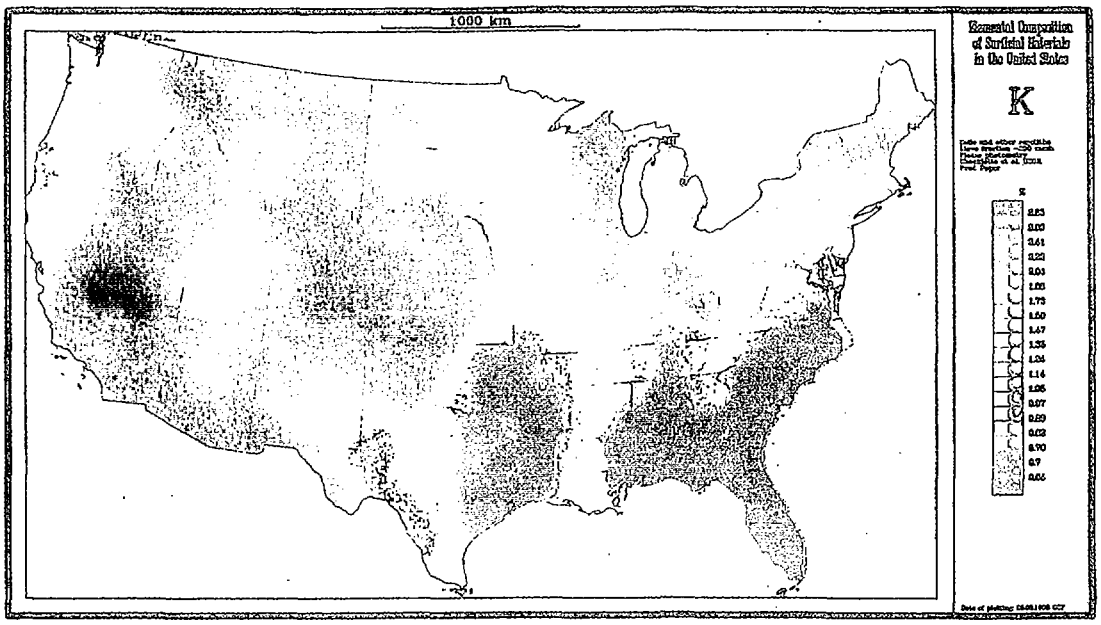

FIG. 1. Potassium in the regolith of the USA; based on 1314 samples (20 cm depth) collected close to major highways; analysed by flame photometry. Prepared by N.Gustavsson et al. (Geological Survey of Finland) from data by Shacklette and Boerngen.

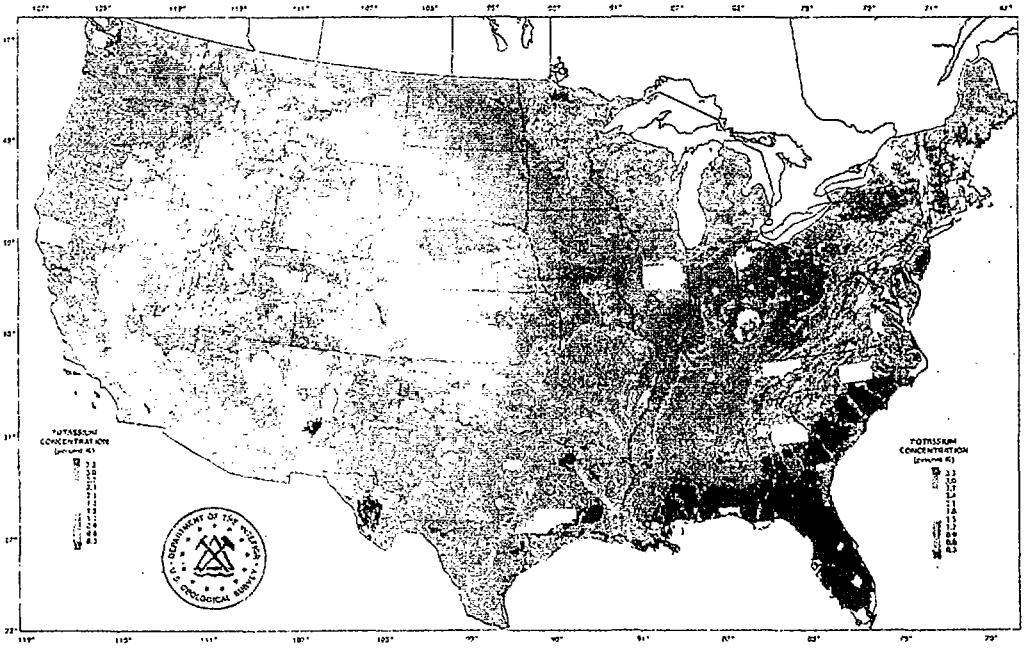

FIG. 2. Potassium in the regolith of the USA; from airborne gamma ray spectrometry; E. half of country mostly 10 km line spacing, W. half mostly 5 km. From Duval (1991).

4. RELEVANCE OF AGRS PROFILES TO GEOCHEMICAL BASELINES

AGRS systems are calibrated by determining the surface layer concentrations of K, eU and eTh along specially selected test strips (there are several in different parts of the world, see [21]) using calibrated portable gamma ray spectrometers, and overflying the strip with the airborne system. Methods were developed in Canada during the late 1960s [6]. Later, test lines several km in length were delineated in several countries, using an alluvial plain, or dry lake bed. A linear correlation is established between ground and airborne count rates for each installation, thus providing the basis for quantitative surveys elswhere (subject to a number of conditions and corrections; for details see IAEA [19,20,21]. Grasty et al. [14] have recently demonstrated the correlation obtained between ground and airborne gamma ray measurements along a 10 km calibration line in an area of rubber plantations in NE Malaysia.

Given that the relationship between ground and airborne count rates provides the basis for AGRS system calibration, this suggests that AGRS measurements can be used for the reverse process, to monitor the validity of otherwise uncertain or unstandardized ground data involving the radioelements. The conterminous United States constitutes a large test area over which K data are available to allow a comparison to be made between AGRS and conventional surface sampling. During the 1960s Shacklette et al. [24] sampled regolith material, principally soil, from a depth of about 20 cm from locations approximately 80 km apart along major highways over the whole country (1314 sites). The -200 mesh fraction was analysed for K by flame photometry and the results plotted as sample-point symbols on a map [24, p.72-73]. These data have recently been digitised, smoothed and computer plotted by Gustavsson et al. at the Geological Survey of Finland, (pers.com.). The result is reproduced as a K map in Fig. 1. Shacklette and Boerngen report the arithmetic mean for K over the whole US as 1.5% K. They report the western half of the country (W. of Long.97^0) has a geometric mean of 1.8% K; the eastern half, 0.75% K.

Fig. 2 shows a K abundance map of the conterminous US, based on AGRS data obtained during the National Uranium Resource Evaluation program [from 10]. The AGRS data were collected with most of the flight lines either 5 or 10 km apart. Given the reconnaissance nature of the two totally independent data sets and the wide spacing of the ground-data sample sites (approximately 1 per 6000 km^2), the spatial patterns, the location of high and low values, and the values obtained are surprisingly similar. From visual inspection of Duval's colour map, the median K value from AGRS is between 1.8 and 2.1% west of Long.97^0 and between 0.6 and 0.9% east of 97^0. These numbers bracket Shacklette's geometric means quoted above. It is important to note that both the Shacklette and Duval datasets were each acquired and processed as single tasks, with adequate quality control, resulting in quantitative consistency across the continent and the concordance of the two maps. If either of the datasets had been assembled from unstandardized information the map products could have been grossly discordant.

A comparison of Th datasets, obtained by AGRS and by conventional ground sampling, can be made with respect to an area of 120,000 km^2 between Calgary and Edmonton, in Canada. An airborne survey, with E-W flight lines 30 km apart, was undertaken in 1977 [17]. Fig. 3 shows the eTh profiles along the individual flight lines, superimposed on contoured eTh values. In 1992 soil samples were collected over this region as part of a wide-spaced survey, planned around a 40 km grid, covering a large part of the prairie provinces [13]. Approximately 180 soil sample sites were taken within the block where the airborne survey was carried out; Th was determined by neutron activation analysis. The two datasets provide the following results (values in ppm, rounded-off):

	Range of Th values (5% to 95%)	**Median value**
Airborne gamma spectrometry (eTh):	3 to 7	5
Neutron activation analysis (Th):	5 to 9	7

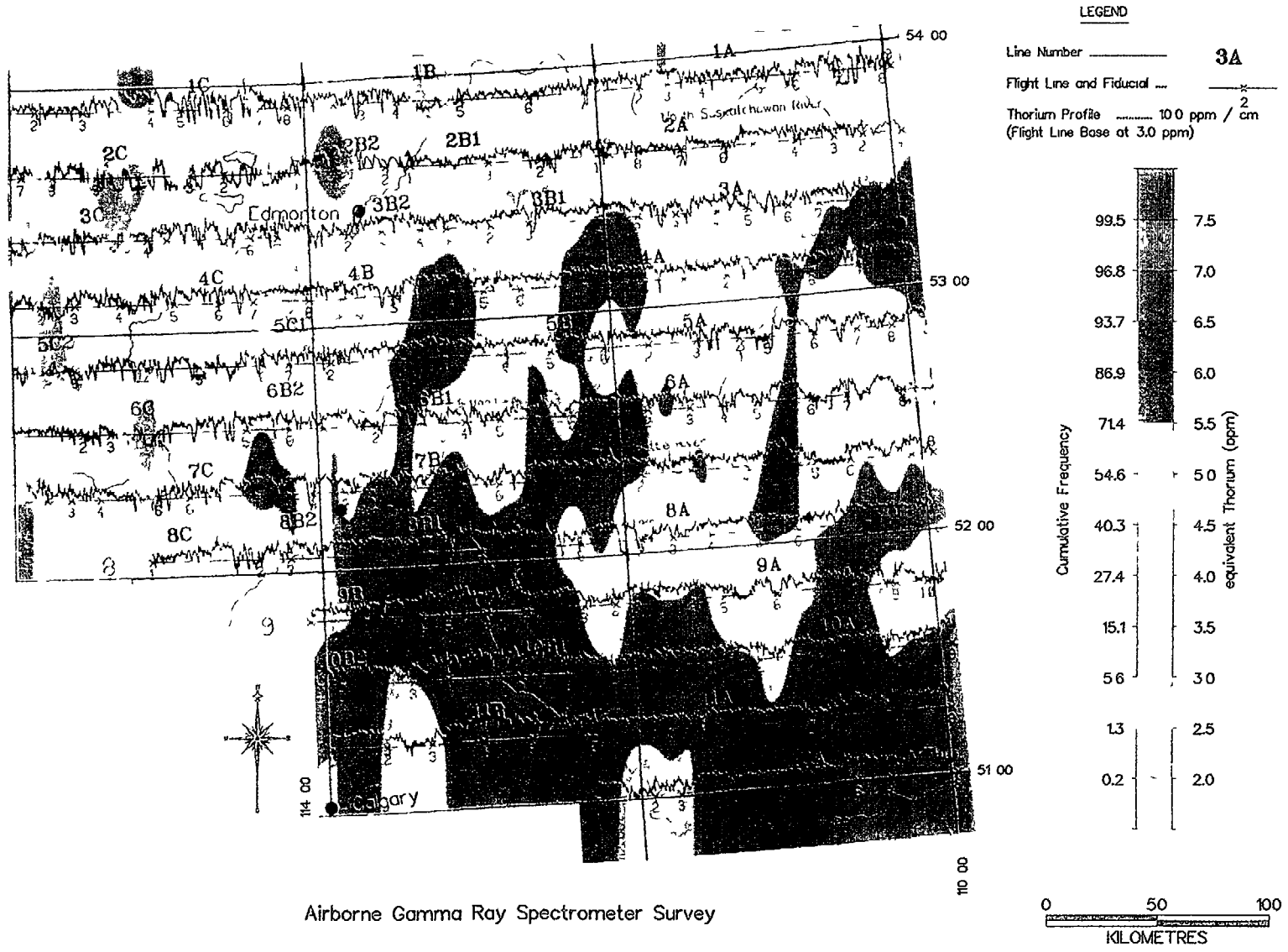

FIG. 3. Thorium in the regolith, SE Alberta, Canada; profiles and contours from airborne gamma ray spectrometry. From Hetu (1991).

The AGRS values are 2 ppm lower than the neutron activation analyses of soil from the same region. It is relevant to note that the airborne and ground surveys were undertaken 15 years apart, with separate objectives. As with the K data in the USA discussed above, the regolith was measured with different analytical methods, at nominally representative but non-coincident sites. No correction has been applied to the AGRS data for a possible soil moisture effect; taking the variables into account, the agreement between these datasets is considered to be within reasonable limits.

The concordance between ground and airborne gamma ray data which can be observed on test ranges and, with less precision, over much larger regions, provides the evidence for believing that AGRS can assist in geochemical levelling. AGRS equipment gathers data continuously in a uniform way whatever the nature of the surface and so it offers a method of linking and comparing disparate data blocks. Extensive surveys over the past 20 years in regions ranging from the arctic to equatorial rainforest have provided many opportunities to examine the relationship between AGRS and ground data [7]. In cold dry climates where there is negligeable chemical weathering the correlation between AGRS data and data from conventional ground sampling appears to have been generally satisfactory for all elements. For Th, the correlation between airborne eTh and ground eTh (or Th) in the A_{25} horizon, shows consistency in all environments. Potassium correlation tends to be somewhat inferior to that observed for Th because more corrections are required in order to derive K abundance from AGRS data, and errors in the correction factors may be cumulative. Also K minerals, particularly micas, are more susceptible to weathering than Th minerals. Data reduction procedures are discussed in the relevant IAEA Technical reports. Uranium correlation, arising from the geochemistry of the element, is inherently the most uncertain, depending upon mineralogy and climate. The correlation observed between airborne and ground eU determination (i.e. both determinations by gamma ray spectrometry) can be good provided both measurements are obtained when a similar soil moisture profile applies [Grasty, pers.com.]. Where a direct method of U analysis (e.g. XRF or NAA) has been employed for determination of U in ground samples, discrepancies are present where chemical weathering has caused parent and/or daughter element migration and separation over distances of more than a few cm. The influence of chemical weathering depends in part on the mineralogical assemblage. Because ^{214}Bi is used as a proxy for U (and expressed as eU) in gamma ray mapping, there is the potential for gross discrepancies between chemically determined U and eU, in part because of gross differences in sample size. In conventional geochemistry the sample weight is measured in gm; in AGRS, tonnes. Because each AGRS sample is very large, migration of constituents can take place and still remain within the sample. However, for the reasons indicated, quantitative estimation of U by AGRS is inherently more uncertain than is the case for Th and K; AGRS responds to ^{214}Bi not U. Thus, discrepancies in U abundance obtained by direct (U) and indirect (eU) methods of analysis do occur, and because of the number of factors which may be involved, if a problem is suspected a detailed investigation may be needed to find the reason.

The use of AGRS to "flag" the existence of suspect data blocks is well within the current state of the art. It involves flying AGRS profiles at a line-spacing determined by the dimensions and complexity of the data blocks to be checked. For example, AGRS profiles at 10 km line-spacing provide continuous sampling over a 250 m strip along each line, representing 2.5 per cent of a block's total area. Thirty km line-spacing, as in the Alberta example referred to above, samples 0.8 per cent. For the reasons given above, median Th and K abundances determined by AGRS and conventional soil sampling along common profiles should normally be expected to agree within ± 2 ppm Th and ± 0.5 per cent K, provided that the soil is not abnormally wet or dry at the time of the airborne measurements and that geochemical analyses of surface soil samples are based upon natural gamma ray spectrometry, neutron activation, XRF or other total estimation methods. Regrettably, Th determinations have rarely been included in past analytical work on soils or regolith. Potassium is often determined for agricultural purposes, but has seldom been included in geochemical mapping where mineral exploration has been the prime objective. Thorium and K determinations are essential if AGRS eTh and K profiles are to be used for reference purposes. It must be possible to compare airborne and ground analyses of A_{25} regolith material.

A problem with data quality may be indicated where there is an abrupt change in the Th/K ratio of ground versus airborne data. This would occur where there is a level change in either Th or K ground survey data which is not reflected in coincident airborne data. This may be an indication of methodological inconsistencies with respect to the ground data, involving a change in sample collection, sample preparation or analytical techniques. In this case it is probable that inconsistencies will apply to other elements in addition to Th and K, depending upon the details of the work. This is important information with respect to the establishment of geochemical baselines, because as previously indicated, the lack of consistency in past data collection methods can make it difficult to distinguish between real and apparent regional differences. By continuously observing the relationship between airborne and ground Th and K data, discrepant blocks of data may be identified. If a consistent serious discrepancy is observed over some clearly defined area, if it is not possible to verify this on the ground (e.g. access is impossible), consideration could be given to calculating and applying a normalization factor to data in this block. Subject to further research, the use of AGRS to compare and correlate resistate element levels (Th being a resistate element) in survey blocks where different sample media have been employed for conventional geochemical mapping may prove to be a useful extension of the level-monitoring technique.

5. RECOMMENDATIONS RELATING TO THE USE OF GAMMA RAY SPECTROMETRY IN ESTABLISHING GLOBAL GEOCHEMICAL BASELINES

This section summarises the relevant section of the report "A Global Geochemical Database: recommendations for International Geochemical Mapping", [8]. It is based on the work of several IAEA consultants' and technical committees, established in support of the radioactive element component of the IGM project. These committees have published their own reports, the contents of which extend beyond what is included here [20, 21, also 22].

5.1. GENERAL STATEMENT

1) Radioactive elements are of special public concern. Data to show their spatial distribution should be an essential part of any comprehensive global (and also regional) geochemical databases.

2) The technique of gamma ray spectrometry enables the abundance of radioactive elements to be determined quantitatively. Its principal advantage is that in addition to being a laboratory technique, determinations can be undertaken rapidly, in situ, from a moving vehicle or from a low-flying aircraft. Gamma ray spectrometry is a standardised technique which can provide a continuous quantitative profile of radioelement abundance over any type of land surface. If profiles are closely spaced, an entire surface can be mapped. In addition to profiling or mapping natural radioelement distribution, radioactive fallout can be identified, measured and delineated. The relevant data should be acquired as part of the collection of baseline information.

3) Airborne gamma ray spectrometry can be used to provide an inter- and trans-continental Th reference datum to assist in levelling geochemical maps from geographically diverse regions.

4) In order to obtain standardized data, methodologies recommended by and promulgated through the publications of the International Atomic Energy Agency should be followed (see references).

5.2. USE OF EXISTING DATA

It is recognised that in many countries there has been a significant past investment in radiometric (gamma radiation) surveys of various types, especially during the 1960s and 70s, primarily related to uranium exploration. Much of this work was sponsored by national governments or international agencies; in general, where surveys were sponsored by the mineral industry, attention was focussed on small areas selected according to suspected mineral potential. This often resulted in overlapping patchwork coverage of priority areas. The early work, and most industry-sponsored surveys, were of a qualitative nature. Standardized methodology began to be introduced into some of the national/international agency large-area surveys during the 1970s. In the interests of economy, before new work is commissioned, there should be a review of existing data:

1) Countries should make an inventory of all regional airborne and car-borne gamma ray spectrometric surveys, and note all the relevant information (date of survey, system used, calibration, type of data processing and storage used, type of map produced, availability of the data). Data quality and completeness of documentation is more important than age, although older data is likely to have been obtained with low-sensitivity equipment. Note that it is important to make a repository of all records and assure adequate storage of the data to prevent damage. The shelf life of most magnetic tapes is 10 years and where possible data should be transferred to an optical disk type of storage medium.

2) If radiometric calibration facilities exist, but they have not been compared (intercalibrated) with internationally recognized facilities, this should be arranged through the IAEA.

3) Where several separate areas have been surveyed, numerical data should be normalized/levelled, using the nearest available recognized calibration facility. If results of these surveys were not presented in terms of radioelement abundances (concentration of the three radioelements), a back-calibration exercise should be carried out so as to allow the preparation of quantitative geochemical maps.

4) For environmental health radiation monitoring puposes, a map of air dose rate (Gy s^{-1}) or effective dose equivalent (mSv a^{-1}), should be produced.

5) Where sufficient data are available, they should be sub-sampled onto an appropriate grid suitable for the production of a regional or national atlas and ultimately the radioelement map of the world.

5.3. COLLECTION OF NEW DATA

Although it is desirable from the point of view of minimising costs to make the maximum possible use of existing data, it should be recognized that many past surveys were undertaken with inadequate equipment and insufficient quality control. At best, they were qualitative rather than quantitative. There is often incomplete information concerning equipment, survey and data reduction parameters. If the data were not digitally recorded in a readily recoverable format the difficulty and cost of retrieving information can greatly exceed its value. In these circumstances, and for the many parts of the world where no gamma ray surveys have been carried out, it is necessary to collect new data, following recommended procedures.

1) Many of the comments made above are applicable to newly collected data. Particular attention must be paid to calibration and standardised data reduction procedures, according to IAEA guidelines.

2) *In situ ground measurements*. In order to link airborne with ground measurements, including conventional sampling for the non-radioactive elements, in situ measurements with a field

portable gamma ray spectrometer (GRS) should be made at each sub-site where a geochemical regolith reference sample is collected. Thus, several measurements should be made at each site in the 160 × 160 km primary sampling grid.

3) With a modest increase in the equipment required, useful additional information can be obtained by using the same portable GRS to obtain a continuous profile whilst in transit in a road vehicle between sample sites (i.e., a car-borne survey). If the 160 km cell sample sites are located close to surface transportation routes, then a continuous profile could be recorded along these routes where conditions are suitable, as a modification of the method used for reconnaissance purposes by Shacklette et al. [24].

4) *Airborne gamma ray spectrometry*. The preferred method of obtaining comprehensive radioelement baseline data over a large region is by means of airborne gamma ray spectrometry. Widely spaced profiles are of comparable significance to widely spaced surface samples, but with the important advantage of being continuous along-line and not restricted or diverted by difficulties of surface travel or access. Continuous profiles enable the boundaries encountered en route to be identified as gradational or sharp, and in the latter case, their exact position can be located. In order to complement the 160 × 160 km primary sampling reference grid it is recommended that flight-line spacing must not be less than 160 km, and preferably 80 km, 40 km or 20 km in populated areas, so that most points in the ground sampling network (which may be irregularly spaced for reasons of access) can be overflown. Where the ground sampling follows a straight (or nearly straight) corridor, it is obviously much simpler to arrange to overfly the sample sites. For the purpose of checking for possible level problems between isolated blocks of ground geochemical data it may be desirable and advantageous to insert additional flight lines whilst a suitably equipped aircraft is in the region.

5) Irrespective of the flight line-spacing, data are normally collected along each line at constant 1s intervals. In order to produce a map which is not directionally biassed, along-line data must be smoothed over a distance proportional to line spacing. This reduces the amplitude of features. For this reason contoured maps are progressively less satisfactory as line spacing increases, so that when this exceeds 10 km profile maps are usually the preferred product.

6. CONCLUSION

Subject to proper calibration and use, gamma ray spectrometry is a unique tool for mapping the distribution of all radioactive elements, whatever their origin, in the surface of the regolith (termed the A_{25} horizon); the data which are acquired are an essential part of the description of the geochemical environment. In addition to providing baseline data for radioelements, the use of gamma ray spectrometry facilitates the acquisition of a common database with non-radioactive elements and offers a partial solution to a fundamental problem associated with the concept of international geochemical mapping, namely, that of establishing a standardized base for all measurements.

ACKNOWLEDGEMENTS

The recommendations for A Global Geochemical Database referred to in this report have been prepared as a result of a prolonged joint effort by members of the IGCP 259 Steering Comittee: A.J.Bjorklund, Finland, leader Global Sampling Committee; B.Bolviken, Norway, leader Fennoscandian Regional Committee; N.Gustavsson, Finland, leader Data Management Committee; P.Koval, Russia, co-leader Russian Regional Committee; J.A.Plant, UK, leader European Community Regional Committee; A.Steenfelt, Denmark, leader Field Methods Committee; Xie Xuejing, China,

leader Analytical Methods Committee and Chinese Regional Committee. In particular, thanks are due to M.Tauchid, IAEA, leader Radiometric Methods Committee for obtaining the support of the IAEA for activities pertaining to nuclear minerals exploration. The writer (A.G.Darnley) is chairman of the Steering Committee.

REFERENCES

[1] BOLVIKEN, B., BERGSTROM, J., BJORKLUND, A., KONTIO, M., LEHMUSPELTO P., LINDHOLM, T., MAGNUSSON, J., OTTESEN, R.T., STEENFELT, A. and VOLDEN, T., Geochemical Atlas of Northern Fennoscandia, Scale 1:4,000,000, Nordkalott Project, Geological Survey of Sweden (1986) 170pp.

[2] DARNLEY, A.G., International geochemical mapping: a new global project. Journal of Geochemical Exploration, 39 (1990) 1-13.

[3] DARNLEY, A.G., The development of airborne gamma ray spectrometry: a case study in technological innovation and acceptance. Journal of Nuclear Geophysics, 5 (1991) 377-402

[4] DARNLEY, A.G., News item: International Geochemical Mapping, Journal of Geochemical Exploration, 48 (1993) 97-104.

[5] DARNLEY, A.G., Uranium exploration data, international geochemical mapping and the environment. (this volume), (1994).

[6] DARNLEY, A.G. and FLEET, M., Evaluation of airborne gamma ray spectrometry in the Bancroft and Elliot Lake areas of Ontario, Canada. In Proc. 5th Symp. Remote Sensing of the Environment. pp 833-853. University of Michigan, Ann Arbor (1968).

[7] DARNLEY, A.G. and FORD, K.L., Regional airborne gamma-ray surveys: a review. In Proceedings of Exploration '87; Third Decennial International Conference on Geophysical and Geochemical Exploration for Minerals and Groundwater, ed. G.D. Garland, Ontario Geological Survey, Special Volume 3 (1989) 229-240.

[8] DARNLEY, A.G., BJORKLUND, A.J., BOLVIKEN, B., GUSTAVSSON, N., KOVAL, P., PLANT, J.A., STEENFELT, A., TAUCHID, M., and XIE, XUEJING, A global geochemical database: recommendations for international geochemical mapping. Final report for IGCP project 259. ICSU (1994) (in press).

[9] DAVENPORT, P.H., A comparison of regional geochemical data from lakes and streams in northern Labrador: implications for mixed-media geochemical mapping. Journal of Geochemical Exploration, **39** (1990) 117-151.

[10] DUVAL, J.S., Modern aerial gamma ray spectrometry and regional potassium map of the conterminous United States. Journal of Geochemical Exploration, **39** (1990) 249-253.

[11] GARRETT, R.G., BANVILLE, R.M.P. and ADCOCK, S.W., Regional geochemical data compilation and map preparation, Labrador, Canada. Journal of Geochemical Exploration, **39** (1990) 91-116.

[12] GARRETT, R.G., BEAUMIER M. and DAVENPORT, P.H., Quebec-Labrador geochemical transect, James Bay to the Labrador Sea 53-55°N. in Current Activities Forum, Program with Abstracts, January 1991, Geological Survey of Canada, 8 (1991).

[13] GARRETT R.G., Ultra-low density geochemical mapping on the Canadian prairie. Abstracts, 16th International Geochemical Mapping Symposium, 1-6 September 1993, Beijing, China (1993) p.50.

[14] GRASTY, R.L., WHITTON, R.M. and DUFFY, A., Back calibration and reprocessing an airborne gamma ray survey, Malaysia. Expanded Abstracts with Biographies, 1992 Technical Program, 62nd Annual International SEG Meeting, New Orleans (1992) 550-551

[15] GREEN, B.M.R., HUGHES, J.S. and LOMAS, P.R., Radiation atlas, national sources of ionising radiation in Europe. Environment Directorate, Nuclear Safety and Civil Protection, Commission of European Communities, Luxembourg (1991) 34pp.

[16] GREGORY, A.F. and HORWOOD, J.L, A laboratory study of gamma ray spectra at the surface of rocks. Mines Branch Research Report R 85, Department of Mines and Technical Surveys, Ottawa (1961) 52p.
[17] HETU, R.J. (Compiler), Airborne geophysical survey of the Edmonton-Calgary reconnaissance area, Alberta. GSC Open File 2442 (1992).
[18] INTERNATIONAL ATOMIC ENERGY AGENCY, Radiometric Reporting Methods and Calibration in Uranium Exploration, Technical Report Series No. 174, Vienna (1976) 57p.
[19] INTERNATIONAL ATOMIC ENERGY AGENCY, Gamma ray surveys in uranium exploration, Technical Report Series No. 186, Vienna (1979) 90p.
[20] INTERNATIONAL ATOMIC ENERGY AGENCY, The use of gamma ray data to define the natural radiation environment, IAEA-TECDOC-566, Vienna (1990) 48pp.
[21] INTERNATIONAL ATOMIC ENERGY AGENCY, Airborne gamma ray spectrometer surveying. Technical Report Series No. 323, Vienna (1991) 97p.
[22] MELLANDER, H., Airborne gamma spectrometric measurements of the fall-out over Sweden after the nuclear reactor accident at Chernobyl, USSR. Internal report IAEA/NENF/NM-89-1, IAEA, Vienna (1989) 41.
[23] PLANT, J.A. and RIDGWAY, J., Inventory of geochemical surveys in Western Europe. In A.Demetriades, J.Locutura, R.T. Ottesen (compilers), Geochemical Mapping of Western Europe towards the year 2000, Pilot Project Report, Appendix 10, NGU Report 90-105, Geol. Surv. Norway (1990) 400pp.
[24] SHACKLETTE, H.T. and BOERNGEN, J.G., Elemental concentrations in soils and other surficial materials of the conterminous United States. U.S. Geological Survey Professional Paper 1270, United States Government Printing Office, Washington (1984).

CONSISTENCY OF RADIOMETRIC DATA

(Abstract)

M. MATOLIN
Charles University, Prague, Czech Republic

Radiometric data of uranium exploration and data of other field radiometric measurements are applicable for studies of the radiation environment. Quantitative data on radiation field and radon concentration in rocks are requisite to the assessment of environmental radioactivity. Consistency of radiometric data, which is essential in this procedure, has been studied. Total count (TC) measurements, reflect also the used detectors, energy rays of the natural environment, reflect also the used detectors, energy thresholds of instruments and the way of their calibration. TC results, expressed in units of air dose rate, are further dependent on ratios of K, U and Th in rocks. Current TC instruments, calibrated with Ra-226 point source, indicate air dose rate values that can exceed acceptable limits of errors, instruments calibrated over extensive U source can differ from the correct value of the air dose rate up to 25% relatively. Gamma ray spectrometry analyses of K, U and Th in rocks has been improved substantially by introducing the IAEA laboratory reference materials for geological analyses (RG-set), and by research, development and establishment of world net of calibration facilities for field radiometric equipment. Experience shows that K, U and Th concentrations in rocks can be determined with relative differences in the range of 1 - 5%. Air dose rate values, calculated from K, U Th concentrations in rocks, can be influenced by differences of the element composition and moisture of applied theoretical model and real rock environment. Radon risk mapping employs data on Rn-222 in rocks. The dispersion of attainable quantitative data on Rn-222 volume activity in soil air, reported by single organizations, is caused by differences in soil air sampling, depth of sampling, methods of radon detection, methods of measurement and the way of equipment calibration, in addition to radon climatic variation. Experimental results of the 1991 — 1993 comparison measurements, realized under the programme of radon risk mapping in the Czech Republic, on 5 test areas of various radon levels (10 - 100 $kBq.m^{-3}$), exhibit the relative spread of reported average Rn-222 volume activity in the range 0.55 - 1.43 with most cases in the range 0.8 - 1.2 (well acceptable limits).

Next page(s) left blank

DATA PROCESSING AND MAPPING IN AIRBORNE RADIOACTIVITY SURVEYS

G.F. SCHWARZ, L. RYBACH, E. E. KLINGELÉ
Institut für Geophysik, Eidgenössische Technische Hochschule, Zurich, Switzerland

Abstract

Methods and software have been developed for processing and corrections to allow a routine treatment of airborne radiometric data acquired even in areas with high topographic relief. In order to identify possible radiation level changes around the five Swiss nuclear installations (four power plants and one research facility) the surrounding regions of each site are surveyed annually. In addition, regions with elevated natural radioactivity are mapped within the framework of the Swiss National Geophysical Survey. Mapping is done by pixel (125 × 125 m) representation, which is better suited than isolines to account for the statistical nature of radiometric data. For maps with considerable data range a to 3D-representation was chosen. The results for the areas processed so far show a very good fit with geology and can be used for geological overview mapping. The measurements in the environs of the Swiss nuclear installations performed since 1989 show that all sites (with the exception of the Gösgen power plant) can be identified clearly on the radiometric maps. No artificial radioactivity, that could not be explained by contamination from the Chernobyl event or nuclear weapon tests, was detected outside of the fenced sites of the nuclear installations.

1. INTRODUCTION

Regional and local gamma-ray radiation maps are of key importance for a variety of purposes: location and monitoring of contamination, basic data for radiation biology (variation of the natural exposure rate in the context of the effects of low doses), information relevant to prospecting for raw materials (for example potassium alteration) and geological mapping.

Since areal radiometric surveys are expensive and time consuming, they are advantageously carried out airborne. Airborne surveys permit rapid evaluation of radiation levels of large areas. In inaccessible regions, surveys with complete areal coverage are only possible from the air. Because of the larger ground clearance and the higher speed, the coverage per unit time of an airborne system is about 2500 times larger than of a comparable ground system. This is of key importance in radiological accidents. Although the costs for the measuring instruments and the flights are relatively high, the resulting cost per surveyed area is clearly lower than for a comparable terrestrial survey. Three projects actually make use of airborne radiometric measurements in Switzerland.

The first project aims at a better evaluation of the natural radiation level in Switzerland. The Swiss Geophysical Commission (SGPK) decided to map selected regions with elevated natural radioactivity within the framework of the Swiss National Geophysical Survey [1]. The main attention was given to the crystalline rocks of the Central Massifs of the Swiss Alps because of their relatively high natural radioactivity. The area covered by this survey is about 3000 km^2.

The second project financed by the Swiss Federal Nuclear Safety Inspectorate (HSK) concerns on artificial radioactivity. The surrounding regions (approx. 50 km2) of the four nuclear power plants (Beznau, Gösgen, Leibstadt and Mühleberg) and the Swiss nuclear research facility (Paul Scherrer Institute) are surveyed annually since four years. The measurements aim to monitor the dose-rate distribution and to provide a documented reference base [2]. From 1994 on the surveys will be carried out biannually.

In addition to the mentioned two projects the airborne measuring system will be mobilized in case of accidents with radioactive material or from debris of nuclear-powered satellites. The

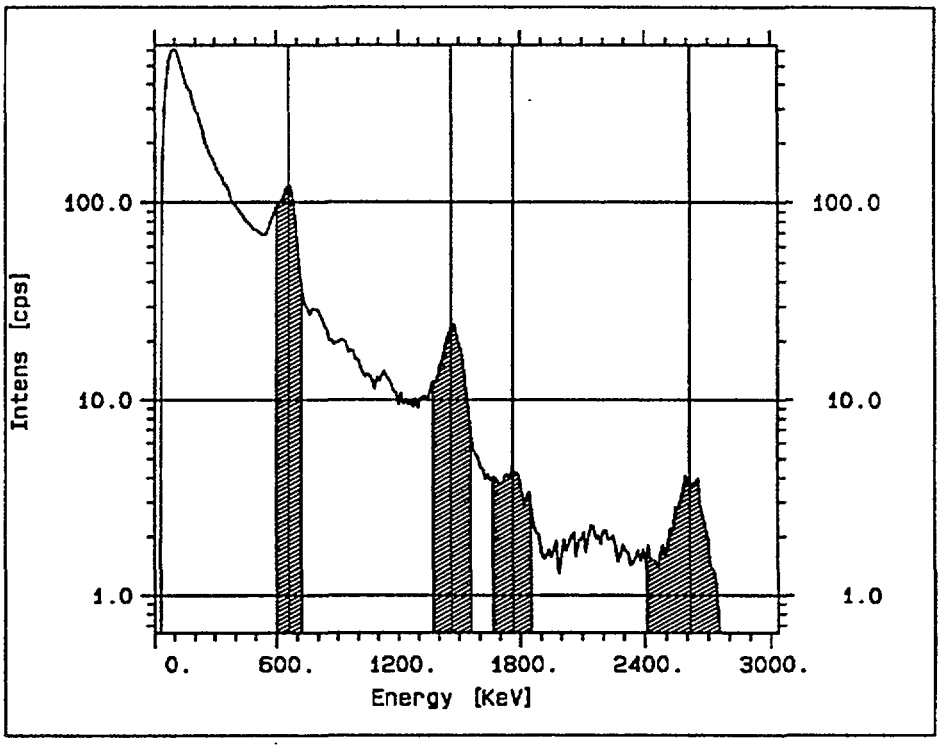

FIG. 1. Spectrum of the γ-radiation in the Magadino plain (TI) as measured in July 1991.

emergency measurements will be done by military helicopters under the control of the Swiss National Emergency Operation Center (NAZ).

The methodology developments [3] as well as the measurements were carried out by the Institute of Geophysics of the Swiss Federal Institute of Technology (Zürich). The measuring equipment was developed, calibrated and put together at the Institute of Geophysics (see [4]).

2. PROCESSING OF RAW DATA

Since NaI-detectors have a relatively poor energy resolution the data processing is based on specified energy windows in which the registered counts are integrated. The energy windows are centered on spectral regions of special interest. The energy windows have to be sufficiently separated from each other to keep interactions small.

The region centered at the 1460 keV peak of K40 is used for the determination of the potassium content. Uranium is detected using the 1765 keV line of the daughter product Bi214. For thorium the 2615 keV line of Tl208 is used. The energy windows are located at higher gamma ray energies where the absorption by air is less important. The artificial isotopes Cs^{137} and the Co^{60} are determined using energy windows centered at 660 keV and 1250 keV. Fig. 1 shows a spectrum measured in the Magadino plain (TI). The peak at 660 keV which can be identified in the spectrum is mainly caused by release of the Chernobyl accident.

Three additional windows cover larger parts of the spectrum. The total count window covers the complete spectrum and is representative for the total amount of gamma radiation. The low (below 1400 keV) and the high energy part of the spectrum are registered in separate windows as an indicator for artificial radiation (see chapter 3).

The gamma radiation registered by the detector in a helicopter is composed of the contributions from soil, atmosphere, aircraft and cosmic radiation (see Fig. 2):

Cosmic radiation: During the absorption process of the cosmic high energy particle radiation gamma radiation is produced, which is registered by the spectrometer. The intensity of the cosmic radiation depends mainly on the thicknes of the atmosphere above the measurement location and therefore on air pressure and altitude above sea level.

Atmospheric radiation: The most important radiation source in the atmosphere is the isotope Rn^{222} of the inert gas radon. It originates from the decay of uranium. The concentration of radon in the air depends on meteorological conditions and is strongly variable [4].

Background radiation from aircraft and detector: In the aircraft as well as in the detector material itself small amounts of radioactive material are present. The helicopter background is assumed to be constant.

Terrestrial radiation: Terrestrial radiation is mostly produced by the decay of the four natural radio isotopes U^{235}, U^{238}, Th^{232} and K40. Sometimes contributions of long living decay- and activation-products from nuclear weapon tests and/or nuclear facilities as Cs^{137} and Co^{60} add to the natural contributions.

The aim of airborne radiometric measurements is the determination of the radionuclide content of ground using the information of the direct terrestrial gamma radiation. All other contributions are perturbing and have to be removed.

These contributions are determined by flights above large lakes, where the ground radiation is completely absorbed by water. Whereas the helicopter background and atmospheric radiation is assumed constant, the contribution of the cosmic radiation increases with increasing height. Therefore the calibration flights are carried out at different altitudes above sea level.

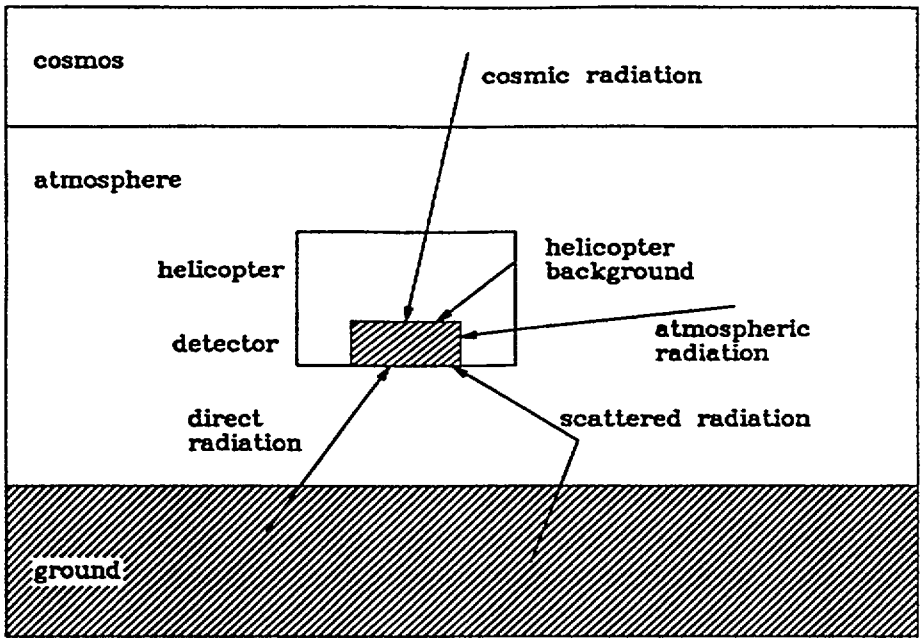

FIG. 2. Situation encountered during airborne radiometric measurements.

The gamma ray spectrum received during field measurements is very complex. It is composed of the contributions of several radio isotopes. The spectrum is further complicated by scattering and absorption, which can occur in the ground, in the air and in the detector itself. To reduce the radiation intensities measured from the air to the ground activity a second set of corrections is needed. These corrections are called normalization corrections and are carried out applying the following steps:

Spectral stripping: Gamma rays are scattered in the detector crystals, in the air and also in the soil. The scattering changes the energy of the radiation and therefore the original spectrum. The spectral stripping reduces the data to the primary (direct) radiation contribution by removing the effects of scattering and contributions from other isotopes.

Altitude correction: The effects of a varying flight altitude are removed with the altitude correction. These variations represent the most significant perturbation to airborne radiometric measurements. The gamma ray intensity decreases rapidly with increasing ground clearance because of absorption of gamma rays in the air.

Topographical correction: The effects of topographic relief can be neglected in flat or slightly hilly areas. In narrow valleys, which are abundant in the Swiss Alps, topography can produce a strong increase of the count rates by as much as 100%. These effects can be corrected adequately in most practical circumstances with the topographical correction [6].

Conversion to general units: In a last step the detector-specific count rates are converted to the corresponding soil activity or radionuclide concentrations. For this conversion the detector sensitivity is needed. In case of uranium and thorium, radioactive equilibrium is assumed.

TABLE I. OVERVIEW OF THE SOFTWARE MODULES

Module	**Function**
Define	Define energy windows, systems and survey parameters
Prepare	Read Raw data, check plausibility and backup
Reduce	Spectrum visualization, energy calibration, dead time correction and reduction of energy windows
Analog	Editing visualization and calibration of radar altitude, barometric altitude, attitude data and temperature
Geometry	Processing of positioning data from GPS receiver and flight path camera
Strip	Background and spectral stripping corrections
Normal	Altitude correction, topographical correction and conversion to general units
Grid	Gridding of the data and processing of the grids (filters, ratios)
Map	Map generation (pixel maps, scatterograms)
Output	Plotting of the maps and charts

Contrary to the background corrections, the normalization corrections need assumptions on the distribution of the radioactive source(s). The topographical and the altitude corrections as well as the conversion to general units can only be carried out when the activity distribution is known. Normally the natural radioisotopes are homogeneously distributed in the ground. Their activity distribution can therefore be considered as known, which is not the case regarding artificial isotopes. This is the reason why the normalization corrections with exception of the spectral stripping and the altitude correction generally apply only to the natural isotopes.

The methods developed for processing and correction allow a routine processing of airborne radiometric data acquired even in areas with high topographic relief. The complete processing software including the modules for corrections and map outputs has been implemented on a personal computer. This enables not only the quality control of the acquired raw data, but also the complete processing directly in the field, a facility of great importance in the event of a radiological accident. The software is menu driven and easy to use and easy to learn even for non computer specialists. It contains a total of 32'000 lines of source code. An overview of the software modules is given in Table I. Details are given in Schwarz [3].

3. MAP GENERATION

Radiometric measurements always show a large statistical scattering. Additionally the corrections applied to a measurement contribute essentially to the total error. The total error of a corrected measurement can be approximated by:

$$\Delta I_{corr} = 1.5.\sqrt{I_{corr}+\Sigma |I_{CT}|}$$

Where Icorr is the error of the corrected measurement, I_{corr} is the corrected count rate and $\Sigma|I_{CT}|$ is the sum of the corrections applied. The error of single measurements typically ranges between 10% for the total-count-window and up to 50% in windows with low count rates like the cesium window.

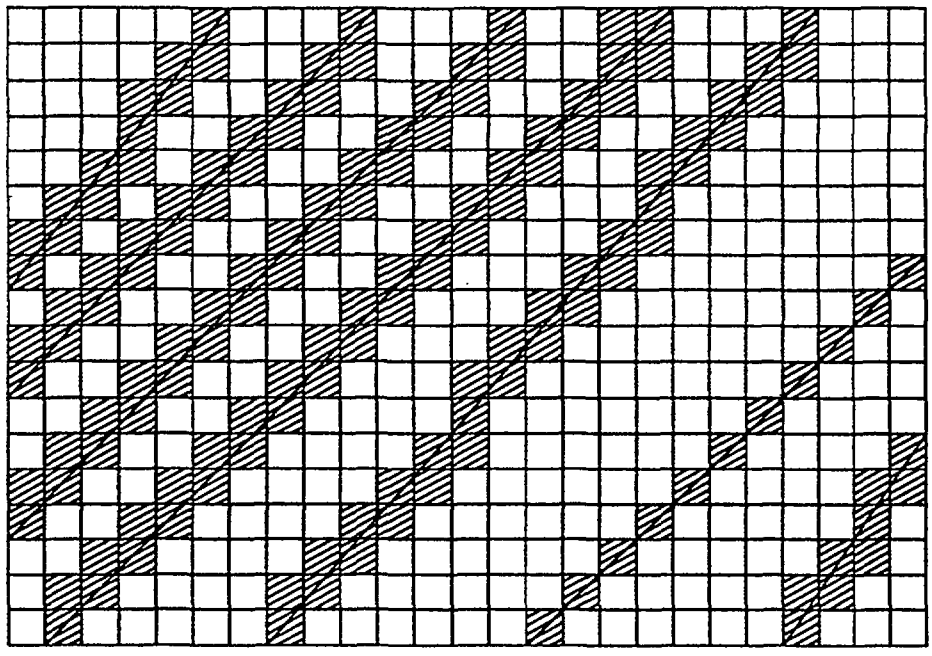

FIG. 3. Grid and flight path.

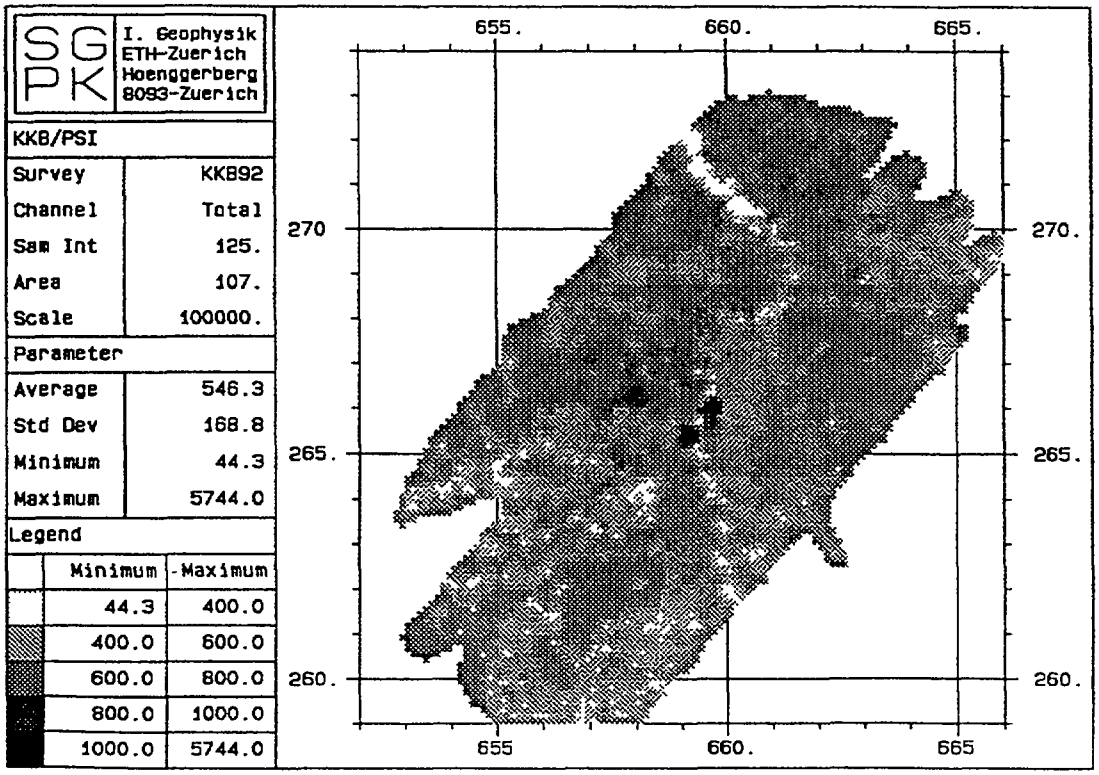

FIG. 4. Total count map of the KKB/PSI survey.

Because of the large error of airborne radiometric measurements the classical data representation using isolines is not very well suited in this case. We decided to use the pixel representation instead. To reduce the error only an average of several single measurements is displayed on the radiometric maps.

In our case the data are recorded at a flight speed of 25 m/s and a flight altitude of 90 m. For these flight parameters a pixel size of 125 × 125 m is used for the representation. Since the distance between two measurements is 25 m a pixel represents the average of five measurements. The pixel size of 125 × 125 m corresponds also roughly to the field of view of the detector at a flight altitude of 90 m [7].

The generally used line spacing is 250 m, so only half of the pixels will contain data without interpolation (see Fig. 3). Since the gamma ray field contains abrupt steps and the statistical error of airborne radiometric data is very large, the interpolation cannot be performed with standard methods. A simple method proposed by Green [8] was therefore chosen for the interpolation.

The remaining pixels are filled with the average of the surrounding neighbours if they have at least three already assigned neighbors. This procedure is repeated until the grid is completely filled. It has to be mentioned that the original values are not changed by this interpolation procedure.

Fig. 4 shows the total activity map of the surroundings of the nuclear power plant Beznau (KKB) and of the research facility Paul Scherrer Institut (PSI). The total intensity of (gamma)-radiation as measured from the helicopter is plotted in detector specific counts per second. For reproduction reasons the map is plotted in black and white. Of course, color maps can also be produced. The highest intensities (the two black spots) are measured over the two sub-units of the PSI. They are caused by the direct radiation of the storage areas for radioactive components (PSI-West) respectively for radioactive waste (PSI-East). The water of the river Aare strongly absorbs

the ground radiation, which is why the course of the river stands out in white. Even differences in vegetation cover are visible; meadows (light grey) show generally higher values than forests (dark grey).

Only the error of the count rate has been discussed so far. When converting the airborne count rates to ground activities additional perturbing effects have to be considered. For a constant ground activity a lower count rate is measured over forests than over meadows due to the additional absorption by trees. This attenuation varies between 5% and 25% depending on the biomass of the forest. Soil humidity and rain also influence the measurements up to 10%. This second effect is especially troublesome because the soil humidity varies with time.

Both effects can be distinctly reduced with the aids of ratios. The ratio of two windows is less affected by an additional absorber than the single window values, since the ratio is only affected by the difference of the attenuation coefficients in the two windows. Especially sensitive to artificial radiation is the so called Man Made Gross Count (V_{MMGC}) ratio [9].

$$MMGC1 = \sum_{400keV}^{1390keV} I_E$$

$$MMGC2 = \sum_{1400keV}^{3000keV} I_E$$

$$V_{MMGC} = \frac{MMGC1}{MMGC2}$$

It uses the fact that the common artificial radio nuclides all radiate at gamma energies below 1400 keV, the natural isotopes on the other hand emit gamma quanta of higher energy too. The ratio of the low energy part of the spectrum (MMGC1) to its high energy part (MMGC2) corresponds

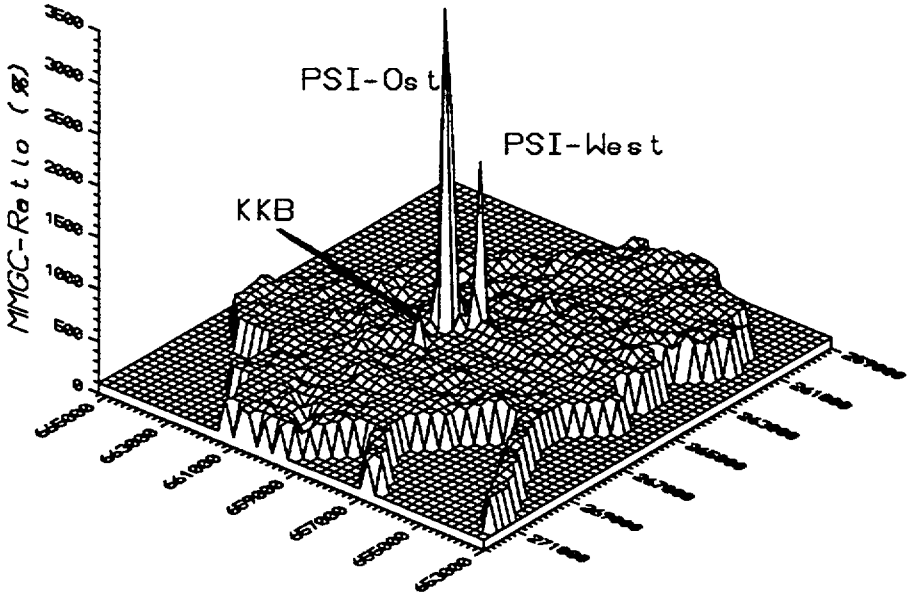

FIG. 5. 3D-representation of the MMGC-ratio of the region of Würenlingen/AG (looking from north-west). The highest peak corresponds to a ground dose rate of 2 mSv/a.

therefore to the ratio of artificial to natural radioactivity. An example of representation of MMGC ratio is shown on Fig. 5.

Because of the strong correlation between the radioelements due to geochemical reasons, the maps of the natural radioisotopes are all very similar. Working with ratios of natural radioisotopes will therefore not only reduce disturbing effects, but also reduce the contrast of the image. An appropriate method to increase the contrast and with it the interpretability of an image is called histogram equalization [10]. After histogram equalization every color covers the same area on the map. The visual impression of such a representation is optimal. As a consequence the color scale becomes nonlinear.

The histogram equalization is particularly useful producing ternary maps. In this representation the maps of potassium, uranium and thorium are merged into a single map. The color red is assigned to the potassium window. Uranium and thorium are colored green and blue respectively. Regions with a high relative potassium content will appear in red color shades on the map. Correspondingly areas with a high relative uranium or thorium content will appear in green or blue shades. Regions with equally balanced radioisotopes will be plotted as gray or white shades depending on the total activity. Ternary maps can almost be read like a geological maps, especially in regions with crystalline rocks [1].

4. CONCLUDING REMARKS

The methods developed for processing and correction allow a routine treatment of airborne radiometric data acquired even in areas with high topographic relief. The results for the areas processed so far show a very good fit with geology and can be used for geological overview mapping.

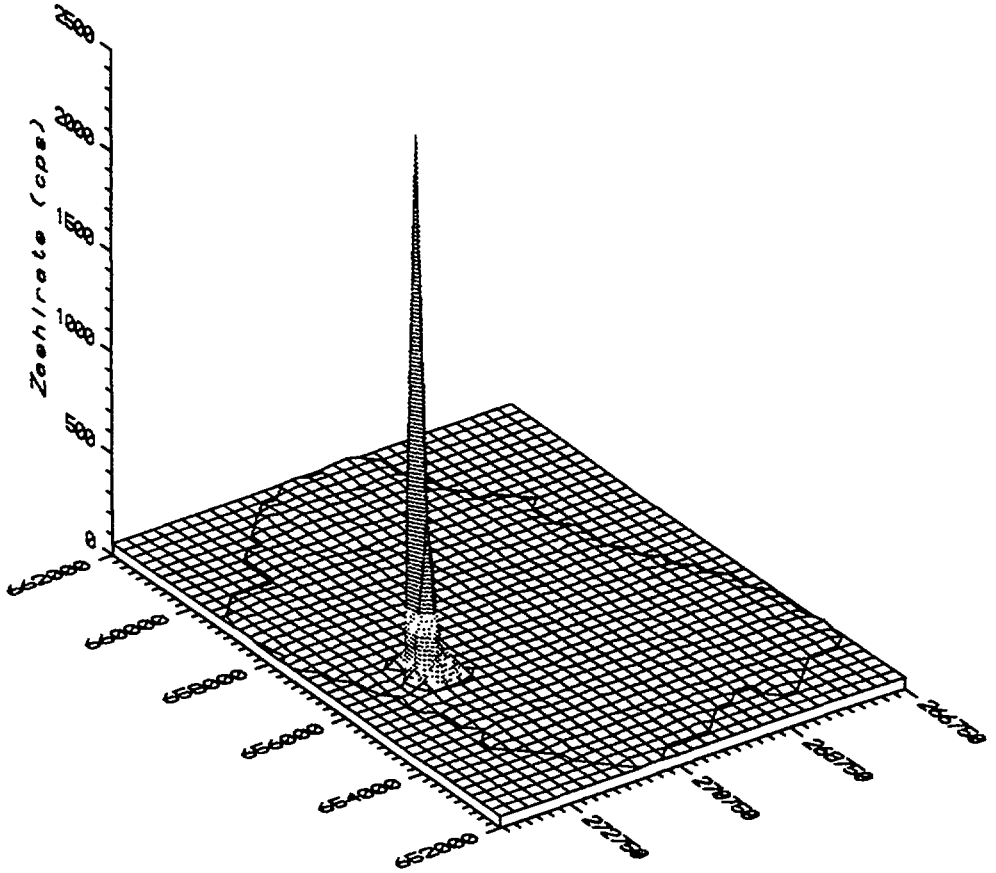

FIG. 6. 3D-representation of the direct upward radiation, caused by N^{16} at the power plant site Leibstadt (looking from north-west).

The airborne radiometric survey conducted so far covers about ten percent of the area of Switzerland. The results of the survey allow to describe the mean radioactivity level in Switzerland and its variation in broad outline [1]. Together with in situ ground measurements and data from rock samples the airborne survey can serve as a good base for the compilation of a radiometric (dose rate) map of whole Switzerland including the contributions of artificial isotopes and cosmic radiation.

The measurements in the environs of the Swiss nuclear installations showed that all sites (with the exception of the Gösgen power plant) can be identified clearly on the MMGC-ratio maps.

Fig. 5 shows a three dimensional representation of the MMGC-ratio of the surroundings of Würenlingen/AG (looking from north east). The two locations of the Paul Scherrer Institute PSI-Ost and PSI-West show up particularly well. The signal is caused by the direct radiation of the storage areas for radioactive components (PSI-West) and radioactive waste (PSI-Ost). The smaller peak is caused by the Beznau nuclear power plant. The highest peak corresponds to a ground dose rate of 2 mSv/a.

At sites of operating boiling water reactors (BWR) the high energy radiation of the activation product N^{16} is clearly visible in the data. The N^{16} (from the reaction O16 (n,p) N^{16}, $T_{1/2}=7.3$ s) reaches the machine building through the steam line. Since the roof of this building is comparatively less shielded, the high energy gamma radiation of the N^{16} (two gamma ray lines at 6.13 MeV and 7.11 MeV) can be detected easily by airborne measurements. The scattered radiation of the emitted N^{16} quanta can be observed in the whole spectrum. Fig. 6 shows a three dimensional representation of the direct upward radiation, caused by N^{16} at the power plant site Leibstadt.

No artificial radioactivity, that could not be explained by Chernobyl or nuclear weapon test, was detected outside of the fenced sites of the nuclear installations. The repeated measurements in the last four years [2] showed that the radioactivity level in the environs remained more or less constant within the measurement errors.

REFERENCES

[1] SCHWARZ, G.F., KLINGELE, E.K., RYBACH, L., Airborne radiometric mapping in Switzerland, Beiträge zur Geologie der Schweiz, Geophysik Nr.25, Schweizerische Geophysikalische Kommission (1992a).

[2] SCHWARZ, G.F., KLINGELE, E.K., RYBACH, L., Aeroradiometrische Messungen in der Umgebung der schweizerischen Kernanlagen; Bericht zuhanden der Hauptabteilung für die Sicherheit der Kernanlagen, Interner Bericht, Institut für Geophysik ETHZ, Zürich (1989, 1990, 1991 and 1992b).

[3] SCHWARZ, G.F., Methodische Entwicklungen zur Aerogammaspektrometrie. Beiträge zur Geologie der Schweiz, Geophysik Nr. 23, Schweizerische Geophysikalische Kommission (1991).

[4] SCHWARZ, G.F., KLINGELE, E.K., RYBACH, L., these Proceedings.

[5] KOGAN, R.M., NAZAROV, I.M., FRIDMAN, S.D., Gamma Spectrometry of Natural Environments and Formations, Atomizdat, Moskau, (English Translation: Israel Program for Scientific Translations Ltd., Jerusalem, 1971, Microfiche-TT-70-50092) (1969).

[6] SCHWARZ, G.F., KLINGELE, E.K., RYBACH, L., How to handle rugged topography in airborne gamma-ray spectrometry surveys, First break 10 (1992c) 11-17.

[7] PITKIN, J.A., DUVAL, J.S., Design parameters for aerial gamma-ray surveys, Geophysics 45 (1980) 1427-1439.

[8] GREEN, A.A., Leveling airborne gamma-radiation data using between-channel correlation information. Geophysics 52 (1987) 1557-1562.

[9] HOOVER, R.A., An aerial radiological survey of the River Bend Station and surrounding area, National Technical Information Service, U.S. Department of Commerce, Springfield (Virginia) (1988).

[10] HABERAECKER, P., Digitale Bildverarbeitung, Grundlagen und Anwendungen. Hanser Studienbücher, München/Wien (1985).

ENVIRONMENTAL APPLICATIONS OF AIRBORNE GAMMA SPECTROMETRY

D.C.W. SANDERSON, J.D. ALLYSON, A.N. TYLER
Scottish Universities Research & Reactor Centre,
East Kilbride

E.M. SCOTT
Department of Statistics, University of Glagow, Glasgow

United Kingdom

Abstract

Over the last few years the Scottish Universities Research & Reactor Centre has conducted a programme of developmental and baseline radiometric surveys aimed at quantifying existing levels of anthropogenic, natural and technologically enhanced activity in the environment. This has included an epidemiological study of variations in natural sources, searches for lost sources, a series of surveys of upland areas of the UK affected by the Chernobyl accident, and detailed investigations of the local radiation environment of several nuclear sites. These include the Sellafield reprocessing site, the Springfields fuel fabrication plant, and power reactors at Hinkley Point, Trawsfynedd, Calder Hall, Chapelcross and Hunterston. Emergency response plans have been prepared for some sites to provide rapid environmental monitoring in the event of an accident. The surveys have been conducted using a combination of standard geometry prismatic NaI detectors, a thin NaI and CsI scintillation geometry and, most recently Ge spectrometers utilized to supplement spectral resolution. Spectrometers have been developed which incorporate ^{40}K gain monitoring, multidetector spectral recording, real time data analysis, and facilities for rapid mapping immediately on landing. It has been necessary to extend the international standard (IEC,1992 IAEA,1991) calibration methods to include anthropogenic and technologically enhanced natural nuclides. This has been achieved using a combination of laboratory and field measurements of system parameters together with Monte-Carlo simulation of the spectral response of airborne gamma spectrometers. The methods developed, and main findings, are described here with an emphasis on case studies which demonstrate the ability of aerial radiometrics to define the radiation background and it's composition. Examples will be presented illustrating the contributions from aged fallout, Chernobyl derived activity, dynamic signals in the estuarine and coastal environment, and technologically enhanced natural signals. The results are highly complementary to those obtained using ground based methods. However the mobility, cost effectiveness and speed of airborne approaches offer a unique contribution to environmental studies where large scale mapping, inaccessibility, or the presence of dynamic sources limit other approaches.

1. INTRODUCTION

Airborne gamma ray spectrometry has a number of key features of value to studies of environmental radioactivity. The technique originated in uranium exploration and geological mapping, where the abilities to provide effective and economical radiometric data covering large scale surveys of remote areas, and to direct the more costly ground based effort to places of greatest interest, have proved highly successful [1-6]. The potential of using existing uranium exploration data to define the natural radiation background has been recognized [7], as have the potential of utilizing standard geophysical spectrometers [8,9] in source searches [10,11], and in response to accidents [12-15]. However recent developments in instrumentation and technique have taken place which considerably enhance the utility of airborne gamma ray spectrometry methods for resolving and mapping different components of the radiation environment. These developments have taken place against a post-Chernobyl background of increased appreciation of the importance of recording changes in the radiation environment, of providing clear comparisons between natural and other sources of radiation, and of the need for rapid preparation and dissemination of radiometric results, including under emergency response conditions. This paper aims to show that aerial gamma ray surveys can separate and define natural, anthropogenic and technologically enhanced natural radiation sources in the

environment, to highlight the main strengths of this approach, AND to demonstrate its complementary nature to conventional methods. Areas where capabilities have been strengthened by recent technical developments are indicated together with advances which may be expected to further enhance the method in the future.

2. METHODS

Conventional environmental core sampling and high resolution laboratory spectrometry can be highly accurate and sensitive, and are essential for studies of speciation, vertical profiling and measurements by alpha, beta or mass spectrometry. However this is an essentially time consuming approach which is more appropriate to detailed characterization of environmental radioactivity than to large scale surveys or monitoring schemes. Furthermore since the concentrations of environmental radionuclides are generally low, core samples may be prone to high subsampling variability, and are not always representative of the complete ground level radiation environment. In-situ measurements at ground level can improve spatial averaging, at the expense of knowledge of vertical profile. On individual sites in-situ methods can be highly effective; for large scale studies adoption of either ground based approach inevitably leads to a low sampling density, and can be hampered by local obstacles and hazards (peat bogs, irate bulls, barbed wire etc). In a situation where large scale mapping is required at short notice aerial gamma spectrometry has many advantages.

When a gamma ray spectrometer is elevated above the ground it's field of view [16,17] is enlarged; for high energy photon sources the 90% circle of investigation of a static detector is approximately 4-5 times the height above ground. In practice useful spectroscopic information is most readily available at ground clearances of 100 m or less, although in emergency response conditions higher altitude flights may still be useful. Thus the signal recorded at 100 m height are spatially averaged over some 1.2×10^5 m^2; whereas those from 50 m survey correspond to 3×10^4 m^2. By contrast ground level spectrometers record a signal from some 50-100 m^2, whereas core samples represent perhaps 10^{-2} m^2. The sampling scale, of some 10^6-10^7 times larger than cores, and 10^2-10^3 times greater than ground based readings can be extremely beneficial in large scale surveys. It provides the means of conducting effectively total environmental sampling, if flight lines are spaced with parallel separation of a few hundred metres or less. High sensitivity spectrometers capable of making measurements in a few seconds or less from helicopters or fixed wing aircraft, provide the means to conducting large scale surveys describing the major spatial variations in terrestrial radioactivity distribution with total sampling where needed, and a measurement rate of at least 2 orders of magnitude greater than ground based observations. The method of recording data directly together with positional and ground clearance information leads to unsurpassed potential for rapid mapping of environmental radioactivity. This is particularly effective in studying remote, or upland areas where ground based access is limited, or in the estuarine or marine context, where surface level access may be complex or hazardous. The high speed of sampling means that dynamic environmental sources, for example gaseous or aqueous discharges, or active sedimentary systems can be studied, and short term changes revealed.

A series of developmental and application surveys was initiated at SURRC in 1987, inspired by the recognition of the scale of the problems posed in attempting to mount an effective ground-based national response to the Chernobyl fallout. The facilities and techniques have been continually developed through these studies. The earliest work was conducted using large volume cylindrical whole body monitoring NaI (Tl) detectors from fixed and rotary wing aircraft, together with relatively simple navigational and recording systems. Since 1989 an array of prismatic NaI detectors was adopted of standard geophysical geometry. The use of computer-based acquisition systems with multiple distributed pulse height analyzers has been in use since 1989, allowing direct combination of spectral data, positional information and radar-altimetry within the primary flight records. On line GPS, in stand alone (50-100 m precision) and differential ($<$5m precision) has been used since 1992 for navigational purposes. As noted previously in 1990 [18,19] there are many attractions to the

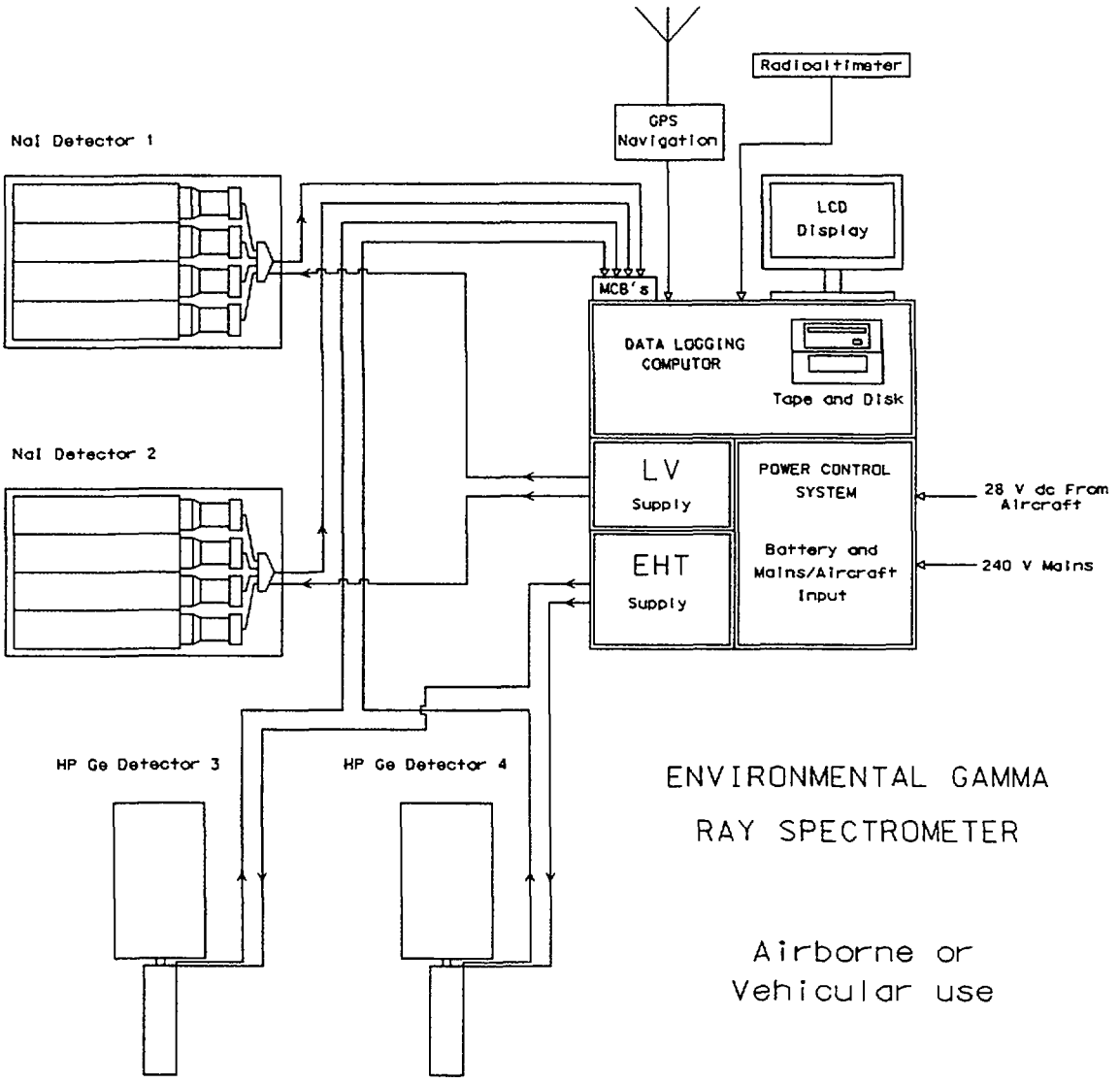

FIG. 1. Schematic diagram of an SURRC airborne gamma ray spectrometer. The system can be configured for one to four detectors, comprising NaI and/or Germanium detectors.

concept of a hybrid detector with both scintillation and semiconductor elements. A set of 6 "n" type Ge detectors was obtained in 1992, comprising two >50% relative efficiency GMX detectors and four LoAx type detectors to develop the concept of such a system. It is planned to develop external mounts for the LoAx array for mapping ^{241}Am, ^{234}Th and ^{226}Ra; in the meantime the GMX detectors have been successfully flight tested on an internal baseplate. Fig. 1 shows a schematic diagram of a recent SURRC spectrometer, which can be configured for single or multi-detector use, and is suitable for airborne or vehicular operation. The system can be powered from mains, batteries or aircraft supplies, and are kept in the laboratory in a state of readiness for survey. Installation times using a CAA approved mounting system for Aerospatiale helicopters, are less than 30 minutes. This provides an extremely effective basis for low cost emergency stand-by. Survey methods are similar to standard geological procedures [8,9], with extension to suit environmental objectives. Modern computer based analysis and recording methods are adopted allowing real-time analysis of spectra during flight and rapid mapping [19]. Longer integration times (5-10 seconds or more per reading) have been used to improve statistics for extraction of environmental gamma peaks, and a varied range of nuclides has been analysed depending on circumstances. Table I summaries the projects undertaken, which include surveys for baseline definition, fallout mapping, emergency response purposes, source searches and specifically developmental studies. More than 30,000 gamma ray spectra have been recorded in these studies from a wide range of environmental contexts.

TABLE I. ENVIRONMENTAL AERIAL SURVEYS CONDUCTED BY SURRC

Location	*Date*	*Area / ha*	*Flying Time / hrs*	*Resolution*
Whithorn, Mull of Galloway [1,4]	*Feb. 1988*	*30,000*	*5*	*1 mile*
N. and S. Uist, Benbecula [1,4]	*Mar. 1988*	*30,000*	*5*	*1 mile*
West Cumbria [1]	*Aug. 1988*	*45,000*	*36*	*500m*
Upper Clyde Valley [1]	*Dec. 1988*	*8,000*	*2*	*1km*
Central Highlands [1]	*Dec. 1988*	*5,000*	*5*	*line*
Grangemouth (source search)	*Dec. 1988*	*>3,000*	*5*	*500m*
Eaglesham Moor [1]	*Jan. 1989*	*8,000*	*1*	*1km*
N. Wales [1]	*Jul. 1989*	*32,000*	*20*	*500m*
SW. England [2]	*Sep. 1989*	*225,000*	*51*	*500m/ 1km*
Ayrshire [1,2]	*Jul. 1990*	*250,000*	*50*	*1km*
Sellafield [2,3]	*Oct. 1990*	*>25,000*	*10*	*1km*
Nigeria (source search)	*May 1991*	*>25,000*	*12*	*300m/500m*
Chapelcross and Solway Firth [2,3]	*Feb. 1992*	*52,500*	*12*	*500m*
Springfields and Ribble Estuary [2,3]	*Sep. 1992*	*24,000*	*12*	*300m*
SW Scotland and Solway Firth [1,2]	*Feb. 1993*	*375,000*	*40*	*500m/1km*
SURRC semiconductor trials [4]	*Mar. 1993*	*500,000*	*15*	*5km*
BNF plc Exercises [3]	*Mar. 1993*	*>75,000*	*10*	*line*

1 Chernobyl fallout **2 Baseline definition**
3. Emergency response **4. Developmental**

3. APPLICATION STUDIES

Fig. 2 shows the locations of the main UK surveys undertaken. The following sections summarize the findings of projects illustrating the application of aerial radiometrics to mapping natural, anthropogenic and technologically enhanced activity. The ability of aerial radiometrics to record detailed variations in natural and modern additional nuclides, and to indicate spatially which makes the dominant contribution to local dose rates is important. Environmental radioactivity is most commonly expressed as activity concentrations (Bq kg^{-1}), for uniform sources or as integrated activity per unit area (Bq m^{-2}) for deposited activity. It is useful on occasion to present natural sources in the latter unit, referred to a depth range of 0-30 cm, to assist with comparisons between anthropogenic and natural sources.

3.1. DEFINITION OF NATURAL BACKGROUND LEVELS AND VARIATIONS

Natural background components have been quantified and mapped using the standard K, eU, eTh gamma ray lines in all SURRC surveys [18-31]. As well as placing other more recent additions to the radiation background into context, and allowing geological and geomorphological interpretations, this provides an indication of the main contributions to estimated dose rates in the environment. This is of interest to a number of disciplines, including epidemiology. Natural sources provide the majority of the radiation exposure to the general public [32], there have been many statistical attempts to relate environmental radiation levels to health effects [33]. In the UK national background maps have been published based on over 3000 ground level measurements at a density of approximately 1 sample for each 10 × 10 km grid [34]. The EC have recently published an atlas of natural sources of ionizing radiation summarizing average data for each member state, or in some cases local administrative regions [35], with the aim of enabling users to "..recognize the degree to which exposure is determined by the accidents of geography and geology" and "..to judge the significance for human health of other exposure to radiation of artificial origins". Data of these sorts have been used in conjunction with regional or national incidence data (eg [36]) to form hypotheses concerning the health effects of natural radiation. It is extremely desirable to attempt to measure the effects, if any, of exposure to varying sources of background radiation; indeed ICRP 60 calls specifically for such studies [37]. However there are concerns that (i) the spatial variations of natural sources occur on a dimensional scale which is not represented by low density regional or national data and (ii) that any study with real statistical power will need to investigate population groups of 10^6 or more individuals for which reliable medical records are available.

A preliminary investigation of the variations in natural background sources, and their potential use in studying leukaemia incidence was undertaken by SURRC with sponsorship from the Leukaemia Research Fund [26]. Three disjoint grids in SW England, selected on epidemiological grounds, and comprising some 2500 km^2 were surveyed by aerial gamma spectrometry in 1989. The results have subsequently been used for methodological pilot studies of case-control and radiation stratified incidence rate analysis using clinically validated diagnostic results. The survey itself was conducted at 1 km line spacing in two of the areas, and 500 m line spacing in the third, using a 24 litre combination of two NaI detectors. The fieldwork was completed in a 2 week period and required some 50 hours of flight time. This resulted in a set of over 4,800 gamma spectra representing a 50% sampling density for the 1 km line spaced grids and approximately total sampling for the 500 m grid. These figures compare with the national ground based mapping, which has an estimated area sampling density of 10^{-6}, and roughly 200-400 times fewer observations per unit area. The regional mean levels for the gamma dose rate however are in approximate agreement. The radiometric data were used to prepare maps indicating the activity concentrations (Bq kg^{-1}) of K, eU and eTh, the estimated ground level gamma dose rate, derived from spectra, and calculated environmental infinite matrix alpha and beta dose rates. The radiometric variables all show coherent spatial distributions from which local geomorphological and geological features can be clearly observed. All variables show a greater than fivefold range, and derived variables indicating the relative availability of high and low LET environmental sources, and the U series contribution to alpha energy, show a factor of three variation.

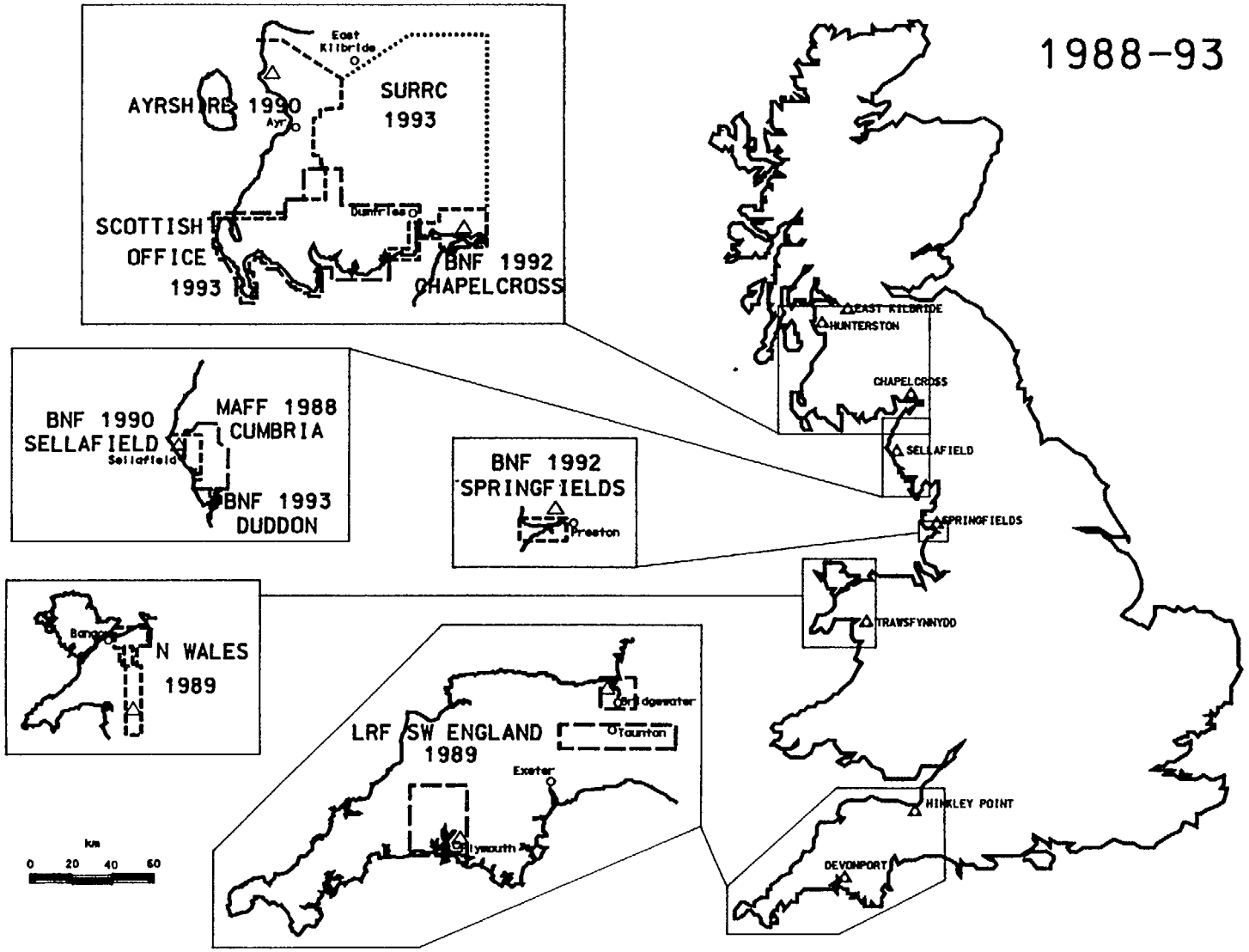

FIG. 2. Locations of main UK surveys from 1988-93.

The variations observed within each grid are thus as great as those demonstrated throughout the UK using low density national maps. It is clearly important that these sources of local variability should be taken into account in future epidemiological studies of environmental radiation. The epidemiological pilot study demonstrated that radiometric data could be readily used for both case-control studies and for preparing radiation stratified incidence rate data from which unbiased risk estimates could be derived. Despite low statistical power in the pilot study there is tentative support for a link with U series activity, which might be suggestive of either a ^{226}Ra association or lend support for the ^{222}Rn hypothesis. In either case further work to examine the relationship between environmental observations of this sort and personal integrated radiation exposure is needed. However there is no doubt that aerial radiometrics are capable of revealing spatially representative and detailed local variations in the natural radiation environment, and could, if necessary, be applied to sufficiently large area studies to encompass the large population groups required to gain statistical power in epidemiological studies. Unfortunately there appears to be far less scope for ground based studies to achieve either of these two objectives.

3.2. FALLOUT MAPPING

Fallout mapping has been conducted since 1988 in a range of terrestrial and upland contexts in the UK [21-25]. Feasibility studies in 1988, SW Scotland and the outer Hebrides confirmed that the ^{137}Cs signal from levels above approximately 1-2 kBq m^{-2} could be readily extracted from data at 100 m ground clearance; regarded as a practical survey height for fixed wing aircraft. Subsequent studies have used helicopters allowing routine fallout mapping at 50 m ground clearance or less; with the exception of built up areas. Up until 1989 it was possible to detect Chernobyl derived ^{134}Cs from the air, although levels for this nuclide fell beneath minimum detectable levels on the less contaminated areas. Upland areas of northern and western Britain received the highest levels of Chernobyl deposition as a result of their high rainfall over the course of a few critical days. Subsequent recycling in organic-rich upland soils and vegetation led to the sustained imposition of livestock movement restrictions on hill farms in North Wales, NW England and parts of Scotland. Game species such as venison have also shown elevated levels of ^{137}Cs. SURRC surveys have been conducted in the effected areas of N. Wales, West Cumbria, and in parts of Scotland which have demonstrated the high degree of local spatial variability which wet deposition over the course of a few days can exhibit. Again dealing with high spatial variability, particularly in relative inaccessible locations, using ground based methods is problematic. It is widely recognized that the precise definition of boundaries for counter-measures of the sort implemented in the UK using ground based approaches is highly contentious. Aerial radiometrics are again highly capable of generating large scale, highly detailed maps which can be used to direct ground based resources to the places of greatest need. They also have an important role in helping to alleviate unnecessary public anxieties, which are too often the consequence of inadequate information.

The extraction of fallout nuclides from standard geological NaI detectors, and their rapid quantification and mapping is described in more detail in [20]. However it is perhaps relevant to note here that the ^{137}Cs full-energy peak is partially interfered with by ^{208}Tl, ^{214}Bi and ^{134}Cs, and that such interferences must be disentangled by stripping. Any deficiencies in stripped count rate data, for example arising from the difficulties in fully accounting for field level scattering, can be compensated for by appropriate calibration procedures involving ground to air comparisons across a range of activities. However minimum detectable levels are effected by such processes. ^{134}Cs by contrast can be detected (at 796 keV) on a primarily scattered background; here the residual counts are to some extent influenced by the amount of ^{40}K scattering within the environmental field of view, including in the air path. The 1988 survey of West Cumbria revealed a complex and highly detailed deposition pattern from the Chernobyl plume; it also suggested that two areas — in the northern and southern extremities of the livestock restriction zone — had deficient ^{134}Cs relative to the ^{137}Cs. The possibility of fractionation between these two nuclides during the Chernobyl discharge, and subsequent transport

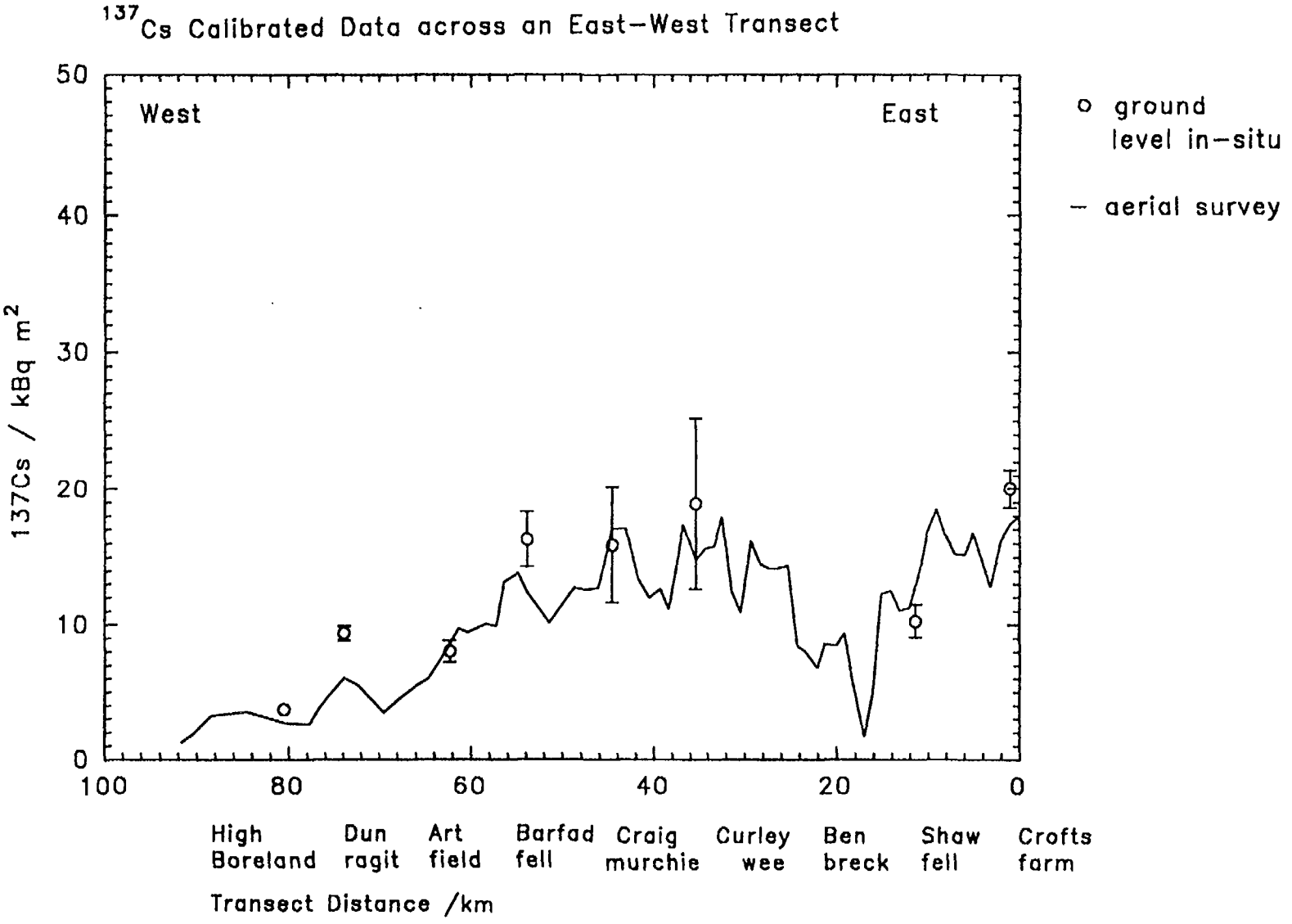

FIG. 3. A comparison between aerial and ground level estimates of ^{137}Cs in SW Scotland.

was considered. However it has subsequently been noted that these two areas are locations affected by historic discharges from the Windscale piles, including the 1957 Windscale fire, which seems a more tenable explanation. Further interpretation is limited by the precision of the original 1988 survey data, and by the subsequent decay of ^{134}Cs; however there may be prospects for using semiconductor detectors to further define the outlines of the Chernobyl and historic components. Aged deposition of ^{137}Cs was also noted on estuarine salt marshes, and is attributed to past marine discharges from Sellafield.

To minimize any interpretational difficulties arising from aged fallout, it is extremely desirable to conduct baseline studies of the existing background, including anthropogenic sources, so that future changes can be clearly assessed. Both the baseline definition task, and the potential for rapid regional mapping are illustrated by a recent large scale survey of SW Scotland conducted in February 1993 [25]. The survey took place within a two week period in February, and covered the majority of Coastal and Inland parts of Dumfries and Galloway; excluding areas in the immediate vicinity of the Chapelcross reactor and inner Solway, which were surveyed in a three day period the previous year. During the fieldwork a total of over 17,000 gamma ray spectra were recorded and analysed, from a 40 hour flight programme with 500m line spacing in coastal areas and 1 km lines spacing inland. The survey was conducted from a fieldbase within the survey area. The aircraft was refuelled without virtually no off-survey flying, using a series of strategically located drum supplies. Preliminary maps of the survey were prepared at the fieldbase during the field programme, and the preliminary report [25] including full colour maps was completed within a month of the fieldwork. A series of some 60 soil cores was collected from coastal calibration sites (defined by the expanding hexagonal pattern discussed in [20] during the survey. This was supplemented by ground based investigation of an inland transect where further in-situ measurements and core samples were taken later in the summer.

The ^{137}Cs map produced shows the terrestrial distribution of activity mainly attributed to the Chernobyl fallout, reaching maximum levels of over 30 kBq m^{-2} in pasture land on the Wigton peninsular, and in upland areas of the Cairnsmore of Fleet and Rhins of Galloway mountains. The variable patterns of deposition, and the fragmented nature of the plumes themselves are clearly visible. On the western extremity of the Mull of Galloway the ^{137}Cs levels are at the lower levels consistent with global weapons testing fallout in the West of Scotland ($<$2-4 kBq m^{-2}); therefore the western extremity of the Chernobyl fallout zone in Dumfries and Galloway has been clearly located. The eastern limit was also observed in the previous survey of the surroundings of Chapelcross and the inner Solway. Fig. 3 shows a comparison between the ^{137}Cs activity per unit are estimates derived from in situ gamma spectrometry across the inland transect and the corresponding aerial gamma spectrometry estimates. Both data appear to be concordant within the error estimates derived from replicate in-situ measurements of up to 4 spectra per site separated by 30 m from the central location. Preliminary results from cores collected from the same sites also support the aerial survey calibration.

Elevated levels of ^{137}Cs are also noted in tide-washed pastures associated with the major river systems of the Solway Firth. Activity levels of up to 100-200 kBq m^{-2} are observed, which the aerial survey has underestimated using a terrestrial calibration derived from recently deposited activity. The cores samples collected from calibration sites demonstrate a pronounced sub-surface maximum, and also provided evidence of the presence of actinides, as expected given the attribution of this activity to past marine discharges from Sellafield into the Irish Sea. The peak discharges occurred over 10 years ago, and the subsurface maxima observed on the major merse sites of the Solway system are probably the result sedimentary transport and deposition processes, perhaps coupled to on-site mobility. The effect of a pronounced sub-surface maximum is to reduce the full-energy photon fluence rate above ground level per unit areal activity. For this reason the calibration factors for correctly quantifying these aged sources are different from those applicable to recent terrestrial sources.

Examination of the gamma dose rate maps from the survey zone shows that the Chernobyl and weapons testing components are generally a minor contributor to overall dosimetry. The natural granite intrusions within the area are dominant sources within their local environment; the aged Sellafield derived activity produces the dominant contribution to tide washed pastures.

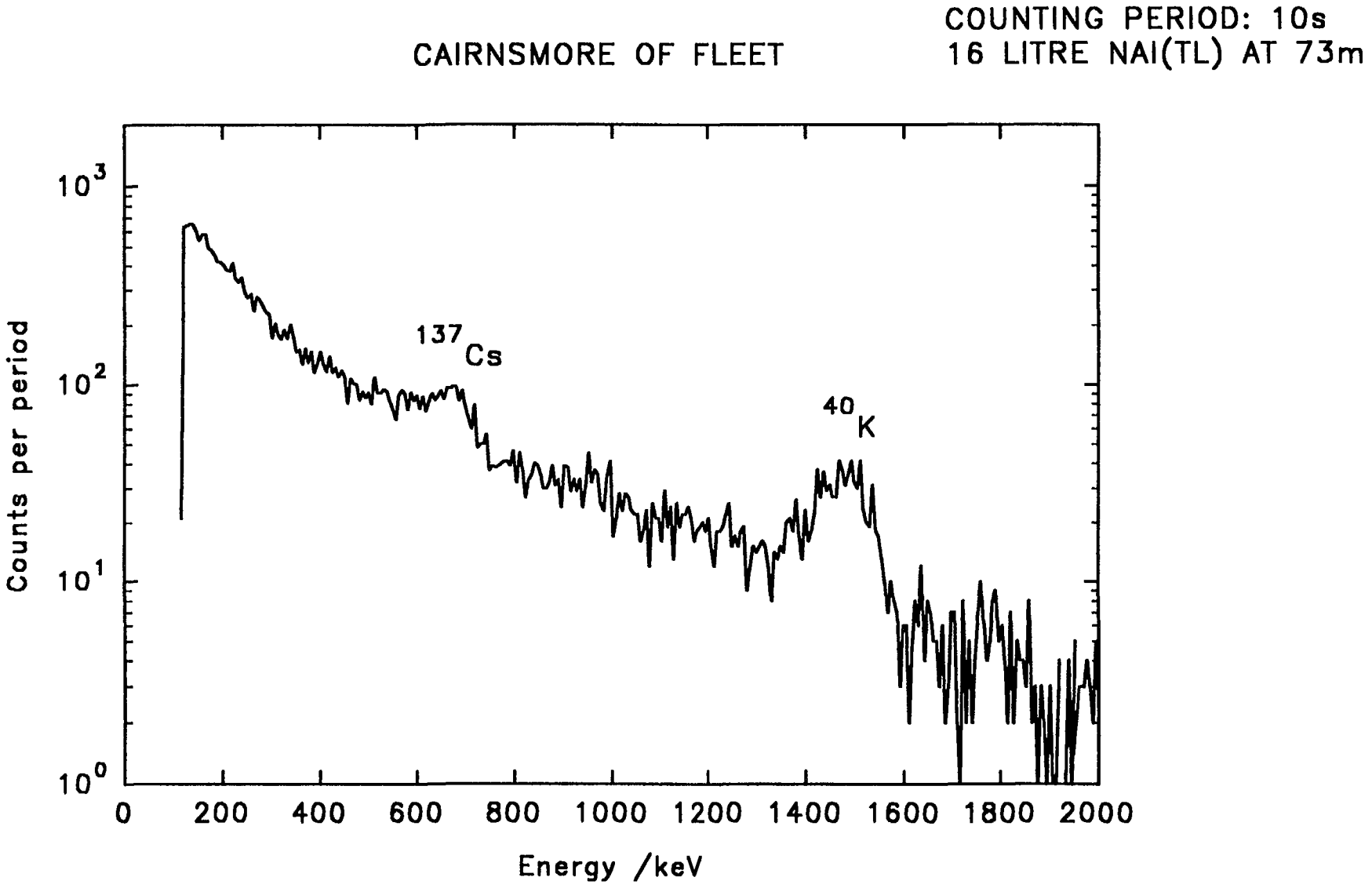

FIG. 4.a Aerial gamma ray spectra at Cairnsmore of Fleet, showing natural sources and Chernobyl derived ^{137}Cs NaI detector.

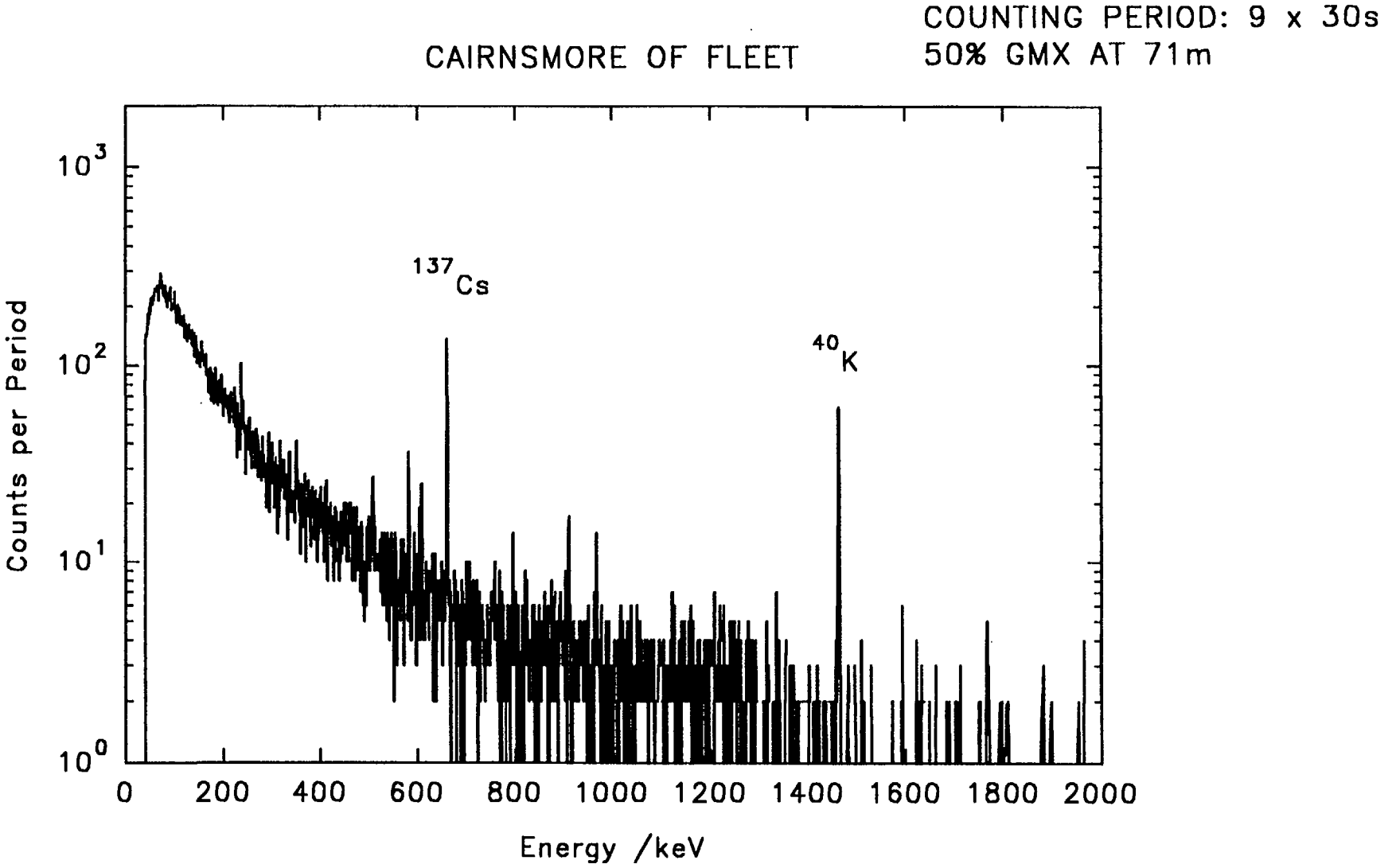

FIG. 4.b Aerial gamma ray spectra at Cairnsmore of Fleet, showing natural sources and Chernobyl derived ^{137}Cs 50% relative efficiency GMX.

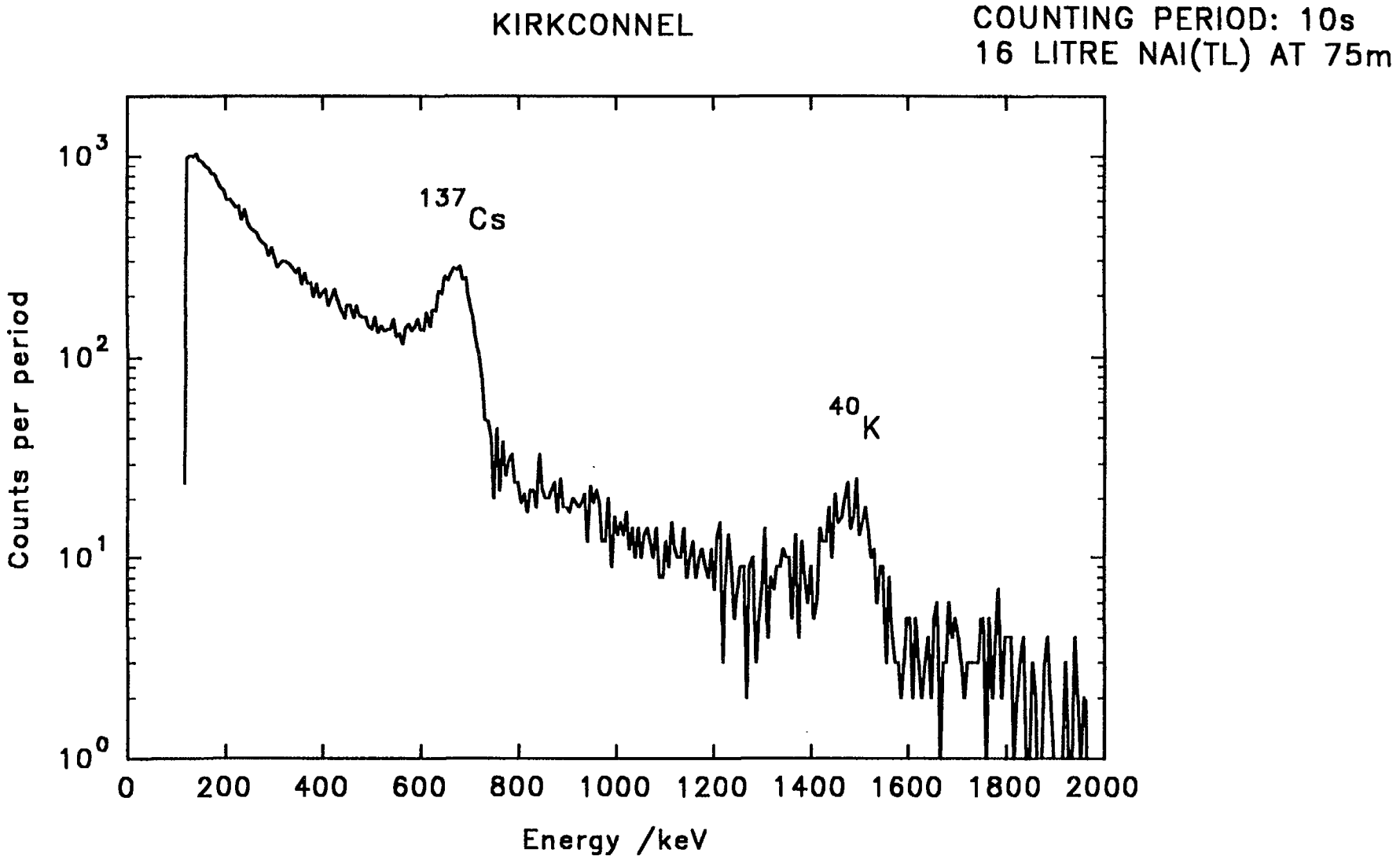

FIG. 5.a Aerial gamma ray spectra at Kirkconnel Merse, showing natural sources and Sellafield derived ^{137}Cs NaI detector. Note the enhanced forward scattering and higher ^{137}Cs/^{134}Cs compared with Fig. 4.

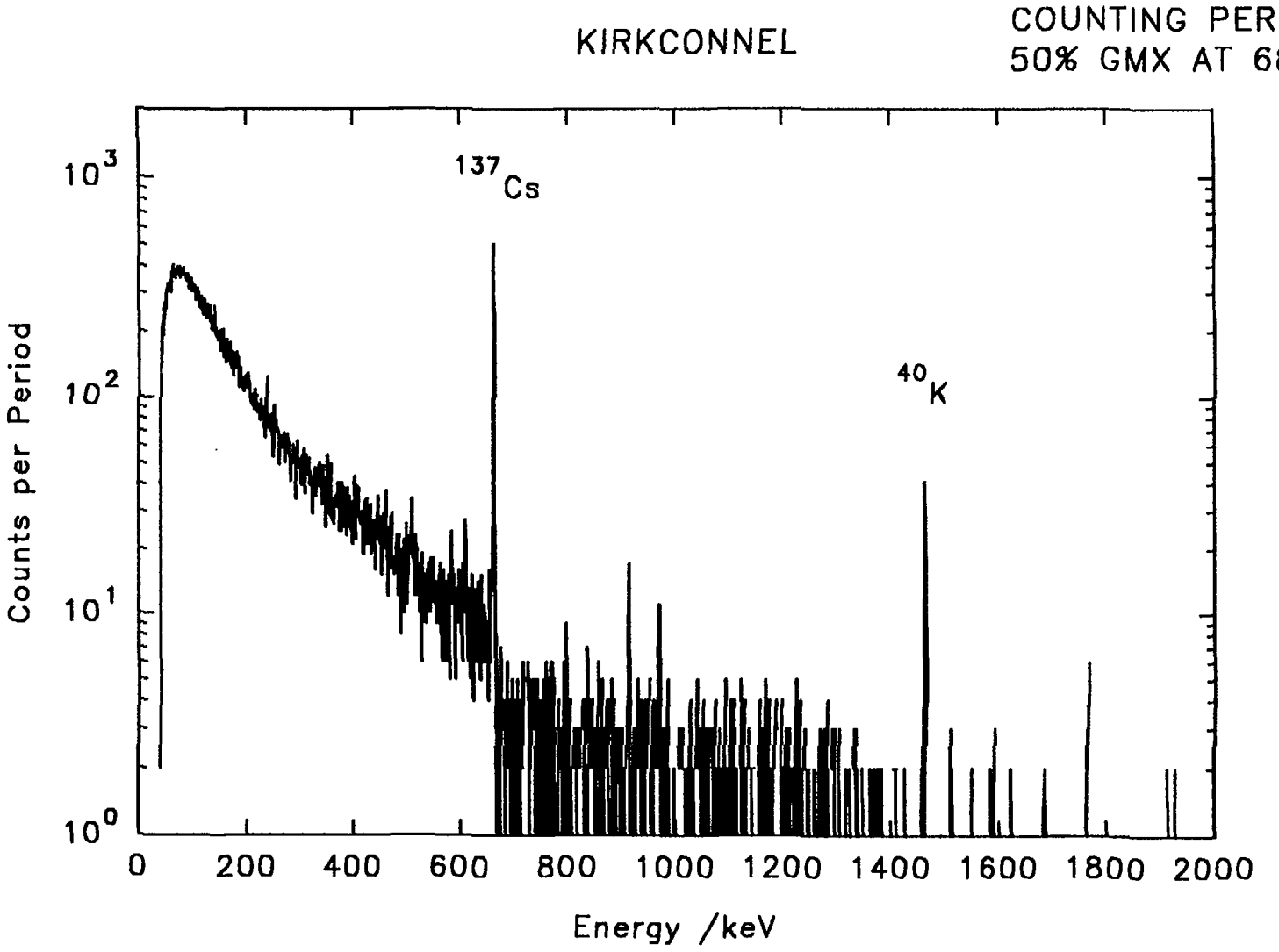

FIG. 5.b Aerial gamma ray spectra at Kirkconnel Merse, showing natural sources and Sellafield derived ^{137}Cs 50% relative efficiency GMX. Note the enhanced forward scattering and higher $^{137}Cs/^{134}Cs$ compared with Fig. 4.

Separate flight trials of a composite NaI, Ge spectrometer were conducted in SW Scotland and NW England by SURRC in late March, demonstrating the successful operation of such a system from a helicopter. There are encouraging signs that the semiconductor data may be of use in distinguishing between aged and recent anthropogenic activity. Examples of spectra recorded from both detectors at aerial survey heights above Cairnsmore of Fleet (predominantly Chernobyl) and Kirkconnel Merse (aged Sellafield marine discharge) are shown in Figs 4 and 5 respectively. Despite the lower count rates the semiconductor spectra add considerable information. The ^{137}Cs peak at 662 keV is clearly resolved from ^{214}Bi at 609 keV and ^{208}Tl and 583 keV. It is still possible to discern the 796 keV ^{134}Cs signal on both sites, and to recognize the different ratio arising from the distinct source age. Furthermore the enhanced levels of scattering, and particularly forward scattering associated with the aged ^{137}Cs source can be clearly identified in the semiconductor spectra, and thereafter recognized in the NaI spectra from the tide washed pasture. This leads to important possibilities for recognizing buried profiles using aerial survey results alone, and potentially for correcting calibration factors using scattered information.

It is clear that aerial radiometrics can provide detailed regional mapping which produces concordant results with ground based measurements. It is further notable that the fieldwork timescale to map the complete region was similar to that needed to investigate a single upland transect of some 12 sites using ground based methods. Quantitative interpretation using NaI detector depends on understanding the recent and aged sources within the mapping zone, which at present is approached by considered sampling during and after the survey. However there are signs that semiconductor detectors may be of assistance, both in reliable identification of individual nuclides in complex spectra, and potentially in recognizing and correcting for source burial effects on calibration.

3.3. ENVIRONMENTAL RADIOACTIVITY NEAR NUCLEAR SITES

Several SURRC surveys have incidentally included the environment of nuclear sites; for examples the Trawsfynydd, Hinkley Point and Hunterston power stations, and the Devonport Naval Dockyard fell within the scope of fallout mapping and general baseline studies. Where necessary permission to fly within air exclusion zones was obtained to enable off-site mapping.

More specific surveys of the environment of BNF nuclear sites have been conducted to define existing levels as part of an emergency response development programme. As has been pointed out the self powered spectrometers developed by SURRC can be rapidly installed in helicopters, and deployed within the time span of a few hours. Maintaining spectrometric equipment in a state ready for use is in many ways more effective in a laboratory environment than as part of a permanent installation in an aircraft. This minimizes delays due to aircraft unavailability, and reduces the need for regular spectrometer inspection and servicing in an aircraft hangar. Adoption of this model for emergency response purposes thus leads to an extremely economic, and effective way of providing for the eventuality of needing a survey at short notice. At present SURRC maintains two independent systems in flight ready condition. Baseline surveys of the Sellafield Works and Calder Hall reactors, of the Chapelcross reactor site, and of the Springfields fuel fabrication plant have been conducted. Rapid response plans have also been prepared for the reactor sites and exercised. The approach adopted is to prepare a flight path which encircles the site at 10 km, 5 km and 2 km distances — based on a series of waypoints which could be recognized visually in the event of failure of navigational instruments. In the event of an incident involving the release of activity from the sites an aerial survey could be mobilized immediately following deposition (thus minimizing risks of contaminating the aircraft). The initial exploratory approach to the site can be conducted within 45 minutes flying time, and would identify trajectories for further investigation, such as retrospective plume tracking.

The detailed investigations of nuclear sites have, unsurprisingly, shown local radiation fields due to the sites. Magnox reactors in particular show readily detectable signals from ^{41}Ar and ^{16}N, plus

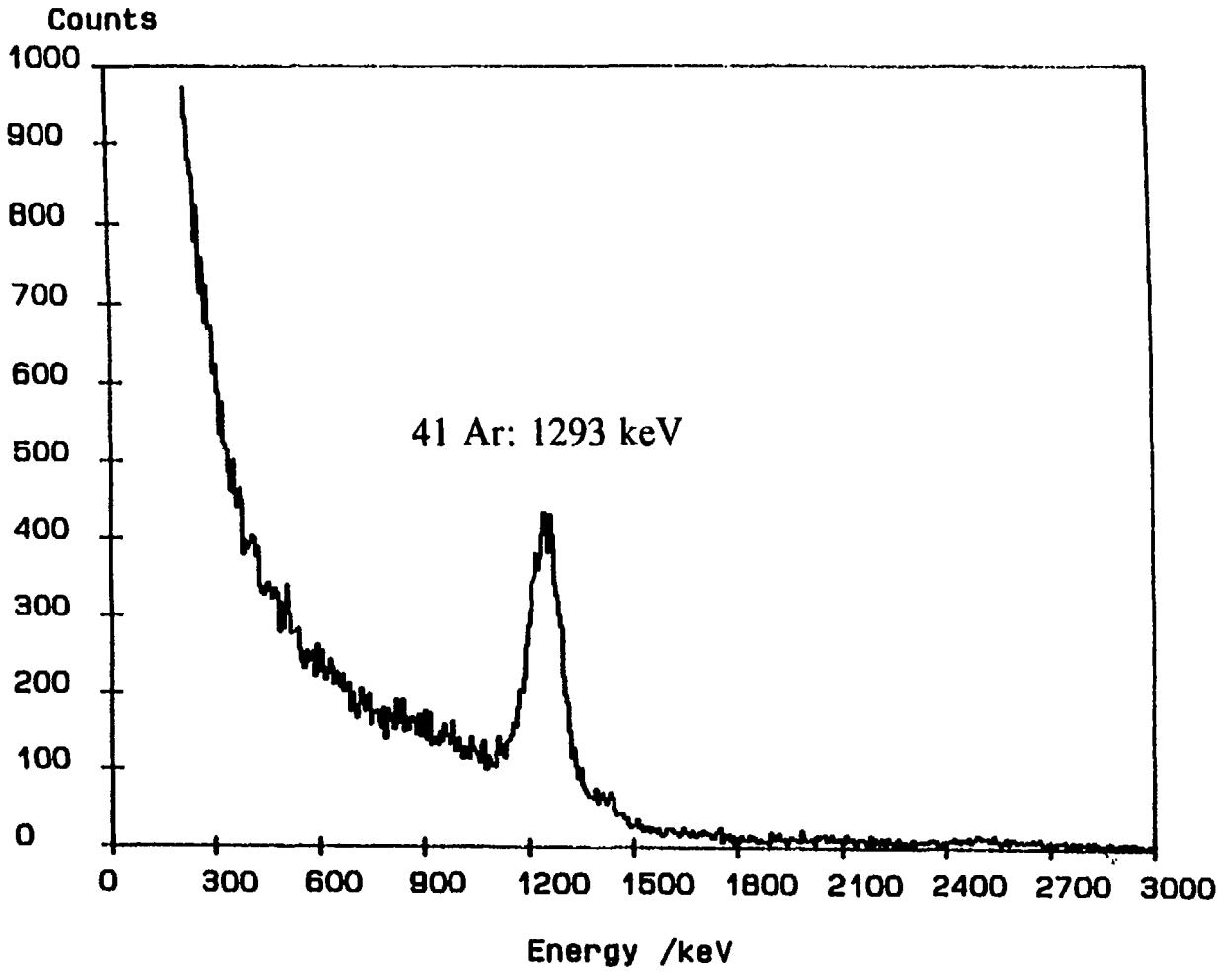

FIG. 6. ^{41}Ar plume close to the Chapelcross nuclear power station.

occasional evidence of residual activity due to fuel handling. Two spectral examples of such signals are presented in Figs 6 and 7, showing the ^{41}Ar plume close to the Chapelcross site recorded in 1992 [28], and a signal recorded near the Hunterston "A" station during baseline mapping in 1990. The second of these shows clear evidence of both ^{137}Cs and ^{60}Co, recorded above a field adjacent to the Magnox station after it had ceased operation. On further investigation in collaboration with Scottish Nuclear [24] it was possible to show that the signal was due to contained activity within an unshielded pipe on-site, which was part of a water treatment facility designed to remove low level radioactivity from cooling pond water.

The environment of AGR-only stations in the UK has not been investigated in detail, although no anomalies due to the Hunterston B station were detected off-site in 1990. The local radiation environment of nuclear sites can be investigated effectively within a single day, producing maps which clearly reveal any local radiation or contamination signals. The incorporation of aerial radiometrics within routine discharge monitoring and environmental quality assurance programmes could play an important additional role in assuring the public that well designed and operated nuclear facilities need not result in extensive environmental contamination.

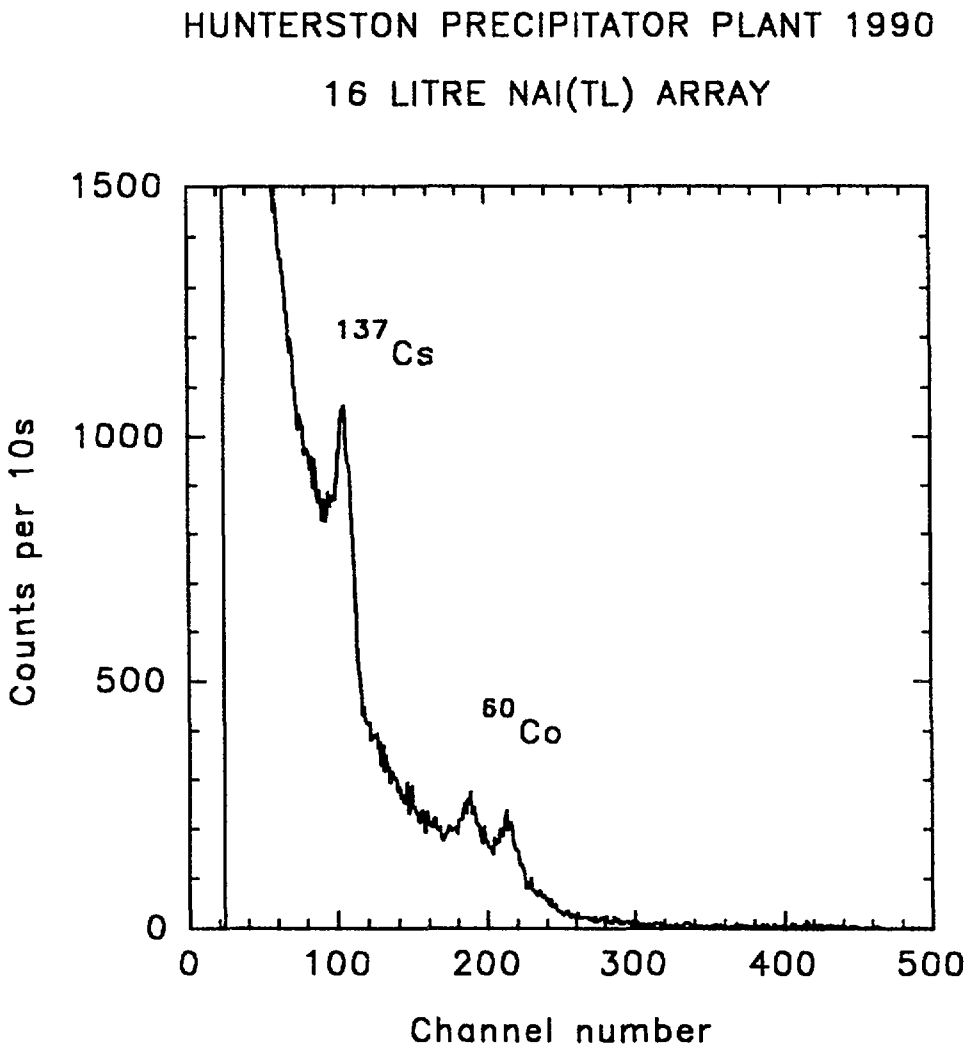

FIG. 7. ^{137}Cs and ^{60}Co signals recorded close to the Hunterston "A" station in 1990.

3.4. TECHNOLOGICALLY ENHANCED NATURAL RADIOACTIVITY

Technologically enhanced natural signals have been recorded during a number of surveys. Two examples were encountered during a source search in the Niger Delta in 1991 [31], in the first case associated with slags at a Steelworks, in the second with a domestic context, possibly containing a stolen gamma ray calibration facility. Flight trials in the Forth estuary in 1991 also showed considerable natural enhancements associated with fly-ash pits at the Longannet coal fired power station. In all these cases the localized enhanced dose rates were comparable with the sorts of enhancements encountered for example on Sellafield contaminated tide washed pastures.

Perhaps a more interesting situation was encountered in the Ribble estuary in 1992 during the baseline survey of the Springfields fuel fabrication plant. In this case one of the aims was to investigate the possibility of detecting unsupported ^{234m}Pa accumulating in the muds of the river Ribble arising from the continuous discharge from the plant. In this case the TENR was only a minor part of the gamma radiation environment; it was also surprising to detect unsupported Th series activity in the same system.

The baseline study was conducted from 1st-5th September 1992, and comprised a 300 m line spacing survey of the Ribble estuary and it's associated salt marsh over a 12 $\times$ 20 km area, together with a more detailed 100 m spacing area on one of the salt marshes. The Springfield works discharges low levels of unsupported uranium series activity in a continuous discharge to the Salwick Brook during production periods, leading to a quasi equilibrium with ^{234m}Pa in the mudflats of the Salwick Brook and Ribble. Since ^{234m}Pa is particle reactive it tends to accumulate in certain sediment traps, in a temporally unstable manner which relates to local rainfall and tidal behaviour. The ground level distribution is monitored frequently using beta probes both by BNFL staff, and by other organizations, and is know to be highly dynamic.

Prior to the survey an additional energy window was defined to attempt to resolve the 1001 keV line associated with ^{234m}Pa, and stripping ratios measured using a depleted uranium source to define the peak. The week before the survey a calibration site was established at Warton Bank on the Ribble; an estuarine salt marsh close to the operating base. An extremely high spring tide covered this site the day before survey operations commenced. The majority of the 2700 gamma spectra recorded during the survey were acquired during a two day period the following week and used to map ^{137}Cs, K, eU, eTh and gamma dose rate using standard methods. The main anthropogenic contribution to environmental gamma dose rates was clearly identified as ^{137}Cs on the salt marshes of the lower Ribble, at levels which were consistent with the ground based monitoring conducted independently by BNFL.

A tentative stripped ^{234m}Pa signal was also mapped and showed a distribution which included the Springfields site itself (as expected), the upper reaches of the Ribble, and the salt marshes in the lower reaches. The last of these areas was surprising, and individual spectra were summed from various locations and examined. Fig. 8 shows spectra from Springfields, and the lower salt marsh together with the window defined for ^{234m}Pa. Detailed examination of these spectra showed that the lower salt marsh showed a slightly lower energy peak than the authentic signal from ^{234m}Pa at Springfields. This was attributed to ^{228}Ac at 911 and 969 keV. A Monte-Carlo simulation of the pure ^{228}Ac spectral shape was then performed and a separate set of overlapping spectral windows defined in an attempt to separate the two potential sources. When the original spectral records were re-integrated into this new set of windows, and stripped with additional terms this resulted in two sets of maps; one of which produced a pronounced distribution in the up-river locations associated with ^{234m}Pa, and correctly identifying the major known sedimentary sinks for this nuclide. The excess ^{228}Ac distribution (bearing in mind that equilibrated contributions from the Th series had already been stripped) was spatially correlated with lower estuarine salt marshes. Possible explanations for this behaviour were that (i) the vertical profile of Th series activity showed a layered distribution with superficial excess, or (ii) that the excess ^{228}Ac represents a super-equilibrated source. The first of these hypotheses was eliminated by examining the vertical profile of Th series activity at Warton

Bank, which showed no evidence of a superficial maximum. This leads to the second interpretation, that Th series activity in the estuarine salt marsh exhibits temporary disequilibrium following spring tides. The mechanism envisaged is one whereby ^{228}Ra may be extracted from estuarine sediments, and the particle reactive ^{228}Ac deposited from solution on the salt marsh during the high tide. This hypothesis requires further investigation at ground level, but seems reasonable on geochemical grounds.

The separation of short lived supra-equilibrated natural series sources from aerial survey spectra probably represents the limits to which spectral analysis could be expected to reach. The sources concerned were not dominant contributions to the gamma spectrum, nor to the radiation environment. The geometry of the upper river sources is small compared with the fields of view of aerial spectrometers at reasonable heights for surveys of semi-urban, and urban areas. This makes accurate quantification difficult. Nevertheless the consistency between the observed ^{234m}Pa distribution lends credence to the results.

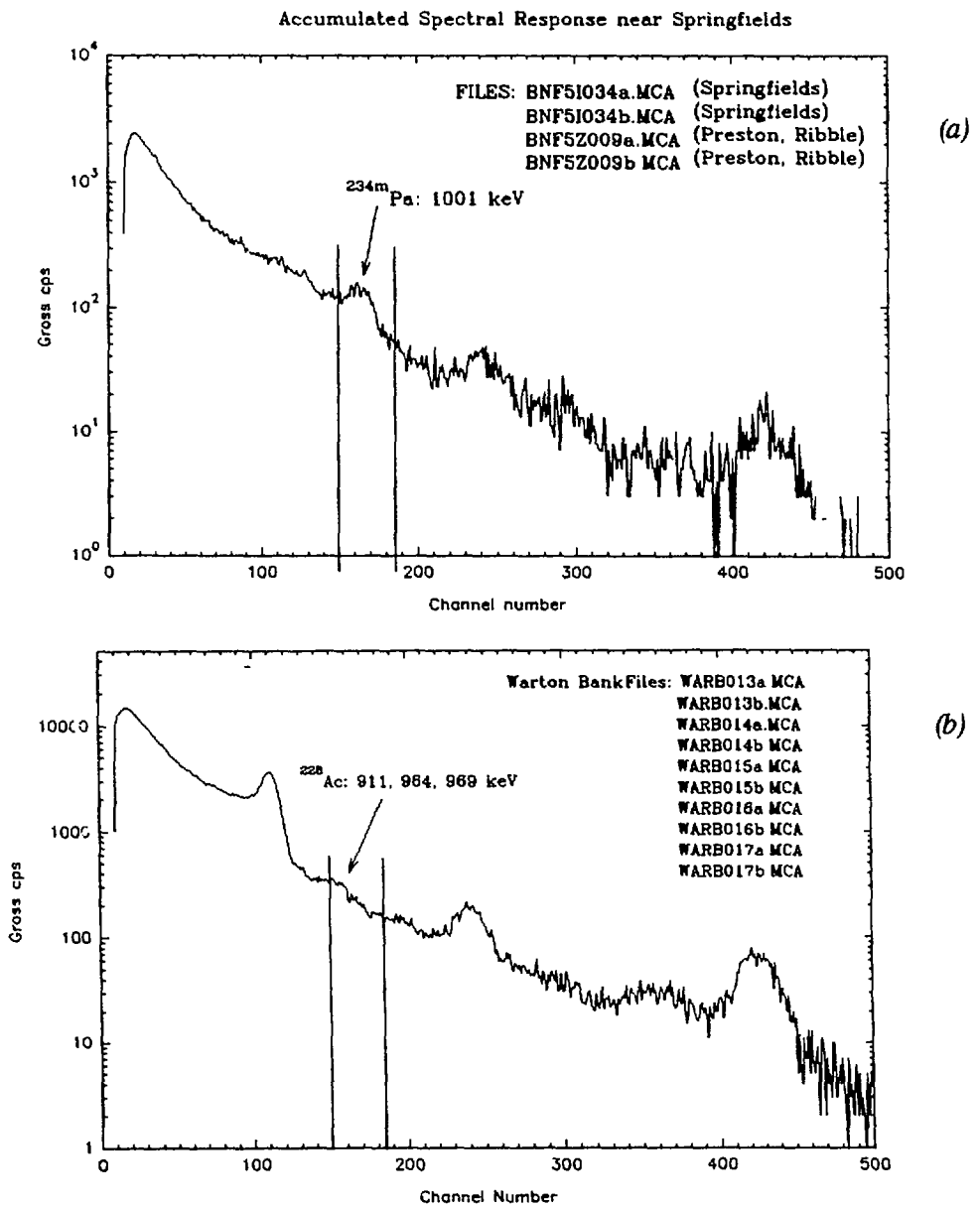

FIG. 8. NaI spectra recorded (a) close to Springfields, showing ^{234m}Pa, and (b) at Warton Bank showing ^{137}Cs and ^{228}Ac.

It appears therefore that aerial radiometrics are not only able to detect pronounced technologically enhanced nuclides, but also to map subtle disequilibria in both uranium and thorium series in timescales which are meaningful compared with the environmental dynamics of tidally driven systems. This also represents a considerable potential capability for investigating environmental systems.

4. DISCUSSION AND CONCLUSIONS

The main strengths of aerial gamma ray spectrometry arise from its ability to produce rapid and large scale data sets which are spatially representative of the total environment. In natural mapping there is considerable potential for utilizing these methods to produce background radiation maps which reveal the inherent variability of environmental fields. such information may be of interest to epidemiological studies. By extending the recording and analytical methods to include the capacity for fallout mapping, unique capabilities for investigating remote upland areas are available. Data can be recorded at a rate which is at least 2 orders of magnitude greater than ground based studies, and can be used to produce complete maps of the deposition patterns of aged and recent fallout in short timescales. This has important implications for both definition of existing levels, and for measuring future changes. The results are compatible with ground based estimates. The same benefits may be applied to definition of the environments of nuclear sites. While nuclear site may present local radiation enhancements, their impact on a wider scale can be readily appreciated by relatively short scale surveys. The emergency response potential is clear. Finally aerial survey methods are also able to put technologically enhanced natural sources into context, and to record dynamic environmental systems where temporary disequilibria may exist for natural or technological reasons.

REFERENCES

[1] DARNLEY, A.G., Airborne gamma ray survey techniques — present and future, Uranium Exploration Methods, IAEA, Vienna, 67 (1973).

[2] INTERNATIONAL ATOMIC ENERGY AGENCY, Recommended Instrumentation for Uranium and Thorium exploration, Technical Report Series No. 158, Vienna (1974).

[3] GRASTY, R.L., Uranium measurement by airborne gamma-ray spectrometry, Geophysics **40**, 503-519 (1975).

[4] INTERNATIONAL ATOMIC ENERGY AGENCY, Radiometric reporting methods and calibration in uranium exploration, Technical Report Series No. 174, IAEA, Vienna (1976).

[5] INTERNATIONAL ATOMIC ENERGY AGENCY, Gamma ray surveys in uranium exploration, Technical Report Series No. 186, IAEA, Vienna (1979).

[6] INTERNATIONAL ATOMIC ENERGY AGENCY, Construction and use of calibration facilities for radiometric field equipment, Technical Report Series No. 309, IAEA, Vienna (1989).

[7] INTERNATIONAL ATOMIC ENERGY AGENCY, The use of gamma ray data to define the natural radiation environment, IAEA-TECDOC-566, Vienna (1990).

[8] INTERNATIONAL ATOMIC ENERGY AGENCY, Airborne gamma ray spectrometer surveying, Technical Reports Series No. 323, IAEA, Vienna (1991).

[9] IEC, Airborne Instrumentation for Measurement of Terrestrial Gamma Radiation, IEC 1134, International Electrotechnical Commission, Geneva (1992).

[10] DEAL, L.J., DOYLE, J.F., BURSON, Z.G., BOYNS, P.K., Locating the lost Athena missile in Mexico by the Aerial Radiological Measuring System (ARMS), Health Physics **23**, 95 (1968).

[11] GRASTY, R.L., The search for Cosmos 954, in "Search Theory and Applications", ed. Hevlev and Stone, Plenum Publishing Corporation, New York (1980).

[12] WILLIAMS, D., Cambray, R.S., Maskell, S.C., An airborne radiometric survey of the Windscale area, October 19-22nd, AERE report R-2890 (1957).
[13] CHAMBERLAIN, A.C., GARNER, R.J., WILLIAMS, D., Environmental monitoring after accidental deposition of radioactivity, Reactor Science and Technology **14**, 155-167 (1961).
[14] LINDEN, A., MELLANDER, H., Airborne measurements in Sweden of the radioactive fallout after the nuclear accident in Chernobyl, TFRAP 8606 (1986).
[15] MELLANDER, H., Airborne gamma spectrometric measurements of the fallout over Sweden after the nuclear reactor accident at Chernobyl USSR, IAEA/NENF/NM-89-1 (1989).
[16] DUVAL, J.S., COOK, B., ADAMS, J.A.S., Circle of investigation of an airborne gamma ray spectrometer, J. Geophys. Res. **76**, 8466-8470 (1971).
[17] GRASTY, R.L., KOSANKE, K.L., FOOTE, R.S., Fields of view of airborne gamma ray detectors, Geophysics **44** (8), 1444-1457 (1979).
[18] SANDERSON, D.C.W., SCOTT, E.M., BAXTER, M.S., The Use and potential of Aerial Radiometrics for Monitoring Water Resource Contamination, in "Nuclear Contamination of Water Resources", Thomas Telford, London, pp 99-106 (1990a).
[19] SANDERSON, D.C.W., SCOTT, E.M., BAXTER, M.S., Use of airborne radiometric measurements for monitoring environmental radioactive contamination, IAEA SM-306/138, 411-421, IAEA, Vienna (1990b).
[20] SANDERSON, D.C.W., ALLYSON, J.D.,TYLER, A.N., Rapid quantification and mapping of radiometric data for anthropogenic and technologically enhanced natural nuclides, This meeting (1993).
[21] SANDERSON, D.C.W, SCOTT, E.M., BAXTER, M.S., PRESTON, T., A feasibility study of the use of airborne radiometric survey for UK fallout, SURRC report (1988).
[22] SANDERSON, D.C.W., SCOTT, E.M., Aerial Radiometric Survey in West Cumbria in 1988, MAFF Report N611 and Technical Annex (1989) 120p.
[23] SANDERSON, D.C.W., EAST, B.W. SCOTT, E.M., Aerial Radiometric Survey of Parts of North Wales in July 1989, SURRC Report (1989) 9p.
[24] SANDERSON, D.C.W., ALLYSON, J.D., MARTIN, E., TYLER, A.N., SCOTT, E.M., An Aerial Gamma Ray Survey of Three Ayrshire Districts, Commissioned by the District Councils of Cunninghame, Kilmarnock & Loudon, and Kyle and Carrick, SURRC Aerial Survey Report (1990) 22p.
[25] SANDERSON, D.C.W, ALLYSON, J.D., TYLER, A.N., NI RIAIN, S., MURPHY, S., An airborne gamma ray survey of parts of SW Scotland in February 1993, SURRC Aerial Survey Report (1993a) 26p.
[26] SANDERSON, D.C.W., SCOTT, E.M., BAXTER, M.S., MARTIN, E., NI RIAIN, S., The use of aerial radiometrics for epidemiological studies of leukaemia, SURRC Report (1993) 165 p.
[27] SANDERSON, D.C.W., ALLYSON, J.D., CAIRNS, K.J., MACDONALD, P.A., A Brief Aerial Survey in the Vicinity of Sellafield, SURRC Aerial Survey Report (1991) 34p.
[28] SANDERSON, D.C.W, ALLYSON, J.D., TYLER, A.N., An aerial gamma ray survey of Chapelcross and its surroundings in February 1992, SURRC Aerial Survey Report, to BNFL (1992) 36p.
[29] SANDERSON, D.C.W, ALLYSON, J.D., TYLER, A.N., MURPHY, S., An aerial gamma ray survey of Springfields and the Ribble Estuary in September 1992, SURRC Aerial Survey Report, to BNFL (1993b) 46p.
[30] SANDERSON, D.C.W., EAST, B.W., ROBERTSON, I., SCOTT, E.M.,The use of aerial radiometrics in the search for a lost 137-Cs source, SURRC report to BP Oil (1989) 8p.
[31] SANDERSON, D.C.W., ALLYSON, J.D., An Aerial Gamma Ray Search for a missing ^{137}Cs source in the Niger Delta, May 1991, SURRC Aerial Survey Report (1991) 29p.
[32] HUGHES, J.S., SHAW, K.B., O'RIORDAN, M.C., Radiation exposure of the UK population -1988 Review, NRPB Report, NRPB-R227 (1989).
[33] ROSE, K.S.B., Clusters of Health Effects associated with radiation around the world excluding the UK, AERE R13776 (1988).
[34] GREEN, B.M.R., LOMAS, P.R., BRADLEY, E.J., WRIXON, A.D., Gamma radiation levels outdoors in Great Britain, NRPB Report, NRPB-191 (1989).

[35] GREEN, B.M.R., HUGHES, J.S., LOMAS, P.R., Radiation Atlas. Natural sources of ionising radiation in Europe, Commission of the European Communities (1992).
[36] HENSHAW, D.L., EATOUGH, J.P, RICHARDSON, R.B., Radon as a causative factor in induction of myeloid leukaemia and other cancers, The Lancet **335** (1990) pp 1008-1012.
[37] ICRP 60, 1990.

Next page(s) left blank

ENVIRONMENTAL MONITORING BY AIRBORNE GAMMA RAY SPECTROMETRY, EXPERIENCE AT THE GEOLOGICAL SURVEY OF CANADA

R.L. GRASTY
Geological Survey of Canada, Ottawa, Canada

Abstract

At the Geological Survey of Canada (GSC), techniques have been developed for detecting and mapping man-made sources of radiation by airborne gamma ray spectrometry. Using a gamma ray spectrum ratio technique, the GSC airborne gamma ray spectrometer detected the first piece of radioactive debris from the Russian nuclear satellite which fell in northern Canada in 1978. In co-operation with the Finnish Geological Survey, a technique has been developed to remove the natural gamma ray contribution from the measured spectrum. This technique was used in Finland for mapping radioactive fallout from the Chernobyl nuclear accident. Using the same technique, an airborne gamma ray survey in the vicinity of the Kozloduy nuclear reactor identified areas contaminated by ^{60}Co and ^{137}Cs.

1. INTRODUCTION

Since 1968, the GSC has been routinely flying airborne gamma ray surveys for mineral exploration and geological mapping. Standardized procedures have been developed to convert the airborne measurements to ground concentrations of potassium, uranium and thorium [1]. Originally these surveys were flown with four channel gamma ray spectrometers to monitor total gamma-radioactivity and natural gamma-radiation from potassium and the uranium and thorium decay series.

In 1977, the GSC developed a 256 gamma ray spectrometer with which it was possible to monitor gamma-radiation from both natural or man-made sources [2]. This development proved to come at an opportune time, since in January, 1978, the nuclear powered Russian satellite crashed in northern Canada [3]. The new spectrometer was flown in the search operation and analysis of the airborne data confirmed that radioactive debris from the satellite had reached the earth's surface.

The nuclear accident at Chernobyl occurred during the night of 25-26 April 1986, contaminating large parts of Europe. The techniques developed for mapping natural sources of radiation were adapted to monitor man-made radiation and once again proved to be very effective for mapping the extent of the contamination [1].

In Canada, there was very little fallout from Chernobyl. However, airborne data collected by the Finnish Geological Survey in contaminated areas of Finland was analyzed at the GSC and resulted in the development of a simple technique for separating man-made and natural radiation [4]. Subsequently, this technique was used in Finland to map the contamination from Chernobyl and was also used to map man-made contamination in the vicinity of the nuclear facility at Kozloduy in Bulgaria [5].

This paper describes the search for Cosmos-954 and the technique developed at the GSC for mapping contamination from the Chernobyl nuclear accident and from the nuclear power plant at Kozloduy, Bulgaria. These three examples demonstrate how airborne gamma ray spectrometry can be an effective tool for environmental monitoring.

2. THE COSMOS-954 INCIDENT

On January 24 1978, COSMOS-954, a nuclear powered Soviet satellite, disintegrated on re-entering the earth's atmosphere and scattered radioactive debris over a large area of northern Canada. The U.S. Government offered the Canadian Government the assistance of their Nuclear Emergency Search Team (NEST) with three gamma ray spectrometers. These three gamma ray spectrometers, together with one from the Geological Survey of Canada were all involved in the search and recovery operation [3,6,7].

Based on computer reentry predictions, the probable impact zone covered an area 800 km long by 50 km wide. For logistical reasons, this initial search area was divided into 8 sectors. To cover this large area, four C-130 Hercules aircraft flew a reconnaissance survey along lines 1 nautical mile apart at an altitude of 500 m (1500 ft). The first of the three U.S. gamma ray spectrometers was airborne early on the morning of January 25. The Canadian system was in the air 24 hours later.

Fission products of a reactor emit gamma radiation with a higher proportion of low energy gamma rays than naturally occurring radioactive isotopes. Gamma rays from the neutron activation

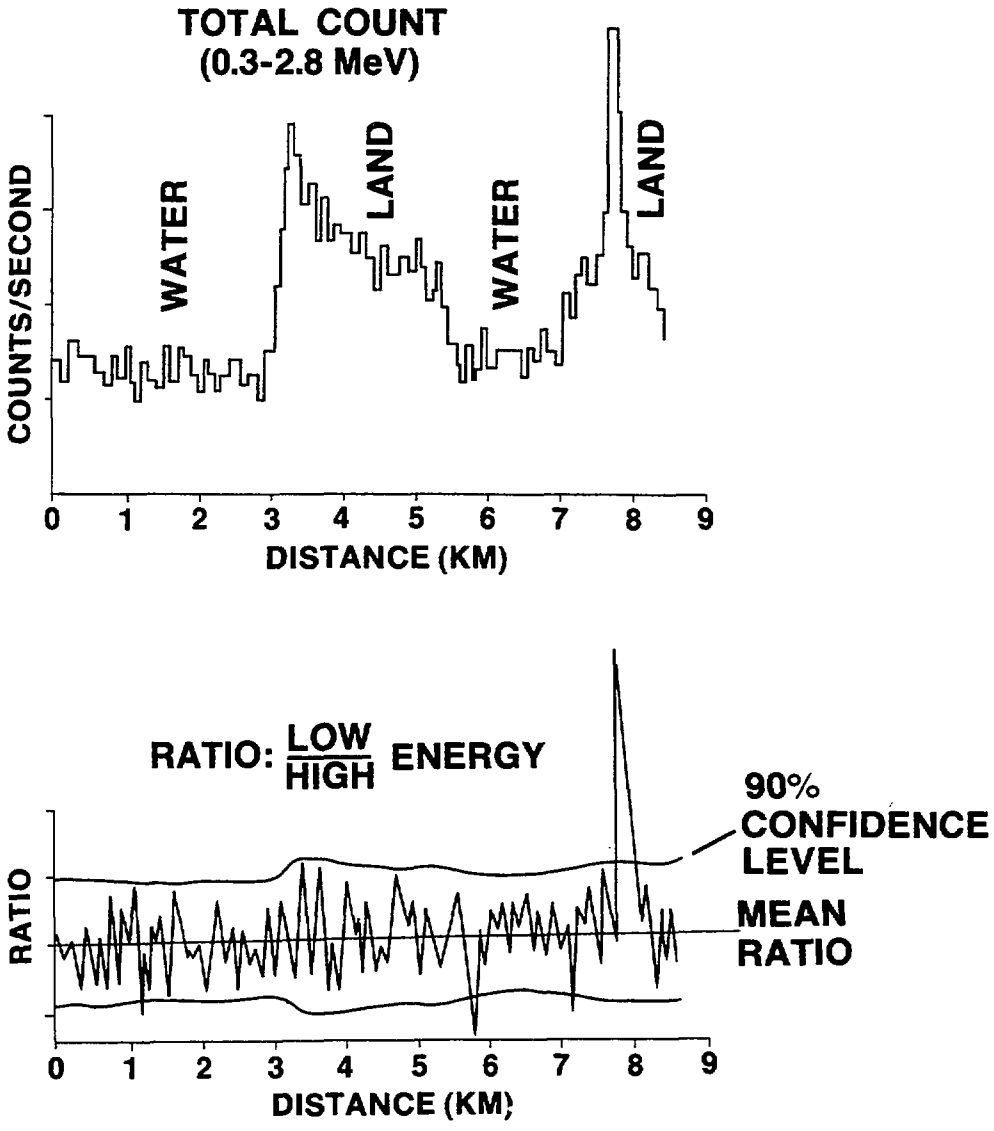

FIG. 1. Total count profile and ratio of high to low energy showing the detection of man-made radiation from Cosmos-954 debris in northern Canada.

of steel are also predominantly of low energy. Table I shows the major gamma rays emitted by fission and neutron activation products which are most likely to be observed soon after reactor shutdown [1]. The half-lives of the various isotopes are also indicated. The more volatile elements such as cesium and iodine were not expected to have reached the ground because of the heat of re-entry.

Because of the high levels of radioactivity of rocks in the search area, a ratio technique was used to detect the artificial sources of radiation. This technique makes use of the fact that the radiation from the satellite debris is predominantly of low energy. The ratio of gamma rays in a 300 to 1400 keV window to those from 1400 to 2800 keV was found to remain constant for all natural sources of radioactivity. Radioactive satellite debris was indicated by an increase in this ratio as shown in Fig. 1.

TABLE I. PRINCIPAL MAN-MADE NUCLIDES

Nuclide	Principal Energies (keV)	Half-life (days)
^{95}Zr	724, 756	65
^{95}Nb	765	35
^{99}Mo	740	3
^{103}Ru	497	40
^{106}Ru	512	368
^{131}I	364	8
^{132}Te	230	3
^{134}Cs	605, 795	730
^{137}Cs	662	11,000
$^{140}Ba/^{140}La$	1596	13

On the night of the 26/27 January, the Canadian spectrometer detected a radioactive source on the ice of Great Slave Lake. Subsequent computer analysis of the data recorded on magnetic tape confirmed the presence of gamma rays characteristic of the products of nuclear fission. The gamma ray spectrum of the source, obtained by subtracting the spectrum from neighbouring points is shown in Fig. 2 together with the total count profile, shows the significant low energy component.

By January 31 the search had shown that all large radioactive fragments from the satellite had fallen within a strip ten kilometers wide along part of the predicted reentry path. As much of the area was north of the tree line with few reference points, considerable difficulty was found in pinpointing the location of radioactive debris detected. In order to provide accurate and systematic coverage of the narrow zone where radioactive debris had been found, two microwave ranging systems (MRS) were employed. Detailed coverage of this narrow search area was flown at a line spacing of 500 m (1500 ft) at a nominal terrain clearance of 250 m (750 ft).

On February 10, by chance, a low flying helicopter discovered many radioactive sources some distance from the original search area. These sources were too weak to be detected at the altitude flown by the Hercules. Later analyses of these minute pieces showed them to be part of the missing reactor core. In the next few days, other low flying helicopters detected more radioactive particles even farther from the satellite track. The reactor core had apparently disintegrated on entering the earth's atmosphere and minute pieces of the core had been carried by the wind to dust many thousands of square kilometers of northern Canada. These minute particles were not considered to be cause for concern [7].

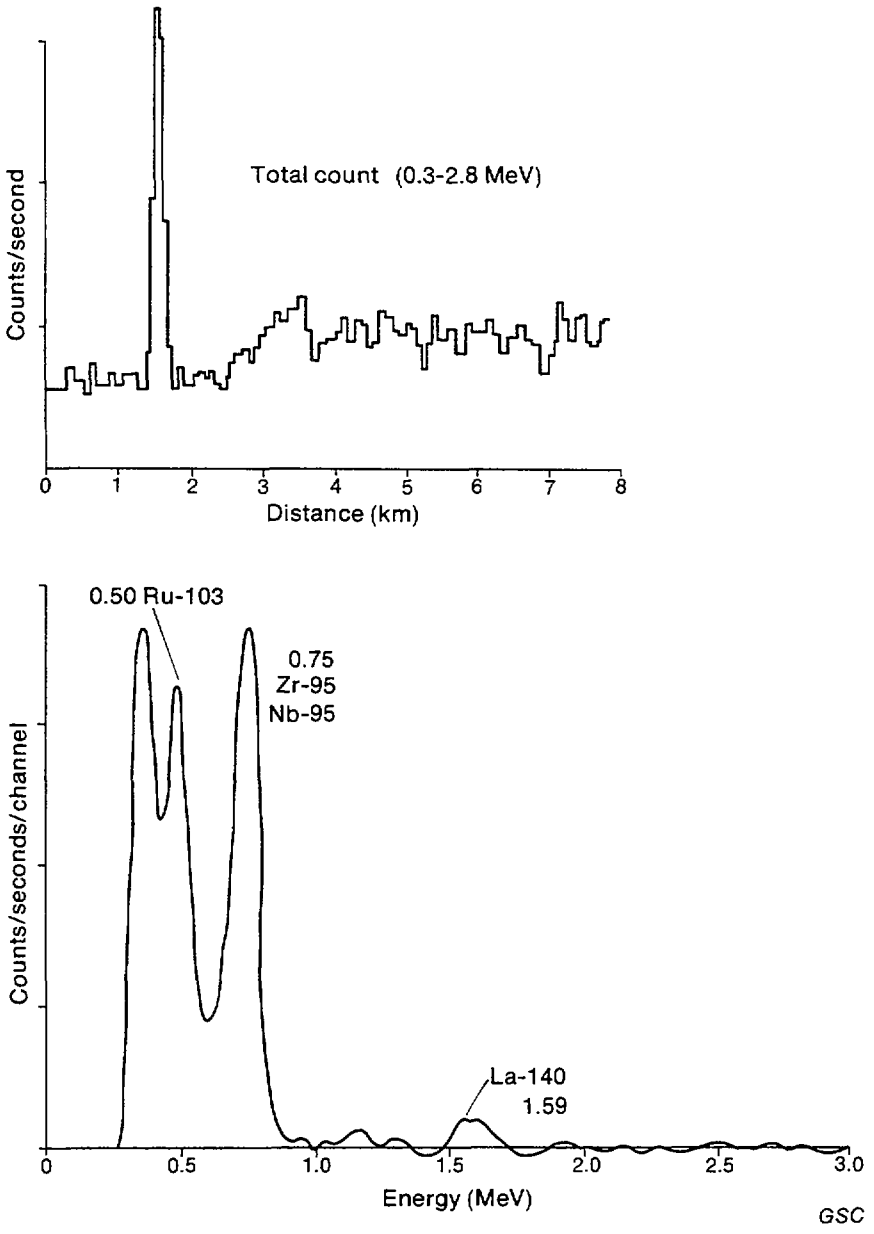

FIG. 2. Total count profile and gamma ray spectrum showing the peaks of ^{103}Ru, ^{95}Zr-^{95}Nb and ^{140}La.

3. THE CHERNOBYL EVENT

3.1. INTRODUCTION

Following a nuclear reactor accident, such as the Chernobyl event of 1986, many man-made radioactive nuclides with a variety of gamma ray energies and half-lives may contaminate the environment. To estimate the significance of any man-made contamination, the contribution due to natural gamma-radiation must first be removed.

In 1989, analysis of airborne gamma ray data collected in 1988 by the Geological Survey of Finland following the Chernobyl nuclear accident showed that the natural gamma ray component could be removed from the airborne spectrum without prior knowledge of the gamma ray spectral shapes of potassium, uranium and thorium [4].

3.2. THEORY

In the technique to separate man-made and natural gamma-radiation, it is assumed that the gamma ray energies due to fallout are below the potassium, uranium and thorium windows normally used for monitoring the concentrations of these elements on the ground [1]. Table I shows that of the man-made gamma ray emitting isotopes from the Chernobyl accident, ^{140}La with a gamma ray peak at 1596 keV is the only nuclide with an energy falling in the standard potassium, uranium and thorium windows [1]. However, it has a half-life of 13 days. Provided the analyses of the airborne spectra are carried out on data collected several months after the Chernobyl accident, the ^{140}La peak will be negligible.

The count rate in a low energy window, such as one centered about the ^{137}Cs peak at 662 keV, will depend linearly on the count rates in the potassium, uranium and thorium windows. Following a nuclear accident, there may be an additional contribution in the low energy window from fallout. Consequently, the relationship between a low energy window count rate L, and the potassium, uranium and thorium window count rates, K, U and Th is given by:

$$L = a_1 \times K + a_2 \times U + a_3 \times Th + C \ldots . \quad (1)$$

where a_1, a_2 and a_3 are constants which give the count rates in the low energy channel L per unit count rate in the potassium, uranium and thorium windows. The constant C represents the contribution in the low energy channel L due to fallout. In this equation, it is assumed that the background contributions in the various windows due to cosmic radiation, the aircraft and airborne radioactivity have been removed. This background would normally be determined from measurements over water.

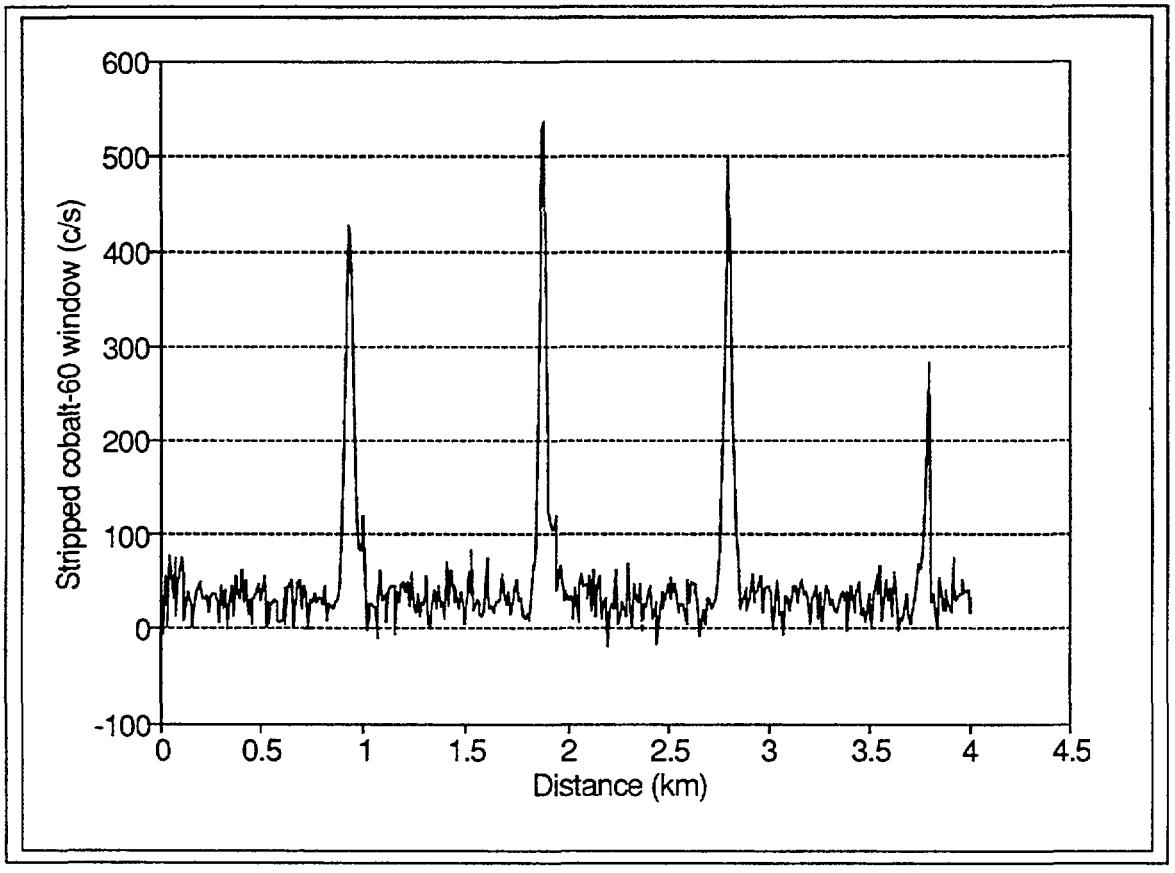

FIG. 3. A profile of a single window, centered around the ^{60}Co peak at 1173 keV with the natural gamma ray components removed. The profile corresponds to four flights over a contaminated area.

From flights over areas with different concentrations of potassium, uranium and thorium, the four constants a_1, a_2, a_3 and C in equation (1) can be determined by simple linear regression. The value of C will be the average contribution from fallout in the low energy channel for the data that is analyzed. Once these coefficients have been determined, the contribution from potassium, uranium and thorium to any low energy channel can be removed [4]. No special flights are required to determine the coefficients a_1, a_2, a_3 in equation (1). However, it has been found experimentally that they are best determined using airborne data collected prior to the Chernobyl accident. For such data, the contribution due to fallout from atomic weapons testing is small and relatively uniform.

In 1989, this technique was successfully tested on airborne gamma ray spectra acquired in 1988 by the Finnish Geological Survey over two areas in Finland which were contaminated by fallout from Chernobyl [4]. This procedure is now used routinely in Finland for mapping radioactive fallout from the Chernobyl nuclear accident.

4. THE KOZLODUY SURVEY, BULGARIA

In 1990, a detailed gamma ray survey was flown by the Airborne Geophysics Department of the Enterprise for Geophysical Exploration and Geological Mapping in Sophia, Bulgaria in the vicinity of a nuclear reactor near the town of Kozloduy. Analysis of the airborne data in Bulgaria had shown evidence for man-made contamination due to cesium-137 and cobalt-60. More detailed analysis of the data was performed at the GSC [5] using the technique described by Grasty and Multala [4].

Fig. 3 illustrates how the technique can be used to identify the presence of ^{60}Co on the ground. It shows a continuous profile from several flight lines over a contaminated area near a canal. The profile shows the count rate from a single window centered around the ^{60}Co gamma ray peak at 1173 keV. The natural contribution to the ^{60}Co window was removed by monitoring the potassium, uranium and thorium windows and applying the appropriate coefficients derived from the entire flight line.

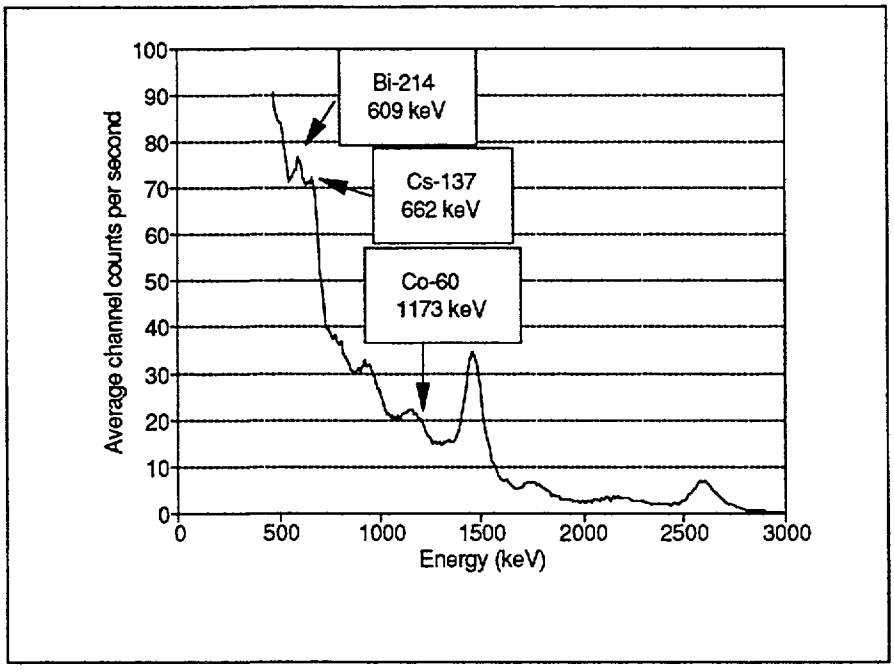

FIG. 4. An average spectrum measured over an area contaminated by ^{60}Co.

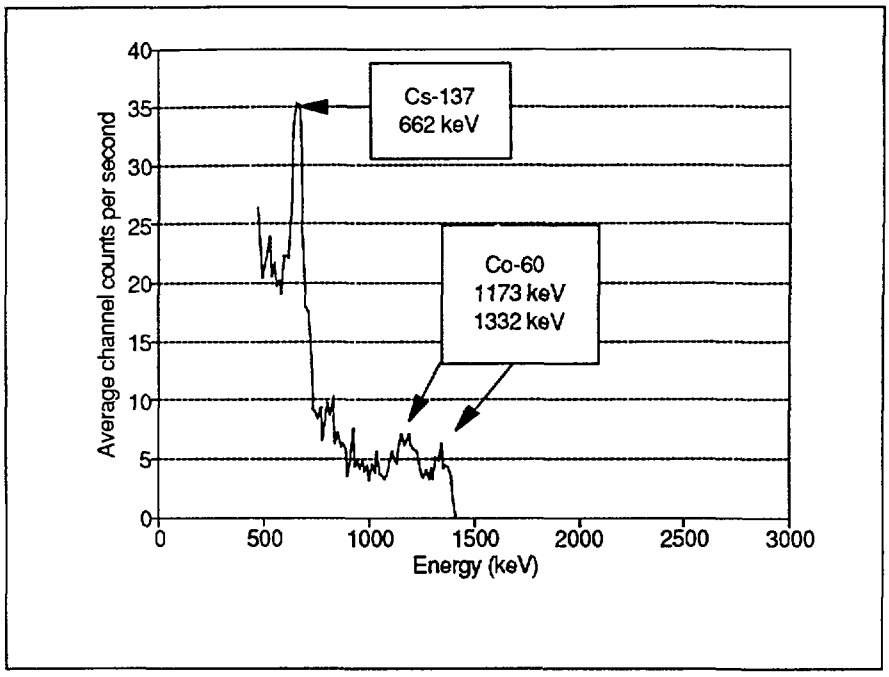

FIG. 5. The same spectrum showing the ^{60}Co peaks at 1173 and 1332 keV, after removal of the natural gamma ray components.

The potassium, uranium and thorium contribution can be also be removed from the entire measured spectrum using coefficients for all low energy channels. Figs 4 and 5 illustrate how a cobalt-60 spectrum can be extracted from the measured spectrum of a small section of line covering an area of cobalt-60 contamination. Fig. 4 shows the average spectrum along this flight section. No clear cobalt-60 peaks can be seen at 1173 and 1332 keV. The coefficients a_1, a_2, and a_3 in equation (1) were derived for each channel of the spectrum using data from the entire flight. Using these coefficients, the natural gamma ray spectrum was removed from all channels below an energy of approximately 1300 keV. In the man-made extracted spectrum shown in Fig. 5, $^{6}0Co$ and ^{137}Cs are clearly identified.

The airborne data from the Kozloduy area was processed in the standard way recommended by the International Atomic Energy Agency [1] to produce potassium, uranium and thorium maps and their respective ratios together with maps showing the distribution of ^{137}Cs and ^{60}Co maps [5]. Fig. 6 is a map showing the deposition of ^{137}Cs which was similar to the distribution of ^{60}Co. The conversion of the ^{137}Cs count rates to kBq/m^2 was carried out using data provided by the Finnish Geological survey and the Scottish Universities Research Centre. In the case of the ^{60}Co map, no conversion factors were available. It should be noted that the higher ^{137}Cs deposition levels indicated on the maps are comparable to those found in large areas of Sweden and Finland due to fallout from Chernobyl.

REFERENCES

[1] INTERNATIONAL ATOMIC ENERGY AGENCY, Airborne gamma ray spectrometer surveying, Technical Reports Series No. 323, IAEA, Vienna (1991) 97 p.

[2] BRISTOW, Q., A gamma ray spectrometry system for airborne geological research, Geological Survey of Canada Paper 79-1C (1979) 55-61.

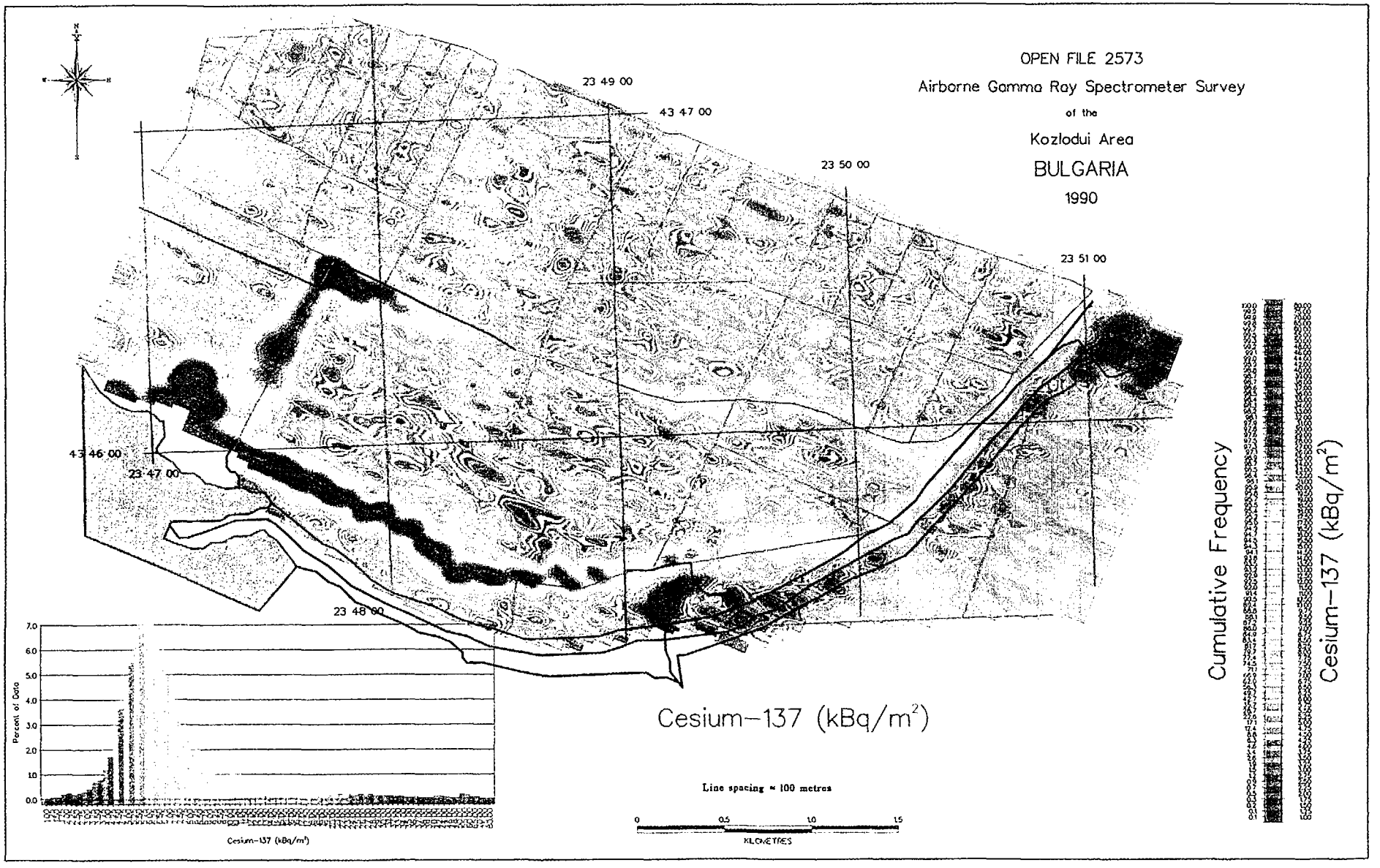

FIG. 6. A map of the Kozloduy area showing the deposition of ^{137}Cs.

[3] GRASTY, R.L., The Search for COSMOS-954, Proceedings of the NATO Conference on Search Theory and Applications, Portugal 1979, Plenum Press, New York and London (1980) 211-220.
[4] GRASTY, R.L., MULTALA, J., A correlation technique for separating natural and man-mae airborne gamma ray spectra, Geological Survey of Canada Paper 90-1D (1991) 111-116.
[5] HETU, R., RANGELOV, R., GRANT, J.A., GRASTY, R.L., GRAHAM, D., Monitoring Natural and Man-made Radiation by Airborne Gamma ray Spectrometry, Kozlodui Area, Bulgaria, 1990. Geological Survey of Canada Open File 2573 (1993).
[6] UNITED STATES DEPARTMENT OF ENERGY, Operation Morning Light, Northwest Territories, Canada - 1978, U.S. Dept. of Energy Report NV-198; United States Department of Commerce, Springfield, Virginia (1978) 81 p.
[7] GUMMER, W.K., CAMPBELL, F.R., KNIGHT, G. B., RICARD, J.L., Cosmos-954, the occurence and nature of recovered debris, Atomic Energy Control Board, Canada, Info-0006 (1980) 60 p.

Next page(s) left blank

AIRBORNE GAMMA RAY MEASUREMENTS IN RADIOACTIVE CLOUD — EXPERIENCE AT THE GEOLOGICAL SURVEY OF FINLAND

J. MULTALA
Geological Survey of Finland, Espoo, Finland

Abstract

On April 29, 1986 the airborne gamma ray measurement system of Geological Survey of Finland flew by misfortune thorough the radiating cloud from Chernobyl accident. The measured gamma ray data shows how the radioactivity varied in different parts of that cloud. Due to that flight it came obvious how seriously the aircraft can contaminate, how difficult it is to clean the aircraft and what kind of technical problems that introduces for measurement systems and techniques

1. THE AEROGEOPHYSICAL EQUIPMENT OF GSF

The second national aerogeophysical mapping program in Finland was started in 1972. The survey is carried out using 200 m line spacing at the nominal altitude of 30 meters. At the moment Geological Survey of Finland (GSF) has covered more than 70 % of the country with these flights and the program is scheduled to run about 2005. The aerogeophysical system of GSF consist of following instrumentation:

- Gamma ray measurement system: 6 NaI crystals total volume 25 liters and multichannel analyser. Nowadays also 2 upward looking crystals has been installed. 120 channels are recorded once in second covering energy range from about 0.2 MeV to 3.1 MeV and the width of one channel is about 24 keV.
- Two Cesium magnetometers.
- Active electromagnetic system.
- VLF system.
- GPS-satellite navigation system.

The instruments are installed on DHC-6/300 Twin Otter aircraft owned and operated by Karair Oy. The nominal ground speed during the survey flights is about 50 m/s. Annually this system flies about 65 000 line kilometers (550 hours) mainly for aerogeophysical mapping.

2. THE FLIGHT THROUGH THE RADIATING CLOUD

Background spectra measured above the sea at the altitude of 60 meters on April 24 in 1986 is shown in Fig. 1. This spectra is from the first test flight which was done in 1986 and it is like all the other background spectra recorded before that. The next flight in 1986 was done on April 27 and the background spectra is also shown in Fig. 1. In the lower energy part of the spectra some new peaks can bee seen around the energies 355 keV and 537 keV. It is estimated that the first part of the radiating cloud from Chernobyl was above the South coast of Finland on that day, but hardly any observations were made on ground level. That means that these peaks in the background spectra are

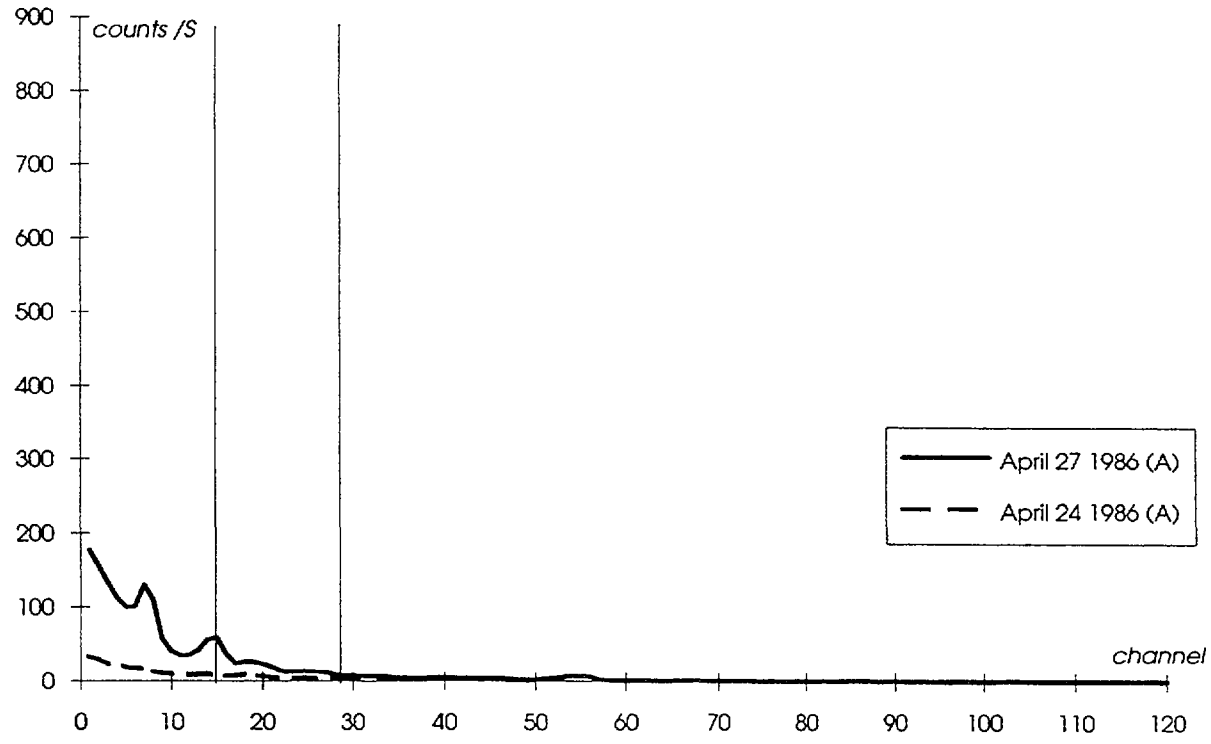

FIG. 1. Two background spectra measured above sea at the altitude of 60 meters. The Cesium window used in Fig. 2 is also plotted.

due to the first stage of the aircraft contamination. Unfortunately these peaks were so small that the operator didn't pay any attention on them during the flight and the aircraft continued its flight from Helsinki to North Finland in order to fly snow surveys.

The first news about the Chernobyl accident was announced April 28 and in the morning on April 29 the crew started the flight back home. The 700 km long flight from Rovaniemi straight South to Helsinki took about 2 and half hours. Figure 2 illustrates the barometric altimeter and the measured count rates of Cesium window (width about 390 keV, sum of 16 channels) from that flight. The aircraft flew on altitudes between 1.5 and 2.5 km. On those altitudes all the measured gamma rays are coming elsewhere than from ground (that is from the aircraft itself and from cosmic). Fig. 2 shows that there is hardly any correlation between the altitude and Cs-window count rates.

During the first hour of the flight the Cs-window counts keep the level around 500 counts/s. That level is mainly due to the aircraft's contamination two days earlier. When the aircraft flies to the first part of the radiating cloud the counts in Cs-window jumps to level 2 000 - 5 000 counts/s and soon after that the counts rise to the level from 5 000 to 10 000 counts/s. Just before landing but still high enough not to measure any radiation originating from the ground, the Cs-window counts drops and maintain at the level about 4 500 counts/s. A test flight above the sea which was done shortly afterwards confirmed that the aircraft contamination just after the flight was around 4 500 counts/s in Cs-window. Based on the measurements done by Finnish Centre for Radiation and Nuclear Safety hardly any fallout was found on ground level around Helsinki on that day. The first of the two most important things in this presentation is to notice the high level of the contamination of the aircraft.

To illustrate some technical difficulties and to show the location of the Cs-window four (A, C, H, and J) different spectra are shown in Fig. 3. They are mean spectra of one minute from the flight thorough the radiating cloud. The locations of each these spectra is marked with corresponding

capital letter on Fig. 2. The spectra A from the beginning of the flight is practically the same as the second spectra in Fig. 1, only Cs-134 and Cs-137 peaks has been come visible due to the contamination that was got from the flight from Helsinki to Rovaniemi on the April 27.

Spectra C is just after hitting the edge of the cloud. The lower energy part of that spectra (channels 1 - 10) is looking distorted or unrealistic. The reason is that the counts in each channel are registered with 3 ascii coded digits and that causes so called overflow problem when the counts in one channel exceeds the value of 999. For example the actual measured value of 1 023 counts/s in one channel is registered as 23 counts/s.

The H spectra is from one of the highest Cesium areas in the cloud. Finally spectra J is just before landing describing the contamination that was stuck on and in the aircraft.

3. THE CONSEQUENCES

Background spectra from different dates after Chernobyl are shown in Fig. 4. The spectra are from measurements over water (large lake or sea) on the altitude of 30 meters on dates shown in Fig. 3. The peaks from Ba-140 and Ba/La-140 disappear quite fast as they have short half time. But Cs-137 and Cs-134 can bee seen even after one year. The aircraft was thoroughly washed and cleaned between 4th and 9th July. The result was that the total counts went down only about 5 - 10 %. The second of the two most important things to notice is how difficult it is and how long it takes to get rid of the aircraft contamination. At the moment it is more than seven years from the accident and we still can see the Cs-137 peak in our background spectra.

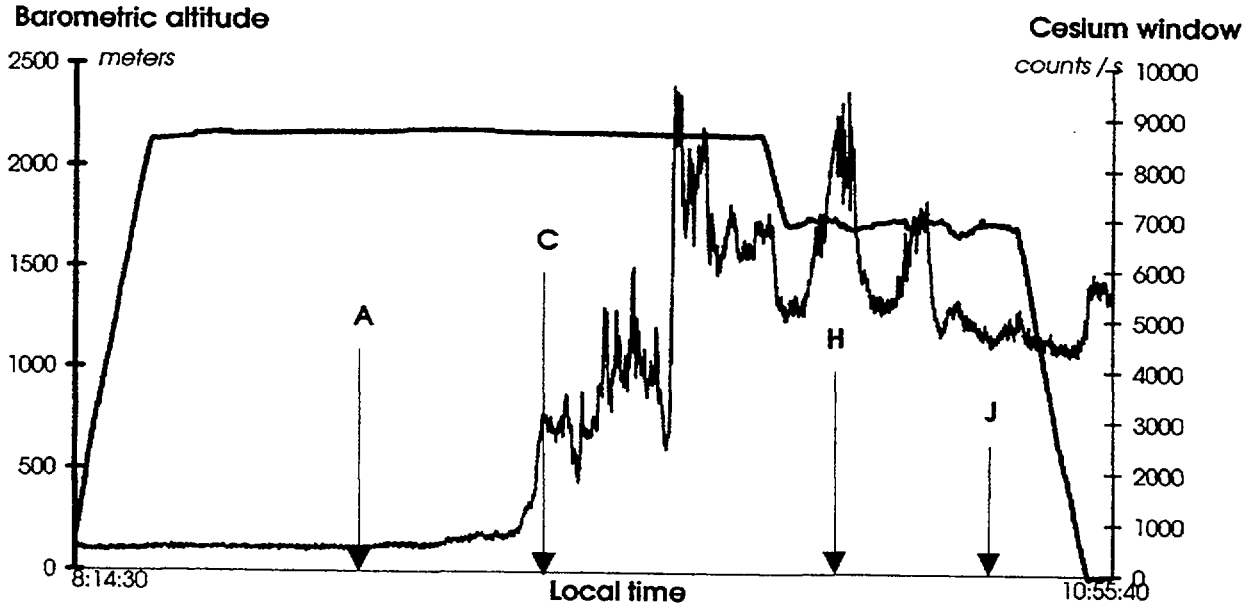

FIG. 2. The barometric altimeter and the measured Cesium window count rates from the flight thorough the radiating cloud from Chernobyl accident on April 29 1986.

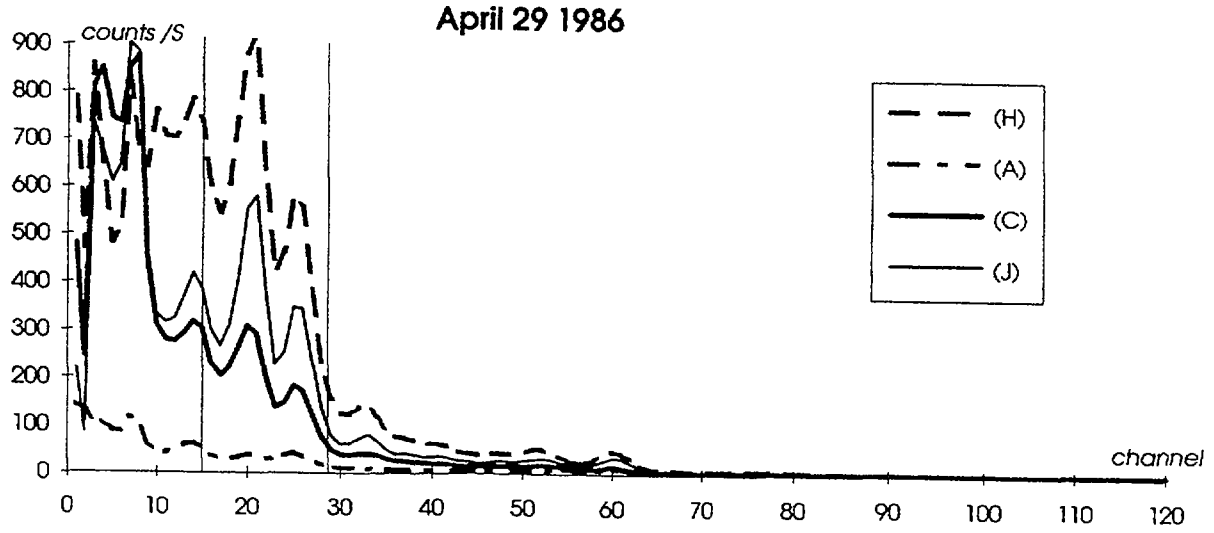

FIG. 3. Four measured spectra from the flight thorough the radiating cloud from Chernobyl accident. The locations (A, C, H and J) respect to the Cesium window count rate profile are show in Fig. 2.

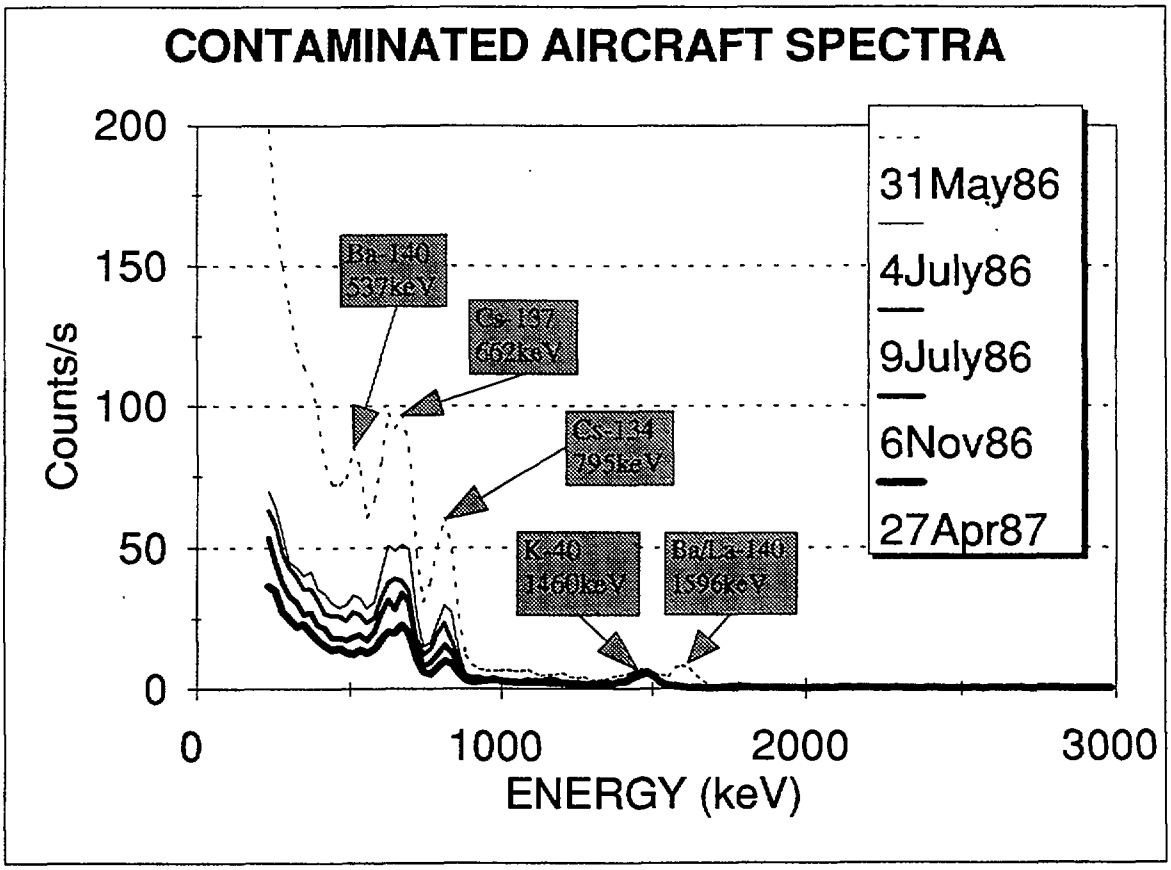

FIG. 4. Background spectra after the Chernobyl accident. Showing the aircraft contamination.

4. CONCLUSIONS

In the case of Chernobyl accident the radiating cloud was not visible and I suppose that is the normal case. If one tries to localize where are the edges of that cloud with airborne measurement system installed in helicopter or in fixed wing aircraft it is sure that the possibility to fly into the cloud is very high. The strong aircraft contamination decreases the accuracy of gamma ray measurements. As it is very difficult to get rid of or to reduce significantly the contamination it takes a long time before that aircraft can be used to map the fallout. The only reasonable way to measure the radioactivity of the air on high altitudes is to take air samples thorough a filter and analyze them rapidly at the ground.

My strong recommendation according to our experience is that if something similar to Chernobyl accident will happen again it is better to take the aircraft and the instruments into a shelter for one or two days. After the air is clean the fallout on the ground can be mapped very easily, with reasonably accuracy, with reasonably costs and fast with this kind of airborne instrumentation.

USE OF URANIUM AIRBORNE SURVEY DATA IN THE PREPARATION OF A RADIOMETRIC MAP OF SPAIN

E. SUÁREZ MAHOU, J.A. FERNÁNDEZ AMIGOT
ENUSA, Spain

Abstract

In December 1991, upon the initiative of the Nuclear Safety Council (CSN), an agreement was signed between the latter and the Empresa Nacional del Uranio, S.A. (ENUSA) for the purpose of mapping a National Radioactivity Map of Spain, i.e. a map of Spain showing gamma radiation in the soil and external cosmic radiation. The MARNA Project, which has been carried out over a period of four years, summarizes and standardizes an important radiometric data bank covering approximately 70 per cent of the country and generated by aerial gamma spectrometrics methods, by car-borne, field prospecting and through investigations, undertaken as part of the former PNEIU (National Uranium Exploration and Research Plan). It likewise generates the necessary data in the 30 % of the country lacking radiometric cover. This publication lists the most important data from the Project, the methodology used and the results obtained. Two universities, eight teachers and several scholarship holders are actively participating in the technological development of the MARNA Project, with a short term increase in university participation being anticipated in addition to that of some regional governments responsive to the Project and eager to boost its budget.

1. INTRODUCTION

The need for knowing the levels of natural radiation in order to be able to use them in future studies has been set forth by the International Atomic Energy Agency and by the EEC Commission which are promoting a research project related to the drawing-up of a Natural Radiation Atlas of Europe.

For the purpose of planning the drawing-up of this atlas, the EEC Commission made a pilot study which showed that the technical difficulties involved in carrying it out were not insurmountable.

Several atlas trials have been performed since then with data provided by a large number of scientists from EEC and neighbouring countries (e.g. EUR 14.470. 1993).

With regard to the aforementioned Atlas, the CSN deemed that Spain ought to approach the matter on the basis of the information available to it as well as of complementary field measurements in areas with little or no cover. The Spanish contribution will therefore refer to natural radiation due to the cosmic component and to that related to gamma radiation from external soil, all of which should be carried out in accordance with the relevant EEC standards in such a way that information on Spain may subsequently be integrated with that obtained by the other participating countries.

Law 15/80 of 22 April and Royal Decree 1157/82 of 30 April entrust the CSN with setting up R + D plans for matters within its sphere and, therefore, this body is interested in drawing up a Natural Radioactive Map of Spain.

Royal Decree 296/1979 of 7 December (Official State Gazette 14.01.80) entrusted ENUSA with carrying out the National Uranium Exploration and Research Plan which had hitherto been

the responsibility of the Nuclear Energy Board (JEN). Therefore, all documentation produced by the successive programmes related to this matter can currently be found in the files of ENUSA. Likewise, ENUSA has the necessary means and technology to carry out the project.

As a result of the above, in December 1991 the two bodies signed an agreement for carrying out the MARNA Project, the outline of which is set out below:

2. TARGETS OF THE PROJECT

The Project targets are to produce the following maps:

- A natural radiation map and a dosimetric map of Spain on a 1/1 000 000 scale.
- A natural radiation pilot map and a pilot dosimetric map on a 1/200 000 scale of two Spanish regions in which sufficient data are available prior to carrying out the Project.
- A natural radiation pilot map and a dosimetric map, on a 1/50 000 scale, of four particularly interesting areas of Spain.

3. DATA BANK

There are abundant data available in Spain as regards natural radiation, as a result of 30 years' work, and they cover a large part of the country. They have been obtained using different techniques and methodologies and they are expressed in different units and are not of uniform quality. They were taken from the following sources:

- Radiometric flights, without energy discrimination, carried out by the JEN.
- Radiometric flights with multichannel spectrometers contracted by the JEN.
- Car-borne radiometric prospecting campaigns.
- Field prospecting campaigns either general, regional or detailed.
- Appraisals of "hot" areas.
- Sundry reports.

4. PROJECT DEVELOPMENT

The stages and sub-stages developed during the course of the Project are, from a schematic standpoint, as follows:

4.1. PREPARATION STAGE

a) Creation of a specific file with the documentation applicable to the project existing in ENUSA.

b) Capture and drawing-up of the radiometric data necessary to complete the file in areas with deficient information.

c) Computering of the file data.

d) Setting-up of correlations between measurements obtained with different equipment, homogenizing and standardizing them in microroentgens/hour (μR/h).

4.2. DRAWING-UP AND RESULTS STAGE

e) Drawing-up of the maps referred to in paragraph 2.

5. BASIC FEATURES OF THE AIRBORNE PROSPECTING CAMPAIGNS

The various airborne prospecting campaigns may be grouped into three blocks:

- Flights undertaken by the JEN with its own means between 1967 and 1977.
- Flights contracted with the Hunting firm (1978-1979).
- Flights contracted with the Geodata firm (1980-1981).

The basic characteristics of these flights were as follows:

5.1. JEN FLIGHTS

-	Navigation.....	visual, flight line position on map 1:50,000
-	Grid.....	1 km
-	Flight line control.....	= every 14 km
-	Restitution.....	Manual, sometimes backed by serial photography
-	Radioaltimeters.....	AN/APM - 1 BONZER TRN - 10
-	Aircraft.....	CESSNA 180 PIPER CHEROKEE ARROW CESSNA 337 "SUPER SKYMASTER" OTHERS
-	Recorders (graphic).....	ESTERLINE ANGUS A - 601 - C MECHANICS FOR ELECTRONICS MFE-2

- Detectors

a) Scintillometer SPAT - 3 T (Saphimo) with

Detector.....	I Na (TI), 151.4 mm × 127 mm
Scales.....	300 - 1 000 - 3 000 - 10 000 cps
Time constants.....	1.2 sec in scale of 300 0.6 sec in scale of 1 000 0.3 sec in scale of 3 000
Sensitivity.....	± 4%
Gamma energy.....	0.5 Mev - 2.8 Mev

b) Scintillometer Mount Sopris SC - 160 - 124 A (US)

Detector.....	I Na (TI), 127 mm × 91.6 mm
Scales.....	20 - 50 - 100 - 200 - 500 - 1 000 . 50 000 cps
Probable selection error.	1 - 2 - 4 %
Most used integration constant	Scales 1,000 and 2,000 with 2% error and constants of 0.56 and 0.28 sec.

Possibility of discriminating energy with attenuation controls

c) Other apparatus

5.2. FLIGHTS CONTRACTED BY THE JEN WITH THE HUNTING COMPANY

FLIGHT INFORMATION

NAVIGATION BY MEANS OF DOPPLER RADAR

Position of flight lines: by means of continuous photographic and photo to photo recording.

Direction of flight lines	N30°N
Direction of control lines	N60°E
Height of pattern flight	120 m
Average separation between flight lines	1 km
Average separation between control lines	7 km

SPECTROMETRIC DATA

Unit of measurement : cps

Counts corresponding to the following windows, with energy expressed in MeV

Total Counts	0.40 - 2.80
Potassium	1.37 - 1.57
Uranium	1.66 - 1.86
Thorium	2.45 - 2.80

Spectrometer model Geometrics Exploranium DiGRS 3001 (gamma ray spectrometer, 4-channel differential)

Sensor: ..... 1,280 inches = 20,975 l

Spectrometer data are corrected by :

i) Height and references at a pattern height of 120 m
ii) Background variation in the aircraft system
iii) Cosmic background variation observed every day at 750 m above ground
iv) Interchannel contribution by applying suitable coefficients

Aeroradiactivity maps :

Total Counts (cps)
Uranium (ppm)
Thorium (ppm)
Potassium (%)
Ratios

5.3. FLIGHTS CONTRACTED BY THE JEN WITH GEODATA INTERNATIONAL

FLIGHT INFORMATION

NAVIGATION BY MEANS OF DOPPLER RADAR

Position of flight lines: by video-camera recording.

Direction of flight lines, bearings	030° - 210°
Direction of control lines, bearings	120° - 300°
Average separation between flight lines	1 km
Average separation between control lines	14 km

SPECTROMETRIC DATA

Counts corresponding to the following windows, with energy expressed in Mev

Thorium	2.41 - 2.81
Uranium	1.66 - 1.87
Potassium	1.36 - 1.57
Total counts	0.40 - 2.81

Spectrometer model Geodata Int. LAMA 4 (512 channels)

Sensor: 33.5 l (2,048 inches) of I Na (TI)

Spectrometer data corrected and standardized by:

1 Cosmic radiation every second
2 Dispersion due to the Compton effect
3 Background and dead time
4 Contribution of atmospheric Bi - 214
5 Pattern height of 120 m, at 760 mm and 0°C
6 eTh (ppm); eU (ppm); K (%)

Aeroradiactivity maps :

Total Counts (cps)
Uranium (ppm)
Thorium (ppm)
Potassium (%)
Ratios

Regression Analysis — Linear model: Y = a+bX

Dependent variable: ESMICR — Independent variable: SPPUND

Parameter	Estimate	Standard Error	T Value	Prob. Level
Intercept	- 17.2725	3.24978	-5.31498	.00000
Slope	0.160999	1.44189E-3	111.658	.00000

Analysis of Variance

Source	Sum of Squares	Df	Mean Square	F-Ratio	Prob. Level
Model	9259599.3	1	9259599.3	12468	.00000
Error	87638.356	118	742.698		
Total (corr.)	9347237.6	119			

Correlation coefficient = 0.995301 R-squared = 99.06 percent
Stnd. Error of Est. = 27.2525

FIG. 1. Correlations between values measured by different instruments.

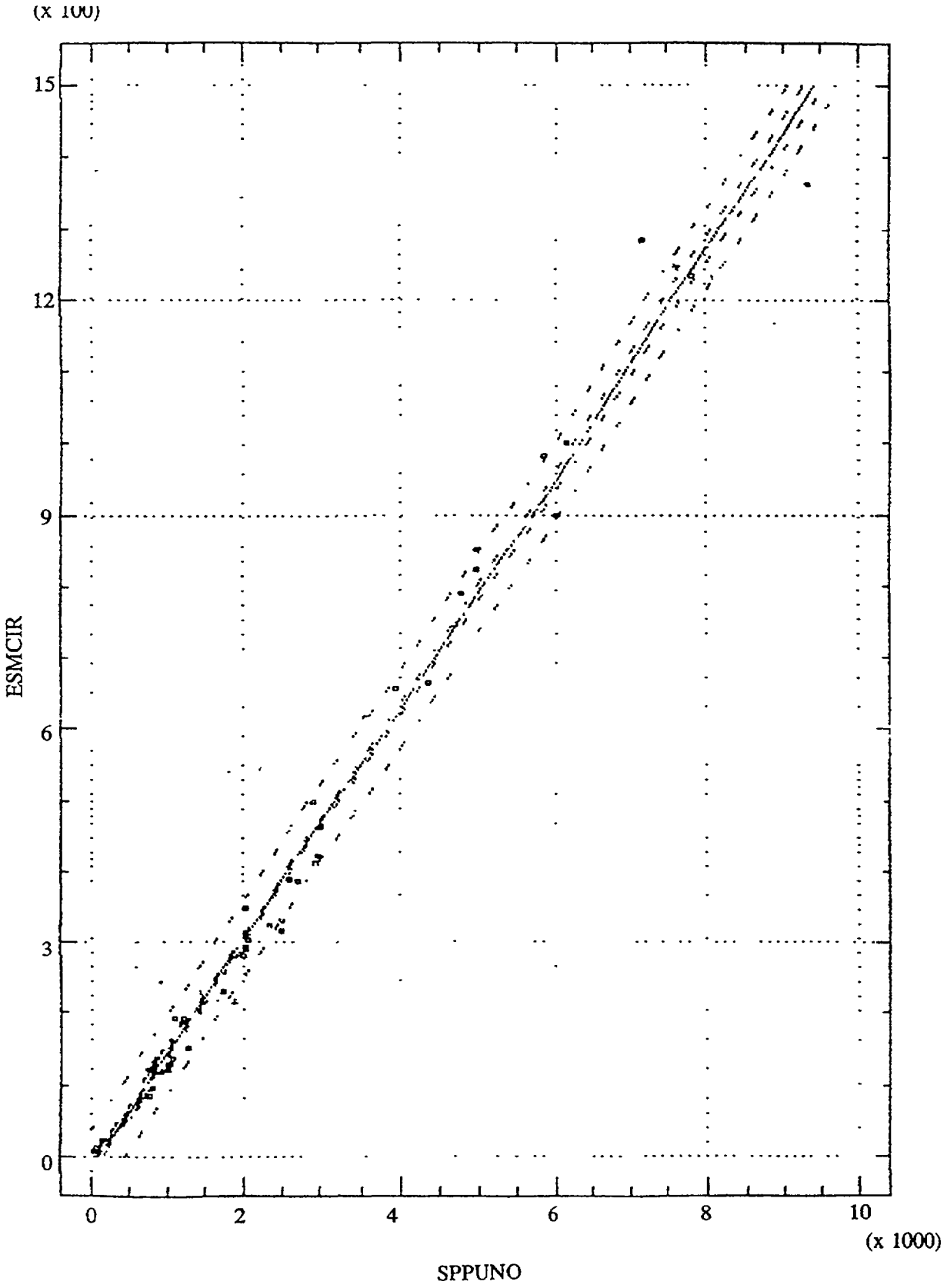

FIG. 2. Regression of ESMICT on SPPUNO.

6. SETTING UP OF METHODOLOGIES

The following have been perfected:

6.1. MEASUREMENT SYSTEM

For measurement taking, ES-3 apparatus (μR/h) manufactured and gauged by CIEMAT, Saphimo Srat SPP-2 apparatus (cps) and ES-4 apparatus (cps) likewise manufactured by CIEMAT were available.

For taking readings and establishing correlations it was expedient to use the ES-3 type apparatus, but as far as carrying out on-site gauge checking was concerned it was sufficient to repeat the readings with another, cps-measuring piece of apparatus, provided there was a good cps-μR/h correlation. The ES-3 is a very reliable device for measuring μR/h, while the SPP-2s is very stable, especially when measuring on the slow scale.

On the basis of the foregoing, the high and low correlations between the different apparatus were established, with the following correlation results being obtained, with 29 degrees liberty, in low (Figs. 1,2 and 3):

CORRELATION COEFFICIENTS

	ES-3 / SPP-2 (N° 1)	ES-3 / ES-4 (N° 1)
LINEAL	0.987	0.996
POTENTIAL	0.996	0.998
EXPONENTIAL	0.961	0.960

Similar results were obtained for high activity, with a prior matter of equivalences thus being solved.

In order to neutralize the effect on the apparatus of statistic fluctuation, experiments were performed on the same by taking blocks of measures 10 at regular time intervals and later calculating the mobile averages and the separate averages for different blocks of readings. The conclusion reached was that the average for five instantaneous readings produced individual reliability limits below 0.5 μR/h with an absolute error below 5% which, for the average of a few samples, is close to zero. Lastly, a multiple of the greatest time constant of the apparatus was taken into consideration in order to establish a simple standard for beginning the readings.

6.2. METHODOLOGY FOR ESTABLISHING EARTH (MR/H) — AIR (CPS) CORRELATIONS

This was a basic issue for the MARNA Project since the latter's viability depended on its being solved. There are several approaches to the problem and, due to the characteristics of our data bank and budget optimization, the most straightforward was chosen, namely to take the radiometries in μR/h in the soil and try to correlate them with the measurements in the air of total gammas. Since the initial experiment was going to be performed over the Extremadura region ($\approx$ 50 000 km^2), because there was an aeroradiometric cover greater than 90% and most of this surface had been flown over by Geodata, it was essential to establish the correlation between these flights (cps) and earth (μR/h). First of all a point-to-point correlation was attempted and was shown to exist. However, this procedure was considered unsuitable on account of the great effort required in order to achieve acceptable parameters. The study immediately moved on to take in radiometric

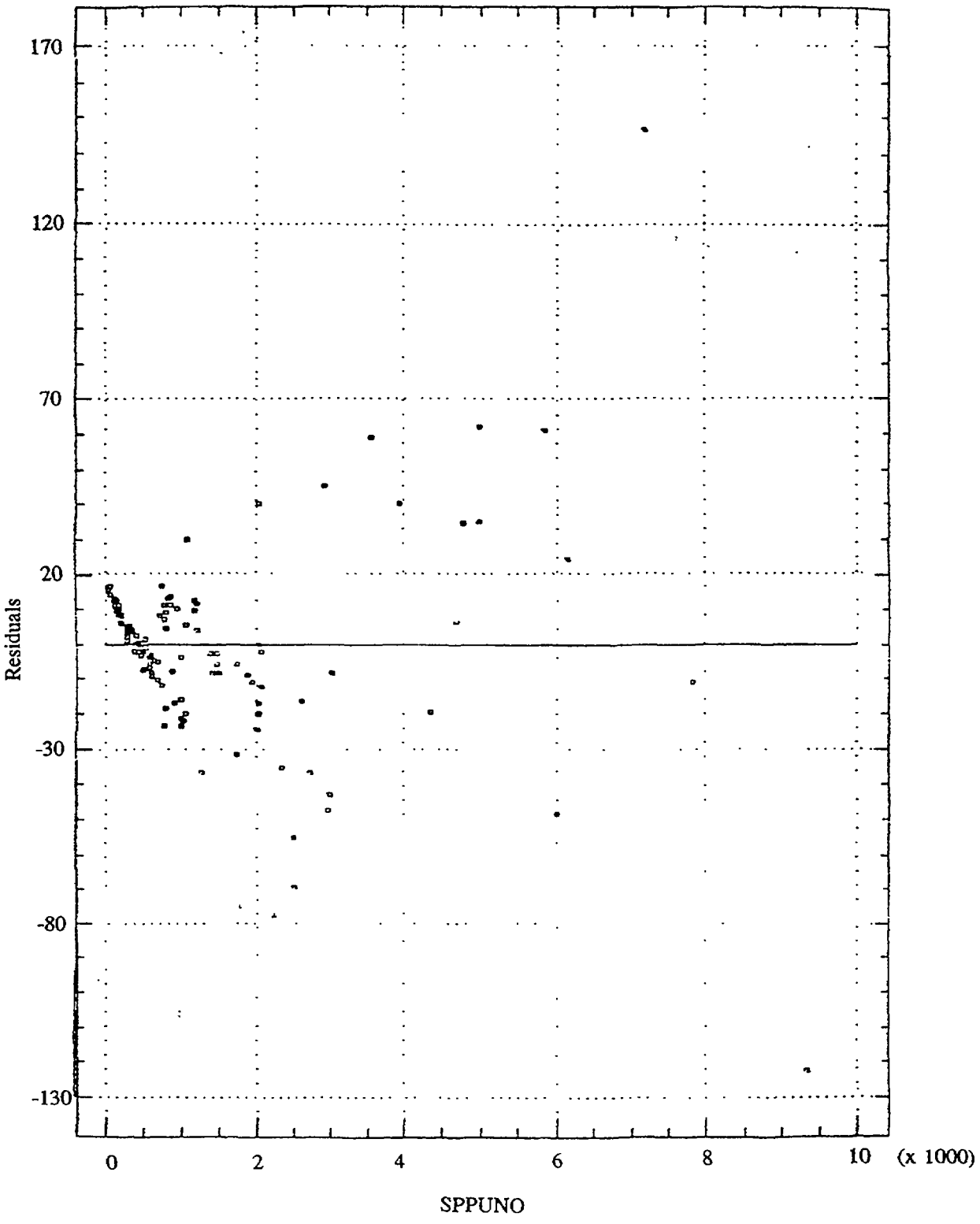

FIG. 3. Correlation between residuals and SPPUNO.

plateaux of various categories, and finally the study of plateaux was combined with that of other areas of radiometric interest provided the average values complied with certain standards as regards reliability limits.

The plateaux study was essential in order to prove that the field-air correlation was a good one, and the averages for certain areas of interest helped to perfect this correlation in intervals in which no plateaux existed. Those values which showed reliability limits $> 1\mu R/h$ for n - 1 degrees of liberty were discarded, or else the number of measurements was increased until the limit had been lowered. This criterion is closely related to the geology of the area that was studied (6.4).

More than 2 000 measurements were taken on the field, attaining correlation coefficients of 0.92 and 0.94 for lineal and potential correlations and achieving signification intervals of 1 μR/h which were so important, not only from an absolute point of view but also as regards the choice of the data support grid for the MARNA Project.

6.3. METHODOLOGY FOR ESTABLISHING AIR-AIR CORRELATIONS BETWEEN FLIGHTS OF DIFFERENT TYPES

Approximately 70 per cent of the Extremadura air cover (90%) was carried out with Geodata flights and the remaining 20 per cent with Hunting flights. It was of great interest for the MARNA Project that the radiometric equivalencies (correlations) between the Geodata (cps) and Hunting (cps) measurements be known. Sheet 1:50 000 n° 623 (Malpartida de Plasencia) was chosen as an area of interest due to there being a good overlap ($\approx$ 250 km^2) of radiometric flights by Hunting and Geodata. By means of a transparent centrimetric mesh (equivalent to 250 $\times$ 250 m), the radiometric data corresponding to the co-ordinates referring to the south-west vertex of the sheet were extracted. These data were used for the point-to-point correlation studies, with the best level of representativeness being achieved in the 0.7915 correlation, significant at a level higher than 999‰.

So as to increase the support surface for each piece of data and improve the proportion of real common surface in both flights the "5-point average" was used, whereby each point is represented by its average with those of the closest four. The representative surface rose to 0.5 km^2 and the lineal correlation coefficient rose to 0.878. Using the "9-point average" the representative surface rose to 1 sq km while the lineal correlation coefficient rose to 0.902. These studies were performed simultaneously with readings taken directly on site (μR/h).

6.4. GEOLOGY-RADIOMETRY CORRELATIONS

The correlation between geological formations and radiometry is obvious for any radioactive-mineral prospector. Acid hypogenic rocks (granites, adamellites, granodiorites, etc.), due to their higher U, Th and K content, show a greater level of radioactivity than basic rocks. Sedimentary, chemical precipitation rocks usually show a lower level of radioactivity than the rest. Recent detrital rocks, having fewer signs of organic components, are usually less radioactive than the more reduced varieties. They may also have a high radiometric relation with the base of the source rock. Highly tectonic, low-grade (green schists) metamorphic rocks show a great deal of radiometric variability. The metamorphic contact fronts may superpose their radioactive gradients to those pre-existing.

This general norm is followed in Extremadura, and the granitic batholiths of the Sierra de Gredos, Cabeza de Araya, Montánchez, La Haba and even stocks such as that of Trujillo may be observed perfectly from a radiometric point of view. The palaeozoic metamorphics may likewise be observed with their intermediate radiometries, as well as the radiometric lows of the calcareous

plains of Tierra de Barros. The radiometric low of the Tagus reservoirs may also be observed along tens of kilometres.

In the Castilla-León region the Research Group of Salamanca's University which is collaborating in the MARNA Project is carrying out car-borne prospecting tasks in order to complete the radiometric cover of this region. This work is being done simultaneously with two end-of-course tasks on the subject of geology-radiometry correlations in Castilla-León.

6.5. DEFINING THE BASE GRID. METHODOLOGY FOR EXTRACTING DATA FROM AIRBORNE PROSPECTING CAMPAIGNS

The Base Grid is defined as a quadrilateral, the sides of which are approximately proportional to those of a 1:50 000 topographical sheet, and whose surface is approximately equivalent to 1:16 of such a sheet. The purpose of this grid is to carry the average radiometric data of its surface and which oscillates, approximately, between 30 and 35 km^2. This Base Grid was defined originally due to its fulfilling two conditions:

1) There is a computerized base with the vertices of this grid in the Spanish Geographical Institute.

2) It is considered to be a good data for taking the first steps on the definitive Base Grid which will serve to draw up the plan (1/1 000 000), since there is a high density of radiometric data.

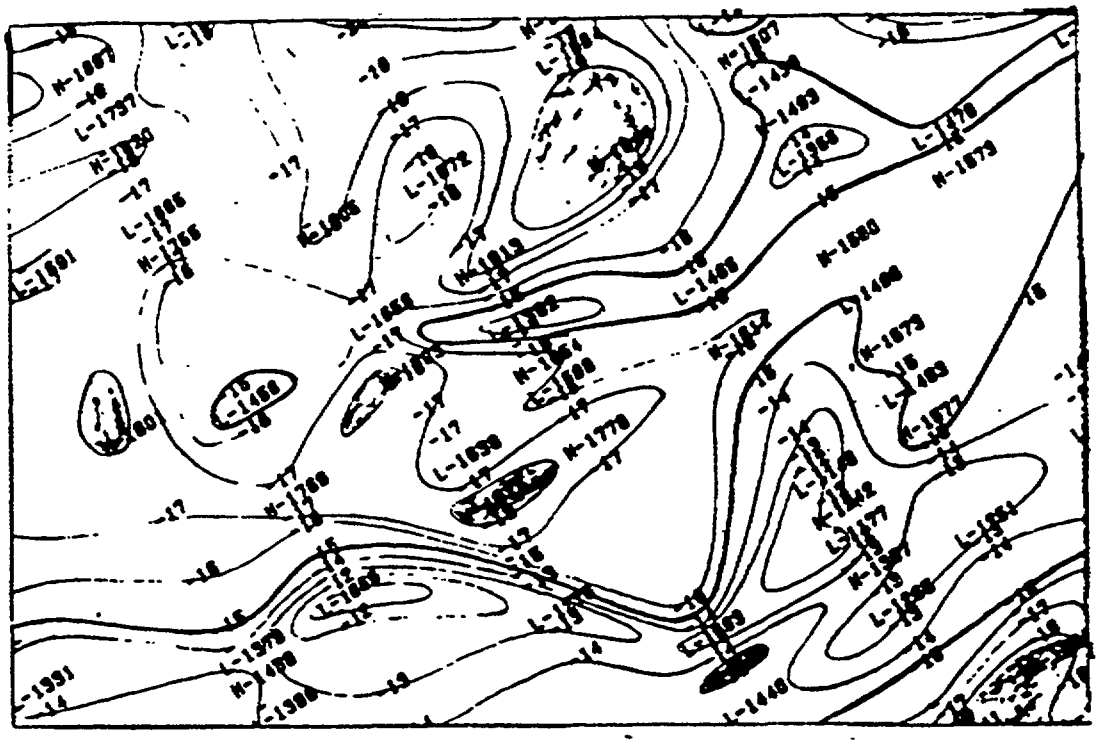

H - 628 (TORRIJOS)
CUADRICULA Nº 1 (HUNTING-79)

FIG. 4. Variabilities of radiometric data from a calculated Base Grid of a HUNTING survey.

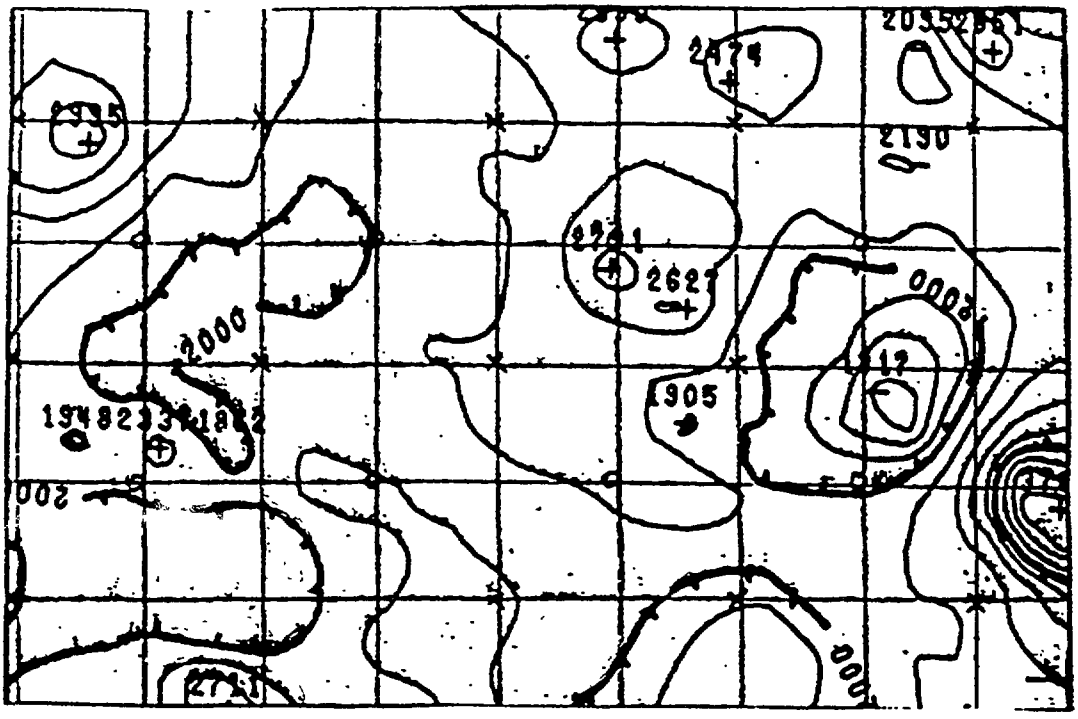

H - 628 (TORRIJOS)
CUADRICULA Nº 12 (GEODATA-80)

FIG. 5. Variabilities of radiometric data from a calculated Base Grid of a GEODATA survey.

The first steps towards applying an economical and reliable methodology for extracting data from airborne prospecting campaigns were made by using the Base Grid as a point of departure. Data extractions were carried out according to eleven extraction mesh models, starting from the four vertices of the grid or from the centres of the quadrilaterals resulting from dividing one grid into four subgrids, followed by successive centrings. All the parameters of interest (points per sq km, average, typical deviation, variance for n and n - 1 grades of liberty, variation coefficient and reliability limits) were calculated for each grid. Studies were made of eleven grids (Figs 4 and 5) showing various radiometric variabilities (5 from Hunting and 4 from Geodata). In all cases in which a 25-point mesh per grid was used the result was reliability limits, in cps, lower than an equivalent of 1 μR/h. On the basis of the foregoing, and after a severe appraisal of the method, the criterion of performing the data extraction with an equivalent, regular, two-centimetre mesh, approximately, with 32 points per grid was established. Subsequently, the data would be filtered by computer so as, if appropriate, to close the extraction grid in grids exceeding the reliability limit equivalent to 1μR/h.

6.6. METHODOLOGY FOR COMPUTERISING DATA AND DRAWING UP MAPS.

All the data corresponding to the approximately 100, 1:50,000 sheets for Extremadura have been extracted on individual DBase III files compatible with Symphony, Golden and StatGraph, with each flight sheet being reproduced on the basis of the data extracted (Fig. 6). By means of a small program all the data have been reduced to a single database, with the co-ordinates being unified and the Hunting and Geodata values (cps) being rendered in μR/h. This has resulted in a base for Extremadura with a total of around 50 00 items of data.

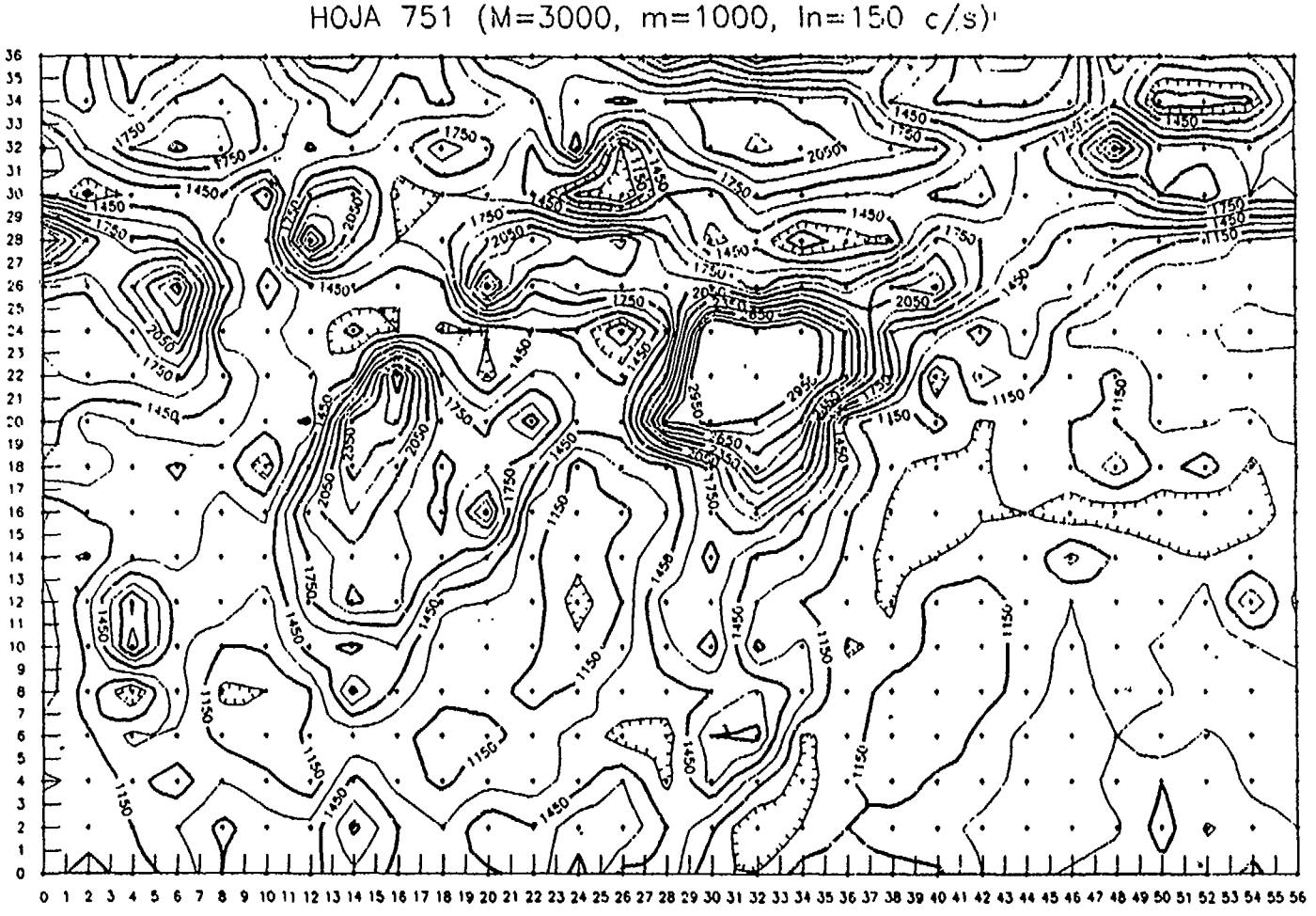

FIG. 6. Example of map produced from the reprocessed and levelled data.

The maps are being drawn up with the collaboration of Computer Science teachers from the Polytechnic University School of Cáceres (E.U.P.C.) and, in addition, teachers of Physics from the Cáceres Faculty of Veterinary Science and their associates from the E.U.P.C. are helping to perfect equivalences.

Value ranks and isocurves of 1 μR/h in 1 μR/h have been drawn up for the interval ≥ 4 - ≥ 20 μR/h, with a first solution being observed for the maps with a scale of $1:10^6$ using all the data.

On a scale of 1:50 000 the use of around 500 data per sheet is extremely attractive, especially if a detailed analysis of the geology-radiometry correspondence is to be made.

On a scale of 1:200 000 the information is excessive, and so tests were made with base grids equivalent to 1/64, 1/16 and 1/4 of the 1:50 000 sheet.

In principle, one solution to the $1:10^6$ problem is that described above. However, in the event of using isocurves, recourse must be had to a base grid which, furthermore, is more representative in dose terms.

BIBLIOGRAPHY

Atlas of Natural Radiation Levels in the European Communities. Phase II. Final Report - Nov. 1988, CEC Contract Nr 85.420 (1988).

BETTENCOURT, A. O. de, GALVAO, J. P., LOWDER W., OLAST, M., SINNAEVE, J., Eds; Natural Radiactivity, Proceedings of the Fourth International Symposium on the Natural Radiation Environment held at Lisbon, Portugal, December 7-11, 1987, Conf 871208; EUR 11895 Radiation Protection Dosimetry 24, (1 - 4) Publ. by Nuclear Technology Publishing (1988).

Book of Abstracts, Int. Conf on High Levels of Natural Radiation, 3-7 Nov, Ramsar, Islamic Republic of Iran. AEOI, IAEA, WHO, UNEP, INTS (1990).

BRADLEY, E.J., GREEN B.M.R., Outdoor gamma-ray dose rates in Great Britain - Preliminary Results, Radiol. Prot. Bull. 59 (1987) p 16.

BROWN, et. al. Radón en España, Forum Atómico Español, Madrid (1992).

CAULCUT, R., Statistics in Research and Development (2nd ed.), Champman and Hall, London (1991).

CEC, Radiation protection, exposure to natural radiation in dwellings of the European Communities, CEC, Luxembourg (1987).

CERRAJERO, J. C., Investigación de minerales radiactivos en España mediante prospección aérea, Tesis doctoral, ETSIM, Madrid (1973).

CSN, La vigilancia de la radiación, Consejo de Seguridad Nuclear, Madrid (1992).

DAVIES, O. L., Metodos estadísticos para investigación y producción, Aguilar, Madrid (1960).

FERNÁNDEZ AMIGOT, J. A., Valoración estadística del yacimiento uranífero Mina FE. JEN., Ciudad Rodrigo (1968).

FERNÁNDEZ AMIGOT, J. A., Valoración estadística de trece yacimientos uraníferos en la provincia de Salamanca, JEN., Ciudad Rodrigo. (1969).

FERNÁNDEZ AMIGOT, J. A., Desmuestres y sus tipos. Studia Geológica, U, Salamanca (1975).

GARZÓN RUIPÉREZ, L., Radiactividad y medio ambiente, Serv. Publ. Universidad Oviedo, Oviedo (1979).

GEODATA, Prospección Aérea. Proyecto AR - 1 / 80, Características de los equipos empleados en la campaña, Geodata, Madrid (1981).

GEODATA, Prospección Aérea. Proyecto AR - 1 / 81. Características de los equipos empleados en la campaña Geodata, Madrid (1982)

GMURNAN, V. E., Teoría de las probabilidades y estadística matemática, MIR. Moscú (1983).

GREEN, B.M., HUGHES J. S., Lomas, P. R., Natural sources of ionising radiation in Europe, Radiation Atlas, Commission of the European Communities, Luxembourg (1991).

GREEN, B.M.R., Atlas of natural radiation levels in the European Community Pilot Study, Report to the CEC, Oct. 1986.

GREEN, B.M.R., LOMAS P. R., BRADLEY, E. J., WRIXON, A.D., Gamma - radiation level outdoors in Great Britain, NRPB Chilton, R - 191 (1988).

HUNTING, Prospección Aérea. Proyecto AR - 1 / 78. Características de los equipos empleados en la campaña, Hunting, Madrid (1979).

I.T.G.E., Proyecto de reprocesado e interpretación de varias campañas de geofísica en el Macizo Hespérico. I.T.G.E. Madrid (Oct. 1992).

KNOLL, G.F., Radiation detection and measurement, John Willy & Sons, New York (1979).

LOWDER, W., External terrestrial and cosmic radiation. Proceeding of the Fifth International Symposium on the Natural Radiation Enrivonment, Salzburg (1991).

MORO B., Mª. C., CEMBRANOS, Mª. L., PÉREZ del V., L. Aplicación de la prospección aereo-radiométrica y litogeoquímica del uranio a la localización de indicios de fosfatos silúricos en la Provincia de Zamora. Reunión de la Sociedad Geológica de España, Madrid (1993).

MORO B., Mª. C., PÉREZ del V., L. Estudio de la distribución de K, U y Th en el batolito de Cabeza de Araya mediante prospección aéreo-radiométrica. Implicaciones petrogenéticas y metalogenéticas. Libro Jubilar de Figuerola L. D. Omega, Madrid (1988).

MERINO, J. L., JOSA, J. M., Study of Spanish uraniferous sandstones. En: Jones, M. J. (ed), Geology, Mining and Extractive Processing of Uranium, I.M.M. London (1977) 63 - 70.

QUINDOS, L. S., FERNÁNDEZ, P. L., SOTO, J., Exposure to natural sources of radiation in Spain. En Int. Conf on Implications of the New ICRP Recomendations on Radiation Protection, Practices and Interventions, Salamanca 26 -29 Nov. 1991, CIEMAT, Madrid, Vol 2 (1992) 273 - 282.

QUINDOS, L., S., FERNÁNDEZ, P. L., SOTO, J., NEWTON, G., PEÑA, J., ARTECHE, J., VILLAR, E., Radón principal fuente de radiación natural. Rev. Española de Física 3 (2) 22 - 27 (1989).

SÁNCHEZ LEÓN, J. G., Radiactividad y medio ambiente, Estratos (26) Invierno 93, 12 - 18.

SCHEAFFER, R. L., MENDENHALL, W., OTT, L., Elementos de muestreo, G. E. Iberoamericana, México (1986).

Seminar on the Radiological Burden of Man from Natural Radiactivity in the Countries of the European Communities, CEC, V/2.408/80 (1980).

SIERRA, M. A. Ejercicios resueltos de estadística, CENRA, Madrid (1987).

SOCIEDAD NUCLEAR ESPAÑOLA. Jornada sobre el control del fondo radiactivo ambiental. Barcelona, 15 Diciembre 1992 (1992).

STEINHAUSLER, F., The natural radiation environment: future perspective. Proceedings of the Fifth International Symposium on the Natural Radiation Environment, Salzburg (1991).

SUÁREZ MAHOU, E., CERRAJERO H., J., CREGO, A. Relación Interna JEN. Prospección aérea sistemática de Cuenca y Guadalajara, Madrid (1964).

SUAREZ MAHOU, E., CERRAJERO H., J., CREGO, A. Relación Interna JEN. Prospección detallada de la zona de Huete-Saelices-Montalvo, Madrid (1964).

SUAREZ MAHOU, E., CERRAJERO H., J., CREGO, A. Relación Interna JEN. Prospección aérea sistemática del valle del Guadiana, Madrid (1064).

SUAREZ MAHOU, E., CERRAJERO H., J., CREGO, A. Relación Interna JEN. Prospección aérea sistemática de la zona de la Sierra de la Demanda, Madrid (1965).

SUAREZ MAHOU, E., CERRAJERO H., J., CREGO, A. Relación Interna JEN. Prospección aérea sistemática del Valle del Tajo, Madrid (1965).

SUAREZ MAHOU, E., CERRAJERO H., J., CREGO, A. Relación Interna JEN. Prospección aérea sistemática del valle del Duero, Madrid (1965).

SUAREZ MAHOU, E., CERRAJERO H., J., CREGO, A. Relación Interna JEN. Prospección aérea sistemática de la zona de Córdoba, Madrid (1966).

SUAREZ MAHOU, E., CERRAJERO H., J., CREGO, A. Relación Interna JEN. prospección aérea sistemática de la zona de Almería, Madrid (1966).

SUAREZ MAHOU, E.: CERRAJERO H., J., CREGO, A. Relación Interna JEN. Prospección aérea sistemática de la zona de Sevilla, Madrid (1966).

SUAREZ MAHOU, E.: CERRAJERO H., J., CREGO, A. Relación Interna JEN. Prospección aérea sistemática de la zona de Badajoz, Madrid (1967).

SUAREZ MAHOU, E.: CERRAJERO H., J., CREGO, A. Relación Interna JEN. Prospección aérea sistemática de la zona de Ciudad Real, Madrid (1967).

SUAREZ MAHOU, E., CERRAJERO H., J., CREGO, A. Relación Interna JEN. Prospección aérea sistemática de la zona de Valencia, Madrid (1967).

SUAREZ MAHOU, E., CERRAJERO H., J., CREGO, A. Relación Interna JEN. Prospección aérea sistemática de la zona de Atienza, Madrid (1068).

SUAREZ MAHOU, E., CERRAJERO H., J., CREGO, A. Relación Interna JEN. Prospección aérea sistemática de la zona de Belchite-Caspe, Madrid (1968).

SUAREZ MAHOU, E., CERRAJERO H., J., CREGO, A. Relación Interna JEN. Prospección aérea sistemática de la zona de León, Madrid (1968).

SUAREZ MAHOU, E., CERRAJERO H., J., CREGO, A. Relación Interna JEN. Prospección aérea sistemática de la zona de Burgos, Madrid (1969).

SUAREZ MAHOU, E., CERRAJERO H., J., CREGO, A. Relación Interna JEN. Prospección aérea sistemática de la zona de Orense, Madrid (1969).

SUAREZ MAHOU, E., CERRAJERO H., J., CREGO, A. Relación Interna JEN. Prospección aérea sistemática de la zona de Zamora, Madrid (1970).

SUAREZ MAHOU, E., CERRAJERO H., J., CREGO, A. Relación Interna JEN. Prospección aérea sistemática de la zona de Cuenca, Madrid (1970).

SUAREZ MAHOU, E., CERRAJERO H., J., CREGO, A. Relación Interna JEN. Prospección aérea sistemática de la zona de Calatayud, Madrid (1971).

SUAREZ MAHOU, E., CERRAJERO H., J., CREGO, A. Relación Interna JEN. Prospección aérea sistemática de la zona de Montalbán, Madrid (1971).

SUAREZ MAHOU, E., CERRAJERO H., J., CREGO, A. Relación Interna JEN. Prospección aérea sistemática de la zona de Albacete. Madrid (1971).

Mapa de radiometría aérea de España (parcial), Escala 1/1000.000 (1972).

Mapa de radiometría aérea de España (parcial), Escala 1/200.000 (1972).

Mapa de radiometría aérea de España (parcial), Escala 1/50.000 (1972).

UNSCEAR, Sources, effects and risks of ionizing radiation. United Nations Scientific Committee on the Effects of Atomics Radiation. 1988. Report to the General Assembly with annexes. United Nations, New York (1998).

THE NATURAL RADIOACTIVITY MAP OF PORTUGAL

L.M. TORRES
Instituto Geologico e Mineiro, Lisboa, Portugal

R. L. GRASTY
Geological Survey of Canada, Ottawa, Canada

Abstract

Hundreds of thousands of total count scintillometric car-borne and foot-borne data, collected in Portugal in the 1960s and 1970s as part of uranium exploration and assessment efforts are being compiled to produce exposure rate maps, under a Government programme. Recently flown 256 channel spectrometric data, combined with the available total count data, now cover the majority of mainland Portugal, enabling the production of good 1:200 000 scale natural radioactivity exposure rate maps. Data collection, from paper maps and analog records to numerical maps, as well as the quality of the different data sets and density of coverage are presented and discussed.

1. GAMMA RAY DATA FROM MINING EXPLORATION

Exploration work for uranium started in Portugal before 1957. At that time airborne gamma ray surveys were not reliable, and most of the country was covered by car-borne total count surveys. The data collected was used to select areas for further detailed work. The uranium mines of Urgeirica and the Nisa prospect, were discovered on the basis of those systematic surveys. Most of the work was conducted in the crystalline areas as the metallogenic concepts prevailing at that time suggested those areas held higher potential to bear uranium deposits.

Further exploration work was pursued at a slower pace in the 1970s, with emphasis on the Meso Cenozoic sedimentary basins of western Portugal. The areas were surveyed, using hand held SPP2 scintillometers. Altogether the data collected represent some 55 000 line kilometres of car-borne data and several tens of thousands of hand held scintillometer readings.

By the end of the 1980s a considerable amount of data existed in archive. At that time an attempt was made to cover part of the centre of Portugal (some 8000 km^2) with an airborne spectrometric survey in a multidisciplinary project aimed at mining exploration (Sn, W, Au, Ag, Phosphates) and environmental monitoring. An actual test survey in the Gois-Segura area, comprising 5 000 line kms was made in 1989-90, contracted by the IGM, and jointly supported by Gabinete de Proteccao e Seguranca Nuclear (GPSN) and the IGM.

Unfortunately a dramatic fall in the price of metals, especially of tungsten, tin and uranium, created an unfavourable situation to proceed with the airborne surveys.

In 1989 one of the authors (L.Torres) under a suggestion of the IAEA, initiated the compilation of data to produce exposure rate maps.

In 1991, a mining company holding permits in the South of Portugal, contracted a survey of a total of about 22 000 line kilometres of gamma ray spectrometry, including the Portuguese part of the Pyrite Belt. The existence of this project, and the fact that the costs of adding a gamma ray spectrometer to the planned fixed wing aeromagnetic survey were not significative, helped persuade the management of the company to take such a decision. This dataset is of very high quality and interestingly complements and enhances the global gamma ray coverage (Figs 1a and 1b).

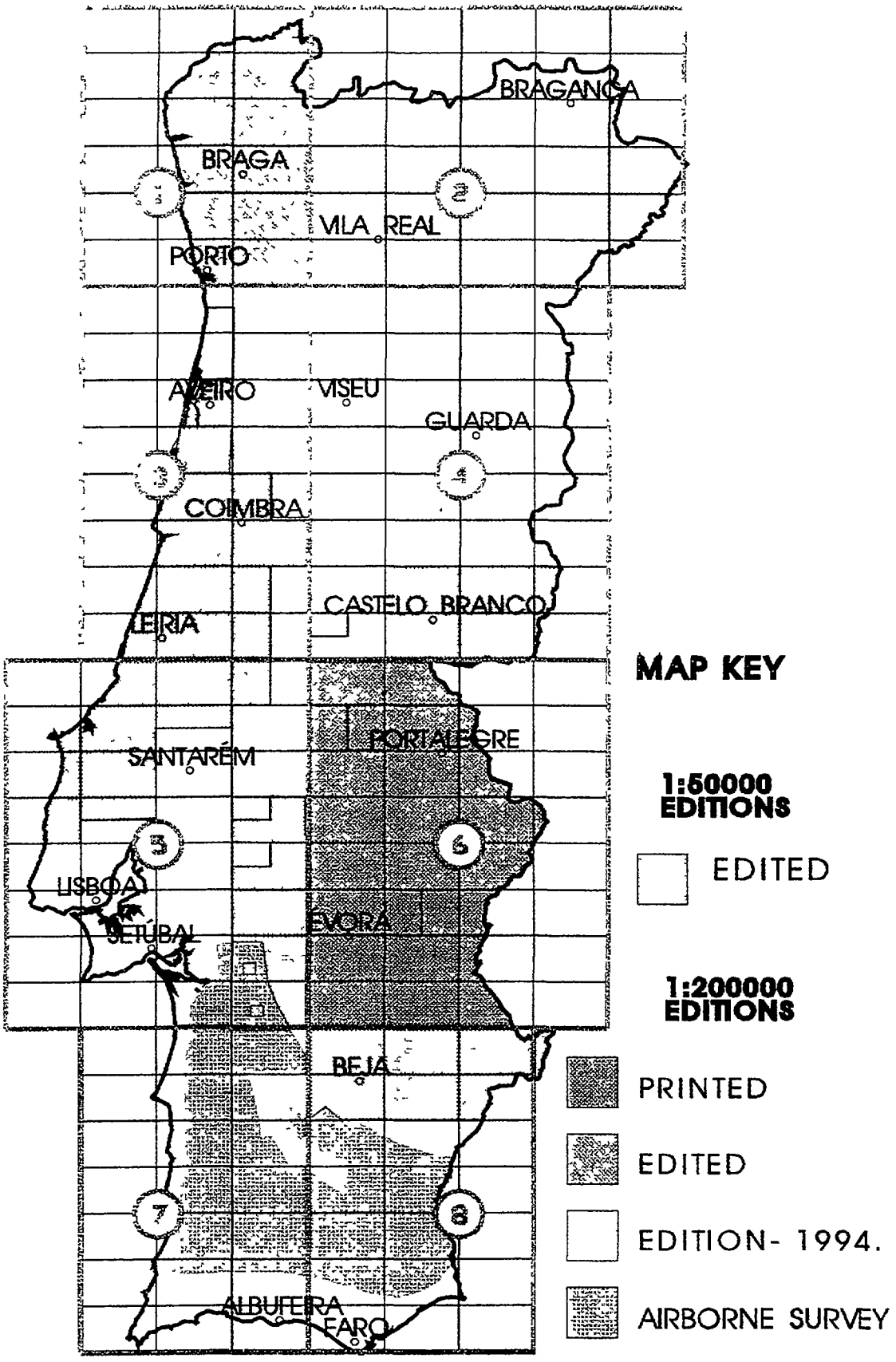

FIG. 1a. Map of mainland Portugal showing radiometric data coverage and mapping progress. Maps were based on car-borne (see Fig. 1b) and foot-borne surveys. The blank areas in this figure without any tracks (compare with Fig. 1b), lack gamma ray data.

All airborne work, was made with fixed wing aircraft, 256 channel spectrometers, 32 l volume crystals without upward looking detectors, 120 m terrain clearance and 500 m line spacing and is available in digital form at the IGM. Unfortunately none of the surveys was presented in concentrations of equivalent radioisotopes as recommend by the IAEA.

The foot-borne data exists as 1:25 000 topographic maps with the location of the readings, which are presented in counts per second. The car-borne data is archived in folded 1:25 000 with truck itineraries and fiducial marks along the tracks. A complementary set of analog charts pertaining to the itineraries, and tied to the location maps by the fiducial marks is also available. Those records are in arbitrary units (millimetres), and from the instructions of the car-borne system, supplied by the manufacturer, the function to convert scale units of the analog charts to counts per second was obtained.

2. PRODUCTION OF THE EXPOSURE RATE MAPS

2.1. FIRST PHASE OF THE PROJECT

Before the start of the project a feasibility study was carried out. The first point to test was how reliable the old car-borne records were. The good quality was confirmed by reproducing the analog charts, driving a GAD-6 Scintrex spectrometer at about 20 km/h along the same tracks used by the old car-borne system of the 1960s. Dirty roads, practically in the same virgin state as at the time of the former surveys, were used for the tests. A second point concerned the development of economically efficient procedures to digitize the data and an assessment of the work involved in the production of suitable cartographic products and reliable digital data. As a result a decision was taken to digitize only the fiducials and not the complete records, to reduce the costs.

So, by 1989 the project actually started, under a protocol of GPSN and Servico de Fomento Mineiro (now part of IGM). As both institutions wanted quick results the first maps were produced at 1:50 000 scale. However it was soon, realized that the data coverage was too coarse for a comprehensive national coverage at that scale. It was decided that as soon as back calibrations of the different sensors were available and reliable exposure rate maps could be produced, mapping scale should be changed to 1:200 000. The experience obtained so far was invaluable in the production of 1:200 000 maps.

2.1. BRIEF DESCRIPTION OF THE MAP MAKING PROCEDURES

First, analog records are sorted by 1:25 000 base maps, enabling easy control of the digitizing and keying in of data.

Simplified base maps (at 1:50 000 or 1:200 000) are accurately digitized and organized in layered Autocad drawing files, with roads, railways, hydrography and toponymy. Simultaneously, a database of anomalies from paper records collected in uranium exploration work, was created and is also included as a layer of the respective map sheets. Separate data, grid and drawing files with coloured isolines, are generated for the radiometric data by 1:50 000 map sheet. Data is posted and verified at this scale, enabling checking and easy correlation with published geological maps. A number of routines were coded to automate some of the tasks, to keep track of data files, organizing a database with records sorted by sensor type, year of collection, map sheets, coordinates and values, allowing easy update, import and export and calibration of data in exposure rate units.

Simple routines were coded to produce fast and inexpensive printer plots of uncovered areas, enabling quick planning for fill in field work. Suspect values, which do not match known geology, or present abnormally low or high values are checked, as part of the fill in work.

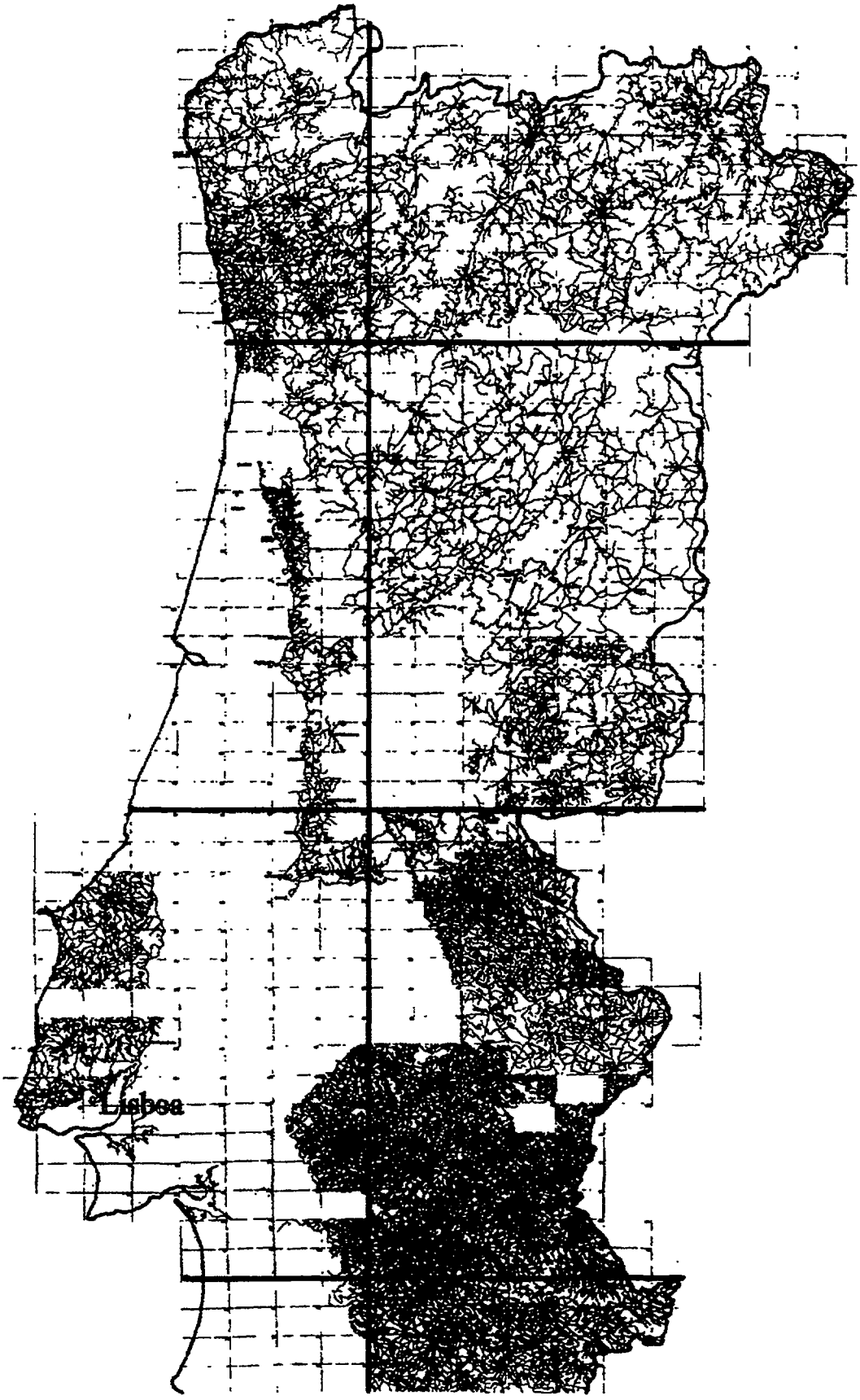

FIG. 1 b. Partial map of mainland Portugal showing the tracks of the car-borne scintillometric system used in the uranium exploration surveys. Please compare with Fig. 1a.

The foot-borne data was organized by 1:25 000 map sheets. Some of the data for the sedimentary areas existed in digital form, and was validated. Owing to the multiple surveys of disparate quality, oversampling in some areas (readings every 2 m, for instance) and lack of data in adjacent areas, some simple criteria was adopted, to get a more evenly distribution of data to ensure 1-2 samples per km^2. Some fill in work was done, to get a better representation of the background while depicting the anomalous zones known from previous surveys.

Compilation is done in-house, while digitizing and cartography is contracted, relieving IGM from the most time consuming phases. Calibrations were made under the methodology devised by one of us (Grasty [1]). Data organization and reprocessing allows full control at all stages of the process.

A National database of all the anomaly locations, calibrated in mR/h and with a short description of the geology was also built from the exploration archives and included as a layer in the numerical maps both at 1:50 000 and 1:200 000 scales. Mineral occurrences were also organized in a database and fed as a layer to the correspondent base maps.

Final raster copies and colour separations were produced for map sheet nQ6 (Fig. 2), at the Geological Survey of Canada, while one of the authors (L.Torres) was at the GSC under an IAEA fellowship.

3. CALIBRATION PROCEDURES

Using a calibrated a GR-256 Exploranium spectrometer a dozen sites previously surveyed by the car-borne and foot-borne scintillometers, covering a large range of values and encompassing diverse geological units, were reoccupied. Exposure rates were calculated from the concentrations of equivalent Uranium, Thorium and Potassium supplied by the GR-256. Exposure rates calculated from those concentrations were linearly correlated with the values in counts per second of the scintilometers. The reader is referred to [1], for further details. The linear relationships established for the different sensors are used to calculate the exposure rates from the original data. The authors also calibrated the Gois-Segura airborne survey detector, and more recently the Pyrite Belt airborne survey detector was also back calibrated.

4. GENERAL COMMENTS ABOUT SHEET NQ6

Taking in consideration the limitations of the original data the final map is surprisingly good. A simple comparison of the exposure rate map with the most recent edition of the geological map of Portugal at 1:500 000 (in press), easily allows correlation between several geological and radiometric units.

Careful examination of the map shows an East-West artificial lineament, at the border between foot-borne and car-borne survey areas, which are clearly outlined in the legend of the map. This is indicative that users should be warned of some limitations of the original data and the recovering process used. Actually it must be pointed out that at least two different car-borne systems and several dozens of hand held SPP2 scintilometers were used in those surveys, which span more than 35 years.

One source of error in the car-borne data is the non-linearity of the analog unit response in the low and high end ranges of the scale owing to electronic and mechanical problems. Larger relative errors are expected in such areas.

Perhaps the principal source of error results from the interpolation itself, owing to poor sampling. Average density of readings used in the map is about 1.5 point per km^2. The interpolation

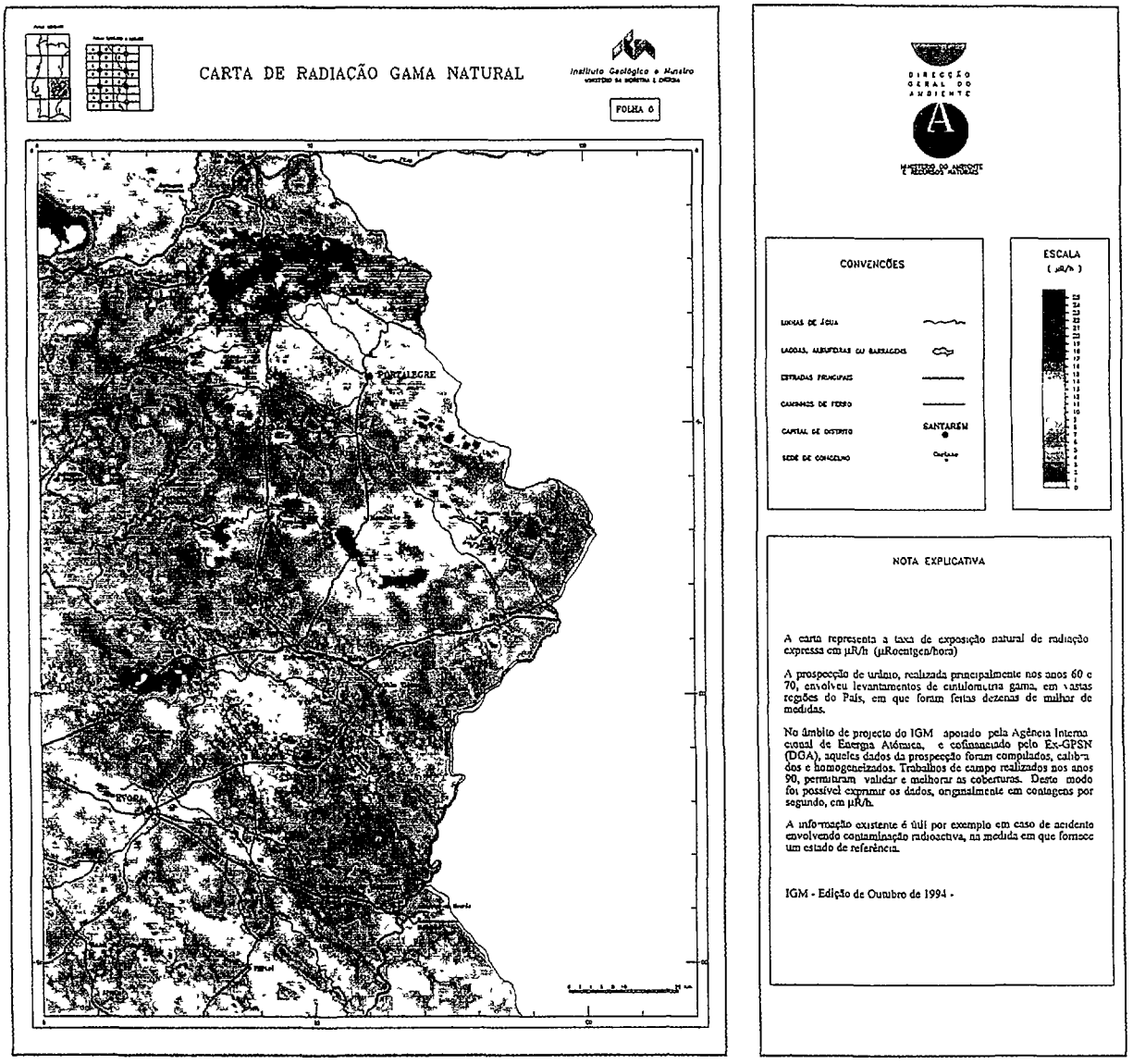

FIG. 2. Map sheet n. 6 of the Natural Radioactivity Map of Portugal at 1:200 000, reduced to fit page (scale approx. 1:1000 000). Map was based on car-borne and foot-borne data. Please compare with Fig. 1b.

algorithm used is based on bicubic splines, but kridging methods gave very similar results, except for greater smoothing of contours. As expected the degree of confidence decreases as we move away from the measured points. Some areas might be represented differently with more measurements.

5. CONCLUSIONS. FUTURE DEVELOPMENTS

The project is scheduled to be finished in 1996. In the meantime we proved that reliable exposure rate maps can be obtained by the procedures just described. As an immediate result a significative part of the country was mapped at a fraction of the cost of a new airborne survey. The reprocessing of the southern airborne survey will further increase the coverage and overall quality and usefulness of the final maps. Independent efforts proceed in Spain [2] to compile gamma ray data,

and it will soon be possible to produce homogeneous exposure rate maps of the Iberian Peninsula, an important base line information for environmental studies.

Byproducts of the mapping project, like numerical base maps, databases, etc, will be useful by themselves in other projects.

Another interesting development of the project is that a new truck mounted Environmental Monitoring System, comprising an 256 channel spectrometer, a 4 l volume crystal and a GPS navigation system will start to operate in the beginning of 1994. The system will be used to fill in areas without any radiometric data, and enable the monitoring of man-made radiation in environmental studies.

ACKNOWLEDGEMENTS

This project is the result of teamwork, but we must stress some important contributions.

The key role of Jaime Leote, formerly with Junta de Energia Nuclear, with his remarkable knowledge of the radiometrics of Portugal and his commitment in the field work and compilation of old data.

The technical and financial support of the IAEA under biennial assistance programmes, of which the enthusiastic support of M. Tauchid is not a minor point.

Last but not least, the professionalism of the cartographic unit of the Geological Survey of Canada under Gary Labelle, which produced the final version of map sheet nQ6 and the colour separations.

REFERENCES

[1] GRASTY, R.L., TAUCHID, M., Standardization of old gamma ray survey data. (IAEA, Tech. Committee Meeting 9-12 November 1993.)

[2] MAHOU, E.M., AMIGOT, F., Use of uranium airborne survey data in the preparation of radiometric map of Spain.

URANIUM RESOURCE ASSESSMENT AND EXPLORATION DATA FOR GEOLOGIC RADON POTENTIAL ASSESSMENTS IN THE UNITED STATES

J. K. OTTON, L.C.S. GUNDERSEN, R. R. SCHUMANN, G. M. REIMER
U.S. Geological Survey, Denver, Colorado, United States of America

J. S. DUVAL
U.S. Geological Survey, Reston, Virginia, United States of America

Uranium resource assessment and exploration programmes funded by the United States Government since the late 1940s have yielded a substantial body of earth science data, much of which is now maintained by the U.S. Geological Survey (USGS). These data have been used since 1987 to assess the geologic radon potential of various counties, States, and regions throughout the entire United States Included in the database are three distinct types of data that have been used in radon assessments: (1) aeroradiometric data, covering the continental United States and parts of Alaska, that include potassium (derived from K-40 spectra), uranium (derived from Bi-214 spectra), and thorium (derived from Tl-208 spectra) coverage flown at a nominal 166-m altitude at flightline spacings of 1.6, 5, or 10 km; (2) uranium occurrence and deposit data that contain detailed geologic and geochemical descriptions and production information; and (3) rock geochemical data, including uranium and thorium analyses of rocks and related soils from many regional geochemical studies. The spectral aeroradiometric survey of the entire United States was produced during the National Uranium Resource Evaluation (NURE) program funded by the U.S. Department of Energy. Some of these data were compiled and combined with estimates of soil permeability from county soil surveys to develop a preliminary evaluation of radon potential in the Pacific Northwest (Duval and Otton, 1990; Otton and Duval, 1990). In a later, modified version of this methodology, the NURE aeroradiometric data were used with indoor radon data, geology, soil permeability estimates, and house-construction data to provide semiquantitative estimates of radon potential of geologic provinces in individual States as part of a national assessment (Schumann, 1993). In more recent studies, detailed evaluation of the NURE aeroradiometric data for Florida provided quantitative estimates of the radium concentrations of near-surface soil layers that were used in a mathematical model to assess geologic radon potential in Florida (Nielson and others, 1993a,b: Holt and others, 1993a,b,c; Otton and others, this volume). The NURE data and the total-count data from a USGS survey of northern Florida (Grosz and others, 1989) also were used with drillhole descriptions to estimate the radium content of underlying geologic units for the mathematical model. The uranium deposit and occurrence data identify small, specific localities where anomalous concentrations of uranium are present in soils and rocks and where high indoor radon levels may therefore occur (Otton, 1993, Henry and others, 1991). Areas such as Grand Junction, Colo. where mine and mill wastes are present, define areas of elevated radon concentrations in soils (Landa, 1991). The rock geochemical data identify specific geologic map units, like the extensive marine black shales in the Central United States (Coveney and others 1987; Harrell and others, 1991) and the granites in the Northeast (Boudette and Olszewski, 1986) and the Rocky Mountains (Castor and others, 1977), that, on the basis of their radioelement content, are likely to yield high average indoor radon. Each of these data sets has some limitations. None of them directly account for the other factors that control radon availability, such as soil permeability, soil moisture, and radon emanation coefficient. Aeroradiometric surveys are limited by a relatively shallow depth of view (about 90 percent of the gamma signature is from the upper 40 cm). The national coverage is fairly widely spaced and provides detailed coverage only in limited areas. Uranium deposit and occurrence descriptions usually do not describe the dispersion of lower-grade uranium enrichment, if any, surrounding the mineralized rock. Rock formations with high uranium content may be masked by transported soils of lower uranium content. Despite these limitations, uranium resource assessment and exploration data are the most useful sources of information on the distribution of uranium-rich rocks and soils that create radon hazards and other environmental problems in the United States.

BIBLIOGRAPHY

BOUDETTE, E.L., and OLSZEWSKI, W.J., Jr., Generalized bedrock geologic map of New England, with emphasis on uranium endowment and radon production: Concord, New Hampshire Water Supply and Pollution Control Commission and U.S. Environmental Protection Agency, scale 1 : 1 000 000 (1986).

CASTOR, S.B., BERRY, M.A. and ROBINS, J.W., Uranium and thorium content of intrusive rocks in northeastern Washington and northern Idaho, In Bendix Field Engineering Corporation, 1977 NURE uranium geology symposium; abstracts and visual presentations, Grand Junction, Colo., Dec. 7-8, 1977: U.S. Department of Energy Report No. GJBX-12(78) (1977) 167-172.

COVENEY, R. M., JR., HILPMAN, P. L., ALLEN, A. V., and GLASCOCK, M. D., Radionuclides in Pennsylvanian black shales of the midwestern United States, in Marikos, M. A. and Hansman, R. H., eds., Geologic causes of natural radionuclide anomalies, proceedings of the GEORAD conference, St. Louis, Mo., Apr. 21-22, 1987: Missouri Department of Natural Resources Special Publication 4 (1987) 180 p.

DUVAL, J.S., and OTTON, J.K., Radium distribution and indoor radon in the Pacific Northwest: Geophysical Res. Letters, v. 17, n. 6 (1990) 801-804.

GROSZ, A.E., CATHCART, J.B., MACKE, D.L., KNAPP, M.S., SCHMIDT, WALTER, and SCOTT, T.M., Geologic interpretation of the gamma-ray aeroradiometric maps of central and northern Florida: U.S. Geological Survey Professional Paper 1461(1989) 48 p.

HARRELL, J.A., BELSITO, M.E., and KUMAR, A., Radon hazards associated with outcrops of Ohio shale in Ohio: Jour. of Environmental Geology and Water Science, v. 18., n. 1 (1991) 17-26.

HENRY, M.E., KAEDING, M.E., and MONTEVERDE, D., Radon in soil gas and gamma-ray activity of rocks and soils at the Mulligan Quarry, Clinton, New Jersey, in Gundersen, L.C.S., and Wanty, R.B., Field studies of radon in rocks, soils, and water: U.S.Geological Survey Bulletin 1971 (1991) 65-76.

HOLT, R.B., NIELSON, K.K., and ROGERS, V.C., Soil radon potential mapping of nine counties in northern Florida: Salt Lake City, Rogers and Associates Engineering Report RAE-9226/1-6 (1993a) 152 p.

---, 1993b, Soil radon potential mapping of fourteen counties in central Florida: Salt Lake City, Rogers and Associates Engineering Report RAE-9226/1-9, 219 p.

---, 1993c, Soil radon potential mapping of fourteen counties in south Florida: Salt Lake City, Rogers and Associates Engineering Report RAE-9226/1-13, 203 p.

LANDA, E.R., Radon emanation from uranium mill tailings, in Gundersen, L.C.S., and Wanty, R.B., Field studies of radon in rocks, soils, and water: U.S.G.S. Bulletin 1971 (1991) 145-154.

NIELSON, K.K., HOLT, R.B., and ROGERS, V.C., Soil radon potential mapping of twelve counties in northcentral Florida: Salt Lake City, Rogers and Associates Engineering Report RAE-9226/1-1 (1993a) 267 p.

---, 1993b, Soil radon potential mapping of eighteen counties in the Florida Panhandle: Salt Lake City, Rogers and Associates Engineering Report RAE-9226/1-5, 271 p.

OTTON, J.K., and DUVAL, J.S., Geologic controls on indoor radon in the Pacific Northwest: U.S. Environmental Protection Agency, Proceedings of the 1990 EPA Symposium on Radon and Radon Reduction Technology, Atlanta, GA., Feb. 19-23, v. III (1990) unpag.

OTTON, J.K., Preliminary geologic radon assessment of Washington, in Schumann, R.R., editor, Geologic radon potential of USEPA Region 10: U.S. Geological Survey Open-File Report 93-292J (1993) 125-146.

SCHUMANN, R.R., ed., Geologic radon potential of USEPA Regions 1-10: U.S. Geological Survey Open-File Report 93-292 (A-J) (1993) 1799 p.

THE USE OF URANIUM EXPLORATION DATA FOR MAPPING RADON POTENTIAL IN THE UK - ADVANTAGES AND PITFALLS

T.K. BALL, D.G. CAMERON, T.B. COLMAN, P.D. ROBERTS
British Geological Survey, Keyworth, Nottingham, United Kingdom

Abstract

Radon is generated during the decay of uranium and thorium and knowledge of uranium concentrations may be of help in identifying areas with high radon emissions. The primary determinant for a potential radon problem is the mineralogy of the uranium bearing phases in bed-rock or overburden. The controls over radon escape from the mineral is governed by the effective specific surface area of the uranium phases. Once in the disperse phase radon migration is controlled by the dispersion characteristics of the fluids. The uranium-rich province of the south-west peninsula has undergone many campaigns of uranium exploration. The techniques include drainage geochemical surveys, airborne total count radiometric surveys, more limited airborne gamma spectrometric surveys, soil geochemical surveys which have included gamma spectrometric measurements, non-systematic drilling etc. There is a very large data-set for house radon levels in the area and this is examined in relation to the geochemical data. In granitic areas the relationship between high uranium background and radon in house measurements is close, but this relationship is obscured in mudstone dominated, low permeability lithologies. There are other areas where the permeability of the ground is high, the uranium concentration close to or below the crustal abundance, yet having a high proportion of buildings above the action level. Limestones in the U.K. are usually low in uranium, but a limited uranium exploration programme in Derbyshire identified uranium mineralization in reef limestones in contact with uraniferous black shale. However radon generated from non-radioactive limestones is close to the values observed in uraniferous varieties and a high proportion of buildings are above the 200 Bq/m^3 action level. The three main controls on radon generation are the source mineralogy, the concentration of uranium and the permeability. The first two factors are usually addressed during uranium exploration. Generally the question of permeability is irrelevant to prospecting, but essential to the assessment of radon potential.

1. INTRODUCTION

Radon is now recognized as a major human health hazard. Radon emanates from bed-rock and overburden and may accumulate in houses. As in many countries, the main impetus for uranium exploration stemmed from the requirements for nuclear raw materials to support the defence effort and for the nuclear electricity industry. The main periods of uranium exploration were during the late 1950s and late 1960s. In the early 1970s the main effort in finding domestic supplies of uranium came to an end. An understanding of the major controls on uranium mineralization suggested that large tonnages of uranium ore were unlikely, whilst the finding of very large deposits in Canada, Australia and in Southern Africa reduced the requirement for secure domestic supplies.

Much of the uranium exploration effort and techniques were subsumed by two other programmes:

1. The Mineral Reconnaissance Programme, incorporated techniques developed for uranium search into a large scale exploration programme for other metals, within which uranium was but one of the large range of elements sought.

2. The Geochemical Survey Programme which investigates the distribution of many elements including uranium. The collection is systematic, started in the north of Great Britain and has currently covered about two thirds of the main island. This has been mainly a drainage based survey, stream sediment and water samples being the main sampling media.

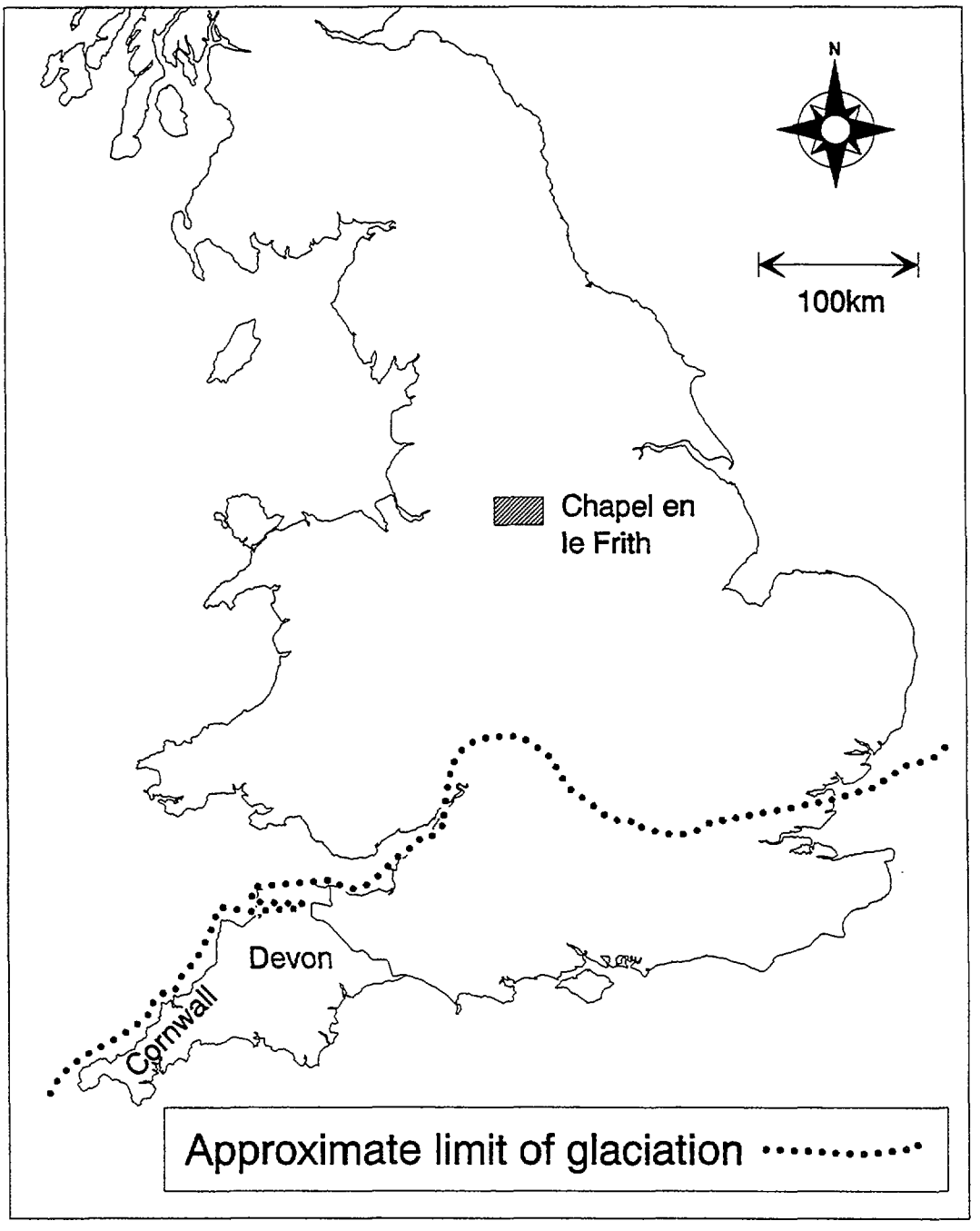

FIG. 1. Location map also showing the approximate southern limit of Pleistocene ice.

Because of the decline of interest in the early 1970s there has been no extensive airborne gamma spectrometric survey programme, although some early seminal work had been undertaken using total count instruments. The main source of data for assessing uranium distribution is therefore geochemical and of this most data is for stream sediments, supplemented by soil geochemical and ground gamma spectrometric surveys in selected areas. Boreholes, mostly for stratigraphic purposes, may be radiometrically logged with both total count and more rarely gamma spectrometric measurements, supplemented by chemical analyses where appropriate. Large area radon in overburden gas surveys were not used in reconnaissance uranium exploration, although more detailed follow-up investigations frequently used these techniques. Large area radon surveys have awaited the recognition that radon enters houses and in the UK at least, this approach is proving a very effective method in predicting areas with potential for high radon in houses.

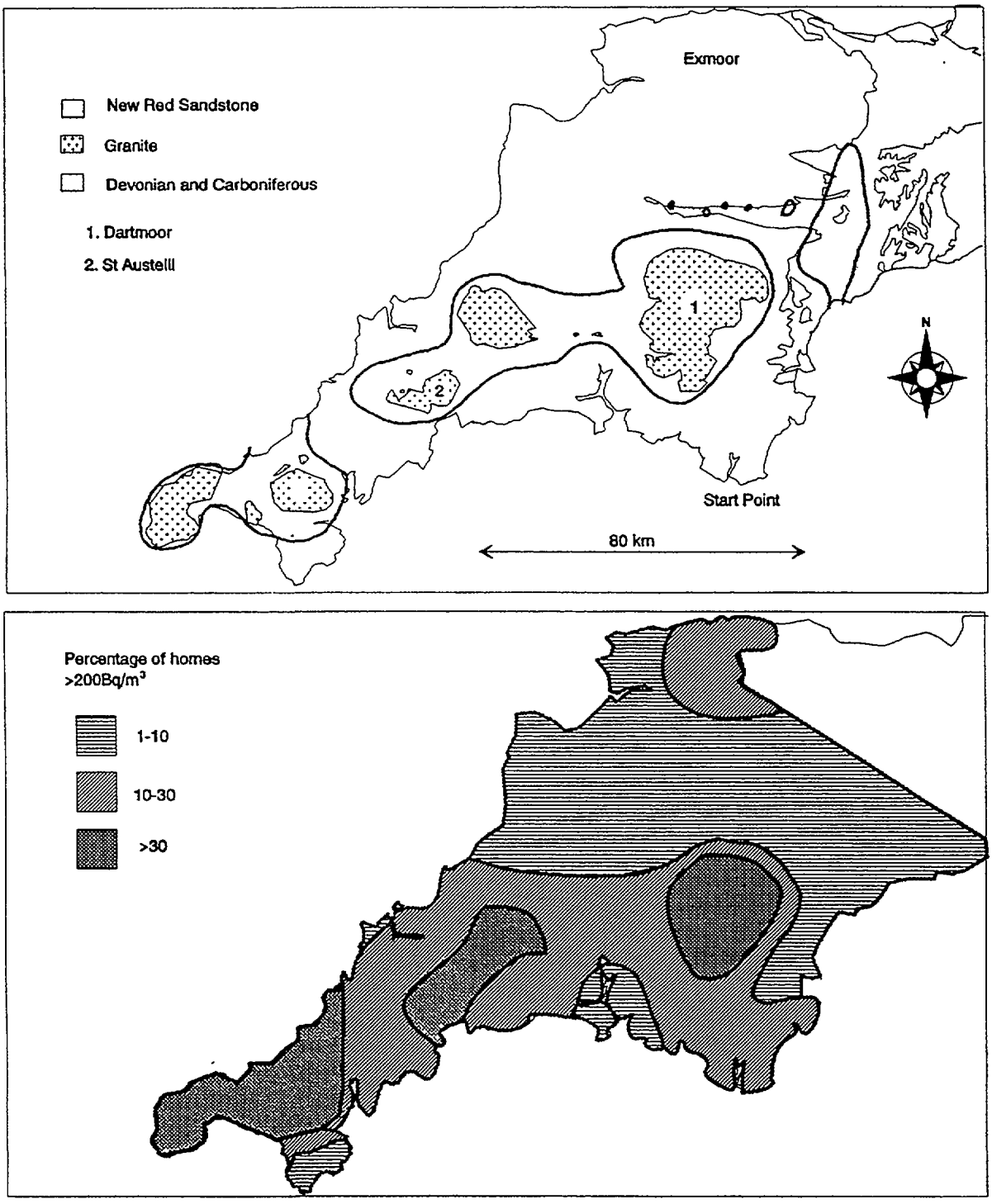

FIG. 2. Map of Cornwall and Devon. The upper part shows the location of the major granite plutons and the Permo/Triassic New Red Sandstone beds. The heavy line marks the approximate limit of uranium enrichment, based upon observations from the uranium exploration programme, mining records and drainage geochemical surveys. The lower portion summarises the house survey data as the proportion of houses with radon levels above the "Action Level" of 200 Bq/m³.

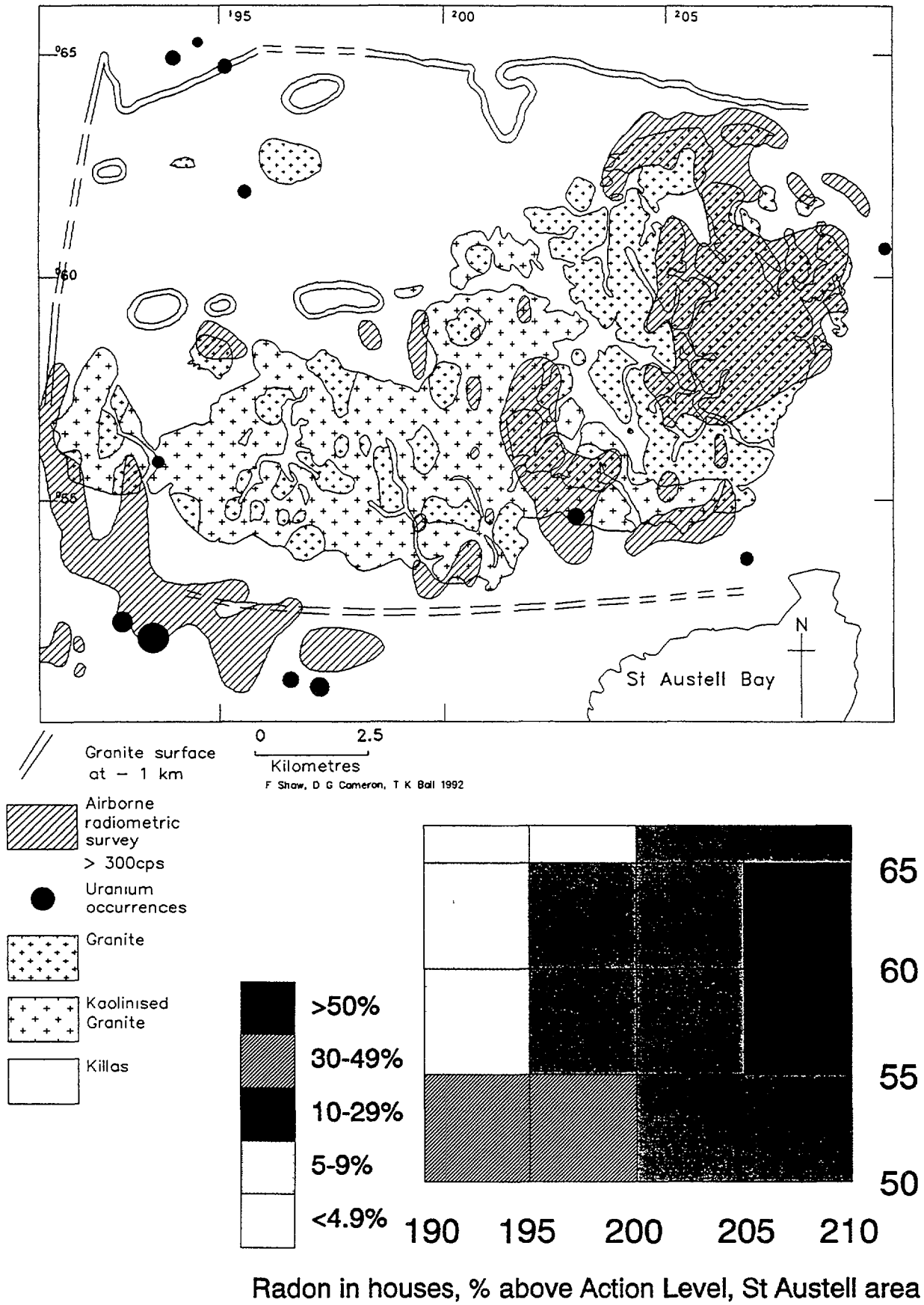

FIG. 3. Geological sketch map of the St Austell Granite. The upper portion shows the distribution of the main granite variants and also the results of an airborne total gamma radiometric survey. The lower part shows the proportion of houses above the action level in 5km squares for the same area.

Radon is mainly a problem when it enters houses. The levels in houses are affected by the construction and maintenance of the building and the life style of its occupants. In order to determine the extent of the radon problem in relation to geological features, a large house data set is required to overcome some of the sources of variation. There are only two areas in the U.K. where there are sufficient surveyed houses and enough data from uranium exploration studies to enable valid comparisons to be made.

2. RADON MAPPING IN CORNWALL AND DEVON

2.1. GEOLOGY, GEOCHEMISTRY AND URANIUM MINERALOGY

Ball and Miles [1] have compared geological and geochemical datasets for Cornwall and Devon, with the data from radon surveys in houses (Figs 1 and 2).

A granite batholith intrudes folded and faulted Devonian and Carboniferous sedimentary rocks which are dominantly argillaceous and arenaceous with very minor volcanic rocks and limestones. In the Exmoor area (Fig. 2) the Devonian contains a greater proportion of deltaic sandstones and conglomerates. The area was further folded and faulted, uplifted, and Permo-Triassic red-bed sequences (The New Red Sandstone) deposited upon the eroded land surfaces. Present day granite outcrops reveal only the uppermost few hundred metres of the batholith.

The granitic rocks are uraniferous with concentrations ranging from 6-25 ppm, although higher values occur rarely [2, 3, 4, 5].

There are extensive areas of alteration within the granites: tourmalinization, greisening, haematitization, and kaolinization all affect substantial volumes of rock. Kaolinization is the most important because it was very widespread and usually resulted in a substantial decrease in the uranium concentration [5].

It has been shown that the greatest proportion of the uranium in the granites occurs in the mineral uraninite [4, 5]. This is often weathered near the surface, the uraninite being pseudomorphed by aggregates of various mineral phases ranging from plumbogummite to mixed clay and iron oxides. Much of the uranium is removed by weathering but a large part of the radium remains in the relict minerals and, because of the greater specific surface area, these minerals in the weathered rock become more efficient radon generators than expected from the remnant uranium [7].

Uranium mineralization has been known in the area for at least a century and the minerals were mined, originally for glass colouring, before reworking of some deposits for their radium content [8]. Two types of uranium occurrence are recognized: within high temperature tin/tungsten/copper lodes and in later "crosscourses" (for summary see [5]).

Spatially most of the uranium vein mineralization occurs within about 2 km either side of the granite contact. Uranium mineralization ranges from small, high-grade, to more disseminated occurrences [9]. In south Devon small uraniferous mineral occurrences near Start Point, and also the uraniferous/vanadiniferous nodules in the New Red Sandstone are not related to a granite contact.

Comprehensive data sets for uranium in stream sediments are available for much of the Cornwall and Devon area. The data are summarized in Fig. 2 where it is clear that the granites are surrounded by a zone in which uranium in stream sediments is high.

Uranium is high in the rocks, and in the derived stream waters and sediments of the New Red Sandstone. The area, corresponding to the suboutcrop of one of the mudstone formation, gives extremely high values for uranium related to extensive zones of uranium/vanadium mineralization (Fig. 2).

The Devonian rocks of the Exmoor area show a low and restricted range of uranium values. 747 samples of stream sediments give a geometric mean of 2.6 and a median of 2.7 ppm U.

2.1. HOUSE SURVEYS

House survey data for the two counties are summarized in Fig. 2. For detailed discussion of the procedures for estimating and smoothing the data see [10]. The data are considered in relation to a 5 km grid in order to maintain confidentiality.

There is a close correspondence between areas where more than 30% of the house radon levels are above the 200 Bq/m^{-3} Action Level, and the granites. The granites are characterized by high uranium concentrations, a deep weathering profile, and uranium in a mineral phase that is easily weathered; however, whilst the uranium may be removed, the radium can remain in situ. Radon is thus easily emanated from the host rock and high values of radon have been detected in ground and surface waters and soil gases.

One of the zones where 10-30% of houses exceed the Action Level surrounds the >30% contour and is broadly coincident with rocks in which sub-economic grade uranium mineralization is common. This usually occurs as small high-grade discrete veins but there are also numerous disseminated uranium occurrences. This area is further underlain by microgranitic intrusions and small granite plugs which also contribute to the overall moderate to high levels of radon. This zone is also characterized by high values of uranium in stream sediments.

There are subtleties in house distribution features, within the granite zone, which are also explained by the uranium exploration data. The St Austell Granite Pluton has two major variants (Fig. 3). The western section is largely kaolinized and uranium depleted, whereas the eastern portion is relatively unaltered. Later work has shown that there is relatively little variation otherwise in the potassium and thorium distributions in rock and overburden, most of the changes in gamma activity are due to uranium variation. The airborne total count survey reflects this relationship with higher values of total gamma over the eastern section of the pluton and also over the aureole rocks to the south west. Here there is evidence of a large volume "soak" of uranium mineralization, culminating in one large high grade uranium vein at the South Terras Mine [8].

House data (Fig. 3) reflects these relationships with a higher frequency of affected houses over the eastern granite, slightly lower frequencies over the mineralized aureole and lower values over the western granite.

There are other areas, however, within the 10-30% category (Fig. 2), which are more difficult to explain, since they are not characterized by anomalous values of uranium in drainage samples. This may be partly due to the cover of thick overburden over a deep weathering profile where the underlying geology is poorly known. The area south of the Dartmoor granite for example, has no known uranium mineralization apart from that exposed at the coast near Start Point. There is no evidence for uranium enrichment either from the stream sediments or the airborne surveys. Yet there are zones with high radon in soil gases.

Another zone difficult to explain is the 10-30% incidence in Exmoor where, despite extensive investigations, only one anomalous concentration of uranium was found in the whole of the area, all other values were very close to the crustal average of 2.7 ppm [11].

Very high values of uranium occur in stream sediments and waters related to sub-zones within the Permo-Triassic mudstones. Based purely upon the uranium concentrations in surface drainage samples, a comparable frequency of houses above the radon action level to granitic areas would be expected. In reality the proportion of houses above the action level is about 1%. The mudstones are

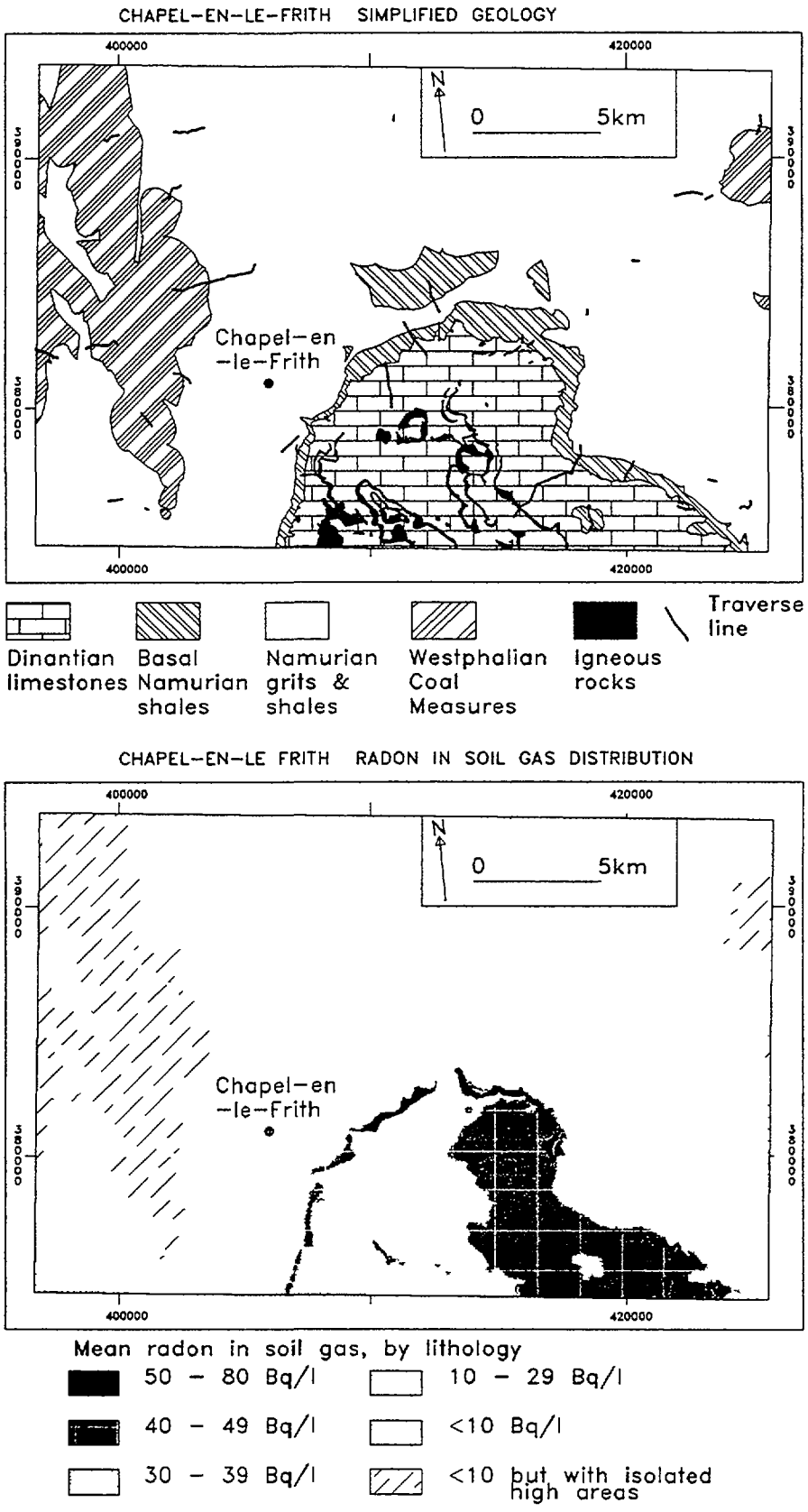

FIG. 4. Simplified geological map of the Chapel-en-le-Frith area in Derbyshire. The lower map shows the distribution of radon emanation for the different rock types under summer conditions.

relatively impermeable; there is therefore little transport of radon despite the high uranium, radium and consequently radon content of the rocks.

By contrast, there are areas such as in Exmoor, underlain by rocks that have uranium levels at about the crustal average, but which still give rise to high radon levels in houses. Ball and Miles [1] suggested that the reason was that the whole of the S.W. Peninsula was south of the maximum Pleistocene glaciation ice-front. North of the ice-front there was efficient removal of weathering profiles, and deposition of the glacial drift onto lower ground. South of the ice fronts, despite semi-permanent snow-fields and small ice caps on the high moors, the very deep weathering profiles initiated during the Mesozoic and Tertiary periods are retained. These along with soliflucted head deposits, can result in a high gas permeability in the soil substrate. The deltaic sedimentary rocks of Exmoor weather to give a well drained sandy overburden, whereas the Carboniferous rocks to the south tend to produce poorly drained clay-rich soils.

3. RADON MAPPING IN LIMESTONE AREAS IN DERBYSHIRE

3.1. GEOLOGY, GEOCHEMISTRY AND URANIUM MINERALS.

The Chapel-en-le-Frith area is underlain by a range of rocks of Carboniferous and Pleistocene age (Fig. 4). Dinantian limestones with basic intrusive and extrusive igneous rocks are overlain by Namurian black mudstones and sandstones, in turn succeeded by Westphalian Coal Measures comprising interbedded coals, mudstones and sandstones. Uranium exploration studies have shown that uranium is high in the limestone marginal reef facies, where it is found in sedimentary nodules and other phosphatic concentrations. Some of the fluorite/barite/galena mineral veins include sparse uranium/hydrocarbon associations whilst uraniferous sedimentary enrichments occur widely within the lower Namurian pyritic black shales and in relatively narrow marine bands within the Westphalian. The whole area was glaciated, and boulder clay and glacio-fluvial sands and gravels deposited in the valleys. There was also a mantle of loess rich drift.

Fig. 3 shows a simplified geological map of this area and also the geological map re-interpreted as a radon in soil gas map based upon selected traverses carried out in summer conditions. Clearly the radon levels over the various rock units do not correspond to the uranium levels in the rock types.

The highest soil gas radon occurs over the Dinantian reef limestones and where the Namurian mudstones overlie the reefs. Radon in soil gas was found to vary with lithology. Statistical analysis shows highly significant differences for radon emanation over the various lithologies. The soil gas radon values are also independent of the uranium concentration in the bed-rock. The uranium rich marginal reef limestones only emanates about twice as much radon as shelf facies limestones with typically less than 2 ppm uranium. The reef limestones typically exhibit ranges of 1-25 ppm U, whilst the basal Namurian mudstones have 10-60 ppm U. The non-reef limestones however also give rise to high radon in soil gas, whilst the radon from the less permeable Namurian mudstones may be regarded as only moderate. The Westphalian outcrop is characterized by isolated high concentrations of radon in soil gas corresponding to marine bands within the sequence.

Studies of the distribution of uranium in the constituent minerals have shown that uranium is uniformly distributed within the limestones, being largely confined to the organic matrix. The following relationships have been identified [12]:

- Uranium is mostly associated with finely divided organic matter in the matrix of bio-clastic limestones (usually < 10 ppm). Uranium is also concentrated in stylolites, which are abundant, and which typically have 20-60 ppmU.

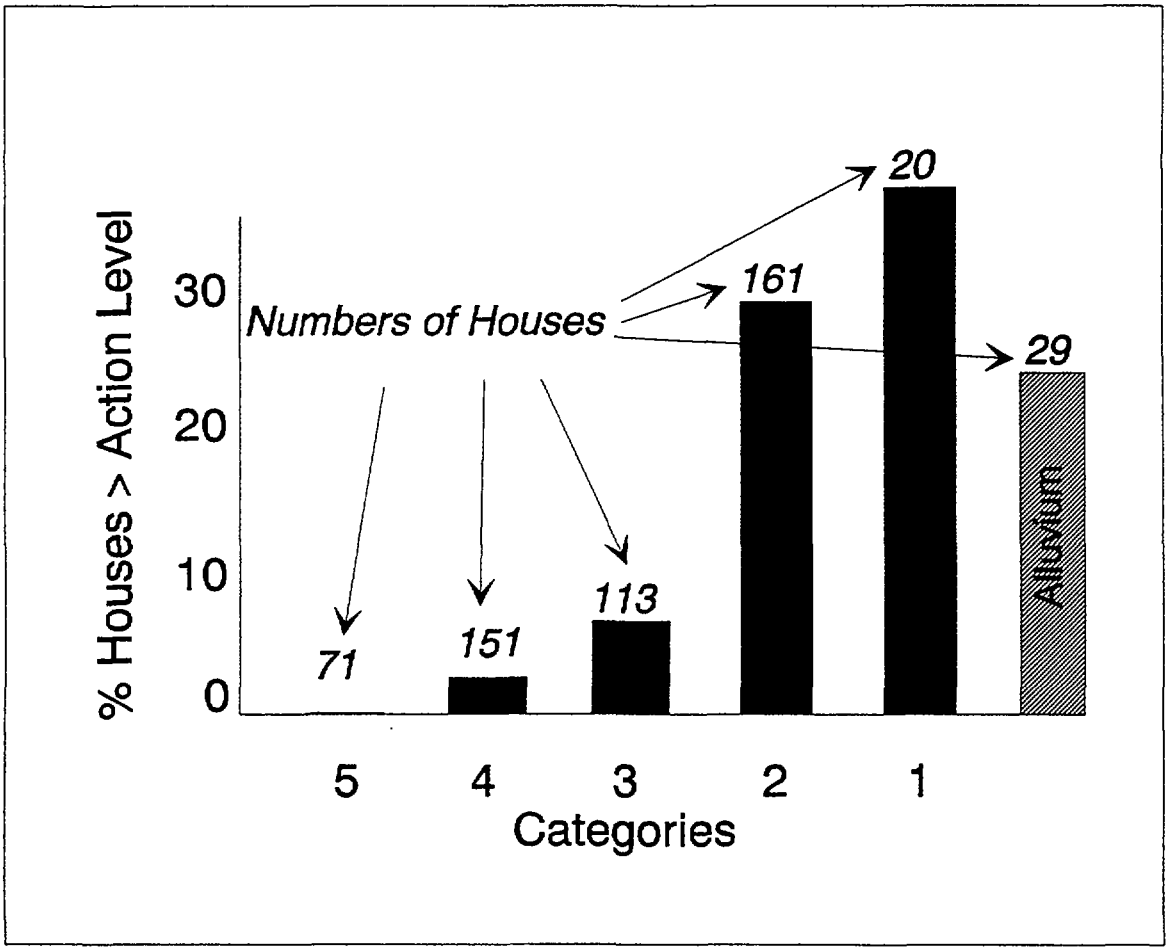

FIG. 5. The data from Fig. 4 are divided into 5 categories, with one additional. The proportion of houses above the action level are given for these categories.

- Quantitatively less significant are concentrations in larger fragment of organic detritus and scattered hydrocarbon globules where levels of several hundreds of ppm may be found.

In the Namurian black shales uranium is located mainly in the fine grained mud matrix, where it may be present at levels up to 20 ppmU, and also in organic rich bands at concentrations up to 40 ppmU. Uranium is rare in primary detrital phases and may also be remobilized and relocated on iron oxides.

In the sandstones the main uranium hosts are in primary detrital minerals (apatite, zircon etc.) where it is present as 100s of ppm. Uranium may also be sorbed onto Fe-oxides which may be present as cements or as weathering products.

3.2. HOUSE SURVEYS

House data correlates reasonably well with the radon in overburden gas determinations (Fig. 5). Five major categories have been identified based on the radon value in soil gas and permeability considerations:

1. Reef limestones
2. Shelf limestones
3. Namurian black shales

4. Coal measures (identified as being mostly low with isolated zones of high potential).
5. Namurian grey shales and sandstones.

A further category of river terrace alluvium was added at a later stage. This relates to those fossil terraces that are currently well above the present flood plain. Material in the terraces are derived from adjacent areas and these features usually result in a much higher proportion of houses being above the action level than do the parent materials. The figure shows the proportion of houses above the action level of 200 Bq/m^3 for each geological feature.

4. CONCLUSIONS

There are two considerations in considering the mobility of radon:

1. the extent to which radon can escape from the primary mineral phase;

2. the nature of transport mechanisms that are governed by permeability and carrier fluid transport in bed-rock and overburden.

In many rocks despite uranium being present as a trace element it is frequently found in trace minerals in which the uranium is a major component. The emanation from such minerals will depend upon the density, the number of imperfections in the mineral and most importantly upon the surface area. The surface area of the uranium bearing phases is thus of considerable importance in radon emanation and this is only partly a function of the uranium concentrations in rocks. Whether the radon rich ground gas moves into zones within the influence of a house is dependent upon the fluid flow characteristics of the ground.

In conclusion, regional geochemical distribution patterns for uranium, as obtained during geochemical surveys and /or by airborne gamma spectrometric measurements, can be an useful first indicator of high radon potential in such areas as South West England. However there are environments where sole reliance on such data can be misleading. This is because radon potential is a function not only of uranium concentration, but also of the nature of the minerals and permeability. High permeability can result in high radon potential, even where the bed-rock uranium concentrations are at or even slightly below the average crustal abundance. Soil gas radon measurements gives the most useful indication of radon potential and this is also in accord with the findings in Sweden [13]), and the eastern USA [14].

REFERENCES

[1] BALL, T.K., MILES, J.C.H., Geological and geochemical factors affecting the radon concentration in homes in Cornwall and Devon, UK, Environmental Geochemistry and Health **15** 1 (1993) 27-36.

[2] TAMMEMAGI, H.Y., SMITH, N.L., A radiogeologic study of the granites of SW England. Geological Society of London Journal. **131** (1975) 425-427.

[3] SIMPSON, P.R., PLANT, J., COPE, M.J., "Uranium abundance and distribution in some granites from northern Scotland southwest England as indicators of uranium provinces", Geology, mining and extractive processing of uranium (JONES, M.J. Ed.), Institution of Mining and Metallurgy, London (1976) 126-139.

[4] BALL, T. K., BASHAM, I.R., Radioactive accessory minerals in granite from south west England, Proceedings of the Ussher Society **4** (1979) 432-438.

[5] BALL, T.K., BASHAM, I.R. & MICHIE, U.McL., "Uraniferous vein occurrences of south-west England - paragenesis and genesis", Vein-type and similar uranium deposits in rocks younger than Proterozoic, (Proc Int. Conf. Vienna, 1982) IAEA, Vienna (1982) 113-156.

[6] ASHAM, I.R., BALL, T.K., BEDDOE-STEPHENS, B. & MICHIE, U.McL. "Uranium-bearing accessory minerals and granite fertility: 1. Methods of identification and evaluation", "II. Studies of granites from the British Isles", Proc. Int. Symposium on Uranium Exploration Methods - review of the NEA/IAEA R & D programme, Paris (1-4 June 1982).

[7] BALL T.K., CAMERON D.G., COLMAN T.B. & ROBERTS P.D. Behaviour of radon in the geological environment: a review. Quarterly Journal Of Engineering Geology. **24** (1991) 169-182.

[8] DINES H.G., The metalliferous mining region of South West England, Memoir Geological Survey Great Britain, HMSO, London (1956).

[9] BOWIE, S.H.U., OSTLE, D. & CAMPBELL, C.B., Uranium mineralisation in N. Scotland, Wales, the Midlands and S.W. England, Transactions Institution of Mining and Metallurgy, Section B, **82** (1973) B177-179.

[10] MILES, J.C.H., GREEN, B.M.R., LOMAS, P.R. & CLIFF, K.D., Radon affected areas: Cornwall and Devon, Documents of the National Radiological Protection Board, **1**, 4 (1990).

[11] TAYLOR, S.R., Abundance of elements in the continental crust: a new table, Geochimica et Cosmochimica Acta **28** (1964) 1273-1284.

[12] HYSLOP, E.K., Uranium distribution studies of potential radon source rocks from the Ashover area, Derbyshire UK, British Geological Survey Technical Report WG/92/4C (1993) 32pp.

[13] ÅKERBLOM, G., ANDERSSON, P., CLAVENSJÖ, B., Soil Gas Radon - A source for indoor radon daughters, Radiation Protection Dosimetry. **7** (1-4) (1984) 49-54.

[14] REIMER, G.M. & GUNDERSEN, L.C.S., A direct correlation among indoor Rn, soil gas Rn and geology in the Reading Prong near Boyertown, Pennsylvania, Health Physics, **57**, (1989) 155-160.

THE ROLE OF AIRBORNE GAMMA SPECTROMETRIC DATA IN THE RADON PROGRAMME OF THE CZECH REPUBLIC

I. BARNET
Czech Geological Survey, Prague, Czech Republic

Abstract

During 40 years of uranium prospecting in the Czech Republic the airborne gammaspectrometric mapping has covered about 60% of the state territory in the working scale of 1 : 25 000. In the 1990s the gammaspectrometric maps occured to be a very useful tool for environmental applications. The K, U and Th data, reflecting both the natural characterictics of the bedrock and the environmentaZ impact of intensive U-mining were also used as the input data for the radon risk mapping. Due to the prevailing crystalline and granitic basement, the radon problem was highlighted in the Czech Republic since 1989. First indices, obtained by the Hygienic Survey (radiation departments) referred to indoor radon in the houses built from U-contaminated materials (e.g. the special case of Jachymov — the long term use of material from U-waste dumps for centuries of Ag and adjacent U exploitation or the case of START family prefab houses, built in the 1960s and 70's from the slag concrete). In some of these houses, the internal U sources were not so intensive to explain high indoor Rn values. Later the attention was given to the radon potential of geological environment. In 1989 the Czech Geological Survey carried a proposal for radon risk mapping of the state territory. The geological units as well as the rock types were characterised from the soil gas Rn point of view. The radon risk maps were published in the scale of 1 : 200 000 and widely distributed to the state authorities and private companies dealing with radon problematics. The regional maps were based on the following data: soil gas Rn measurements, grain-size analyses at the testing areas, U-gammaspectrometric data (both airborne and ground measurements), and geological, soil and hydrogeological maps.

1. RADON PROGRAMME IN THE CZECH REPUBLIC

The radon programme is coordinated by the Interministerial Radon Commission (IRC) joining the experts from the state sector (geology — soil gas Rn, Hygienic Service — indoor Rn, Ministry of Finance — state subvention for mitigation) and private sector (Rn measurements, mitigation projects and technologies). The IRC is in the close contact with the Association Radon Risk (private companies involved in practical measurements). In 1991 the Decree of Ministry of Health 76/91 [2] was issued, setting the limits for radiation protection from natural sources:

Soil gas Rn limits in the Czech Republic:

Radon risk	Soil gas radon ^{222}RN [kBq.m^{-3}]		
	Permeability low	Permeability medium	Permeability high
low	< 30	< 20	< 10
medium	30-100	20-70	10-30
high	> 100	> 70	> 30

cit. par. 4, sect.2: "The houses built in the areas except of those with low risk, proved by in situ measurements, must be protected against radon".

Building materials < 120 Bq.kg^{-1} 226Ra, gamma dose > 0.7 μSv.h^{-1} can be used in extravilan with approval of the General Hygienist

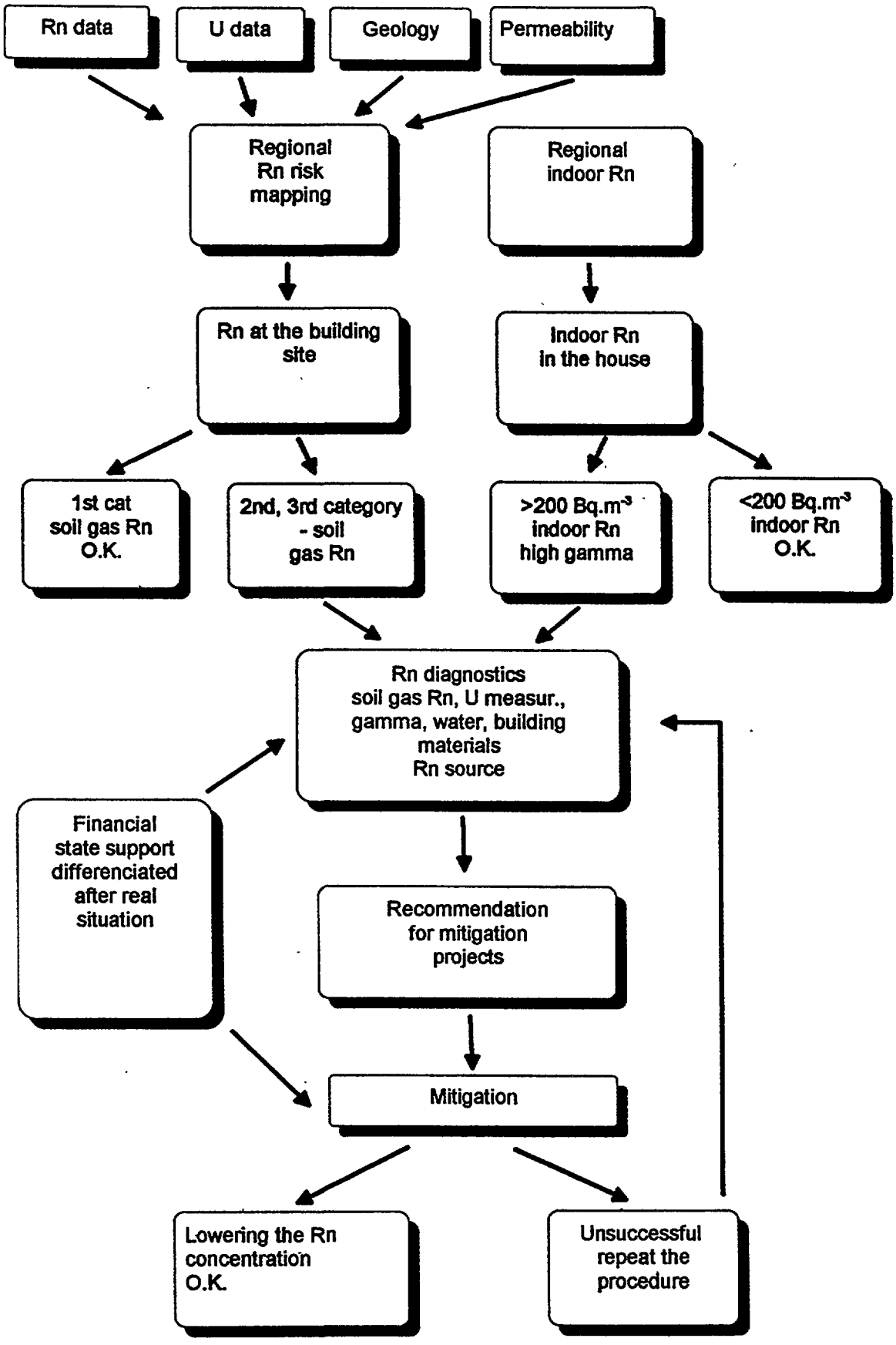

FIG. 1. The scheme of mitigation procedure for existing houses in the Czech radon programme (existing = for those, where building permission was issued before February 1991).

Indoor radon	existing houses < 200 Bq.m^{-3} EER newly built houses < 100 Bq.m^{-3} EER
Water	< 50 Bq.l^{-1}, higher only with the permission of the district hygienist > 1000 Bq.l^{-1} not permitted for indoor use

The scheme of mitigation procedure in existing houses is presented in Fig. 1.

2. THE U-Rn COORRELATION IN THE REGIONAL SCALE

The correlation can be clearly observed in acid magmatites (syenites (durbachites), granodiorites and diorites). The extremely high values of U and Rn correlate fairly in these rock types (see Fig. 2), but within the interval of usual values (U up to 10 ppm and Rn up to 50 Bq.m^{-3}), typical for sedimentary and metamorphosed rocks of the Bohemian Massif, the correlation can be hardly observed (see Fig. 3). In both these figures the centered symbols of the rock types represent the mean values from 15 measurements at each point. It is evident, that the primary U content influences Rn concentration in special geological conditions only, like the granitic rocks and Silurian black shales, but in general the applications of U–Ra–Rn calculations in other rock types can be misleading.

3. THE U-Rn CORRELATION IN THE LOCAL SCALES

The positive U-Rn correlation can be found in the following geological environments:

- tectonic structures. especially when mineralised by uranium
- boundary planes of of rock types
- the occurence of U-contrasting rock types
- the environmental pollution caused by U-mining and by the use of U-contaminated material for building purposes (road construction and building materials)

The following case studies illustrate the U-Rn relation in these environments.

3.1. TECTONIC STRUCTURES — CASE STUDY OF KOVAROV

In Central Bohemian granitic massif the areas of durbachite (biotitic-syenite) represent the highest radon potential. Near Milevsko the durbachite massif is intersected by U+quartz mineralised tectonic zones, reaching the intravilan of village Kovarov. The detailed ground gamma spectrometry and Rn soil gas measurements were carried out across the tectonic planes. The Rn values taken directly at the tectonic planes were over 1800 kBq.m^{-3}, accompanied by U concentration up to 30 ppm. The indoor Rn monitoring, performed in this area by Hygienic Service, has detected the indoor Rn concentration > 200 Bq.m^{-3} in 67.8% of the house stock, > 500 Bq.m^{-3} in 24.8% of houses and > 500 Bq.m^{-3} in 4.4% of houses (pers. communication).

3.2. CASE STUDY OF NURSERY SCHOOL AT JACHYMOV

During indoor Rn monitoring in the house stock of Jachymov extremely high values were detected in the cellar of the nursery school (11 000 Bq.m^{-3}). The indoor Rn concentration in the upper floors were within the range of the first hundreds of Bq.m^{-3} depending upon the ventilation regime. The geological investigation has proved the presence of U-mineralised zone Geschieber (one of the

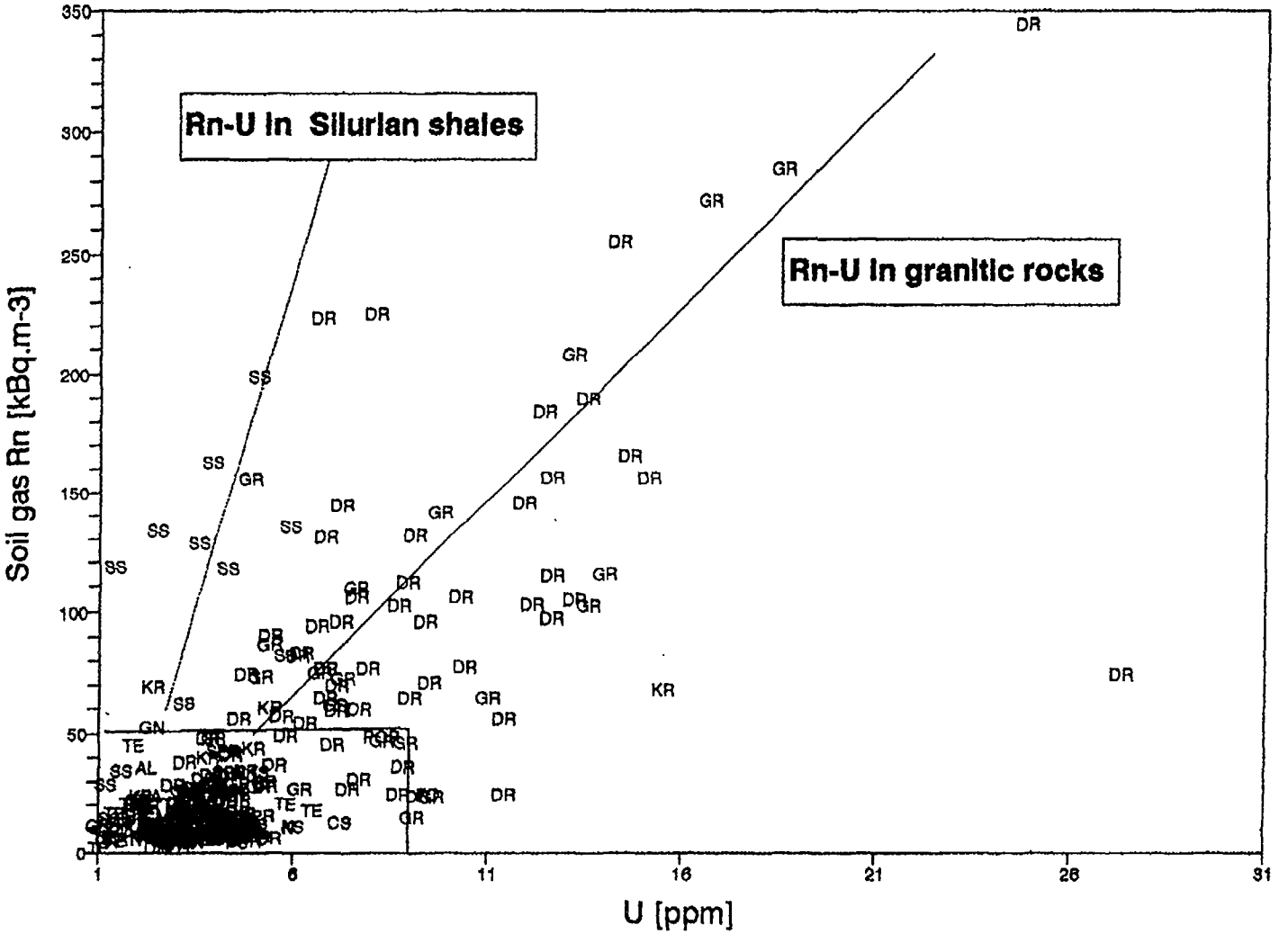

FIG. 2. The Rn-U relationship in the rock types of the Bohemian Massif (DR,GR - granitic rocks, SS - Silurian black shales). Marked area zoomed in Fig. 3.

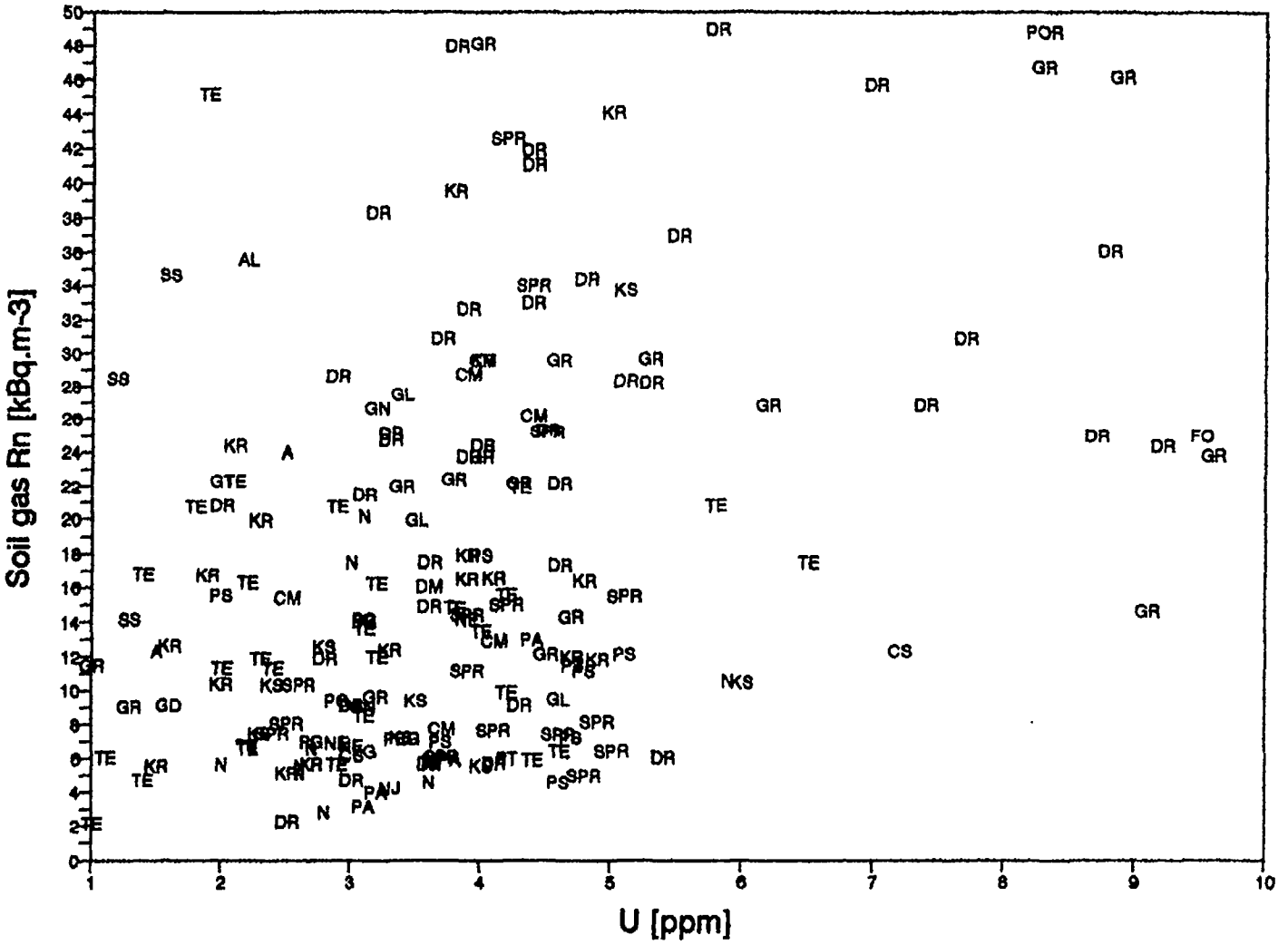

FIG. 3. The Rn-U relationship in the usual ranges of values in the rock types of the Bohemian Massif. Zoomed from Fig. 2 (major codes: DR,GR,GD - granitic rocks, KR - crystalline rocks, TE - river terraces, SPR loess, KS - Cretaceous sediments, GL - glacifluvial sediments).

main U-veins in Jachymov) about 50 m apart from the nursery school [3]. By the test trenches, oriented 10 m from the nursery school, the vein accompaniments was found (46.9 ppm U after the ground gamma spectrometry — see Fig. 4). The mitigation project, realised during the summer holiday season 1992 was based on the antiradon sealing of the cellar floor and door leading to upper floors and the apllication of the overpressure filter-ventilation system, lowering not only the iondoor Rn concentration under 200 $Bq.m^{-3}$ limit, but also the levels of dust and immision aerosol particles.

3.3. CASE STUDY OF PRIBRAM — U IN ROAD CONSTRUCTION

The airborne gamma spectrometric mapping around Pribram (one of the biggest U-mining districts, recently abandoned) has discovered local, mutually isolated U anomalies in the surrounding villages and roads. These anomalies were revised by ground gamma spectrometric measurements, carried out by the Czech Geological Survey in 1992 [4]. From the past years of U-mining there were clear evidences of using the material from the U waste dumps for road construction. The measurements gave a list of impacted villages, which was passed to the regional branch of Hygienic Survey. The levels of U contamination > 20 ppm U were confirmed in all the location of airborne anomalies, the range of 30-50 ppm U was usual for more than 50% of them, in 2 cases the values were over 200 ppm U. The Hygienic Survey checks the places of U-concentration for the gamma dose impact to human health.

4. CONCLUSIONS

The wide scale study of soil gas radon in the Czech Republic yielded the experience of using the relations between U and Rn in environmental studies which can be applied to other regions with similar geological environment:

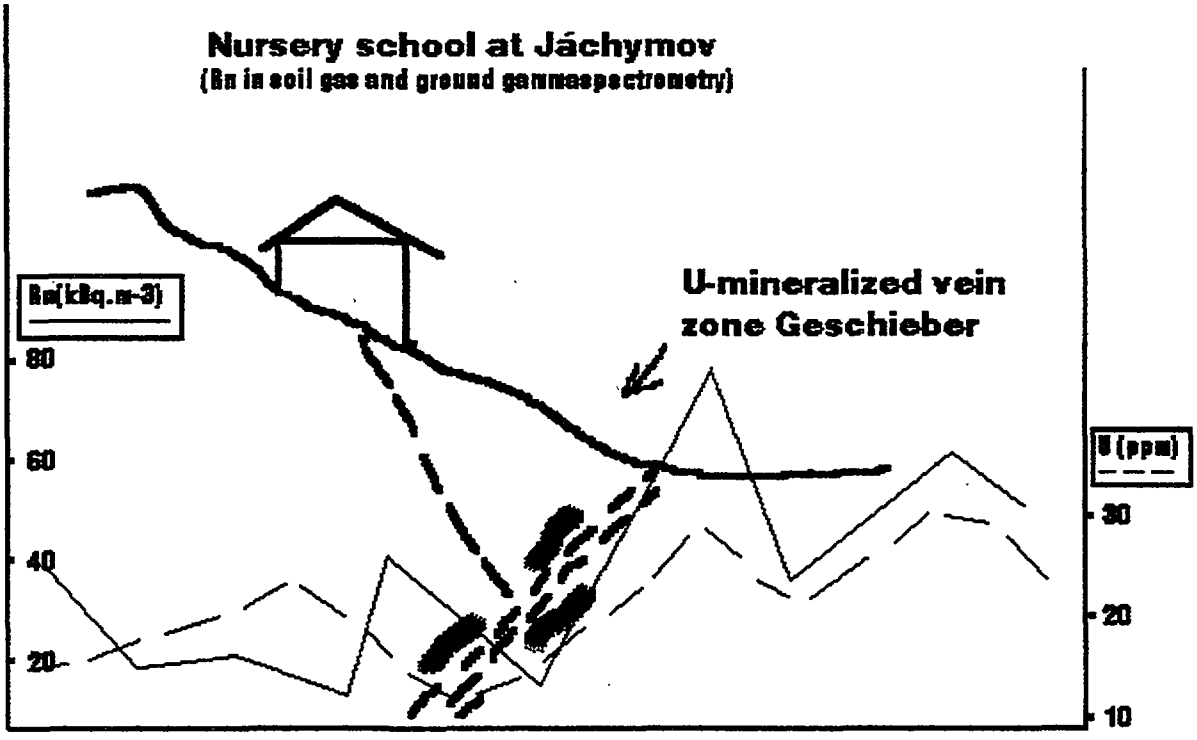

FIG. 4. The Rn and gammaspectrometric profile - case study nursery school Jachymov (Czech Republic).

1. In the regional scales the U-Rn correlation is well expressed in acid magmatic rocks. Therefore the U data can contribute to distinguishing the expected levels of radon in the rock types, especially the contrasting ones, but cannot be used for direct transformation to radon data in the rock types with lower uranium contents. In these rock types, the resulting levels of radon are strongly influenced by local geological environment and soil characteristics (permeability, soil moisture, the vertical profile of the soil cover).

2. In the local scales the U data can be used as additive information for radon diagnostics of the test sites. The strong correlation can be found in specific geological environments like the tectonic zones (especially when mineralized by U), at the boundary planes of the rock types. The U data can also serve as a useful tool for determining the radon sources and migration paths in the houses and for monitoring the environmental impact of U-mining and the use of U-enriched material for building purposes.

REFERENCES

[1] Radon investigations in Czechoslovakia I-III (1990-1992), Radon investigations in the Czech Republic IV (1993), I. Barnet ed., Czech Geol. Survey, Prague (1993).

[2] Decree 76/1991 "on the lowering the radiation risk from radon and natural radionuclides", Ministry of Health, Prague (1991) (in Czech).

[3] BARNET, I., PROCHAZKA, J., Report on the Rn and gamma spectrometry measurements - case study Jachymov, nursery school, Ministry of Environment, Prague (in Czech) (1992).

[4] PROCHAZKA, J., MANOVA, M., BARNET, I., The radioactive pollution of the villages in the vicinity of Pribram uranium mines.- in Radon investigations in the Czech Republic IV, ed. I. Barnet, Czech Geol. Survey, Prague (1993).

THE USE OF AIRBORNE RADIOMETRIC AND EXPLORATION SURVEY DATA AND TECHNIQUES IN RADON RISK MAPPING IN SWEDEN

G. ÅKERBLOM
Swedish Radiation Protection Institute, Stockholm, Sweden

Abstract

Production of Swedish maps for the purpose of showing radon risk at different locations was initiated in Sweden in 1979. The Swedish Radon Commission, working in co-operation with the National Radiation Protection Institute and the Board for Urban Planning and Building, commissioned the Geological Survey of Sweden to produce maps of all areas in which the gamma radiation from the ground surface or in the ground were known to exceed 30 μR/h and of areas at risk of exceeding that level. The bases for the maps were existing geological and geophysical maps and other data. In 1981, we learned that the 30 μR/h level was a crude measure of the risk of radon in dwellings. Actually, there are buildings with high indoor radon levels built on nearly every type of ground, except on soils and bedrock with very low uranium content. A new type of map, Radon Risk Map, was developed. These maps show areas of high radon risk, normal risk and low risk. High risk areas are those where radon concentration in soil air is known to or can be expected to exceed 50 000 Bq/m^3. Radon risk maps covering 65% of Sweden have now been produced. According to the Swedish Building Code, a radon investigation of a building site must be made before construction starts. To a large extent, the Radon Risk Maps are compiled from data based on gamma ray spectrometric airborne surveys and information obtained from uranium exploration surveys. In field investigations for radon risk mapping and detailed site investigations, gamma measurements, gamma ray spectrometric and radon measurements are used. The measurements are made using technology and instruments once developed for uranium exploration.

1. RADON IN SWEDEN

Radon constitutes a serious health risk in Sweden. The Swedish National Radiation Protection Institute estimates that 900 lung cancer cases per year are caused by elevated radon concentrations in dwellings. This from a population of 8.5 million. The arithmetic mean radon concentration in Swedish homes is 108 Bq/m^3. In Sweden, there are 4.1 million dwellings. Of those, 650 000 have indoor radon levels which exceed 140 becquerel per cubic metre (Bq/m^3) and 13 000 have levels exceeding 400 Bq/m^3. More than 1500 houses with radon concentrations above 2000 Bq/m^3 have been located. The two main sources of radon are the ground and light weight concrete made from uranium-rich alum shale. Alum shale concrete blocks have been used in approximately 300 000 houses. Relatively large areas of Sweden (Fig. 1) are covered by rocks containing enhanced levels of uranium. They include the 500 million year old alum shale, with 50-350 ppm U [1], and some types of granites and pegmatites with ages varying in age between 1900-850 million years old, with 10-50 ppm U and in extreme cases 50-100 ppm U [10]. Pegmatites often have concentrations of uranium-rich minerals and locally the uranium content can reach 200-1000 ppm U.

2. RADON RISK MAPPING AND CLASSIFICATION OF LAND

When the Swedish Radon Commission was appointed in 1979, it was expected that the houses that had problems with radon were those that were built in areas where alum shale and uranium rich granites occur. We predicted that 8 000 houses could be affected. However, now we know that more than 70 000 detached houses have indoor radon levels exceeding 400 Becquerels per cubic meter (Bq/m^3) due, to radon from the ground.

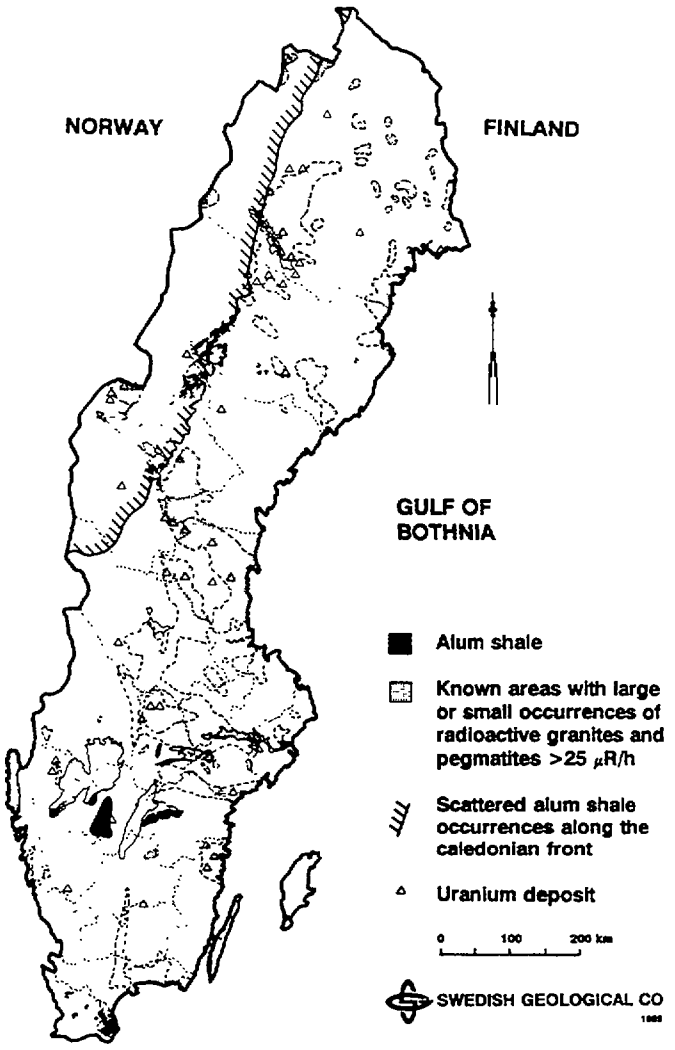

FIG. 1. Distribution of uranium-rich bedrock in Sweden

To prevent new houses from being built on ground which could be a potential radon hazard, the government in 1979 commissioned the Geological Survey (SGU) to produce maps of all known areas with highly radioactive rocks and soils. That is, where the gamma radiation from the soil or bedrock is or would be expected to be higher than 30 micro-roentgen per hour (μR/h). During two years, 240 maps, known as GEO-radiation maps were produced on the scale of 1:50 000 [4].

While we were producing the GEO-radiation maps, the Swedish programme for measuring radon in homes had commenced and houses with up to 20 000 Bq/m^3 had been located. When we examined these houses we found that they were often built on eskers comprised of gravel or coarse sand, or on fill of blasted rock. The gamma radiation was 10-15 μR/h, which is quite normal for soils in Sweden. However, the radon concentration in the soil air was around 80 000 Bq/m^3 and this soil air was being sucked into the houses due to the lower pressure indoors.

In one research programme, we studied the geological and building relationship to indoor radon concentrations of 90 houses with enhanced radon levels [2, 3]. Drill holes were made through the soil layer and into the bedrock around each house, the gamma radiation was measured on the ground and the drill holes were logged. Determinations of the radium, thorium and potassium content of the soil and bedrock was made by use of field gamma ray spectrometric measurements. We also

measured the radon concentration of the soil air around the houses and under the bottom slabs at a depth of one metre or more. The radon concentration in soil air at one metre was never less than 5 000 Bq/m^3. Some houses were obtaining more than one third of their incoming ventilation air from the ground.

The building authorities were eventually convinced that GEO-radiation maps did not give enough information concerning the risk of radon. From the National Board of Planning and Building, I was asked about the possibility of producing maps that could predict where special radon building technical requirements had to be used in building to prevent the problem of indoor radon.

My answer was that it was not possible to make such maps. We had learned that any house anywhere can have indoor radon levels higher than 400 Bq/m^3, the limit (compulsory) for existing buildings in Sweden (Table I). If there is enough available soil air containing radon to maintain a continuous flow of radon into the building, as there would be in the gravel and sand typical of an esker, the limit is easily exceeded.

TABLE I. CURRENT LIMITS (COMPULSORY) IN SWEDEN FOR RADON GAS CONCENTRATION* AND GAMMA RADIATION IN BUILDINGS:

400 Bq/m^3	for existing buildings
200 Bq/m^3	for new buildings
50 μR/h	for new buildings

* The Swedish limits were expressed in units of radon daughter concentration until January 1, 1994. For existing buildings, the limit was 200 Bq/m^3 and for new buildings 70 Bq/m^3.

TABLE II. CLASSIFICATION OF GROUND ACCORDING TO THE RISK OF RADON GAS. RECOMMENDATIONS ISSUED BY THE NATIONAL SWEDISH BOARD OF URBAN PLANNING AND BUILDING, 1982.

Regional Classification	**Examples of ground types**
• High risk areas	Bedrock and soil containing radium rich material, e.g.uranium-rich granites and alum shale. Soils with high emanation, e.g. gravel or gravelly sandy till.
• Normal risk areas	Ground where the radium content is normal, about 25-50 Bq/kg, e.g. gneisses and shales.
• Low risk areas	Ground where the radium content is low, less than 30 Bq/kg, e.g. limestone, sandstone, and basic igneous and volcanic rocks. Soils with low permeability, e.g. clay and silt.

Ground around building	**Radon conc. in soil air (Bq/m^3)**	**Technical construction requirements**
• High radon ground	> 50 000	Radon safe construction
• Normal radon ground	10 000 - 50 000	Radon protective construction
• Low radon ground	< 10 000	None

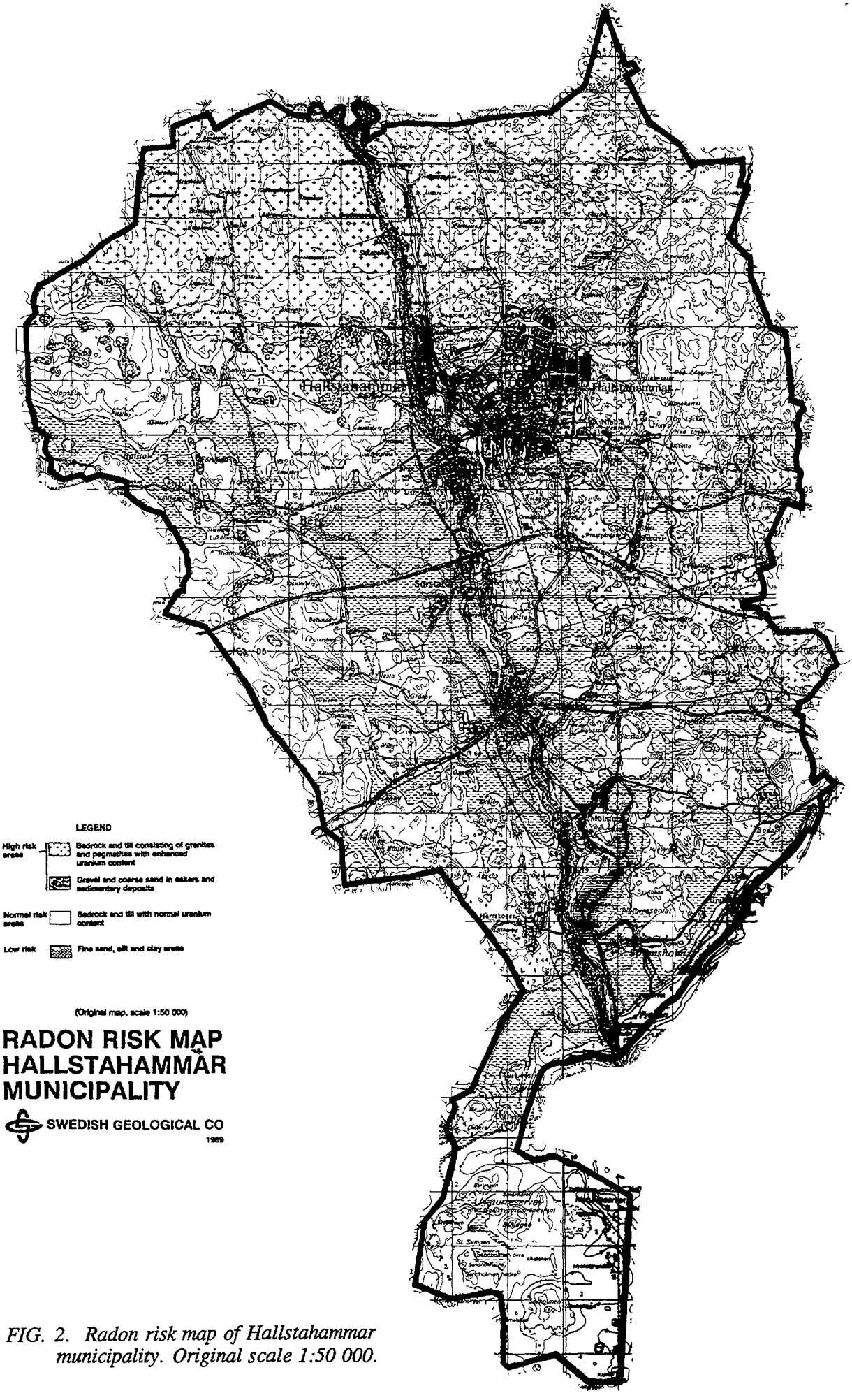

FIG. 2. Radon risk map of Hallstahammar municipality. Original scale 1:50 000.

However, if in the future, new houses could be constructed in a manner which prevents an influx of more than approximately one cubic metre of soil air per hour, the risk of indoor radon attaining levels above 140 Bq/m^3 would be low, as long as the radon concentration in the soil air is less than 50 000 Bq/m^3. (140 Bq/m^3 was the 1981-93 Swedish Building Code maximum allowable radon concentration in new buildings. January 1, 1994 the limit was changed to 200 Bq/m^3). By 1981, we had learned that for levels of over 50 000 Bq/m^3 in soil air to be reached, special geological conditions must exist. We recommended that, in future, it should be normal practice to construct houses limiting the influx of soil air from the ground to less than 1 cubic metre per hour.

It then became possible to set up a classification for the radon risk to be used for planning and building (Table II). This classification is recommended by the National Board of Planning and Building [9]. According to the recommendations, the technical construction requirements are set up to cope with radon concentrations in soil air. Normally, when radon concentration in the soil air is between 10 000 and 50 000 Bq/m^3, houses are required to have *radon protective construction*. When the radon concentration is higher than 50 000 Bq/m^3, *radon safe* construction must be used. If the radon concentration is lower than 10 000 Bq/m^3, there is no restriction on the construction as far as radon is concerned. For comprehensive planning, the ground should be classified into *high, normal and low risk areas*.

TABLE III. DETAILED CLASSIFICATION OF GROUND ACCORDING TO THE RISK OF RADON GAS.

High radon ground		
Bedrock or soil type	^{226}Ra Bq/kg	^{222}Rn in soil air one metre below ground surface, Bq/m^3
Bedrock surface (including a thin layer of remaining blasting rubble)	> 200	
Fill of blased rock	> 80	
Gravel, coarse sand, coarse till	> 50	> 50 000
Sand, coarse silt	> 50	> 50 000
Silt	> 70	> 60 000
Clay, clayey till	> 100	> 120 000
Low radon ground		
Bedrock or soil type	^{226}Ra Bq/kg	^{222}Rn in soil air one metre below ground surface, Bq/m^3
Bedrock surface (including a thin layer of remaining blasting rubble)	< 60	
Blasted rock, till, gravel, sand, coarse silt	< 25	< 10 000
Silt	< 50	< 20 000
Clay	< 80	< 60 000

The classification given in Table II is to rough too be used for site evaluations. At investigations for building constructions a more detailed classification of the radon risk for different types of ground is used (Table III). This classification includes the situation of a building founded on bedrock or fill, and also takes into consideration the permeability of silt and clay. In the latter case higher soil air radon concentrations can be tolerated due to the low permeability of the sediments.

3. RADON RISK MAPS AND INVESTIGATION BEFORE BUILDING

The local authorities are advised to investigate the radon situation within their districts. Today Radon Risk Maps on a scale of 1:50 000 or larger cover more than 60% of Sweden. The maps are made by geological consultants and paid for by the municipalities. Most of the maps represent a whole district, but some cover only the urban sections. More attention is given to urban areas when mapping. The radon risk map of Hallstahammar municipality is shown in Fig. 2.

According to the Building Code of 1988, a geotechnical investigation is required for all buildings, including a report on the radon situation. Today radon investigations are made of most building sites and plans.

The methods used for mapping and more detailed investigations include the following; but I must emphasize that none of these methods alone can predict the radon risk for any given area:

For mapping of larger areas, on a scale 1:50 000 or greater:

- Geological maps
- Results from airborne radiometric surveys, where available
- Results from radiometric surveys on the ground, where available
- Results from measurements of radon in buildings, where available
- Results from earlier geotechnical investigations such as soil composition, thickness and permeability of the soil layer, and the level of the ground water table
- Field surveys including measurements of gamma radiation
- Orientating radon measurements

For detailed surveys, for example a building site:

- Geological examination or mapping of the area
- Gamma radiation measurements
- Gamma ray spectrometric measurements to determine the radium concentration in bedrock and soil
  Measurements of radon concentration in the soil air

All available information and results from the measurements and observations are used to predict the radon potential. The technical requirements needed to build *radon safe houses* are given in the report.

In the report, it is also important to consider changes which are likely during the course of the construction project: soil removal, soil or blasted bedrock fill, and lowered ground water table. Such changes are likely to influence the radon situation.

4. SWEDISH GEOLOGY AND RADON RISK

In Sweden, exploration for uranium ore began in the early 1950s. At that time, most attention was directed to the alum shale formation which was thoroughly investigated and mapped. A

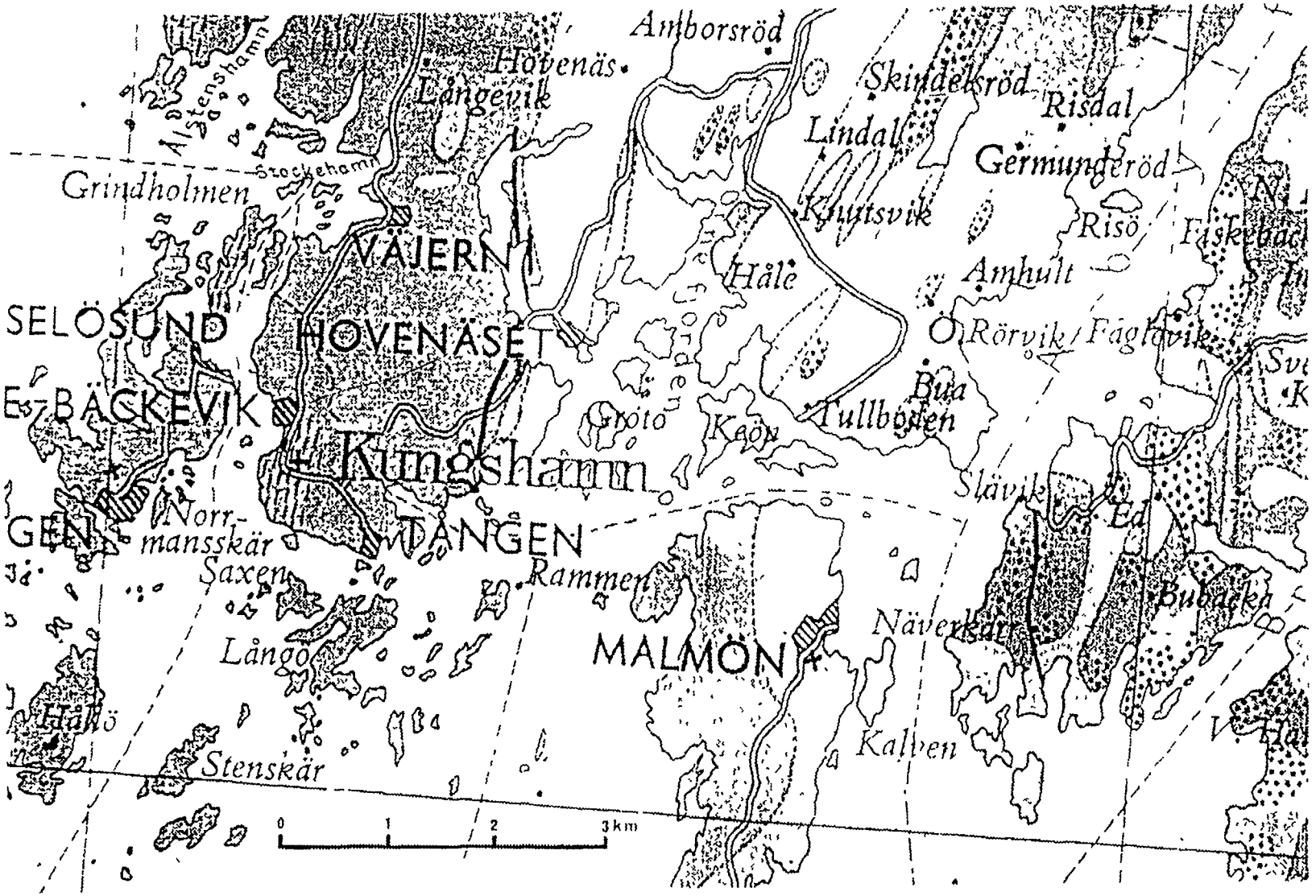

FIG. 3. Bedrock geological map of the Smögen district, which consists entirely of uranium-rich and thorium-rich granites. Dark grey = red granites. Light grey = grey granites. Dotted = porphyritic granites. Original scale 1:50,000. Geological Survey of Sweden, Ser. C nr. 479.

compilation of all known occurrences of alum shale was made for the GEO-radiation maps. However, information was insufficient in some regions. Those areas were surveyed especially to obtain information to make the GEO-radiation maps.

Data on the occurrence of uranium-rich granites and other rocks with enhanced uranium and thorium content have gradually been accumulated through exploration for uranium and the regional programme of geophysical mapping at the Geological Survey of Sweden. The most valuable methods of obtaining information on the occurrence and extent of rocks with enhanced radiation has come from airborne and car-borne surveys, and the follow-up of these surveys on the ground by boulder tracing, regional measurements with hand held scintillometers, in situ gamma ray spectrometers measurements and geochemical investigations.

Airborne gamma ray spectrometric surveys have been completed for 65% of Sweden's 450 000 km^2. Until 1984, when the Swedish programme for uranium exploration was brought to an end, most surveys where carried out for the purpose of uranium exploration. After which time, the measurements were made within the programme for geophysical mapping. The first airborne measurements were made around 1955 when vast areas were searched by small aircraft equipped with GM-counters. Since 1960, all surveys have been made with the use of gamma ray spectrometers. The airborne surveys carried out today by the Geological Survey are made from an altitude of 30 metres. The line spacing is 200 metres and a recording of the gamma spectra is made every 40 metres along the flight path. The gamma spectrometer is of Geometric/SGAB design. It has four crystals providing a total volume of 17 litres. The energy interval between 0 and 3187.5 keV is divided into 255 channels, each 12.5 eV wide. The primary channels are grouped into 24 or 40 channel configurations. The recordings from all separate channels are used to calculate the uranium, thorium and potassium-40 concentrations at the surface level. The concentrations are given as equivalent concentrations of ppm U, ppm Th and per cent K. The results of the measurements are plotted on maps which usually have a scale of 1:50 000. On the maps, the measured concentrations of eU, eTh and eK are marked as coloured lines (eU = red, eTh = blue and eK = yellow), the lengths of which are proportional to the registered equivalent concentration. A full description of the Swedish system for airborne spectrometric surveys is given by Mellander [8].

A problem which has restricted the use of the airborne surveys is that the airspace above towns and villages has a strictly enforced minimum flight altitude of 300 m. At that height, almost all gamma radiation from the surface is shielded by the air. Thus, information on the radioactivity of the ground is lacking where it is most needed. To cope with this problem, the Geological Survey obtained special permission to fly at an altitude of 50 m above densely populated areas, provided the results are used for predicting radon risk.

The technique used by the Geological Survey provides very good ground coverage and enables us to detect, for example, a single outcrop of uranium-rich pegmatite [7]. Combining the results from the airborne measurements with information from geological maps, it is often possible to delimit areas with different potential radon risks and to point out areas of special interest.

Sweden was covered by a continental ice sheet during the ice age, therefore, till is the most common soil type. Generally, glacial drift is derived from the bedrock directly underlying the drift cover, and recorded gamma radiation thus gives a relatively good idea of the extent of a rock containing enhanced uranium. However, when interpreting airborne measurements, the effects of shielding by soil and water must be taken into consideration.

Figs 3 and 4 show an area of uranium- and thorium-rich granite at Smögen, on the west coast of Sweden. The entire district consists mainly of granite outcroppings. In this case, the gamma radiation map may be used directly to determine areas of enhanced radon risk and delimit of such areas. As shown, the south-eastern part of the area consists of uranium-rich granites and the north-western part of thorium-rich granite, which often have fairly low uranium concentrations. The total measured gamma radiation from outcropping granite is almost equal in both areas, 20-40 μR/h.

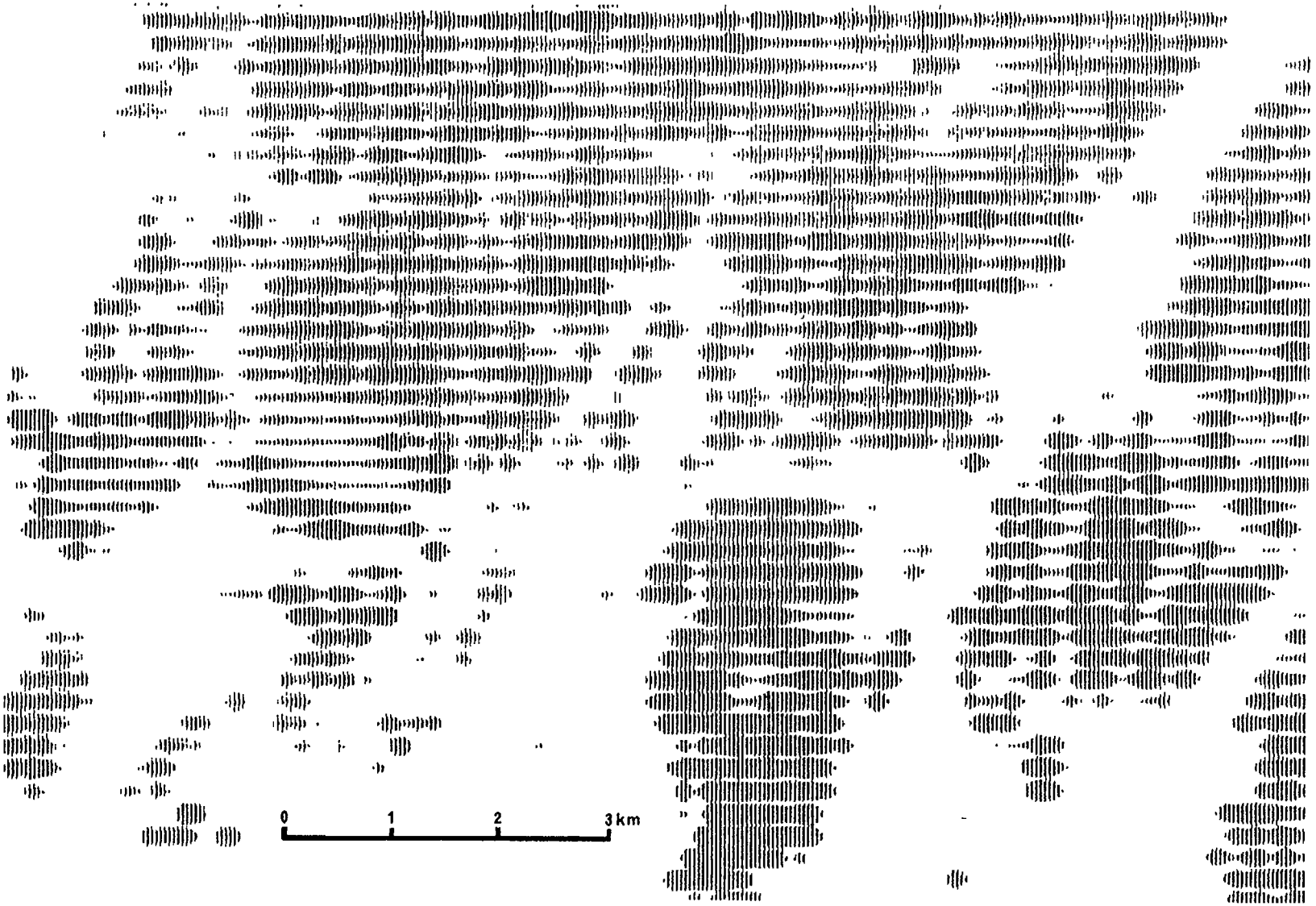

FIG. 4. Gamma ray spectrometric map of the Smögen area. Thin lines = uranium. Thick lines = thorium. Scale 1:50 000. Measurements performed by Geological Survey of Sweden.

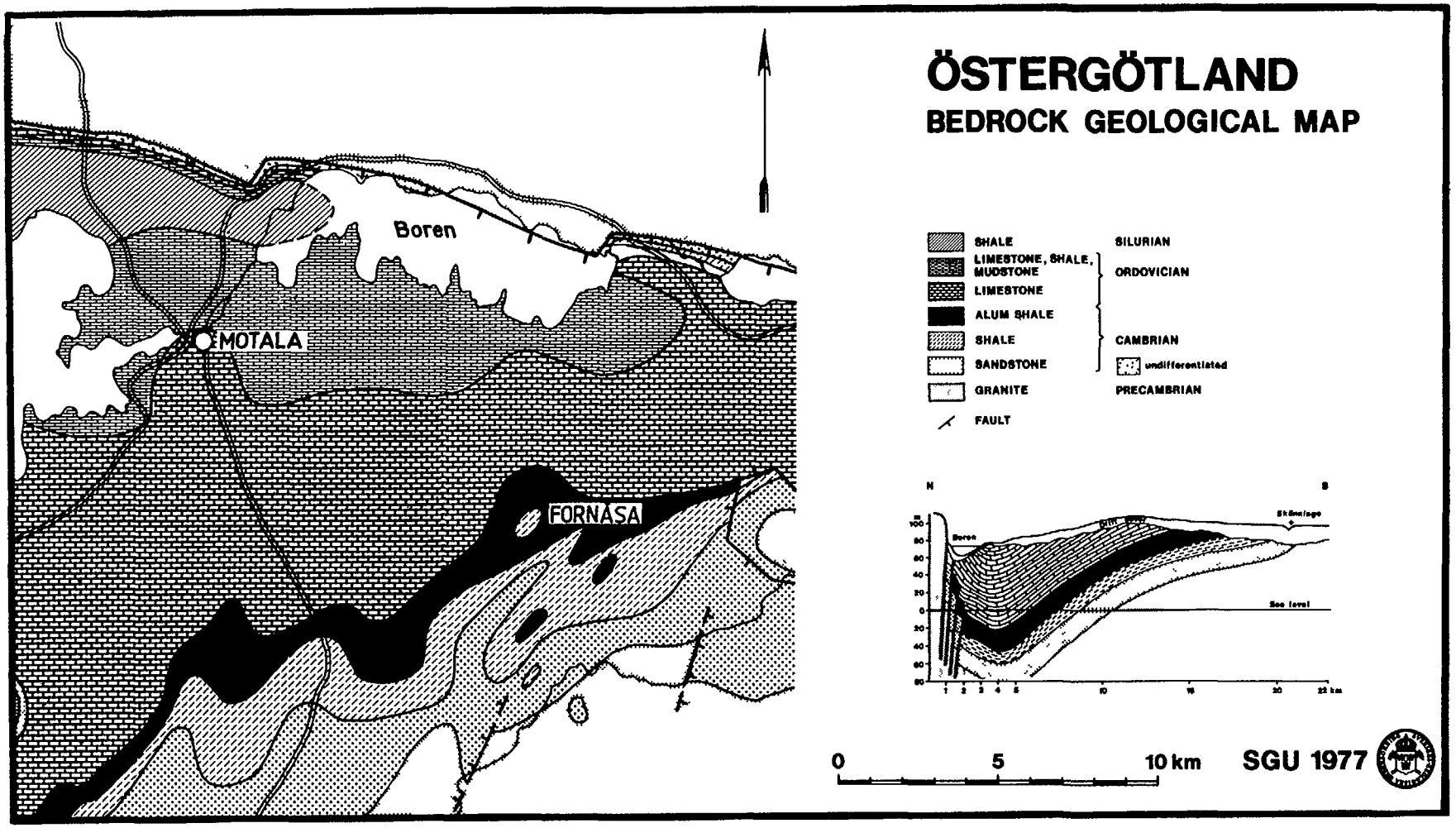

FIG. 5. Bedrock geological maps of the Motala district, Östergötland. Geological Survey of Sweden.

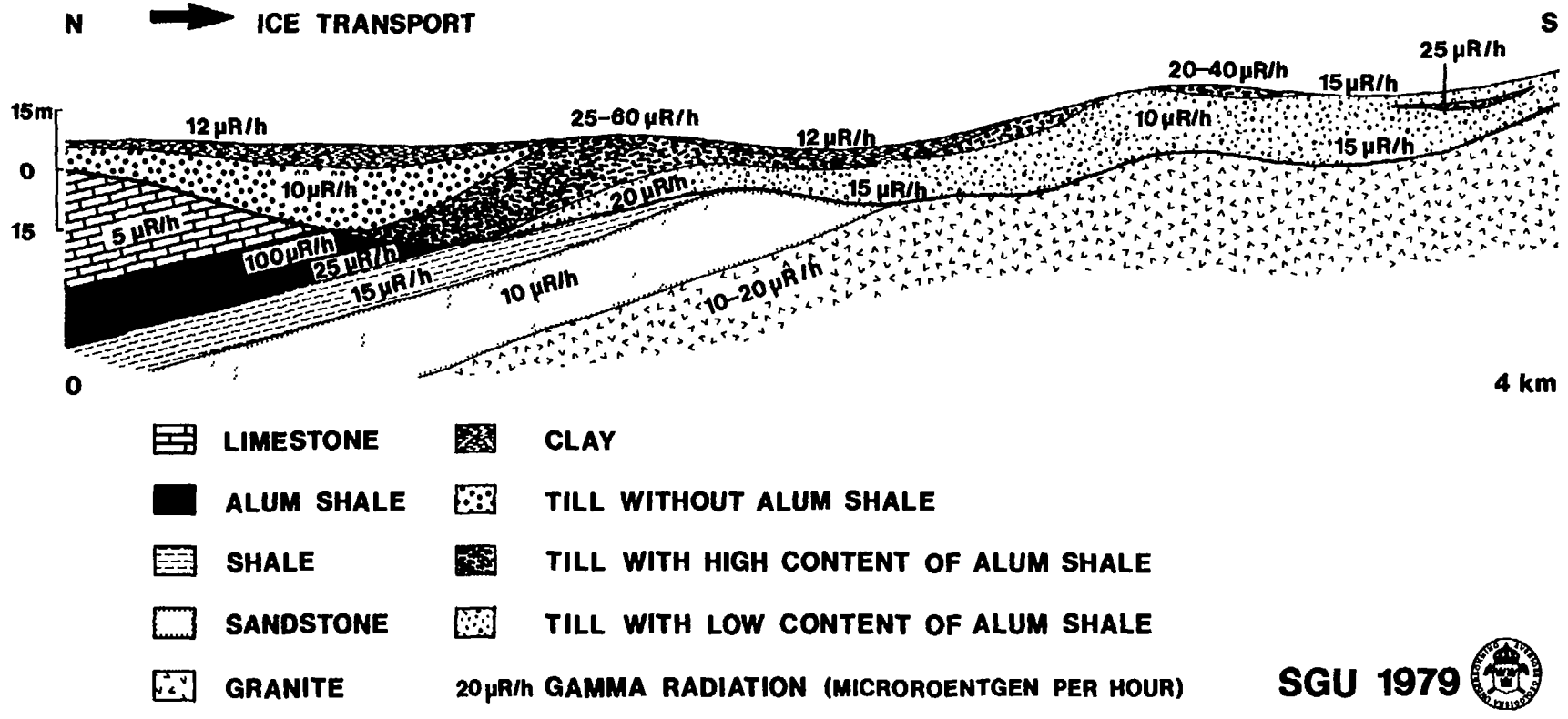

FIG. 6. Profile illustrating the distribution of alum shale fragments in the Quaternary drift cover of the Fornåsa area, Östergötland.

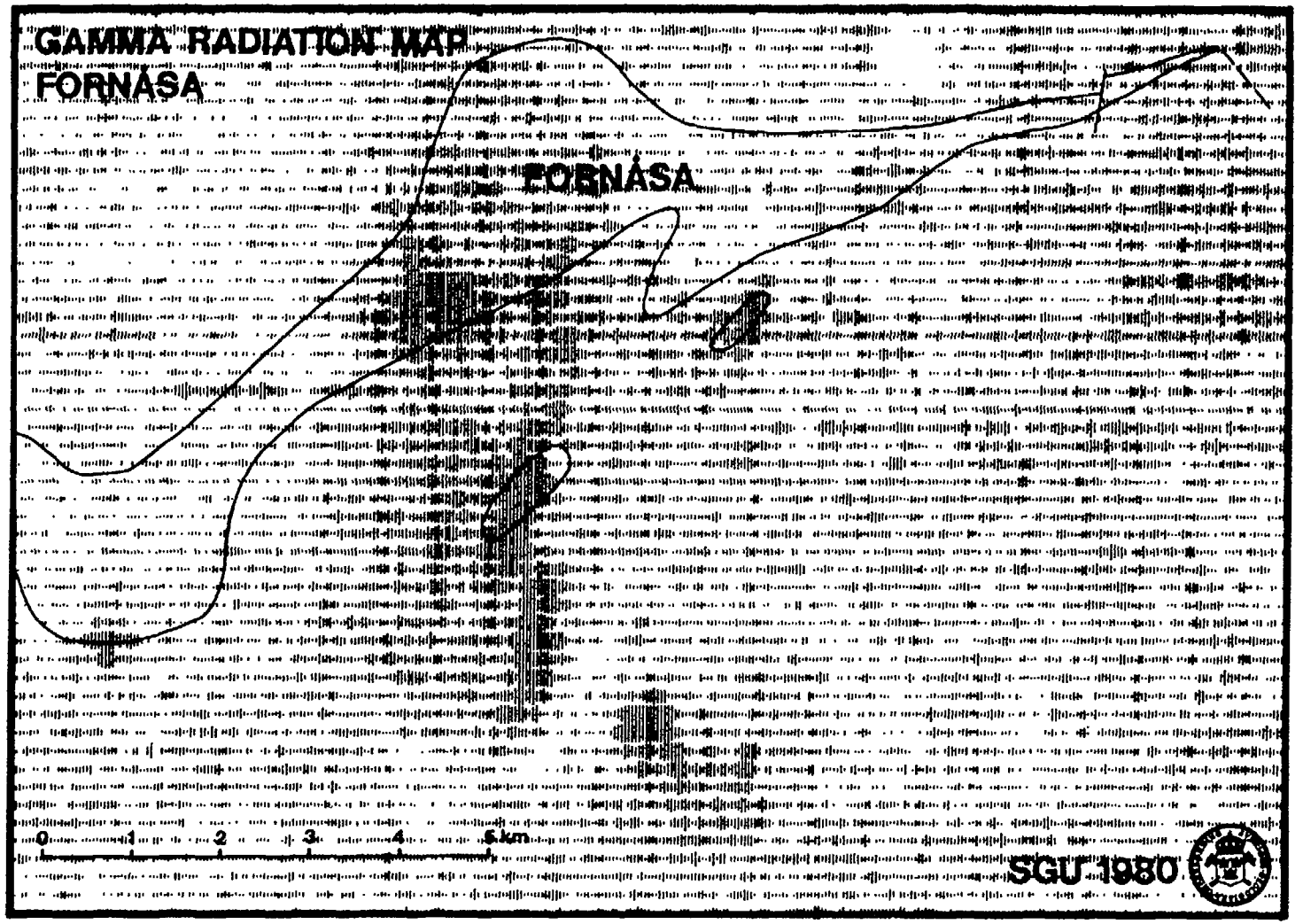

FIG. 7. Uranium-component of the gamma ray spectrometric map of the Fornåsa area, Östergötland. Original scale 1:50 000. The subcrops of the alum shale formation are outlined on the map. Measurements performed by Geological Survey of Sweden.

However, in uranium rich areas, where the uranium concentration is 10-40 ppm U, radon concentrations exceeding 800 Bq/m^3 have been measured in more than 30% of the houses. Within the thorium-rich areas, where the uranium concentration is often not is more than 3-5 ppm U, 1-5% of the houses have more than 400 Bq/m^3.

Fig. 5 shows the geological map covering part of Östergötland in southeastern Sweden. Figure 6 shows the geological profile from north to south for the same area. Fig. 7 is an enlarged detail of the gamma radiation map of Fornåsa in the centre of the area. The bedrock consists of Cambrian — Ordovician sandstones, shales and limestones that overlay Precambrian granite. The alum shale formation lies within the sedimentary sequence. The movement of the glacial inland ice was from north to south. The alum shale is entirely covered by glacial drift, mainly consisting of limestone and aqueous sediments. However, fragments of alum shale are frequent in the glacial drift in some areas. The interpretation of the radon risk in this area must take into consideration that a few decimeters of soil that totally lack alum shale will shield all gamma radiation emitted from underlying alum shale containing soils or rock. Risk of radon may exist south of the northern alum shale border, and where topsoil lacking alum shale is less than 2 metres thick or where the topsoil is penetrated by building foundations.

Fig. 8 shows the geological map covering part of the area south of Söderhamn in central Sweden, and Fig. 9 shows the gamma radiation for the same area. The whole area consists of Precambrian vulcanites and gneiss. These rocks are penetrated by pegmatites which are often uranium rich. Some outcropping pegmatites are recorded by the airborne surveys. Others are covered by glacial drift or sediments, are thus shielded. When interpreting the radon risk, this must be taken into consideration.

Gamma radiation maps are, as shown above, a useful tool for radon risk evaluation. For some areas, they give all the information required for mapping the radon risk and for others they can point to areas where the risk of radon may be high. However, in most cases ground checks need to be made. Special attention is required to define the borderlines between soil and bedrock with differing radon potentials. Fieldwork is largely based on geological observation combined with continuous measurements of gamma radiation by scintillometer. In general, if the gamma radiation is low, it is often possible to classify an area as a low potential radon risk area without any further measurements.

There is a direct correlation between the gamma radiation and the concentration of radium, as follows:

The gamma radiation from a large flat outcrop is [6]:

per	1 ppm U	(12.3 Bq/kg radium-226)	= 0.653 μR/h
	1 ppm Th	(4.0 Bq/kg thorium-232)	= 0.287 μR/h
	1 % K	(310 Bq/kg potassium-40)	= 1.505 μR/h

assuming no disequilibrium within the uranium and thorium series.

(1 μR/h = 0.01 μSv/h)

However, more than 75% of field-measured gamma radiation is derived from the upper two decimeters of soil.

If the gamma radiation is more than 12-15 μR/h, the radium-226 content in the bedrock or soil may be so high that the radon concentration in the soil air will exceed 50 000 Bq/m^3. But gamma radiation can also come from thorium and its decay products, and from potassium-40, (though the concentration of ^{40}K in the bedrock and soil is never high enough to cause gamma radiation levels above 8 μR/h). Enhanced radiation caused by thorium will not result in enhanced radon risk, except

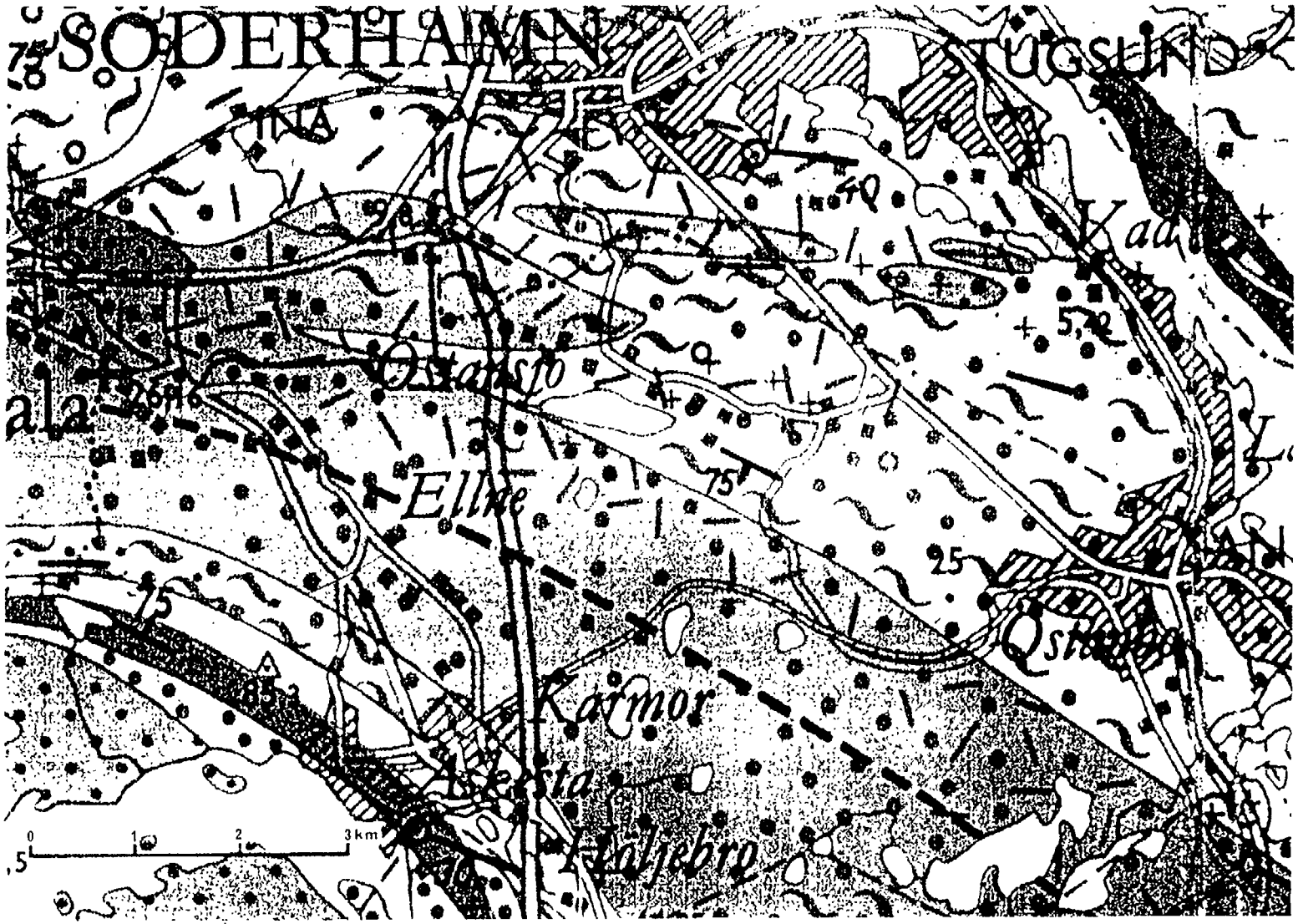

FIG. 8. Bedrock geological map of the area south of Söderhamn. Light grey = paragneiss. Grey = gneissic granites. Dark grey = basic volcanites. Dotted = coarse-grained granite. Original scale 1:200 000. Geological Survey of Sweden, Ser. Ba 22.

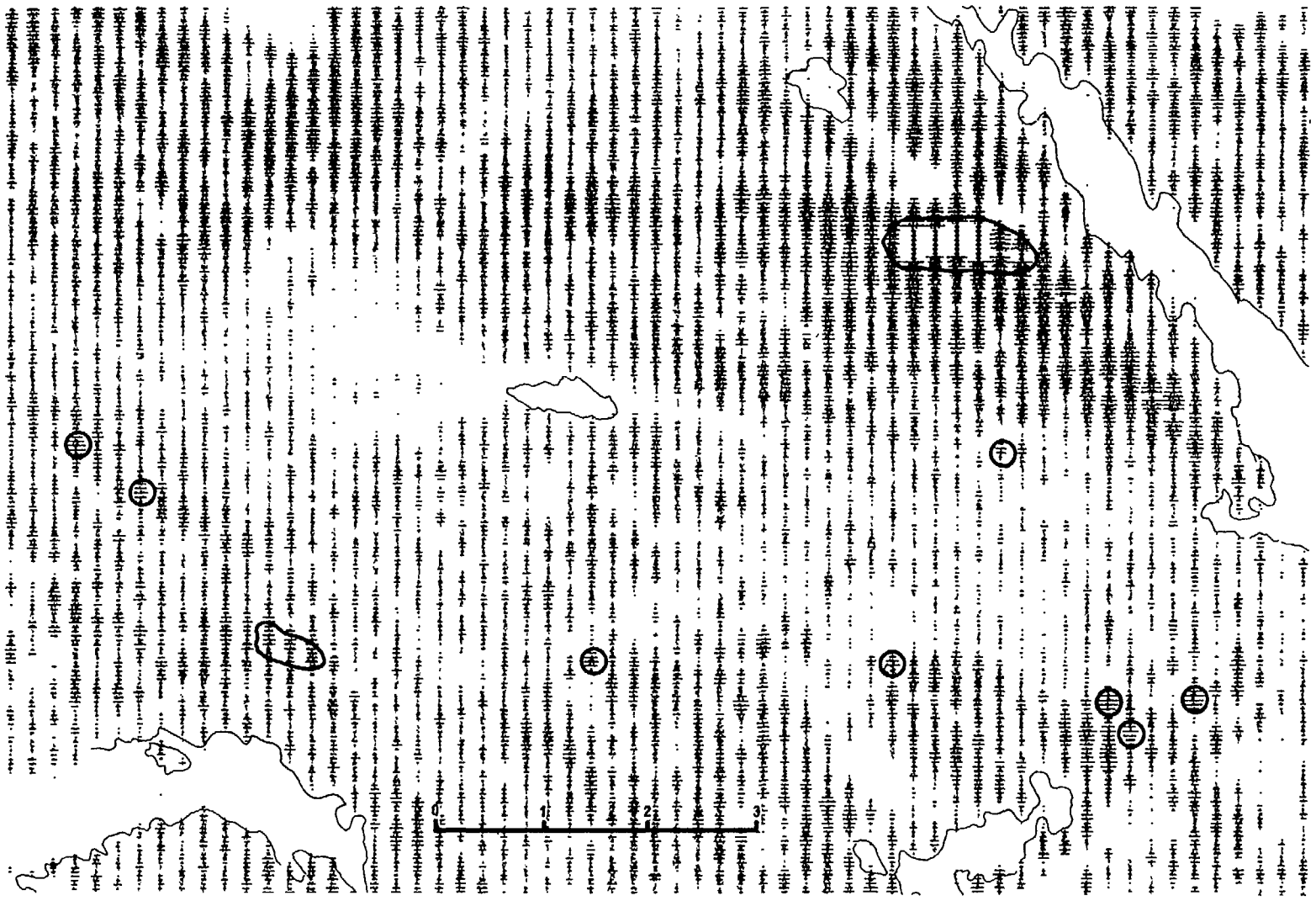

FIG. 9. Gamma spectrometric map of the area south of Söderhamn. Thin lines = uranium. Thicker grey lines = thorium. The ++++ represents recordings of more than 15 ppm eU. Marked positions indicate field locations investigated in the follow-up of airborne measurements. Original scale 1:50 000. Measurements performed by Swedish Geological Co.

where the thorium concentration is high (more than approximately 300 Bq/kg). In this case, thoron gas could present a health hazard.

When mapping large areas, such as a district or county, orienting radon measurements are made. The actual locations of these measurements are chosen on the basis of geological data to give maximum information. However, the number of radon measurements must be rather limited, for economical reasons. One should also remember that measurements of radon in soil air are only relevant for that spot and for a small area around it. At best, the values obtained are valid for a specific soil type with a specific radium content. The latter may vary substantially at different locations.

When investigating small areas, such as building sites, the work begins with measuring the gamma radiation in the area. If enhanced gamma radiation, more than 12 μR/h for soils and more than 15 μR/h for rocks, is encountered the only way to investigate whether the rock poses a risk or not is to determine the radium-226 concentration by gamma spectrometric measurements. If the gamma radiation from a soil is enhanced, the radon potential can be established either by in situ measurements with a gamma spectrometer or by measurements of the radon concentration in the soil air. However, if the bedrock crops out at the site or if the soil layer is less than one metre thick, there is no point in measuring the radon concentration, as the results would have very little to do with the situation after the houses are built. Neither is it useful to make radon measurements in fill of blasted rock. The radon concentration in the fill depends on how much the wind ventilates the layer of fill.

In Sweden, it is generally agreed that radon measurements should be made at a minimum depth of 70 centimeters. However, it is my opinion that the measurements should be made at a depth of one metre or more, in order to reduce both the effect of ventilation of the soil by wind and the effect of percolating rain water. The aim of the radon measurements is to establish a situation similar to that which will exist once the ground has been built upon. After construction, the radon exhalation is greatly reduced due to the fact that the ground surface is covered by concrete slabs, asphalt roads and clayey topsoil. This makes the radon concentration in the pore spaces increase towards its maximum. The maximum radon concentration in the soil air is expressed by equation (1) [2].

Equation (1) for calculation of the maximal radon concentration in *soil air* or *water* in a pore space.

$$C_{max} = A \cdot e \cdot \delta \cdot \frac{1-p}{p} \qquad (1)$$

C_{max} = radon concentration in the pore space at 0 air changes per hour, ach (Bq m^{-3})
A = activity of ^{226}Ra (Bq kg^{-1})
e = emanation (%)
δ = compact density (kg m^{-3})
p = porosity (%)
e cannot exceed p, $e \leq p$

Normally a ^{226}Ra concentration of 12 Bq kg^{-1} (eq. to 1 ppm U) gives a maximum concentration of 20,000 Bq m^{-3} in the pore space.

In Table IV, normal radon concentrations in soil air are given for different Swedish soils.

In Sweden, several methods are used for radon measurements. Emanometers usually give reliable results for permeable soils such as sand and gravel, but they give highly variable results for impermeable soils, such as silt and clay. The wide spread of values is interpreted as due to variation in moisture content, and the availability and mobility of soil air.

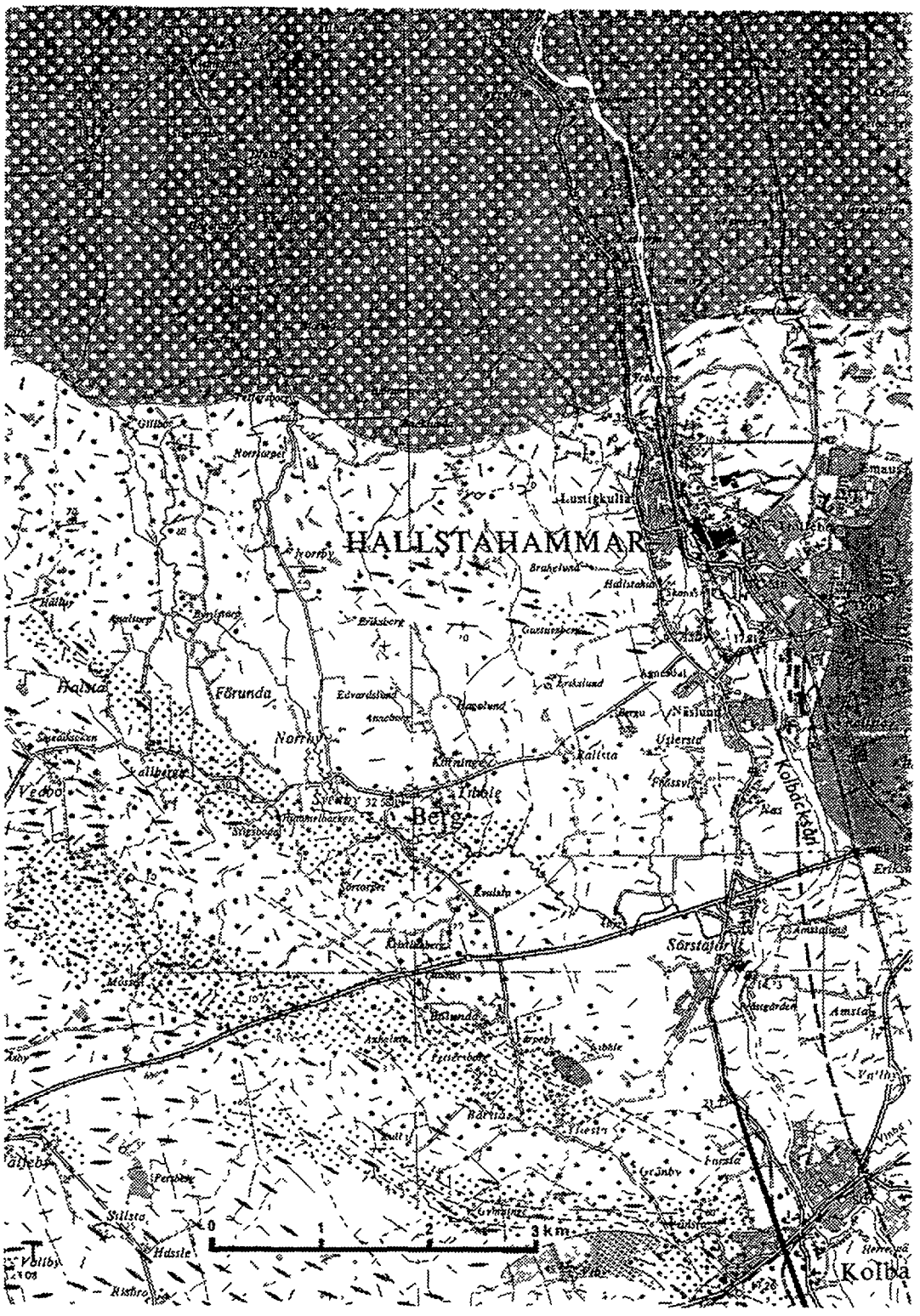

FIG. 10. Bedrock geological map of the western part of the Hallstahammar municipality. Dark grey with white dots = red granite with microcline augen, Grey = non-prophyritic granite. Light grey = granodiorite. Original scale 1:50 000. Geological Survey of Sweden, Ser. Af nr. 122.

FIG. 11. Quaternary geologic map of the western part of the Hallstahammar municipality. Grey with dots = gravel and sand in the esker and other glaciofluvial deposits. Light grey = till. White = clay and silt. Dark grey = outcrops. Original scale 1:50 000. Geological survey of Sweden, Ser Ae nr 35.

TABLE IV. NORMAL RADIUM-226 AND RADON-222 CONCENTRATIONS IN SWEDISH SOILS, MEASURED AT 1 M DEPTH.

	^{226}Ra (Bq/kg)	^{222}Rn (Bq/m^3)
Till, normal	15 - 50	5 000 - 40 000
Till, with granitic material	30 - 75	20 000 - 60 000
Till, with uranium-rich granite material	75 - 350	40 000 - 200 000
Gravel and coarse sand in glaciofluvial deposits	20 - 75	10 000 - 150 000
Sand and coarse silt	5 - 25	4 000 - 20 000
Silt	10 - 50	20 000 - 60 000
Clay	25 - 100	10 000 - 120 000
Soils containing alum shale	175 - 2500	50 000 - >1 Mill.

Note: 12.3 Bq/kg 226Ra is equivalent to a concentration of 1 ppm U.

Charcoal cups (the ROAC, Radon On Activated Charcoal method) are also frequently used. They are reliable in most cases. But in clay and silt, the surface area at the bottom of the sampling hole must be enlarged, so that radon can exhale from a larger soil area, otherwise the result may be too low.

Alpha track films were one of the first methods used. However, these did not produce reliable or reproducible results. The results were often too low, compared with the real radon concentration in the soil air. The use of thoron filters improved the measurements but the errors were still great. One explanation is that condensation creates water droplets on the film surface that prevent the alpha particles from making tracks.

Fig. 2 shows the Radon Risk Map of the Hallstahammar municipality which has the highest average radon concentration of indoor radon in Sweden. Of the houses measured, 9 % had indoor radon concentrations greater than 2 000 Bq/m^3. The houses are, to a large extent, built on granites with enhanced uranium concentrations and on the esker, that runs from north to south through the municipality. In a house situated at the top of the esker, the indoor radon concentration was 60 000 Bq/m^3. The soil in the esker consists mainly of sand, gravel and stones derived from the uranium-rich granite to the north of the municipality (Figs 10, 11 and 12). The esker areas, the uranium-rich granite areas and the areas with uranium-rich granite till form high risk areas. The areas with clay and fine silt form low risk areas, and the areas with normal uranium content in the till and bedrock form normal risk areas. The results from gamma measurements, gamma spectrometric measurements and radon measurements in the central part of the municipality are shown in Figure 13. The highest radon concentration measured in the gravel air within this area is 78 000 Bq/m^3. However, in the till beyond the northern boundary of the map, levels of 100 000 to 300 000 Bq/m^3 were measured.

4. EVALUATION

Radon Risk Maps have now been in use since 1982. They may be of different qualities. However, our experience is that they give valuable information for planners and builders. Even

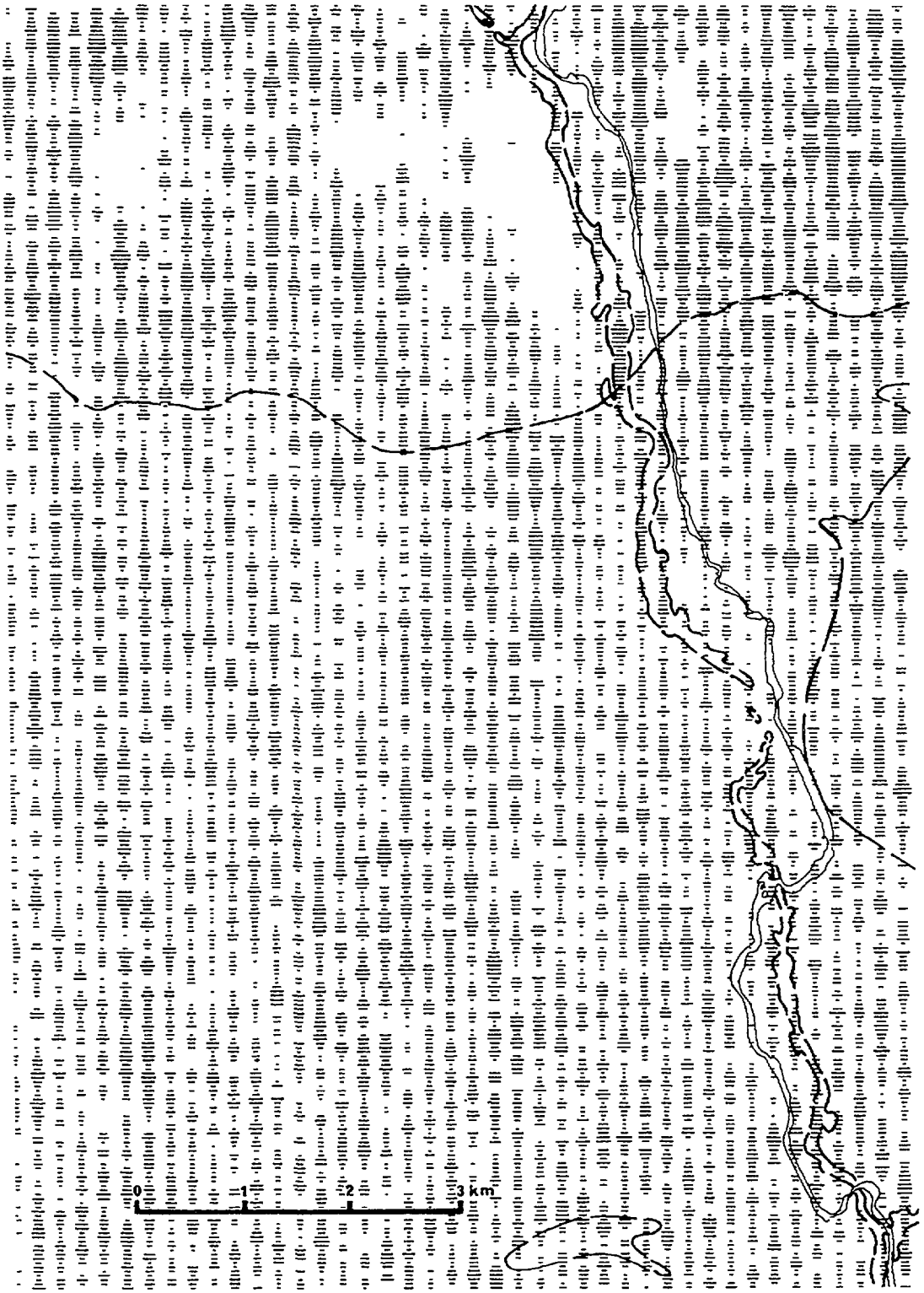

FIG. 12. Map of airborne gamma ray spectrometric measurements (uranium-component) over the western part of the Hallstahammar municipality. Marked on the map are the borders of the uranium and thorium rich granite areas, the esker and the Kolbäcksån river. Original scale 1:50 000. Measurements performed by Swedish Geological Co.

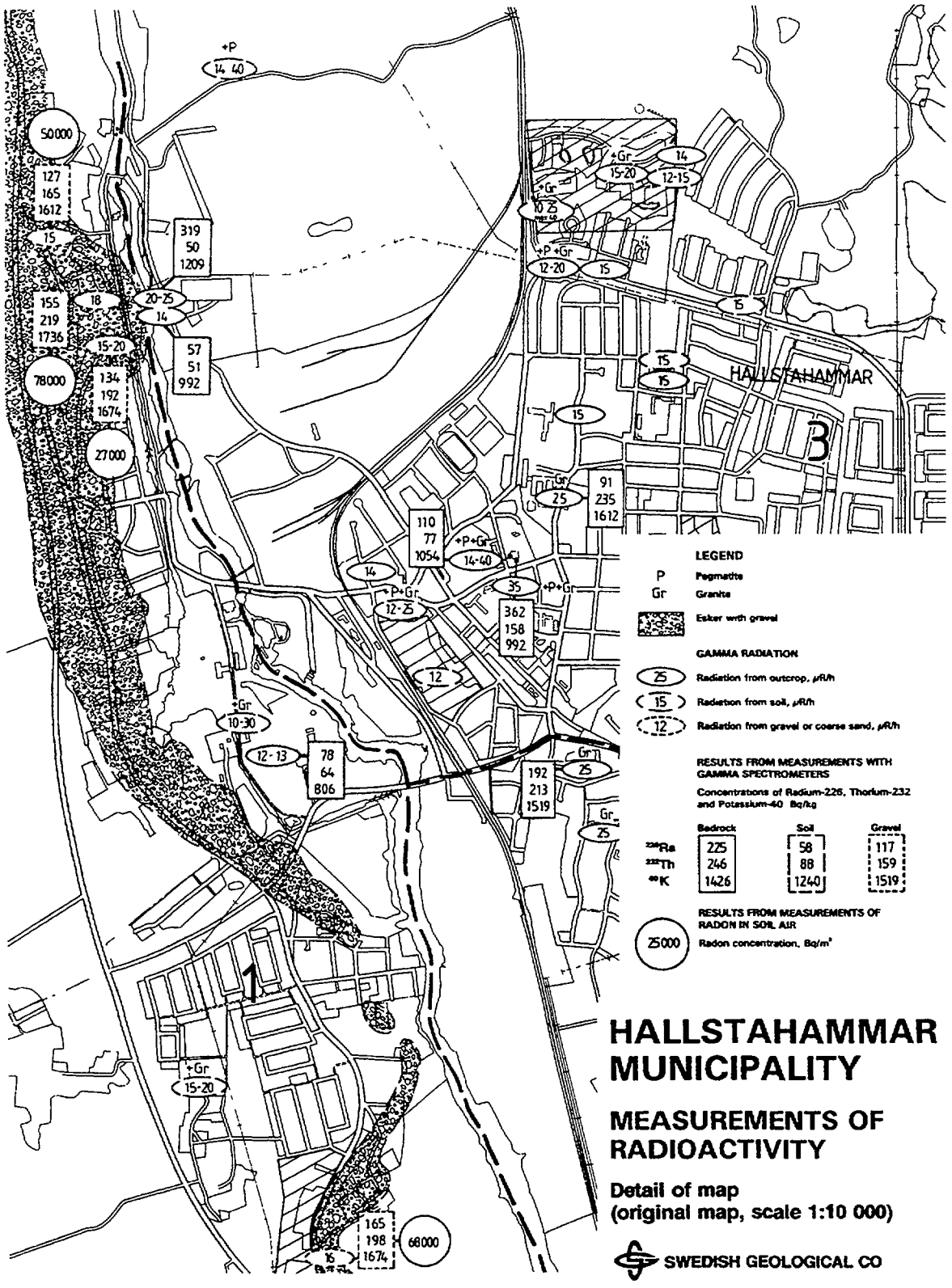

FIG. 13. Map of the central part of Hallstahammar municipality showing results obtained by total gamma, gamma ray spectrometric and radon measurements from the field made when mapping the radon potential of the ground.

though the main purpose of the maps was to provide information for the planning and building of new houses, they have also proved to be useful in pointing out areas where existing houses have enhanced levels of indoor radon.

REFERENCES

[1] ANDERSSON, A., DAHLMAN, B., GEE, D.G., SNÄLL, S., The Scandinavian Alum Shales. Geological Survey of Sweden Ser. Ca, nr 56, Uppsala (1985) 50 p. ISBN 91-7158-334-3.

[2] ANDERSSON, P., CLAVENSJÖ, B., ÅKERBLOM, G., The effect of the ground on the connection of radon and gamma radiation indoors. Report R 9:1983, Swedish Council for Building Research, Stockholm (1983) (in Swedish), 442 p. ISBN 91-540-3866-9.

[3] ÅKERBLOM, G., CLAVENSJÖ, B., ANDERSSON, P., Soil gas radon — a source for indoor radon daughters. Radiation Protection Dosimetry. Vol. 7. No. 1-4 (1983) 49-54.

[4] ÅKERBLOM, G., WILSON, C., Radon - geological aspects of an environmental problem. Papers presented at the International Meeting on Radon - Radon Progeny Measurements, Montgomery, Alabama, August 27-28 (1981) Geological Survey of Sweden, Reports and communications no. 30, Uppsala (1982) 47 p. ISBN 91-7158-271-1.

[5] ÅKERBLOM, G., Investigation and mapping of radon risk areas. Paper presented at the International Symposium on Geological Mapping in the Service of Environmental Planning: Subcommission for Maps on environmental Geology, Trondheim, Norway. May 6-9 1986. In: Geology for Environmental Planning, edited by Wolff F C. Geological Survey of Norway. Special papers 2 (1986) 96-106. ISBN 82-7385-029-3.

[6] INTERNATIONAL ATOMIC ENERGY AGENCY, Airborne Gamma Ray Spectrometer Surveying, Technical Reports Series No. 323, IAEA, Vienna, (1991).

[7] LINDEN, A., ÅKERBLOM, G., Method of detecting small or indistinct radioactive sources by airborne gamma ray spectrometry. In: Geology, mining and extractive processing of uranium. Editor: Jones M J, Institute of Mining and Metallurgy. London (1976) p. 111-120.

[8] MELLANDER, H., Airborne gamma spectrometric measurements of the fall-out over Sweden after the nuclear reactor accident at Chernobyl, USSR. IAEA/NENF/NM-89-1, Internal report (1989).

[9] THE NATIONAL SWEDISH BOARD OF URBAN PLANNING AND BUILDING, Radon — planning, building permit and protective measures. Statens planverk report 59, Stockholm (1982) (in Swedish), p. 28.

[10] WILSON, M.R., ÅKERBLOM, G. V., Geological setting and geochemistry of uranium-rich granites in the Proterozoic of Sweden, Mineralogical Magazine, Vol 46 (1982) 233-45.

QUANTITATIVE MODELLING OF RADON POTENTIAL IN FLORIDA AND THE USE OF AERORADIOMETRIC DATA

(Summary)

J.K. OTTON
US Geological Survey, Denver, Colorado

K.K. NIELSON
Rogers and Associates Engineering, Salt Lake City, Utah

R.B. BROWN, P.D. ZWICK
University of Florida, Gainesville, Florida

T.M. SCOTT
Florida Geological Survey, Tallahassee, Florida

United States of America

In April 1991, the Florida Radon Research Program of the Florida Department of Community Affairs began a statewide quantitative assessment of radon potential. As part of this assessment a mathematical model (Eq. (1), in steady state form) was developed by Rogers and Associates Engineering (RAETRAD) to describe the radon concentration (Cb) at any given location in a multilayered volume of soil and underlying sediment that extends from the surface to 5 m depth (Nielson and others, 1991).

$$\nabla \times f_a D \nabla (C_b / f_s) - \nabla \times [9K/\mu)(C_b/f_s) \nabla P] - \lambda C_b + R \rho \lambda E = 0 \qquad (1)$$

where

∇ = gradient operator
f_a = $p(1S + Sk_H)$
p = soil porosity (dimensionless: cm^3 pore space per cm^3 bulk space)
S = soil water saturation fraction (dimensionless)
k^H = ^{222}Rn distribution coefficient (water/air) from Henry's Law (dimensionless)
D = diffusion coefficient for ^{222}Rn in soil pores ($cm^2\ s^{-1}$)
C_b = $f_S C_a$ = ^{222}Rn concentration in bulk soil space (pCi cm^{-3})
Ca = ^{222}Rn concentration in air-filled pore space (pCi cm^{-3})
fs = $P(1-S+Sk_H)+\rho k_a$
ρ = soil bulk density (g cm^{-3}, dry basis)
k_a = $k_{ao}\ exp(-bS)$
k_{ao} = dry-surface adsorption coefficient for ^{222}Rn ($cm^3\ g^{-1}$)
b = adsorption-moisture correlation constant (g cm^{-3})
K = bulk soil air permeability (cm^2)
μ = dynamic viscosity of air (Pa s)
∇P = air pressure gradient (Pa cm^{-1})
λ = ^{222}Rn decay constant ($2.1 \times 10^{-6}\ s^{-1}$)
R = soil ^{226}Ra concentration (pCi g^{-1})
E = total ^{222}Rn emanation coefficient (air + water, dimensionless).

The model accounts for the diffusive and convective components of radon movement in soil gas. The model equation requires data for the radium content of the layers of soil and underlying substrate, the emanating power of soil materials, the soil moisture content, seasonal water-table fluctuations, and soil permeability, density, and porosity.

The assigned radium concentrations (R in Eq. (1)) in surface layers (0-2 m, number and thickness of layers are defined in soil datasets) are average equivalent radium values that are calculated from 214Bi gamma-ray intensities recorded along aeroradiometric flightlines in the National Uranium Resource Evaluation (NURE) Survey. The lower layers (2-5 m) are assigned radium values based on the NURE aeroradiometric signature of surface exposures, a total-count survey from the northern 40 percent of the State (Grosz and others, 1989), radium analyses of archived samples, and drillhole descriptions of the abundance of phosphate in underlying geologic units. Other model parameters are estimated from measured physical properties, descriptions of the soil map units, and empirical relations (between radium content and emanating power, for example) established by experimental studies.

The model results describe the radon concentrations (Cb values) at various points beneath a reference Florida slabon-grade residence (Fig. 1). A separate radon entry model (Eq. (2)) based on house parameters calculates the rate of entry in pCi/s (or mCi/yr).

$$Q = 10\ [(C_s\ p_s\ D_s\ A_h)t_c + (C_c\ p_s\ D_s\ A_c)/t_c + A_c\ C_c\ v] \qquad (2)$$

where

Q = indoor radon entry rate (pCi s^{-1})
10 = unit conversion
C_s = area-weighted average sub-slab radon concentration (pCi L^{-1})
p_c = concrete effective total porosity
D_c = concrete radon diffusion coefficient ($cm^2\ s^{-1}$)
A_h = house floor area (m^2)
t_c = concrete floor thickness (cm)
C_c = radon concentration at the base of the floor crack (pCi L^{-1})
p_s = effective total porosity of the surface soil layer
D_s = radon diffusion coefficient, surface soil layer ($cm^2\ s^{-1}$)
A_c = floor crack area (m^2)
v = air velocity through the floor crack (cm s^{-1})

Values for the house parameters are given in Table I.

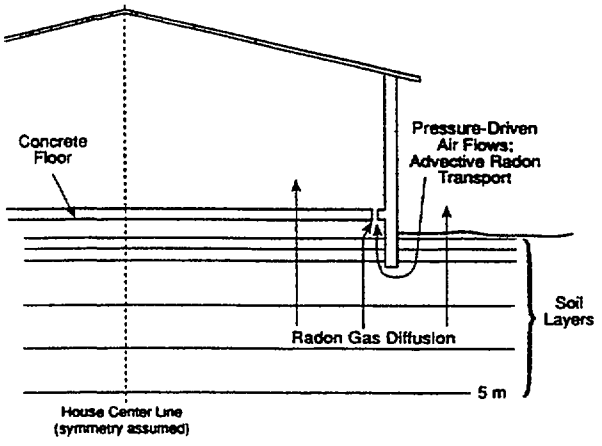

Fig. 1. Diffusive and advective radon entry into a reference house from the underlying soil profile.

TABLE I. NOMINAL VALUES OF PARAMETERS USED IN RADON ENTRY CALCULATIONS FOR THE REFERENCE HOUSE

House area	143 m^2
Fill soil thickness	30 cm
House dimensions	8.6 × 16.5 m
Indoor pressure	-2.4 Pa
House length/width	1.9 (ratio)
Concrete slab thickness	10 cm
Hose volume	350 cm^3
Concrete slab porosity	0.22
House ventilation rate	0.25 h^{-1}
Concrete slab ^{226}Ra. emanation	0.07 pCi g^{-1}
Floor crack width	0.5 cm
Exterior footing depth	61 cm
Floor crack location	slab perimeter
Concrete air permeability	1×10^{-11} cm^2
Crack area fraction	0.002
Concrete Rn diffusion coefficient	8×10^{-4} cm^2 s^{-1}

The radon entry values (Q) can then be used in a third model Eq. (3) to calculate expected average annual indoor radon levels.

$$C_h = 114\ Q\ /\ (V_h \lambda_h) \tag{3}$$

where

C_h = indoor radon concentration (pCi L^{-1})
114 = unit conversion (pCi L^{-1} h^{-1}/mCi m^{-3} y^{-1})
Q = potential radon entry rate (mCi y^{-1})
V_h = house volume (m^3)
λ_h = house ventilation rate (h^{-1}).

Calculated radon entry values for a defined typical reference house are determined for each of several hundred map polygons. The polygons are defined by the merging of a digital geologic map of Florida with a generalized digital soil map for the State. Each soil/geology polygon is given a unique name to which the radium and soil data are attributed.

The radium signature for surface layers in each polygon is directly calculated from flightline eU values for intersected polygons. Radium values for polygons not overflown are represented by the overall geometric mean for the geologic unit in which the polygon was classified. The result is a GIS ARC/INFO map of the State that can display either radon entry values (Q, Eq. (2)) or means of expected indoor radon values (C_h, Eq.(3)). The map can be verified either by comparing calculated radon entry values (flux into a reference house) with field soil-surface radon flux measurements or

by comparing expected indoor radon values with observed indoor radon measurements. For the State of Florida, the 10-km flightline spacing of the NURE dataset is a primary limitation of the resolution achievable for the radon potential map. The minimum permitted size of a geology/soil polygon will probably be in the range of 2.56 to 10 km^2.

BIBLIOGRAPHY

GROSZ, A.E., CATHCART, J.B., MACKE, D.L., KNAPP, M.S., SCHMIDT, WALTER and SCOTT, T.M., Geologic interpretation of the gamma-ray aeroradiometric maps of central and northern Florida: U.S. Geological Survey Professional Paper 1461 (1989) 48 p.

NIELSON, K.K., ROGERS, V.C., BROWN, R.B., HARRIS, W.G., and OTTON, J.K., Prototype mapping of radon potentials in Florida: The 1991 Annual American Association of Radon Scientists and Technologists National Fall Conference: Preprints volume I (1991) 145-162.

RADON LEVELS OF ROCK FORMATIONS IN ISRAEL

(Summary)

U. VULKAN
Soreq Nuclear Research Center, Yavne, Israel

M. SHIRAV (SCHWARTZ), Y. SHILONI
Geological Survey of Israel, Jerusalem, Israel

Radon concentrations of rock formations (and soils) were measured directly at more than 70 sites, representing stratigraphic units which constitute the main rock exposures in Israel. The purpose of this project is the production of a map indicating radon levels in rocks, as a planning means for the pertinent authorities. In order to meet local conditions, a modified alpha-track detection system was implemented, consisting essentially of a polycarbonate foil within a PVC pipe. The detectors are inserted into shallow ($\sim$50 cm) drillholes at the test sites (usually 20-30 detectors for each location). The detector is attached to a plastic cup which serves as a thermal isolator and minimizes vapour condensation. Thoron (^{220}Rn) signal is reduced by a membrane placed in front of the polycarbonate foil. The detectors are buried for a period of up to 28 days (according to the radon level). After removal, the foils are electrochemically etched and track densities are counted. Calibration of the track density versus absolute activity is accomplished by a special designed calibration cell with a known radon source. Nearly all stratigraphic units which were studied (Precambrian basement; Cenomanian — Turonian limestones and dolomites; Eocene carbonates and Neogene to Recent basalts, sediments and soils) exhibit radon levels (less than 250 pCi/l) which do not require any special sealing in buildings founded on these rocks' exposures (based on Swedish guidelines). Average radon levels in southern outcrops of the Campanian — Maastrichtian Mount Scopus Group, which consists of chalks, cherts and phosphoritic layers, are usually higher than 1000 pCi/l, demanding appropriate sealing during construction. Rock units within the Mount Scopus Group in northern Israel show intermediate radon levels (250-1000 pCi/l), calling for local, specific studies in limited areas before construction. Summary of the radon levels which were determined for each group is given in Fig. 1. The radon source in the Mount Scopus Group rock units is the apatite (calcium phosphate) content — from $\sim$2 Wt.% P_2O_5 up to $\sim$30% in the phosphate layers, corresponding to uranium concentrations of up to 150 ppm. These rock units, which are down-faulted and buried along the Dead Sea Rift Zone, are believed to be also the source for high radon emanations in the vicinity of some faults and thermal water springs in this area.

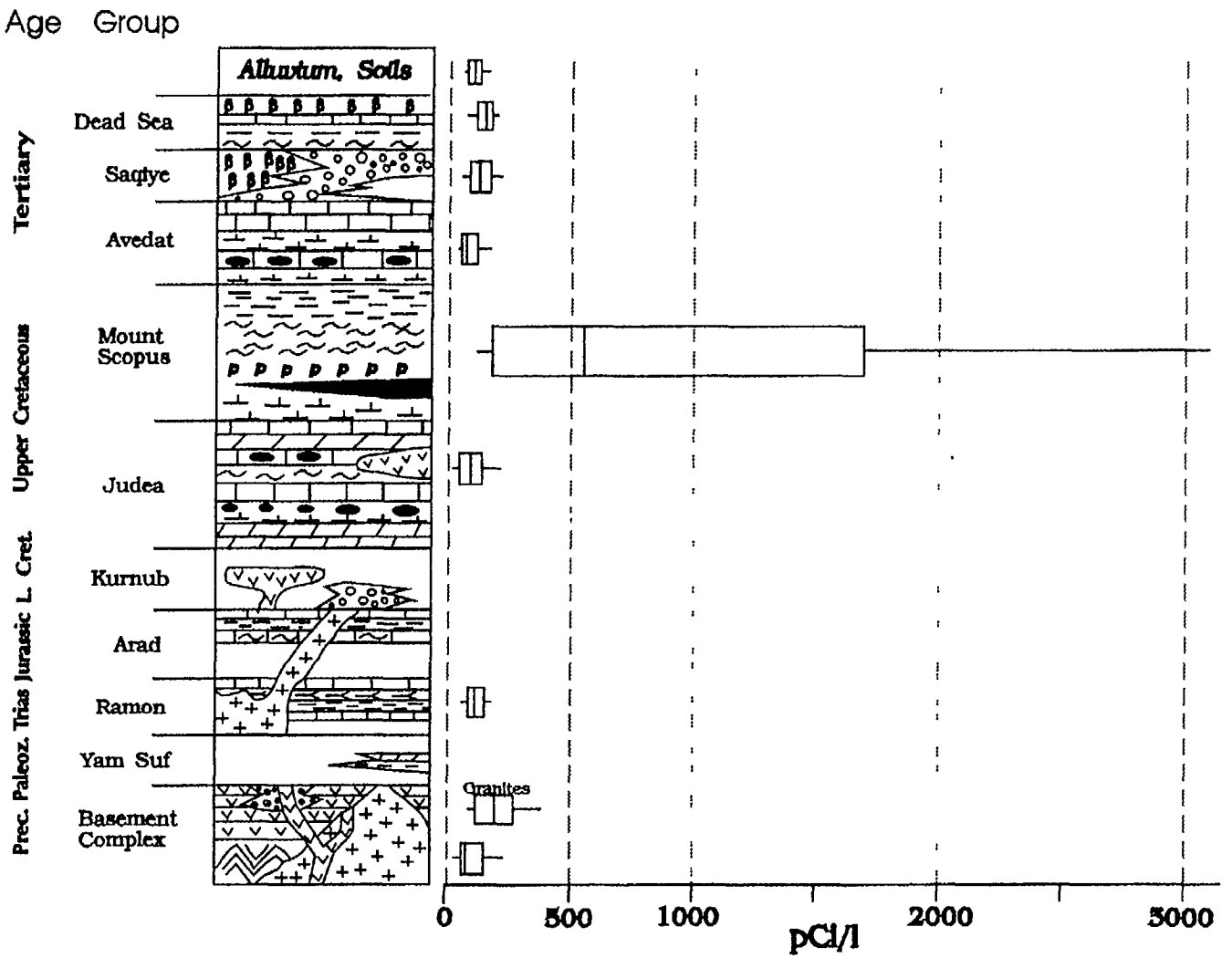

FIG 1. Box plots indicating radon levels of rock formation in Israel. The vertical spread in each box represents 50% of the data between the 25 and 75 percentiles; the line in each box is the median. Vertical lines extending from the boxes are bound at the 10 and 90 percentiles.

THE ROLE OF MOBILE GAMMA SPECTROMETRY IN THE SWEDISH EMERGENCY RESPONSE PROGRAMME FOR NUCLEAR ACCIDENTS — EXPERIENCE AND FUTURE PLANS

H.MELLANDER
Swedish Radiation Protection Institute,
Division of Environmental Radiology,
Stockholm, Sweden

Abstract

The airborne gamma spectrometry measurements in Sweden after the 1986 Chernobyl accident are widely acknowledged as having been of significant importance in all stages of the radiation protection work following the accident. The Swedish Radiation Protection Institute (SSI) and other government organizations, local and regional Swedish authorities and scientists have been working on the effects of the accident for years. Maps and data produced from the airbome radiometric measurements are often used as background material. The airborne measurements were carried out without proper preparation and calibration due to the urgency of the task and the unexpected situation. Many problems were encountered, some of them affecting the quality of the results. The scientific work performed since 1986 has revealed some errors in the data and maps. The experience can be used to make the mobile gamma spectrometry resource significantly more powerful than the one available in 1986. Changes in the Swedish emergency response organization is presented and the proposed use of additional light weight moveable and mobile gamma spectrometry systems is described.

1. BACKGROUND — THE EVENTS IN 1986 SUMMARIZED

At the time of the Chernobyl nuclear power plant accident in April 1986 the emergency planning in Sweden was primarily focused on the possibility of a fault in one of the twelve domestic light water reactors. The fixed station monitoring system consisted of 25 [7] ionization chambers. The stations were not automatic. Results were usually reported weekly unless the local operator decided otherwise. Seven ultra high volume air sampling devices were operated by the Swedish Defense Research Establishment (FOA) characterized by an extremely low detection limit for airborne radioactivity. The gamma measuring instrumentation suitable for environmental monitoring were high resolution solid state gamma spectrometers operated by FOA and a few other organizations and a large number of scintillation counters and a few NaI gamma spectrometers owned and operated by the Swedish Geological Company (SGAB).

SGAB had two airborne gamma spectrometer systems, one of them barely returned from a mission in Botswana.

The first alarm came from the nuclear power plant at Forsmark (100 km north of Stockholm) on Monday morning, 28 April, where activity was detected on personnel entering the plant. The gamma station at Olands Sodra Udde showed an activity increase already on Sunday morning [8] but due to the delayed reporting this was not known at the time. After a few hours of confusion it was concluded that the activity source must be outside Sweden [11] and probably in the Soviet Union. A chain of frantic efforts had been started aiming at getting a good picture of the accident and its consequences in Sweden.

The airborne division of SGAB in Uppsala was contacted by SSI on Wednesday 30 April, and was asked if one airborne system could be used for mapping of fallout in Sweden. The SGAB systems were at that time not in use and it took approximately 24 hours to get the requested system in air.

Meanwhile SSI had received some information on the extent of the fallout. Measurements had been reported to SSI from various parts of the country. The quality of these measurements was sometimes questioned but nonetheless clearly the eastern middle part of the country was affected by significant fallout.

SSI had conducted a car borne survey with scintillation counters starting in Stockholm, going north, almost to Gavle and then west, southwest and back to Stockholm. This route missed the "hottest area" by a few kilometres but passed some semi-hot areas in northern Uppland and Vastmanland. One of these areas was considered so interesting that the SGAB aircraft was directed to it on the first mission on I May. A small area was mapped and reported the following morning to SSI. The fallout was significant but no hot spots were detected and no indications on increased or decreased activity in any direction.

After this initial effort the measurements were aimed at a large scale survey and the country was covered by flight-lines giving a good overall picture of the fallout and also in the hottest areas where the line distance was smaller a fairly good detailed picture. A total of approximately 36000 line kilometres were measured and numerous maps showing the fallout in exposure rate units of μR/h and Cs-134 and Cs-137 in kBq/m^2 were produced (Fig. 1) [10].

2. THE SGAB AIRBORNE SYSTEM — DESIGN AND CALIBRATION

The SGAB airborne radiometric system is integrated into a geophysical system comprising radiometric, magnetic, and electromagnetic instrumentation (Fig. 2). The system has been in operation since 1967 but has been completely changed over the years. The radiometric equipment used in 1986 replaced the original equipment in 1978/79. The detector is a 17-litre temperature stabilized NaI detector. The electronics is partly of Geometrics design and partly made by SGU. The MCA has 256 12.5 keV channels. If any of the primary channels exceeds 256 counts a flag is set and the counter is reset to zero. The 256 channels were usually grouped into a smaller number (i.e. 24) to slow the data flow. A spectrum is recorded every 300 ms corresponding to about 20 metres of flight. The radiometric equipment has been used primarily for uranium prospecting resulting in several discoveries of potential uranium mines. Nowadays it is used for the mapping of natural nuclides which, i.e. is of interest for geological mapping, mineral prospecting and radon potential mapping.

The system is calibrated for the mapping of natural nuclides by measurements on large calibration pads combined with test flights over areas with different natural nuclide composition. Instead of the more common practice of using windows, stripping and sensitivity SGU/SGAB uses the technique of normal (standard) spectra that are fit to the measured spectrum by least square fitting of all channels above a cut off (usually 500-800 keV). This technique was considered advantageous due to the larger apparent sensitivity you get when using a larger part of the spectrum. Its major drawback is the more difficult calibration technique.

The fallout measurements were different when compared to the natural background mapping in several ways:

- the gamma spectrum was very different and the count rates were much higher
- the area to be mapped, the line distances, and the flight altitude were much larger
- the results had initially to be reported daily.

Although the system was calibrated for natural nuclides covering the entire spectrum above 500 keV it had to be further calibrated. Initially a flight line was established. It was measured on the ground with exposure rate calibrated scintillation counters. The line was simultaneously overflown with the system on survey altitude (150 metres) and reflown once or twice a day for the coming weeks. This procedure made it possible to recalculate all exposure rate values to the day of

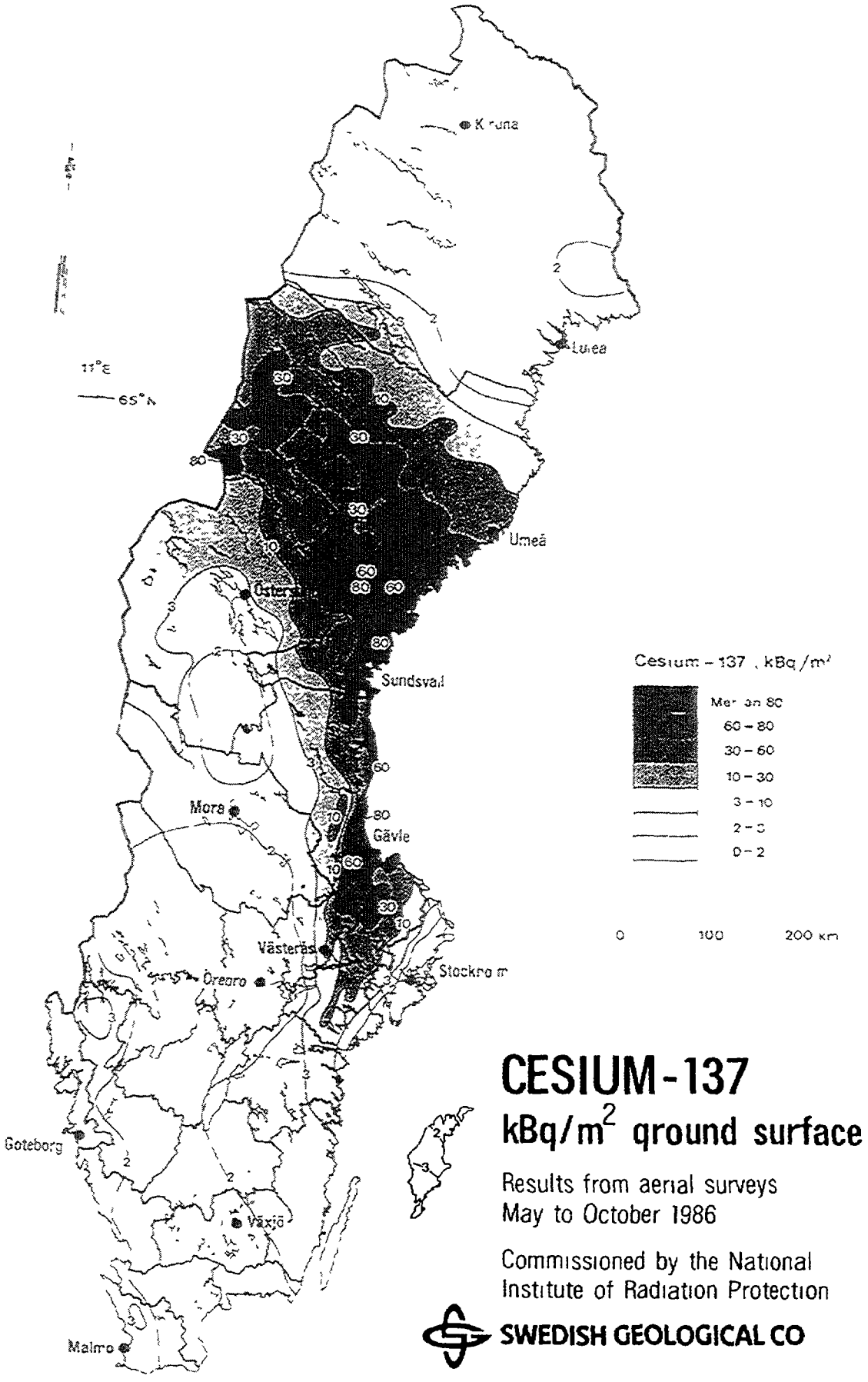

FIG. 1. Cesium-137 kmBq/m² — Results from aerial surveys, May to October 1986.

Geological Survey of Sweden
Airborne Surveys

PLATFORM: TWIN-ENGINED AIRCRAFT

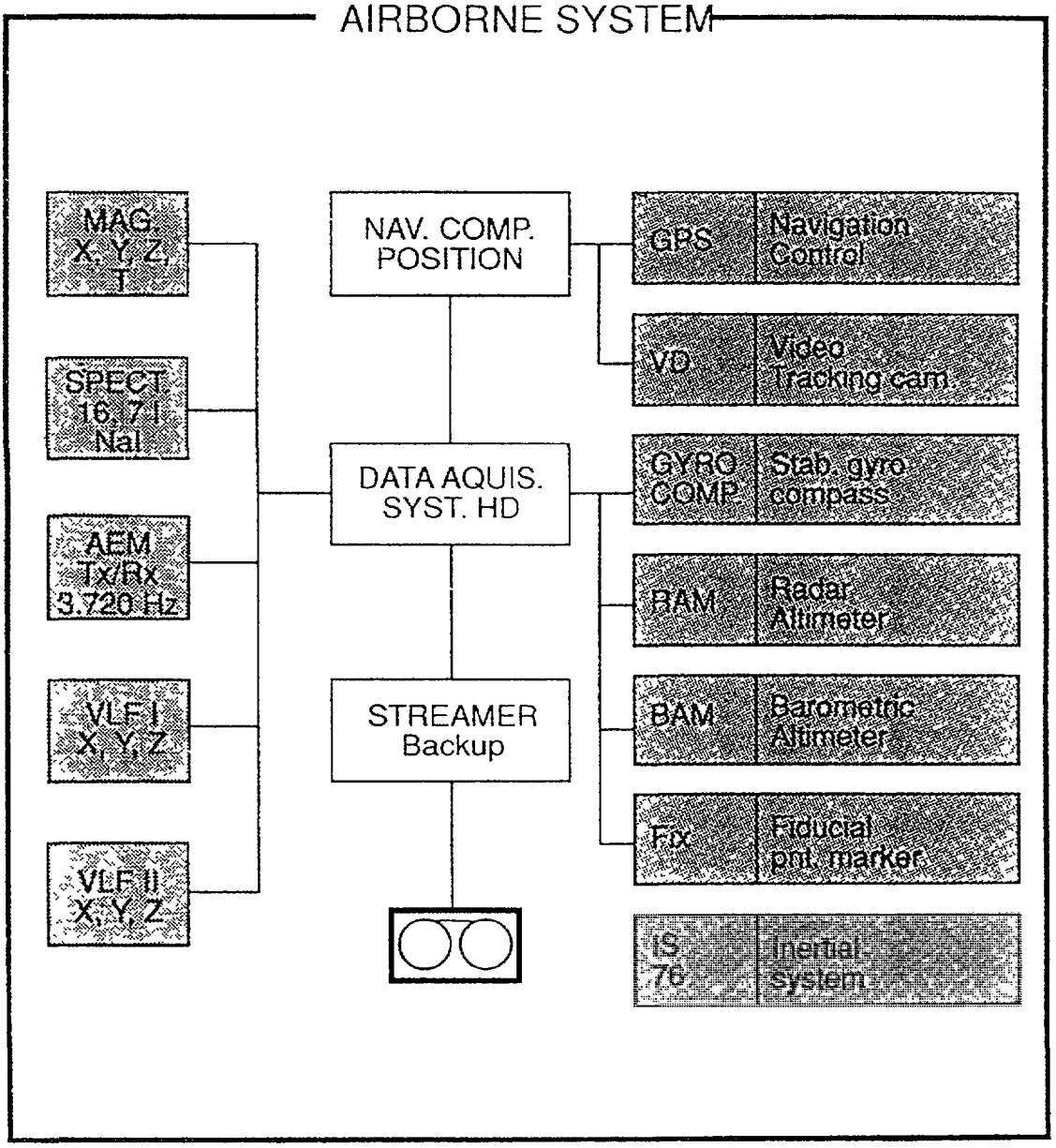

FIG. 2. The present geophysical system operated by the Swedish Geological Survey.

establishment of the line (assuming similar nuclide composition everywhere). This calibration was used to produce total exposure rate maps including the natural background and contamination maps (without the natural background).

A cesium calibration of the SGAB system was first made in May by comparing one ground point measured with a high resolution system situated under one of the flight lines. In September the calibration was remade using a well-documented grass airfield that was measured from the air at different altitudes and on the ground with HPGe- and NaI-systems. Spectra measured after 15 May could be used to calculate activity levels of Cs-134 and Cs-137. Before producing the final maps in the autumn of 1986 a set of long inter calibration lines were flown that covered the country from north to south. These were used to level the data.

3. HOW WERE THE MEASUREMENTS USED?

The aim of the airborne measurements was to locate and quantify, map, the fallout. Other monitoring resources were not suitable for that task. Within a week the entire country had been mapped with a wide line spacing. At this stage the measurements were reported daily to SSI and at press conferences. The final maps produced during the autumn of 1986 were used to inform the public directly and via media. The maps comprised a general background material for local and regional authorities and researchers studying the effects of the Chernobyl fallout during the years following 1986. Another important use of the data was the calculation of the population dose in various parts of the country and for the entire population [2]. These calculations had to include the high resolution ground spectrometry and soil sampling made by the Swedish Defense Research Establishment. The latter measurements were used to correct the airborne measurements in certain areas (see below).

4. THE CHERNOBYL FALLOUT MAPPING IN PERSPECTIVE — PROBLEMS AND ERRORS

Some of the problems encountered by SGAB were related to the gamma spectrum and its rapid change in time initially. The gamma emitting nuclides in the fallout were numerous and most of them were short lived resulting in a rapid dose rate decrease in affected areas. Gamma peaks were seen in the spectrum up to 1.6 MeV. Most peaks were however in the lower part of the spectrum. This fact was used to subtract the natural part of the measured spectra by calculations based on the upper half of the spectrum and knowledge of spectral shapes based on the calibration as described above. The Ba/La-140 peak at 1.6 MeV interfered with these calculations and had to be handled by applying a special "unit spectrum" for this nuclide.

The presence of other (not accounted for) emitters above cesium-134 at 795 keV made the cesium calculations uncertain in the dry deposited areas where the cesium concentration was relatively low compared to the interfering nuclides. The cesium deposition in these areas was often overestimated by a factor 2-3 [2]. In the wet deposited areas with a high relative cesium deposition and the highest activity levels the agreement was much better, usually within 20% when compared to ground measurements with HPGe detectors.

The fallout nuclides initially deposited on the ground surface soon migrated into the ground making all nuclide specific measurements uncertain since the vertical profile of each nuclide depends on the soil and its chemistry. The presented deposition values of Cs-137 are an underestimation by, on an average, a factor of 1.6. This fact shows that it is very important to use ground measurements with high resolution gamma spectrometers as well as soil sampling to adjust the areal measurements.

If information on the vertical nuclide soil profile is missing, it is recommended to report nuclide activities as surface equivalent activities, which always will be an underestimation when analyzing gamma spectra of an aged fallout [6].

5. CHANGES IN THE EMERGENCY RESPONSE ORGANIZATION

The Swedish emergency response organization has been changed since the Chernobyl accident. Many improvements have been made that influence the importance and use of mobile gamma spectrometry units based on NaI detectors. The most important of these monitoring resources added or changed since 1986 can be summarized:

1. An improved network of fixed gamma stations 11 new stations, all 36 fully automatic. The primary use of this network of stations is for early warning especially if the treaty based notification system fails and for dose calculations and prediction. The density of the network is such that all plumes originating abroad and resulting in deposition in Sweden are expected to be detected by at least one station.

2. All local communities now have one simple but well calibrated dose-rate instrument which can be used to measure dose-rate at selected stations. During the initial face of an accident the instrument will be used for measurements at one location each hour. Later it will be used for daily measurements at max 4 different locations. This means that 286 points will be reported to SSI once an hour during the first face of the accident and approximately 800 points once a day in the second face. These data can be used to produce dose rate maps covering the entire country.

3. The number of high purity germanium in-situ systems has been increased and will be an important resource for nuclide specific measurements and dose predictions as well as support for semi nuclide specific systems like those presented below.

4. The radiometric components of the airborne system, nowadays operated by the Swedish Geological Survey, is essentially the same as the ones used in 1986. The Swedish Radiation Protection Institute is a large contributor to a modernization taking place now and during the winter of 93/94. A new detector of the same volume and a new gamma spectrometer has been ordered. It is the modern Exploranium GR800 that will facilitate an increase in measurement quality. The system is equipped with GPS navigation which gives a better position accuracy and a greater freedom to change the flight line setup during flight. Improved calibration routines are planned as well as the possibility to install the real time data processing and presentation system described below.

5. A number of small light weight mobile gamma spectrometer systems including GPS positioning, NaI detectors and real time data processing and presentation are being developed and will be in operation in 1994, according to present plans. They will be used for car measurements and/or helicopter measurements These systems are further described in the next section.

6. THE DEVELOPMENT OF SMALL UNITS FOR MOBILE GAMMA SPECTROMETRY

An important background material to the following discussion on the benefits of mobile gamma spectrometry units is the possible types of nuclear accidents that can be anticipated in Sweden. These are briefly summarized below [4].

1. A major accident in a domestic nuclear power plant. All Swedish reactors are nowadays equipped with a filtering system that will significantly limit the release of nuclides to the environment in most accident types. The fallout can therefore be expected to be much smaller than from a plant not equipped with filters, but nevertheless quite significant.

2. Accidents in nuclear power plants in neighbouring countries. Within a distance of 1000 km, the distance to Chernobyl, 40 nuclear facilities with 1-4 units each are located. Most of these reactors do not have any filtering facilities and a number of reactors do not even have a containment. To this category should be added the risk for military nuclear power accidents and nuclear device accidents in neighbouring countries and on ships and aircraft in the Baltic Sea region.

3. Re-entry of nuclear powered satellites. The probability is small for this event but it cannot be excluded. This type of accident will result in highly radioactive fragments and particles that must be located.

4. Accidents in domestic temporary or final repository for spent nuclear fuel. An unlikely event with limited effects.

5. Accidents when transporting radiation sources.

6. Illegal handling of radioactive sources and nuclear material.

The usefulness of the airbome gamma spectrometry measurements after Chernobyl is well documented. But considering the changing threat spectrum and the added monitoring resources described above, how will mobile gamma measurement resources be used in future accidents? This question is of course difficult to answer since no accidents can be fully foreseen regarding their nature, extent and effects and therefore it is difficult to be entirely prepared for them.

The present policy of the Swedish Radiation Protection Institute in this area is to maintain the radiometric capabilities of the airborne system operated by the Swedish Geological Survey and, if possible, initiate further development of the technique to achieve more accurate dose rate and nuclide activity estimates as well as shorter processing time. It has been discussed to add one similar system that should be dedicated to emergency response and that could be installed in a fixed wing aircraft or a helicopter on a relatively short notice. This system would probably have been maintained by the Swedish Geological Survey. A system like this would, perhaps, never be used except on exercises and still be quite costly to maintain.

Instead of this single extra system it is likely that a few small low cost systems will be purchased based on present development of a prototype system. These systems will be maintained by different contract laboratories in the country. 'They are designed to be used in measurements on foot, in a cars, with helicopters or small fixed wing aircraft. They can also be used for stationary logging of time events or other tasks where gamma spectrometry is required. The primary use will, however, be mobile car or helicopter measurements.

They are based on a light weight 256 or 512 channel gamma spectrometer with a 3 × 3" (maybe one or two systems will be equipped with a larger detector as well) NaI detector, a satellite positioning system (GPS) and a portable computer. The whole system shall be powered by internal battery systems that should last for a day or by an external DC source. It is easily installed in available cars and helicopters, which can be changed if contaminated. The portable computer is powerful enough to facilitate real time data processing including various dose rate calculations and nuclide estimates. It also presents the results in real time on the computer screen on maps that includes some geographic information, i.e. roads. Thus it facilitates a useful tool for in-field decision making which can be of significant importance in an emergency when support from the base sometimes is limited due to overloading of various tasks. If future telecommunication development

allows, the systems can transfer the data almost in real time to a central processing office where data from all mobile and in-situ systems can be pooled and interpreted with only minor delay.

A car mounted system has advantages and many disadvantages when compared to an airborne system (helicopter or fixed wing). In table I this is summarized. It is however important to stress that the car system cannot fully replace the airborne system and vice versa - they are intended to be used together.

TABLE I. A SUMMARY OF ADVANTAGES AND DISADVANTAGES OF USING DIFFERENT PLATFORMS FOR MOBILE GAMMA SPECTROMETRY FOR FALLOUT MEASUREMENTS

	Car 40-60 km/h	Helicopter 50-150 km/h	Fixed wing aircraft 150-250 km/h
Achievable capacity km/24h	400-1000	600-1000	1500-2500
Advantages	A car is easy to find or change Weather & daylight irrelevant Anyone can drive Low cost per km Easy to calibrate Easy to train	Ideal for search Simple installation Can be changed if contaminated	Ideal for mapping Potential for good quality results
Disadvantages	Can only measure along roads Accuracy problems with aged fallout Inaccurate along the road if geometry is difficult Easily contaminated	Limited availability of helicopters Relatively high cost per kilometre Complicated calibration	Difficult to change if contaminated (SGU) High cost per kilometre Complicated calibration

The main advantage of the car-borne system is the easy installation and wide spread support that are available. Any car will do the job as long as roads are used. A four-wheel car may be a better choice in winter or if rough roads are used. If the car is contaminated, it can be changed almost anywhere and anytime. A car can be used day and night almost independent on weather conditions.

The mapping power of a car system is of course inferior to an airborne system, if counted as output per line kilometre, since roads are not made up as orthogonal straight lines. Nevertheless the output is useful and the fact that the road net is dense in densely populated areas makes these areas fairly easily mapped with a car system.

It has not been exactly planned how these systems will be used and how they will cooperate with the airborne system. But allow some speculation on this matter. Assume that the airborne system is available and that it produces 500- 1500 km of high quality measurements per day. It should be used for large scale surveys covering the entire contaminated area within days or weeks depending on the situation. The car systems should at this stage be used for detailed mapping of densely populated areas. They can, if the airborne system fails (for example due to bad weather conditions) also be used for large scale surveys. The car system can be expected, if each of them is run by two crews, to produce 1000 km daily of measurements if large roads are used and 400-800 km daily if minor or intermediate roads are used.

All mobile systems must be calibrated to produce dose rate values referring to both natural and fallout nuclides. The car system can easily and frequently be checked by measuring on a grass field and comparing with a well calibrated dose rate instrument. All systems should also use a more general dose rate calibration that can accept widely different energy spectra. All systems should also have the possibility to calculate nuclide concentration assuming a two dimensional perfectly plane source. This is only possible for some nuclides due to the poor energy resolution of these systems. Since all systems are logging the entire gamma spectrum all data can be reprocessed if the systems are recalibrated in the midst of operations. The car measurements along roads are affected by a varying geometry that will result in a larger spread of the data. The averages can however be expected to be fairly accurate, especially if the data are "levelled""by frequent stops at "perfect geometry fields". The final map production should include data from all mobile systems as well as high resolution in-situ gamma spectrometry and soil sampling.

The combined efforts of all these mobile systems, the in situ HPGe systems, the gamma stations and the dose rate measurements in each local community has the potential of being a powerful mapping tool in case of a nuclear accident. The mobile systems can also be used for search of lost sources or radioactive debris from a crashed nuclear powered satellite. The small light weight systems are also useful for various other nuclide specific monitoring tasks and research.

REFERENCES

[1] ARNTSING, R., BJURMAN, B., DEGEER, L.-E., EDVARSSON, K., FINCK, R., JAKOBSSON, S. and VINTERSVED, I., Field gamma ray spectrometry and soil sample measurements in Sweden following the Chernobyl accident. A data report. National Defense Research Establishment (1991).

[2] EDVARSSON, K., Fallout over Sweden from the Chernobyl accident. In "The Chernobyl fallout in Sweden" edited by L Moberg, The Swedish Radiation Protection Institute (1991) 47-66.

[3] EDVARSSON, K., External doses in Sweden from the Chernobyl fallout. In "The Chernobyl fallout in Sweden" edited by L Moberg, The Swedish Radiation Protection Institute, Stockholm (1991) 527-546.

[4] FINCK, R., PERSSON, A., Overview of monitoring programmes and strategies in Sweden. Swedish Radiation Protection Institute. Internal report (1988).

[6] FINCK, R., High resolution field gamma spectrometry and its application to problems in environmental radiology, Department of Radiophysics, Malmö and Lund University, Malmö (1992).

[7] KJELLE, P-E., Nedfall från Tjernobyl (in Swedish), SSI-rapport 86-07, ISSN 0282-4434, May (1986).

[8] KJELLE, P-E., First registration of the Chernobyl accident in the west by the gamma radiation monitoring stations in Sweden. In "The Chernobyl fallout in Sweden" edited by L Moberg, The Swedish Radiation Protection Institute, Stockholm (1991) 21-28.

[9] MELLANDER, H., Airborne gamma spectrometric measurements of the fallout over Sweden after the nuclear reactor accident at Chernobyl, USSR. IAEA/NENF/NM-89-1, Vienna (1991).

[10] SGAB deposition maps published in 1986.

[11] VINTERSVED, I., DEGEER, L.-E., BJURMAN, B., MELLANDER, H., Early measurements of the Chernobyl fallout in Sweden, IEEE vol NS-34, No 1, February 1987, 590-594.

RAPID QUANTIFICATION AND MAPPING OF RADIOMETRIC DATA FOR ANTHROPOGENIC AND TECHNOLOGICALLY ENHANCED NATURAL NUCLIDES

D.C.W. SANDERSON, J.D. ALLYSON, A.N. TYLER
Scottish Universities Research & Reactor Centre,
East Kilbride, United Kingdom

Abstract

The environmental contribution which aerial radiometrics can make to baseline mapping and measurement of future changes to the radiation environment has been increasingly recognized in recent years, particularly in countries affected by fallout from the Chernobyl accident. In emphasizing the environmental role, the international standard methods for reporting uranium exploration data [1,2] require extension to a broader range of nuclides of environmental interest. Methodologies for rapid extraction and quantification of ^{137}Cs, ^{134}Cs, ^{234m}Pa, ^{41}Ar, ^{16}N and supra-equilibrated ^{228}Ac from airborne gamma ray spectra have been developed, and are discussed here. Particular attention has been paid to the form of the altitude dependence of stripping ratios for anthropogenic nuclides, which have been determined using a combination of transportable calibration pads, extended area layered sources, perspex absorbers and Monte-Carlo simulation. No previous values for these parameters are known from the literature. Sensitivity factors and altitude correction constants have been determined on calibration sites, whose inventories were defined by high resolution gamma spectrometry of environmental core samples, supplemented by in situ gamma spectrometry. It is important to take the spatial variability of results from core samples, and the centre weighted field of view of the radiation spectrometer into account when defining calibration sites. For anthropogenic nuclides in particular the sensitivity depends on the vertical distribution of the source, which can be determined from the calibration sites using core data. Monte-Carlo simulation of spectral response supports the calibration procedures derived in this manner, and supplements them with sensitivity factors for other, particularly short-lived nuclides which are not usually present in the environment. System sensitivities determined over a series of surveys are quite stable, and are consistent with theoretical values for the detector geometries. The procedures could therefore be applied to existing uranium exploration data to define baseline levels for a broader range of environmental nuclides.

1. INTRODUCTION

The aim of this paper is to illustrate methodologies developed at SURRC for analysis and mapping of environmental γ-ray spectra. There have been significant developments in the application of airborne gamma spectrometry since its origins in geological exploration [1-9]. It has been necessary to extend the standard methods to encompass a wider range of nuclides and applications.

The approaches outlined here illustrate techniques for rapid spectral reduction and calibration procedures, developed for environmental mapping and emergency response applications. Near real-time spectral processing can identify features requiring priority investigation and provide maps to assess environmental impact. In addition to natural radionuclides, ^{137}Cs, ^{134}Cs and ^{234m}Pa have been successfully investigated and mapped. The technique can also be readily applied to ^{131}I mapping and ^{41}Ar plume dispersion. Current developments include the use of germanium detectors in combination with NaI systems to assist with spectral interpretation. An array of externally mounted low energy semiconductor detectors is being developed for mapping ^{241}Am and complex low energy emitting radionuclides. Semiconductor detectors can overcome the difficulties associated with determining accurate stripping ratios for scintillation detectors; however they are inherently less sensitive.

Data can be calibrated in Bq kg^{-1} or Bq m^{-2} on the basis of ground to air comparisons with spatially matched areas which have been subjected to sampling and high resolution gamma

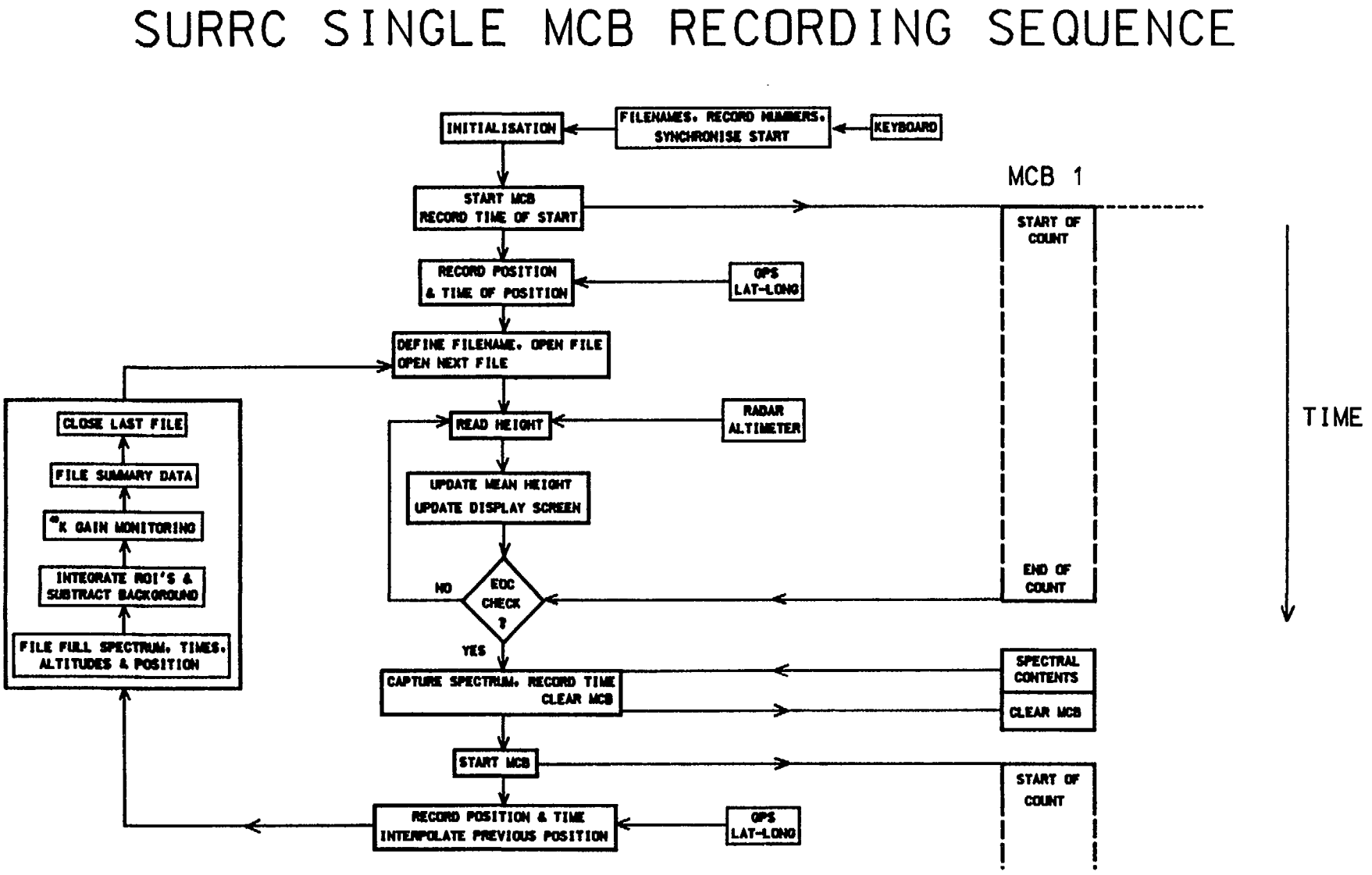

Figure 1. Flow diagram illustrating the recording procedure used to acquire data for rapid quantification and mapping.

spectrometry. These approaches have been verified by Monte Carlo simulation and other numerical methods, which also have the potential to provide working calibration values for nuclides which are not currently present in the environment. The calibration and mapping methods presented here can be used to extend the range of nuclides quantified from existing exploration data, thus for example defining the global ^{137}Cs background. However when used with new data recorded in an appropriately structured manner with navigational and radar altimetry information it is possible to produce calibrated maps on an extremely short time scale after each individual survey flight. This has important implications for emergency response, and is also valuable within a wider environmental context.

2. RAPID QUANTIFICATION OF ENVIRONMENTAL NUCLIDES

2.1. RECORDING METHOD

The SURRC spectrometer has been described elsewhere [10]. The use of multi-channel buffer (MCB) architecture lends itself to flexibility to single or multi-detector use, and also allows the data logging computer to perform real time spectral analysis without introduction of system dead-time. The recording procedure for a single MCB is illustrated in the flow diagram of Fig. 1. A similar, but somewhat more complex sequence can be used for multidetector operation. Additional inputs into the system are from the GPS system and the aircrafts radar altimeter. The GPS can also be used as a navigation aid by programming way points into the system prior to the flight.

The startup procedure involves input from the keyboard. The spectral response characteristics are checked directly through the MCB, and initial detector gain and energy resolution verified by the operator. Thereafter a data logging programme is initialized and use to record and pre-process data for mapping. A root filename, which is common to all data for the individual flight line, and the number of records to be collected are entered into the datalogging computer via the keyboard. This then initializes the system and starts the first acquisition period. The position (latitude and longitude) is read in, since 1992 directly from a GPS system along with the time of the positional reading. The computer defines the first filename and open it to receive spectral, region of interest data, and quality assurance data. During spectral acquisition the radar altimeter is read and averaged whenever the computer is free from other tasks. Once the measurement has finished the MCB sends an end of count (EOC) signal to the computer, which captures the spectrum from the MCB, records the time, clears and then restarts the MCB. The computer then updates the positional estimate from the GPS and interpolates the mean position for the previous spectrum. The full spectrum labelled with times, mean position and altitude is recorded in the open file on either hard disc or floppy drive. The computer then integrates the spectrum into 8 defined regions of interest, subtracts a stored background estimate from these regions of interest and stored the compressed data. ROI data are displayed on the LCD monitor to inform the operator. The NaI(Tl) detector gain is monitored by measuring the symmetry or otherwise of the ^{40}K photopeak. This is also displayed to the operator and recorded with the spectral and data files. These first set of files is then closed and the computer selects the next filename and opens it ready to receive the next data set. It then resumes reading the radar altimeter, updating the mean height and the screen information until the second MCB measurement is complete. This cycle continues until the defined number of spectra have been collected.

Once this is complete, summary files, comprising a line by line record of filename, position, altitude and six spectral integrated count rates, are generated using a search and compression programme; usually on the flight back to base. All summary data are backed up to multiple floppy disks. Multiple backup copies are made of the full spectral data and regions of interest data to tape streamers. Thus on landing, providing that the detector operation has been validated in flight, the summary data can be used for rapid ground based mapping. The availability of the full spectral record allows for retrospective variation in regions of interest, or the use of full spectral analysis procedures.

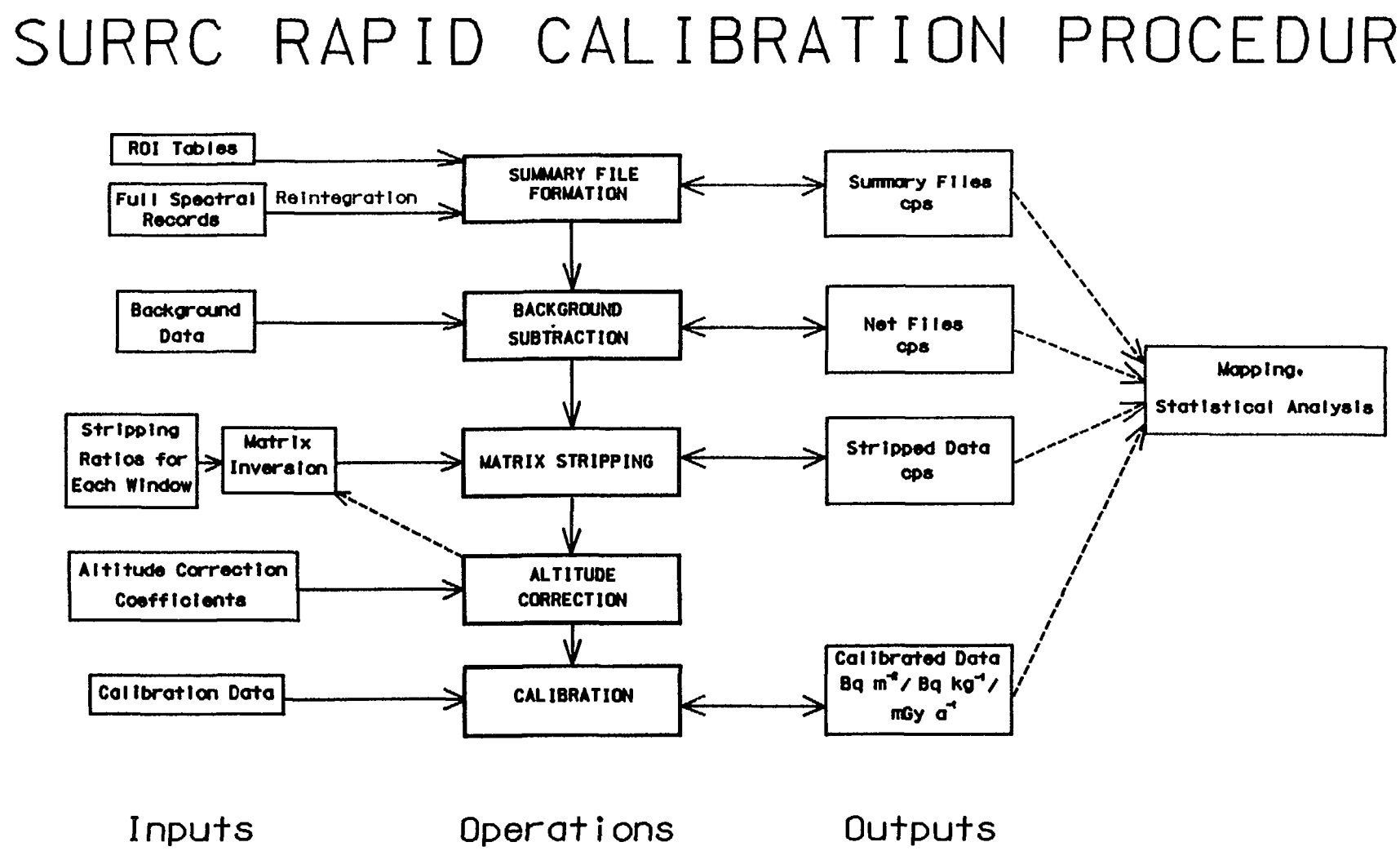

Figure 2. Flow diagram illustrating the rapid calibration procedure.

2.2. WINDOWS AND FULL SPECTRAL PROCESSING

The analysis of spectral information has been developed by quantifying peak energy count rates at an early stage, and relating them through a calibration procedure to estimated concentrations of radionuclides or dose rates. The use of predefined windows, in an analogous manner to the international standard 3 window methods for K, eU, and eTh, is arguably the simplest means of extending calibration to a wider suite of environmental nuclides. Interferences from Compton scatter and nearby peaks contribute to window count rates and therefore must be separated to height correction and calibration. This could be achieved by peak shape fitting, but the window method, coupled to matrix stripping remains the preferred means for rapid quantification. This method can be applied to both scintillation and semiconductor detectors, although in the latter case it is possible to estimate full-energy peak count rates using an interpolated continuum subtraction, rather than adopting matrix stripping methods. IAEA recommends specific windows for the measurement of potassium, uranium and thorium [9], but general guidelines for the definition of other peaks have not yet been agreed. The selection criteria for regions of interest must be based upon detector resolution. For multi-crystal array systems it may be necessary to allow a greater tolerance to take account of spectral broadening and small gain drifts. As a result of drift, either underestimates or overestimates of true window count rates may occur. Continuous monitoring of gain drifts during survey provides a means of ensuring data integrity, at the outset. In practice it is easily possible to maintain better than 1% gain stability using the methods developed. It would be possible to recover data showing gain drifts survey during post-processing, with appropriate energy calibration and re-integration procedures, however again this would be achieved at the expense of rapid quantification.

Full spectral deconvolution has become increasingly feasible in the field with fast, powerful, compact PC based systems becoming available. With successive stripping from high to low energies, of pure spectra from net data (determined by experiment, spectral analysis, interpolative methods and simulation), the residual data may lead to information regarding individual sources and source burial depth characteristics.

2.3. QUANTIFICATION PROCEDURE

The rapid calibration procedure is illustrated in the flow diagram in Fig. 2. For small scale surveys the detector background can be measured over large bodies of water or at ground clearances above 1500-2000 feet altitude. For large scale surveys in areas of considerable relief it may be necessary to adopt the full procedures recommended elsewhere [2]. In either case it is advantageous to define, and preload, the background at the start of survey, and to conduct regular checks during the survey to ensure that the values are representative.

Upon landing at the base, if not already done so, summary files are formed from the regions of interest files. The summary files can also be regenerated automatically by reintegrating the spectra if necessary, although this of course adds to the processing time. The background is then subtracted from the summary data, and used to form an identically structured file of net count rates.

The stripping ratios are determined as appropriate for the mean flying altitude for the survey and tabulated in a matrix. This matrix is inverted and used to estimate stripped count rates from the net count rate data. The stripped count rates are again stored in an identically structured file to the summary and net records. A case could be made for modifying the stripping matrix for each observation to take account of individual radar altimetry observations. However the inversion of the stripping matrix for each data point would add significantly to the computing time, and there are doubts as to whether this would make a practical difference to survey data which do not generally show extreme altitude variations. If it were necessary to make individual adjustments for altitude dependence of stripping then a more efficient approach would be to parameterize the effects on the inverse stripping matrix. The absolute determination of the stripping coefficients is in any case problematic given the finite geometry involved in concrete calibration pads and the determination of

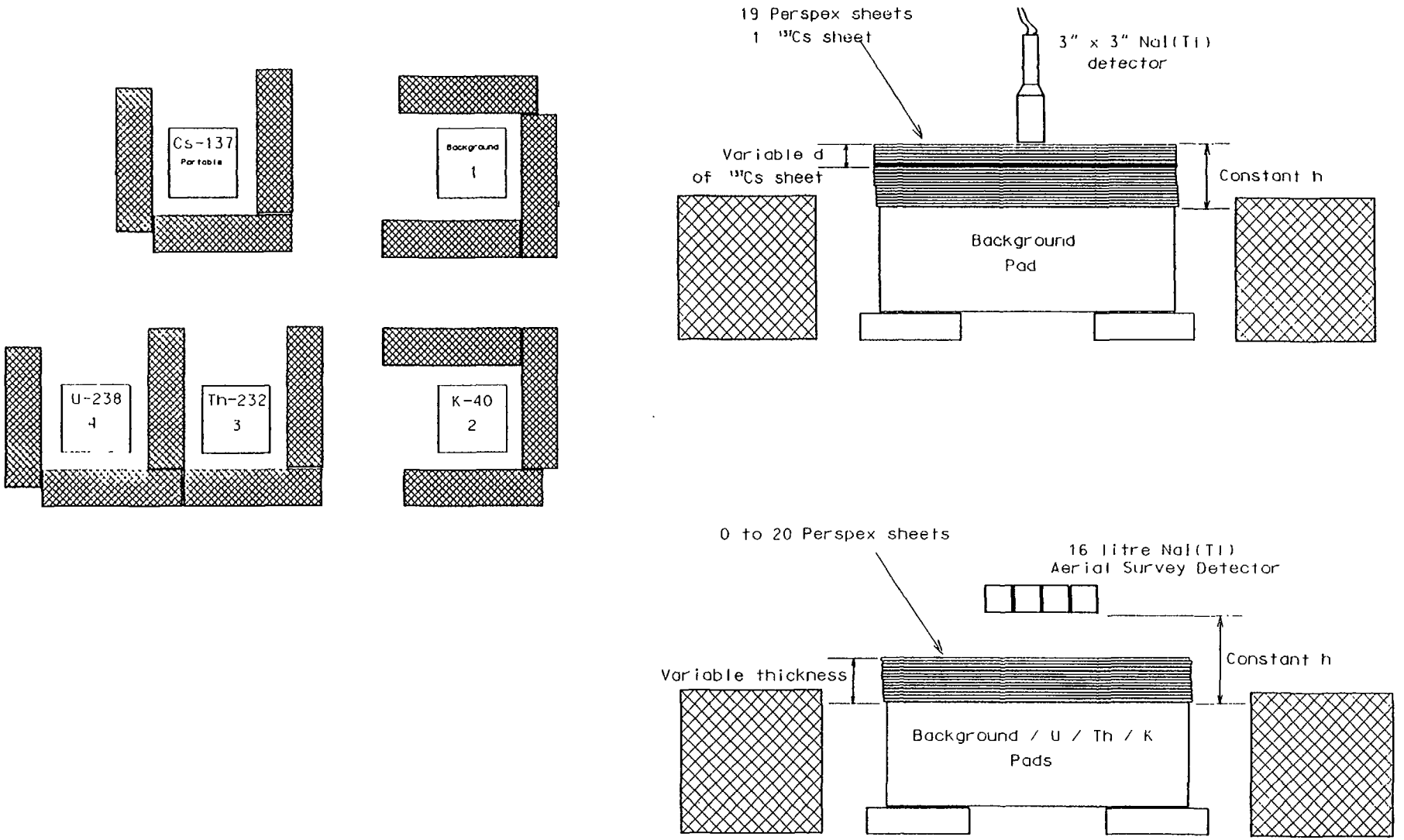

Figure 3. Diagram illustrating the SURRC gamma ray calibration facility.

the altitude dependence. This is discussed in further detail below. However, by calibrating the system relative to a range of activities on different calibration sites, it is possible to overcome any systematic errors in stripped count rates using an intercept. Similarly the measurement of a non-zero intercept in calibrations using a range of activities could be taken as an indication of deficiencies in the stripping procedure. The incorporation of HPGe detectors in the system removes the need to strip data, and thus removes a potential source of uncertainty in calibrated data.

Altitude correction coefficients are determined by making sequential measurements over a range of heights above a calibration site. The profile can be approximated by an exponential form above approximately 30 m. Problems incurred through spatial variability in the calibration site can be accounted for as described below. These correction coefficients are used to normalize the data to a standard altitude before calibration.

The data are then converted to activity per unit area (Bq m^{-2}), activity concentration (Bq kg^{-1}), or dose rate (mGy a^{-1}) based on linear relationships between ground based estimates from calibration sites and the altitude corrected stripped count rates. Again the standard file format is maintained, so that subsequent statistical analysis and mapping routines can operate on raw, net, stripped or calibrated data.

3. STRIPPING SPECTRAL INTERFERENCES

3.1. STRIPPING METHOD

The stripping of net spectral data can be extended to many radionuclides, providing that pure reference spectral shapes can be determined. The fractional contributions between energy windows corresponding to each individual source are calculated and assembled into a stripping matrix. Net window count rates are deconvoluted by their multiplication with corresponding inverse stripping matrices. Whereas for geological mapping a great deal of attention has been paid to the construction of calibration pads from which approximate stripping ratios can be determined, there are few examples of the extension of such facilities to environmental nuclides. It is possible to supplement calibration pads for natural sources by additional laboratory scale facilities; initial SURRC surveys used pure reference materials in point source, or as pure radiochemical solutions. However it is important to attempt to account for the scattering conditions within the environmental sources being mapped, and in the intervening air path it realistic stripping ratios are to be determined.

Unfortunately experimental simulations of ground-air interfaces, between sources and detectors are limited to an artificial geometry which is not encountered under full scale field conditions. The use of calibration pads, with absorbers goes some way towards simulating air-path scattering, and in the absence of any other information, then corrections of this sort are valid, but not ideal. Although in principle it may be possible to conduct full scale experimental simulations of pure spectra using arrays of many sources at ground level, or by geometrically reconstructing the response to an accurately flown trajectory over a single strong point source, there are practical limitations in attempting to determine stripping ratios in this manner. Therefore Monte-Carlo simulation of pure spectral response appears to offer the only means of overcoming the limitations of experimental stripping ratios. Examination of residuals after stripping can lead to semi-empirical optimization of some stripping coefficients, above some suitable test sites [11], but must be used with caution.

3.2. THE USE OF PADS AND SHEETS

Doped concrete calibration pads provide a convenient source of activity to represent natural radionuclides to determine spectral characteristics. Additional sheets of anthropogenic spikes have been produced by SURRC on $1m^2$ plywood boards to represent fallout activity (Fig. 3). This

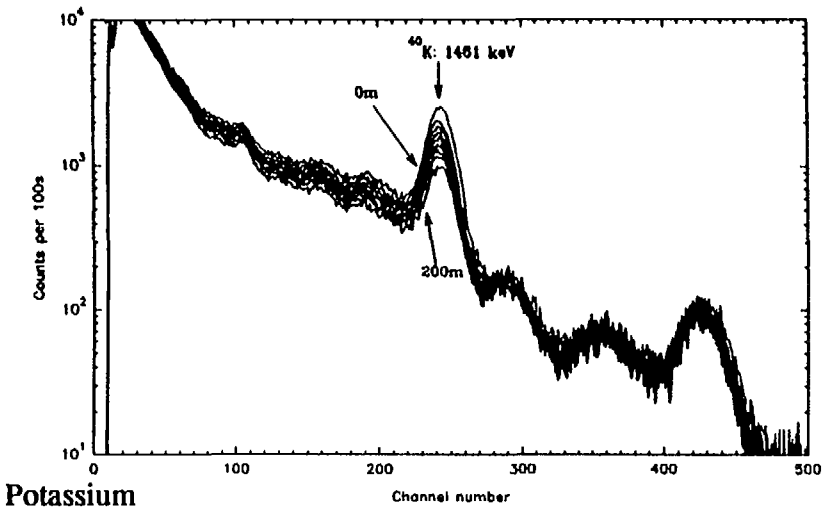

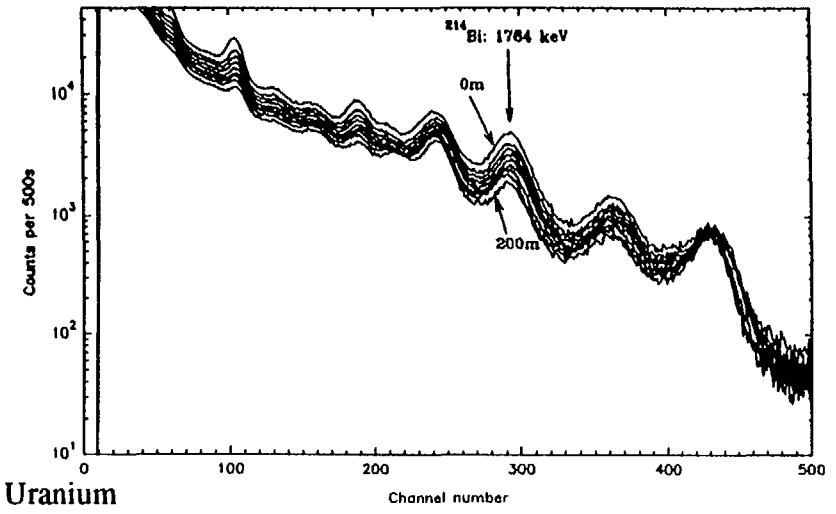

16 litre NaI(Tl) aerial survey detector array above calibrations pads

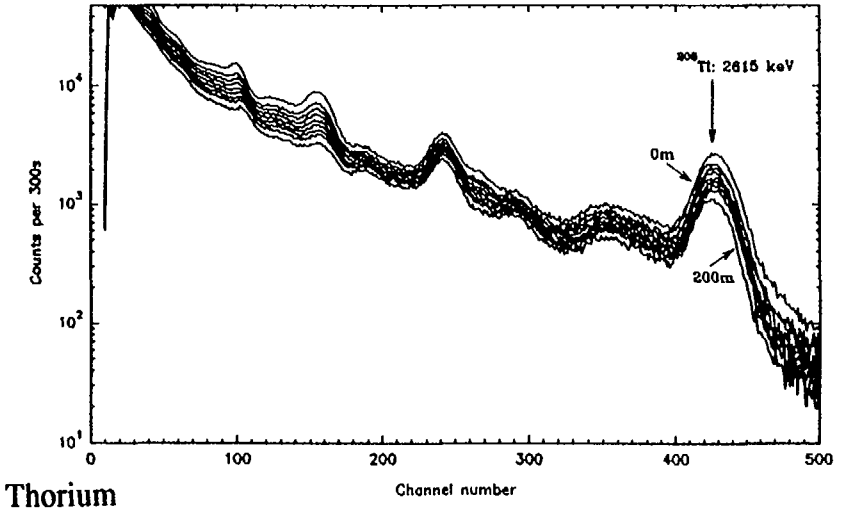

Figure 4. Diagram illustrating the use of perspex absorbers to simulate the variation of spectral response of an aerial survey detector.

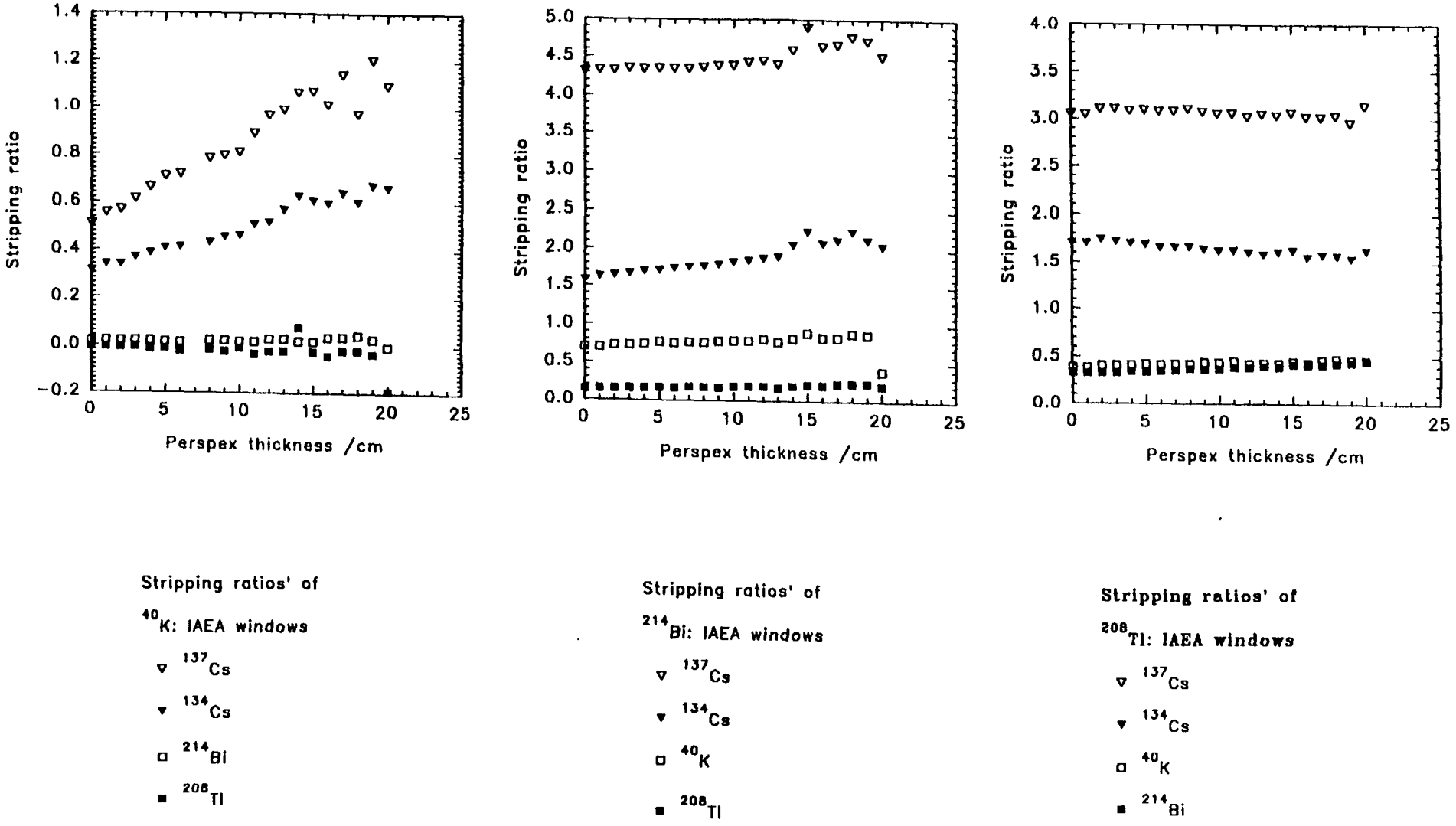

Figure 5. Diagram showing the altitude dependence of stripping ratios using perspex absorbers.

represents a straightforward extension of the conventional use of pads for radioelement mapping, and has the attractions of simplicity and reproducibility in use. As stated above such facilities can only approximate environmental sources; the use of uniform K, eU and eTh concrete blocks cannot of course take account of environmental stratification of soils, substrata and particularly water contents, which may influence the scattering conditions. Anthropogenic sources may show a vertical profile with depth including sub-surface maxima or pronounced burial. In simple form neither system takes account of spectral modifications due to interactions in the intervening air path from source to detector. Whereas the main effect on the high energy photons used for natural radioelement mapping is to increase scattered continua, and hence to increase stripping ratios from high energy sources to lower energy windows, more complex effects are observed at the lower energies used for example for fallout mapping of ^{137}Cs and ^{134}Cs.

Spectral behaviour of calibration pads can be modified by the addition of absorbers to simulate air path lengths, low activity soil overburden and water, between source and detector (Fig. 4). The use of such absorbers is recommended to minimize understripping of ^{134}Cs and overstripping of ^{137}Cs. Absorber composition was chosen by calculating mass attenuation coefficients for a variety of readily

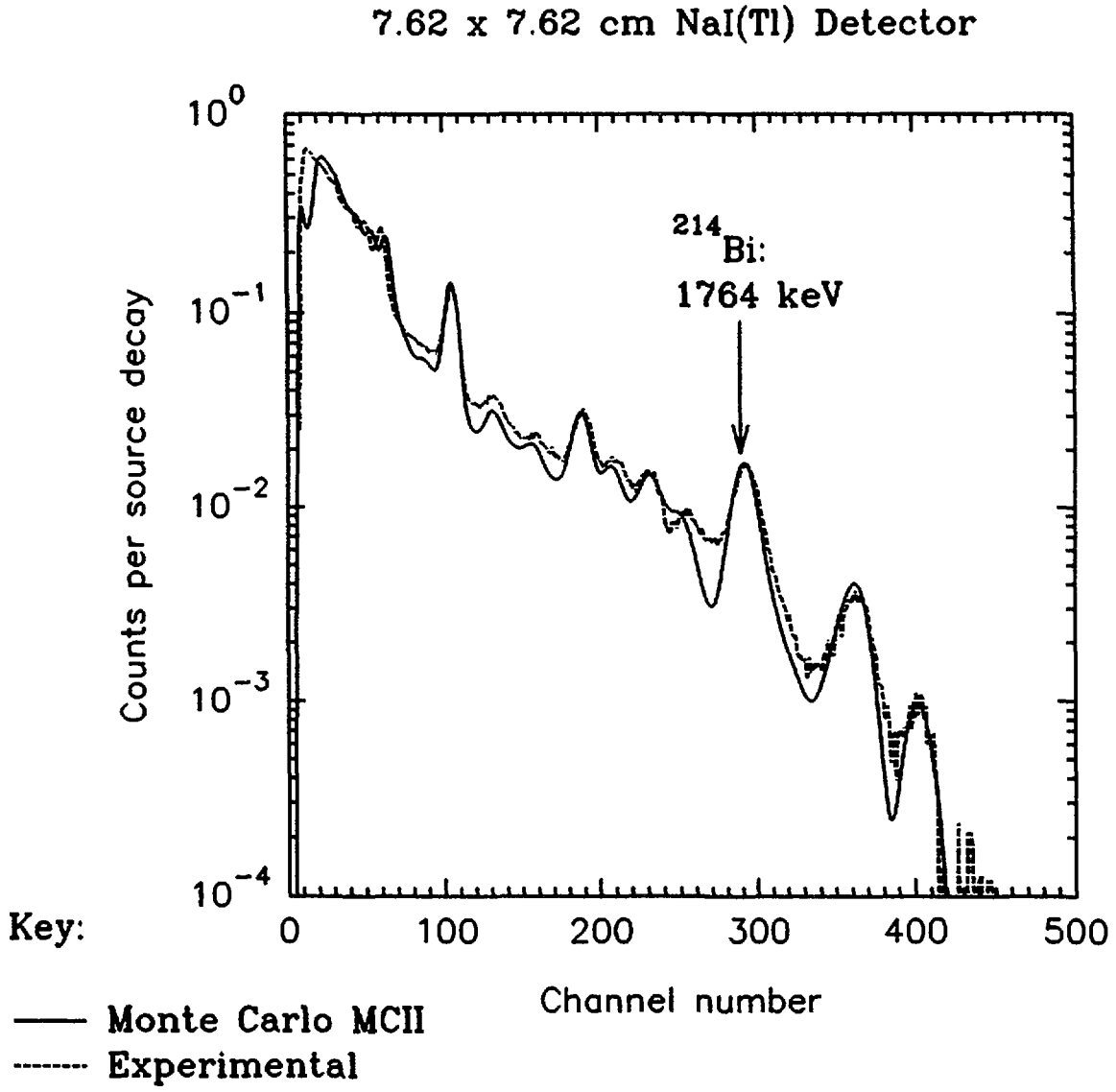

Figure 6. Comparison of Monte-Carlo and experimental spectra above a Uranium calibration Pad for a field based detector.

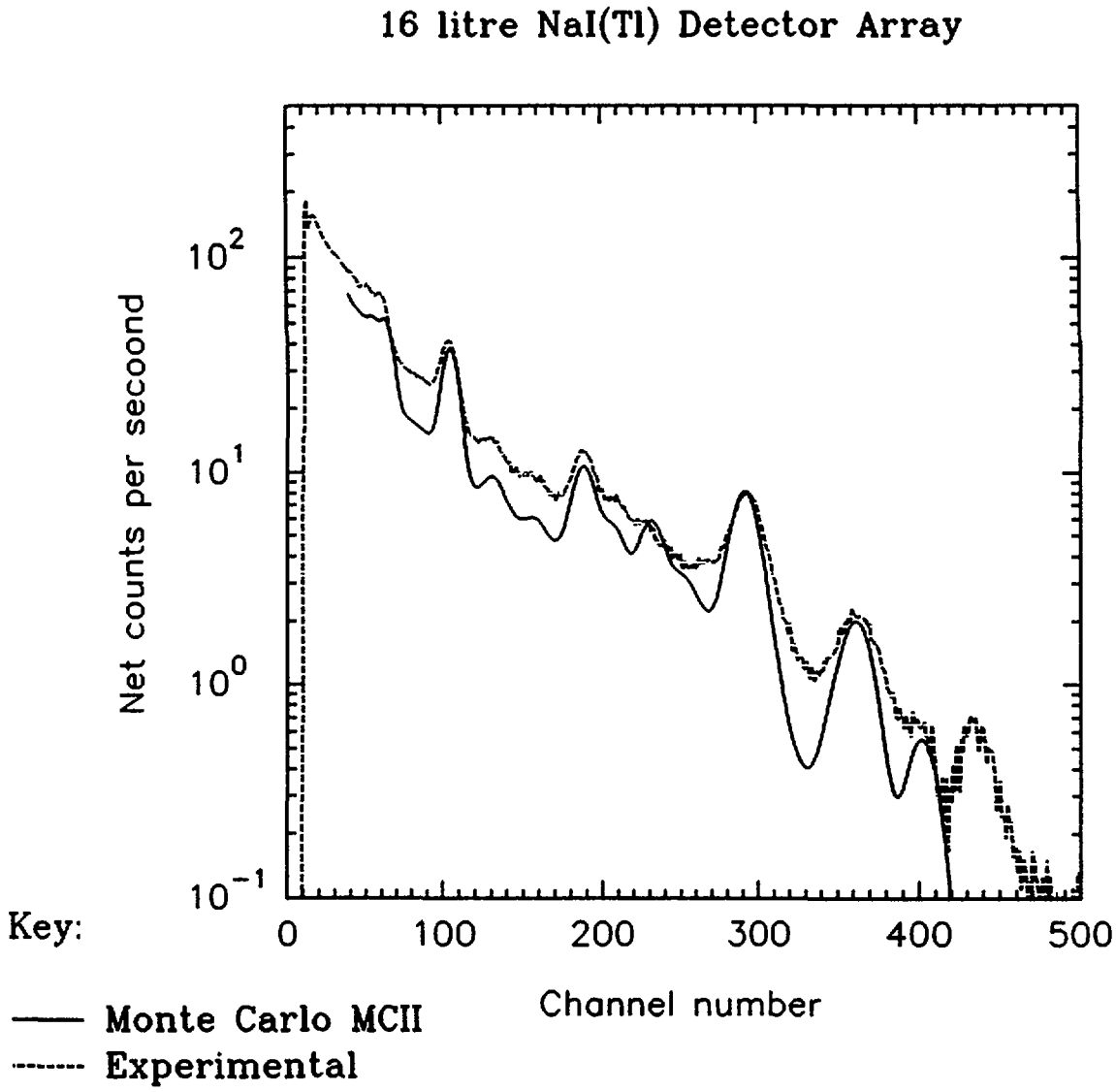

Figure 7. Comparison of Monte-Carlo and experimental spectra above a Uranium calibration Pad for an aerial survey detector.

available materials. Perspex and wood were found to have similar mass attenuation coefficients to that of air, Beck soil [12] and water. Although plywood has been chosen for previous work [13], perspex was used in the SURRC facility since it is chemically well defined, and has uniform thickness and density. The calibration facility based on Grasty transportable K,eU,eTh 1 m^2 pads and supplementary sources, has been enhanced by the addition of 20 1 m^2 perspex absorbers, each of 9.6 metres equivalent standard air. The absorbers can be placed between source and detector, or above the detector, or both. In this way experiments have been devised to simulate source-detector path lengths comparable with air path lengths found at aerial survey heights. Also, with the use of anthropogenic sheets (eg. ^{137}Cs) source burial characteristics can be reconstructed to determine spectral response. The altitude dependence of stripping ratios can be determined with the use of absorbers (Fig. 5), but the results are constrained in the absence of skyshine and proper geometrical considerations. However, trends observed in these measurements show a linearly increasing dependence with altitude for ^{40}K into ^{137}Cs and ^{134}Cs windows. A much slower dependencies are seen from ^{214}Bi and ^{208}Tl into the lower energy windows.

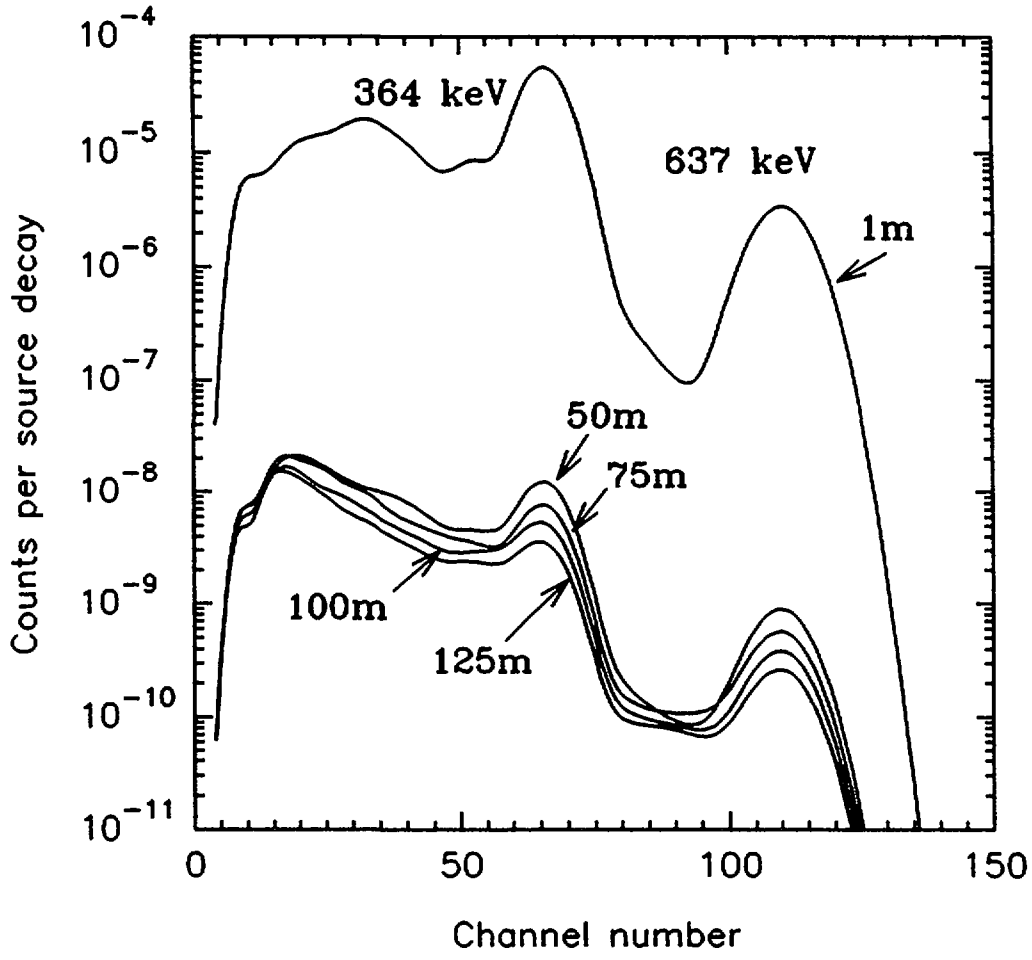

Figure 8. Diagram showing the predicted aerial survey detector response using Monte-Carlo methods of an extended ^{131}I source.

3.3. SIMULATED SPECTRA

In principle, there is much to commend the full simulation of dispersed activity, γ-ray transport and detection mechanisms. Activity distributions and spatial variability can be represented in a realistically defined manner. Certainty in uniformity, if required, is absolute over extended regions. Further to this, the geometrical scale of simulated gamma transport can be defined to match proper aerial survey conditions, unlike that of pad-absorber combinations. Sources for which pads or calibration sheets are not available (eg short lived nuclides) can be simulated.

Provided that simulation methods and code can be validated with known and measurable data, it is possible both to define pure spectral shape, for stripping ratio determination, and to calibrate γ-ray spectrometers for sources that are not usually found in the environment. In addition, understanding detector response from an unlimited number of source configurations is of considerable advantage, enabling simulation of realistic environmental profiles. This also applies to the pre-calibration of detectors for multi-nuclide sources which might be encountered in accidental conditions, and for which rapid early estimates would be needed. Although peak sensitivities can be estimated by alternative and faster numerical methods (section 4.1) in limited applications, the full spectral response, including Compton scattering effects, can be only determined accurately by Monte Carlo simulation.

Figs 6 and 7 show Monte Carlo simulations of hand held and aerial survey detectors above a transportable uranium calibration pad. Comparisons are made with experimental measurements and differences that can be attributable to both approaches [14]. Such comparisons are beneficial for validation of codes. Stripping ratio estimates by Monte Carlo methods have been made for standard geometry detectors [14] and compared with determinations from pads.

Fig. 8 shows the 16 litre NaI(Tl) detector response predicted by Monte Carlo simulation of an extended plane source of ^{131}I, as would probably be observed after an accidental release. Other radionuclides may be treated also. The response of a 16 litre aerial survey detector to a pure source of ^{228}Ac has been simulated and stripping ratios derived. This enabled, the separation and mapping of ^{228}Ac and ^{234m}Pa in an estuarine environment [24].

4. SENSITIVITY DETERMINATION

4.1. ANALYTICAL AND NUMERICAL ESTIMATION

It is possible to calculate fluence rates from line emissions of radionuclides, and to predict the count rates observed per unit activity concentration in detectors whose energy and angular efficiencies have been determined with laboratory sources [12]. Such analytical and numerical methods can be readily developed to determine detector sensitivities for a wide range of anthropogenic sources. Scintillation and semiconductor detector sensitivities can be easily estimated by these means although for full detector calibration, Monte Carlo methods provide a more comprehensive approach. Numerical integration of analytical transport equations in combination with measured or Monte Carlo derived detector response characterization can yield rapid sensitivity estimates for short lived environmental radionuclides.

Stepwise integration of analytical or numerical expressions can also be used to estimate the detector fields of view [15-16]. The angular response of the detector may be important aspect in this, especially for non-spherical geometries. For commonly used prismatic NaI(Tl) arrays, the effect of angular response is to narrow the effective field of view. Field of view is dependent upon the altitude of the detector, γ-ray energy and source depth characteristics, and therefore is a relevant parameter to use in survey designs [17].

The problems with using this approach to sensitivity determination for aerial surveys are that (i) any systematic errors due to imperfections in stripping ratios are maintained in calibrated data, and (ii) it is necessary to know the environmental depth distribution and form to predict fluence rates accurately. The conventional assumption of an exponential burial profile is not justified on many sites, and therefore it may be necessary to extend the equations normally used to deal with generalized source distributions.

4.2. GROUND-TO-AIR COMPARISONS

Historically, ground-to-air comparisons have been made with in situ spectrometer systems calibrated from the same concrete calibration pads as aerial based spectrometers, and used to characterize calibration areas [4-8, 18, 19]. Whilst providing good traceability between similarly calibrated systems [20], which is useful for geological characterization, and being a relatively rapid field approach, there are circumstances where uncertainties in source distribution characteristics may lead to correlated errors in both in situ and aerial measurements. Under these circumstances apparent agreement between both data sources does not guarantee freedom from systematic errors.

As indicated above it is possible to estimate detector calibration parameters (as in the conventional in situ method) using analytical photon transport equations, and assuming a fixed vertical

activity profile. However, the assumption of a constant negative exponential distribution of activity within the soil, for example, does not in many cases correspond to a physically meaningful description of the environmental characteristics prevailing, and may lead to under or over estimation of environmental radioactivity due to changes in soil depth distributions. As noted above this approach also would require error free stripped count rate estimates for each nuclide.

A more direct comparison between spectrometer derived measurements and laboratory analyzed soil samples provides the only means of overcoming such problems, but is more time consuming, and must take account of variations in soil density, and the heterogeneity of source distribution both in the spatial vertical and horizontal planes. This also provides a simple basis for traceability of results back to international standard reference materials.

This is therefore best achieved by direct experimental comparisons with soil sample derived estimates of environmental radioactivity [21]. This approach allows meaningful calibration estimates to be derived whilst also allowing spectral effects of vertical source profiles to be investigated and quantified.

Sampling and sub-sampling errors have been improved by between 30 and 50 % by increasing sample volume collected from a 38 mm diameter soil corer to a 105 mm diameter soil corer. Soil samples are typically collected to 30 cm depth and subdivided into sections of between 2 and 5 cm to determine the mean mass depth. Subsurface maxima are observed to be between 1 cm for atmospheric fallout, to above 20 cm in salt marsh environments. This potential depth variation coupled with changes in soil density has considerable implications on detector sensitivity estimations for both in situ and aerial survey spectrometer systems. However, experimental observations have illustrated the possibility of determining mean mass depth from spectral characteristics.

With ^{137}Cs concentrations in soil typically between 10^{-15} and 10^{-12} parts by weight, coupled with spatial variability, comparisons between soil samples of about 2 kg weight and in situ (1 m height) and aerial survey detectors (100 m height) which typically sample 10^5 and 10^7 times more volume will lead to considerable errors. As uniform distributions of activity do not exist, matching soil samples to in situ and aerial spectrometric measurements should take account of spatial variability and spatially match the field of view of the detector.

4.3. HELICOPTER CALIBRATION SITES

Early 16 point calibration areas sampled with soil corers were weighted to match the field of view of an airborne spectrometer at 100 m altitude [22]. However, the spatial pattern proved inflexible for determining spectrometric sensitivities for a range of altitudes. The 31 point expanding hexagon illustrated in Fig. 9 was developed to take an economic number of samples with increased sample spacing to enable:

1) Spatial variability to be determined for a range of sampling scales

2) The calibrations to be determined for spectrometers at any height above the pad by weighing the contribution from each shell appropriately for the field of view of the detector.

3) Spatially compensated height correction coefficients.

Four expanding hexagons have been successfully developed for three aerial surveys [23-25]. An example from Caerlaverock Natural Nature Reserve (Dumfries) is illustrated in Table I and Fig. 10. Hexagonal shells were sampled at 0, 2, 8, 32, 128 and 256 m spacings. Table I illustrates the ^{137}Cs mean activities with statistical error for each shell. As sample spacing increases, so the statistical error increases. By weighing each shell appropriately for the field of view of the detector, then an

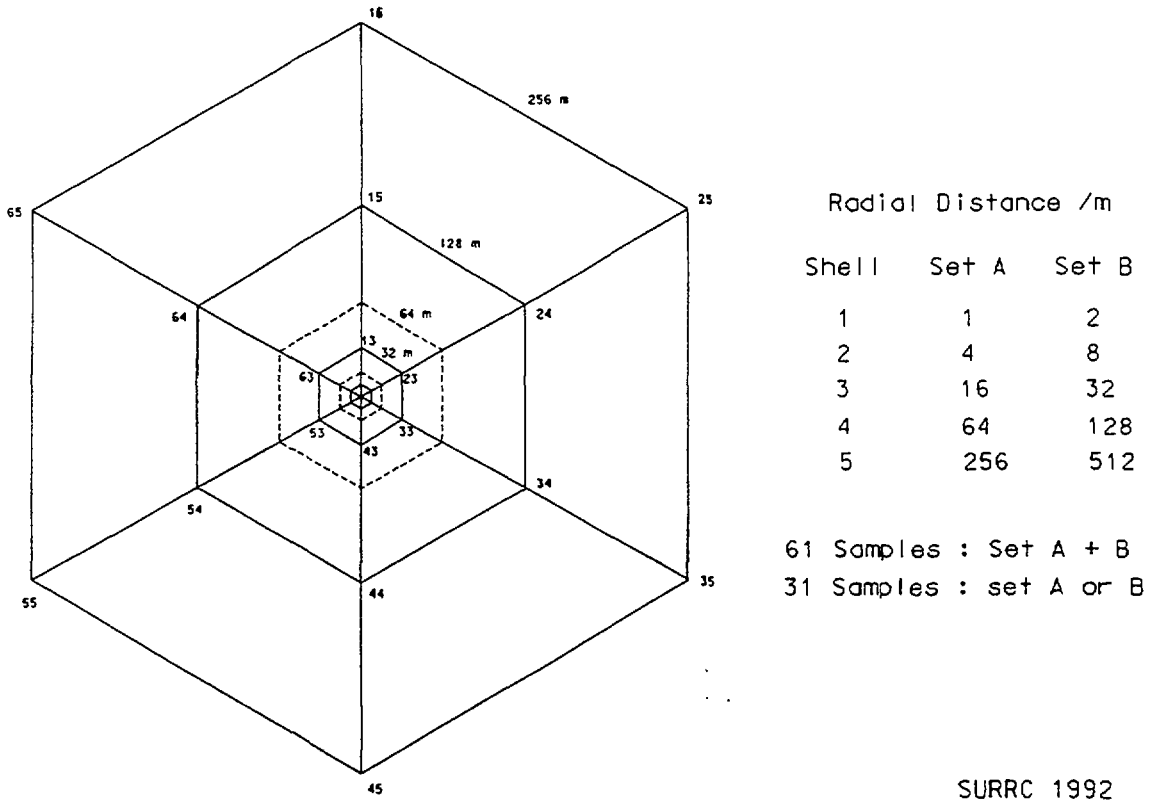

Figure 9. Diagram illustrating the expanding hexagonal sampling plan.

TABLE I. DEMONSTRATING THE SPATIALLY WEIGHTED MEAN ACTIVITIES FOR ^{137}CS AT THE CAERLAVEROCK SAMPLING SITE

Radius metres	Percent Weighting	Cumulative Percentage	Activity Bq/m2	St. Dev. 1 σ	St. Err. of Mean
Detector Height 1 m					
0	10	10	86020	1727	1727
2	70	80	84039	5189	2118
8	17	97	83376	7515	3068
32	3	100	83360	7140	2915
		Weighted Mean	**84104**	**5502**	**2301**
Detector Height 50 m					
2	2	2	84039	5189	2118
8	7	9	83376	7515	3068
32	48	55	83360	7140	2915
128	35	90	78754	33594	13715
256	10	100	39375	19907	8127
		Weighted Mean	**79031**	**21531**	**8790**
Detector Height 100 m					
2	1	1	84039	5189	2118
8	3	2	83376	7515	3068
32	32	35	83260	7140	2915
128	45	80	78754	33594	13715
256	20	100	39375	19907	8127
		Weighted Mean	**73299**	**25272**	**10040**

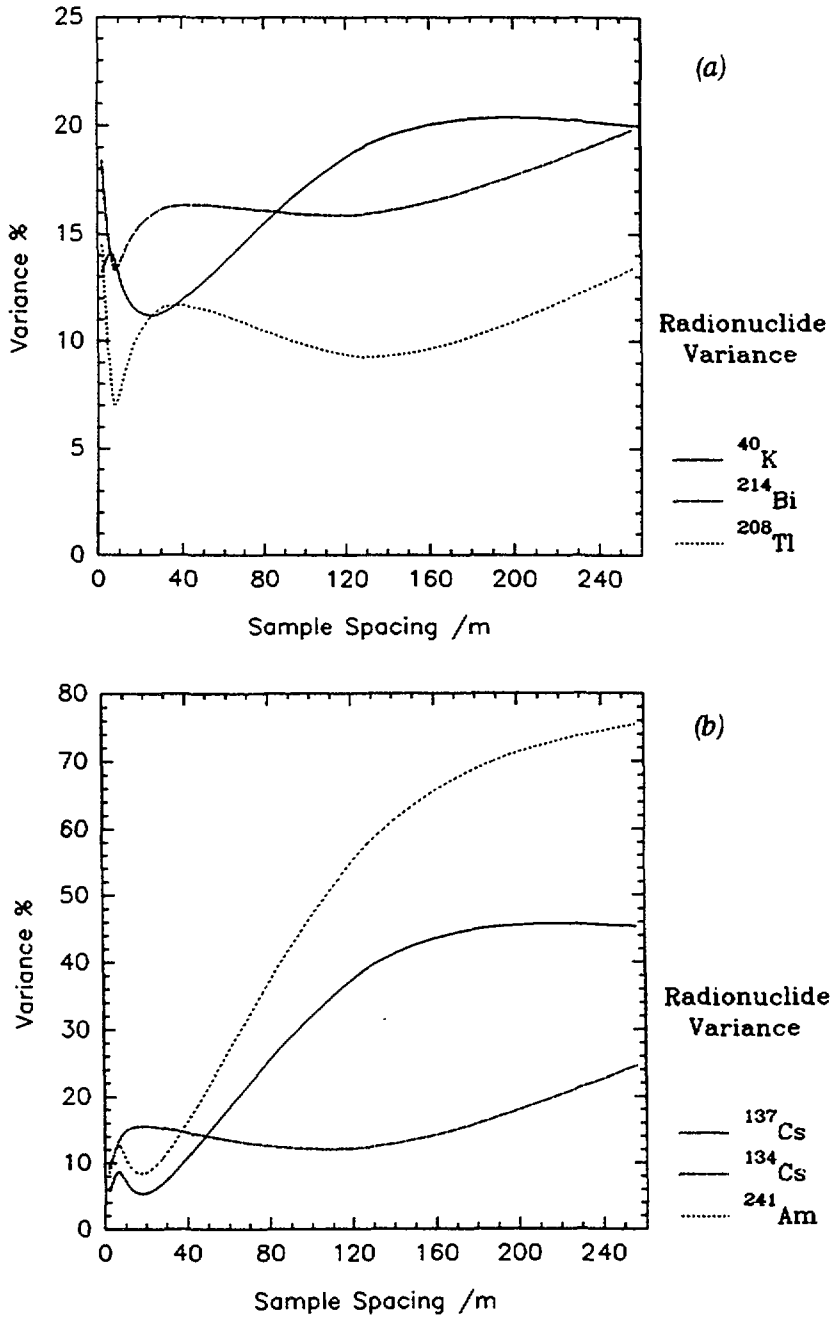

Figure 10. Diagrams demonstrating the sampling variance across the Caerlaverock calibration site for a) natural radionuclides, and b) anthropogenic radionuclides.

weighted mean activity can be determined. As the detector height increases then more of the outer hexagonal shell is effectively viewed by the detector and the spatially weighted mean falls.

Fig. 10 illustrates the sampling variance across the calibration site. It is apparent that the natural nuclides show a modest increase in variance at greater distances from the site centre. By contrast the anthropogenic nuclides on this tide washed pasture site — which have been deposited from marine sediments — show much greater spatial variation due to the influence of tidal and temporal deposition variations. Similar calibrations sites on inland zones affected by the Chernobyl fallout show even greater variations - due to the more uneven distribution of rain-deposited nuclides.

The use of such spatially weighted sampling patterns for ground to air comparisons, while recommended particularly with core samples is also appropriate to in situ measurements, and provides a means of both characterizing and overcoming the inevitable spatial variability of radioactivity in the environment.

5. RAPID MAPPING

Fig. 11 illustrates the rapid mapping procedure. All spectrometric and flight recorded measurements are copied before full data processing to ensure storage integrity of the original data which will require frequent reference. Quality assurance procedures must be adhered to at all stages of processing to minimis corruption risks. After compilation of calibrated results, the datasets are organized and prepared for mapping and contouring. A coordinate transformation is made from the latitude and longitude system, to a national relative X-Y system (British National Grid). Selection of one of the radionuclides or variables is made at this point and is attached to a Z variable. In so doing, XYZ files are produced that can be imported into many different software packages. SURRC has developed its own mapping software however which is constantly updated and reviewed. Statistical analysis of the Z variable can be performed and displayed using standard statistical tools (histograms, summary statistics and regression analysis). For the radiometric data, a range of values and number of colours can be attached for mapping purposes. Displaying information in this manner is the most easily understood form of presentation. Maps can be displayed showing raw radiometric data or smoothed with interpolative functions. For the latter, the concept of field of view has again some significance, and can be related to smoothing and search range parameters. Care must be taken in selection of smoothing parameters to avoid over-interpretation of exploratory data sets. It is recommended that smoothed maps be used to provide an environmental overview of survey results, but that detailed predictions for individual locations, or for comparison with other environmental data sets be based on raw data. Hardcopies of maps can be produced by capture of the displayed data using appropriate software, and output to colour printers.

6. CONCLUSIONS

The methodology described here has enabled aerial survey data to be mapped and demonstrated within 30 minutes following landing during emergency response exercises at nuclear sites. This has benefit in the regular monitoring of nuclear facilities and in particular emergency response situations [22,23,26], where speed of monitoring and data presentation are of prime importance for radiological assessments. In environmental fieldwork it has been possible to complete studies where up to 17,000 gamma ray spectra have been recorded, and to examine preliminary data on screen before the completion of fieldwork. This is important in that it allows re-investigation of specific features identified in the survey before returning to base.

The standard methods have been shown to be extendable to other anthropogenic radionuclides such as ^{137}Cs, ^{134}Cs, ^{60}Co, ^{41}Ar and ^{16}N, in addition to technologically enhanced natural radionuclides eg. ^{234m}Pa, ^{228}Ac. The adoption of theoretically based calibration parameters supplements experimental, semi-empirical approaches [14].

Traceability in an environmental context can be achieved by basing calibration on comparison with soil-core derived information. These comparisons are best made when spatial variability is considered and sampling plans match the spatial response characteristics of airborne detectors. The expanding hexagonal pattern provides a suitable approach and could be extended to form calibration ranges for fixed wing aircraft [21].

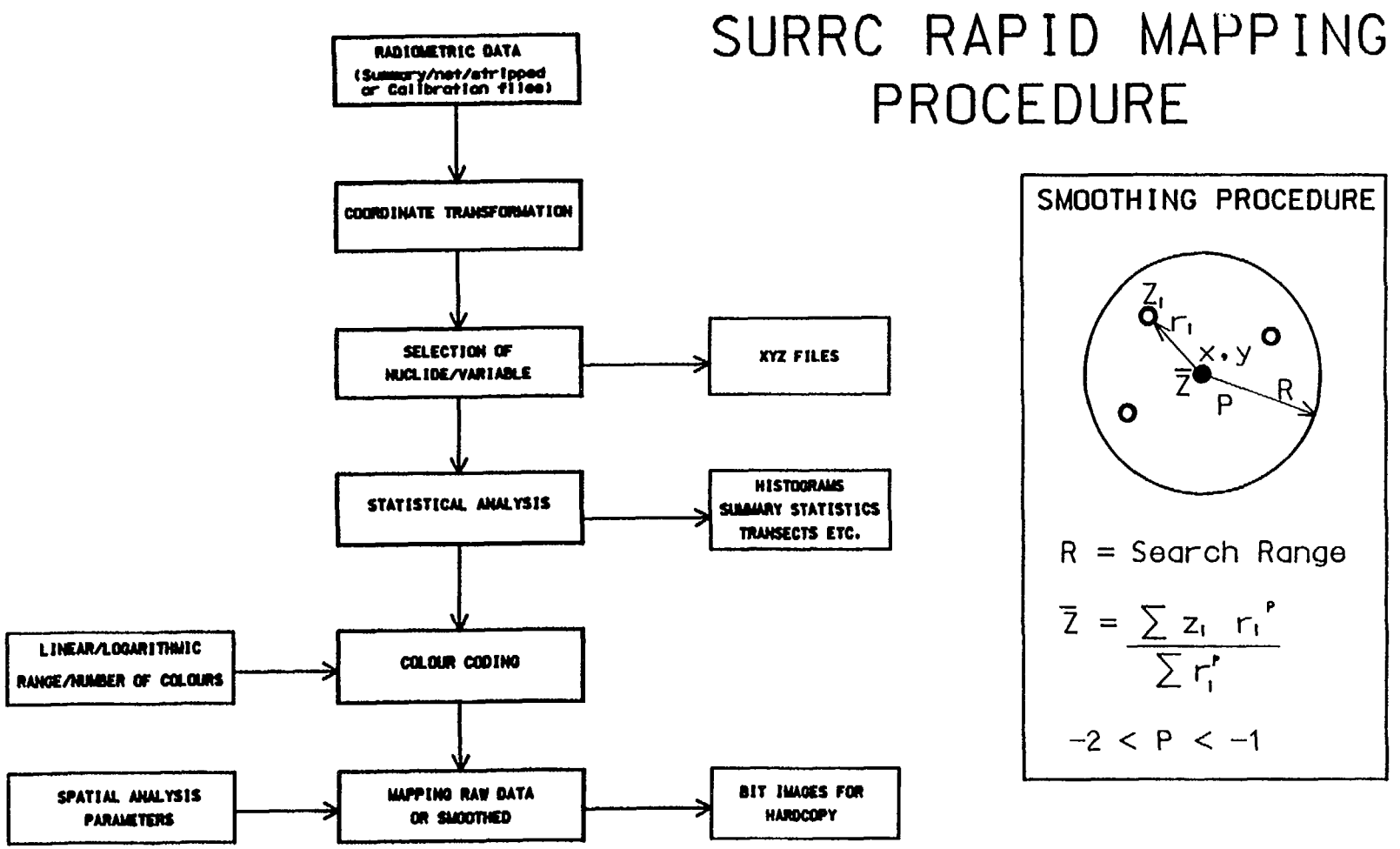

Figure 11. Flow diagram illustrating the SURRC rapid mapping procedure.

Current developments include the incorporation of high efficiency, multi-semiconductor detector arrays to aid interpretation of source burial, complex decay series and low energy photon emitting radionuclides.

REFERENCES

[1] IEC, Airborne Instrumentation for Measurement of Terrestrial Gamma Radiation, IEC 1134, International Electrotechnical Commission, Geneva (1992).

[2] INTERNATIONAL ATOMIC ENERGY AGENCY, Airborne gamma ray spectrometer surveying, Technical Reports Series No. 323, IAEA, Vienna (1991).

[3] DARNLEY, A.G., Airborne gamma ray survey techniques — present and future, Uranium Exploration Methods, IAEA, Vienna, 67 (1973).

[4] INTERNATIONAL ATOMIC ENERGY AGENCY, Recommended instrumentation for Uranium and Thorium exploration, Technical Reports Series No. 158, IAEA, Vienna (1974).

[5] GRASTY R.L., Uranium measurement by airborne gamma-ray spectrometry, *Geophysics* **40**, 503-519 (1975).

[6] INTERNATIONAL ATOMIC ENERGY AGENCY, Radiometric reporting methods and calibration in uranium exploration, Technical Report Series No. 174, IAEA, Vienna (1976).

[7] INTERNAIONAL ATOMIC ENERGY AGENCY, Gamma ray surveys in uranium exploration, Technical Report Series No. 186, IAEA Vienna (1979).

[8] INTERNATIONAL ATOMIC ENERGY AGENCY, Construction and use of calibration facilities for radiometric field equipment, Technical Report Series No. 309, IAEA Vienna (1989).

[9] INTERNATIONAL ATOMIC ENERGY AGENCY, The use of gamma ray data to define the natural radiation environment, IAEA-TECDOC-566, Vienna (1990).

[10] SANDERSON, D.C.W., Allyson, J.D., TYLER, A.N., SCOTT, E.M., 1993, Environmental Applications of Airborne Gamma Spectrometry, IAEA Vienna (??)

[11] SANDERSON, D.C.W., Allyson, J.D., Search for a missing ^{137}Cs source in the Niger Delta, SURRC aerial survey report (1991) 29pp.

[12] BECK, H.L., DECAMPO, J., GOGOLAK, C., In-situ Ge(Li) and NaI(Tl) Gamma-ray spectrometry, HASL-258, USAEC, Health and Safety (TID-4500) (1972).

[13] GRASTY, R., Skyshine and the Calibration of Ground Gamma-ray Spectometry, Geological Society of Canada. Current research part A, 80-1-A (1981).

[14] ALLYSON, J.D., In-situ and aerial environmental radioactivity measurements: An investigation of some factors relating to calibration by simulation and experiment, University of Glasgow (1974).

[15] DUVAL, J.S., Cook B., Adams J.A.S., Circle of investigation of an airborne gamma ray spectrometer, *J. Geophys. Res.* **76**, 8466-8470 (1971).

[16] GRASTY, R.L., KOSANKE, K.L., FOOTE, R.S., Fields of view of airborne gamma ray detectors, *Geophysics* **44**(8), 1444-1457 (1979).

[17] DICKSON, B.H., BAILEY, R.C., GRASTY, R.L., Utilizing multichannel airborne gamma-ray spectra, *Can. J. Earth Sciences*, **18**(2), 1793-1801 (1981).

[18] ALEXANDER, P., KOSANKE, K., The Quality of Airborne Radiometric data. Nevada Section - American Nuclear Soc. Aerial Techniques for Environmental Monitoring, Top. symp. proc. (1978).

[19] LØVBORG, L., GRASTY, R.L., KIRKEGAARD, P., A Guide to the Calibration Constants for Aerial Gamma-ray Surveys in Geoexploration. Top. Symp. Proc. Nevada Section - American Nuclear Soc. Aerial Techniques for Environmental Monitoring (1978).

[20] LØVBORG, L., Error Analysis of Calibration and Field Trials with Spectrometers and Counters. Symp. on Uranium Exploration Methods. OECD Nuclear Energy Agency in collaboration with IAEA, Paris 1-4th June (1982).

[21] TYLER, A.N., Environmental Influences on Radionuclide Inventories and Activity Estimations through Laboratory Based, In-situ and Aerial Gamma Spectrometry. The University of Glasgow (1994).

[22] SANDERSON, D.C.W., AlLYSON, J.D., MARTIN, E., TYLER, A.N., SCOTT, E.M., An Aerial Gamma Ray Survey of Three Ayrshire Districts, Commissioned by the District Councils of Cunninghame, Kilmarnock & Loudon, and Kyle and Carrick, *SURRC Aerial Survey Report* (1990) 22p.

[23] SANDERSON, D.C.W, ALLYSON, J.D., TYLER, A.N., An aerial gamma ray survey of Chapelcross and it's surroundings in February 1992,*SURRC Aerial Survey Report*, to BNFL (1992) 36p.

[24] SANDERSON, D.C.W, ALLYSON, J.D., TYLER, A.N., MURPHY, S., An aerial gamma ray survey of Springfields and the Ribble Estuary in September 1992,*SURRC Aerial Survey Report*, to BNFL (1993a) 46p.

[25] SANDERSON, D.C.W, ALLYSON, J.D., TYLER, A.N., NI RIAIN, S., MURPHY, S., An airborne gamma ray survey of parts of SW Scotland in February 1993,*SURRC Aerial Survey Report*, to the Scottish Office (1993b) 26p.

[26] SANDERSON D.C.W., ALLYSON, J.D., CAIRNS, K.J., MACDONALD, P.A., A Brief Aerial Survey in the Vicinity of Sellafield, *SURRC Aerial Survey Report* to BNFL (1991b) 34p.

NATURAL BACKGROUND RADIOACTIVITIES AND GEOCHEMICAL MAP OF SLOVENIA

M. ANDJELOV, J. TOMŠIČ
Institut za geologijo, geotehniko in geofiziko, Ljubljana, Slovenia

M. PEČNIK
International Atomic Energy Agency, Vienna, Austria

Abstract

In 1990, a programme was initiated as an alternative to airborne survey to obtain the background radiometric map of Slovenia using a very modest resources. The radiometric mapping was performed using portable gamma ray spectrometer on 5 × 5 km grid. Five gamma ray measurements were taken at each of 816 locations. Soil samples of the upper 10 cm were collected for laboratory analysis. Uranium in samples was determined by delayed neutron method. Other 35 elements: Ag, Al, As, Ba, Be, Bi, Ca, Cd, Co, Cr, Cu, Fe, K, La, Mg, Mn, Mo, Na, Nb, Ni, P, Pb, Sb, Sc, Sn, Sr, Th, U, V, W, Y, Zn, and Zr were analysed by plasma emission spectrometry (ICP). The distribution of man-made radiation caused by nuclear weapon tests and the Chernobyl fallout was not the subject of this study. Essential for production of representative map of radioelements was the calibration of spectrometer on concrete pads which were kindly made available by the Geological Survey of Austria at the airfield near Vienna. The data were partly processed at Geological Survey of Canada in Ottawa. The field gamma ray measurements were converted to ground concentrations of potassium, uranium and thorium. The results show a good correlation with the laboratory analyses of soil samples. The ground radioelement concentrations were used to produce maps showing the natural distribution of radioelements, the radioelement ratio map and the maps of individual radioelements. Regardless of the wide spaced sampling, the maps show a relatively good correlation with major geological units in the country. The results have proven that the selected methodology gives good results at minimum costs in a relatively short time. The method demonstrated that it can be successfully implemented in environmental monitoring, geological mapping and mineral exploration. The product of this project represents the first natural background radioactivities and geochemical map of Slovenia covering the entire country.

1. INTRODUCTION

Environment monitoring and meaningful interpretation of man-made pollution is impossible without knowledge about natural abundance of elements in the environment. The main purpose of this study was to produce the geochemical maps showing the distribution of natural radioelements and 35 other elements on the territory of Slovenia. It is also hoped that the results of this study will contribute to the UNESCO International Geological Correlation Programme (IGCP), project 259 — International Geochemical Mapping.

The distribution of chemical elements in the environment in Slovenia has been studied in the past primarily in the context of geological exploration for base metals and nuclear raw materials. Such exploration projects were usually devoted to the specific geological environments and associations of base metals, therefore, they were task oriented. For this reason the territory of Slovenia has never been systematically covered with geochemical exploration using the unique methodology.

The most systematical study of distribution of radioelements was carried out during the uranium exploration programme in 1969, when a fifth of Slovenia's territory was covered by airborne gamma ray spectrometry. Unfortunately only contour maps of the airborne data are now available.

Schematic geological map of Slovenia

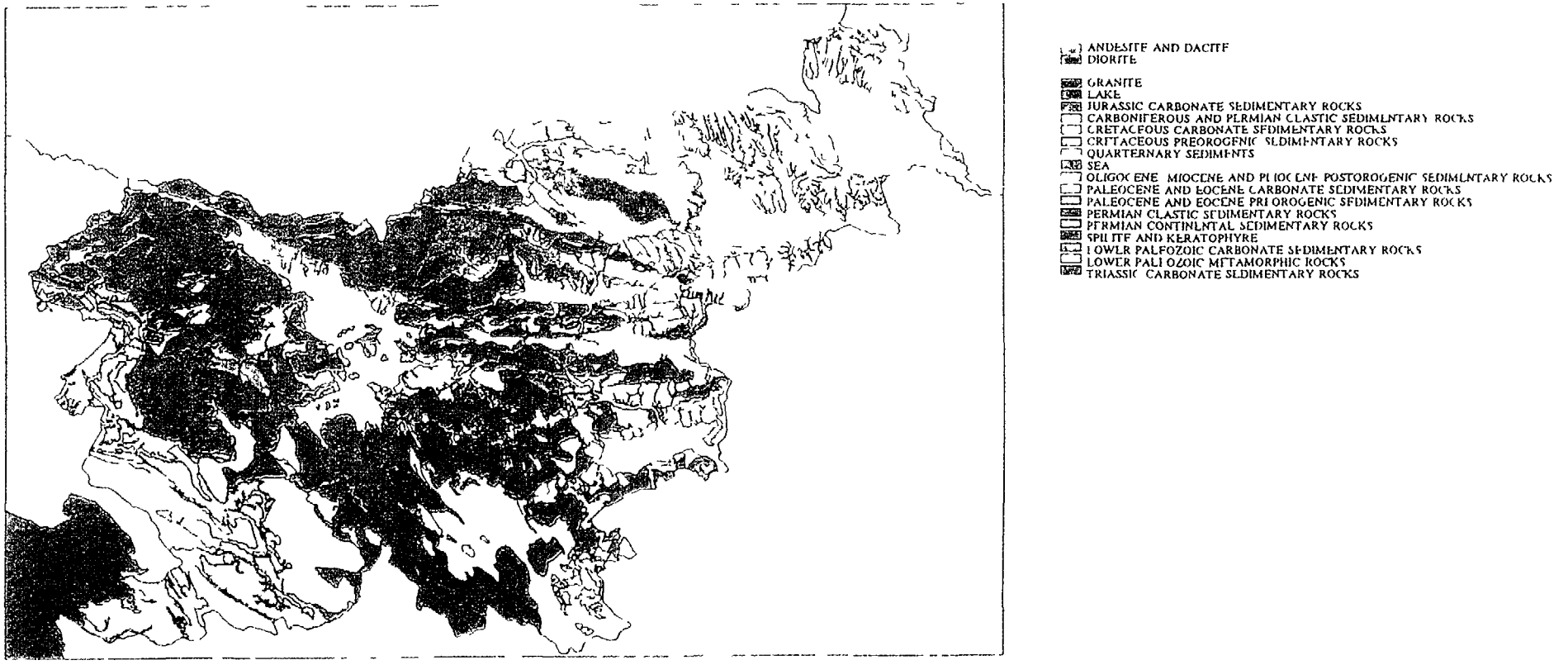

FIG. 1. Schematic geological map of Slovenia.

By M.Poljak (1987)

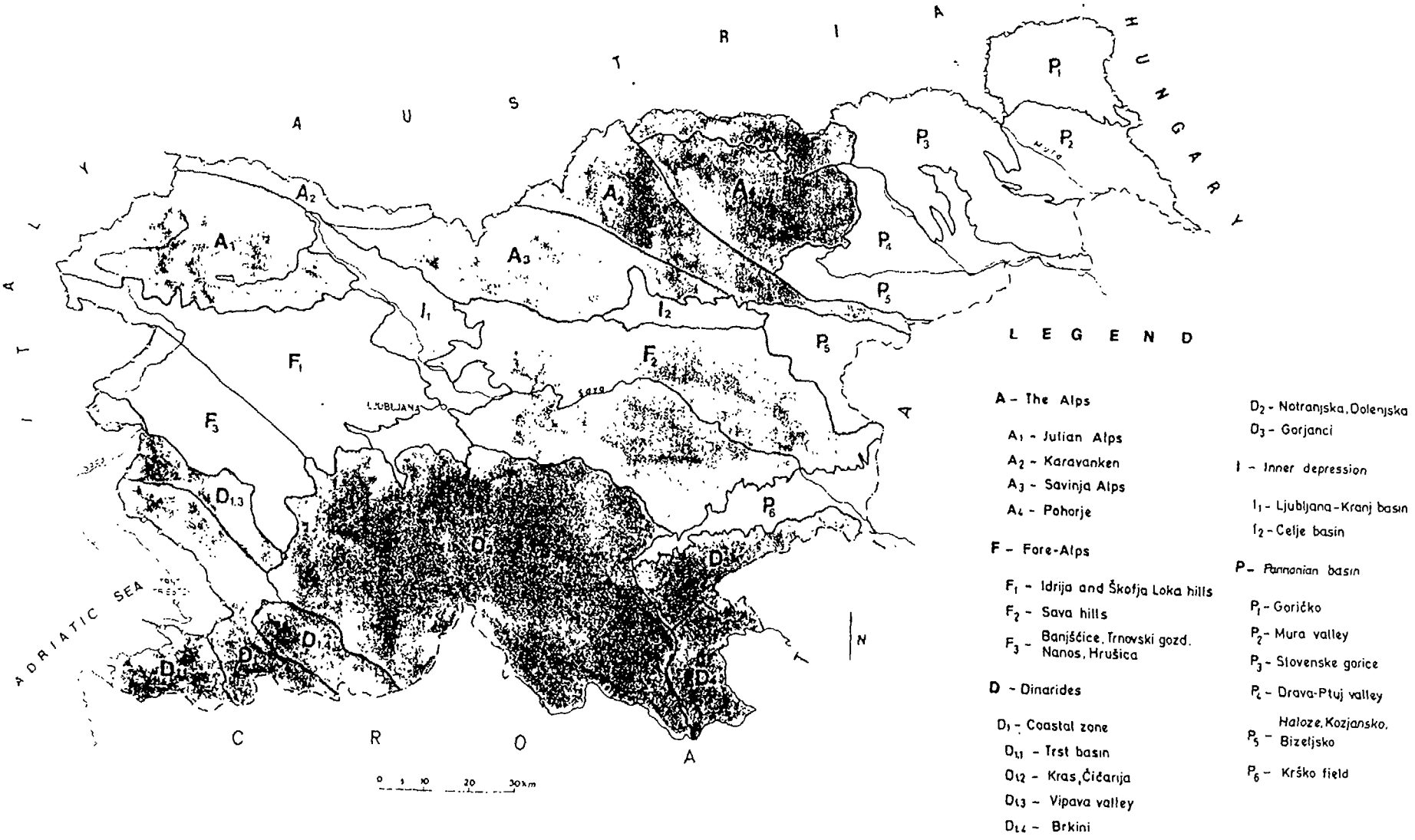

FIG. 2. Geographical-geological units of Slovenia prepared for the land use purpose (remote sensing) (multispectral classification of satellite images).

Attempts to convert the contour data to a digital database were only partially successful because of level problems between flight lines and the limited number of contour intervals on the maps. Parts of Slovenia have also been covered by gamma ray spectrometry on particular rock units favourable for uranium exploration.

In the frame of the UNESCO International Geological Correlation Programme (IGCP), the IAEA co-ordinates the production of the world map of natural radioelements. It was initially planned to produce the map on the basis of airborne gamma ray surveys. As the airborne data are not everywhere available, the use of the ground radiometric surveys was studied for the production of the maps. For this reason the Geological Survey of Ljubljana has performed, with the assistance of the IAEA, the study on use of ground radiometric measurement for the production of natural background radiation maps. The work, which started in 1991, was accomplished in 1993 when the measurement was extended over the entire territory of Slovenia (Fig. 1) [2]. Measurements in a grid 5 × 5 km were performed. Altogether 4 080 measurements on 816 stations covering 20 251 km^2 were carried out. For the comparative analytical determination of K, U, Th and number of other chemical elements soil samples were collected at every measurement point.

2. GEOLOGY

The geological structure of Slovenia is complex. The territory consists of Paleozoic, Mesozoic and Cenozoic beds and igneous rocks of various ages (Fig. 1). Structurally, the territory belongs to the Alps, Dinarides, Fore-Alps and to the Pannonian basin (Fig. 2) [8].

The Alps occupy the northern part of Slovenia. They consist of several physiographic and geologic parts: the Julian Alps, Karavanke, Savinja Alps and Pohorje. The Julian and Savinja Alps are built predominantly of carbonate rocks that strongly influence relief, erosion and vegetation. The Karavanke and Pohorje on the contrary are mostly built of metamorphic and volcanic rocks. These rocks produce rich soils with very dense vegetation cover.

The Fore-Alps occupy the central part of Slovenia. They are divided by the Kranj-Ljubljana valley into eastern and western part. Geologically these terrains belong to the so-called Inner Dinarides. They are mostly built of clastic sediments like shales, marls and sandstones. Vegetation here is very dense due to abundance of water. Mixed forest and grass lands with a lot of cultivated land dominate. The exception is the area south of the Idrija fault i.e. Banjščice, Trnovski gozd and Nanos. This area is built mostly of carbonate rocks. Therefore, we have here a typical karst relief with karstic hydrological regime.

The Dinarides occupy south part of Slovenia. Geologically, the area belongs to the so-called Outer Dinarides. The terrain is predominantly built of carbonates (limestones and dolomites) except for some areas at the coast which consist of flysch deposits. It represents the well-known dinaric karst region. The vegetative cover consists of mixed forest to broad leaf-wood and grass lands with very scarce cultivated land.

Inner depressions lie among previously described regions. The largest are the Ljubljana-Kranj valley and Celje valley. The Ljubljana-Kranj valley is filled up with clay, sand and gravel, fluvio-glacial and limno-glacial origin. The Celje valley represents a flat land of fluvial and proluvial origin of sediments.

The Pannonian basin occupies the eastern part of Slovenia and represents a pattern of broad flat-lands and hilly regions. The flat-lands represent in fact broad river valleys filled up by alluvial deposits (sand, gravel and clay). Hilly regions are mostly built of clastic sediments as marls and sandstones. The land here is highly cultivated, especially the Mura and Drava valleys.

3. DEFINITION OF GRID AND SAMPLING SITES

The density of sampling was limited with the budged allotted for the project. As an optimum for the production of the geochemical maps covering the entire country, the 5 × 5 km grid was selected. The reference point of this grid is located near Ljubljana Castle and is defined with the Gauss-Krueger coordinates 5 100 710 m E and 5 462 520 N.

The measurements were performed as close as possible to the grid intersections. The measuring site was selected outside of narrow ravines on the soils not being cultivated for at least ten years [2]. In total, during the study 816 measuring sites at 5 × 5 km spacing and 226 sites at 1 × 1 km spacing were measured.

4. USED INSTRUMENTS AND METHODOLOGY

The measurements were performed with the four-channel Scintrex GAD-6 spectrometer using the 348 cm^3 NaI crystal. The selected instrument did not allow to measure the effects of man-made radiation caused by nuclear weapon tests and by the Chernobyl fallout which are known to be present in the country.

Five points were measured on each locality: the central point, and four points each at 10 meters N, E, S and W from the central point. During the measurement, the detector was placed on the ground. Time interval of measurement at a locality was five times 100 seconds.

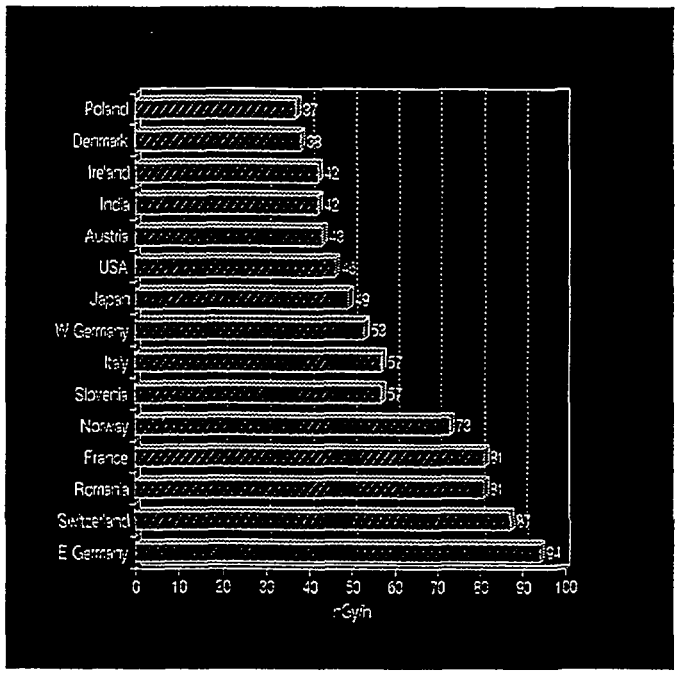

FIG. 3. Outdoor absorbed dose for some countries (UNSCER 1982).

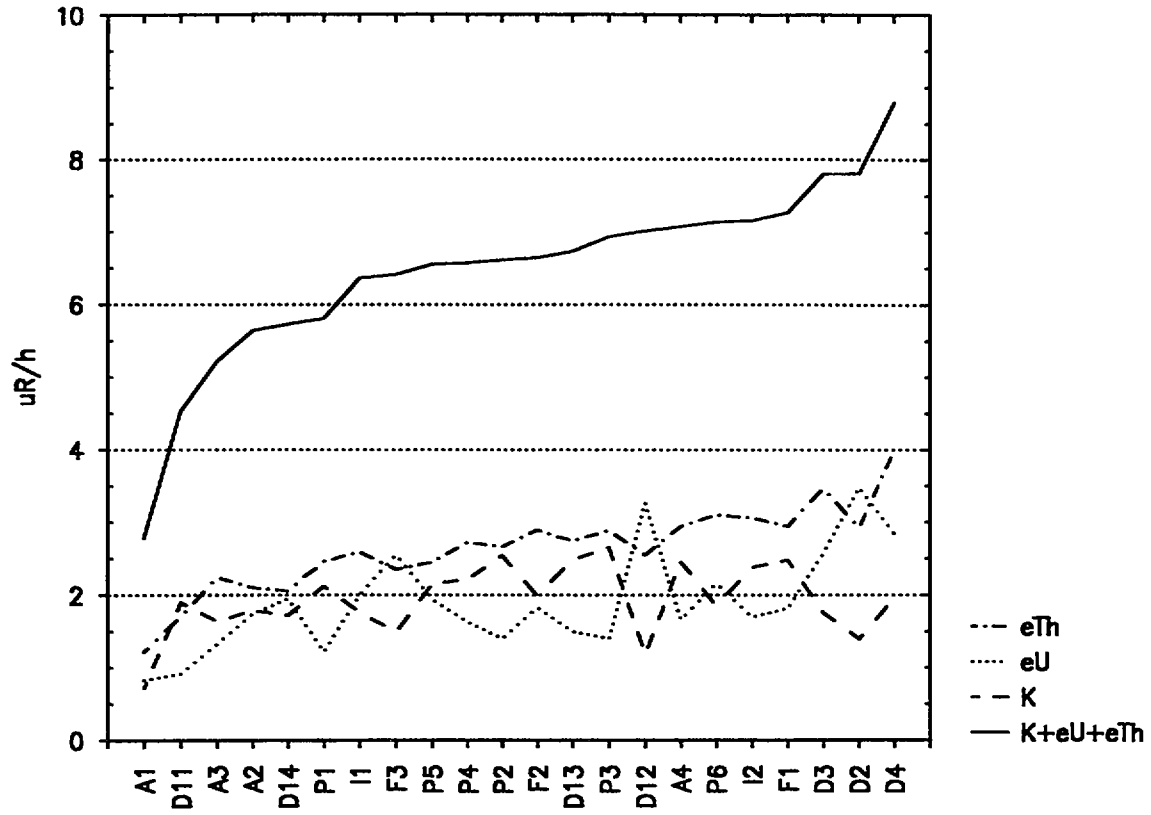

Legend:
A1 - Julian Alps, A2 - Karavanke, A3 - Savinja Alps, A4 - Pohorje, F1 - Idrija in Škofja Loka hills, F2 - Sava hills, F3 - Banjščice, Trnovski gozd, Nanos, Hrušica, D11 - Trst basin, D12 - Kras, Čičarija, D13 - Vipava valley, D14 - Brkini, D2 - Notranjska, Dolenjska, D3 - Gorjanci, D4 - Bela Krajina, I1 - Ljubljana-Kranj basin, I2 - Celje basin, P1 - Goričko, P2 - Mura vally, P3 - Slovenske gorice, P4 - Drava-Ptuj valley, P5 - Haloze, Kozjansko, Bizeljsko, P6 - Krško field.

FIG. 4. The average radiation exposure rate for each natural unit of Slovenia.

Potassium was measured directly in the 1.46 MeV energetic region of gamma radiation emitted by ^{40}K. Uranium and thorium were measured indirectly via gamma radiation of their daughter products. Uranium radioactivity was measured by average gamma radiation at approximately 1.76 MeV emitted by ^{214}Bi, and thorium by average gamma emission at 2.61 MeV of ^{208}Tl. The utilized energy windows are:

potassium	^{40}K	1.38-1.56 MeV
uranium	^{214}Bi	1.66-1.90 MeV
thorium	^{208}Tl	2.44-2.77 MeV

Background radioactivity level caused by the activity of the equipment, cosmic radiation and activity of radon fission products in the air was controlled by periodic measurements in the wooden boat on the Bled Lake. Three year averages were used in computation.

For the production of the representative map of radioelements (Figs 5-8), the spectrometer was calibrated on concrete pads of the Austrian Geological Survey at the airport close to Vienna. Field measurement results were recalculated by using known formulas [4] into concentrations of potassium, uranium and thorium on the basis of results obtained by measurements on concrete pads with known concentrations of radioelements.

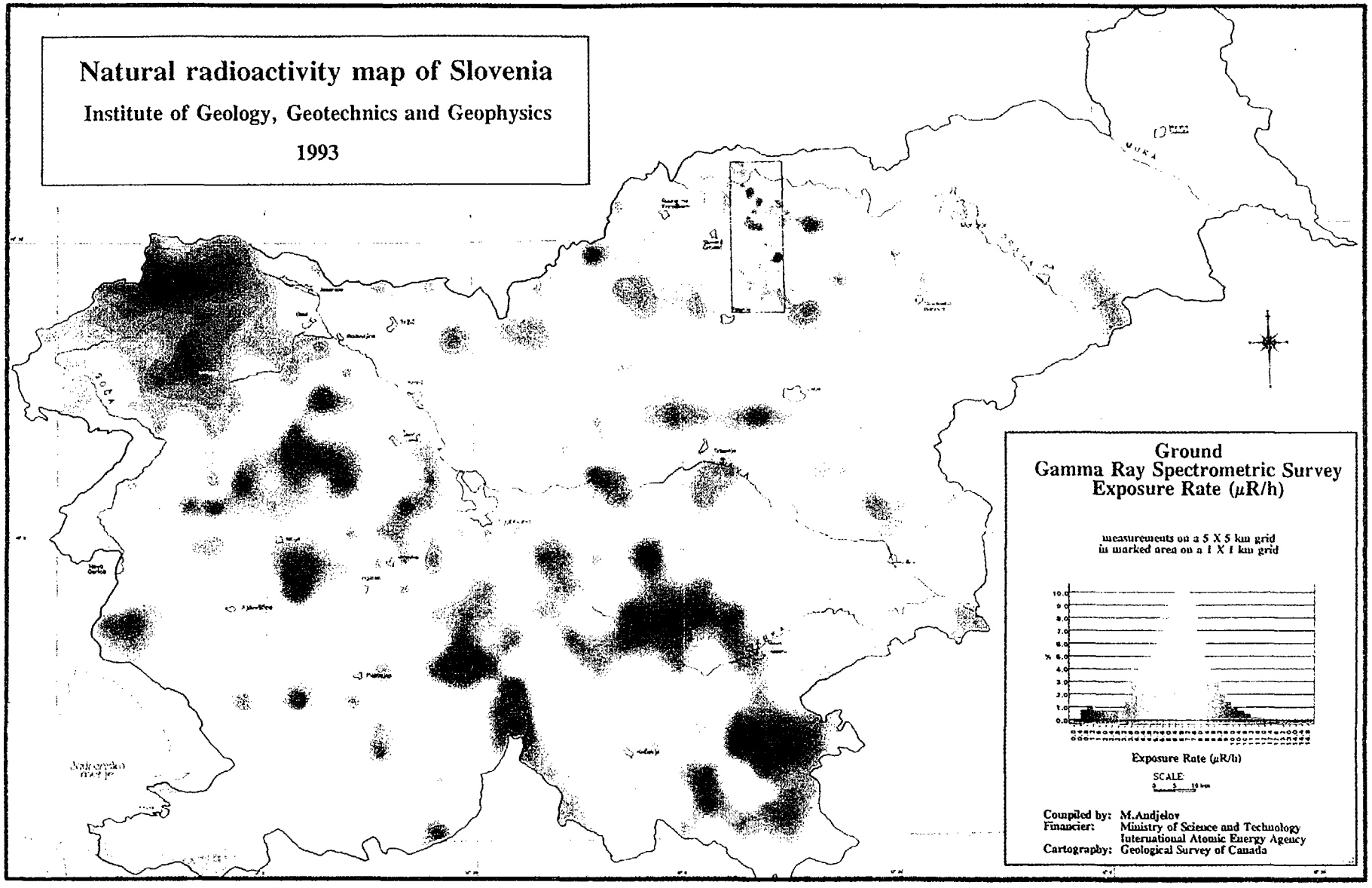

FIG. 5. Natural radioactivity map of Slovenia, Institute of Geology, Geotechnics and Geophysics, 1993; ground gamma ray spectrometric survey — exposure rate (μR/h).

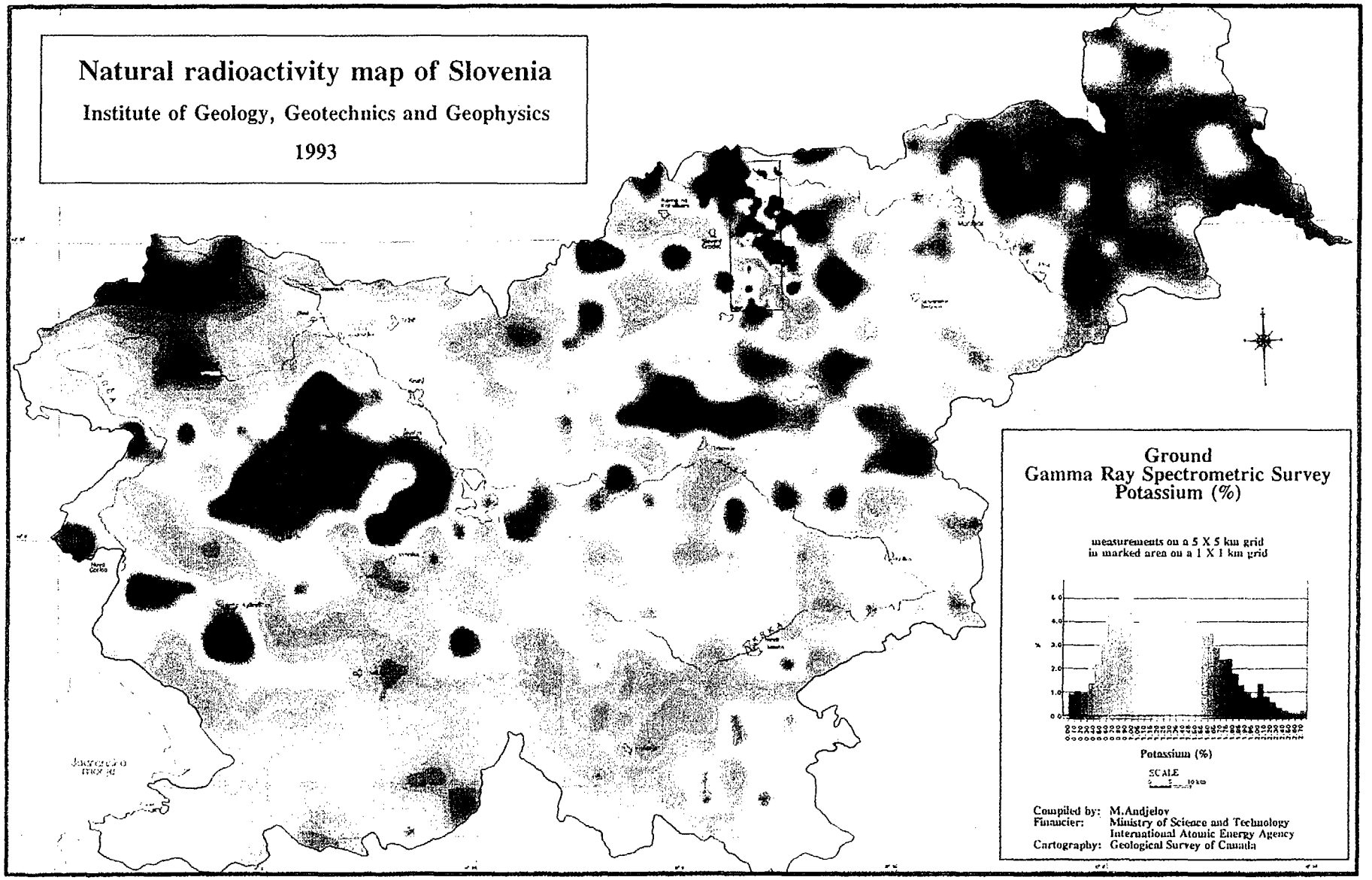

FIG. 6. Natural radioactivity map of Slovenia, Institute of Geology, Geotechnics and Geophysics, 1993; ground gamma ray spectrometric survey — potassium (%).

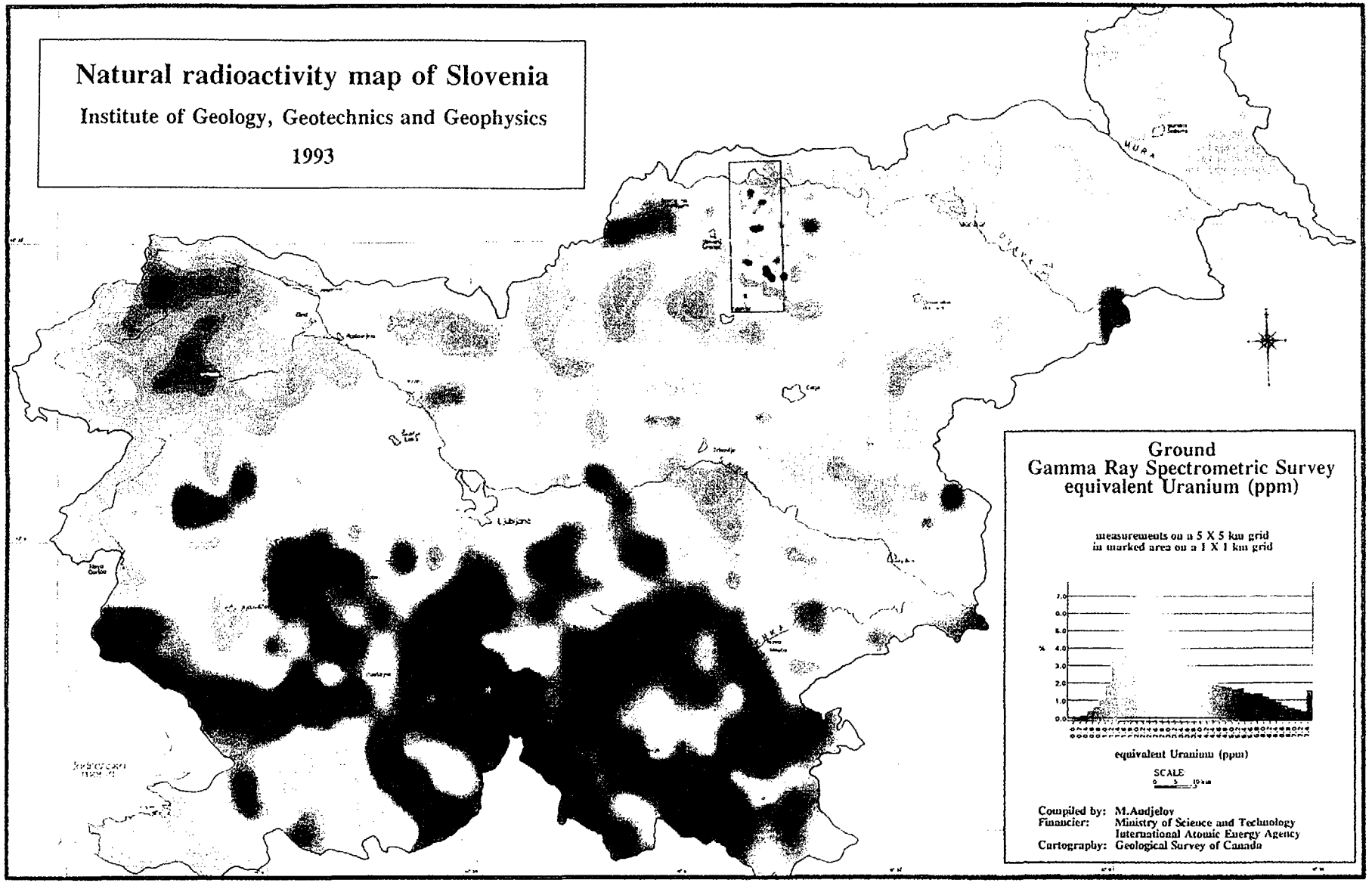

FIG. 7. Natural radioactivity map of Slovenia, Institute of Geology, Geotechnics and Geophysics, 1993; ground gamma ray spectrometric survey — equivalent uranium (ppm).

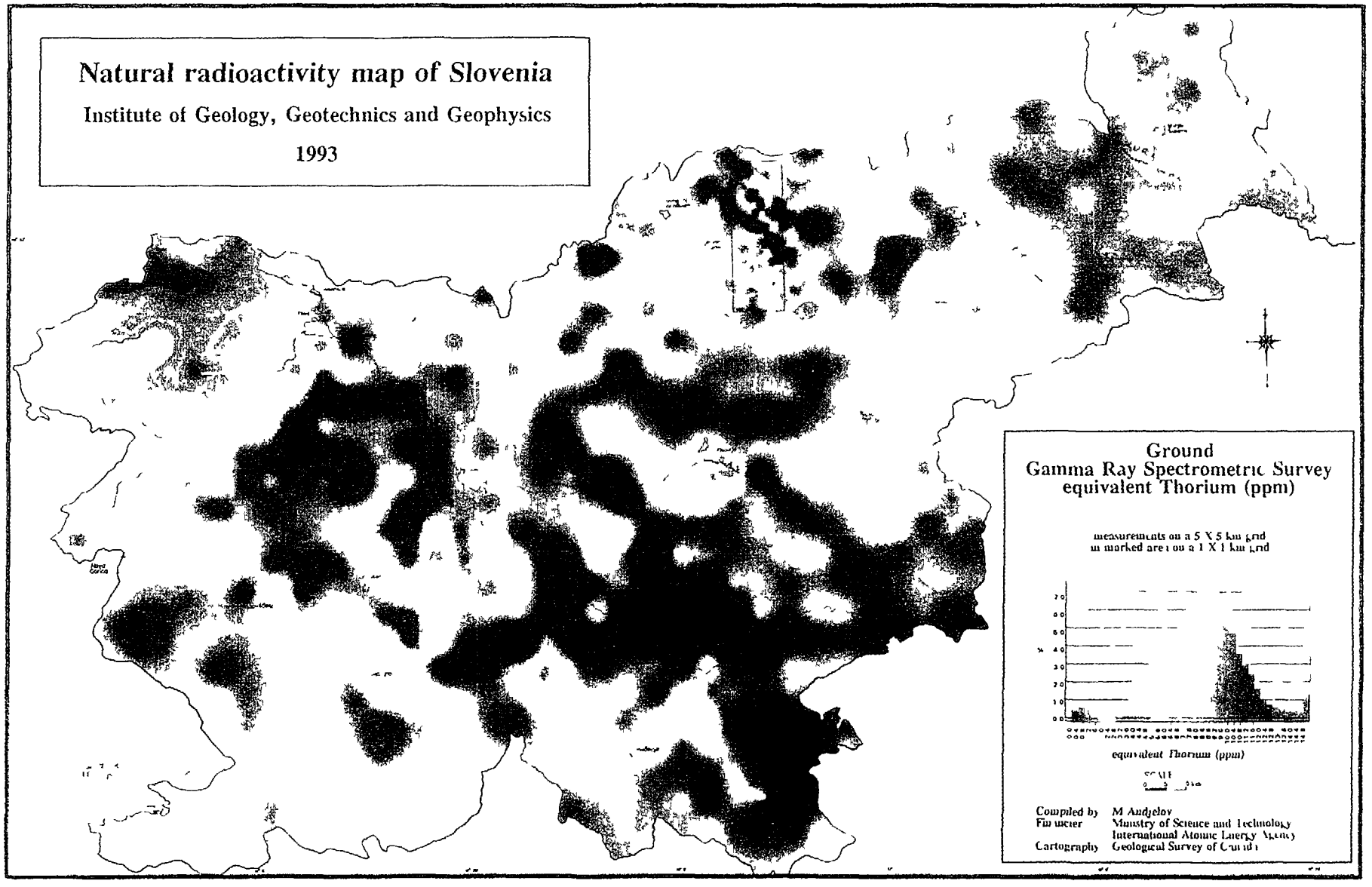

FIG. 8. Natural radioactivity map of Slovenia, Institute of Geology, Geotechnics and Geophysics, 1993, ground gamma ray spectrometric survey — equivalent thorium (ppm)

TABLE I. ELEMENTAL MEANS IN SLOVENIA WITH RESPECT TO THE CLARKE VALUES

Element	Limit of detection		Soil in Slovenia 5 × 5 km				X_{slo}	Clarke value		
	D1	D2	N	min	max	X	$clark_{soil}$	soil	sed.	lith.
Al	0.01	0.01	819	0.39	11.12	**6.69**	0.93	**7.13**		8.05
Fe	0.01	0.01	819	0.21	11.76	**3.75**	0.98	**3.8**		4.65
Ca	0.01	0.01	819	0.02	28.92	**2.58**	1.88	**1.37**		2.96
Na	0.01	0.01	819	0.02	2.54	**0.52**	0.82	**0.63**		2.5
K	0.01	0.01	819	0.06	4.09	**1.45**	1.06	**1.36**		2.5
K*			816	0.05	4.63	**1.23**	0.9	**1.36**		
Mg	0.01	0.01	819	0.09	10.87	**1.35**	2.25	**0.6**		1.87
Ti	0.01	0.01	818	0.02	2.23	**0.38**	0.82	**0.46**	0.39	0.45
P	0.001	0.002	819	0.05	0.46	**0.07**	0.87	**0.08**	0.061	0.093
As	2	4	722	4	131	**8.17**	1.63	**5**		1.7
Ba	2	1	819	12	2261	**370.91**	0.74	**500**	470	650
Be	0.2	1	616	1	5	**2.02**			3.4	3.8
Cd	0.2	0.4	571	0.25	10	**1.16**	(2.32)	**(0.5)**	0.25	0.13
Co	1	2	818	3	99	**27.56**	3.45	**8**	15	18
Cr	1	2	819	7	406	**90.33**	0.45	**200**	78	83
Cu	1	2	818	3	270.5	**27.85**	1.39	**20**	37	47
La	2	2	816	3	104	**31.33**			78	
Mn	1	5	819	24	7187	**1043.99**	1.23	**850**	740	1000
Nb	2	2	709	2.5	21	**7.21**			8.8	
Ni	1	2	816	3	200	**52.85**	1.32	**40**	56	58
Pb	2	4	818	4	181	**38.28**	3.82	**10**	17.5	16
Sc	0.2	1	815	1.6	41.45	**13.22**			11	
Sr	1	4	819	12.5	1016	**98.19**	0.32	**300**	270	340
Th	2	2	795	3	26	**11.02**	1.83	**6**	9.9	13
Th*			816	0.31	21.86	**8.47**	1.41	**6**		
U+	0.01	0.01	816	0.3	12.1	**3.73**	3.73	**1**	3.1	2.5
U*			816	0.11	16.79	**3.3**	3.3	**1**		
V	2	2	819	5	357	**118.07**	1.18	**100**	110	90
Y	2	2	811	3	116	**17.83**			2.8	
Zn	1	2	818	10	1409.5	**113.42**	2.26	**50**	79	38
Zr	1	2	818	2	227	**49.23**	0.16	**300**	160	170

Principal elements in weight % and trace elements in μg/g were determined by ICP, elements marked with the asterisk (*) by gamma-spectrometry, (+) by DNC. D1 detection limit for first 595 samples, D2 for 224 samples. N number of determinations, min-max range, X — arithmetic mean. Clarkes after Vinogradov [9] for soils and lithosphere, and after Judovic & al. [6] for sedimentary rocks.

5. RESULTS

5.1. ABUNDANCES OF RADIOACTIVE ELEMENTS POTASSIUM, URANIUM AND THORIUM IN SOILS IN SLOVENIA

Concentrations of potassium in Slovenia vary between 0.05 and 4.63%, with a mean of 1.23%, and the ratio of this average to the Clarke value is 0.9 (Table I). The highest potassium contents were measured in the Idrija-Škofja Loka territory consisting of predominantly clastic rocks, in the eastern part of the Sava Hills which is built of similar rocks, and in the Pohorje Mountain with mostly igneous and metamorphic rocks. Higher potassium concentrations were also measured in the Pannonian basin where tops of elevations consist mainly of clastic rocks, and in lowlands where the broad river valleys are filled with alluvial deposits. All these areas are covered with rich soils and dense vegetation. The potassium abundances are much lower in the territory of the Dinarides and the Julian Alps which are built mainly of carbonate rocks (Fig. 6).

Uranium in Slovenian soils varies from 0.11 to 16.79 μg/g with an average of 3.23 μg/g, and the ratio of this value to the uranium Clarke is 3.3 (Table I). Higher values of uranium in soil occur in the Idrija-Škofja Loka area and in the Dinaric region on the carbonate rocks with typical karstic relief. Higher uranium abundances were measured also on Pohorje. The lowest uranium values were measured in the Julian Alps region where the carbonate rocks are also karstified, but due to high mountain erosion most of the territory has a very thin regolith cover (Fig. 7).

Occurrence of thorium in Slovenia is found to be in the range between 0.31 and 21.86 μg/g, on the average 8.47 μg/g, and with the ratio to the thorium Clarke 1.4 (Table I). Thorium is the most abundant in soil in the northwestern part of the Outer Dinarides, in the Idrija-Škofja Loka region and on Pohorje. The lowest values were measured in the flysch basins of the Outer Dinarides, and in the Julian Alps where the weathering crust is very thin (Fig. 8).

5.2. EXPOSURE DOSE RATES OF NATURAL RADIOACTIVE ELEMENTS IN SLOVENIA

Factors for conversion of concentrations of natural radioelement potassium, uranium and thorium into the exposure dose rate or the absorbed dose rate in air are almost identical for rocks and for soils, and they are listed in Table II [5].

TABLE II. CALCULATED FACTORS FOR CONVERTING RADIOELEMENT CONCENTRATIONS OF AN INFINITE HOMOGENEOUS PLANE INTO ABSORBED DOSE RATE IN AIR OR EXPOSURE RATE AT AN ALTITUDE OF 1 M ABOVE THE SOIL PLANE.

Conversion into	1 % K	1 ppm eU	1 ppm eTh
Absorbed dose rate (pGy/s)	3.633	1.576	0.693
Exposure dose (μR/h)*	1.505	0.625	0.310

* Factors according to Grasty [4]

Comparison of results of this study with absorbed dose rates elsewhere in Europe and in the world indicates the gamma radiation in Slovenia is very close to the world average which is 45 nGy/h (Fig. 3). As mentioned before, cosmic radiation is not included in the present results. Cosmic radiation in Slovenia, with an average altitude of approximately 530 m, is estimated to be around 35 nGy/h. In the calculation of the absorbed dose rate also climatic factors need to be taken into consideration, especially the seasonal variation of moisture in the soil. In the samples collected for comparison the average humidity in soil was estimated at 22 %.

Important factors governing the exposure dose are in first place the geologic characteristics of the terrain, especially the lithology and the structure, and the geographic characteristics such as the relief and vegetation, as well as the climate. For the land use management in Slovenia, so-called 'natural areas' were defined using the topographic, geologic, pedologic, forestry and climatic maps and the satellite images. The 'natural areas', shown in Fig. 2, were defined on the basis of geographical-geological characteristics which differ from the usual geological and geographical subdivisions of the Slovenian territory [8]. The average radiation exposure rate calculated for each 'natural area' of Slovenia are shown on Fig. 4.

5.3. ANALYSIS OF SOIL SAMPLES

For the comparison of measurements with the chemical composition of soils and its moisture, in the central point of each measurement site a soil sample from the uppermost 10 cm of soil profile was collected. The average weight of the sampled material was 1.5 to 2 kg. Samples for geochemistry were air dried. By weighing the humidity of soil sample was determined (22 weight per cent on the average). The material was gently disintegrated and passed through a 2 mm sieve, and subsequently reduced and ballmilled to grain size below >0.063 mm. Uranium was determined by delayed neutron counting (DNC), and 35 chemical elements (Ag, Al, As, Ba, Be, Bi, Ca, Cd, Co, Cr, Cu, Fe, K, La, Mg, Mn, Mo, Na, Nb, Ni, P, Pb, Sb, Sc, Sn, Sr, Th, U, V, W, Y, Zn, and Zr) were determined by plasma emission spectrometry (ICP).

The results of 819 chemical analyses of soil samples at a 5 $\times$ 5 km grid in Slovenia were used to calculate the averages for 28 chemical elements listed in Table I. About equal to Clarke ($\pm$25%) are means for 8 elements, Al, Fe, Na, K, K*, Ti, P, Mn and V. Higher (up to 100%) are means for 6 elements: Ca, As, Cu, Ni, Sr, Th and Th*, and much higher (above 100%) means of 6 elements Mg, Cd, Co, Pb, U, U* and Zn. Lower are means of 3 elements Ba, Cr and Zr. We do not have data for Clarke values of Be, La, Nb, Sc and Y in soil.

Generally it appears that the elemental averages in soils in Slovenia exceed the world averages. These first data on distribution of chemical elements represent a challenge for further geochemical investigations of the Slovenian territory.

For some of the elements the geochemical maps were produced. Each elemental distribution was subdivided into 9 classes corresponding to 0-5, 5-10, 10-20, 20-40, 40-60, 60-80, 80-90, 90-95, 95-100 percentiles of the given distribution.

The comparison of field measurements and soil analyses of the radioelement shows a relatively good correlation. The correlation of radiometrically determined K and ICP determined K is good, the correlation coefficient is 0.72. The correlation coefficient between radiometric U and ICP U is 0.65, and the slope of the regression line is about 45 degrees. However, some of the measurements show poor correlation. This is because of the disequilibrium between uranium and its decay products which were actually measured by the gamma spectrometer. The correlation between the two methods of Th determination is low, probably because of low sensitivity of the ICP method for Th.

6. CONCLUSIONS

The average total exposure rate for potassium, uranium and thorium in Slovenia is 6.54 $\pm$2.32 μR/h. This result is not corrected for soil humidity which is on the average 22%, and which either increases or reduces the calculated exposure rate in the areas. Of the total mean exposure rate

6.54 μR/h 28% is related to potassium, 32% to uranium and 40% to thorium. The contribution of potassium is lower than the world average for the Earth's crust. The reason is probably the lithology, since more than half of the Slovenian territory consists of carbonate rocks for which lower potassium abundances are typical, and higher (in insoluble residue) abundances of uranium and thorium.

The applied methodology has provided useful information for environment monitoring and geological mapping. The product of this project represents the first natural background radioactivities and geochemical map of Slovenia covering the entire country (Fig. 5). The maps show the baseline information of distribution of elements in the country and represent a good base for the study of consequences of eventual radioactive and other pollution. It is hoped that the information obtained through this project will meet the UNESCO/IGCP and IAEA standards for the production of the Geochemical maps of the world.

Regardless of the relatively large spacing between measurement sites, the principal geological units and trends of the distribution of radioactive elements potassium, uranium and thorium in geological structures are well differentiated on the maps. However, 5 × 5 km density of observation provides just a general impression about the distribution of elements in the country. It is well known that some smaller litostratigraphical units are significantly enriched with particular elements. For this reason it will be necessary to increase the density of sampling in the areas where more detailed information on distribution on natural radio elements and other elements will be needed.

REFERENCES

[1] ANDJELOV, M., TOMŠIČ, J., BRAJNIK, D., Osnove za pripravo radiometrične karte Slovenije, Onesnaževanje in varstvo okolja. Geologija in tehnika za okolje, Zbornik, Zavod za tehnično izobraževenje, Ljubljana (1992) 222-225.

[2] ANDJELOV, M., Use of ground gamma ray spectrometric survey for elaboration of radioelement geochemical maps, Manuscript, Final report for 1993, Research Contract No. 6793/R1/RB, IAEA, Vienna (1993).

[4] GRASTY, R. L.,CARSON, J. M., CHARBONNEAU, B. W., HOLMAN, P. B., Natural background radiation in Canada, Bulletin 360, Geological Survey of Canada, Ottawa (1984).

[5] INTERNATIONAL ATOMIC ENERGY AGENCY, The use of gamma ray data to define the natural radiation environment, Technical Reports Series No. 566, IAEA, Vienna (1990).

[6] JUDOVIC, JA. E., KETRIS, M. P., MERC, A. B., Elementi-primesi v iskopajemih ugljah, Nauka, Leningradskoje otdelenije, Leningrad (1985) 239 p.

[7] PIRC, S., ZUPANČIČ N., Geokemična karta Istre in Slovenskega primorja. Manuscript, Geokemija kamnin Slovenije. FNT Montanistika, Ljubljana (1989).

[8] POLJAK, M., Homogone naravne enote, bazirane na geografsko-geoloških značilnostih SR Slovenije, Uporaba satelitskih metod teledetekcije za ocenjevanje izrabe tal in za potrebe kmetijstva in gozdarstva, Projekt: FAO:TCP/YUG/4502(T), Ljubljana (1987) 7 p.

[9] RÖSLER, H. J., LANGE, H., Geochemical tables, Elsevier Publishing Company, Amsterdam (1972).

[10] UNSCER, Sources and biological effects of ionizing radiation, United Nations Scientific Committee on the Effects of Atomic Radiation 1982, United Nations, New York (1982).

USE OF GAMMA RAY SPECTROMETRIC SURVEY FOR RADIOECOLOGICAL MAPPING IN POLAND

R. STRZELECKI, S. WOŁKOWICZ, J. SZEWCZYK, P. LEWANDOWSKI
Polish Geological Institute, Warsaw, Poland

Abstract

A large spacing ground radiometric survey was carried out over the entire territory of Poland to map the surface concentrations of natural as well as artificial radioelements. The survey was done along N-S lines at approximately 17 km spacing using a 256 channel gamma ray spectrometer. Results of the survey are the productions of, for the first time, gamma dose rate and cesium pollution maps of Poland. The gamma dose rate map reflects largely the geological make up of the country. The cesium map, while indicating very low concentration (from 0 to 8 kBq/m^2) in most parts of the country, shows areas in the country that are polluted. The patterns of the polluted areas have no correlation with the underlying soil types nor vegetation covers. It is deduced that metereological conditions during deposition was the main controlling factor of these patterns.

1. INTRODUCTION

The cover of the Quaternary postglacial sediments is the dominating element in the image of surface geology of Poland. Quaternary sediments represented by moraine clays, fluvioglacial and eolian sands are covering 70 percent of the territory. Their thickness is varying from few up till 300 meters. Older formations are exposed in southern and south-western part of Poland in form of: metamorphic, granitoid massifs and sedimentary Palaeozoic formations in the Sudetes (SW Poland), Palaeozoic and Mesozoic sedimentary formations in the Holy Cross Mountains, Upper Silesian Coal Bassin and Małopolska Highland (Middle and south Poland), Cretaceous–Paleogene flysch sediments exposed in the Carpathians (along souther border of Poland), older granitoid and metamorphic rocks exposed in the Tatras (Inner Carpathians).

The radiometric and gamma ray spectrometric methods were applied in Poland since 1950 for the purpose of uranium exploration in the Sudetes and at the smaller scale in Carpathians and in Holy Cross Mountains. The above mentioned regional surveys covered only 10% of the territory of Poland. Gamma ray spectrometric and radiometric survey of the whole country has been yet not carried out. Since 1990, after stopping the construction of nuclear plant in Zarnowiec (near Gdansk) and restraining up till the year 2000 the concept of development of nuclear power industry in Poland, all uranium prospection programmes in Poland carried out up till then by the Polish Geological Institute were stopped.

In 1989 Polish Geological Institute proposed studies and gamma-ray spectrometric survey covering the territory of the whole country under the national programme entitled "Protection of the Lithosphere". The main tasks of this survey are:

- mapping of the cesium pollution after the Chernobyl accident:
- compilation of individual radioelements distribution maps which are necessary to prepare the radon risk maps and to calculate effective dose equivalent:
- estimation of concentration and distribution of pollution (with uranium and radium) of the recent river sediments of the Vistula and Odra rivers, provoked by dropping of the polluted mine-waters from the coal mines of Upper Silesian Coal Bassin area.

The dose rate map and Cs concentration maps are already compiled and will be soon printed while the map of the distribution of natural radionuclides is now compiled.

2. WORK METHODOLOGY

The accident at the nuclear plant in Chernobyl, disturbed very significantly the terrestrial gamma ray over the big area of Europe.

The spectrometric survey conducted by Polish Geological Institute in 1986 in the Sudetes directly before as well as after the Chernobyl accident, delivered very interesting and unique at the European scale experimental data [1]. The few years period between the accident and the beginning of the field works resulted in decrease of the amount of radionuclides from several tens presented in the fallout just after the accident to only two - ^{137}Cs (T 1/2=30 years) and ^{134}Cs (T1/2=2 years) as well as in the change of the spatial distribution of these elements from surface distribution just after the accident to spatial distribution depending from many factors such as the type of soil, soil permeability and type of vegetation cover.

The results of the above mentioned field works have been used among others to work out the effective methodology of determination of "in situ" total concentration of Cs isotopes. This method determines the gamma radiation dose rate related to the above radionuclides expressed as the difference between the measured total dose rate and the total dose rate from the natural gamma radiation emitters. The concentration of the latter is determined by the measurements covering respectively for potassium, uranium and thorium the decay energies of: 1.46 MeV, 1.76 MeV and 2.62 MeV and decay energy higher than 0.56 MeV for the TC window. Concentration of the latter decay energies does not influence the gamma spectrum in this energetic areas. The calibration coefflcients are determined by measurements with gamma-ray spectrometer at the calibration pads in Bratkovice near Prybram (Czech Republic).

Cosmic background was measured on the Zegrze lake, 100 m from the nearest bank. Calibration of the spectrometer with respect to Cs is more difficult due to lack of possibilities of creation spatial calibration standards meeting the field standards. Here the method of approximate calibration, based on point measurements, used by the Central Laboratory of Radiological Protection was used.

Concentration of the natural isotopes was determined using the known formula:

$$Qi = \sum_{p+1}^{3} a_{ip} \; x \; N_i^p \qquad (1)$$

where: Qi - percentage concentration for K, ppm concentration for U and Th for i - of this isotope

a_{ip} – calibration coefficients
N^p – count rate in energic windows

Concentration of cesium Q_{Cs} isotopes was determined using the formula:

$$Q_{Cs} = K_{Cs} \; x \; d \; (N^T - N^{NAT}) \qquad (2)$$

where: K_{Cs} – calibration factor determining relation between count rate from Cs and their dose rate

d – calibration factor determining relation between ^{137}Cs dose rate and its concentration in soils. The value of this factor is depending of the deep distribution of radionuclide concentration in soils, in the interpretation process usually the average value characteristic for each type of soil is used

N^T, N^{NAT} – measured (N^T) count rate in TC energic window and calculated (N^{NAT}) on the basis of concentration of natural radionuclides.

3. FIELD MEASUREMENTS

Measurements were made along N-S oriented profile lines spaced 15' (about 17 km). Measurements were made each 1 000 m. In the case of certifying in the TC window of the value higher than 5 500 counts/2 minutes, measurements were made each 500 m in order to recognize more precisely the anomalies. Measurements were also made each 500 m or even less in the places of intersection of the profile lines with the Odra and Vistula rivers valleys so, that at least 1 measurement point was located on the flood- or over-flood terrace. The purpose of such procedure was to collect water pollution with radioactive elements transported by mine-waters data [2].

Measurements were made using hand held type gamma-ray spectrometer, model GS-256 produced by "Geofizyka" Brno with 3" × 3" Na (T1) detector. 2 minute time of measurement was used. The detector was placed 1.5 m above the terrain in order to eliminate the influence of the terrain denivelations.

The field works were carried out in the period from June till December, 1992. Out of 20 000 measurements made during this period 19 528 was used for the map compilation.

Data were collected in the DBase system. For map compilation Surfer computer program and GIS Arc/Info system were used. Calculations were made using the SPSS/PC statistical system.

4. RESULTS OF INVESTIGATIONS

4.1. GAMMA DOSE RATE MAP

Gamma dose rate is the compilation of gamma radiation related to the natural radionuclides of: uranium ^{238}U, thorium ^{232}Th and potassium ^{40}K and artificial isotopes of cesium $^{137+134}Cs$ introduced into the environment and considered as elements polluting the environment (Fig. 1).

The average gamma dose rate for Poland is 34.2 nGy/h however it is varying from 23.3 nGy/h for the Zielona Góra voyevodship (W Poland) to 62.25 nGy/h for Wałbrzych voyevodship (SW Poland).

Highest gamma radiation is noted in S Poland (The Sudetes and Carpathians regions) as well as in the Holy Cross Mountains and Lublin area. The central and northern part of the country is characterized by the low total gamma dose rate except for some small areas in the region of Mazury and Suwałki. Such distribution of the gamma dose rate is related to the geological surface image of Poland. It has been changed only on a small part of the territory after the Chernobyl accident.

Highest values of the gamma dose rate — over 70 nGy/h are observed in the Sudetes and are related to the presence on the land surface of rocks containing higher concentration of natural radionuclides presented by: granitoides, gneisses and crystalline schists in Karkonosze and Izery Mts, sedimentary (shales and sandstones) and vulcanic rocks (ryolites) of Permian and Carboniferous in

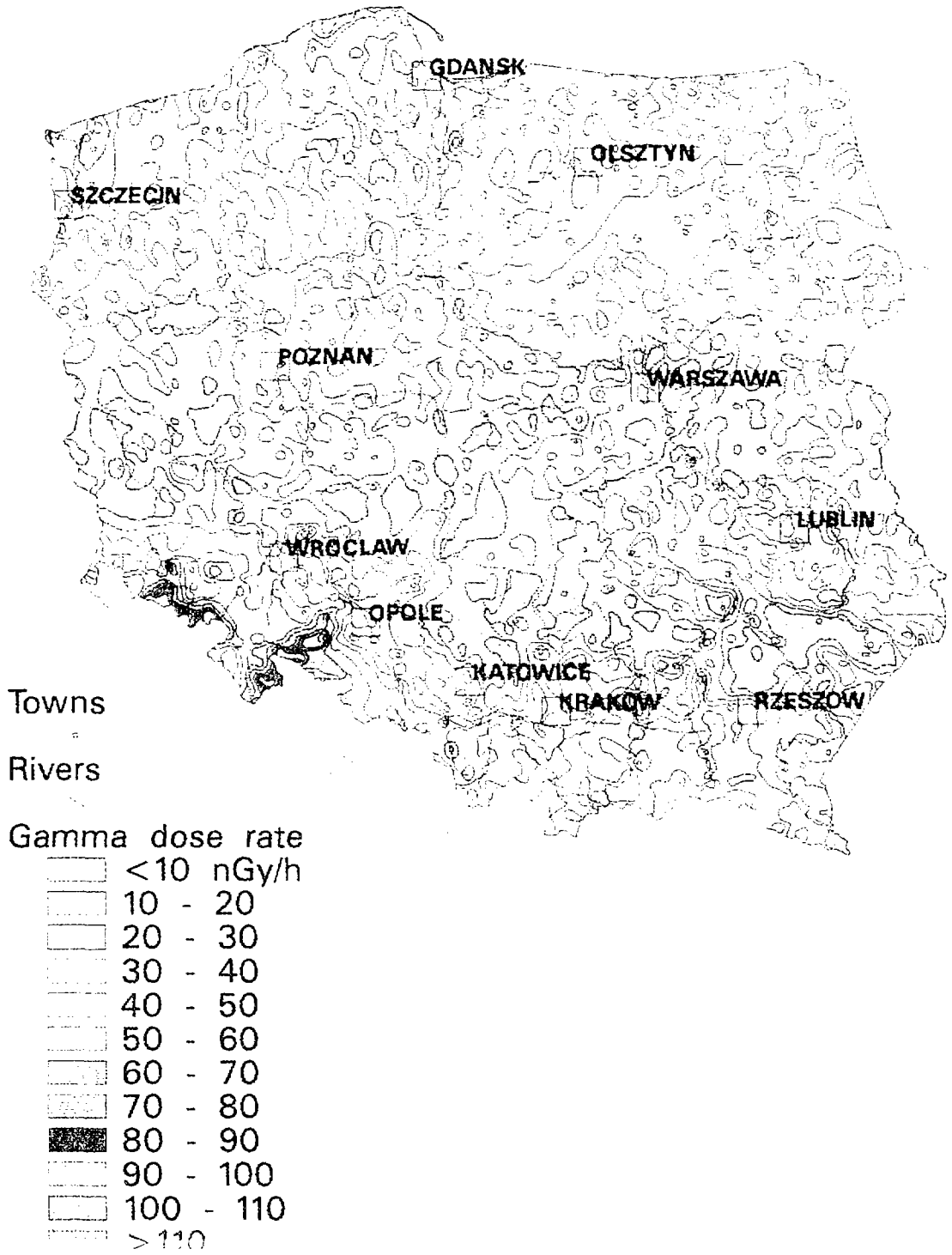

FIG. 1. Map of gamma dose Rate in Poland.

the Intra-Sudetic Depression, Precambrian metamorphic and magmatic rocks in Złote Góry and Śnieznik Massif. Few small uranium deposits and few-tens of indices of uranium and thorium mineralization are known from this area. High values of gamma dose rate in western part of Opole region (SW Poland) is related to the post-Chernobyl pollution.

Another area characterized by relatively high values of gamma dose rate - over 40 nGy/h is the region of Carpathians. This high value is related to the occurrence on the surface of the flysch sediments represented by silt shales and fine-grained sandstones.

The gamma dose rate varying from 40 to 70 nGy/h is also noted from the Lublin area (SE Poland) and from Holy Cross Mountains. In the Lublin area it is related to Creataceous sediments and Quaternary loess cover. The higher gamma dose rate noted in loesses is very interesting as loesses due to their high permeability present a good collector properties and can collect radon emitted from the subsoil [3]. In the Holy Cross Mountains high gamma dose rate are noted from the outcrops of the Palaeozoic sediments covered with thin loess cover in the eastern part of the region.

The middle and northern part of Poland is characterized by relatively low values of the gamma dose rate varying between 20 and 40 nGy/h. This area is covered with the Quaternary sediments. The mosaic image of the gamma dose rate value corresponds in general with the variable lithology. Due to the scale of the map only big lithological units are presented. The lowest gamma dose rate values of 20 - 30 nGy/h are recorded from the areas covered with fluvioglacial and eolian sands. Among the river sediments highest gamma dose rate is described from the Vistula river sediments and can be related to the above mentioned pollution of the waters by the mining industry of the Upper Silesia region.

Moraine uplands build of clays are characterized by gamma dose rate of 30 to 40 nGy/h although in some places a higher dose rate of 60 nGy/h is noted from the boulder clay containing granitoids erratics in Mazury (Ketrzyn) and Suwałki (NE Poland) regions [4].

4.2. CESIUM POLLUTION MAP

In examination of the distribution of concentration of radioactive cesium isotopes the following factors should be taken into consideration:

- the main part of Cs was introduced into the environment as the result of Chernobyl accident in April and May, 1986;
- some amounts of Cs may be related to military nuclear bomb tests, carried especially in 1959-1962;
- regional distribution of Cs fallout was depending from the meteorological conditions, other environmental factors such as type of soil seem to be less important.

Results of the field works indicate that more than 90% of the territory is characterized by very low Cs concentration varying from 0 to 8 kBq/m^2 (Fig. 2). The average Cs concentration calculated for Poland is 4.67 kBq/m^2 with standard variation of 5.51 kBq/m^2. Taking into consideration the assumption, that the average value plus the value of 2 standard variations determines the anomalous concentration, 15 kBq/m^2 isoline is considered as indicating the anomalies.

The highest Cs pollution was noted from SW Poland, from E part of Fore-Sudetes Monocline and from Silesia Lowlands. These anomalous concentrations are a part of zone characterized by higher Cs pollution running in SW-NE direction from the Kłodzko Valley area (Czech border) to the region of Warsaw. Three anomalous areas can be distinguished within this zone, mainly: Opole region (surface of 4 500 km^2), vicinity of Radomsko and vicinity of Warsaw.

The highest values of Cs pollution up to 96 kBq/m^2 are noted from the Opole region. Smaller anomalies are also observed from:

- southern Poland - W Carpathians, Cs concentrations up to 25 kBq/m^2,
- small parts of the Sudetes, Cs concentration up to 25 kBq/m^2,

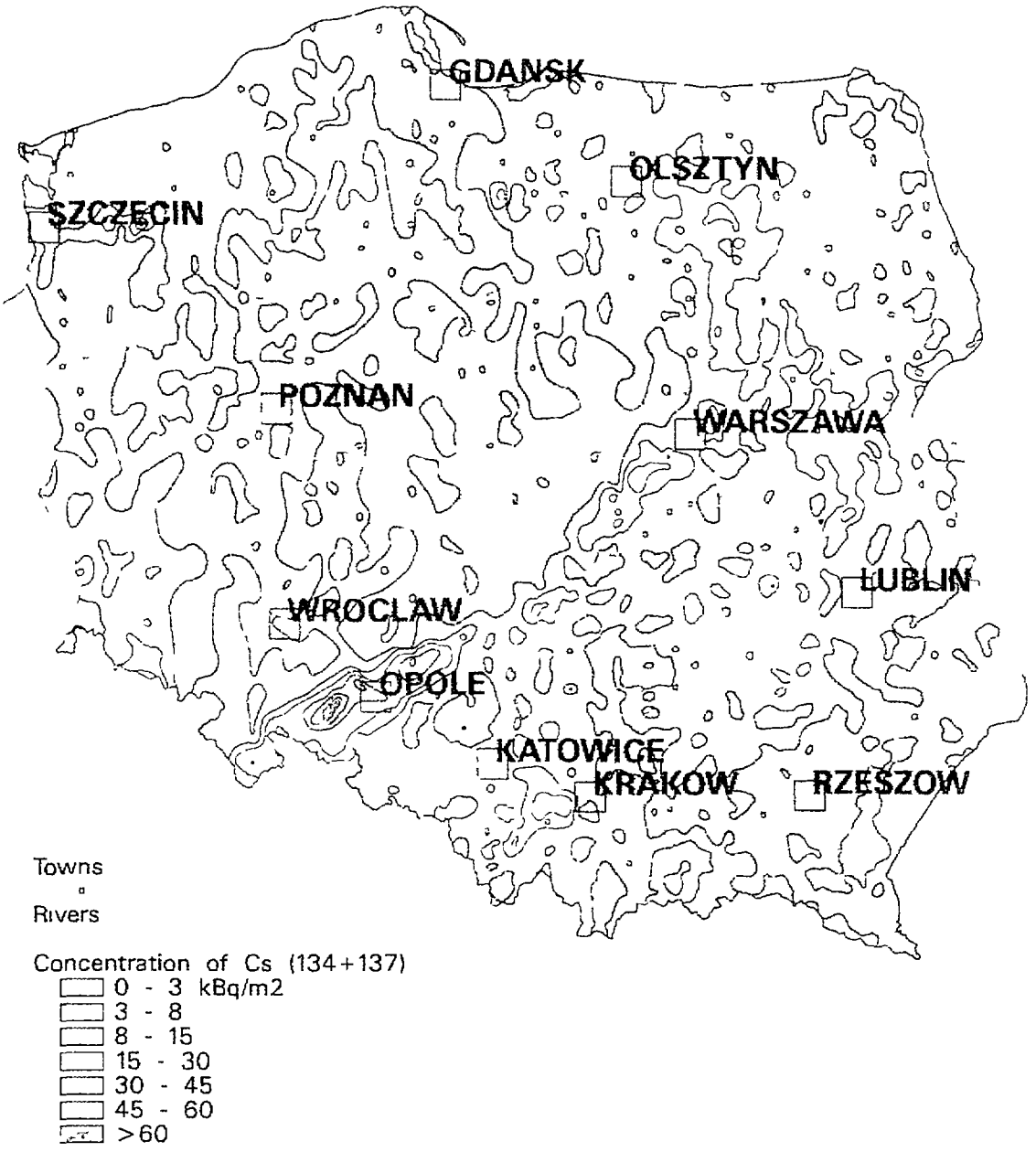

FIG. 2. Map of cesium concentration in Poland.

- few anomalous areas in E Poland, Cs concentration up to 50 kBq/m^2, and their continuation in NW direction - anomaly N of Warsaw,

- separate Cs concentrations (15 kBq/^{2}) in Szczecin voyevodship (NW Poland) and Elblag voyevodship (N Poland).

The statistical analysis of the data did not show any correlation between Cs concentration and the type of soil and vegetation cover.Therefore it can be stated, that the meteorological conditions played the main role in the distribution of Cs pollution in Poland. Statistical frequency distribution of Cs for separate voyevodships characterized with higher Cs pollution [5, in press] show high perturbation, positive skewness and multi-modality what suggests the multi-phase period of the deposition of polluting elements. Unfortunately, lack of meteorological maps for the period of 10 days after the accident does not allow to relate the meteorological elements to the measured cesium concentration.

BIBLIOGRAPHY

SZEWCZYK, J., Wpływ skażeń promieniotwórczych na pole naturalnego promieniowania garnma, Prz. geol. nr 10 (1990).

STRZELECKI, R., SZEWCZYK, J., WOŁKOWICZ, S., JEDRZEJCZAK, Z, Badania promieniotwórczości garnma na obszarze Polski: efekt Czarnobyla, skażenia przemysłowe, promieniotwórczość naturalna, Prz. geol. nr 6 (1992).

STRZELECKI, R., WOŁKOWICZ, S., Radon — zagrożenie wieksze niż "Czarnobyl", Prz. geol. nr 3 (1993).

STRZELECKI, R., WOŁKOWICZ, S., LEWANDOWSKI, P., Wyniki badań promieniotwórczości gamrna na Suwalszczyźnie. Prz. geol. nr 8 (1993).

STRZELECKI, R., WOŁKOWICZ, S., LEWANDOWSKI, P., Koncentracje cezu w Polsce. Prz. geol. 1994 nr 1 (in press).

THE USE OF CAR-BORNE GAMMA RAY DATA FOR THE STUDY ON NATURAL RADIATION

Y. NAGASAKI, Y. OCHIAI, S. SOMA, K. TSUBOTA ,
Power Reactor and Nuclear Fuel Development Corporation,
Izumicho, Toki City, Japan

Abstract

Car-borne gamma ray surveys have been carried out during uranium exploration in Japan by Power Reactor and Nuclear Fuel Development Corporation (PNC) during the last two decades and numerous gamma ray total count rates data were accumulated. 4 channel car-borne system with twelve NaI (Tl) cylindrical crystals was newly introduced to convert the earlier car-borne data into absorbed dose rate because the earlier car-borne system is no longer exist. A good linear relationship between count rates and absorbed dose rates was found by the 4 channel car-borne test survey. This led to the total count rates data successfully converted into absorbed dose rate. The absorbed dose rate distribution in a test area calculated from earlier car-borne data using the linear relationship correlated very well with the geological features within the area. Therefore it is suggested that the earlier car-borne data accumulated during domestic uranium exploration can be effectively used to delineate detailed maps of natural radiation distribution with the help of the detailed regional geological maps obtained during exploration for the future study on natural radiation in Japan.

1. INTRODUCTION

Gamma ray surveys are the most popular and widely used techniques in uranium exploration. Among those surveys, car-borne gamma ray survey system was employed by PNC for domestic uranium exploration during the last two decades mainly because it was the best way to find radioactive anomalous spots rather than by airborne in Japan.

The car-borne survey covered almost all over Japan and several outcrops of uranium occurrence were discovered by the survey [1]. The car-borne data accumulated over two decades are now facing to a decline in the use or even to the loss with the closing of the domestic uranium exploration in 1987. If the data in total count rate could be converted into absorbed dose rate, a large amount of car-borne data would become greatly beneficial for the estimation of natural radiation levels and the delineation of radiation distribution in Japan.

On the other hand, the National Institute of Radiological Sciences (NIRS) of Japan had conducted nationwide a measurement of natural radiation from 1967 to 1977. The measurement was carried out using scintillation spectrometer and ionization chamber at the height of 100 cm from the ground. Totaled 1127 points at large bare areas such as school play grounds were chosen as the measurement sites. The measurement results were compiled and reported by NIRS as exposure rate maps of natural radiation in Japan [2]. Although this study provides a general information about the natural radiation levels and their distribution, more detailed absorbed dose rate distribution maps would be necessary for the environmental assessment around nuclear facilities.

In 1990, the Nuclear Safety Commission (NSC) of Japan projected the five-year national safety research programme. PNC has been concerned with this programme to investigate the detailed natural radiation levels and their distribution in conjunction with geological features with the use of accumulated car-borne data.

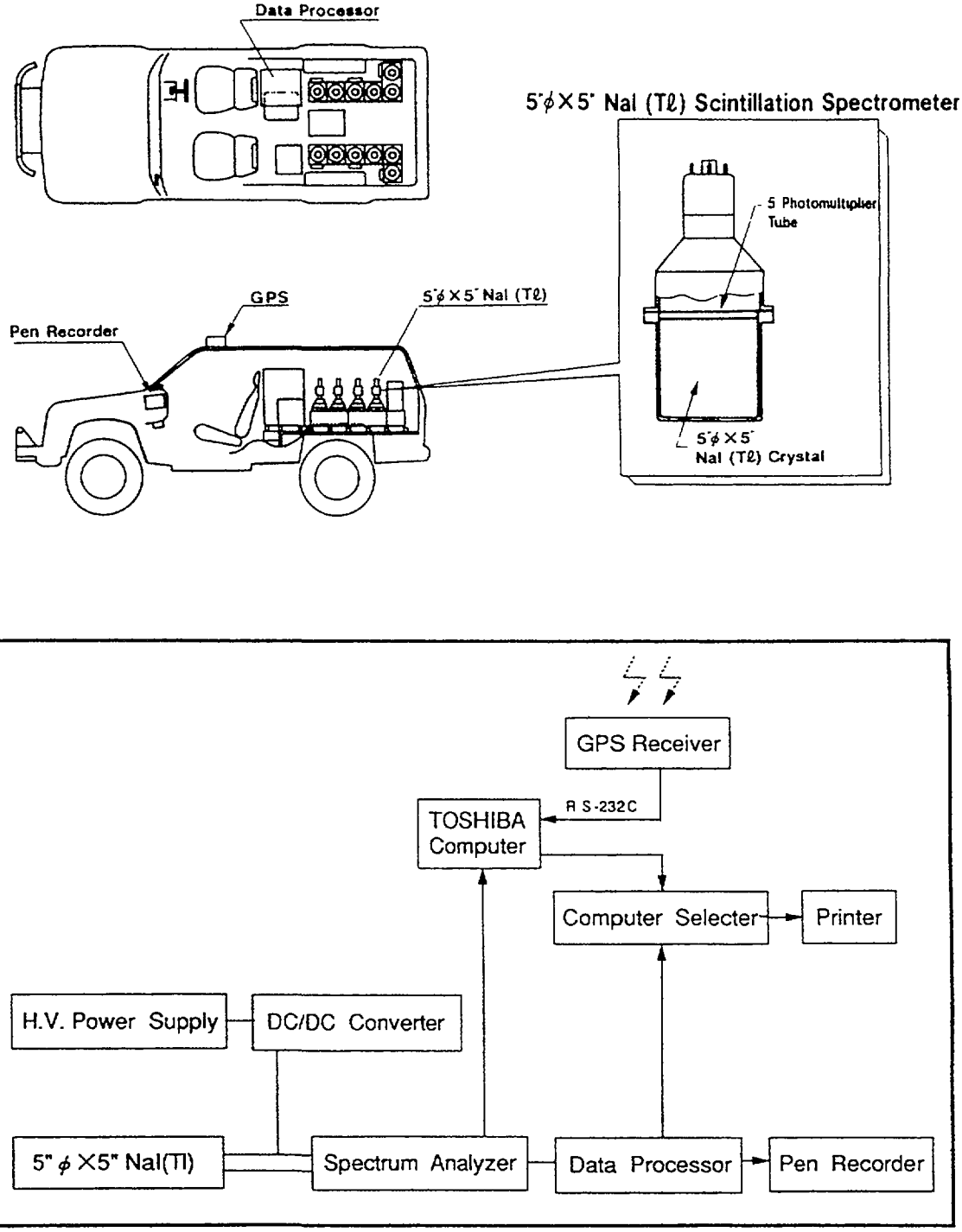

FIG. 1. New 4 channel car-borne system and data acquisition block diagram.

2. THE USE OF CAR-BORNE DATA FOR THE STUDY OF NATURAL RADIATION

2.1. CAR-BORNE DATA ACQUIRED DURING DOMESTIC URANIUM EXPLORATION

Domestic uranium exploration activities began in 1954 and the activities continued for 34 years until 1988 when all activities for domestic uranium exploration were closed. Almost all the exploration areas except city areas in Japan had been covered by car-borne gamma ray survey during this period. The 120 000 km^2 of area and more than 100 000 km of roads and tracks were surveyed. The important outcrops of uranium occurrence in Tono uranium deposits and Ningyo Toge deposits which are main deposits in Japan were also discovered by the car-borne survey.

Since the main task of car-borne survey for exploration was to find the radioactive anomalous outcrops, the data were measured in total count rates and not all the car-borne data were regarded as reasonably calibrated. Moreover, though the domestic uranium exploration began from 1957, the original data such as continuously recorded charts of total gamma counts rate, survey route maps, regional detailed geological maps and other explorational results at hand are only from 1977. Among those data, total 13 000 km of roads length and 17 000 km^2 of area are recognized as the same standard of data qualities. To convert these count rates data into absorbed dose rates, it became necessary to introduce a new car-borne system, since the earlier system does not exit anymore.

2.2. THE CONVERSION OF EARLIER CAR-BORNE DATA

In order to validate and utilize the car-borne data obtained by the earlier car-borne system, a new 4 channel car-borne system (Fig. 1) was introduced and the total count rates of earlier car-borne system were compared with absorbed dose rates which were measured by the new system. The new system is equipped with twelve NaI (T1) cylindrical crystals, each crystal has a dimension of 5 inch in diameter and 5 inch in height. All crystals are calibrated to convert count rates into absorbed dose rates routinely. The global positioning system (GPS) is also equipped so that the measurements of the latitude and longitude at surveyed points are automatically done. Both crystals and GPS are mounted in a car-borne truck which is usually driven at the speed of 7 km/h during the survey.

This new car-borne system surveyed one route (4.5 km) where radiation levels appear from low to high and surrounding condition, pavement and shape remain as before. As a result of survey, good correlation between total count rate data of earlier car-borne system and absorbed dose rate of new car-borne system was obtained as shown in Fig. 2, which means that the data obtained by the earlier car-borne system are still usable for the purpose of assessing environmental radiation distribution as long as a set of original data are available.

From the two car-borne charts in Fig. 2, thirteen representative points were selected and plotted as cpm vs. nGy/h (Fig. 3). As seen from the figure, there was a good linearity between them. The relationship is expressed as follows;

$$(nGy/h) = 18.4 + 0.00075 \times (cpm) \quad (1)$$

By using above equation, the earlier car-borne data in total count rate can be converted into absorbed dose rate.

2.3. AN EXAMPLE OF ABSORBED DOSE RATE DISTRIBUTION MAP

An absorbed dose rate distribution map of natural radiation in a test area of 10 km by 10 km is shown together with the regional geological map in Fig. 4. Here the geological map is the one obtained during domestic uranium exploration and the distribution map is expressed using the earlier

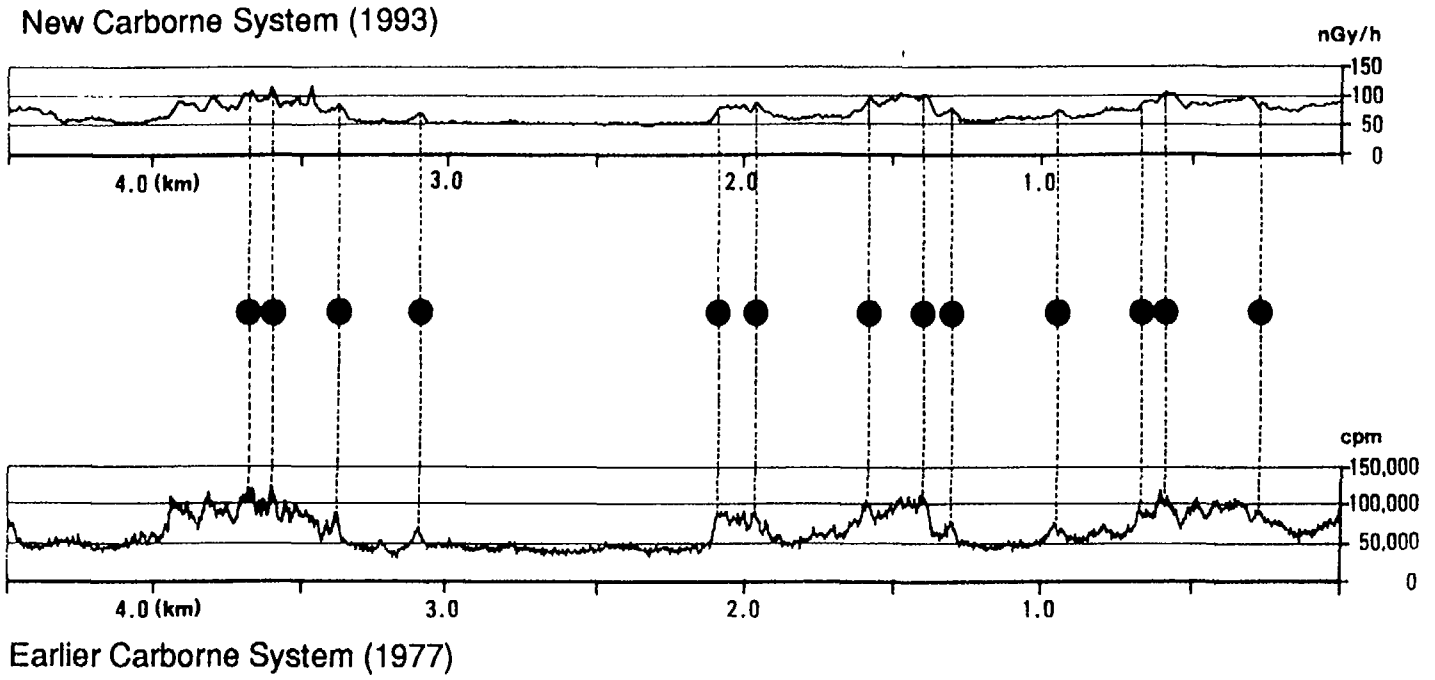

FIG. 2. Car-borne gamma ray charts.

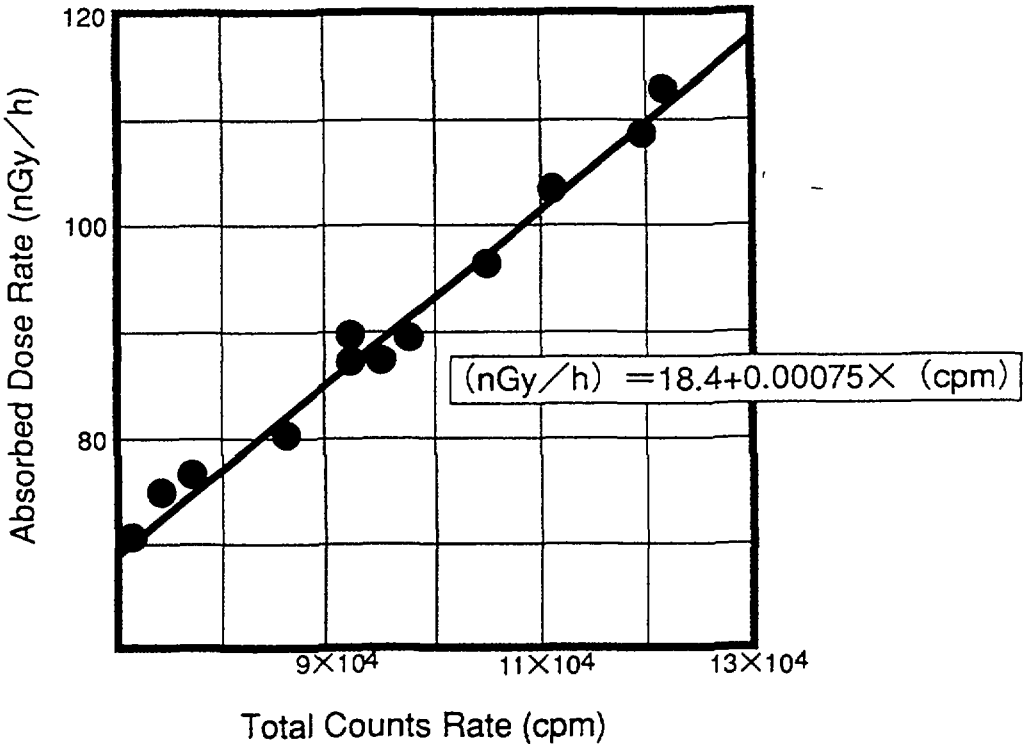

FIG. 3. Correlation between total counts rate data of earlier car-borne system and absorbed dose rate of new car-borne system.

car-borne data in count rates which were converted into absorbed dose rates by the equation (2-1). In the distribution map, a grey scale is shown in the left upper corner, where the darker color represents higher absorbed dose rate level.

The geology of this area is comprised of pre-Tertiary basement rocks and younger sedimentary rocks. The basement rocks are mainly Paleozoic sediments in the western part of the area and late Cretaceous granite in the rest. Miocene sediments unconformably overlie the basements and Pliocene sediments, which are widely distributed in this area, unconformably overlie the older rocks.

When compared two maps, it is seen that the area of high, medium, and low absorbed dose rate levels are well corresponding to the distribution of granitic rocks, Miocene sedimentary rocks, and other sedimentary rocks respectively. This means that natural radiation has close relationship with geological features and lithological characters.

Since car-borne data is taken along lines, it is obvious that the car-borne data is more reliable than point measurements in order to estimate absorbed dose rates distribution which is two-dimensional.

3. OTHER FEATURES OF THE 4 CHANNEL CAR-BORNE SYSTEM

The 4 channel car-borne system is also able to measure 1 cm dose equivalent and exposure rate other than absorbed dose rate.

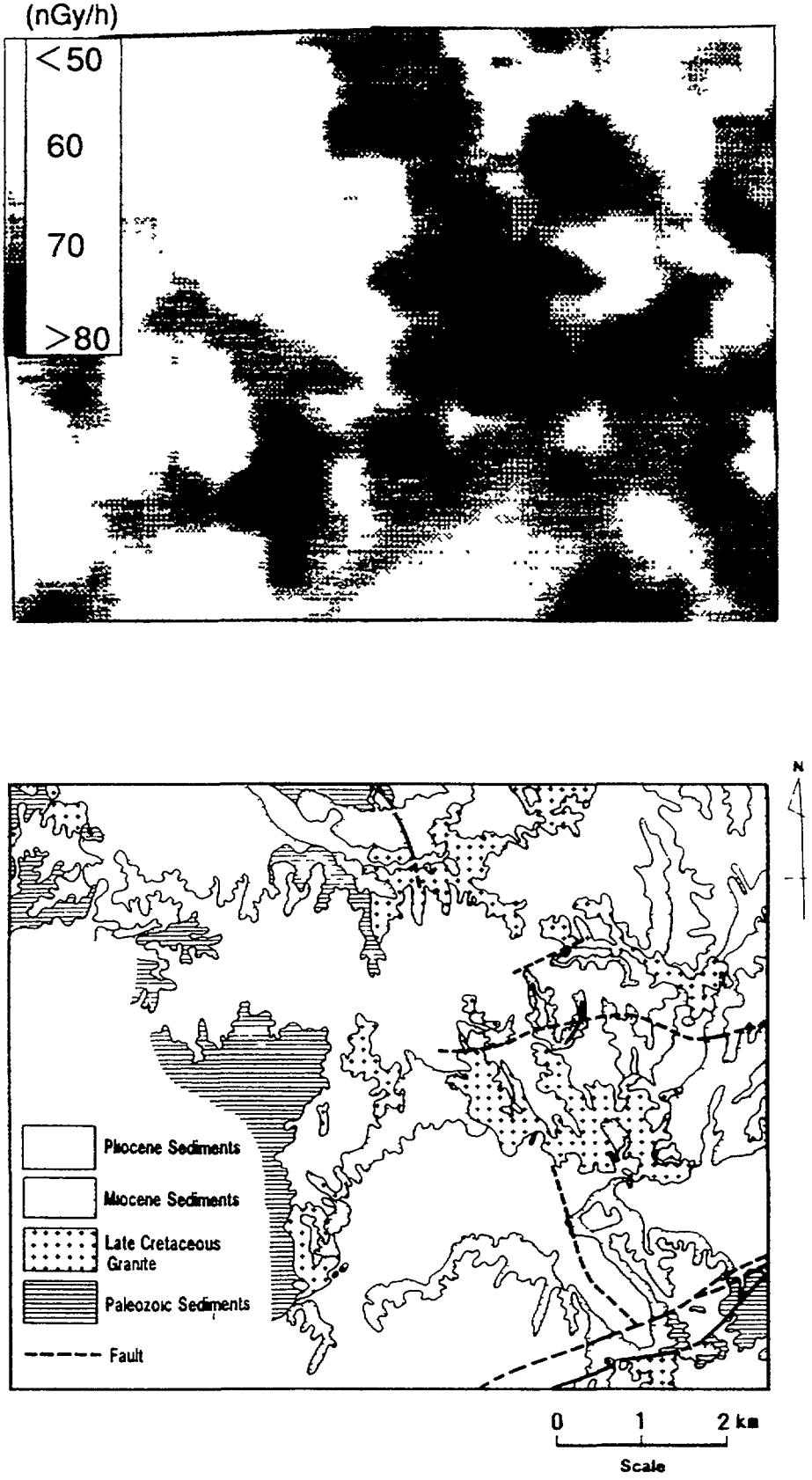

FIG 4. An example of absorbed dose rate distribution map and the geological map of the same area.

The true gamma ray energy spectra are deconvolved from a measured energy spectrum by a mathematical method called unfolding. This unfolding method leads to absorbed dose rates which correspond to each true energy spectrum.

The exposure rate is obtained by dividing absorbed dose rate by a factor of 0.00873. For the 1 cm dose equivalent, true energy spectrum is multiplied by the conversion coefficients which are suggested in the ICRP Publ. 51.

These features contribute greatly to the natural radiation measurements in the areas where no earlier data is available or in the cities.

4. CONCLUSION

The earlier car-borne data in total count rates is successfully converted into absorbed dose rates. It suggests that earlier car-borne data accumulated during domestic uranium exploration can be used to delineate detailed maps of natural radiation distribution in conjunction with the detailed regional geological maps and contributes to the estimation of national background absorbed dose level in Japan.

ACKNOWLEDGEMENTS

We acknowledge gratefully all members of the committee named "Technical Committee on the Study of Geological Features and Environmental Radioactivity" which is organized by PNC. This study was conducted as part of the technical committee's activity.

We would like to express our gratitude and special thanks to Dr. M. Sakanoue, prof. emeritus of Kanazawa University.

REFERENCES

[1] OKADA, S., HASHIMOTO, Y., ITOH, K., Historical review of uranium exploration in Japan. IAEA-TC-543/14 (1985) 193-205.

[2] FUJITAKA, K., ABE, S., FUJIMOTO, M., Distribution of Natural Radiation in Japan in Relation to Geologic Properties. J.Nucl.Sci.Technol. 18 (1981) 222 p.

[3] NELSON, W.R. et al., The EGS4 Code System, SLAC265 (1985).

A CALCULATION OF THE GAMMA RADIATION DOSE FROM RADIONUCLIDE CONCENTRATION IN ISTRIAN SOILS, CROATIA

E. PROHIĆ
Faculty of Natural Sciences, University of Zagreb, Croatia

D. BARIŠIĆ, S. LULIĆ
Ruder Bošković Institute, Zagreb, Croatia

Abstract

The gamma dose-rates were calculated from the results of spectrometric measurements of radionuclide concentrations in soils in the area of Istria peninsula, Croatia. Calculated gamma dose-rate conversion factors (GDRCF) for external exposure above ground give external dose rates per unit natural radionuclide concentration in soil. GDRCF in air at a height of 100 cm above ground are tabulated for ^{40}K, ^{235}U decay series + ^{238}U decay series (up to ^{230}Th), ^{226}Ra decay series as part of ^{238}U decay series, ^{232}Th decay series and complete ^{238}U decay series including contribution from ^{235}U decay series for various source depths in soil between 4 cm and 100 cm. The preliminary results clearly reveal the dependence of natural gamma dose on the lithological characteristics of the bedrock units. The radiometric maps must take into consideration gamma doses from soils as well as from underlaying rocks in the first meters of soil profile. This is of crucial importance especially for the carbonate terrains, where the differences between natural radionuclide concentrations in carbonate derived soils and carbonate bedrock could be of two order of magnitude. Furthermore, for soils itself the role of drainage network in migration processes is undoubtedly very important. All these dependences makes us believe that spectrometric measurements and related dose rate conversions in connection with in situ dose measurements could be the best choice for radiometric mapping at least for carbonate terrains with numerous rock outcrops, poor drainage and lithological variability at local scale. As these parts of Croatia and Slovenia are well known as world recognized locus typicus of karst terrains, our study could be taken as a very first step in solving problems of radiometric mapping in similar carbonate terrains worldwide. The preliminary radiometric map of Istria is our attempt to solve this problem.

1. INTRODUCTION

This work is a part of the national project "General Geochemical Map of Croatia" and also in the frame of the UNESCO International Geological Correlation Programme (IGCP) Project 259 — International Geochemical Mapping.

Airborne gamma surveys which has been applied and recommended for radiometric mapping of most national territories are not suitable method everywhere mostly due to the complexity of the terrains especially in the areas predominantly covered by carbonate rocks. Additionally, the high cost of this technique and some other technical reasons makes this technique unsuitable for the radiometric mapping of the national territory of Republic of Croatia for the time being. In 1969, when part of Republic of Slovenia was covered by airborne measurement, only the negligible part along the Croatian-Slovenian border was included. In 70's, during the uranium explorations in Slovenia and Croatia, a part of Croatia mostly covered by clastic rocks (Lika, Gorski Kotar) and terrains predominantly built of eruptive and metamorphic rocks (Slavonia) were covered by ground gamma ray spectrometry. Unfortunately, this territory is, in general, not accessible for the field work nowadays, as well as some data of this investigations. So, any checking of reliability and usefulness of these data are impossible.

The main goal of this paper is to give a very first insight into the radionuclide distribution in a typical karst terrain. However, we studied the parameters and factors which could influence the radionuclide concentrations in soils overlaying carbonate rocks together with resulting gamma doses.

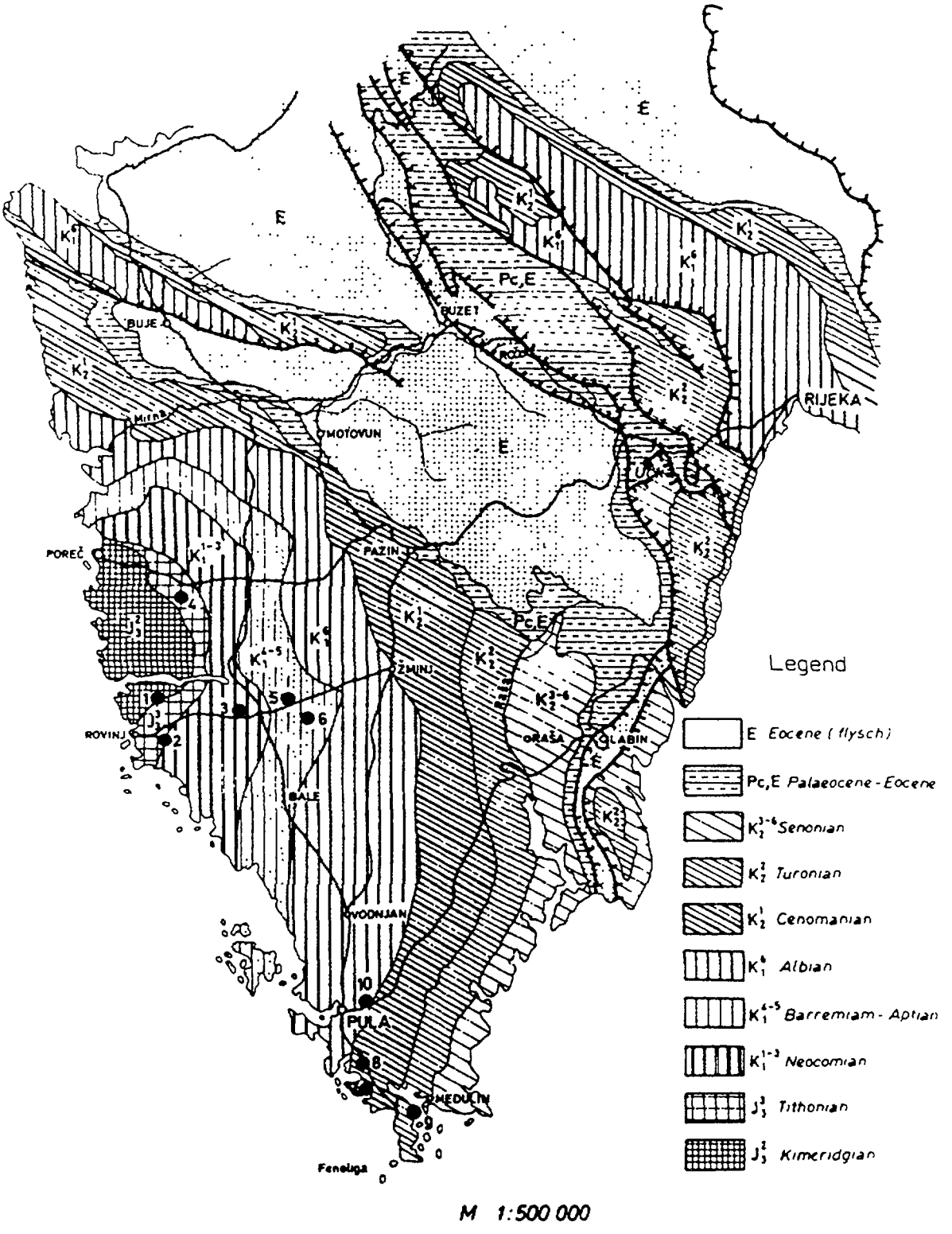

FIG. 1. Geological map of Istria (after Tišljar, J., Velić, I., Radovčić, J., Crnković, B., Upper Jurassic and Cretaceous peritidal, lagoonal, shallow marine and perireefal carbonate sediments of Istria, (From: Excursion guide-book, eds. Babi}, LJ., and Jelaska, V., Contributions to Sedimentology of some carbonate and clastic units of the coastal Dinarides), 4th I. A. S. Regional meeting Split, Zagreb (1983) 13-35.).

Different lithological units, drainage net, thickness of the soil profile, etc, pointed out the influence of various factors upon the radionuclide concentrations in Istrian soils. It is well known fact that the resulted gamma dose in air is a function of the radionuclide concentration in the first meter of the soil profile. In carbonate terrains the thickness of the soil is ranging from few centimeters up to several meters, even completely missing at significant areas. However, the differences between natural radionuclide concentrations in carbonate derived soils and carbonate bedrock could be of two order of magnitude, which additionally complicate the calculations. So, it is necessary to use different gamma dose-rate conversion factors (depend on soils thickness) in carbonate terrains.

2. GEOLOGY AND HYDROGEOLOGY OF ISTRIA

The Istria peninsula is considered to be the western part of a vast Mesozoic carbonate platform today recognized as the Outer Dinarides region. This is the classic karst area, where karst phenomena were first studied and from which the name originated. The relief consists of plains, hills and mountains rising eastwards from the coast to heights of about 1400 m and gradually declining in elevation towards the interior. The belt is characterized by distinct zones of climate, soil development and vegetation. The area is composed of Jurassic, Cretaceous, Tertiary and Quaternary sediments (Fig. 1). While western and southern Istria is mainly characterized by shallow marine Jurassic and Cretaceous carbonate rocks, the rest of the peninsula is composed of Tertiary foraminiferal limestones and flysch.

The oldest strata exposed in Istria are Kimmeridgian in age. A very short emergence took place after this period, thus causing a local deposition of bauxites. Cretaceous sequence consists of carbonate rocks deposited from Tithonian to the Lower Campanian. These sediments had been lifted above the sea level by the Laramian orogeny and since then they were intensively eroded and karstified. The final results of these processes are numerous small bauxite deposits covered by Paleogene sediments.

The Early Paleocene was marked with the sedimentation of fresh-water and brackish "Liburnian strata" with coal in the isolated basin. This strata are specially important to this study due to the high content of radionuclides in coal associated with these strata. These layers are discordant to the intensively karstified Cretaceous base. The large and significant transgression invaded this region entirely in the Early Eocene thus causing the marine sedimentation of foraminiferal limestones and flysch (conglomerates, sandstones, marls and clayey limestones) throughout this period [1].

The total and final emersion occurred at the end of Eocene or at the beginning of Oligocene. The emersion since Early Oligocene until Recent has caused continuous denudation of the Eocene and Paleocene sediments from the greater parts of Istria.

The Quaternary consists of different deposits along the river valleys and in the big karst poljes. These are black and grey soils, terra rossa, talus deposits, various stream deposits, coastal deposits and lacustrine clays and sands.

The main feature of the hydrogeology of investigated area is connected with the presence of carbonate rocks. A regular surface-drainage system is absent or fragmentary (except in the flysch area) because most of the rainfall drains underground.

3. SAMPLING AND METHODS

3.1. SAMPLING PROCEDURE

Soil was sampled by channel sampling the upper 15 cm of the soil profile (below the O1 and Of horizons, if present). The fraction of air-dried material that passed through a 2-mm sieve was

reduced by repeated comminution and quartering to a grain size less then 0.5 mm. The soil types sampled included rendzinas of the A-C soil profile; brown soil on limestone and dolomite, and terra rossa, of the A-(B)-C soil profile (calcocambiosol); leached brown soils on limestone and dolomite, and terra rossa and rendzina on flysch bedrock [2]. Samples were taken in a regular 5x5 km grid with sample points in the middle of the square with the randomly selected position of the grid of the General Geochemical Map of Croatia. On the same samples the content of inorganic constituents were measured for the performing of the geochemical map of Istria. This gives us additional possibilities to compare the element and radionuclide contents in the same samples. In this way 131 samples for whole Istria were collected and 125 of them were analysed by the gamma ray spectrometry.

3.2. GAMMA RAY SPECTROMETRY

Soil samples were placed in the counting vessels, sealed and stored at least for 4 weeks to allow ingrowth period of gaseous ^{222}Rn. At the end of the ingrowth period, the samples were counted on a Ge-Li semiconductor detector joined to 4096 channel analyser "Canberra". The detector system was calibrated using standards supplied by both the National Bureau of Standards (USA) and Amersham International (UK). Precision and accuracy was checked by simultaneous measurement of IAEA standards (IAEA-306, IAEA-313 and IAEA-314). Depending on radionuclide activities, spectra were recorded for times ranging from 80,000 to 150,000 seconds. Activities of ^{40}K were calculated from the 1460.75 keV-peak, ^{137}Cs from 661.6 keV-peak, ^{226}Ra (as a mean value) from 609.3 keV-peak of its ^{214}Bi progeny and 352 keV-peak of its ^{214}Pb progeny, ^{228}Ac from 911.1 keV-peak and ^{235}U from 186 keV-peak (after subtraction of the overlapping ^{226}Ra peak). Concentrations of ^{238}U were calculated from the ^{235}U activity assuming the $^{235}U/^{238}U$ activity ratio of 0.04603 [3].

3.3. CALCULATION OF GAMMA DOSE-RATE

Radionuclides presented in soil can be classified into two main categories; natural radionuclides (primordial with their radioactive daughters) and radionuclides generated by man's activities (in practice, mainly ^{137}Cs from fallout after atmospheric nuclear tests and Chernobyl accident).

Primordial radionuclides can be considered to be relatively uniformly distributed in the first hundred centimeters of vertical soil profile and the natural radionuclides concentrations at any depth in soil is assumed to be uniform over an infinite surface parallel to the ground plane. The dose-rate, at a point on the ground surface from a monoenergetic gamma source, can be found by integrating the plane source over the depth of soil [4]. The calculation of GDRCF, presented in Table I, was based on dose-rate conversion factors in air published by [6] and assumption than soil density is 1.4 g cm^{-3}. Obtained GDRCF are in excelent agreement with previously published [5] and [7] in case of ^{40}K and ^{232}Th decay series while in case of ^{238}U decay series calculated values are about 9% higher. Calculated values are obtained on basis of both, [8] and [9], gamma energy and intensity of emissions and results were practically the same. Radioactive equilibrium in decay series was supposed in all cases although it wasn't found in ^{238}U decay series in Istrian soils [10]. That was reason for tabulating GDRCF for ^{226}Ra including it's decay products.

GDRCF, for exponentially distributed ^{137}Cs in soils, of 112.5 pGy h^{-1} per Bq kg^{-1} was found on the basis of, by [11] published ^{137}Cs dose-rate conversion factor (4.5×10^{-13} Gy h^{-1} per Bq m^{-2}), and assumption that ^{137}Cs concentration of 1 Bg kg^{-1} in the first 15 cm of soil is equivalent to ^{137}Cs contamination of 250 Bg m^{-2}.

4. RESULTS AND DISCUSSION

By referring to the gamma dose-rate conversion factors (GDRCF) shown in Table I, the absorbed dose-rates at one meter above ground from the natural nuclides and from ^{137}Cs were calculated and are tabulated in Table II. Before any discussion one must be aware that all calculated values are based on the assumption that, at each sample point, the soil thickness is one meter. We intentionally included this wrong assumption in our calculation, mostly because, up to now, we have not solved the problem of averaging the soil thickness in carbonate terrains in used regular grid. Data from the pedological map of Istria [12] reveal that the soil thickness is ranging from few centimeters to few meters, but, the majority of area under investigation (excluding flysch) is covered, very probable, by soil less then 50 cm in thickness. So, the reported dose-rates, as a first approximation, are overestimated, especially for the hilly and mountainous areas. In the flysch terrains and areas at lower elevations (valleys, karst poljes, etc) where soil thicknesses are meter or more, the reported values are correct. The ground thermoluminescence dosimetry measurements (TLD) provided at three meteorological stations in Istria, near Rijeka, Pula and Pazin, respectively, and calculations based on real, field approved, soil thicknesses are in very good agreement (Table III).

TABLE I. GAMMA DOSE-RATE CONVERSION FACTORS (GDRCF) IN AIR AT ONE METER ABOVE GROUND FOR UNIFORM SLAB SOURCES BETWEEN THE GROUND SURFACE AND DIFFERENT DEPTHS IN SOIL (DRY SOIL DENSITY = 1.410^3 kg m^{-3})

	GDRCF (pGy h^{-1} per Bq kg^{-1})				
Depth	^{40}K	$^{238}U^a+^{235}U^b$	$^{226}Ra^c$	$^{232}Th^d$	U-chain^e
4 cm	16.0	4.6	182.1	258.3	186.7
5 cm	18.5	5.2	209.8	298.0	215.0
7.5 cm	23.5	6.4	264.8	376.7	271.2
10 cm	27.2	7.2	304.6	434.6	311.8
15 cm	32.6	8.2	360.1	515.5	368.3
20 cm	35.9	8.7	392.3	564.2	401.0
25 cm	38.2	8.9	415.0	598.6	423.9
40 cm	41.5	9.3	442.5	642.7	451.8
60 cm	42.9	9.4	452.6	659.5	462.0
100 cm	43.1	9.4	455.9	661.5	465.3
ref. [5]	43	-	-	662	427

a ^{238}U to ^{230}Th decay series (^{234m}Pa and ^{230}Th)

b ^{235}U decay series (^{235}U, ^{231}Pa, ^{227}Th, ^{223}Ra, ^{219}Rn, ^{211}Bi and ^{211}Pb). ^{235}U gamma dose rate conversion factors are recalculated as ^{238}U gamma dose rate conversion factors on the basis of their natural activity ratio

c ^{226}Ra to ^{206}Pb decay series (^{226}Ra, ^{214}Bi and ^{214}Pb)

d ^{232}Th decay series (^{228}Th, ^{228}Ac, ^{224}Ra, ^{220}Rn, ^{210}Po (64%), ^{212}Bi, ^{212}PB and $^{208}T1$ (36%)

e Calculation on the basis of ^{238}U specific activity in soil assuming radioactive equilibrium in the whole decay chain and contributions from ^{235}U decay series

TABLE II. GENERAL STATISTIC PARAMETERS OF THE TOTAL ABSORBED DOSE-RATE IN AIR AT ONE METER ABOVE SURFACE OF ISTRIAN SOILS (INCLUDING ^{137}Cs) WITH RESPECT TO UNDERLAYING GEOLOGICAL UNITS (in nGy h^{-1})

Geol. unit	No. of samples	Total absorbed dose rate (nGy h^{-1})		
		Average	AM[a]±SD[b]	GM[c]:SD[d]
$E_{2,3}$	26	35-87	50±22	49:1.50
$E_{1,2}$	8	52-97	76±30	74:1.51
Pc,E	7	78-167	120±61	116:1.67
$K_2^{2,3}$	14	75-211	113±76	108:1.78
$K_2^{1,2}$	9	41-148	101±64	95:2.15
K_2^{1}	18	75-157	97±37	96:1.41
K_1^{5}	19	81-150	104±35	103:1.37
K_1^{3-5}	12	80-143	106±56	104:1.43
K_1^{1+2}	6	93-134	111±34	110:1.35
$J_3^{2,3}$	6	80-102	90±16	90:1.22
PALOGENE	41	35-167	67±61	62:2.19
UPPER CRETACEOUS	41	103±59	100:1.71	105:1.38
LOWER CRETACEOUS	37	80-150	106±35	90:1.22
UPPER JURASSIC	6	80-102	90±18	86:2.09
ISTRIA	125	35-211	92±63	

[a] Arithmetic mean
[b] Standard deviation (2σ)
[c] Geometric mean
[d] Standard deviation (2σ)

TABLE III. CALCULATED AND MEASURED ABSORBED DOSE RATE IN AIR (in nGy h^{-1})

Location	Calculated	Measured (TLD)[a]	Distance[b]	Soil thickness
		(nGy h^{-1})	(km)	(cm)
Rijeka	108	116±11	2.5	15
Pula	81	105±24	1.2	>100
Pazin	81	103±16	0.9	25

[a] TDL-measurement includes cosmic radiation
[b] Distance from the nearest point taken in calculation and meterological station where TLD were placed

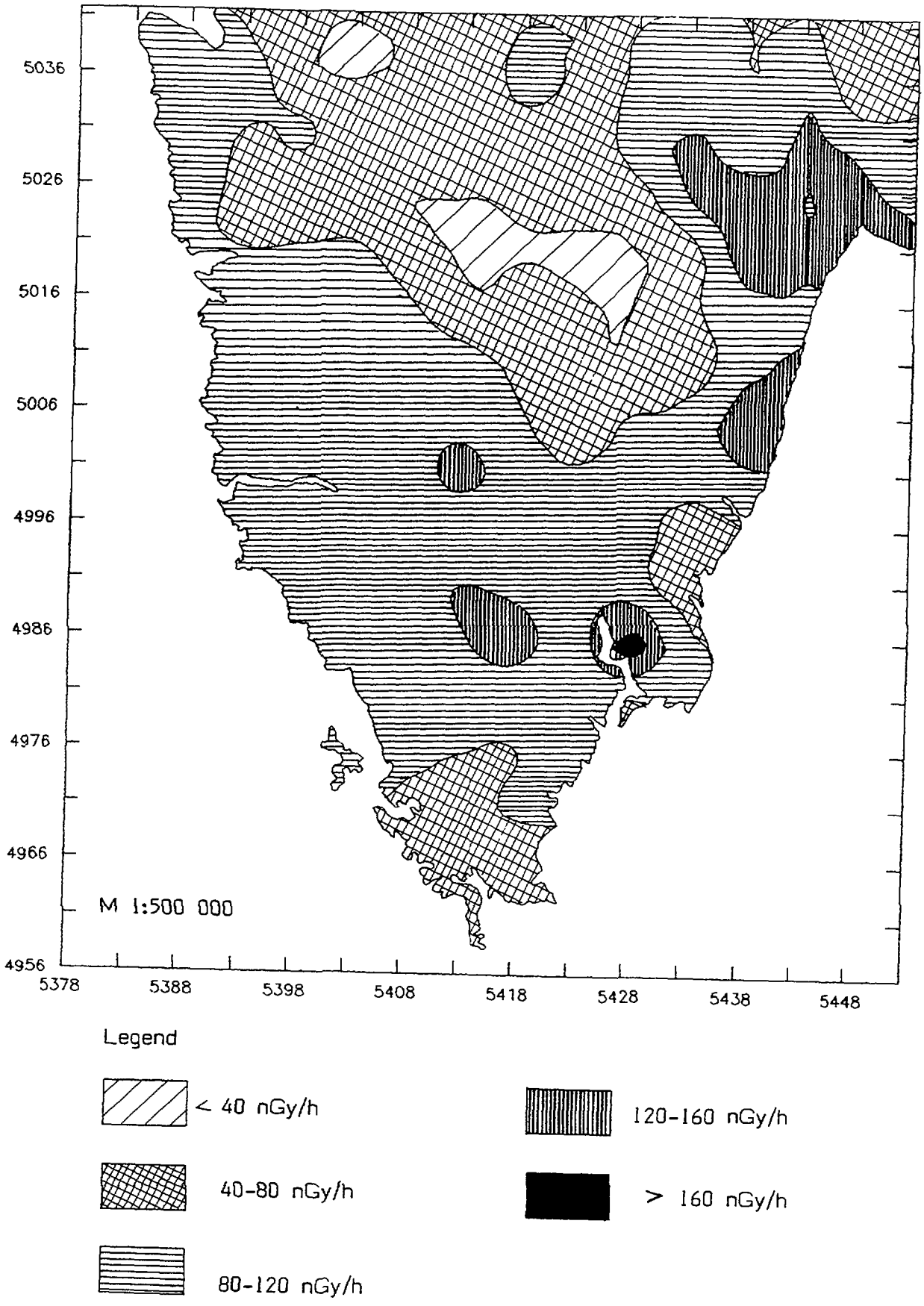

FIG. 2. Total absorbed dose-rate in air one meter above ground surface of Istria peninsula

Data tabulated in the Table III clearly show the influence of the bedrock lithology upon the absorbed dose-rates in air. The best example for study the sources and various factor contributions upon the absorbed doses-rates in air is Paleogene sediments and associated soils. The Paleogene bedrock includes Middle and Upper Eocene flysch deposits, Lower Eocene foraminiferal limestones and Liburnian strata of Paleocene. This complex comprises the areas with the lowest absorbed dose-rates (flysch terrains) as well as the areas with highest absorbed dose-rates (Paleocene terrains) in the whole investigated area (Fig. 2). The increased absorbed dose-rates in air in vicinity of Raša are probable caused by increased radioactivity in soils associated with (underlaying) Paleocene coal strata. Poor surface outflow in that area, as in some other karst areas, additionally increase the possibility of relative accumulation of natural radionuclides in soils vs soil parent materials.

As well known, natural radionuclide concentrations in strata with prevailed clastic rocks, as in flysch, are generally higher then in limestones and dolomites. In soils overlaying flysch and carbonate terrains in Istria, the radionuclide distribution pattern is completely opposite [10]. Consequently, this is reflected in the adsorbed gamma dose-rate in air. Undoubtedly, it is the result of differences in migration due to existing differences in drainage characteristics between flysch, having a very high coefficient of outflow, and limestone and dolomite terrains where the surface drainage network is poorly developed, or even completely missing.

A contribution from various radionuclides to the total absorbed dose-rate in air is given in Table IV. ^{40}K contribution is practically the same in all studied geological units. However, the highest differences are found for the radionuclides of ^{238}U decay series, what was expected. The highest differences in radionuclide concentrations between soil and parent material (especially carbonate rocks), one can expect, in case of ^{232}Th and ^{238}U decay series (including the high degree of radiochemical disequilibrium between ^{238}U and ^{226}Ra, particularly in soils).

TABLE IV. GENERAL STATISTIC PARAMETERS OF GAMMA DOSE-RATE IN AIR ONE METER ABOVE ISTRIAN SOILS WITH RESPECT TO GEOLOGICAL UNITS (in nGy h^{-1})

		(nGY h^{-1} except ^{238}U which is in pGy h^{-1})					
Geol. unit/samples		^{40}K	^{232}Th	^{226}Ra	^{238}U	^{137}Cs	Natural
		ARITHMETIC MEANS $\pm 2\sigma$					
$E_{2,3}$	(26)	15±5	18±8	11±9	39±44	6±14	44±17
$E_{1,2}$	(8)	17±10	29±17	19±19	96±68	11±24	64±17
Pc,E	(7)	13±5	36±10	57±39	171±160	14±19	106±45
Pg	(41)	15±6	23±18	20±39	73±126	9±18	59±53
$K_2^{2,3}$	(14)	15±8	40±12	52±70	152±174	6±7	107±72
$K_2^{1,2}$	(9)	14±4	34±26	46±46	137±96	7±8	93±61
K_2^1	(18)	15±4	41±13	37±32	95±98	4±6	93±35
K_2	(41)	15±6	40±17	44±51	124±136	6±7	98±56
K_1^5	(19)	16±4	41±9	44±30	110±98	4±5	101±31
K_1^{3-5}	(12)	16±1	38±14	46±45	117±126	5±5	101±54
K_1^{1+2}	(6)	15±7	43±14	46±32	146±142	8±8	104±35
K_1	(37)	15±5	40±12	45±33	118±110	5±7	101±32
$J_3^{2,3}$	(6)	16±5	45±16	26±5	50±14	3±6	87±20
Istria	(125)	15±6	35±23	36±47	102±122	6±12	85±61

5. CONCLUSIONS

The presented paper suggests that, for the carbonate terrains, various factors should be considered in order to make a radiometric map of good quality. The main problems are: averaging the soil thickness for the entire sampling grid which the particular sampling point represents; significant difference in radionuclide concentrations between soils and underlaying carbonate rocks and high degree of radiochemical disequilibrium between ^{238}U and ^{226}Ra in soils derived from carbonate rocks.

The airborne gamma survey in carbonate terrains could provide only very general picture of radiometric characteristics of this terrains. For our opinion, the radiometric mapping of carbonate terrains should include data from in situ gamma dose-rate measurements together with laboratory gamma ray spectrometry of samples taken at the same locality. Due to the high variability of soil types and thicknesses and lithologic types of bedrocks at local scale, the much denser sampling grid must be applied.

For the proposed study, as the model area for carbonate terrains, or karst sensus stricto, the area of the Istria peninsula seems to be highly promising. This paper presents the beginning of complex study under the project of Radiometric Map of Croatia.

BIBLIOGRAPHY

TIŠLJAR, J., VELIĆ, I., RADOVĆIĆ, J., CRNKOVIĆ, B., Upper Jurassic and Cretaceous peritidal, lagoonal, shallow marine and perireefal carbonate sediments of Istria, (From: Excursion guide-book, eds. Babi}, LJ., and Jelaska, V., Contributions to Sedimentology of some carbonate and clastic units of the coastal Dinarides), 4th I. A. S. Regional meeting Split, Zagreb (1983) 13-35.

PIRC, S., McNEAL, J. M., LENARĆIĆ, E., PROHIĆ, E., SVRKOTA, E., Geochemical mapping of carbonate terrains, Trans. Instn. Min. Metall. (Sec. B: Appl. Earth Sci.) 100 (1991) B74-B87.

MURRAY, A. S., AITKEN, M. J., Analysis of low-level natural radioactivity in small mineral samples for use in thermoluminescence dating, using high-resolution gamma spectrometry, Int. J. Appl. Radiat. Isot. 39 2 (1988) 145-158.

DICKSON, H. W., KERR, G. D., Dose Rates from Plane Sources of Gamma Rays, Health Phys. 29 (1975) 131-136.

UNITED NATIONS, Sources, Effects and Risk of Ionizing Radiation, United Nations Scientific Committee on the Effects of Atomic Radiation 1988 Report to the General Assembly, with annexes, UN sales publication No. E.88.IX.7. New York (1988).

KOCHER, D. C., SJOREEN, A. L., Dose-Rate Conversion Factors for External Exposure to Photon Emitters in Soil, Health Phys. 48 2 (1985) 193-205.

UNITED NATIONS, Ionizing Radiation: Sources and Biological Effects, United Nations Scientific Committee on the Effects of Atomic Radiation 1982 Report to the General Assembly, with annexes, UN sales publication No. E.82.IX.8. New York (1982).

ERDTMAN, G., SOYKA, W., The gamma rays of the radionuclides, Werlag Chemie, Weinheim, New York (1979).

INTERNATIONAL COMMISSION ON RADIOLOGICAL PROTECTION, Radionuclide transformations. Energy and intensity of emissions, ICRP publication 38. Pergamon Press, (1983).

BARŠIĆ, D., Radionuclides in soils of Istria, PhD Thesis, Zagreb University, Zagreb (1993). (in Croatian, extended abstract in English)

LEUNG, K. C., LAU, S. Y., POON, C. B., Gamma Radiation Dose from Radionuclides in Hong Kong Soil, J. Environ. Radioactivity, 11 (1990) 279-290.

ŠKORIĆ, A., ADAM, M., BAŠIĆ, F., BOGUNOVIĆ, M., CESTAR, D., MARTINOVIĆ, J., MAYER, B., MILOŠ, B., VIDAČEK, Ž., Pedosfera Istre, Mladost, Zagreb (1987).

GEOCHEMICAL EXPLORATION AND DEVELOPMENT OF MONITORING FOR ENVIRONMENTAL CONTROLS

M.A. GAMBA, G. TOMELLINI
Doctor Baulíes Uranium Deposit, Sierra Pintada District, San Rafael, Mendoza, Argentina

Abstract

During the exploration-evaluation stages of the Sierra Pintada Uranium District in the Province of Mendoza, Argentina, different studies such as radiometric airborne (gross-count gamma ray surveys) and geochemical surveys with stream sediments, surface and spring water sampling were performed. These data have given the background references for planning the development of environmental monitoring conditions in the district from the earlier stages of its production. The objective of this paper is to show the results obtained in the early stages of exploration, and the methodology carried out for controlling the environmental impact associated to mine production. The data obtained in the radiometric airborne survey are expressed in total-counts per seconds of gamma rays multiplied by background. The geochemical samples from stream sediments and water, have been analysed by extractable uranium method. This last technique was chosen for performing the monitorage over the district. The geochemical survey was carried out during 1974 (July-September) over the drainage pattern at the south of the Diamante River, and covered all the streams that drain the mine district. The first stage of this survey was a preliminary reconnaissance, to define the best sampling method. In each sampling point conductivity and pH measurements were taken from the water samples. The results of uranium (as labile uranium) were expressed in microgram/gram (ppm) for stream sediments, and as microgram/litre (ppb) for water samples. The samples were not analysed for radium because of lack of an adequate methodology. Mining work began in 1979 with the exploitation of the Tigre III orebody. The environmental control started in September 1979 with the samplings of stream sediments and water around the mine, analysing uranium and radium in both type of samples. The radium results were expressed in pCi/g for stream sediments and in pCi/L for water samples. Stream sediments were analysed by extractable and total uranium. Since 1991, the Diamante River has been sampled every six months. This is the main river of the district, which drains water of the entire basin that contains the ore deposits. Finally, the advantages and limitations of the applied geochemical methodology are delineated in this paper, and a summary of uranium and radium migrations to the surrounding environment is done.

1. INTRODUCTION

The Sierra Pintada Uranium District is situated in the Province of Mendoza, Argentina, 35 km west of the city of San Rafael and 200 km south of the city of Mendoza, the capital of the province. It is located between 34°15' and 35° 30' S and 68° S (Fig. 1).

The Sierra Pintada belongs to the northern sector of the geomorphological unit called "Bloque de San Rafael" with an area of 3500 km^2 in the San Rafaelino-Pampeana Geological Province, located between 33°-30° S and 65°-69° W, with a NNS–SSE trend.

The relief is characterized by a hilly environment, 800 to 2000 m a.s.l., separated by deep gorges and steep flanks that reflect the block-faults structure. Within the area, the Cordon del los Mesones is the highest elevation with 1680 m a.s.l., located at the western sector of the district. At the eastern sector there is and extended and monotonous peniplain called Sanrafaelina Plain; it is separated from the other sector by an abrupt morphological throw.

2. HYDROGRAPHY

At the northern part of the district, the drainage basin is formed by the Diamante River, an allochthonous river, whose headwaters are located in the Cordillera Occidental. It is supplied by

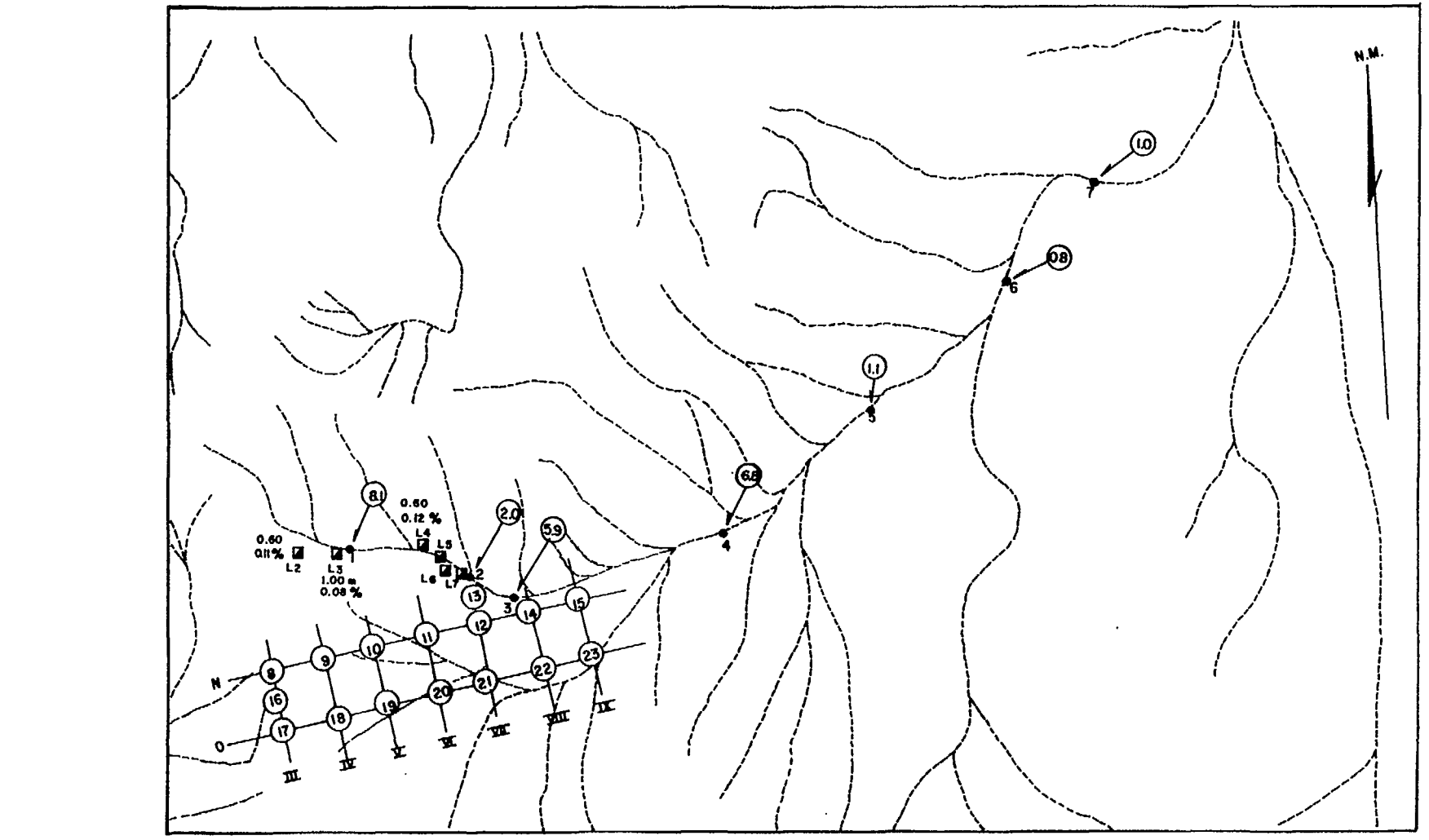

FIG. 4. Geochemical Reconnaissance survey of los Chañales Sector, 1968.

TABLE I. SIMPLIFIED STRATIGRAPHIC SEQUENCE IN THE SIERRA PINTADA DISTRICT (LLAMBIAS ET AL. 1993).

AGE		FORMATION		LITHOLOGY
QUATERNARY		Several Formations		Alluvial, aeolian and piedmont sediments, etc Basaltic and andesitic flows.
TERTIARY	PLIOCENE	Rio Seco del Zapallo		Mainly fine grained sandstones Interbedded basaltic and andesitic sheets
	MIOCENE	Aisol		Mainly sandstones Interbedded basaltic and andesitic sheets
TRIASSIC	Upper			peneplanation
	Middle	Puesto Viejo		Continental sandstones rhyolitic tuffs Basalts
	Lower	Cerro Carrizalito		Lavas Subvolcanics bodies and rhyolitic ignimbrites
PERMIAN	Upper			unconformity
	Lower	Quebrada del Pimiento		Basandesitic and andesitic intrusives
		Meosilicic intrusives		
		Agua de los Burros		Ignimbrites,breccias Rhyolitic and dacitic tuffs. Subvolcanic bodies Sandstones, conglomerates.
		COCHICO Gr.	Arroyo Punta del Agua	Andesitic breccias, dacitic ignimbrites. Sedimentary rocks : sandstones and conglomerates.
			Yacimiento Los Reyunos	Toba Vieja Gorda Member Atigradas Sandstone Member Psefitic Member Andesitic Member
		Arroyo Agua de las Yeguas : stock		
CARBONIFEROUS	Upper	El Imperial		Sandstones and mudstones Marine and continental sedimentation
	Lower			
		Agua de la Chilena stock		Tonalites,granodiorites, spessartites
DEVONIAN		La Horqueta		Metamorphic rocks : greenschist facies Micaceous schists, Greywackes, etc.

meltwaters from the high mountain range. The Diamante River runs in general towards the east, following the original slope of he ancient accumulation plain of Tertiary age. Several intermittent and ephemeral streams and creeks drain toward its margins, north and south. From the west, and downstream on its left hand, we can mention: Carrizalito, Hondo, Las Vacas, Imperial, Salado, La Chilena, Los Reyunos. Downstream, on its right hand we have María Josefa, Alumbre, Horqueta, Chorreado with its tributary La Totora, Atamisqui, Pedernera, Tigre and Pavón.

The ore mine is drained by El Tigre stream. It is formed by El Durazno and La Pintada creeks, and during its short run, 10.3 km, receives the waters of ephemeral creeks that only drain rainwaters. Whereof, the Diamante River is the principal course that joins the ore district with the urban centers located downstream.

Upstream from El Tigre stream outlet several hydraulic complexes have been built at the Diamante River that bring electric power to the zone. These numerous dams act as restraints for the load of the river. Likewise, the Galileo Vitale dam is located downstream of this point and acts as a restraint to the fluvial debris too. From this point onwards the river is an anastomosing stream and has several islets. Finally, at the limits of the city of San Rafael it loses this characteristic and flows as a narrow stream in the Sanrafaelina sedimentary plain.

At the southern part of the district, the Atuel River drainage basin is located. It is an allochthonous river, too, with intermittent and ephemeral tributaries. The flow runs in SE-NE direction and, in the Rincón del Atuel it changes to WE. Both drainage basins — Diamante and Atuel — constitute the principal hydric resources of the region. These waters are used for agricultural and cattle raising developments and as a domestic water supply. South of the city of San Rafael both rivers approach at a distance of some 15–20 km.

3. CLIMATE

The climate of the region is a continental type (warm to tempered and semiarid) with similar characteristics to the Andean Pediment (dry, scarce rainfall and arid). The annual average temperature is about 15°C, in winter it is about 7°C and in summer 22°C. The absolute minimum temperature is -5°C for the winter months and the absolute maximum temperature is 36°C during the summer. The annual average relative humidity is about 60%, with the minimum in summer and the maximum in winter, whereas the annual average rainfall is 342 mm, with the highest values between October and March and the lowest values between April and September. There are fluctuations depending on the year. The prevailing winds are from the NE and in less proportion from the SE, E, SW, N and NW. The quiet atmosphere has a percentage of 20%.

4. GEOLOGY

Table I shows a simplified geological scheme, and a brief description of the local geology after Nicolli et al. [1], Rodrigo and Belluco [2], Llambías et al. [3] follows.

Small outcrops of Precambrian rocks (amphibolites, micacites, horblende schists etc.) and very small outcrops of Cambrian-Ordovician limestones that unconformably overlie the Precambrian metamorphic rocks occur in the geomorphological unit, but not in the area of the Sierra Pintada uranium district. In this area, the stratigraphic sequence is as follows (Fig. 2):

Devonian: La Horqueta Formation. This is a complex sequence composed of grey wackes, quartzites, mica schists, mica quartz schists, sericitic argillites and chloritic and seritic schists, corresponding to a typical flysh deposit, which shows variable degrees of metamorphism decreasing

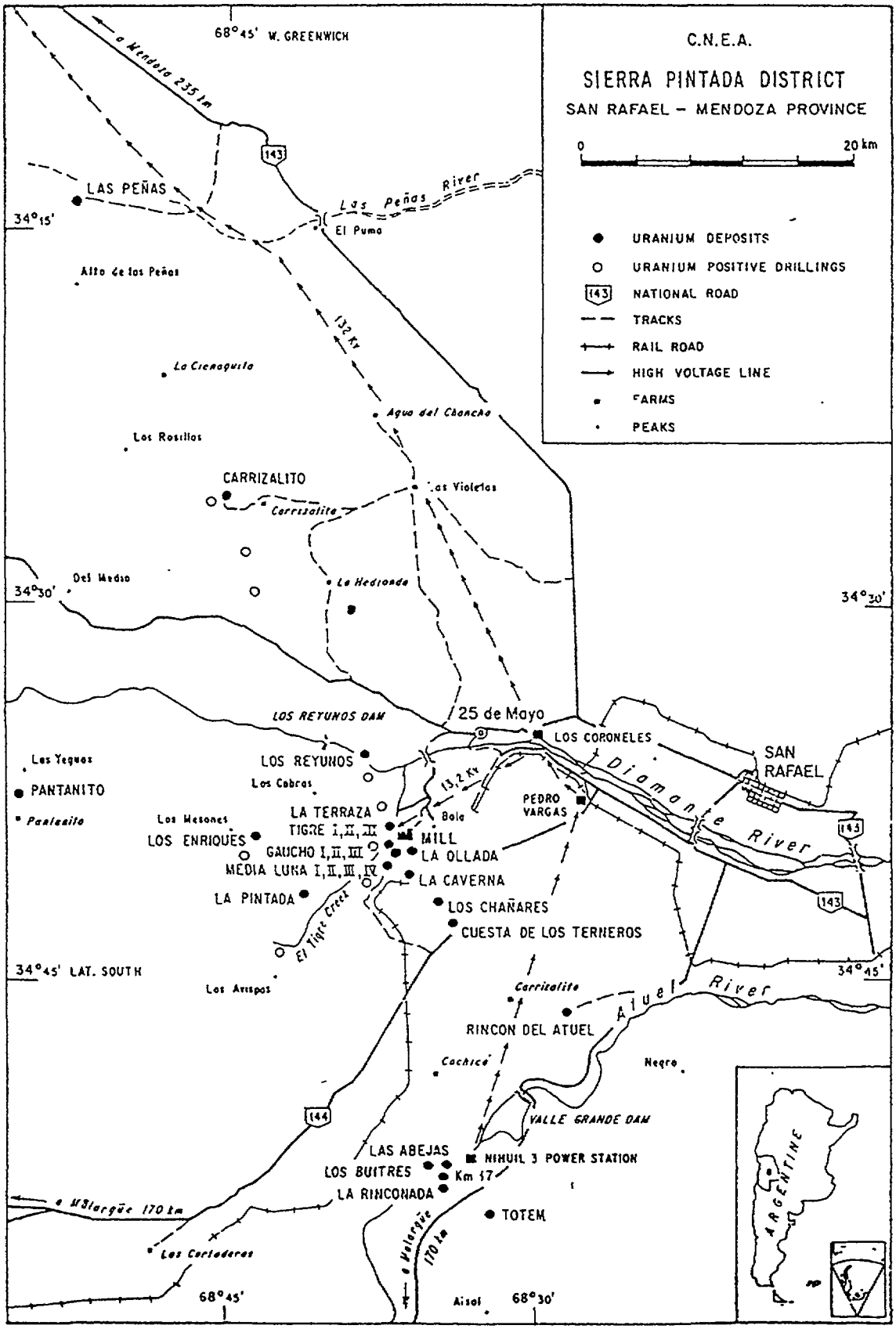

FIG. 1. Sierra Pintada District, San Rafael — Mendoza Province.

from north to south in the Block. Plutonic rocks (granodiorites and diorites) intrude into those metamorphites.

Carboniferous: El Imperial Formation. Extended outcrops of siltstones, green and carbonaceous shale and bituminous rocks characterizing a sea coast environment, gradually turning, in the upper part, to quartzitic sandstone, conglomeratic reddish sandstones and conglomerates which indicate a transition to a continental depositional environment.

Permian: Cochicó Group. Detritic sediments with intercalated pyroclastics. It comprises two formations:

a) Yacimiento Los Reyunos Formation. It is integrated by four members which are interbedded laterally and repeat in the vertical sequence [3]: 1) Andesitic, 2) Psefitic, 3) Atigradas Sandstones and 4) Toba Vieja Gorda.

The sequence begins with andesitic breccias which are interbedded with the basal sections of the Toba Vieja Gorda Member. This Member is formed by dacitic and rhyolitic ignimbrites with some levels containing abundant rock fragments. Meza [4] describes 7 effusive units and locates the possible center of emission at the Loma Colorado del Infiernillo. Some of these units are about 200 m thick.

The Psefitic Member (150 m of thickness) is intercalated in the lower part of this sequence and is constituted by polymictic conglomerates deposited in an alluvial fan environment and/or debris flows [5].

The Atigradas Sandstone Member is integrated by feldspathic sandstones with abundant volcanic material and constitutes the epiclastic facies of the Toba Vieja Gorda Ignimbrite. It is interbedded from the base to the top, of the sequence with greater thickness eastward.

b) Arroyo Punta del Agua Formation. It is a volcaniclastic sequence with intercalated conglomerates and sandstones in the lower part. It rests, in erosional unconformity, over the preceding sequence or over substratum rocks. It is made of andesitic breccias and dacitic ignimbrites.

Agua de los Burros Formation. This sequence is formed by polymictic conglomerates or andesitic laharites at the base, dacitic ignimbrites, with less crystals than the preceding sequence, breccias and rhyolitic ignimbrites. It is intruded by basandesitic and andesitic dykes and sills from the Quebrada del Pimiento Formation.

Upper Permian-Triassic. Cerro Carrizalito Formation. It is constituted by an important volume of subvolcanic bodies together with lavas and high silica rhyolitic ignimbrites.

Triassic. Puesto Viejo Formation. Succession of continental sediments from coarse conglomerates to ignimbrites tuffs. Intercalated basic to andesitic sills and sykes.

Tertiary-Quaternary. After the peneplanation stage, during the Jurassic, Cretaceious and Lower tertiary periods, thick Miocene (Aisol Formation) and Priocene (Rio Seco del Zapallo Formation) continental clastic sediments are deposited. They occur interbedded with basaltic and andesitic sheets. Continental sediments: alluvial, aeolian and piedmont sediments etc; basaltic and andesitic flows, pyroclastic levels and calcareous rocks of hydrothermal origin in the Quaternary stage.

Rodrigo and Belluco [2] described a brief and consistent scheme of the structural and geological history of the area.

5. EXPLORATION WORKS

Rodrigo and Belluco [2] made a brief description of all exploration works in the area to conclude in the discovery of the ore deposits that form of the Sierra Pintada uranium district, and the subsequent development of the mining. Donatti and Galluci [6] described the mining works and the development of the San Rafael Complex Mill-Plant.

From our point of view, the most important exploration works in order to contain the background in the area previous to the beginning of the mill-plant complex operations are:

1. Total gamma airborne survey

2. Geochemical exploration for uranium

5.1. TOTAL GAMMA AIRBORNE SURVEY

During 1968 a total airborne prospecting survey was performed on the Permian Cochicó Group outcrops, specially on the Atigradas Sandstone Member, over an area of 3450 km^2 [7]. The technical specifications, main equipment and operating conditions were as follows:

- Conventional topographic maps at scales of 1:100 000 and 1:50 000 were used for the flights and data plotting;

- Scintillometer MP-10 equipment manufactured by CNEA (Comisión Nacional de Energía Atómica) consisting of one-head 5 in. × 2 in. NaI (Ta) crystal with a lead colimator;

- Radio-altimeter AN/APN 1;

- The strip camera was a continuous French Camaflex, model S, with 35 mm film.

- Synchronized recorders, in tandem, with fiducial mark devices Two Esterline Angus.

The line flight intervals were 250 m and the radiometric points taken at the same distance gave information at square network. The flight directions were, in general, normal to the main structure (E–W) except when the topographic conditions did not allow it. The data recovery from the records were punctual and were plotted after the correction at 100 m base level.

The contour maps (Fig. 3) were made at intervals of BG × 1.10, 1.40, 1.70 and up. In this form, several anomalies were detected and in El Tigre anomaly constellation an exceptional value of 6 × BG was obtained.

Considering that this type of survey gave values only in gamma total counts over the uranium district, it was not taken into account for the monitorage control of the environmental conditions.

5.2. GEOCHEMICAL SURVEY

5.2.1. Preliminary Geochemical Survey (mid 1968)

As long as the climatic and hydrological characteristics of the area appeared to be unfavourable to perform an investigation through the geochemical survey of uranium during mid 1968, a preliminary geochemical survey was carried out at the Sierra Pintada district [8].

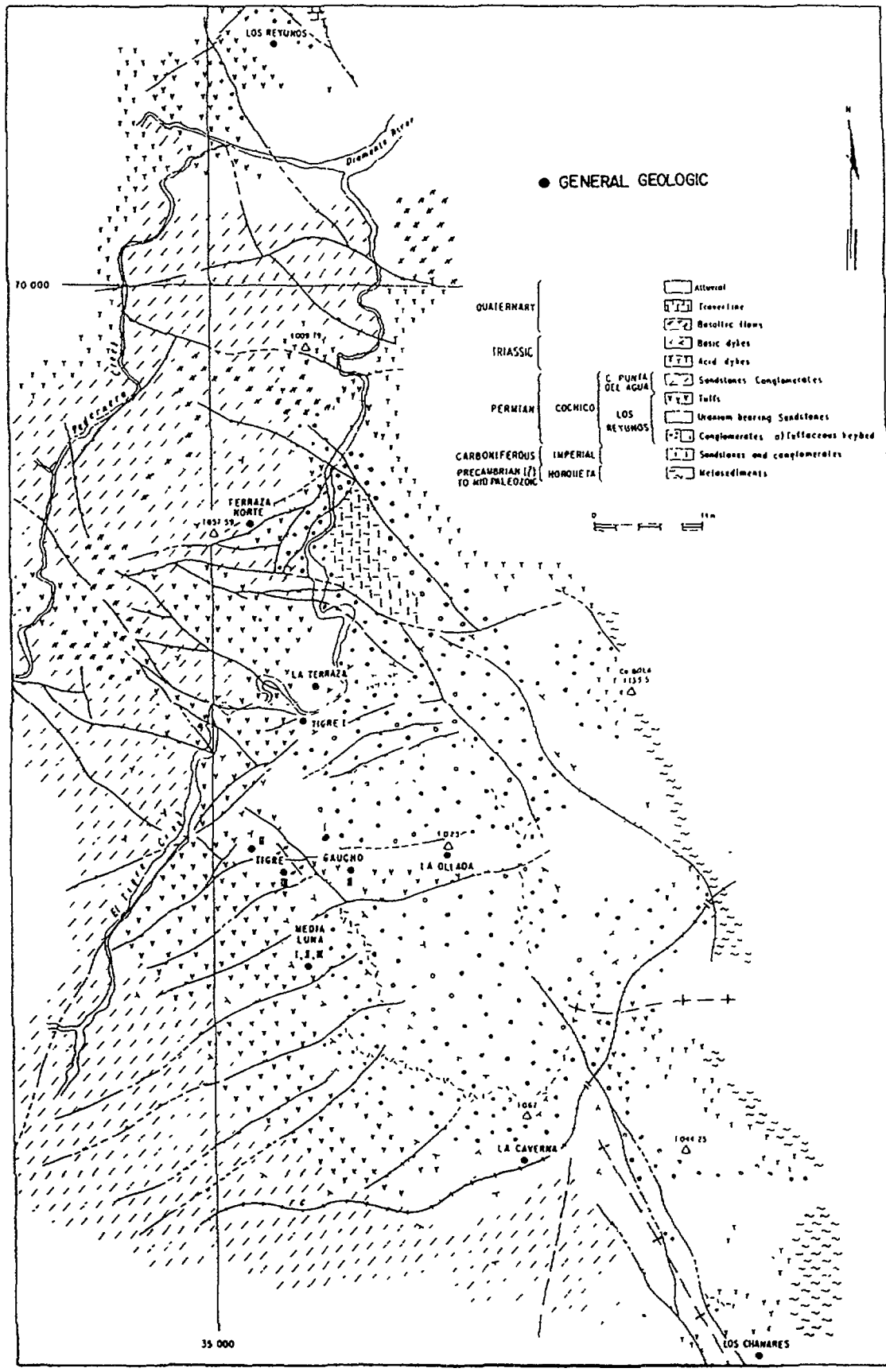

FIG. 2. General Geology of the Sierra Pintada District.

The first phase consisted of a reconnaissance survey over ore deposits (prospects) known up to that moment in the zone, previous to the discovery of the Dr. Baulíes ore. Among the most favourable anomalies the following were chosen: Las Peñas, Los Chañarès and Cuesta de los Terneros (Fig. 1).

Drainage sediments and soil sampling were performed according to the possibilities of each sector. A total of 97 samples were taken, 52 of which correspond to stream sediments and 45 to soil samples.

Sampling techniques

a) **stream sediment samples:** 200 g to 300 g of the finest fraction were taken, preferably the clay fraction over the river bed which was dry at the moment of sampling, avoiding the deposits of eolian origin. Sampling interval was between 50 an 200 m.

b) **soil samples**: Using a soil auger 200 g of the soil sample were taken at different depths of 10, 20, 25, 30 and 50 cm, according to the possibility of each profile. Those soils are characterized as arid soils without a developed soil profile. The sampling pattern was two lines according to the structure of the ore deposition.

Sample preparation and analytical techniques

The stream sediment and soil samples were dried 80°C in a stove, sieved and stored. The sieving was made in a stainless steel sieve of -150 mesh after Tyler norms. The portion +150 mesh was discarded.

For the uranium analysis, the sample was attacked with HNO_3 2.5 N. The uranium was separated to avoid the quenching effect by an organic solvent (ethyl acetate) and analysed by the fluorimetric method. The Jarrell Ash Fluorimeter, type 26010 was used. The sensibility of the analytical method was of 0.3 μg/l (0.3 ppm U).

Results

The data of Los Chañares sector (Fig. 4) were the best obtained in this work. The stream sediments had a scattered over the creek, downstream the prospect, with values ranging from 8.1 ppm U, near the prospect, down to 0.8 ppm U (background value) 400 m downstream. The conclusion was that, in these conditions, the uranium dispersion over the stream was only 150 m from the mineralized sector.

The data on soil samples have an uranium dispersion more limited than the stream sediment samples. The values obtained were slightly over the background (1 ppm U), between 1.3 and 2.1 ppm, except for the samples taken directly over the mineralized material.

5.2.2. Reconnaissance Geochemical Survey (mid 1974–1976)

A new stage of geochemical prospecting was carried out in different years. It began in July 1974 and was continued in April–July 1976. In this opportunity, besides the stream sediment samples, an hydrogeochemical sampling was carried out, with collection of surficial and spring water samples [9].

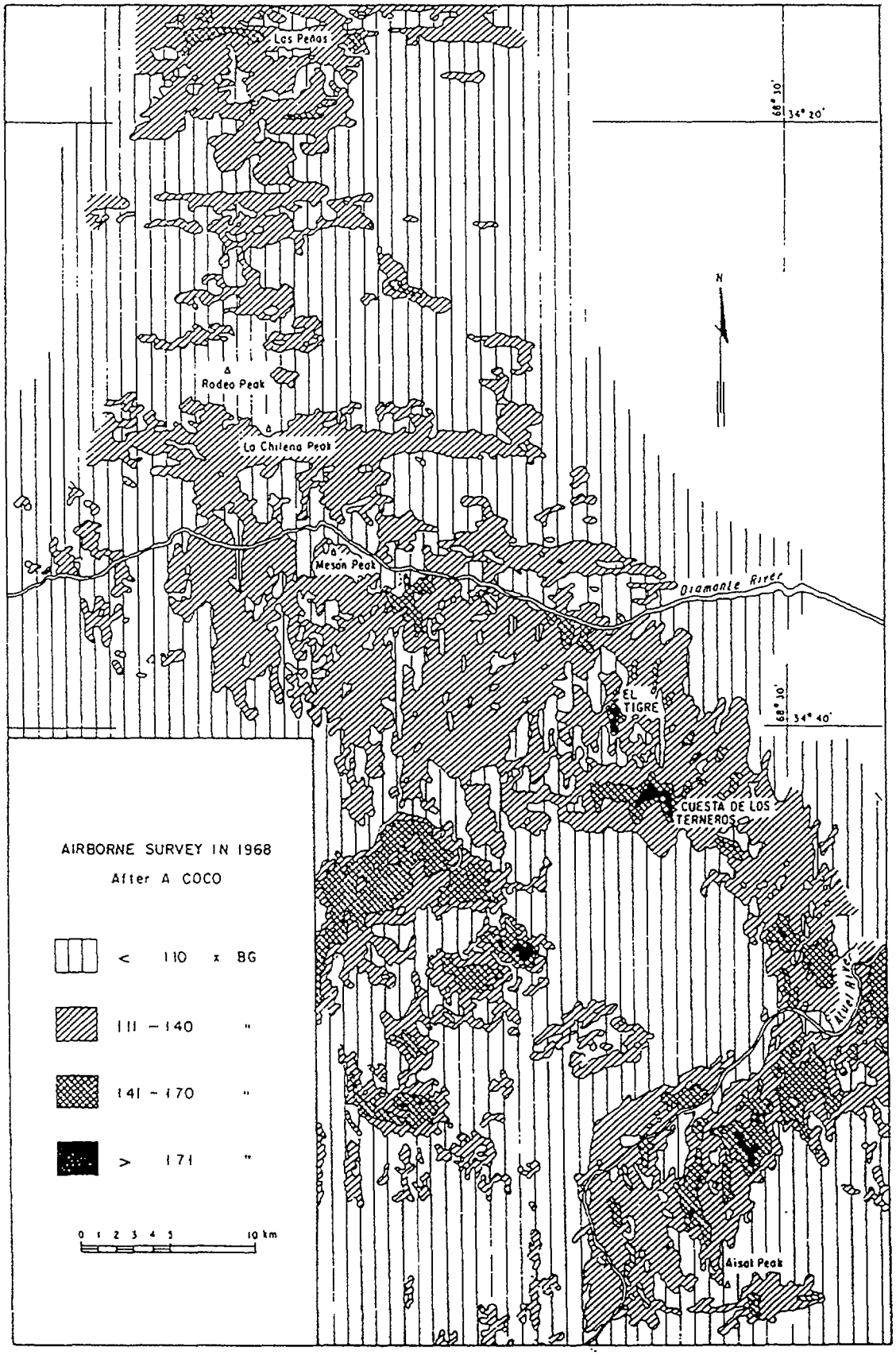

FIG. 3. Airborne Survey of the Sierra Pintada District, 1968.

In the initial stage, a preliminary sampling was performed near the "Doctor Baulíes" ore, in "El Tigre" stream, in order to observe the answer to hydrogeochemical sampling in the region where the stream and creeks are intermittent.

The teams, following common instructions for sampling, obtained at the end of work 1427 samples (977 stream sediment and 450 water samples) in 977 station points in the streams and creeks, over the area of 450 km^2 with a density of 2 samples per 1 km^2.

Sampling techniques

a) **stream sediment samples:** 200 to 300 g of the finest fraction was obtained in each point. In the preliminary stage samples were collected surficially and at different depths (20, 40 and 60 cm) in order to obtain vertical variations of uranium in the river bed and to determine the best depth of sampling. 90% of data did not show noticeable variations at different depths, for this reason, only the surficial samples were taken. In some locations also spring sediment samples were obtained.

b) **water samples**: where it was possible a water sample was obtained following the general instructions of the best sampling. In some cases spring water samples were obtained together with a spring sediment. Immediately after its extraction the following systematic measurements were made in each water sample:

- pH determinations with a portable Methrom device with standard electrodes;
- oxidation-reduction potential (Eh) with a portable Methrom device with hydrogen and Pt electrodes;
- conductivity measurements with a portable conductimeter WTW device, type LF-54 and a type cell LTA-100;

Sample preparation and analytical techniques

a) **stream sediment samples**: they were dried in a stove at 80°C and then, to test the behaviour of uranium in the samples, some of them were sieved at different mesh in stainless steel sieves. 80, 120 and 150 mesh after Tyler norms were used. The best results for uranium were obtained in the finest fraction (150 mesh) and, for this reason, this size was adopted.

b) **water samples**: after 12 hours of decantation, an aliquot was concentrated by evaporation over chromatographic paper Whatman N. 1 bands, using an evaporator manufactured by CNEA.

Uranium determinations. In this opportunity, a portable laboratory situated in the area of surveying was used. The analytical technique was based on the Berthollet method [10]. Labile uranium was analysed by fluorimetry, after acid attack with HNO_3, 2.5 N and separated to avoid the quenching effect by paper partition with tri-n-butyl phosphate in white spirit. The upper part of the paper was calcinated in an infrared drier and its ashes melted with NaF-Na_2CO_3 flux in platinum discs. The flux discs were measured in a portable Fluorimeter "Nucleometre" type F.P.D.T.U.1. The sensibility was 0.3 μg/g (ppm U).

The water samples on the chromatographic paper bands were attacked directly with dilute nitric acid (2,5 N) and then treated in the same way as the stream sediment samples. The sensibility for the water samples was 1 μg/L (ppb U).

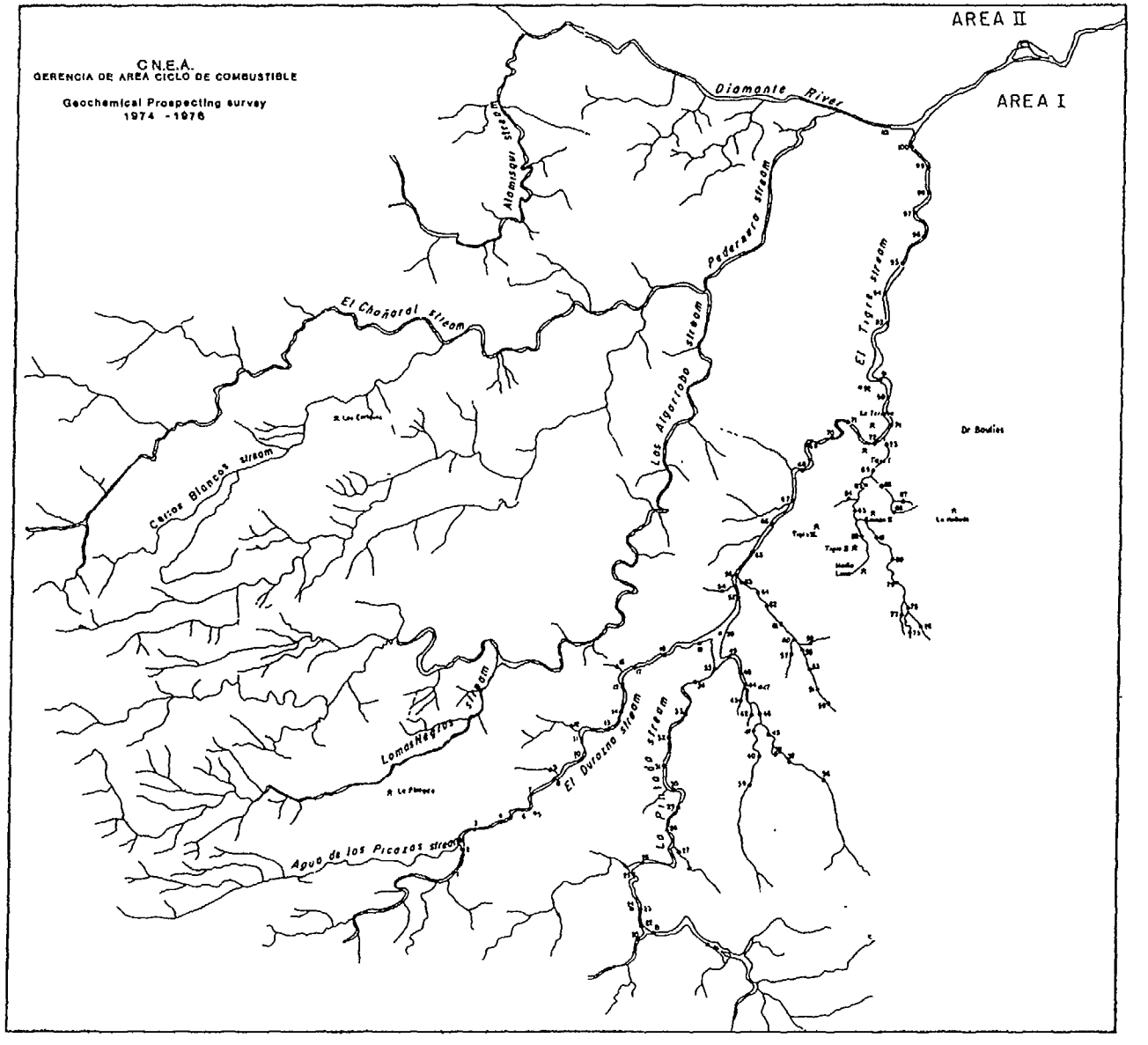

FIG. 5. Geochemical survey of El Tigre Drainage System, 1974 - 1976.

Results

All data were statistically treated and the geochemical background, standard deviation coefficients and geochemical threshold were determined by the Lepeltier graphic method [11].

The whole sampled area was separated in two zones according to their content of uranium prospects: a) zone 1, under the influence of the "Dr. Baulíes" ore, south of the Diamante River, it included all sampling over "El Tigre", "Pedernera" and "Seco de Pavón" streams and b) zone 2, included the sampling carried out over "Chorreado", "Atamisqui" and "Reyunos" stream and all samples taken at the northern sector of the Diamante River (Fig. 5).

Santomero [9] assigned the geochemical background and threshold as follows:

	Waters	Stream sediments
• ZONE 1		
Background	3.4 ppb U	0.5 ppm U
Threshold	12.3 ppb U	1.8 ppm U
• ZONE 2		
Background	2.8 ppb U	0.5 ppm U
Threshold	8.0 ppb U	1.2 ppm U

Taking into account the objective of this work, all data were revised and then only the sampling over "El Tigre" and "Pedernera" streams were statistically treated in order to obtain the geochemical background and threshold in the area under the influence of the Mill-Plant Complex. The parameters are as follows:

	Water	Stream sediments
• "EL TIGRE" stream and its tributaries"		
Number of samples	123	247
Minimum value	1.3 ppb U	< 0.3 ppm U
Maximum	270.0 ppb U	73.0 ppm U
Background	3.2 ppb U	0.4 ppm U
Threshold	10.0 ppb U	1.0 ppm U
• "PEDERNERA" stream and its tributaries		
Number of samples	158	158
Minimum value	1.0 ppb U	< 0.3 ppm U
Maximum value	500.0 ppb U	0.4 ppm U
Background	3.1 ppb U	0.4 ppm U
Threshold	7.5 ppb U	1.0 ppm U

If we restrain only to samples over "El Tigre" stream, which is the nearest point to the present mill-plant complex, we have a background value of 3.7 ppb U and 0.3 ppm U for the water and stream sediment samples, respectively. These are the background data for the area, before activities of the mill-plant complex began.

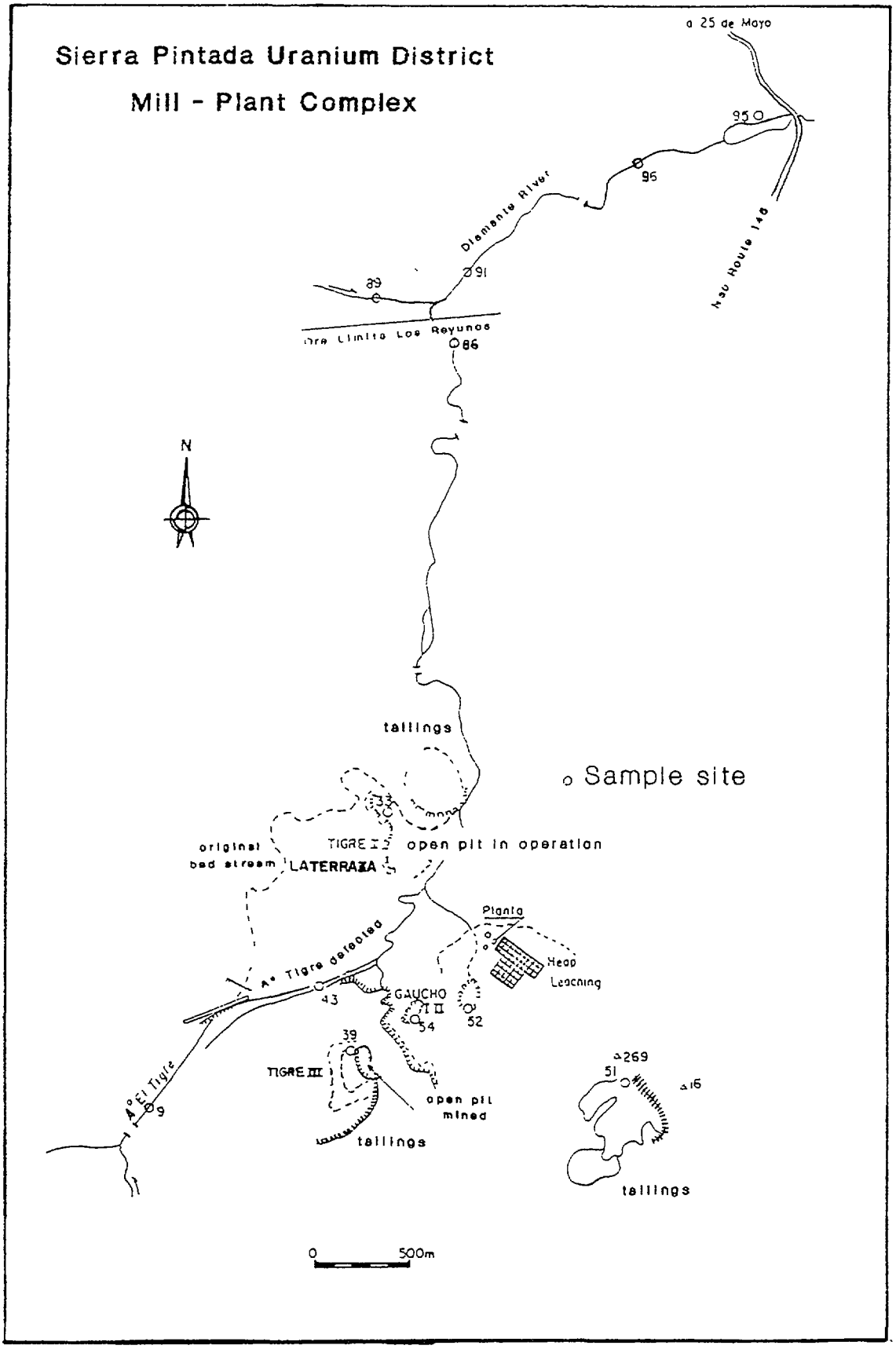

After Donati and Gallucci 1984

FIG. 6. El Tigre stream, Sierra Pintada Uranium District, Mill-plant complex.

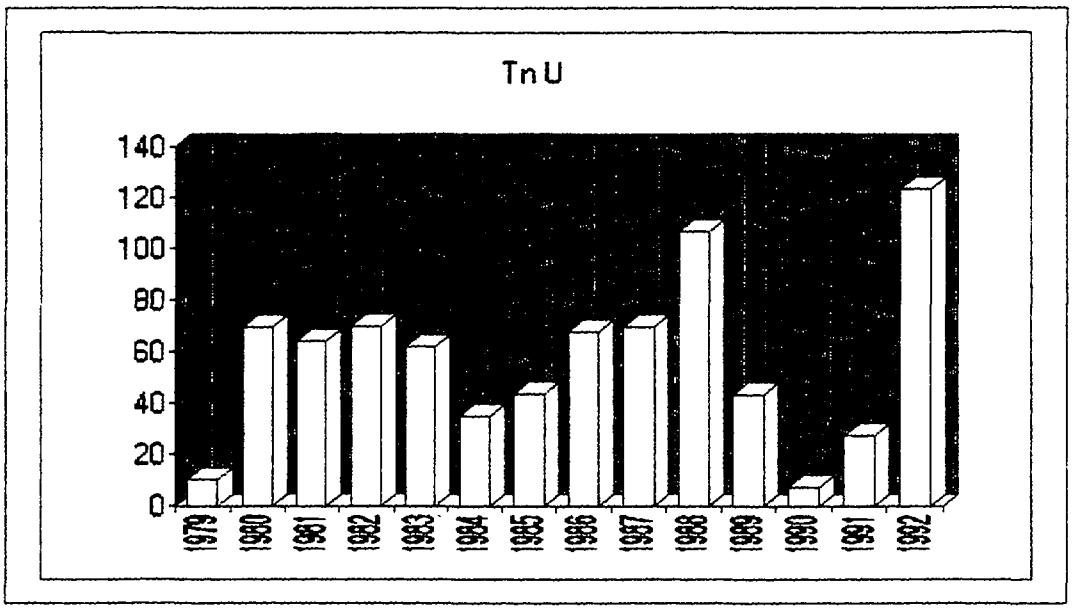

FIG. 7. Annual production of San Rafael mill-plant complex.

Water data are lower than those quoted by the bibliography for the mineralized areas. The maximum values obtained in the zone are 270 and 500 ppb U in "El Tigre" and "Pedernera" streams in waters with pH between 7.4 and 8.4 (slightly alkaline and bicarbonate waters). The stream sediments values are the lowest and its dispersion trends the shortest due to quality of sampling materials (medium to coarse grained) and climatic conditions.

In this geochemical survey the samples were not analysed by radium because of lack of an adequate methodology.

6. MILL–PLANT COMPLEX

The mine began production of uranium concentrates in 1979. The Dr. Baulíes - Los Reyunos orebodies have been mined by open pit methods. The plant uses the heap leaching method, and the recovery of uranium is made by ion-exchange resins.

The course of "El Tigre" stream was deflected to allow the exploitation of Tigre I -La Terraza Sector in 1979 (Fig. 6).

The annual production of the Mill-Plant Complex up to 1992 can be observed in Fig. 7.

7. ENVIRONMENTAL CONTROLS

From the beginning of the works in the Mill-Plant Complex, there has been a Radiological Protection and Safety Service. His duty is to perform the controls according to the norms specified by the competent authority in the country. This service performs control determinations inside and outside the Complex area.

As the objective of this report is to apply the geochemical prospecting techniques to the environmental control we will show the results obtained up to now.

7.1. CONTROL ENVIRONMENTAL POINTS

We already mentioned that "El Tigre" stream is the water course that passes and drains the whole Complex area. Several control points were established in different years, but only four of them are considered as fixed control points: two at the El Tigre stream (samples 9 and 86) and two at the Diamante River of which it is a tributary (samples 89 and 95) (Fig. 6).

Sample N. 9: is situated at "El Tigre" stream, 1500 m before entering the mining works area. The data of this point are considered as the environmental background.

Sample N. 86: is situated at "El Tigre" stream, 300 m before its outlet in the Diamante River and 7.5 km downstream from the Mill-Plant Complex. Its data are compared with that of the preceding point in order to do the migration balance from the Complex to the environment.

Sample N. 89: is located at the Diamante River, 100 m upstream from the "El Tigre" stream mouth. It is the reference background point before the entrance of the waters arising from the Complex.

Sample N. 95: is located at the Galileo Vitale Dam (Diamante River), several kilometers downstream from "El Tigre" stream mouth.

7.2. SAMPLING TECHNIQUES

The sampling techniques were developed during the different geochemical prospection surveys. The stream sediment samples were taken and prepared in the same form that was explained in point 5.2. The water samples are obtained directly in a plastic bottle and do not require preparation because since 1977, we use the laser induced fluorescence method.

7.3. ANALYTICAL TECHNIQUES

Natural Uranium. After the appropriate drying, crushing and sieving steps of the stream sediment samples, a hot acid digestion is used to bring uranium into solution (total uranium). The resultant leach is neutralized and diluted to the normal operating levels; an aliquot is treated with a "fluoran" solution to correct the matrix effects, and measured in the UA-3 Uranium Analyser which is calibrated using certified standards of known concentration. To detection limit is 1 μg/g (1 ppm U). The water samples are analysed directly and its detection is 0.1 μg/L (0.1 ppb U).

^{226}Radium. The Rushing method [12] is used. The water samples are treated with $BaCl_2$ after a sulfation, that forms a precipitate containing radium, generally $Ba(Ra)So_4$. This precipitate is separated by filtration and dissolved, and after a convenient intergrowth time (approx. 15 days) the radon gas is flushed into a ZnS coated counting cell and an alpha counting of the precipitate is performed in a Canberra equipment.

The stream sediment samples are melted with Na_2CO_3 after an appropriate sieving and put into solution with HCl. Then the method used is the same as the one for the water samples.

The detection limits are 0.10 ^{226}Ra pCi/g and 0.10 ^{226}Ra pCi/L for the stream sediment and water samples, respectively.

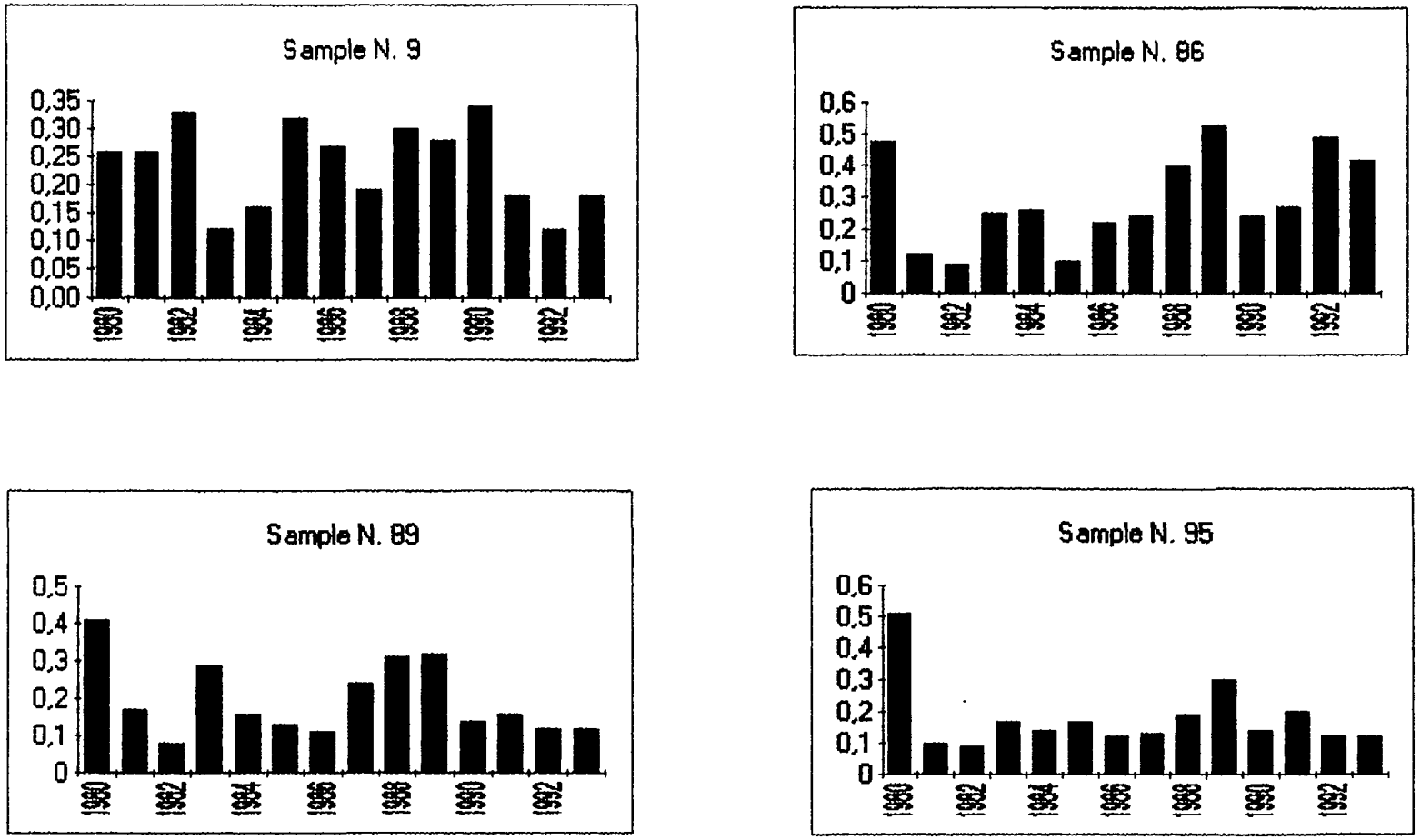

FIG. 8. Radium concentration (p Ci/L) in water samples, 1980 – 1993.

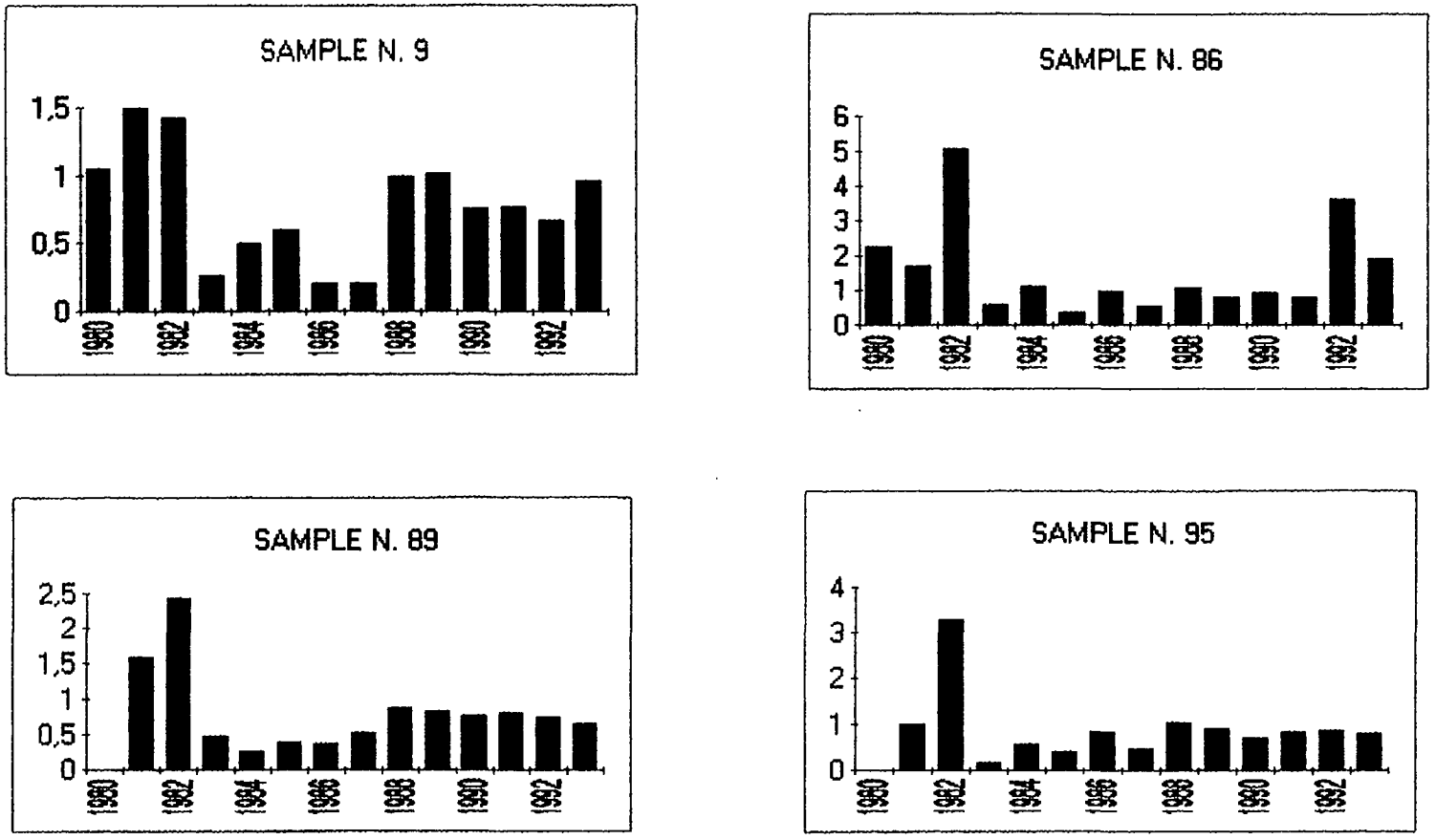

FIG. 9. Radium concentration (pCi/g) in stream sediment samples, 1980 – 1993.

7.4. HYDRIC CHARACTERISTICS OF "EL TIGRE" STREAM AND THE DIAMANTE RIVER

El Tigre. This stream is formed by the confluence of "El Durazno" and "La Pintada" creeks, about 2 km before the uranium mining district and runs with a SE–NE trend to outlet in the Diamante River. Its drainage basin has an extension of 297 km^2. Originally, the middle part of its course bisected the Tigre I — La Terraza ores. For that reason it was necessary to deflect its natural course. Its drainage basin is characterized by a great amount of alluvial deposits in its high and medium course and is dangerous during the short torrential rainfalls. The sediments are of fluvial, alluvial and detrital origin; sand and silty sand fractions are predominant with abundant gravel and blocks. Its normal flow is low, 0.10–0.30 m^3/s and, fundamentally, it depends on the pluviometric regime: distribution, frequency and type of rainfall precipitations. During the rainy season, the contribution from the eastern mountain range increases its flow in a disproportionate form in a short interval of time. These freshets principally occur from November to March with low annual frequencies.

Diamante River. It forms the principal drainage basin of the mill-Plant Complex. It has a permanent current with an average flow of 40 m^3/s and maximum values form November to March which seldom are more than 100 m^3/s.

7.5. MIGRATIONS OF NATURAL URANIUM AND ^{226}RADIUM FROM THE SAN RAFAEL MILL-PLANT COMPLEX TO THE ENVIRONMENT

Figs 8 to 11 show the annual average (median) values of natural uranium and ^{226}Ra for the water and stream sediment samples in the four control environmental points for the period between 1980 and 1993. From these, we can deduce the following:

Sample N. 9: The natural uranium content in the water samples is similar to that measured during the geochemical prospection survey in 1974, whereas the ^{226}Radium values are fluctuating and low. No ^{226}Ra measurements were done before 1980.

The stream sediment samples increased this natural uranium content 6-fold according to the background obtained in 1974. The ^{226}Radium values are fluctuating and low.

Sample N. 86: The natural uranium content of the water samples increased between 8 up to 30 times over 1974 values, but they are not higher than the maximum value obtained at the moment. If we compare with sample N. 9 values, the maximum increase is 20-fold and, on an average, only 9 times the background value. The ^{226}Radium values are fluctuating, low and without significant increase.

The natural uranium content in stream sediment samples increased 6-fold according to the background in 1974 and twice with respect to sample N. 9. The ^{226}Radium values are fluctuating and increased 4 times in relation to sample N. 9.

Sample N. 89: The natural uranium content in the water samples is similar to the 1974 background, while the ^{226}Radium contents are fluctuating and low.

In the stream sediment samples we observed a low increase in the natural uranium contents in relation to the 1974 background. It is necessary to say that the number of determinations in the geochemical prospecting were limited and for that reason the statistic confidence is low. As for the water samples, the ^{226}Radium values are fluctuating and low.

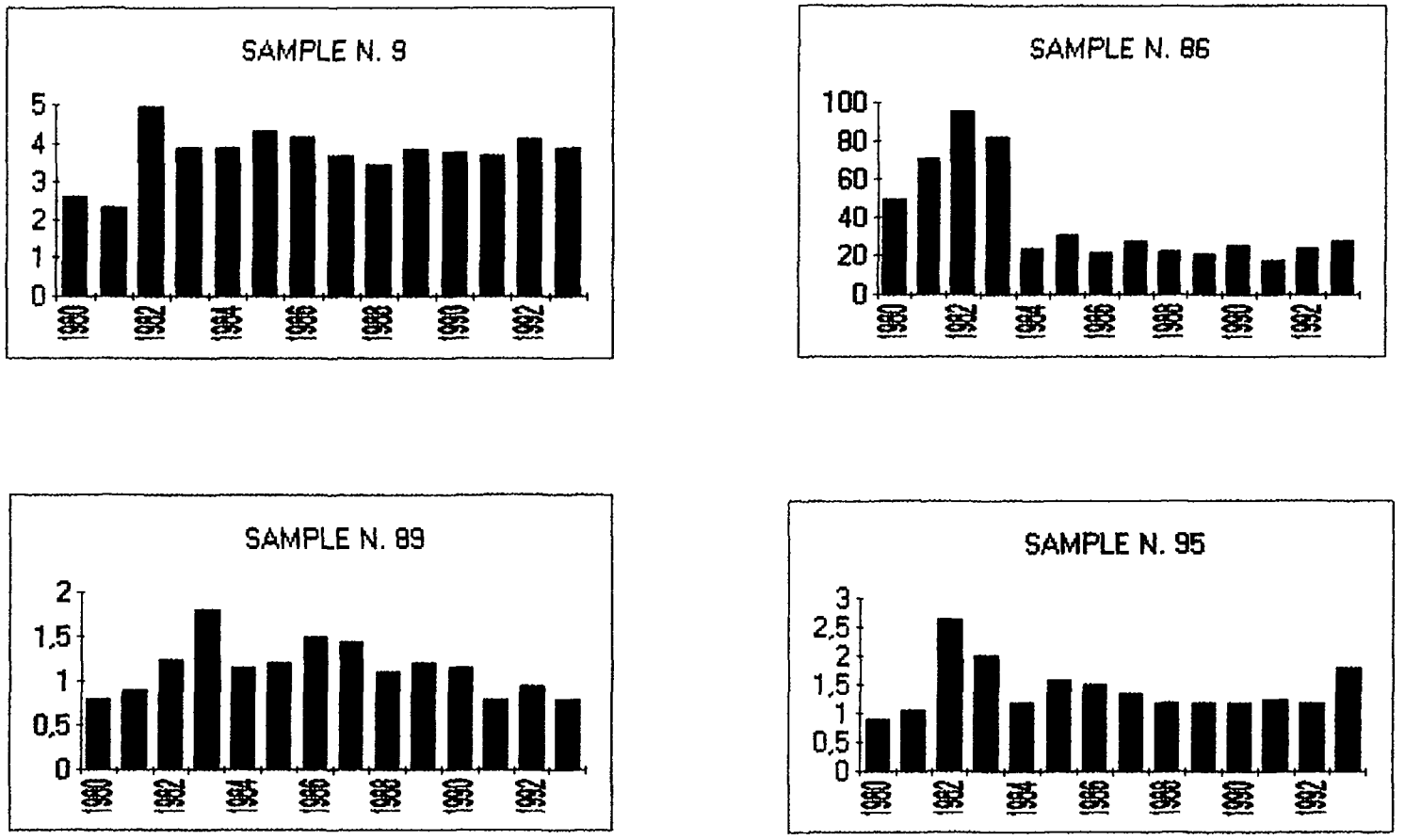

FIG. 10. Uranium (ppb) concentration in water samples, 1980 - 1993.

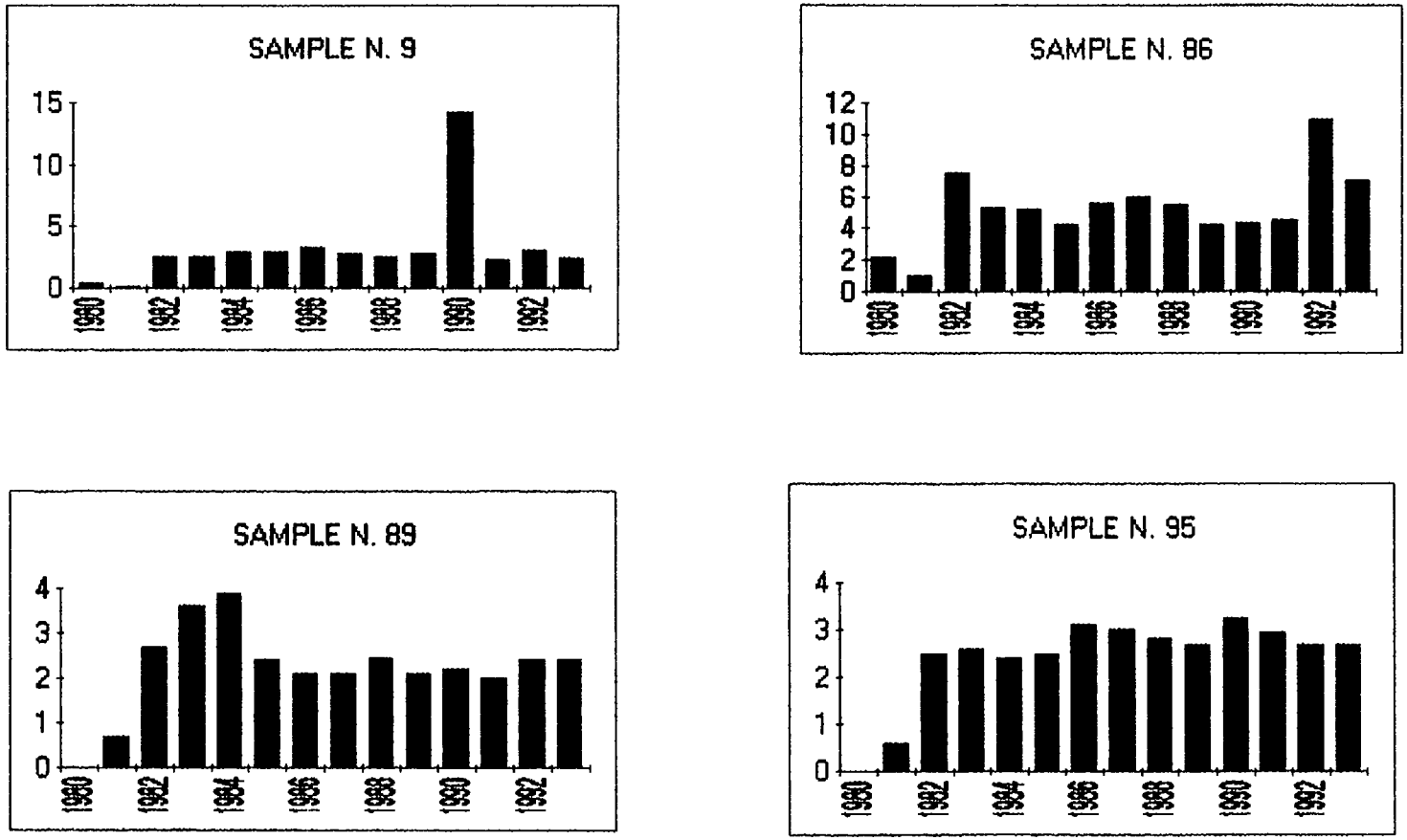

FIG. 11. Uranium (ppm) concentration in stream sediment samples, 1980 - 1993.

Sample N. 95: There are no data from 1974. The natural uranium content in the water and stream sediment samples has a slight increase between this control point and sample N. 89, whereas the ^{226}Radium values are similar.

8. CONCLUSIONS

- There is an increase in the natural uranium content in the water samples of "El Tigre" stream after passing through the Mill-Plant Complex. When its waters outlet to the Diamante River the flow is 140 times more than El Tigre, and do not produce a significative increase in the uranium content. We come to the same conclusion considering the natural uranium values in the stream sediments.

- The values of ^{226}Radium are fluctuating, low and they are within the analytical method trends.

- The sampling techniques, sample preparation, analytical methods and laboratories that were developed in the Geochemistry Section for the geochemical survey, were completely adaptable for carrying out the environmental control of the Mill-Plant Complex at the Sierra Pintada uranium mining district. The human resources of this sector were trained in the first stage of this control and they carried out the training of the new staff.

- The data obtained in the environmental control do not exceed the limit values given by the basic norms of Radiologic and Nuclear Safety of the CNEA or by the international norms. The natural uranium and ^{226}Ra contents that enter the environment surrounding the mine complex, are lower than the annual levels admissible for human ingestion [13].

ACKNOWLEDGEMENTS

The authors would like to thank the authorities of the Fuel Cycle Area of CNEA (Argentina) for the nomination to write this paper and would also like to thank Ms. Laura Kleiman and Mr. Raúl Ferreyra for a critical review of the paper and Mr. Luis López for their assistance during the writing of this work.

REFERENCES

[1] NICOLLI, H.B., GAMBA, M.A., FERREYRA, R.E., Geochemical Characteristics and Genesis of Sandstone-type Uranium Deposits, Sierra Pintada District, San Rafael, MEndoza, Argentina, in Metallogenesis of URanium, Proc. 26th Int. Geol. Cong., Section 13, Theme 2.2, Paris (1980/Pub. 1981) 163-184.

[2] RODRIGO, F., BELLUCO, A.E., Discovery of the Sierra Pintada Uranium Dicstrict, Mendoza Province, Argentina, in Uranium Exploration, Case Histories, Proc. Adv. Group MEeting Vienna (1079), IAEA (Pub. 1981) 23.

[3] LLAMBIAS, E.J., KLEIMAN, L.E., SALVARREDI, J.A., Magmatismo Gondwanico de Mendoza, in Geología y recursos naturales de Mendoza, Relatorio XII Cong. Geol. Arg., II Cong. Explor. Hydrocarburos (1933) 53-64.

[4] MEZA, J.C. (per com.) (1993).

[5] MALOBERTI, A, Análisis estadístico de imbricaciones del Miembro Psefítico Inferior de la Formación Cochicó, Flanco oriental de la Sierra Pintada, Dpto. San Rafael, Mendoza, CNEA, Inf. inéd., DDE (1983) 22-83.

[6] DONATI, B., GALLUCCI, A.R., Trabajo de invetigación sobre migración de Ra-226 y uranio natural desde el Complejo Minero Fabril hacia el medio ambiente, Contrato OIEA-CNEA N. 3123/RB (1984) 45 p.
[7] COCO, A. Relevamiento radimétrico aéreo, San Rafael, Mendoza, CNEA, Inf. int. (1969) 20 p.
[8] SANTOMERO, A.O.M., Ensayo de prospección geoquímica por uranio en el area de la Sierra Pintada-Depto. de San Rafael, Prov. de Mendoza, CNEA, Inf. int. (1968) 17 p.
[9] SANTOMERO, A.O.M., Prospección geoquímica estratégica en el distrito uranífero de Sierra Pintada, San Rafael, Mendoza, CNEA, Inf. int. (1978) 19 p.
[10] BERTOLLET, P., Méthodes d'analyses utilisées par la section de géochimie: Uranium, Radon, Radium, Centre d'Études Nucleaires de Fontenay-aux-Roses, Rapport CEA R-3557 (1968).
[11] LEPELTIER, C.A., A Simplified Statistical Treatment of Geochemical Data by Graphical Representation, Econ. Geol. Vol. 64 (1969) 538-550.
[12] RUSHING, D.R., GARCIA, W.J., CLARK, D.A., The Analysis of Effluents and Environmental Samples from Uranium Mills and Biological Samples for Radium, Polonium and Uranium, in Radiological Health and Safety in Mining and MIlling of Nuclear Materials, Proc. Symp., Vienna, Austria (1963), vol. 2, (Pub. 1964), 187.
[13] ESCRIBANO, T.L., CIALELLA, H., ZARBO, S., Informe de la misión a la zona del Complejo Minero Sierra Pintada y sus zonas de influencioa, CNEA, Inf. Int. (1979).

THE CONTRIBUTION OF APPLIED GEOPHYSICS FOR THE ESTIMATION OF THE RADIOELEMENT CONTAMINATION OF THE ENVIRONMENT

G.N. SIDERIS
I.G.M.E., Athens, Greece

K.N. PAPACONSTANTINOU
Colorado School of Mines, Dep. of Geophysics, Golden, Colorado,
United States of America

N.N. PAPADOPOULOS
N.C.S.R. "Demokritos", Athens, Greece

Abstract

One of the most significant advances in uranium exploration has been the development of nuclear geophysical methods. It has been proved that, under certain conditions, it is possible to use such techniques to estimate the radioactive pollution of the Natural Environment. Portable gamma-ray spectrometers, threshold type, are instruments which have been used for many years for the research of both uranium and radioactive raw materials deposits. During the disaster at the Chernobyl nuclear facility, this kind of equipment contributed effectively to the recording and estimation of radioactive pollution not only of the environment but of various products of the food chain as well. Besides this, a HpGe spectrometer system which has been obtained from an IAEA-TC programme for radiometric measurements of uranium and for multielement neutron activation analysis of geological and other samples, has also been used for measurements of the radiation effects from the Chernobyl accident. Furthermore a short-lived nuclide activation analysis system, which has been used extensively for uranium exploration by delayed neutron counting, can also be used for environmental pollution studies. By the use of the technique which is presented in this report, it became possible to determine with accuracy and speed the radioactivity burdening to various primary food products like milk, meat and fruit (cherries, etc.). On the other hand, the extent of the radioactivity burdening of the Environment has been calculated through the difference among the rates of total count gamma-ray intensity obtained with the gamma-ray spectrometers, threshold type, before, during and after the nuclear accident at Chernobyl, Ukraine. The measurements of the environmental radiation have been obtained before the accident of Chernobyl through the calibration of the equipment at the calibration pads for instruments of applied geophysics at the N.C.S.R. "Demokritos" campus, in order to use them in any geoscientific exploration project. Therefore, we were aware of the background radiation recorded under normal conditions and it was easy to determine the level of any radioactive contamination and to estimate the percentage of burdening in Greece.

1. INTRODUCTION

The accident at the Nuclear Reactor No. 4, of Chernobyl, Ukraine, according to the information given by the I.A.E.A. in Vienna, Austria, happened on the 26th of April 1986. The radioactivity cloud which has been formed, moved towards the Greek territory following two (2) main directions. One of them moved through the Black Sea and the other one moved through the Territory of the Former Republic of Yugoslavia. Finally, the radioactivity cloud reached Athens, Greece on May 3rd, 1986 around 12:00 GMT. This was the first time that the instruments of the National Centre for Scientific Research (N.C.S.R.) "Demokritos", Athens, Greece, indicated high levels of radioactivity [1].

The danger of the abnormal radioactivity values made necessary to check the radioactivity pollution levels not only of the natural environment but also of various products of the food chain that

TABLE I DATA FOR THE ESTIMATION OF THE RADIOACTIVITY BURDENING OF THE ENVIRONMENT AT THE CALIBRATION FACILITIES FOR GEOPHYSICAL INSTRUMENTS

Date			Total count gamma ray intensity on calibration pads for geophysical instruments		
			Pad of low radioelement concentration GR/AL-5	Pad of medium radioelement concentration GR/AM-6	Pad of high radioelement concentration GR/AH-4
1	March	1986	36 25	730 00	2425 00
24	April	1986	37 25	735 00	2400 00
08	May	1986	126 25	820 00	2595 00
09	May	1986	126 25	812 00	2550 00
10	May	1986	125 00	815 00	2517 50
11	May	1986	136 25	900 00	2547 50
12	May	1986	123 75	825 00	2495 00
13	May	1986	116 25	810 00	2480 00
14	May	1986	111 25	790 00	2465 00
15	May	1986	112 50	800 00	2477 50
17	May	1986	97 50	790 00	2437 50
18	May	1986	95 00	787 50	2450 00
19	May	1986	91 25	785 00	2467 50
26	May	1986	80 00	777 50	2462 50
30	May	1986	67 75	767 50	2437 50
02	June	1986	70 00	760 00	2450 00
06	June	1986	69 00	770 00	2427 50
09	June	1986	64 75	767 50	2425 00
11	June	1986	61 50	760 00	2420 00
13	June	1986	70 50	735 00	2445 00
16	June	1986	70 00	752 00	2462 50
18	June	1986	58 25	750 00	2430 00
20	June	1986	57 75	755 00	2437 50
30	June	1986	54 25	740 00	2447 50
11	July	1986	53 75	745 00	2422 50
25	July	1986	55 75	755 00	2425 00
19	August	1986	53 50	757 50	2417 50
22	August	1986	53 75	752 50	2410 00
18	Sept	1986	48 00	737 50	2422 50
24	Sept	1986	47 25	740 00	2422 50
06	Oct	1986	49 75	745 00	2452 50
14	Oct	1986	46 00	735 00	2427 50
20	Oct	1986	58 00	750 00	2437 50
30	Oct	1986	44 25	740 00	2435 00
10	Nov	1986	44 00	740 00	2410 00
24	Nov	1986	43 50	752 50	2415 00
22	Dec	1986	39 75	742 50	2405 00
12	Jan	1987	40 50	732 50	2400 00
20	Jan	1987	39 75	750 00	2400 00
10	Feb	1987	38 50	740 00	2392 50
19	Feb	1987	40 00	725 00	2425 00
10	April	1987/	40 75	737 50	2455 00
04	June	1987	42 00	732 50	2427 50
18	Sept	1987	39 25	727 50	2400 00

were existing at that period of the year. For this reason we have developed a technique based on rather simple measurements obtained with light, non expensive, portable geophysical instruments of the specific gamma-ray spectrometer, threshold type.

The radioactivity pollution levels have been measured by the GIS-4 of Scintrex Geophysical Company, threshold type gamma-ray spectrometers:

- At the calibration facility for the geophysical radiometric instruments which were located at the N.C.S.R. "Demokritos" campus [2].

- In the Laboratory for Measuring the Radioactivity of the Environment (L.M.R.E.) of the N.C.S.R. "Demokritos".

TABLE II. MEASUREMENTS SHEET

	Eγ	A cps	(I.3)-1 Filter	Bq	Bq/kg	corrected Bq/kg
I-131	364.5	0.095	27.9	2.65	66.26	89.45
I-132	667.0		43.8			M.A.
Cs-137	661.6	0.470	40.9	23.92	598.07	907.40
	604.7	0.230	40.0	9.29	230.00	310.50
Cs-134	795.8	0.250	60.2	15.05	376.25	507.94
Te-132	228.0		17.6			M.A.
La-140	487.0	0.090	69.4	6.25	156.15	210.80
Ba-140	537.3	0.090	145.0	13.05	326.25	440.44
Ru-103	497.1	1.360	36.2	49.20	1230.80	166 1.58
Ce-141	145.0		24.3			M.A.
	T O T A L					**3619 Bq/kg**

Sample No.: 7583 L.M.R.E./N.C.R.P.S. "Democritos"

Date of sampling:	03.06.1986	Comments:	soil sample
Date of measurement:	05.06.1986	Weight of sample:	40 g
Instrument:	Canberra-90		

M.A.:	non detectable element
Instrument:	GIS-4 (Scintrex)
Counting:	C = 255 c/30 sec
Background:	Bg = 45 c/30 sec
Net count:	Nc = 210 c/30 sec
Nc/sec:	= 7 c/30 sec
Nc/sec.kg	= 175 c/ sec.kg

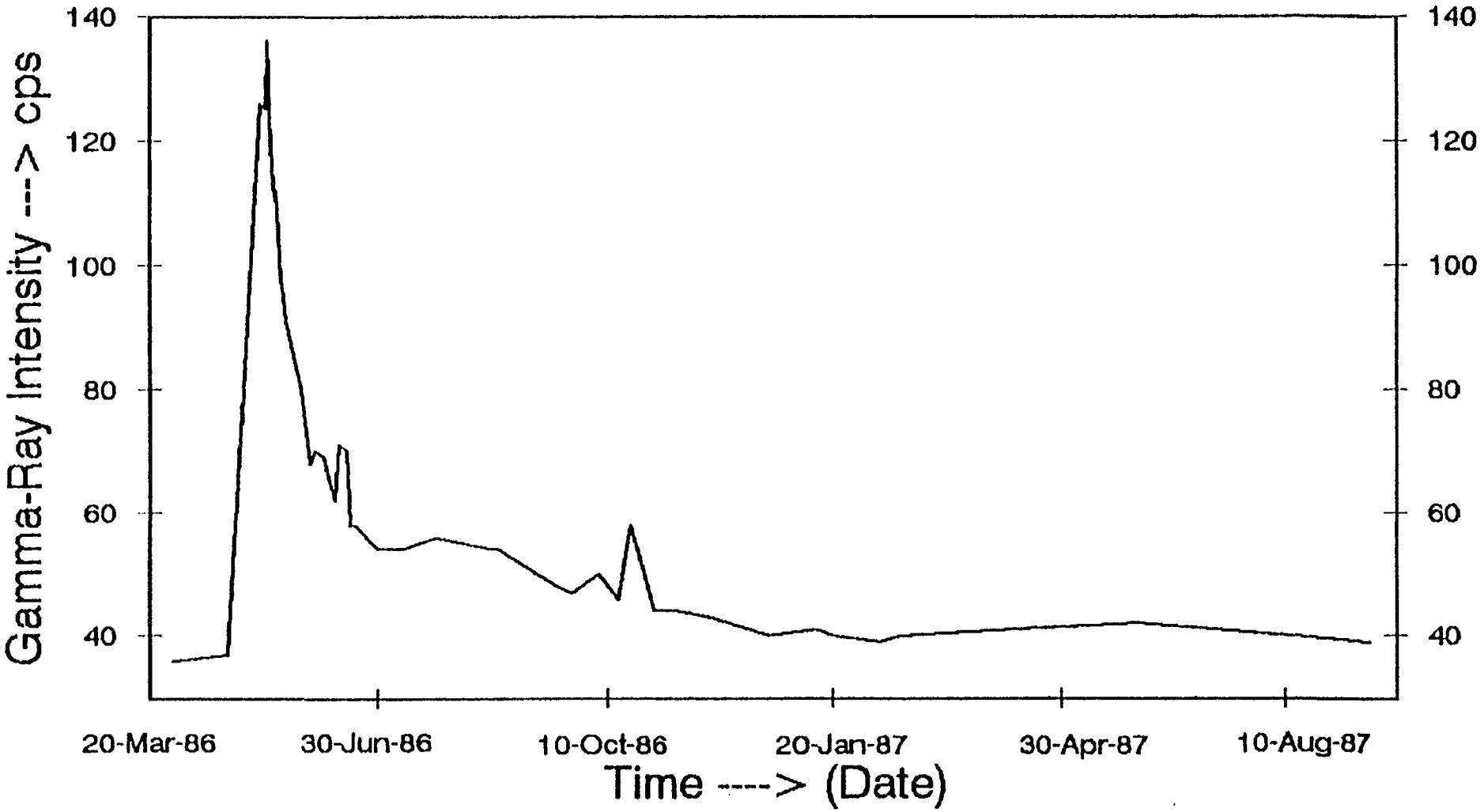

FIG. 1. Gamma ray intensity menasurements on the geophysical calibration facilities.

TABLE III. DATA FOR THE CONSTRUCTION OF THE REGRESSION LINE AND THE RADIOACTIVITY BURDENING IN DAIRY PRODUCTS

Sample identification	Date of sampling	Date of measurement	Volume/weight of sample ml, g	Radioelement content given (Canberra-90) Bq/l, kg	Measurement c/30 sec	Background c/30 sec	Net count per sec/per kg or per l cps/l, kg	Corrected radioelement contents Bq/l, kg
21444 / milk	10.06.1986	13.06.1986	400 ml	276.5	98	57	3.42	
No. 1 / cheese	06.06.1986	14.06.1986	397 g	323.0	97	54	3.61	
11168 / cheese	06.06.1986	14.06.1986	407 g	535.0	139	50	7.29	
11161 / cheese	06.06.1986	14.06.1986	405 g	610.0	172	44	10.53	
11163 / cheese	06.06.1986	14.06.1986	390 g	830.0	218	41	15.13	
No. 2 / milk	11.06.1986	13.06.1986	400 ml	1381.0	312	52	21.70	
No. 3 / milk	11.06.1986	14.06.1986	230 ml	278.0	79	48	4.49	
9432 / milk	14.06.1986	16.06.1986	400 ml		120	45	6.25	435.16
21432 / milk	10.06.1986	13.06.1986	400 ml		69	58	0.75	70.97
Σ1 / milk	15.06.1986	16.06.1986	400 ml		122	46	6.33	439.92
Σ2 / milk	15.06.1986	16.06.1986	400 ml		139	98	7.58	513.23
A1 / milk	15.06.1986	16.06.1986	400 ml		146	51	7.92	532.86
2 / milk	15.06.1986	16.06.1986	400 ml		121	55	5.50	390.09
3 / milk	15.06.1986	16.06.1986	400 ml		75	55	1.67	140.75
81 / cheese	15.06.1986	16.06.1986	322 g		170	53	11.22	717.43
No. 2 / cheese	15.06.1986	16.06.1986	300 g		147	49	10.14	658.36
No. 3 / cheese	15.06.1986	16.06.1986	258 g		64	40	3.10	238.36
10614 / milk	20.06.1986	25.06.1986	400 ml		806	140	16.65	1005.95

2. METHODOLOGY — INSTRUMENTATION

Measurements of the radioactivity levels in the Greek territory have been recorded before the Nuclear Accident at Chernobyl, Ukraine. These measurements have been performed with portable, GIS-4 (Scintrex Geophysical Company), threshold type, gamma ray spectrometer instruments, during their calibration procedure at the N.C.S.R. "Democritos" calibration facility for radiometric instruments of Applied Geophysics [3]. The calibration of gamma ray spectrometers, as every portable radiometric instrument, is necessary to be applied prior to the beginning of each geoexploration project [4]. These data enabled us to localize and estimate the magnitude of the radioactivity pollution of the natural environment in Greece, during that Nuclear Accident.

Measurements with the GIS-4 instruments were taken, systematically, in the calibration facility at the N.C.S.R. "Demokritos", during the radioactivity burdening in Greece. These measurements (Table I) have given a diagram of the change of the gamma ray intensity values with respect to time (Fig. 1.).

On the other hand the calculation of the magnitude of the radioactivity contamination of the food chain products was based on the remark that there is a relation between the radionuclide concentration, in Bq/kg or l, and the gamma ray intensity, in cps/kg or l. According to that remark the pairs of the values which have been recorded, correspond, graphically, to points of a line (regression line) traced with the least square fitting method. The value of the radioelement concentration of each product, in Bq/kg or l, has been measured in the Laboratory for Measuring the Radioactivity of the Environment (L.M.R.E.) at the N.C.S.R. "Demokritos" with the Canberra-90 type, Gamma ray Spectroscopy instrument (Table II). The measurements of the gamma ray intensity have been taken with the geophysical radiometric instruments of the Scintrex company, type GIS-4 gamma ray spectrometers, threshold type. The measurements recorded by these particular instruments are given in units of counts per second over the time during which the product is exposed to measurement. The duration of the measurement varies from one (1) to one hundred (100) seconds. The GIS-4 geophysical instruments which have been used are light, easy to carry and sensitive towards the influence of the gamma ray intensity. They are composed of probes equipped with NaI crystals connected with photomultiplier tubes. With the GIS-4 gamma ray spectrometer, threshold type, one has the possibility to record the gamma ray intensity of the pre-selected energy level according to the seeking target cut-off level, in the energy spectrum.

In order to keep the background radiation level as low as possible we have placed the whole instrument within a lead castle, properly shaped with lead bricks (of the known 10 cm $\times$ 5 cm $\times$ 3 cm size). Within the lead castle there was enough space for the measuring sample as well. In this way we succeeded to bring the background level as low as one count per second (1 cps). Consequently, even samples with low radiation levels could easily be measured, because of the extremely low background radiation achieved. The values of the gamma ray intensity were converted to corresponding values of counts per second over kg or l (cps/kg or l) with respect to the condition of the product, solid or liquid (Table III).

On the basis of these measurements we have constructed regression lines for each particular instrument and for each food product, separately. For the construction of each regression line we used various, randomly selected samples from each product of which we have measured both the radioelement concentration (in Bq/kg or l) with the Canberra-90 system and the gamma ray intensity with the GIS-4 instrument of Scintrex.

After the construction of the regression lines, for each particular instrument and each food product, separately, we were in position to estimate the corresponding radioelement concentration for every single sample of any food product. All we had to consider was the gamma ray intensity value (in cps/kg or l) for each one of them.

TABLE IV COMPARISON OF RESULTS OF RADIONUCLIDE CONTENTS DETERMINED BY GAMMA-SPECTROSCOPY AND Gamma ray SPECTROMETRY, THRESHOLD TYPE, METHODS

Sample identification	Date measurement	Net count per sec per kg or l	Calculated content	Content measured by (Canberra-90)	Error
		cps/kg, l	Bq/kg, l	Bq/kg l	%
44 / milk	13 06 1986	3 42	259 81	277 0	6 0
No 1 / milk	13 06 1986	21 70	1261 75	1381 0	8 6
11161 / cheese	14 06 1986	10 53	679 81	601 0	13 6
11163 / cheese	14 06 1986	15 13	926 87	803 0	11 7
11168 / cheese	14 06 1986	7 29	496 36	535 0	7 2
No 1 / cheese	14 06 1986	3 61	272 11	323 0	15 8
No 3 / cheese	14 06 1986	4 49	327 93	278 0	18 0
21432 / milk	13 06 1986	0 75	70 97	116 0	38 8
9432 / milk	16 06 1986	6 25	435 14	449 0	3 1
S1 / milk	16 06 1986	6 33	439 89	402 0	9 4
S2 / milk	16 06 1986	7 58	513 20	509 0	0 8
A1 / milk	16 06 1986	7 92	532 83	550 0	3 1
2 / milk	16 06 1986	5 58	394 92	415 0	4 8
3 / milk	16 06 1986	1 67	140 74	154 0	8 6
No 2/cheese	16 06 1986	11 22	717 73	697 0	3 0
B1 / cheese	16 06 1986	10 14	658 22	678 0	2 8
10614 / milk	25 06 1986	16 65	1005 95	898 0	12 0
8940 / meat	13 06 1986	79 46	4705 79	4429 0	6 2
80003 / meat	21 06 1986	53 50	3189 44	3837 0	16 9
80013 / meat	20 06 1986	15 00	913 48	1016 0	10 1
80566 / meat	08 07 1986	7 91	486 90	449 0	8 4
80572 / meat	08 07 1986	18 35	1113 72	1019 0	9 3
80597 / meat	09 07 1986	1 46	92 45	94 0	1 6
80599 / meat	09 07 1986	1 80	113 58	109 0	4 2
80600 / meat	09 07 1986	14 64	891 92	925 0	3 6
2290 / cherries	15 05 1986	25 20	1534 18	1348 0	13 8
3116 / cherries	15 05 1986	18 30	1135 11	1176 0	3 6
3117 / cherries	15 05 1986	15 20	953 10	918 0	3 8
1666 / cherries	16 05 1986	12 50	792 80	828 0	4 2
2515 /cherries	16 05 1986	9 50	612 26	715 0	14 5
4031 / cherries	16 05 1986	3 36	230 09	251 0	8 3
3567 / cherries	17 05 1986	21 75	1335 57	1330 0	0 4
3578 / cherries	17 05 1986	1 25	90 69	55 0	64 5
4166 / cherries	19 05 1986	2 01	141 83	125 0	13 6

During the application of the above mentioned methodology it has been realized that the estimation of the radionuclide contents, below the value of 100 Bq/kg or 1 (total emission of the radioactivity level) was not very "successful". We can say that for the sensitivity and the precision of these particular geophysical instruments we were expecting "better" results. The error in determining the values of the radionuclide contents, in this area, is relatively high. This does not mean that it is a serious disadvantage of this technique since that is a non interesting area as far as values are concerned, in relation to the radioactivity contamination influence of the natural environment.

On the contrary in the region close to the values of 600 Bq/kg or 1, which have been considered from the Ministry of Health as an upper limit, for many food products, for hygiene purposes, the error for the estimation of their magnitudes was less than 10% and in many cases even less than 5% (Table IV).

Besides this, a HpGe spectrometer system with a Canberra 35 PLUS multichannel analyzer and an IBM PC/AT, which was obtained shortly before the Chernobyl accident from an IAEA-TC programme for radiometric measurements of uranium and for multielement neutron activation analysis of geological and other samples, after irradiation at the 5 MW swimming pool reactor of N.C.R.P.S. "Demokritos", has also been extensively used for measurements of the radiation effects from the Chernobyl accident. Using this equipment, thousands of air, water, soil and foodstuff samples have been analysed in plastic 400 ml cylindrical containers, mainly for 131I, 132I, 137Cs, 134Cs, 132Te, 132La, 140Ba, and 103Ru, [5], leading to useful conclusions with regard to the impact of this accident to the country and permitting proper precautions to be taken for the public health [1]. Of main concern were goat and sheep milk, cheese and meat, some vegetables and fruit, wheat and their products. Furthermore a short-lived nuclide activation analysis system, which has been used extensively for uranium exploration by delayed neutron counting [6] can also be used for environmental pollution studies.

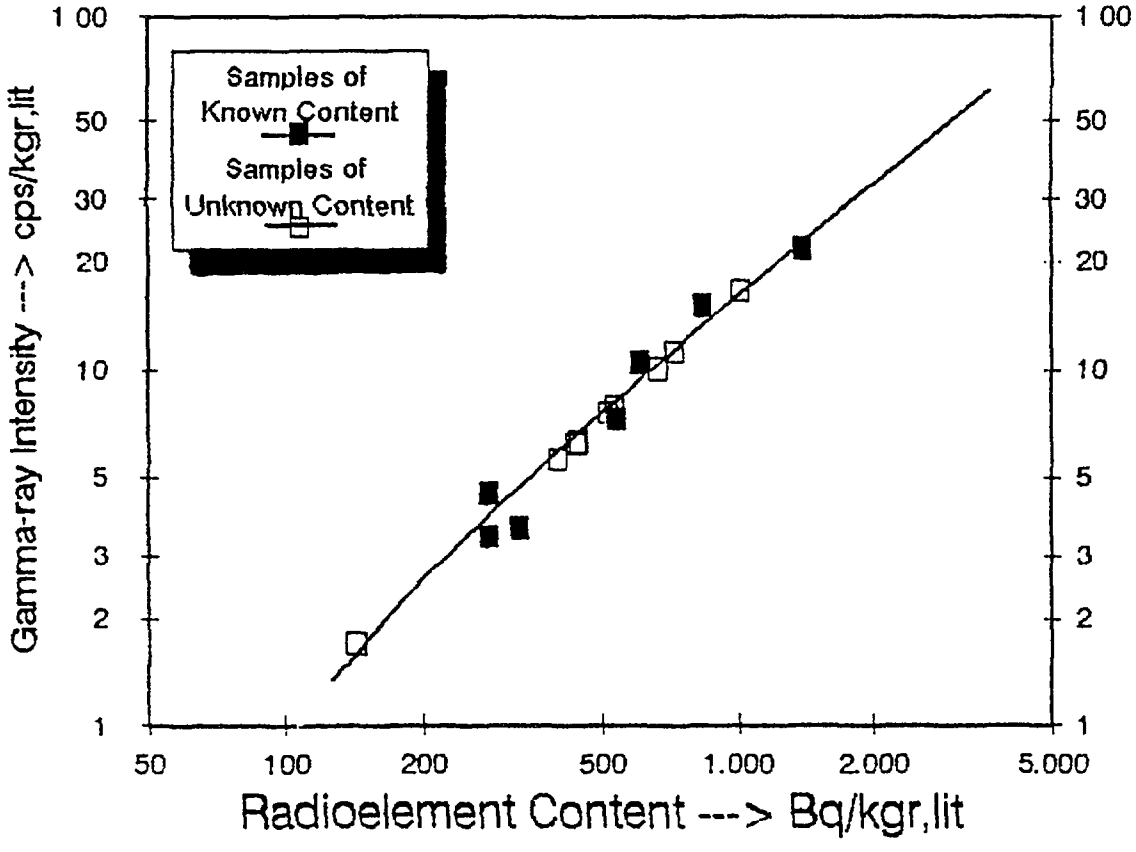

FIG. 2. Regression line from measurements on dairy products.

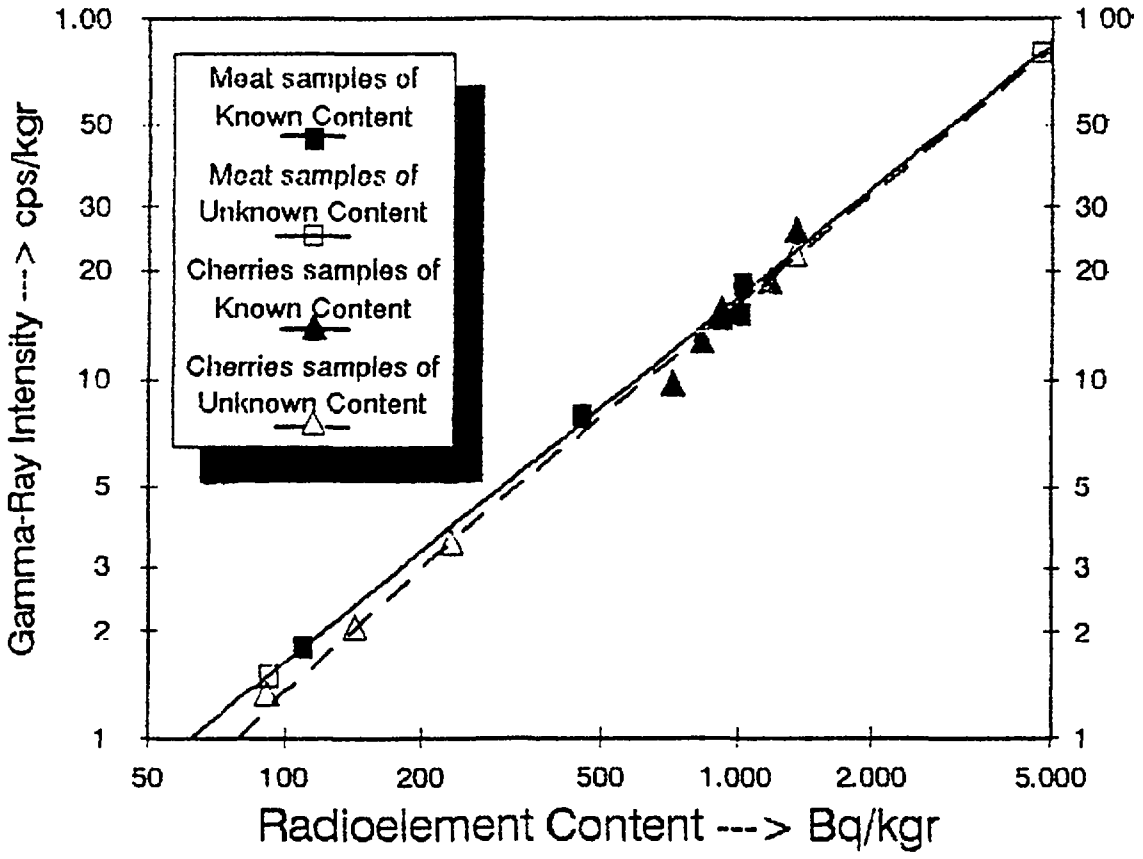

FIG. 3. Regression lines from measurements on meat and cherry samples.

3. RESULTS

With the application of the methodology which has been presented above, the radioactivity pollution level of the Natural Environment (Table I, Fig. 1) has been estimated. Furthermore the radioactivity burdening of various basic products of the food chain, like diary (milk, white cheese, dry cheese, etc.) meat and cherries (Figs 2 and 3) have been determined. This technique has given the chance to measure more samples of the above mentioned products and to determine easily, accurately and rapidly the radionuclide concentration by measuring them with the gamma ray spectrometer, GIS-4, threshold type of Scintrex.

After the estimation of the radioelement content from the measurements of the gamma ray intensity of the products, we have compared these results with those derived from the Canberra-90 Gamma Spectroscopy system. Consequently, we have constructed a comparison table with the calculated radioelement contents and those which have been measured with the GIS-4 instrument. As a result of this work, we have calculated that the mean error of the estimated radioelement concentration is ranging from 10% to 15% (Table IV).

4. CONCLUSIONS

Methods and instruments that have been used in the past for the exploration of radioactive raw materials, have, also, been used effectively to record the environmental contamination in the Greek

territory and to estimate, with precision, the radioelement pollution of various products of the food chain during the period of the nuclear accident at Chernobyl, Ukraine.

The radioactivity pollution of the area, around the calibration facilities for geophysical instruments, being installed in the campus of the N.C.S.R. "Demokritos", was four times greater, in comparison with the "before Chernobyl" period. The greatest value has been measured on the 1st of July, 1986. We can say that the value of the radioactivity pollution was near to the pro-Chernobyl one, close to the end of November 1986 and reached the same level as the one we used to have in the past, very close to October 1987.

The gamma ray spectrometers GIS-4 of Scintrex, threshold type, gave a better estimation of both the radioelement pollution of the environment and the total contamination of the food products, in comparison with instruments like scintillometers, Geiger-Muller counters etc., due to the fact that they have the possibility to measure the total count gamma ray intensity for a period up to 100 seconds.

With the technique that has been developed during the period of "Chernobyl" and has been described above, we have calculated, with accuracy, the radioactivity contamination of a large number of food products as well as of the natural environment, in a simple, quick and inexpensive way.

REFERENCES

[1] ANTONIOU, N., KAPPAS, A., KOLLAS, I., KRITIDIS, P., BARTZIS, I., PANTELIAS, G., PAPANIKOLAOU, E., E., PARADELIS, Th., SIDERIS, E., The Nuclear Accident at Chernobyl, U.S.S.R., and its consequences in Greece: G.A.E.C. Technical Report, Athens, Greece (1986).

[2] SIDERIS, G.N., BARTOSEC J., CHLUPACOVA, M., PAPAKONSTANTINOU, Ek. N., Recent Possibilities of quantitative calibration of Portable Gamma ray Spectrometry in Greece. Paper published in the 1st Hellenic Geophysical Congress Proceedings, Athens, Greece (1989).

[3] SIDERIS, G.N., Evaluation of Uranium Potential of Serres Basin, N. Greece with surface and subsurface Radiometric Methods of Applied Geophysics. Ph.D thesis, University of Athens, Geophysics and Geothermy Division. Athens, Greece (1985).

[4] LØVBORG, L., Total Count Calibration Blocks for use in Uranium Exploration. Riso - R-490, Roskilde, Denmark (1983).

[5] PAPADOPOULOS, N.N., Development of nuclear techniques for national requirements, Int. Symp. on the Significance and Impact of Nuclear Research in Developing Countries, Athens, Greece (1986). Proceedings, I.A.E.A., Vienna (1987), 339.

[6] PAPADOPOULOS, N.N., J. Radioanal. Chem., 72, (1982), 463.

ENVIRONMENTAL AERORADIOACTIVITY LEVELS IN THE SUEZ-CANAL ZONE, EGYPT

A.A. AMMAR, K.M. FOUAD, M.L. MELIEK, A.M. ELSIRAFE, E.M. ELKATTAN
Nuclear Materials Authority, Cairo, Egypt

Abstract

The present study deals essentially with the establishment of the environmental radioactivity levels in the Suez Canal Zone. It will provide basic information that can be used as a reference to detect and determine the amount and extent of any possible future variations in the natural radioactivity level in that part of Egypt, that might result from nuclear testing or accidents involving release of nuclear radiations and fallout of nuclear fission products that might affect both the terrestrial and atmospheric environments. According to the statistical analysis of the radio active measurements recorded over the Suez Canal Zone, it was found that its mean radiometric background is 7.76 millirem/year. Seven lithological units were separated, each was found to be homogeneously distributed, as far as radioactivity is concerned and has its own characteristic statistics. They form the environmental terrestrial aeroradioactivity map of the area. The Suez Canal Zone is characterized by the presence of extensive water surfaces represented by the Gulf of Suez, Bitter Lakes, El Temsah and El Manzalah Lakes. These represent the lowest radiometric level (0.03-5.16 millirem/year) in the studied zone in spite of the presence of a slightly higher level around the rim of the great Bitter Lake. The highest radiometric level was (4.4-15.3 millirem/year) found associated with El Shat formation of Middle Miocene age and which is composed mainly of sandstone, clay, limestone and gypsum. In that regard the present study demonstrated that periodical aerial radiometric surveying for the entire Suez Canal area is highly recommended for monitoring changes in its environmental radioactivity levels.

1. GEOMORPHOLOGY OF THE SUEZ CANAL ZONE

The investigated Suez Canal Zone is characterized mainly by features dominated by low land and water surfaces. The hilly areas are relatively small and extending from the southern part of the zone northward to Fayed. The low land areas are generally covered by gravels, eolian sand, sand dunes, clay, marshes with some scattered low hills of sandstone and limestone especially on the eastern side of the Bitter Lakes (Fig. 1).

1.1. LAKES

The Suez Canal Zone (Fig. 2) is characterized by the presence of extensive water surfaces represented mainly by the Gulf of Suez, Bitter Lakes, El Tamesah Lake and El Manzala Lake. The latter extends parallel to the shore line of the Mediterranean Sea at the north, and stretches to about 15 km to the south, where it is bounded by marshes, shallow water bodies and low lands covered with various salts and evaporites.

1.2. MARSHES AND SABKHAS

Marshes and sabkhas are scattered in the Suez Canal Zone and, especially in the area between El Manzala Lake and El Qantara Town (Fig. 2). Marshes and sabkhas, though of small size, are also encountered around El Temsak Lake and on the eastern side of the Little and Great Bitter Lakes. Marshes differ greatly in the depth of their water and in salinity, the greatest marshes located to the south of El Manzala Lake have the deepest water. El Manzala Lake is more saline as compared to the smaller marshes around El Temsah Lake. The latter is generally surrounded by salty surficial material and evaporates barren of natural vegetation. The small marshes, encountered to the east and

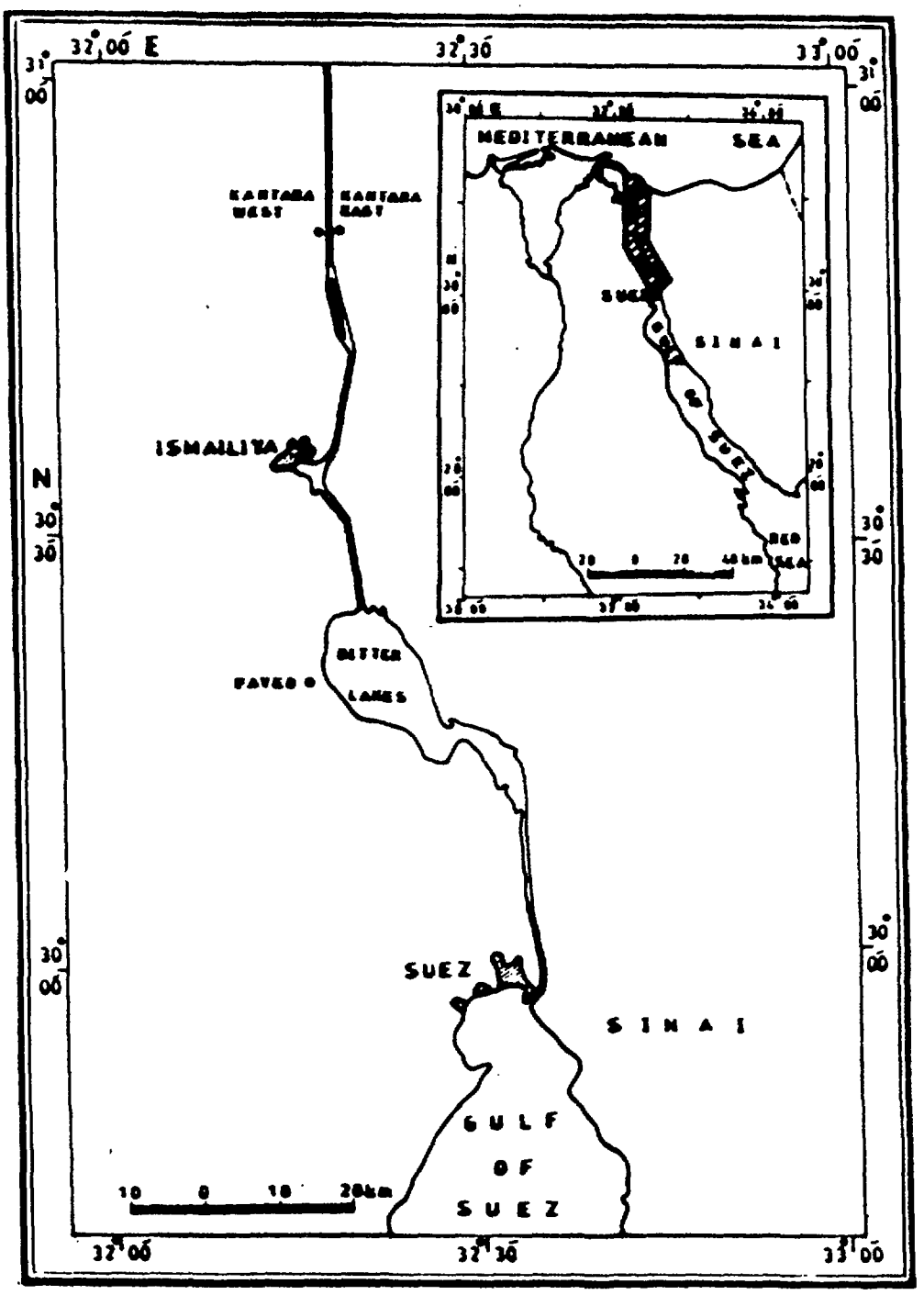

FIG. 1. Key map showing location of the Suez Canal Zone.

west of El Temsah Lake and surrounding the Bitter Lakes, are generally of shallow water and low salinity.

1.3. SAND DUNES

Sand dunes of different types and sizes are covering considerable areas in the eastern part of the investigated Suez Canal Zone and around marshes near El Devreswar, El Ismailiya and El Qantara (Fig. 2). These dunes are generally of low elevation and surrounded by eolian accumulations.

Marshes and vegetation are occasionally found in low lands between these sand dunes, especially to the east and west of El Temsah Lake, near El Devreswar and south of El Qantara El Sharkiya (Fig. 2).

1.4. NATURAL VEGETATION

Natural vegetation growth is encountered around the marshes, Lakes and the lee side of sand dunes. In general, vegetation belongs to two major types, namely short shrubs and taller trees. The shortest shrubs are haphazardly distributed on the surface of the eolian sand, while the taller trees such as tamarex and palm trees are concentrated around the marshes and lakes.

1.5. DRAINAGE

The western side of the Suez Canal Zone is dissected by numerous drainage lines, including some pronounced valleys (wadis) which drain eastward to the Gulf of Suez and the Bitter Lakes. On this side of the Suez Canala, drainage lines are nearly concentrated in the hilly area south of El Devreswar. On the eastern side of the Canal, however, drainage lines are nearly absent except in the area between the Little Bitter Lake and the Gulf of Suez.

2. SURFACE GEOLOGIC ENVIRONMENT OF THE SUEZ CANAL ZONE

The Suez Canal Zone is covered by sedimentary rocks which belong to the Cretaceous, Middle Eocene, Late Eocene, Oligocene, Early Miocene, Middle Miocene, Late Miocene and Pleistocene-Holocene ages. The following is a general outline of the surface geology of the zone under consideration as given by El Shazly et al. [3] and illustrated on the geological map of the zone (Fig. 2).

2.2. CRETACEOUS SEDIMENTS

The Cretaceous sediments in the investigated Suez Canal Zone belong mainly to the Late Cretaceous and partly to the top od the Early Cretaceous. These are exposed in the Gebel Ataqa and Gebel shabrawet areas (Fig. 2). In the former area these sediments are composed mainly of thick, apparently unfossiliferous gypseous marl with variegated caly and limestone bands. In the latter area they are generally constituted of limestone and marl.

2.3. MIDDLE EOCENE SEDIMENTS

These are represented by the Khaboba Formation which is exposed in Gebel Ataqa and Gebel Gineifa areas (Fig. 2). In the first area this formation is composed mainly of limestone beds which are hard massive, white, occasionally dolomitic and sandy, especially in the lower part. In the Gebel Gineifa area, however, the formation in question is mainly composed of thickly bedded limestone which is white to light grey and occasionally dolomitic.

2.4. LATE EOCENE SEDIMENTS

These are represented by the Tanka Formation which is of limited occurrence in the Suez Canal Zone. In the Gebel Ataqa area this formation is composed mainly of grit, marl, sandy limestone, sandstone and conglomerates, while in the Gebel Gineifa area, it is mainly composed of

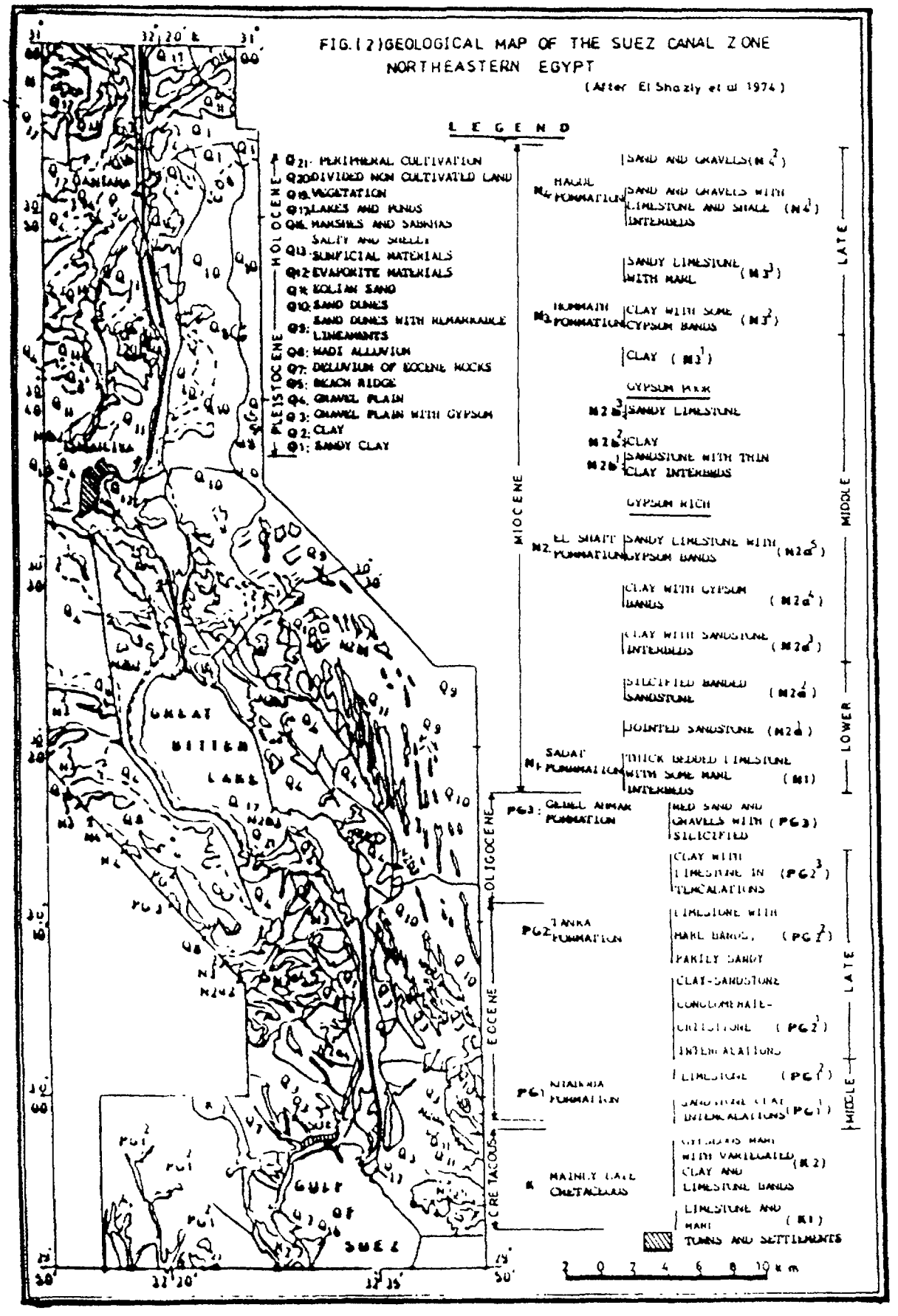

FIG. 2. Geological map of the Suez Canal Zone Northeastern Egypt.

fossiliferous limestone and clay intercalations. The Tanka Formation covers different horizons of the middle rock indicating an unconformable relation between the Late and Middle Eocene.

2.5. OLIGOCENE SEDIMENTS

These sediments are represented in the Suez Canal Zone by Gebel Ahmar Formation which is of wide distribution in the Gebel Geneifa area (Fig. 2). It overlies the Late Eocene sediments with a remarkable unconformity and occupies the low lands in most cases. This formation is composed mainly of dark brown gravels and ill-sorted varicoloured sand with the occasional presence of cross bedded sandstone and silicified wood.

2.6. EARLY MIOCENE SEDIMENTS

The Early Miocene sediments in the Suez Canal Zone are represented by the El Sadat Formation which has been recorded in the El Sadat Locality in the Gebel Ataq area. It is mainly composed of thickly bedded limestone with some marl interbeds. In the Gebel Gineifa area, the Early Miocene sediments consist mainly of limestone with sandstone and gypseous clay interbeds. In this area, these sediments unconformably overlie the Oligocene sand and gravels, while in the El Sadat Locality they lie on different levels of the Middle and Late Eocene sediments. The Early Miocene sediments are not exposed in other parts of the studied Suez Canal Zone.

2.7. MIDDLE MIOCENE SEDIMENTS

These sediments are classified in the zone under investigation into El Shatt Formation and Hommath Formation. The sedimentary units which belong to the El Shall Formation are widely spread in the studied area, and are classified in two types; gypsum-rich and gypsum-poor sediments. The former are generally exposed to the east of the Gulf of Suez and the El Shatt area (Fig. 2). They include essentially sandstone, clay, limestone and gypsum. On the other hand the gypsum-poor sediments are exposed to the east of the Bitter Lakes, the El Devreswar and El Ismailya areas (Fig. 2) and consist of sand and sandstone, clay, limestone and gypsum.

The Hommath Formation exposed in Wadi Hommath, El Sadat Locality, Gebel Ataqa area, is composed of clay, limestone, grit and marl beds, and unconformably overlies the Early Miocene Sediments.

2.8. LATE MIOCENE SEDIMENTS

They are represented by the Hagul Formation which is exposed in some parts of Wadi Hagul and in the Gebel Gineifa areas (Fig. 2). It consists essentially of non-marine sediments, flint and gravels, and some sandy limestone. Moreover, some silicified wood is recorded in these sediments.

2.9. PLEISTOCENE - HOLOCENE SEDIMENTS

The Quaternary sediments cover a considerable part of the Suez Canal Zone. They are composed mainly of sandy clay and clay around the marshes and sabakhas, gravel and without gypsum, beach ridges, beach sand, deluvium of Eocene rocks, wadi alluvium,sand dunes, eolian sand, evaporitic surficial material, salty and shelly surficial material, and salt crust.

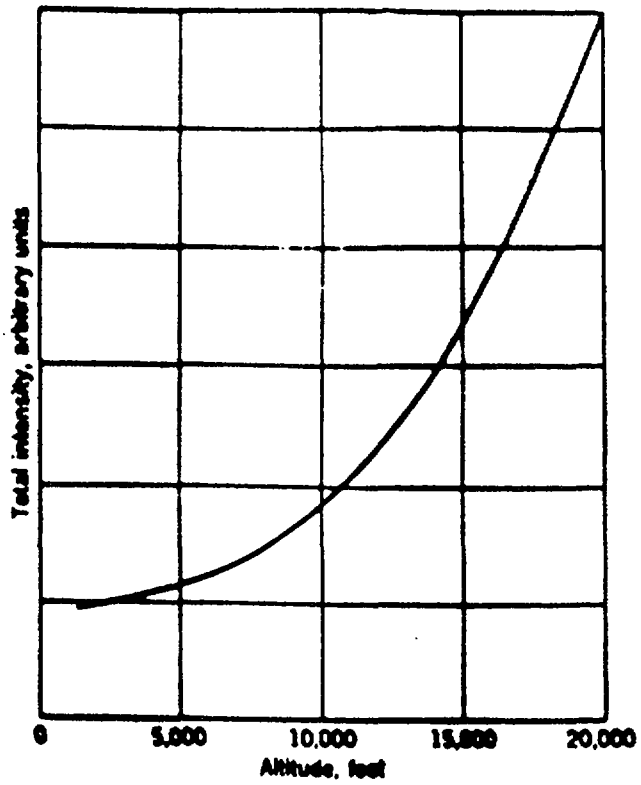

FIG. 3. Total cosmic-ray intensity, plotted as a function of barometric altitude above sea level.

3. ENVIRONMENTAL AERORADIOACTIVITY SURVEY OF THE SUEZ CANAL ZONE

The Suez Canal Zone has been aeroradiometrically surveyed by the airborne exploration group of the Nuclear Materials Authority. This survey covers an area of about 2500 km^2 extending from the apex of the Golf of Suarez to the south and to the Qantara City to the north.

The survey was made using a continuous-recording gamma ray scintillation detection equipment, type ARS-2, installed in an Antonoff-II aircraft. The flight altitude has been kept at a ground clearance of 50 m approximately and the flight traverses at one km apart being oriented mostly in a NE-SW direction. This survey was flown at an average aircraft speed of 170 m/h. The sensitivity of the scintillation equipment calibrated by a radium standard source reached about 180 count/second/one micro Roentgen/hour at one meter (C/S/μ/R/h) or 22 count/second/one millirem/year, for the total count. The registered radiations were compensated for the changes in elevation by a built-in automatic compensating circuit to reduce the obtained aeroradiometric measurement to the ground level (El Shazly et al., 1975).

3.1. ANALYSIS OF THE DETECTED GAMMA RAY FLUX

The gamma ray flux measured at the survey altitude is of a complicated nature and consists mainly of three principal components: (1) gamma ray activity from the three naturally occurring radioelements, potassium 40, uranium 238 and thorium 232, distributed in the surficial layer of the ground and their daughter products that decay by gamma ray emission, (2) gamma ray activity originating from radionuclides in the atmosphere (which are mostly radon-222 daughter products), radioactivity in the aircraft itself and in the instrument materials, as well as (3) cosmic-ray activity which is of particular interest in the environmental radiometric survey. The latter two components are referred to as the residual duration field or, better, the residual background.

Gamma radiation coming from the earth's surface (terrestrial radiation) attenuates fairly rapidly with growing flight attitude (Fig. 3) where it drops to immeasurable values at 600-700 m altitude. With further increase of altitude, the influence of cosmic radiation increases sharply. At the inflection point, the observed region of minimum values corresponds to the magnitude of the "residual background". It is necessary to determine the contribution of the combined effect of both the cosmic and atmospheric gamma radiation to the measured gamma ray flux in order to avoid interference with the aerial measurements of terrestrial radiations. In that regard, it is worth mentioning that the intensity of the cosmic-ray activity is a function of the geomagnetic latitude. It reaches its minimum intensity near the equator and increases gradually northward and southward to reach the maximum intensity around the northern and southern magnetic poles (Fig. 4).

3.2. DATA REDUCTION AND PRESENTATION

Regarding the present survey of the Suez Canal Zone, the intensity of the residual background radioactivity was estimated as 16 millirem/year. It has been determined by flying twice daily at an altitude of 600 m above ground level, and is assumed to be fairly uniform and constant in the geomagnetic latitude of the area under consideration. This value has been subtracted from the registered total radioactivity. Net aeroradiometric measurements were reduced to ground level using a linear reduction coefficient. These reduced data were finally presented in the form of an isorad contour map at a scale 1:100,000 with contour interval 0.5 micro Roentgen/hour. A new version of this map (Fig. 5) at the same scale was prepared but the isorad contours were presented in units of millirems/year.

4. SCOPE AND OBJECTIVE OF THE STUDY

The present study deals essentially with the establishment of the environmental aerial radioactivity levels in the Suez Canal Zone. This work will provide basic information that can be used as a reference to detect and determine the amount and extent of any possible future variations in the natural radioactivity levels in the studied zone that might result from nuclear testing or accidents involving release of nuclear radiations and fallout of nuclear fission products that might affect both the terrestrial and atmospheric radioactivity fields. In addition, this study will be of direct assistance in prospecting for radioactive minerals in the investigated zone as well as geological mapping purposes.

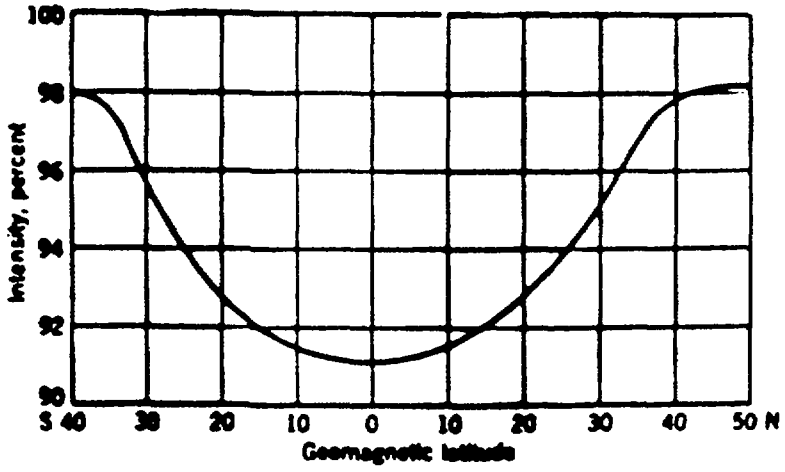

FIG. 4. Total cosmic-ray intensity at sea level, plotted as a function of geo-magnetic latitude. The vertical scale is exaggerated. Modified after Compton and Turner.

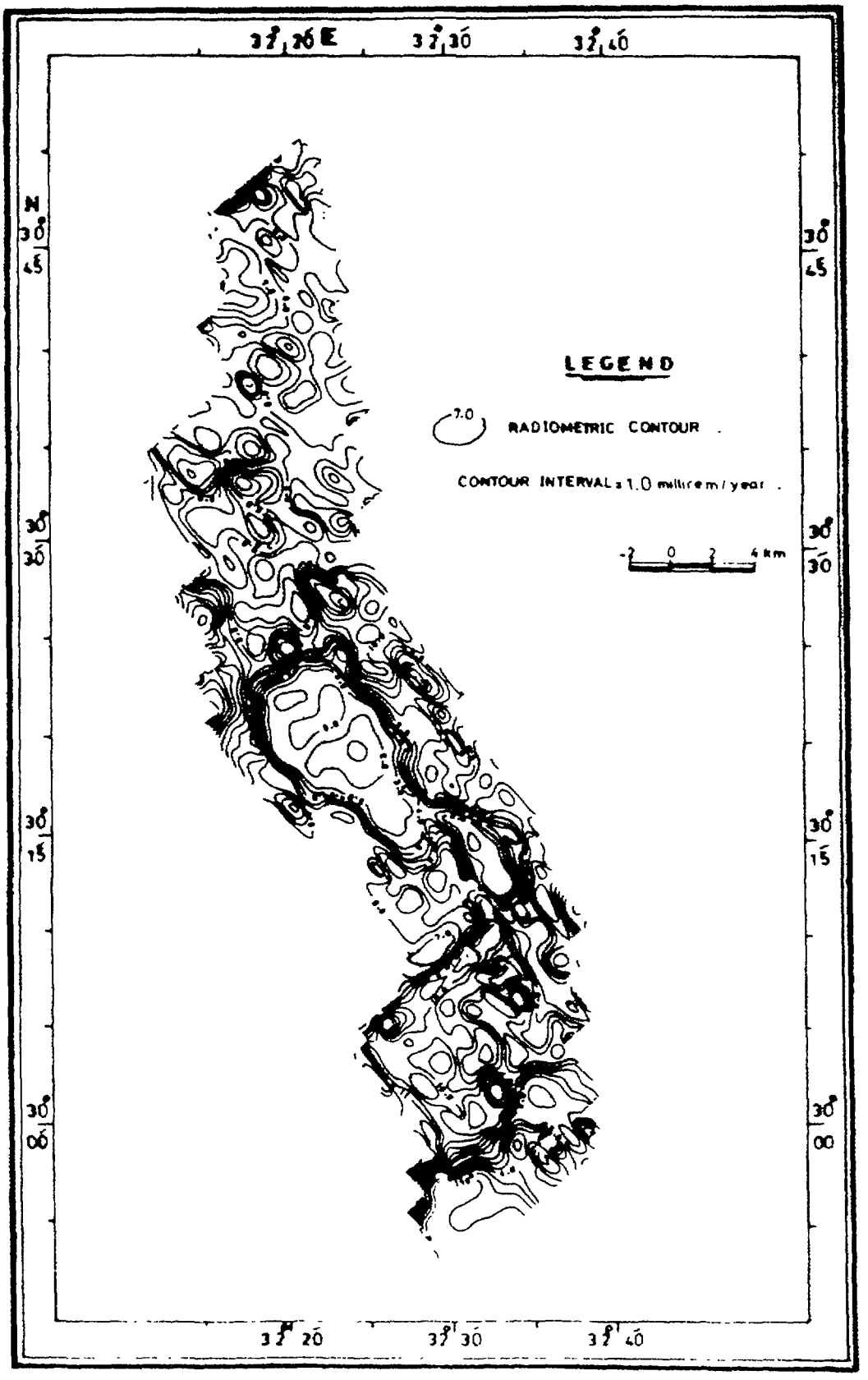

FIG. 5. Environmental total count aeroradiometric contour map of the Suez Canal Zone, Egypt.

5. STATISTICAL ANALYSIS OF THE ENVIRONMENTAL AERORADIOMETRIC MEASUREMENTS IN THE SUEZ CANAL ZONE

Aerial radiometric measurements registered over the Suez Canal Zone have been subjected to conventional statistical methods of analysis in order to facilitate the manipulation of the large volume of the radiometric data and enhance their interpretation. In that regard, the digital aeroradiometric measurements of the individual rock units as well as water surfaces were fed into an IBM, PC/AT Micronet computer. Statistical computations were performed using a software package namely, "STATGRAPHICS". Statistical treatment of the data was executed in the following sequence:

(1) Organization of the recorded radiometric data for each surveyed unit in the form of frequency histogram in order to facilitate the recognition of possible natural grouping or populations within the data set.

(2) Calculation of the statistical characteristics of the distribution of radioactivity in each of the units under consideration. These include measures of central tendency of the data namely: the range, arithmetic mean (X), median (M) as well as measures of dispersion of the data, standard deviation (Sd) and coefficient of variability (CV) which measures the relative dispersion with respect to the mean of the distribution. Table I summarizes the computed statistical characteristics, mentioned above of the various radiometric units. The background environmental radioactivity level of each unit was designated as all values failing within the limits of X + 3S. Radiometric measurements beyond these limits were excluded and were considered anomalous.

(3) The homogeneity of the distribution of aeroradiometric data of each environmental unit was tested numerically by the application of the chi-squared test (χ^2-test), and using the statistical tables [2]. Results of application of this test are presented in Table II.

TABLE I. COMPUTED STATISTICAL CHARACTERISTICS OF THE DISTRIBUTION OF TOTAL RADIOACTIVITY IN THE INTERPRETED ENVIRONMENTAL AERORADIOMETRIC UNITS IN THE SUEZ CANAL ZONE

Rad unit	Min	Max	Range	X	M	S	X + 3S
Q (1,2)	6.25	12.08	5.83	8.33	8.33	1.33	4.25 - 12.25
Q (3,4)	3.75	14.16	10.41	9.03	8.91	1.81	3.63 - 14.43
Q (9,10,11)	4.17	11.66	7.50	8.18	8.33	1.29	1.72 - 14.64
Q (16)	4.58	12.50	7.91	7.83	7.91	1.75	2.58 - 13.08
Q (17,18)	0.83	4.58	3.75	2.58	2.50	0.83	0.03 - 5.16
Q (19,20,21)	4.58	14.16	9.58	8.58	8.33	1.80	3.19 - 14.07
N (2)	5.41	15.41	10.00	9.87	10.00	1.80	4.44 - 15.29

Values of all statistical characteristics are given in units of millirems/year

Min.: minimum
Max.: maximum
Rad.: radiometric
X : arithmetic mean
M : median
S : standard deviation

TABLE II. RESULTS OF APPLICATION OF THE CHI-SQUARED TEST TO THE ENVIRONMENTAL AERORADIOMETRIC UNITS IN THE SUEZ CANAL ZONE

Rad unit	χ^2-test values		Type of distribution
	observed	theoretical	
Q 1,2	1.75	9.49	normal
Q 3,4	17.45	25.00	normal
Q 9,10,11	18.90	27.59	normal
Q 16	3.99	12.59	normal
Q 17,18	13.68	26.30	normal
Q 19,20,21	6.99	26.30	normal
N 2	10.33	22.36	normal

N.B. Theoretical χ^2-test values are at the 95% level of significance.

6. DISCUSSION AND INTERPRETATION

Statistical analysis of the natural gamma ray measurements registered over the Suez Canal Zone indicated that the terrestrial background radioactivity levels (expressed as X + 3S in Table I) in the surveyed zone oscillate between 0.03 - 5.16 to 4.44 - 15.29 millirem/year with grand mean background radioactivity of 7.76 millirem/year. The established background gamma-radiation levels (Table I) are consistent with the nature of the geologic environment of the zone (Fig. 1).

Frequency analysis as well as the homogeneity test (chi-square test) were applied to the aeroradiometric measurements of the surface geological units of similar lithological composition, taken collectively. These units are presented on the surface geological map of the investigated zone (Fig. 2). This statistical treatment has resulted in the construction of the environmental terrestrial aeroradioactivity unit map of the Suez Canal Zone (Fig. 6). Each of the inferred units exhibits a normally distributed aeroradiometric measurements as evidenced from the good fitting between the frequency distribution curve of the observed radiometric data set and the corresponding Gaussian (normal) distribution curve of each of the interpreted radiometric units (Figs 7 and 8). Table I presents a brief description of the different lithologies (lithological units) as well as their computed statistical characteristics in units as well as their computed statistical characteristics in units of millirem per year. A close review of these values illustrates that the investigated area is characterized in general by distinct low levels of environmental background radioactivity. However, it is worth to note that the lowest background radioactivity level in the surveyed Suez Canal Zone (0.03 - 5.16 millirem/year) was recorded mainly over the Great and Little Bitter lakes in addition to some restricted shallow water bodies located to the north of the Gulf of Suez (Fig. 6). On the other hand, the highest background radioactivity level (4.44-15.29 millirem/year) was recorded over the El Shatt Formation (of Middle Miocene age) which is mainly composed of sandstone, clay, limestone and gypsum (Fig. 6).

Here follows a detailed discussion of the results obtained from the statistical analysis of the environmental aeroradiometric measurements made over the various geologic units in the Suez Canal Zone starting from the youngest:

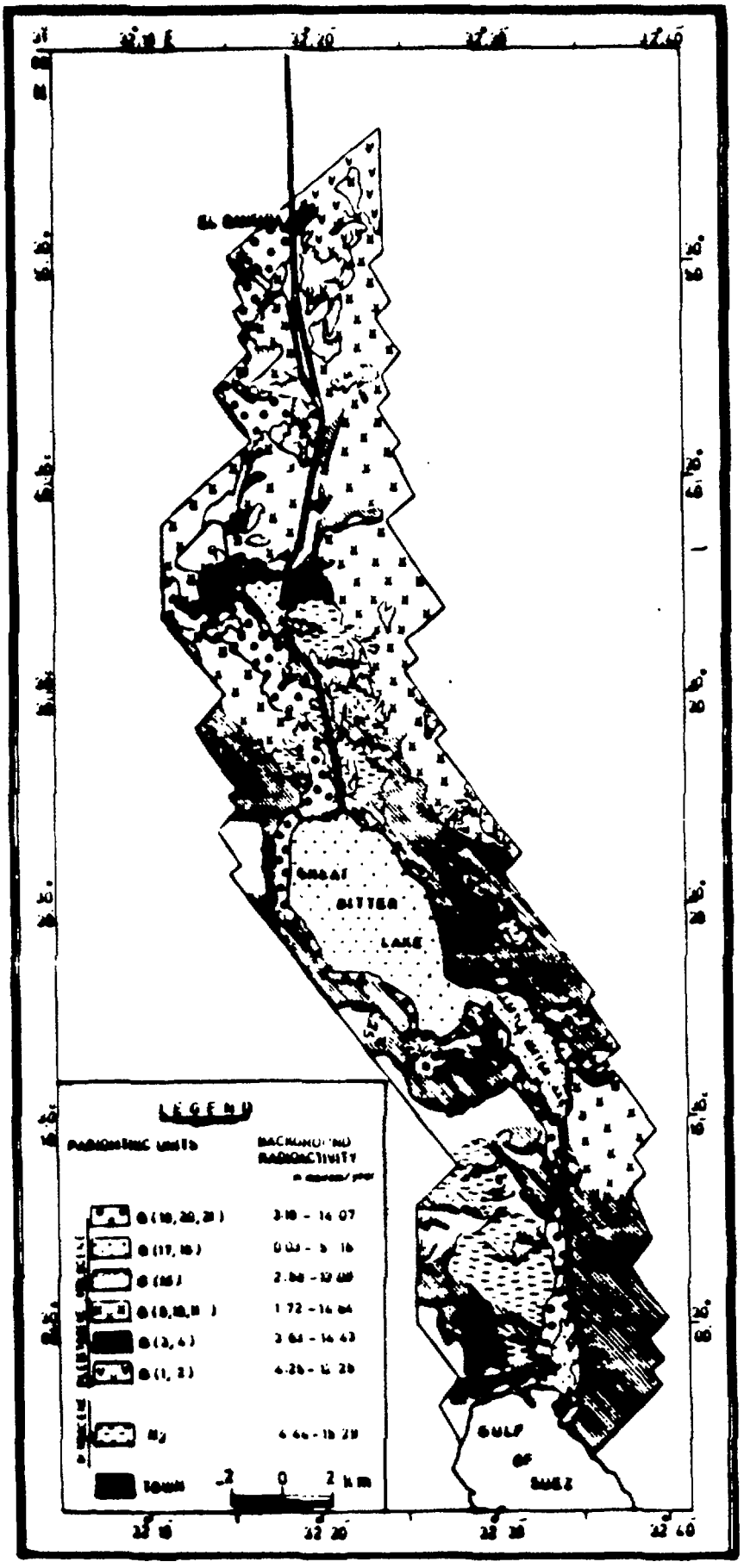

FIG. 6. Interpreted environmental aeroradiometric unit map of the Suez Canal Zone, Egypt.

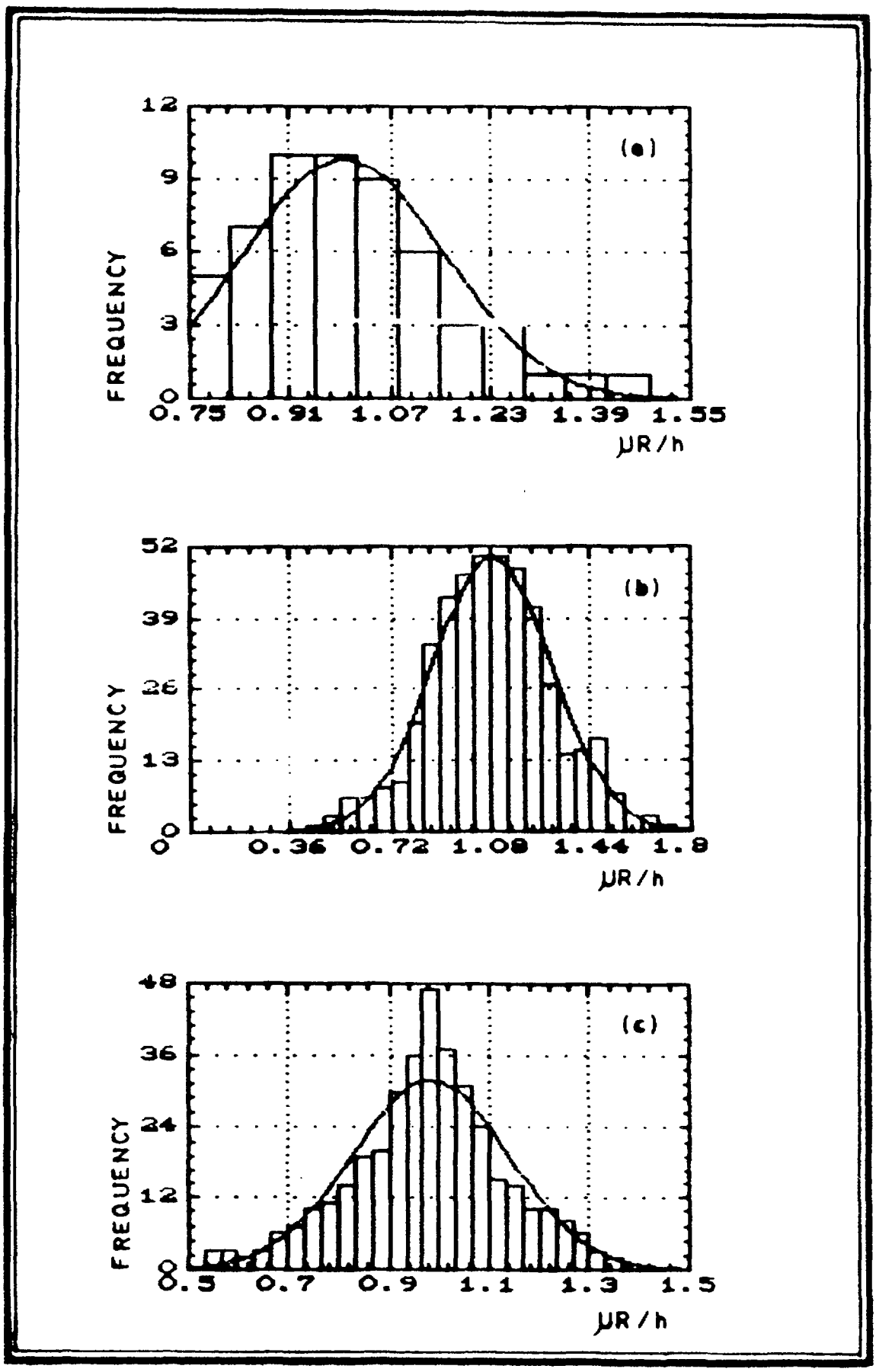

FIG. 7. Frequency histograms of aeroradioactivity data with fitted theoretical curves of the interpreted radiometric units (a) Q 1,2 (b) Q 3,4, and (c) Q 9, 10, 11.

6.1. PLEISTOCENE - HOLOCENE

Statistical treatment of the aeroradiometric measurements acquired over the surface lithological units related to the Pleistocene-Holocene epochs (Plate I) has enabled the recognition and delineation of six environmental aeroradiometric units (Fig. 6.). Each of these units has its own background gamma-radiation level (Table I). The outlines units, however, showed some interfering values of radioactivity levels. The lowest background radioactivity level (0.03 - 5.16) was recorded over lakes and ponds as well as shallow water bodies (unit 17, 18, Table I), whereas the highest background radiation level (3.63 - 14.43 millirem/year) was recorded over plains covered with gravel (unit 3, 4, Table I).

Among the interpreted environmental aeroradiometric units of the Pleistocene-Holocene epochs the lakes, ponds and shallow water bodies proved to have the lowest range (3.75 millirem/year), mean (2.58 millirem/year), median (2.50 millirem/year) and standard deviation (0.83 millirem/year). This may reflect the low abundance and the relatively higher degree of homogeneity of the distribution of radionuclides in such water environment of this radiometric unit. On the contrary, the gravel plains (unit Q3-4 Table I) showed the highest range (10.41 millirem/year), mean (9.03 millirem/year), median (8.91 millirem/year) and standard deviation (1.81 millirem/year). These figures give a quantitative estimate of the degree of dispersion of the values of the natural aeroradioactivity measurement around the mean background radioactivity of this unit. Such high degree of dispersion is a reflection of the high degree of heterogeneous distribution of radioelements in the environment. This may be attributed to the heterogeneities in the lithological composition of the source rocks from which these transported gravel were derived, and/or to the mode of deposition of these rocks during the last 2.5 million years.

6.2. MIOCENE (MIDDLE MIOCENE)

Statistical analysis of the aeroradiometric measurements made over the Middle Miocene outcrops demonstrated that the El Shatt Formation which is mainly composed of sandstone, limestone and gypsum can be regarded as representing a radiometric unit (Fig. 6) of normal pattern of radioactivity distribution (Fig. 5d). Besides, these sediments displayed the highest natural background gamma-radiation level, median and mean in the studied Suez Canal Zone (4.44-15.29, 10 and 9.87 millirem/year respectively). On the other hand, it was observed that this radiometric unit showed a remarkably high range and standard deviation values (10 and 1.B millirem/year respectively). This may reflect the heterogeneous lithological composition of the El Shatt Formation, which may have taken up to 19 million years of deposition.

7. CONCLUSION AND RECOMMENDATION

From the environmental point of view, the established background terrestrial gamma-radiation levels of the various rock types, soils and water bodies in the Suez Canal Zone provided the necessary basic information that can be used as a reference to determine the amount and extent of any possible future variations in the environmental radioactivity of he area, that might result either from accidents involving release of nuclear radiations and radioactive contamination of the ground or introduction of radioactive materials to the area (waste, leakage or fallout), especially taking into consideration that the Suez Canal is traversed by ships that may carry, and/or run by, nuclear materials. Consequently, a periodical airborne radiometric surveying for the entire Suez Canal Zone is highly recommended for monitoring changes in the environmental radiation levels in this zone.

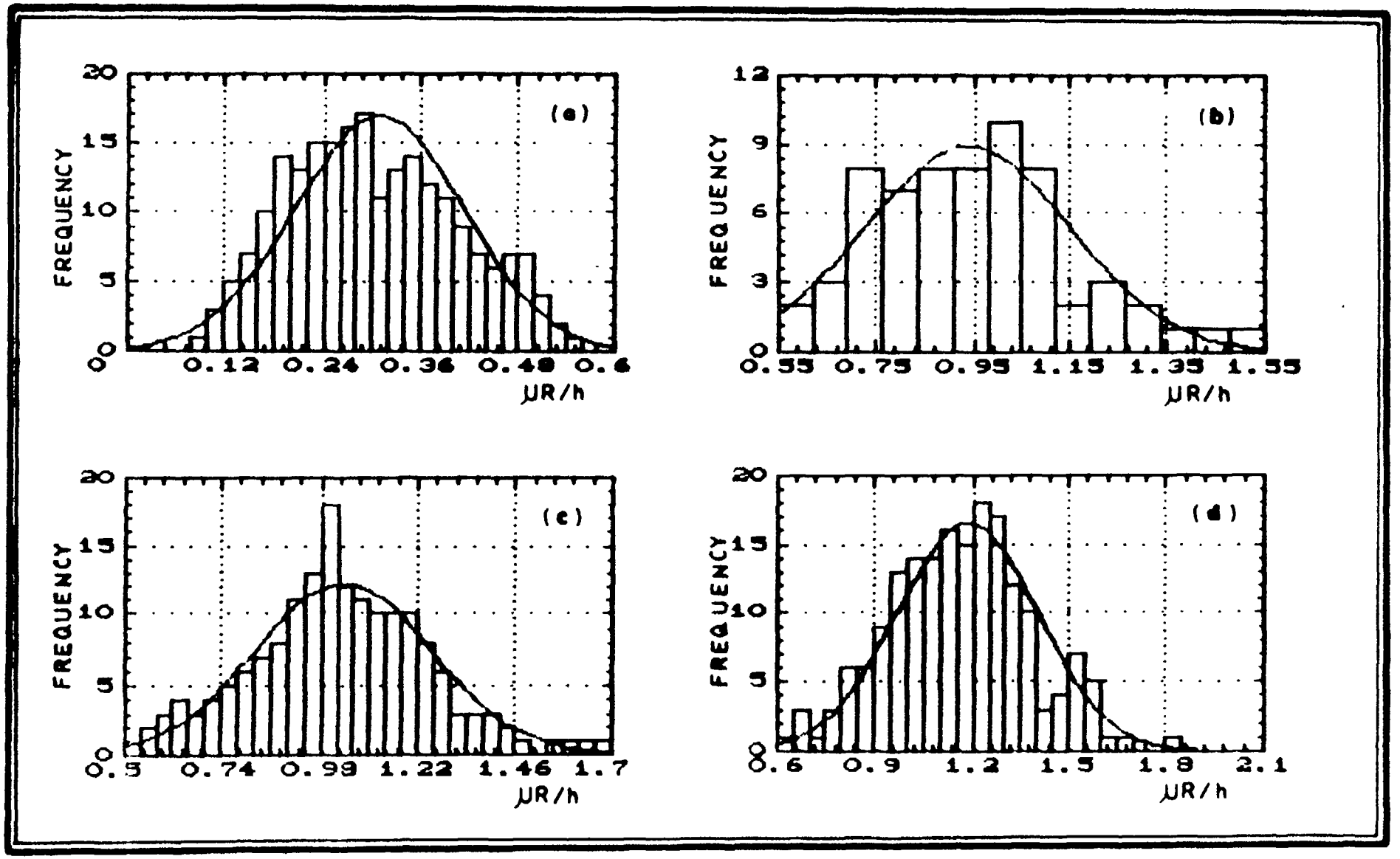

FIG. 8. Frequency histograms of aeroradioactivity data with fitted theoretical curves of the interpreted radiometric units (a) Q 16, (b) Q 17, 18 (c) Q 19, 20, 21 and N 2.

REFERENCES

[1] ADAMS L., The natural radiation environment, Rice University Semicentennial Publications (1965).

[2] CLARK G.M. and CROOK D., A basic course in statistics, English Language Society/Edward Arnold (publishers) (1988).

[3] EL SHAZLY E.M., ABDEL HADY, MESHREF W.M., AMMAR A.A., MELEIK M.L., SALMAN A.B., MORSEY M.A., EL RAKAIBY M.M., EL AASSY I.E.E. and KAMEL A.F., Geological and geophysical investigations of the Suez Canal Zone, Remote Sensing Research Project, Academy of Scientific Research and Technology (1975) 38p.

[4] INTERNATIONAL ATOMIC ENERGY AGENCY, Radiometric reporting methods and calibration in uranium exploration, Technical Reports Series No. 174, Vienna, Austria (1976) 57 p.

[5] INTERNATIONAL ATOMIC ENERGY AGENCY (IAEA), Gamma ray surveys in uranium exploration, Technical Reports Series No. 186, Vienna, Austria (1979) 90 p.

[6] RICHARD V. BLARICAN, Practical Geophysics for tte exploration geologist, Northwest Mining Association, USA (1980).

AGRIGEOCHEMICAL MAPS FROM URANIUM EXPLORATION DATA

G. SANTOS, JR., N. GARCIA
Philippine Nuclear Research Institute, Quezon City, Philippines

Abstract

Trace element data (mainly Cu) obtained during the course of uranium geochemical exploration in Pangasinan province, Luzon were transformed or converted to reflect micronutrient copper distribution. The transformed copper data (their range of values) were plotted as contours in the agrigeochemical map of copper. Soil samples were collected from different parts of the province and were analyzed for copper. The copper analysis results of these soil samples, i.e. range of values were compared with those plotted in the agrigeochemical map. The comparison indicates close agreement between the soil samples and the copper agrigeochemical map with the map having generally slightly higher copper range values than those found in the soil. The high copper range values also show possible extent of copper mine tails siltation in central Pangasinan. It is suggested that the map could be used as an interim guide on the copper micronutrient level in Pangasinan province as copper is one of the essential micronutrients needed for healthy plant growth.

1. INTRODUCTION

As part of the Philippine Nuclear Power Programme, the former Philippine Atomic Energy Commission (PAEC) embarked on a nationwide uranium reconnaissance exploration project in the late 1970s. Considerable geochemical data were accumulated as a result of the exploration in the different parts of the country. The surveys were patterned after the work of Tauchid et al. (1978). The geochemical analysis used the method of Smith and Lynch [12]. Santos et al. (1989) recognized the potential usefulness of the geochemical data in agriculture.

A study on micronutrients in soils of the entire Philippines was made by Agustin et al. [1], however, Santos et al. (1989) noted that the study did not adequately cover large areas. They further observed that the geochemical values obtained from stream sediments could be converted or transformed to reflect the micronutrient element distribution in the soil. This conversion was done by getting the soil-sediment background concentration ratio. By using this ratio, stream sediment geochemical maps could be converted to agrigeochemical maps. These maps indicate the amount of trace elements that could be available to the plant.

In agriculture it is essential to know the areas which have anomalously high or low trace element concentrations especially the essential micronutrients such as zinc, copper, manganese and iron, among others. These micronutrients in soil could significantly affect the growth of plants. According to Castro [4], there are about 5 000 sq km in the Philippines which have soils deficient in zinc. The locations of the zinc-deficient areas, however, are not clear. Iron toxicity in soil is another problem in agricultural production as noted by Benckiser et al. [3]. According to them, this problem is found not only in the Philippines but in other Asian countries as well. Their studies indicate that rice affected by iron toxicity develop poor root system. Of course, other factors such as acidity, alkalinity, salinity and excess organic matter, in addition to iron toxicity could hinder plant growth. Benckiser et al. observed that iron-rich soil could give rise to iron toxicity if phosphorous, potassium, calcium and zinc are deficient. According to Ponnamperuma [7] and Benckiser et al. [3], excess or deficiency in certain minor elements in soil could lead to nutritional disorders in rice plants. The observations of these investigators suggest that the presence of excessive concentrations of an element in soil does not always result in element toxicity in plant. Rosales [8] suggests that application of zinc as zinc sulfate tends to increase rice yield.

The objective of this report is to describe an attempt to produce agrigeochemical maps of essential micronutients in Pangasinan, Luzon using the method developed by Santos et al. (1989). The method converts trace and minor element geochemical data obtained in uranium exploration survey to maps of essential micronutrients in soils.

The study area is located in Pangasinan province, Luzon covering less than 5 000 km^2. The region produces rice, corn, sugar cane, tomatoes and mangoes.

2. PROCEDURES

Geochemical concentration data of copper, zinc, manganese and iron in stream sediments collected from Pangasinan (Santos et al. [10]) were multiplied by a soil-stream sediment background ratio used by Santos et al. (1989). The ratio was obtained by deriving the background concentrations of the elements in the soils using the method developed at the International Rice Research Institute (IRRI) for zinc determination (Castro [4] and that of Smith and Lynch [12].

The IRRI method consists of adding a 10 g soil sample to 20 ml of 0.05N hydrochloric acid and shaking the mixture for 5 minutes. The mixture is then filtered and the filtrate is determined for Cu. Zn, Mn and Fe employing atomic absorption spectrophotometry (AAS). The Smith and Lynch method consists of digesting the soil sample in an acid mixture of 85X nitric acid and 15X hydrochloric acid. The filtrate was similarly analyzed for Cu, Zn, Mn, and Fe by AAS. The results were treated statistically to determine the background values using the method of Lepeltier (1969). Listed in Table I are the background values and ratios of the essential minor elements using the IRRI and the Smith and Lynch methods.

TABLE I. BACKGROUND CONCENTRATIONS (PPM) OF COPPER, ZINC, MANGANESE AND IRON USING THE IRRI AND THE SMITH AND LYNCH METHODS. (SANTOS ET AL., (1989).

Element	IRRI	Smith and Lynch (S & L)	IRRI/S & L
Copper	0.5	45	0.011
Zinc	0.8	50	0.016
Manganese	45	900	0.050
Iron	less than 1.4	3%	0.000047

The soil background concentration ratio of the elements is then multiplied with the respective concentration of these elements obtained in the stream sediments. The resulting values are considered to be the concentrations that are available for assimilation for plant growth.

3. SOIL VERIFICATION

Soil samples from different parts in Pangasinan were obtained from the different town agricultural officers and the office of the provincial agriculturist. Some samples were personally collected in the field. The samples were analyzed using the IRRI method.

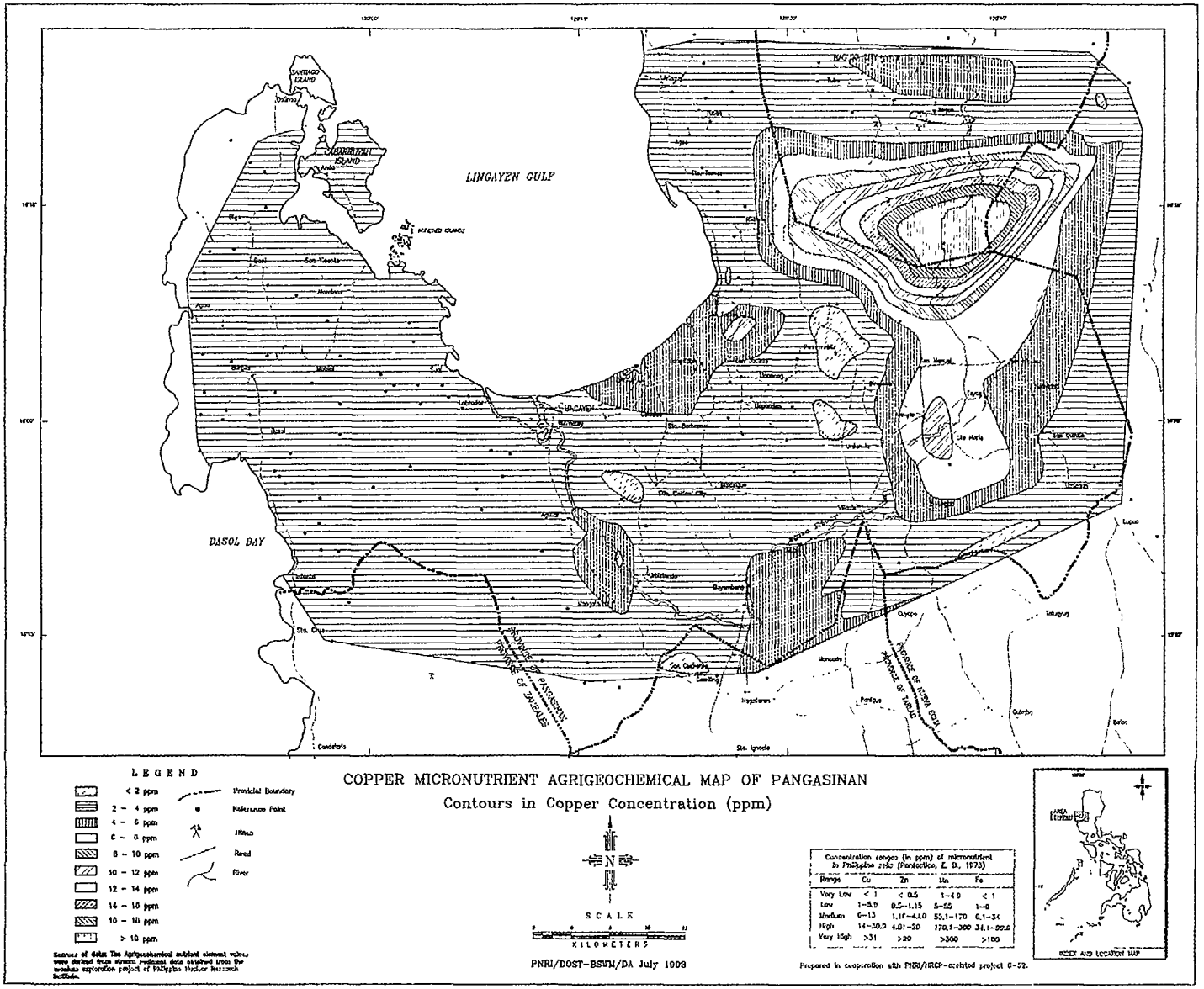

FIG. 1. Copper micronutient agrigeochemical map of Pangasinan.

1.3 PLOTTING OF SAMPLING POINTS

Before data processing, the stream sediment sampling points were re-plotted or relocated midway between the sediment sampling location and the headwater of the stream or midway between sampling points along the same stream. This was considered the better location to reflect the soil values of a drainage area.

In contrast, the work of Santos et al. (1989) did not include the relocation of the stream sediment sampling points before data processing which used the method of moving averages.

4. DATA PROCESSING

Computerized contour mapping of the converted values of copper, zinc, manganese and iron was performed using the Arc/Info mapping software which utilizes the method of moving averages. Map contouring was done in cooperation with the Soils Research and Development Center of the Bureau of Soils and Water Management (BSWM).

5. RESULTS AND DISCUSSIONS

Four preliminary agrigeochemical maps were produced. These were for copper, zinc, manganese and iron. However, in this report the copper map is considered in its final stage. As for the other three agrigeochemical maps, it is hoped that these maps when finalized will be reproduced, demonstrated and distributed to the provincial agriculturist and the different municipal or town agricultural officers. The maps of zinc, manganese and iron are still being reviewed for slight modifications. The contours plotted in the map are ranges of element concentrations, such that any given point in the map could be easily identified as belonging to a certain range of possible values.

Shown in Fig. 1 is the copper micronutrient agrigeochemical map of Pangasinan. The high copper concentration in the northern part is due mainly to the presence of mineralized area enriched in copper (Philex Mines).

This map as compared to the contour map of Santos et al. (1989) is deemed to be more understandable to the municipal agricultural officers and farmer endusers. This map also includes a range of class limits for Philippine soils. These range of class limits by Pantastico [6] is classified as very low, low, medium, high and very high. See Table II.

TABLE II. THE CONCENTRATION RANGES (IN PPM) OF MICRONUTRIENT IN PHILIPPINE SOILS [6].

Range	Cu	Zn	Mn	Fe
Very low	<1	<0.5	1 - 4.9	<1
Low	1 - 5.9	0.5 - 1.15	5 - 55	1 - 6
Medium	6 - 13	1.16 - 4.80	55.1 - 170	6.1 - 34
High	14 - 30.9	4.81 - 20	170.1 - 300	34.1 - 99.9
Very high	>31	>20	>300	>100

Agustin et al. [1] on the other hand categorized the micronutrients using diethelenetriaminepentaacetic acid (DTPA) as extractant. The different categories are: well below

average, below average, average, above average and well above average. Agustin et al. (1988) and Sillanpaa [11] suggested that critical deficiency limit for several plant crops using ethylenediaminetetraacetic acid (EDTA) extractable micronutrients are as follows: Zn -0.5 ppm, Cu -0.2 ppm, Fe -4.5 ppm and Mn -1.0 ppm.

TABLE III. RESULTS OF MICRONUTRIENT ANALYSIS (SOIL RANGE VALUE) OF SOIL COMPARED TO AGRIGEOCHEMICAL MAP RANGE VALUES FOR COPPER OBTAINED FROM DIFFERENT TOWNS IN PANGASINAN.

Location	Map Range Value	Soil Range Value
Aguilar	Low - Medium	Very low
Alcala	Low - Medium	Very low
Asingan	Medium	Very low
Alaminos	Low	Very low
Bayambang	Low - Medium	Medium
Balungao	Low - Medium	Very low
Binmaley	Low	Very low
Bugallon	Low	Very low
Calasiao	Low	Very low
Dagupan	Medium	Very low
Infanta	Low	Very low
Labrador	Low	Very low
Lingayen	Medium	Low
Mangaldan	Low	Very low
Mabini	Low	Very low
Malasiqui	Low	Very low
Manaoag	Low	Very low
Mangatarem	Low	Very low
Natividad	Medium	Very low
Pozorrubio	Very low	Very low
Rosales	Low - Medium	Very low
San Carlos	Low	Very low
San Jacinto	Low - Medium	Very low
San Fabian	Low - Medium	Very low
San Manuel	Medium	Medium
San Nicolas	Medium	Very low
Sta. Barbara	Low	Very low
San Quintin	Low	Very low
Sta. Maria	Medium	Very low
Sual	Low	Low
Tayug	Low	Very low
Villasis	Low	Very low
Umingan	Low	Very low
Urdaneta	Very low	Very low
Urbistondo	Low	Very low

The copper results of the soil verification analysis are closely in agreement with the copper agrigeochemical map produced from geochemical data. The stream sediments which are considered to contain more micronutrients than the soil, tend to give a higher copper range than the soil samples. That is, there is an apparent trend that the "Low" range values in the map correspond to the "Very Low" range values in the soils. Although the work of Agustin et al. [1] did not cover all of

Pangasinan, there is also some general agreement between the micronutrient map of Pangasinan for copper obtained by Agustin et al. [1] and the present work. For instance in western Pangasinan and certain areas in southeastern Pangasinan the range of "Below Average" corresponds to the "Low" range in the present work. However, there are differences between the Agustin map and the present work in the copper distribution for the central part of Pangasinan. This suggests that the map could be used as a guide for predicting copper micronutrient concenration in soil in Pangasinan. The soil analyses for Zn, Mn and Fe are also consistent with their values in the preliminary agrigeochemical maps of the said micronutrients which are not included in this report. The copper map clearly shows the possible extent of mine tails siltation in central Pangasinan.

It is interesting to note that the central part is drained by Agno River and its tributaries which have been affected by copper mine tails siltation (NEPC and NCTAD, 1974).

6. CONCLUSION

We have demonstrated that the conversion or transformation of copper data obtained from uranium geochemical exploration to micronutrient copper agrigeochemical map of Pangasinan has potential application in agriculture. A comparison of the soil analyses from different parts of the Province show close agreement with those range of values in the agrigeochemical map. However, the copper agrigeochemical map tends to exhibit slightly higher values than those obtained in the soils. The possible extent of copper mine tailings siltation in Pangasinan is clearly evident in the map.

REFERENCES

[1] AGUSTIN, L.C., AGNES, P.S. Jr., ANGELES, E.L. and AMURAO, G.G., Micronutrient status in some Philippine soils. Part 1. Special Issue, Soils and Water Technical Bull., Bu. of Soils and Water Management (1988) pp. 196.

[2] Arc/Info, 1979. TIN Users Guide, Environmental Systems Research Institute, Inc., Redlands, Calif.

[3] BENCKISER, G., ATTOIR, J., SANTIAGO, S. and WATANABE, 1., Physicochemical characterization of iron-toxic soils in some Asian countries. IRRI Res. Paper Series No. 85 (1982) 11 p.

[4] CASTRO, R.U., Zinc deficiency in rice: a review of research at the International Rice Research Institute, IRRI Research Paper Series, no. 9 (1977) 18 p.

[5] NATIONAL ENVIRONMENTAL PROTECTION COUNCIL AND NATIONAL COUNCIL ON INTEGRATED AREA DEVELOPMENT, Ecological Profile of Pangasinan. Q.C. (1984).

[6] PANTASTICO, E.B., SISTONA, G.M., DE PADUA, L.S. and NERY, V.S., Trace element status of Philippine soils and its relation to crop production. NRCP Bull., V. 28. No. 4 (1973).

[7] PONNAMPERUMA, F.N., Behavior of minor elements in paddy soils. IRRI Res. Paper Series No. 5, (1977) 15 p.

[8] ROSALES, C.M., The efficiency of fertilizer-zinc by rice grown under wetland condition. Soils Technical Bull. No. 2, Bu. of Soils, Manila (1979).

[9] SANTOS, G. JR. and ILAGAN, L., Uranium geochemical mapping in the Philippines: Explanatory text of the regional reconnaissance geochemistry of Northwestern Luzon and Samar. PAEC Tech. Report (1) IB 85003 (1985).

[10] SANTOS, G. JR., BERNIDO, C. and FERNANDEZ, L., Trace element content of stream sediments in Pangasinan. NSTA Techno. J., v. 11, no. 4 (1986) pp. 30-42.

[11] SILLANPAA, M., Micronutrients and the nutrient status of soils. FAO Soil Bull., v. 48, FAO, ROME (1987) 444 p.
[12] SMITH, A Y., LYNCH, J.J., Field and laboratory methods used by the Geological Survey in Canada in geochemical surveys, No. 11, Uranium in soil stream sediments and water. Surv. Can. Paper 69-40 (1969).
[13] TAUCHID, M., Reconnaissance geochemical survey for uranium deposit in Samar, Report to the Government of the Republic of the Philippines: Unpublished (1978).

ACKNOWLEDGEMENT

We are grateful to Dr. Nora Inchiong, Bureau of Soils and Water ffanagement (BSWM) for advice and encouraging us in the preparation of micronutrient maps as well as to Mr. J. Mundin, Pangasinan Provincial Agriculturist and his staff for assistance in soil sample collection. Thanks are due to R.N, Gonzales, E. Menguito and N. Concepcion of Integrated Soil Resources Information Services in the computer map production. We want to express our thanks to Director C.R. Aleta, PNRI and Director G.N. Alcasid. Jr. for their kind suppart. We are thankful to the AAS group, L. Fernandez, M. Castillo and E. Tabora. Thanks are due to C. Petrache and N. Bugaoisan for computer assistance. This work was partly supported by NRCP-assisted project G-52.

RADIATION DETECTION OF BURIED SHIELDED SOURCES IN VEHICLES LOADED WITH SCRAP STEEL

J.R. COX
Exploranium G.S. Ltd., Bolton, Ontario, Canada

Abstract

There are about 600 000 registered radioactive sources in North America alone. During the past 10 years, there have been a number of documented accidents caused by discarded sources. Some of these sources ended up as scrap material and found their way into steel furnaces. A system using a plastic (PVT) detector was successfully developed to detect sources that might be buried in vehicles loaded with scrap steel.

1. BACKGROUND

In 1983, Auburn Steel, New York accidentally loaded a shielded cobalt-60 source (estimated at 50 Ci) into a steel making furnace, and melted it. The accident was discovered almost immediately, but by the time that 150 tons of contaminated steel had been disposed of and the site cleared of radioactive debris, the clean up bill was over 10 million dollars.

In 1984 a steel plant in Juarez, Mexico melted another cobalt-60 source but unfortunately this was not discovered until 3 months later, when a load of contaminated construction steel tripped a detector on the Los Alamos test site. All the contaminated steel had to be recovered from across Northamerica and several buildings erected with radioactive steel had to be torn down, at an enormous cost.

In 1992 in Taiwan, a research worker brought a survey meter home to demonstrate simple radiometric principles to his son for school, and measured very high radiation readings in his apartment. He assumed that the instrument was defective but next day the instrument was tested and found to be functioning correctly. An investigation showed that the radiation was caused by structural steel imported from the USSR over 7 years ago and many buildings were torn down as a result of this incident, and medical assessments are in progress.

In the USA alone 3 large Cesium-137 sources were melted in the last 18 months and reports from Italy indicate 2 recent incidents there as well. In the last 10 years at least 7 serious accidents have occurred including one in Brazil which resulted in loss of life.

In Moscow more than 200 tons of steel was contaminated from an accident in 1989.

There is some evidence to show that in Northamerica alone there are over 600 000 registered sources and these include sources ranging from very large (200 Ci+ research sources to 1 mCi laboratory sources). Authorities such as the US-NRC admit to a list of over 15 missing sources in excess of 1 Curie!

The data (from Nuclear News) gives an idea of the scale of these incidents which seem to be averaging 5 a year since 1944. However it is not clear that the reporting method is accurate, as recent reports indicate a much higher rate.

As a result of these early accidents (1983/84) many us steel plants rushed to implement radiation protection on their incoming scrap using simple detection systems usually based on small detectors. The basic idea was that if the sources are that dangerous they must be easy to detect. Unfortunately buried shielded sources are heavily shielded by the scrap steel so emitted levels on the outside of the vehicle are very low (as will be shown shortly).

Source size is very variable but all sources are designed to similar safety guidelines, so to a first approximation the exposure rate on the outside of sources are similar.

This means that from a radiation detection viewpoint — all sources emit approximately the same "signature". This is not always the case as the use of over size shields is common (a 100 mCi source in a 1Ci shield), but in principle a system capable of detecting one type of source will have reasonable detection capabilities to the range of sources in use.

In 1985 a steel plant in Canada approached exploranium to see whether such protection was technically possible, and the balance of this paper describes the technical research into this matter and the results.

2. THE PROBLEM

In the majority of cases the furnace in these plants are 100-250 tonne capacity. An Atomic Energy of Canada research group investigated the problem in 1987 and computed the source size vs furnace size, to assess contamination limits. This data indicates that for Cobalt-60, a 60 mCi would contaminate a 250 tonne furnace. Other researchers indicate a very wide range of estimates, but it is clear that even a source as small as 100 mCi could cause significant contamination.

For radio-chemistry reasons — in the event of melting a source, cobalt alloys directly into the steel, cesium contaminates the dust from the furnace and iridium/radium contaminate the slag.

A large source enclosed in the relatively small volume of a scrap vehicle should be easily detectable, but unfortunately (from a radiation detection viewpoint) all these sources are normally in protective safety shields, so emission levels are very low. A typical source may give a 13.5 R/h rate at the source but only 1 mR/h on the outside of the shield.

Since all these sources are originally supplied in safety shields there is a high probability that they will still be inside such shields, so the real problem is to detect the presence of a shielded source buried in scrap material.

Simple calculations made using typical scrap densities and assuming the solid steel equivalent, indicate that such sources increase background by about 0.04% which clearly is undetectable in a field environment.

3. FIELD EXPERIMENTS

The first series of tests involved a 1 curie Cesium-137 source enclosed in a 7 mm steel walled box buried in a railcar of scrap. Emission levels on the outside of the steel container before burial gave exposure rates of 1 mR/h.

A 21 cu. ins sodium-iodide detector was used to take static measurements with and without the source in the rail car. The results were plotted and they show that some increase in radiation was noted, but local changes in radiation of the ground were very dominant.

It became clear that in the inflexible logistics of a scrap yard static monitoring was impractical so a series of tests were initiated using a geophysical airborne system with a xtal array of 768 Cu ins heavily shielded to suppress the ground effects. It was shown that even with such large xtal volume only a marginal response was achieved.

The next series of experiments involved analysis of the effects of scrap material shielding on the spectral shape. Similar experiments were carried out by Lamastra and all these data show clearly that deeply buried sources only have significant emissions at the very bottom of the spectrum essentially below 300 keV.

This data shows clearly that isotopic analysis to enhance signal sensitivity is pointless so the use of expensive sodium-iodide arrays is unnecessary, so system development concentrated on the use of PVT (plastic) detection systems.

4. SYSTEM DEVELOPMENT

The scrap yard environments is an extremely difficult place to work as the detectors must work in all climatic conditions (-40 to +150°C) and remain unaffected by rain/snow/dirt/vibration etc., vehicle size is irregular, speed is highly erratic, personnel are essentially totally unwilling to modify their operating logistics and most hands-on users are totally unskilled in technical matters.

A prototype system was developed so extensive on-site testing could be carried out to closely investigate the various problems likely to occur.

The first major problem was vehicle suppression. The typical radiation profile of a vehicle as it passes a detector shows that the local background radiation is suppressed by absorption in the vehicle, so the actual background significantly reduces. This reduction is enormously variable as it is affected by vehicle size, density, detector spacing/size etc. But ranges typically from 5 to 45%.

Another problem is radon. When long term monitoring is carried out significant increases in background radiation occur during precipitation. These increases have been measured in excess of 100% increase over a short period of time. Thus fixed alarm level systems false-alarm during precipitation unless their alarm threshold are set unacceptably high.

Another problem is that in the busy environment vehicles are everywhere. A simplistic concept indicates where a passing vehicle alarm can be cancelled by another vehicle passing. This problem is easily solved by shielding the rear of the detector which also significantly improves system sensitivity by essentially doubling the signal to background ratio.

To solve these problems statistical analysis methods must be used so very low alarm threshold can be used which can compensate with these practical problems.

A typical profile may show the following: Inside the source it may be 13 R/h, outside the source it may be 2.5 mR/h but on the outside of the vehicle, exposure rate levels as less than 1 uR/h are common.

The final developed system in a typical installation uses a very large detector volume (73L) of plastic (PVT) detectors. The system uses an external console mounted in the scale operators shack and the whole system operates in a 'go — no go' mode, so technically unsophisticated personnel require no special training beyond "call Mr. X is the alarm goes off".

5. TESTING

To verify the performance of the final system a series of experiments were carried out at a local steel plant. Two sources were used;

- A REAL SHIELDED SOURCE — comprising a 100 mCi cesium-137 source in a safety shield encased in a wooden box for protection. This source had an exposure rate of 0.3 to 0.5 mR/h on the outside of its container.

- A SIMULATED SHIELDED SOURCE — comprising a 300 Uci cesium-137 source in an empty thin walled steel container.

These two sources were loaded into a rail car packed with heavy scrap material.

Effort was made to locate the sources in approximately equivalent geometric locations, so that scrap attenuation is hopefully a semi-worst case scenario.

The results indicate system performance, note the depressed vehicle in background caused by vehicle shielding, the computed system reliable detection level and the size of the source responses.

6. USER FEEDBACK

After a few years of operating these systems in the field some interesting results have occurred.

To date these systems have detected the presence of over 7 very large sources and literally thousands of radium contaminated oil-field pipe. Most of the sources were NOT on the NRC missing list.

A common problem is X ray gauging activities. Recently some users reported problems with their system alarming as a result of X ray crack testing 2 kms away from the detectors, but presumably boresited accidentally on the detectors.

Reports have been received of systems alarming as a result of a train carrying legal radioactive waste passing at 60 kph more than 100 m behind the detectors.

A common question asked is we have been melting steel for many years and have never melted a source, so what s the fuss. The "fuss" is that a large number of large sources have been accidentally melted, not discovered and manufactured into a huge array of goods. With the enormous potential legal liability of such accidents many governments are tightening regulations to restrict transport of contaminated material. The current rash of reports of radioactive material being smuggled across the porous borders of European states bordering on the CIS, shows that public awareness of these problems is increasing, and governmental action will follow.

GRAVITY DATA INVERSION AS A PROBE FOR THE 3D SHAPE AT DEPTH OF GRANITIC BODIES

J.L. VIGNERESSE, M. CUNEY
CREGU, Vandoeuvre/Nancy, France

Abstract

Granitic intrusions represent potential sites for waste disposal. A well constrained determination of their geometry at depth is of importance to evaluate possible leakage and seepage within the surroundings. Among geophysical techniques, gravity remains the best suited method to investigate the 3D shape of the granitic bodies at depth. During uranium exploration programmes, many plutons emplaced within different geochemical and tectonic environment have been surveyed. The quality of gravity surveying depends on the intrinsic accuracy of the measurements, and also on their density of coverage. Accuracy depends on the precision of elevation measurements which have to be better than 0.5 meter to reach detection of 0.1 mGal anomaly. A regularly spaced and dense coverage (about 1 point/km^2) of measurements over the whole pluton and its nearby surroundings is needed to represent the gravity effect of density variations. This yields a lateral resolution of about 0.5 kilometre, or less depending on depth and roughness of the floor, for the interpretation of the Bouguer anomaly map. We recommend the use of a 3D iterative method of data inversion, simpler to run when the geometry and distribution of the sources are already constrained by surface data. This method must take into account the various density changes within the granite and its surroundings, as well as the regional effect of deep regional sources. Because the input of the inversion programme may differ, not in raw gravity data, but in density contrasts, surface shape, maximum expected depth, regional anomaly, the result is not unique. Several tests are used that increase the confidence on the result, mainly by looking at its stability. The map of the computed depth of the floor of the pluton is then drawn. A total error in the input data (measurements, densities, regional field) is estimated at 6%. Errors due to data inversion reflect the uncertainties on the density contrasts at depth. We estimate that the total uncertainty on the calculated depth values does not exceed $\pm 15\%$. Because of the good coverage of gravity measurements, the overall shape of the pluton is certainly better constrained than the depth values themselves. We present several examples of gravity data inversion over granitic intrusions displaying various 3D morphologies. Joint studies of the magmatic structures in plutons provide complementary constraints to validate the shape at depth. They mostly record the conditions of emplacement of the plutons and show how their morphology at depth varies according to the regional deformation field. At a smaller scale mineralizations are also observed above or close to the root zones. Those examples demonstrate the adequacy of joint studies in constraining the mode of magma emplacement before further studies focussing to environmental problems.

1. INTRODUCTION

Numerous studies are presently developed in the world to qualify granitic intrusions as potential sites for the storage of nuclear waste disposal. A precise knowledge of the 3D shape of the granitic batholiths represents an important parameter to select more favorable sites and the best appropriated areas within the batholiths.

Granitic intrusions have also been recognized as preferential places for intrusive ore deposits, specially for U, Sn, W and Au [21]. However, veins and mineralized lode are about 10 to 100 m in scale and must be found out from quite larger bodies, the scale of which is about 1000 km^3 for alkaline to 500-1000 km^3 for calcalkaline or peraluminous plutons when volume is estimated from gravity data inversion [56]. Mineralizations largely depend on the chemical evolution of acidic magmas, which are mostly related to the conditions of emplacement and on the movement of residual melts and fluids. The position and number of the root zones that provide magma to the upper levels determine the mode of emplacement of the successive magma batches which also controls the distribution of the mineralization. Thus, determining the 3D shape at depth of a granitic intrusion would inform on the spot places to investigate for mineralizations.

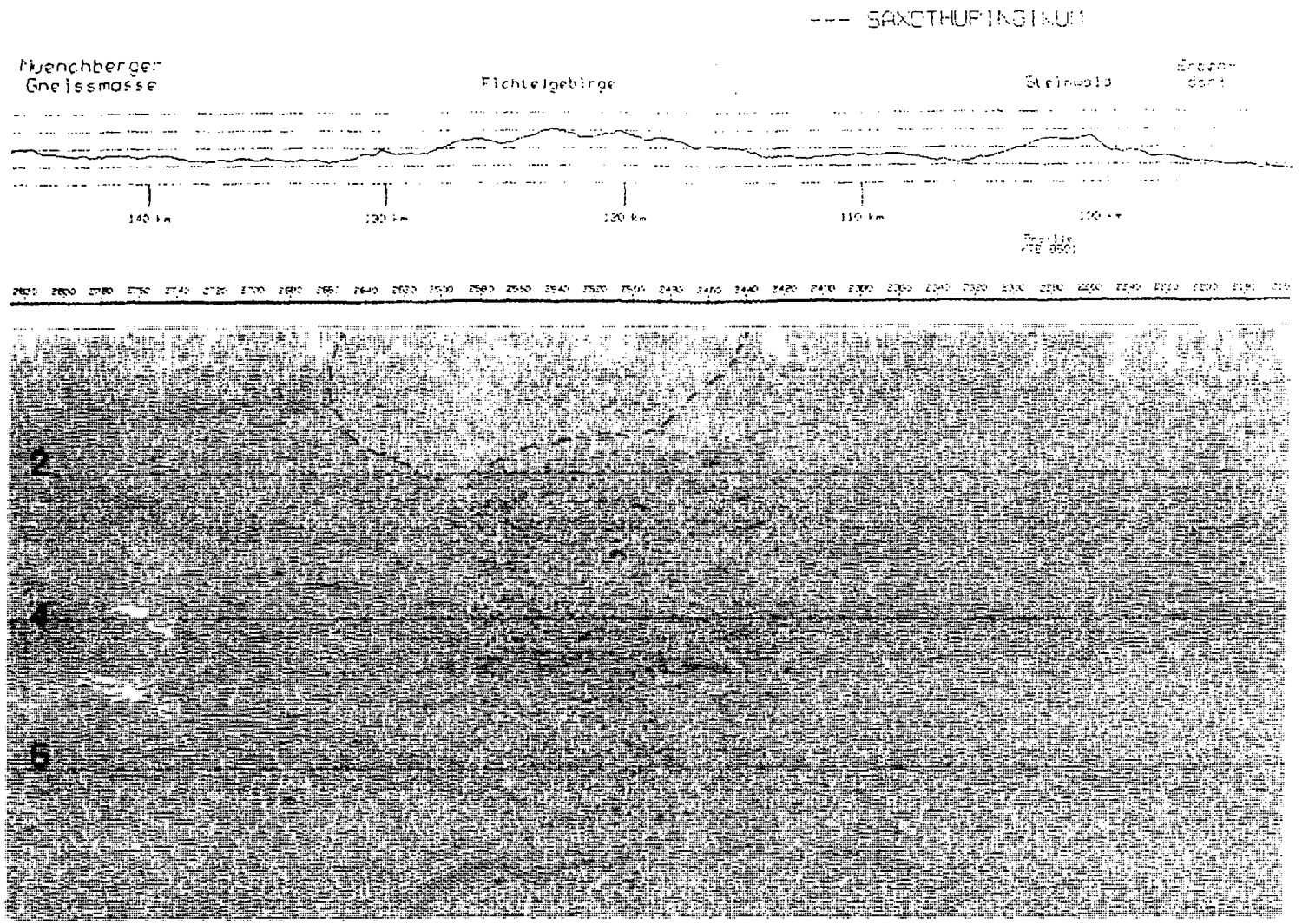

FIGURE 1. Seismic section taken from the Dekorp Atlas, Dekorp 85, line 4N (Meissner and Bortfeld, 1990) that shows the Fichtelgebirge granitic body as a transparent seismic zone. Vertical scale is shown each two seconds, two way travel time, non migrated profile, that is roughly 6 km.

Information on magma emplacement, since it relates to magma dynamics, is not directly accessible by simple observation, but internal structures of the magma record its last movement before it was fully crystallized. They can be observed in the field by usual observations, or by laboratory measurements. Deep structures such as the root zones or the feeding conduits are also too far for direct observation. But, remote sensing methods provide indirect tools to describe such structures. Therefore, an integrated method of surveying granitic intrusions is suggested, in which the shape at depth is obtained by detailed gravity data inversion and then is correlated to internal structures of the magma described by usual structural measurements. This method has been tested for exploration of intragranitic U deposits for more than ten years, mostly in the mid-European Variscan belt.

2. GEOPHYSICAL METHODS

Classic geological observations are limited to the uppermost kilometer through direct observation along erosional cross-sections. Geophysical studies are required to achieve resolution at depth. Seismic data are usually collected along two dimensional profiles because of the high cost of surveying, but this precludes a full three-dimensional shaping at depth. Reflection of seismic waves occurs when impedances, the product of the density by the seismic velocity, are very contrasted at an interface. The ratio of the difference to the sum of seismic impedances indicates the strength of the interface in reflecting elastic waves. Variations in granitic facies result in very small variations in the physical properties of rocks [28]. So, in the case of granitic facies variations, the reflection coefficient remains very low, and the seismic waves are not affected by low reflections coefficients at usual seismic frequencies (up to 10 Hz). Therefore, granitic bodies are essentially transparent (Fig. 1) to seismic waves [35, 47, 37]. To register the facies changes and to produce coherent reflection waves at an interface, provided it is a sharp boundary, higher frequencies (40-120 Hz) are required. Preferential filtering of these frequencies produces a less energetical signal and less efficient depth penetration at depth [24]. This is partly overcome by using a closer seismic array when low resolution is needed at a depth corresponding to the bottom of the granitic intrusions (6 to 8 km, or 2 to 2.5 s two way time).

Other geophysical methods are of lesser use over granitic intrusions. Acidic rocks do not generally show very large amount of magnetic minerals and thus present a weak magnetic signature, except for alkaline granites which are often associated with basic, that is magnetic, components [1]. However, the contrast between granite and metamorphic aureole, often enriched by oxidation in magnetic and opaque minerals can be used to map and to delineate granitic intrusions. The magnetic field is very flat over acid igneous rocks [59, 39], but a magnetic aureole is produced by the metamorphic aureole [50]. The magnetic susceptibility of minerals in acid rocks is more sensitive to variations in the iron and magnesium content of minerals. In granites of the ilmenite-series [34], the more magnetic minerals (biotite, amphibole) are paramagnetic with low susceptibility. Its value increase linearly with the iron content in biotites [12]. In granites from the magnetite-series, ferromagnetic minerals predominate, and magnetic susceptibility values also increase with the total iron content of those minerals. Therefore, at the scale of a pluton, mapping of the magnetic susceptibility represents a complementary tool to map facies within a granitic massif.

Electrical methods are very sensitive to conductors located out of the profiles of measurements. In a granitic massif, late fractures infilled with water and altered minerals greatly influence the trajectory of electric currents. These structures perturbate the measurements to infer the deep structures in a granitic batholith. Conversely, electrical methods are well suited to determine and to map the late fracture zones, infilled with water. As a result, eletromagnetic mapping shows the resistant and unaltered blocks of fresh granite in between altered and water seeping fractures [14]. Magneto-telluric soundings lack of resolution at depth because of the unwanted boundary effects which disturb the penetration of electro-magnetic waves in depth. Thus, those methods can be used as one-dimensional soundings to determine the depth of the floor in one point [7], extended to two-dimensional interpretation, but cannot produce a map of the floor all over the pluton.

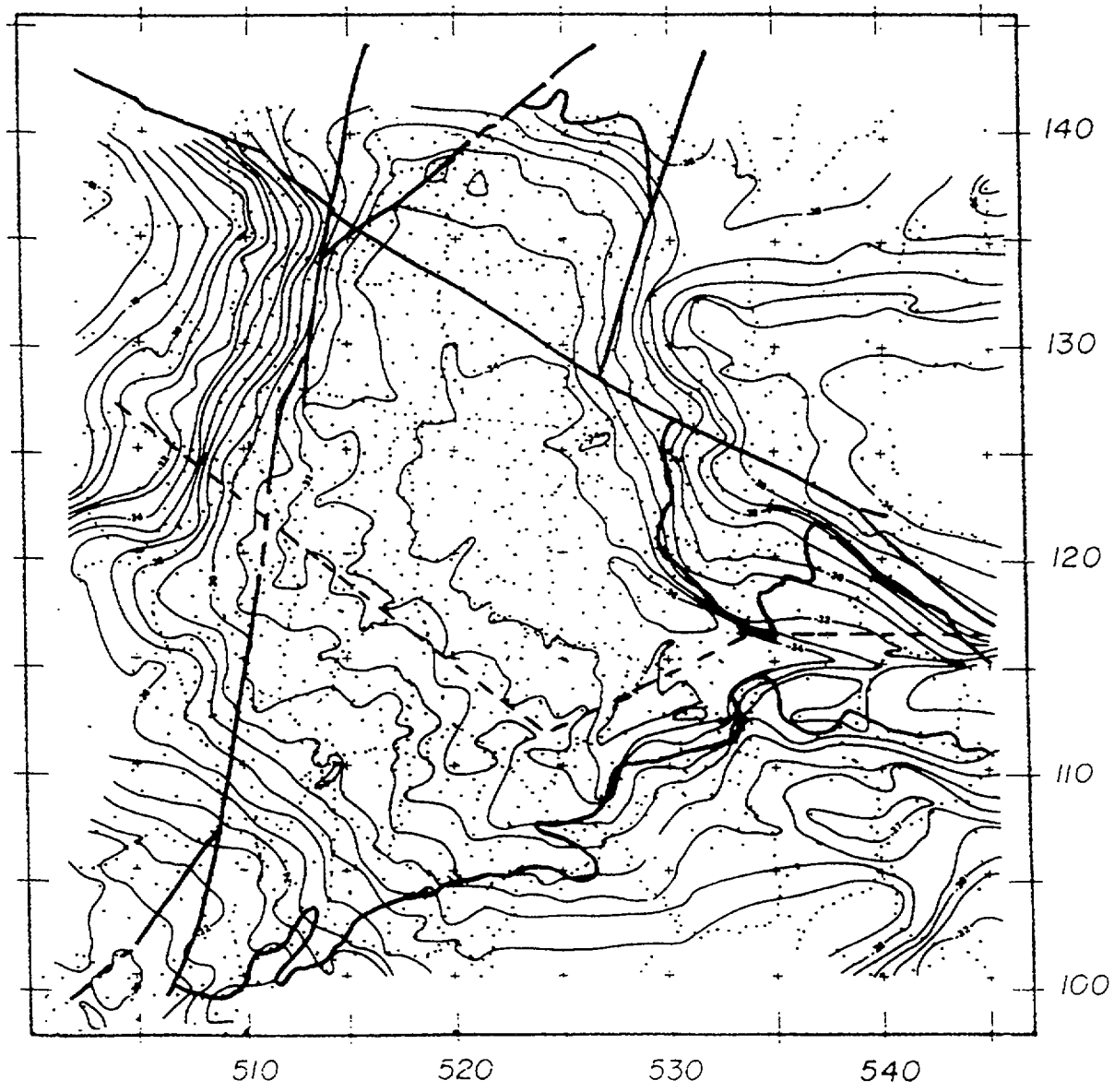

FIGURE 2. Measurements coverage over the massif of Saint Sylvestre, Massif Central, France. Scale on the boarder refers to national grid, in km. Granitic outcrops are shown by a thin line and the cross section in Figure 6 by a dashed line. Contour interval of the Bouguer gravity anomaly are shown each mGal. From this map, no clear trend is evidenced about the position and number of root zones, because of the integrating character of gravity measurements.

The gravific signature of acid intrusions is almost always negative, because of the low density of those rocks compared to the average density of the crust. Due to the more or less forceful emplacement of granites, their walls are often steeply dipping and show a sharp transition with the surrounding. The gravity contrast induced by the granite is thus reinforced and plutons often show a strongly marked negative gravity anomaly. The dimensions of a pluton are about 10 to 20 km in radius, compared to about 5 $\pm$ 2 km in depth. The size of the pluton at the surface is also sufficient to measure the long wavelength component within the gravity signal that corresponds to the deepest part of the pluton. Consequently, gravity data is an excellent candidate for estimating the shape at depth of the plutons.

3. SUGGESTED GRAVITY SURVEY CONDITIONS

Gravity surveying applied to the study of granitic intrusions provided the first geophysical evidence relevant to the "room problem" in the granite controversy [10, 11]. Such surveys have been carried out on isolated massifs to resolve petrological models [41, 15, 30] and represent a valuable contribution to the study of specific plutons. However to infer the shape at depth of a pluton, good quality measurements and detailed gravity coverage are required to achieve a good resolution at depth [57].

Such high standards gravity surveying depends on the density of measurements, but also on the intrinsic accuracy of the measurements. A regularly spaced and dense coverage of measurements over the whole pluton and its nearby surroundings is needed to determine a reliable shape at depth. An appropriated density of measurements is about 1 point/km^2, so that major variations of facies are surveyed (Fig. 2). A lateral resolution of about 0. 5 kilometer, or less depending on depth and roughness of the floor, can thus be expected for the interpretation of the Bouguer anomaly map. Accuracy of gravity data mostly depends on the precision of elevation measurements. It should be better than 0.5 metre to achieve a precision of 0.1 mGal. This is obtained using topographic maps with accurate elevation benchmarks, and a precision baro-altimeter checked several times per day at benchmarks.

Detailed measurements of density contrasts between the many subtypes in the granite and the surrounding rocks are required to perform gravity data inversion that can deal with the changes induced by the varying facies. This requires a systematical measurement of the densities of about five specimens per rock-type, using cored samples, for instance those that have been collected for the measurement of magnetic susceptibility. Cores are better suited since they avoid bias due to surface porosity and fulfill a specific procedure [58]. The cores are weighted, then set under vacuum before being impregnated by water and weighted, then slowly dried to avoid thermal cracks, and weighted again. The difference in weight before and after drying provides an estimates of porosity. The other measurements provide the density of the sample.

4. DATA INTERPRETATION

Because the gravity measurements integrate many sources with varying density values, the resolution presented in the Bouguer anomaly map is low. For instance, the gravity map drawn on Saint-Sylvestre complex (Fig. 2) shows smooth variations over the massif. In particular, no clear trend is shown that allows to determine where there are the local deepest parts of the massif. Two factors have influence on the smooth character of the map. One relates to the regional gravity anomaly, the second comes from the integration of the effects due to specific sources into one global anomaly. Removing the regional gravity anomaly is quite complex, although the principle is simple. It consists in separating the effect of local sources from those located deeper in the crust which show lower frequencies effects [57]. Several techniques exist, from filtering to removing a trend manually. The integrating character of potential fields can only solved by numerical computations. It is in part a consequence of the non-unicity of solutions in potential field methods.

We recommend the use of a 3D iterative method to realize gravity data inversion. Interpretation on profiles cannot be used to infer data which must be correlated on maps with structural data and regional deformation field. A 3D method, adapted from that of Cordell and Henderson [18] is simpler to run when the geometry and distribution of the sources are already constrained by surface data [54, 57]. It also allows the use of specific density contrasts at each point of the mesh, thus taking into account the facies changes. The better the body is individualized with respect to its surrounding, both in geometry and density contrast, the better is defined its gravity anomaly. However, because the input of the inversion programme varies, not in raw gravity data, but

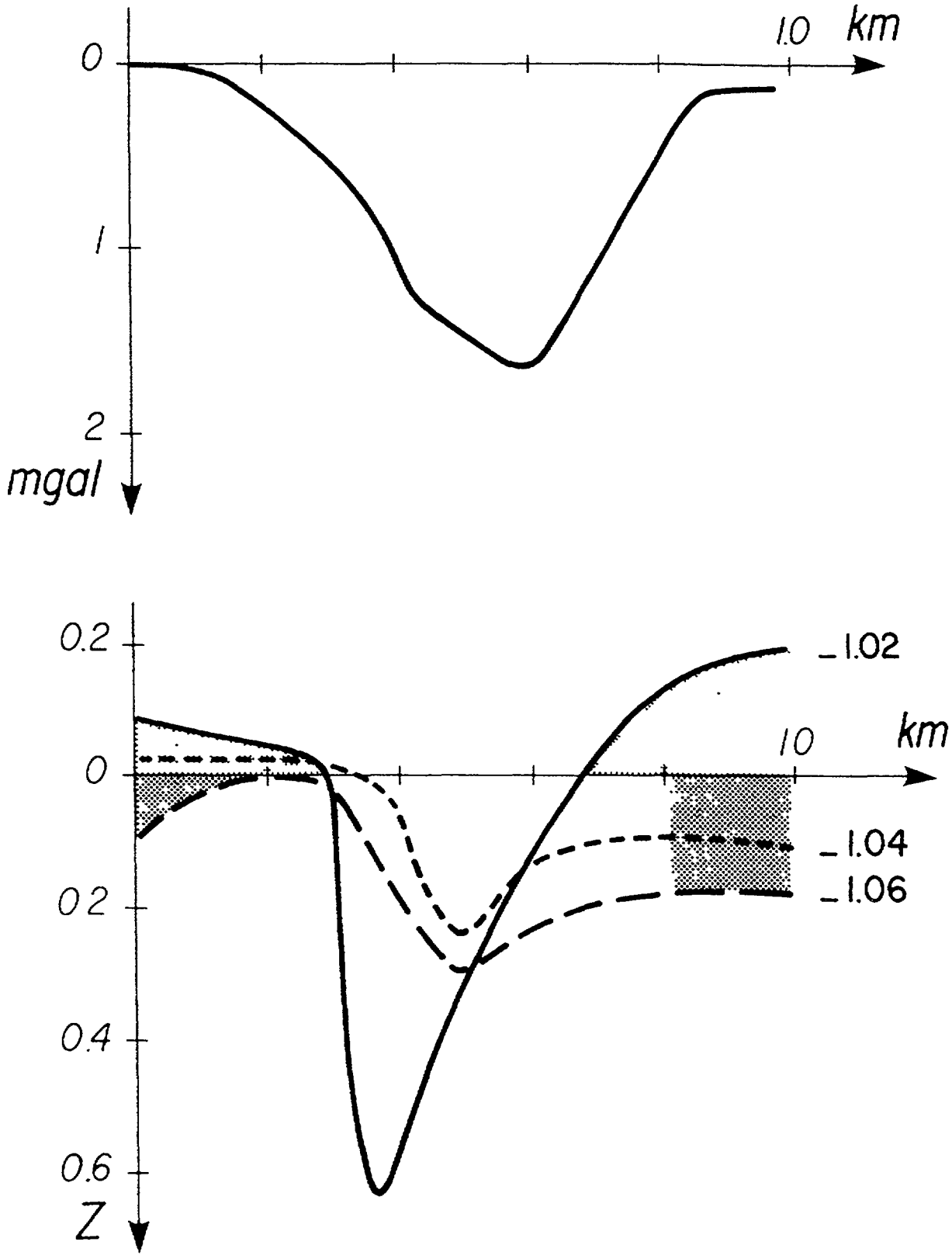

FIGURE 3. Example of a gravity profile (on top) sorted from a 3D data inversion with numerical oscillations (on the bottom) occurring when the density contrast is not adapted to that effectively existing underneath. The expected density contrast (about -1.04) relates to a kaolinized zone at the apex of a granitic stock. In case of too low density contrast (-1.02), then depth increases drastically, whereas spurious reliefs are added on the surroundings. In case of a too large density value (-1.06), the depth is large everywhere, even outside the anomaly.

in density contrasts, surface shape, maximum expected depth, regional anomaly, the result is therefore not unique. Several tests are used that increase the confidence on the result, mainly by looking at its stability.

One major cause of uncertainty is the representativity of the density at depth. During the inversion process, a density is assigned to each prism under the gridded map of the gravity anomaly. The density is assumed to be constant with depth within that prism and the resulting depth is that which better fits the value of the total gravity anomaly. No control exists that can insure the reality of that assumption, since it is impossible to assume neither a density change with depth, nor lateral variations of the density contrast at depth. However, a series of tests can be run during the iterative computation to keep control on the process. When the density is too low, the computer lacks mass and accommodates that mass deficiency by increasing the depth of the prism. But, a deeper source also increases the low frequencies content of the signal, not present in the measurements, and thus, the programme must reduce that low frequencies trend by adding spurious reliefs, to compensate the mass deficiency at depth (Fig. 3). This phenomenon creates numerical oscillations that are easily recognized when examining the successive iterations. Conversely, when the density is too large, the computer has too much masses and cannot deal with that extra mass underneath. So, it tries to place as much as possible that extra mass outside the place of the expected body which creates the anomaly (Fig. 3). As a result, the body is thick everywhere, even outside its limits estimated from the shape of the contours of the anomaly on the map. Again a close inspection at the various steps of iteration easily eliminates those unexpected values and thus allows an indirect test on the distribution of densities at depth. The map of the computed depth of the floor of the pluton is then drawn.

These depth values give a good first-order picture of the pluton. Error on the input data, shared by the gravimeter and the precision in elevation data, is estimated to be about 2%. Error in the estimation of the far-field gravity anomaly may exceed 3%. Therefore, after estimating the error on the densities to be less than 1%, a total error on the input data is estimated at about 6%. It is more difficult to estimate the errors due to the inversion of the data. They reflect the uncertainties on the density contrasts at depth. We consider, however, that the total uncertainty on the calculated values of the depths does not exceed $\pm 15\%$. Because of the good coverage of gravity measurements, the overall shape of the pluton is certainly better constrained than the depth values themselves. The main consequence is the uncertainty on the depth of the deepest parts of the floor, and also on the dips of the walls of the pluton.

5. STRUCTURAL DATA

Structural studies describe the present geometry of granitic bodies, from which inferences are made on how they have been emplaced into the upper crust, thus perturbing the regional deformation field. The strain field is recorded in the schistosity of the surrounding rocks [29, 44] or is shown by the interference between internal granitic structures and regional deformation [17]. Mapping the internal structures in granites [8, 25, 27] relates to deformation recorded by the magma as it intrudes the surrounding crust. They are commonly restricted to surface observations, or in a few cases to structures eroded down to 1 or 2 km, still limited compared to the inferred thickness of granitic plutons, which averages about 5 ± 2 km [56]. Information on the magma flow is obtained by measuring the preferred orientation of crystals. Early anisometric crystallized minerals define a planar fabric, or foliation, through the average orientation of their most developed face. These crystals are mostly Fe ($\pm$ Mg) bearing silicates (biotite, amphibole), but plagioclase and K-feldspar megacrysts are also used to determine the internal fabrics of a granite pluton. Within the foliation plane, a lineation is defined as parallel either to the average elongation of the crystals, or to the zone axis of their orientation. In the field, a compass is used to measure the planar and linear orientations of the crystals [42]. The results become approximate on equigranular and fine-grained rocks. Grain by grain studies are also realized, using a U-stage mounted on a microscope [46, 13], but they are time consuming, hence not applicable in routine.

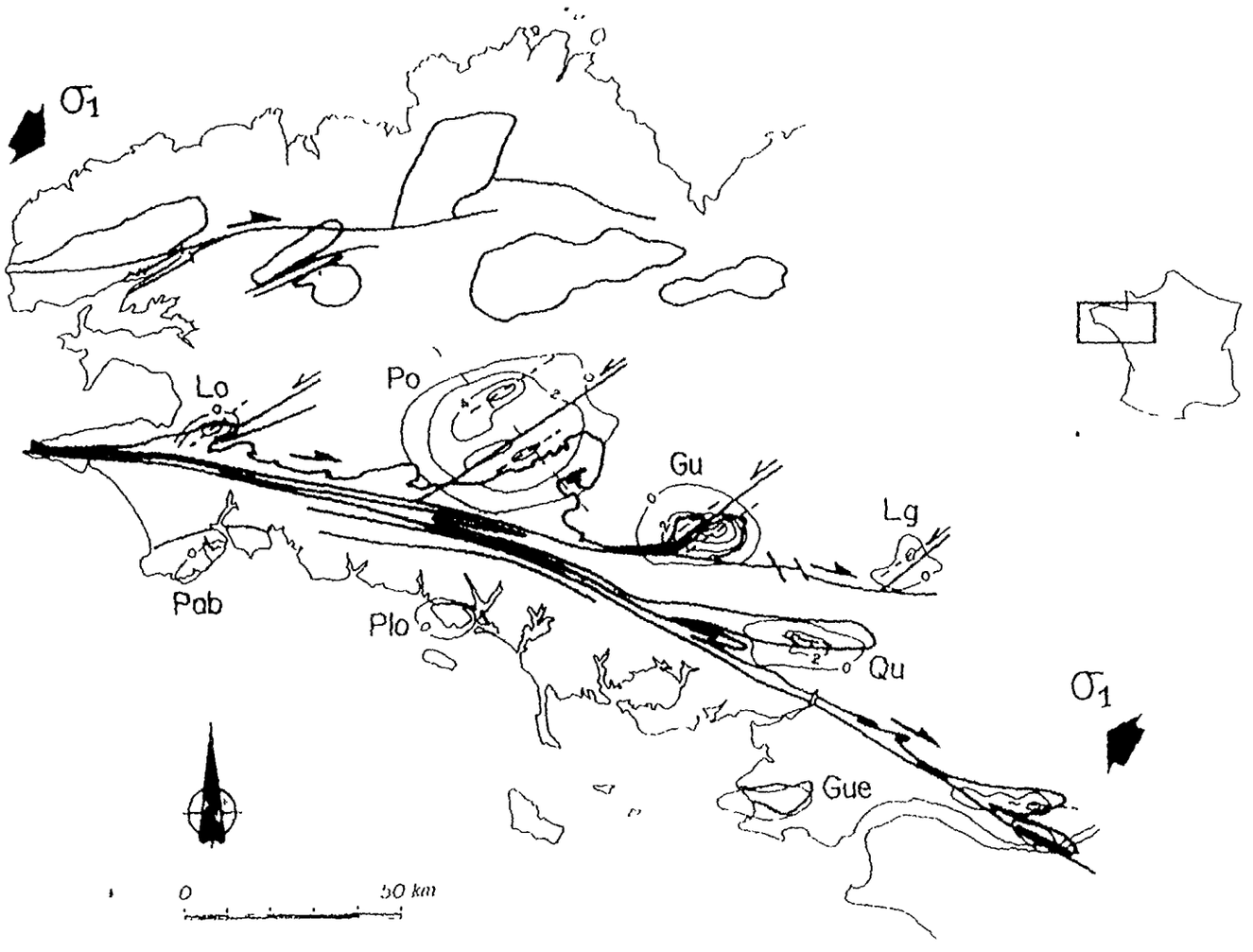

FIGURE 4. Depth (in km) of the floor of the granitic bodies in Brittany, western France, deduced from gravity data inversion (modified from (Vigneresse, 1983). The root zones trend (dashed line) within the extensional area related to the major strain component associated to the main dextral fracture zone. Granitic massifs from the west to the east: Lo Locronan, Po Pontivy-Rostrenen, Gu Guéhenno, Lg La Gacilly, Qu Questembert, Pab Pont l'Abbé, Plo Ploeumeur, Gue Guérande.

Fabrics computed from the anisotropy of magnetic susceptibility [32, 9] are now commonly applied to determine structures in granites [52, 26, 12]. The pluton is sampled on a regular grid, about 1 kilometre in spacing. At each site, two cores are drilled and oriented with respect to north and vertical. Each core yields two specimens 25.4 mm in diameter and 22 mm in height. From this procedure, each site is represented by four specimens, totalizing a volume of about 43 cm^3 of rock. Low alternative-field susceptometers are used, either the Molspin ($\pm$ 7 10^{-4} T at 10 kHz) or the Kappabridge ($\pm$ 4 10^{-4} T at 920 Hz). These apparatus allow the systematic measurement of the specimens, providing the magnitudes and orientations of the principal axes of the ellipsoid of the anisotropy of magnetic susceptibility. The bulk susceptibility magnitude of the specimen serves as a normalization factor. For a given site, the long axis of the averaged ellipsoid of magnetic susceptibility is called Kmax or magnetic lineation, and the short axis Kmin or normal to the magnetic foliation.

Obviously, the magnetic susceptibility and its anisotropy depend on the magnetic mineralogy [49]. Hopefully, in both paramagnetic granites, i.e. belonging to the ilmenite-type series, and the ferromagnetic granites, i.e. the magnetite-type series, the magnetic fabric compares favorably with the classically measured structural preferred orientation [26, 48, 4]. An advantage of paramagnetic granites is that the magnitude of the bulk magnetic susceptibility is directly proportional to the iron weight content, at least in a first approximation [49], allowing correlation of its magnitude with the petrographie types, hence possibly with magma evolution [23].

6. ROOT ZONES IN GRANITES

Combination of both structural and geophysical data helps in understanding the shape at depth of a granite pluton [25, 27, 5, 6, 16]. When erosion of the pluton only affects its uppermost part, the observed magmatic structures reflect the interaction between pluton emplacement and its surrounding rocks [29]. For a more deeply eroded pluton, zones where magmatic lineations are vertical often correlate to the deepest zones computed from gravity data inversion. Conversely, zones where lineations are weakly dipping often denote areas of shallow to medium depth. The deeper zones deduced from gravity data inversion, provided they also show vertical lineations, are interpreted as magma feeding zones. They may be active during all time of pluton emplacement and they are often reflected in the outcrop by chemically more evolved magma or late intrusive facies. For instance (Fig. 5), such root zones have been shown in the Cabeza de Araya complex, Estramadura, Spain, by a more leucocratic magma, whereas the remaining part of the massif is richer in biotite [2, 5]. The location and geometry of the root zones are not biased by the nature of the specific magma associated with that area since changes in density contrast induced by facies variations are taken into account during the inversion process. These zones can be determined on cross sections drawn through a massif, because the slope of the granitic pluton floor severely steepens when approaching the root zone. Root zones are located between 6 to 12 km depth and have a moderate extension of 1 to 10 km^2, compared to several hundreds of km^2 for the surface area of a massif.

7. DEFORMATION REGIME AND ROOT ZONES IN GRANITES

Some granitic intrusions are spatially associated with major strike slip shear zones as in Brittany, Western France [55], in Galicia, NW Spain [19, 3], or in Estramadura, Spain [5]. Such plutons have a moderate volume, about 1000-1500 km^3, with an outcropping surface of a few hundred of km^2 [56] (Fig. 6), the elliptical shape of which reflects shear deformation acting during the emplacement. In those plutons, only one single root is observed, two in larger plutons, despite the high density of gravity measurements. The floor plunges gently down to about 5 $\pm$ 2 km, and then a sharp increase in the dip of the floor corresponds to the root zone which extends down to 6-12 km.

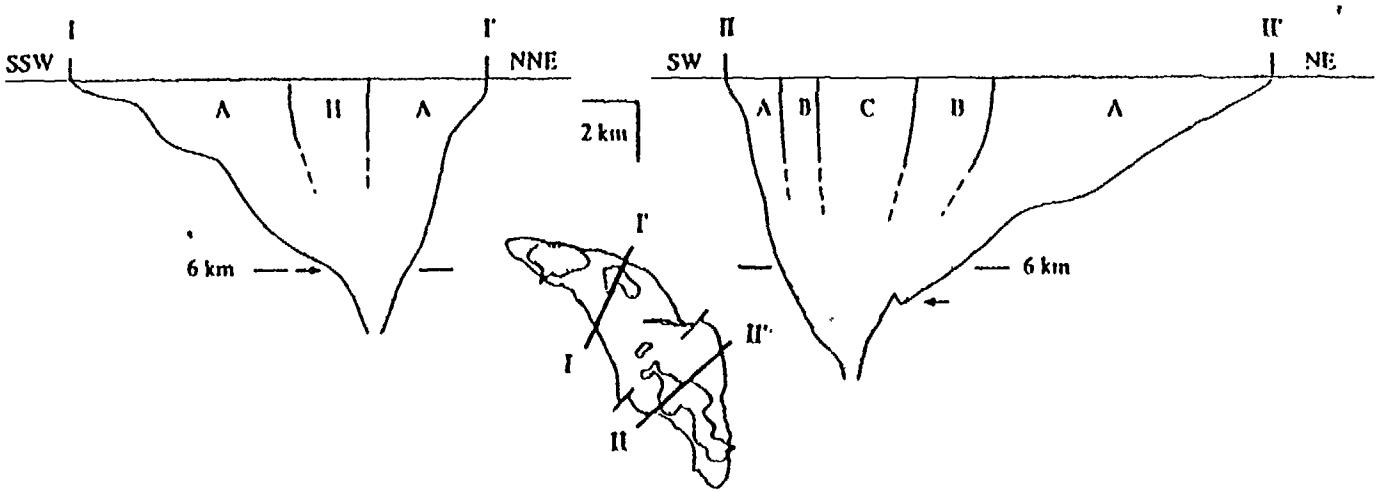

FIGURE 5. Cross-sections across the massif of Cabeza de Araya, Spain (from Audrain et al., 1989a) showing the change of the slope of the iloor (below 6 km) when approaching the root zones. Letters refer to the facies A (mostly biotitic) evolving to B (biotite ± muscovite) then to C (muscovite dominant). H refers to an heterogeneous facies.

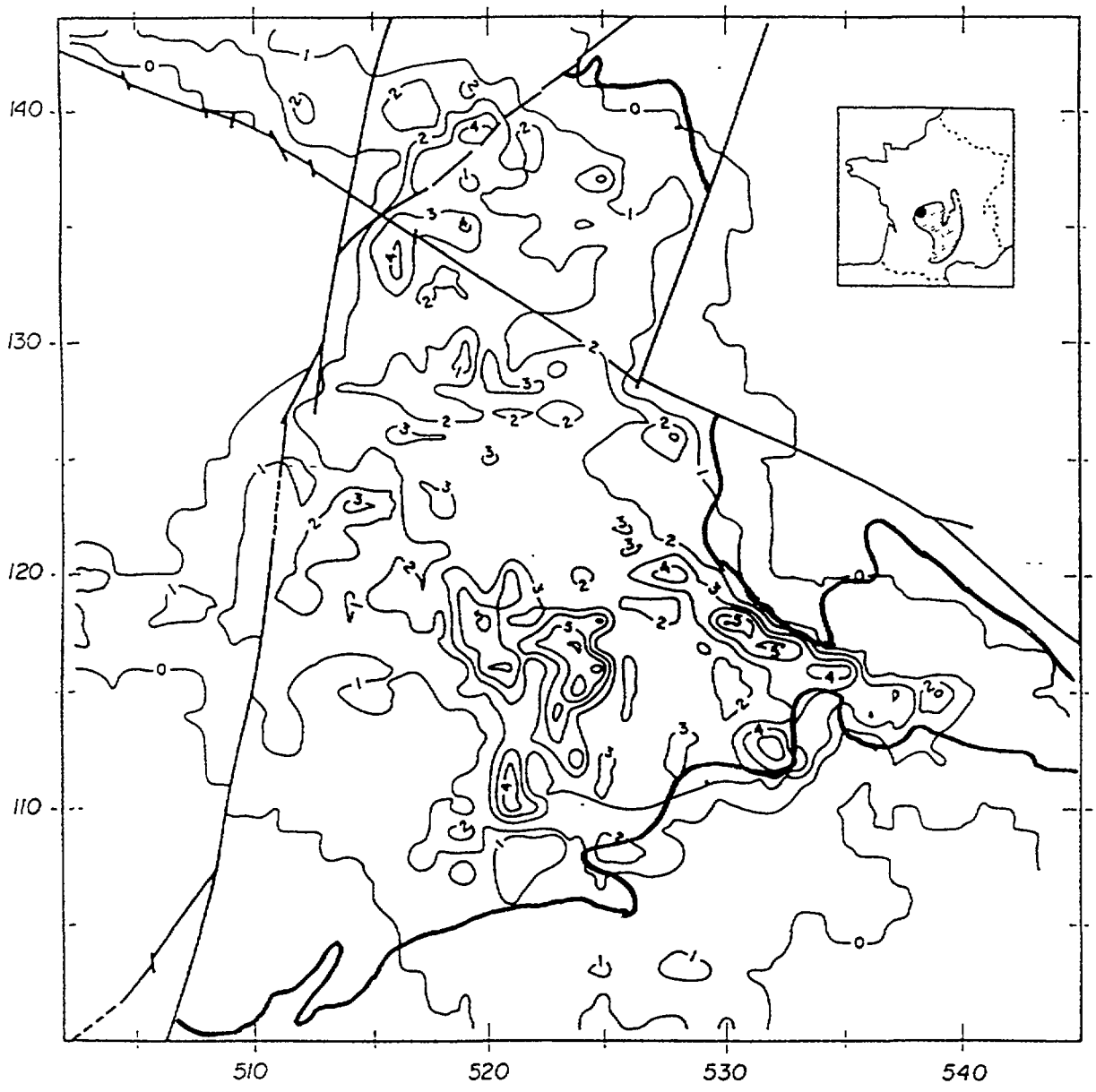

FIGURE 6. Map of the depth (in km) of the floor in the Saint Sylvestre granitic complex (French Massif Central) deduced from gravity data inversion. Note the overall shallow depth of the floor and the great number of small areas with a deeper floor interpreted as secondary root zones.

When magma infills anamostosing shear planes, the amount of granite is generally small and deformation is apparently enhanced [31]. When the shear zone is wider or non continuous, with en échelon relay faults, or when a tensional component exists, magma fills the room created by the opening of pull-apart like structures at retreating bends [27, 33, 51]. The granitic pluton of Mortagne, Brittany, France, represents a good illustration of that situation [27]. In that case, the granitic body has steep walls associated with the shear zone. The average depth of the floor is generally greater than the one of plutons connected with non overlapping shear zones. This situation is restricted to transtensive environment which provides simultaneous shear and place due to the extensional component.

In the remaining cases, which are the majority, the root zones are always located off the major deformation plane, with no connection between the root and the shear plane. Numerous

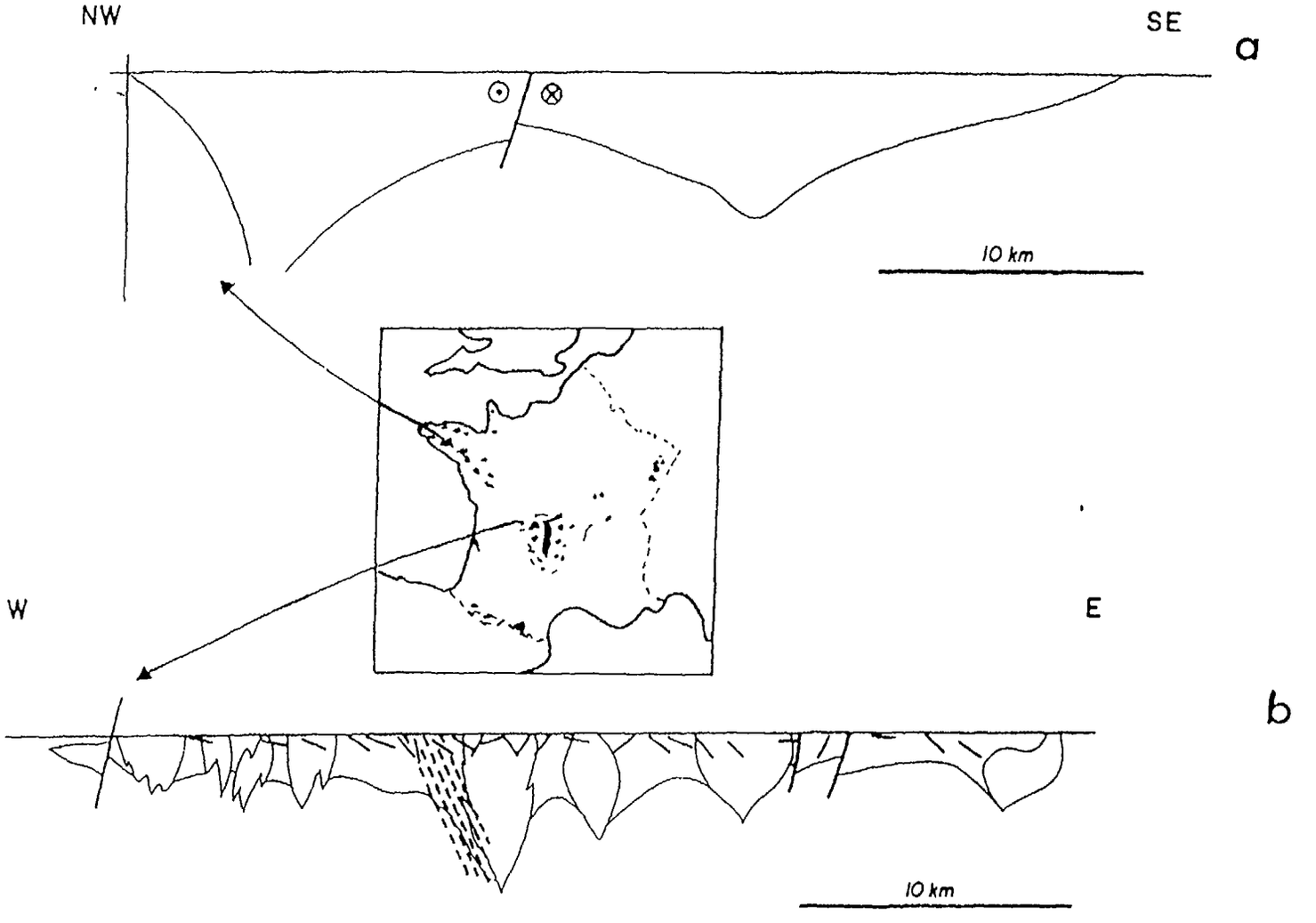

FIGURE 7 a) Cross section oriented EW across the Pontivy massif (see location on Fig. 4). Two distinct roots are present, one for each lobe of the complex. b) Cross section EW oriented within the Saint Sylvestre granitic unit (Fig. 6). A very thin main facies is stippled, in which vertically structured discording facies are intrusive. The foliation planes (adapted from (Mollier and Bouchez, 1982)) are also represented. In both cross sections, vertical and horizontal scales are identical.

examples are provided in Brittany, where most plutons do not show any root connected to the shear zone (Fig. 4), or in the granitic complex of La Marche, French Massif Central. In most cases, the root zones are at high angle with the major stress component (σ_1). The position and orientation of the roots reflect granitic intrusion in a plastically deforming crust. For instance in Brittany, the roots trend to the Northeast relative to a dextral shear zone oriented N110. According to the regional stress field, the roots are at high angle to the major stress component, and are aligned with the stretching direction. When conjugated shear zones exist, the root zones are in the locally extensional area (near field) relative to the regional (far) deformation field. This is observed on single plutons (Brittany, Galicia) or even at a larger scale. For instance, the intrusion pattern of Proterozoic granites from the North-eastern Brazil clearly relates to east-west oriented dextral shear zones [4]. Though some granites present evidence of intense deformation and reorientation due to their intrusion within the shear zone, all massifs are oriented along N045 structures, that is within the stretching direction as expected during plastic deformation. This is not conform to the Andersonian theory of fracture which would predict N135 oriented tension gashes, that is parallel to the major stress component. On a very large scale, massifs were intruded within the local extensional region related to deformation.

In most situations, conjugate shear zones affect the granitic pluton on its border, but no connection is observed from gravity data inversion between the root zones and the deformation planes. This precludes a direct relation between the zone of intense deformation and the place where magma has been preferentially intruded. However, those fracture planes show well-developed mylonites displaying low-temperature C-S structures, with broken quartz on those planes, attesting that intense deformation lasted longer than the emplacement of granites [29, Paterson and Fowler, 1993].

Granites may also be intrusive at the end of a compressional phase or during an extensional regime, as the Saint Sylvestre complex in the French Massif Central [6], Pont l'Abbé and Guérande (Fig. 6) in the southern French Armorican Massif [55], or the Mykonos massif in Greece [22]. Those massifs are very thin, with subhorizontal foliation planes [40]. Their average thickness may be as little as 2.6 km (Fig. 7) for Saint Sylvestre [6, 53]. The floor remains flat on average, but sharp deepenings, as deep as 5-6 km, are locally observed on vertical cross sections through the massif (Fig. 8). In the field, these zones of restricted area (less than 5%) compared with that of the whole unit also show vertical lineations. They are also interpreted as magma feeding zones, shown by fine grained intrusives [6] or variously evolved magmas at the outcrop. Most are not randomly oriented as revealed by their overall pattern. In the Saint Sylvestre massif, the late intrusives as well as the deeper zones are controlled by N020 and N120 structures [6, 21]. The deformation field at that time, which involved a vertical shortening and a maximum horizontal stretching oriented towards the NW-SE [36], indicates that the root zones have formed in regions locally in extension.

8. MAGMA EMPLACEMENT AND MINERALIZATION

After emplacement, granitic magma still evolves, slowly crystallizes as soon as each mineral crosses its proper phase transition boundaries. Large displacement of liquid is therefore enhanced, but crystallizing conditions can be drastically modified by squeezing residual liquid out of the backbone of yet crystallized minerals. In a similar way, emplacement of new, that is hot and liquid, magma into a crystallizing one, induces an important disequilibrium in the crystallization sequence.

The Hercynian granitic complex of Saint Sylvestre-Saint Goussaud (French Massif Central) is known as an important uranium deposit in France. Its thickness is small (2.6 km on average) [6] and it shows horizontal foliations [40]. Locally, fine grain intrusives form vertical sheets, 0.5 to 1.5 km in width, with vertical foliations trending NS to N020 [40]. Other local late intrusive outcrop at sharp contact with the main facies. They also correspond to deeper zones from gravity data. Those areas of greater depth are quite potential sites for U mineralizations [21, 20].

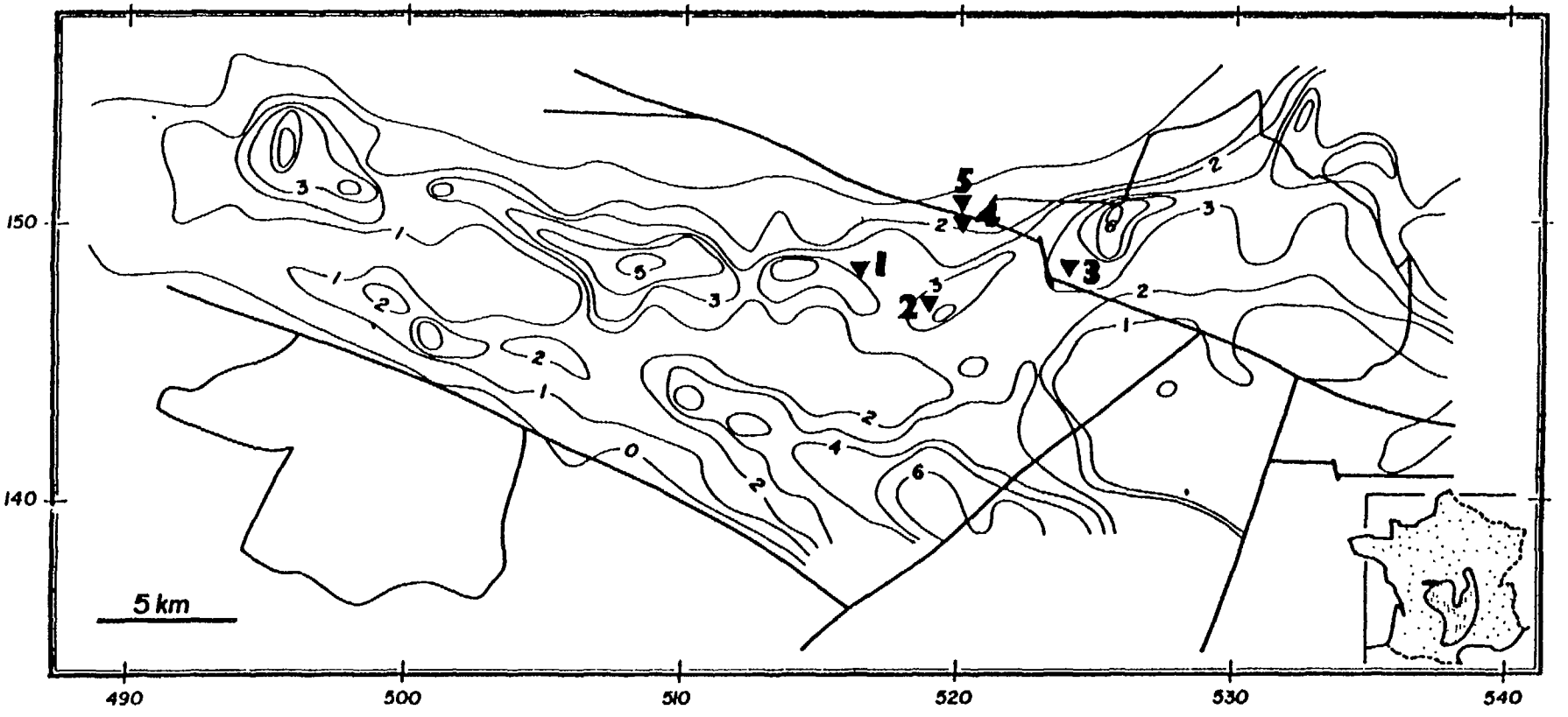

FIGURE 8. Map of the floor (in km) in the granitic complex of La Marche, French Massif Central. Triangles are the major sites for uranium mining 1. Le Bernardan, 2. Les Loges, 3. Les Mas Grimauds, 4. La Cote Moreau, 5. Piégut. The later are associated to movements on the Marche fault.

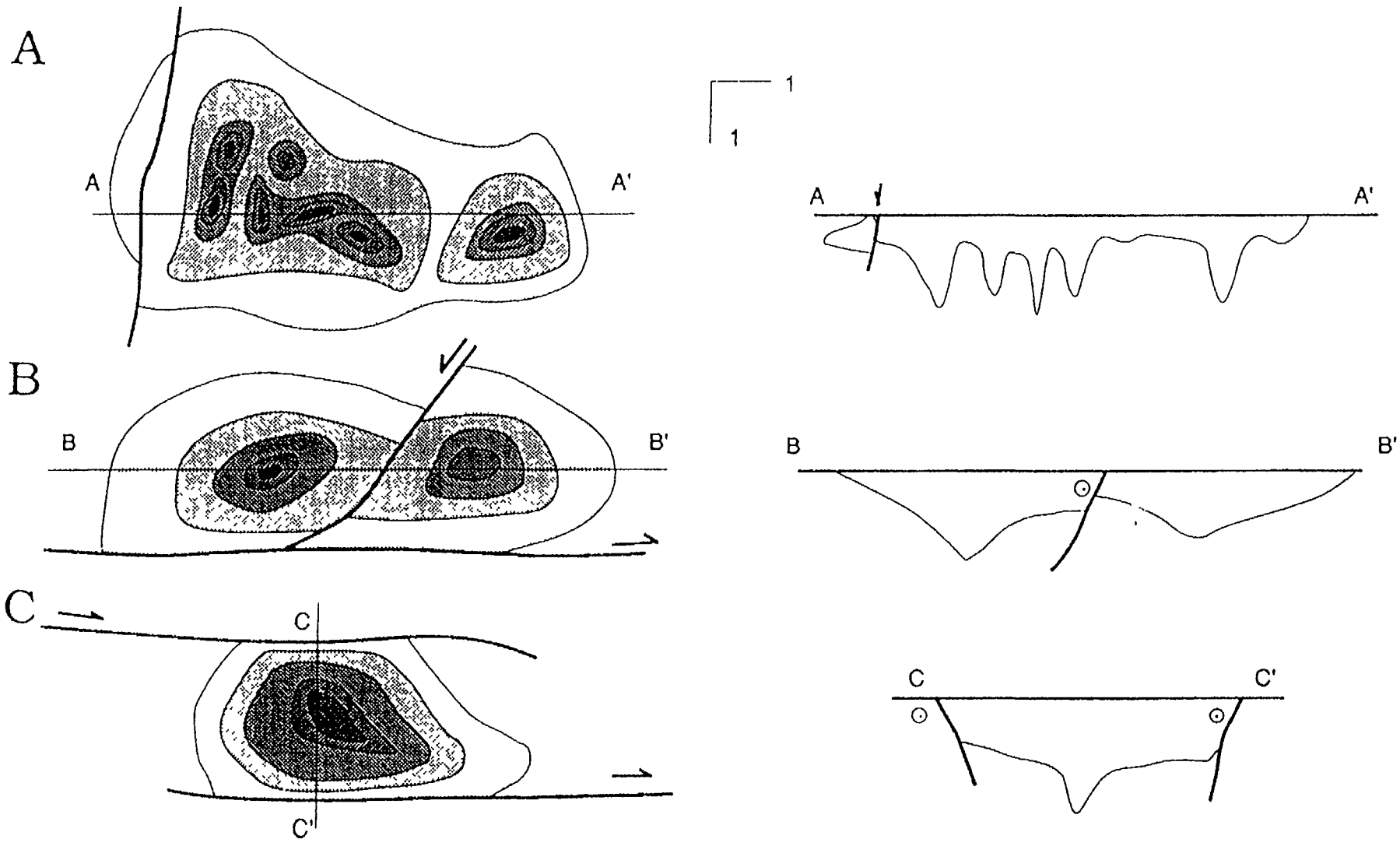

FIGURE 9. Schematic morphology of granitic plutons according to the regional deformation field. A map (on the left) and a cross section (on the right) with no vertical exageration are represented that show the style of pluton which can be expected according to the regional deformation regime: A) extension, B) wrench deformation, C) jog within overlapping shear zones.

Close to that complex, the granitic complex of La Marche is presently the last place of active mining for uranium in France (Fig. 8). It shows a very thin cross-section, in which late fine grain intrusives, richer in biotite are definitively thicker. Zones of uranium deposits have been mined, connected with very late movements on faults, but also within the complex, in relation with fluid movements. Those sites are associated to the zones of deeper roots, and probably represent the effect of late fluids circulation, in relation with the late intrusive.

9. CONCLUSIONS

An integrated method of observations has been tailored to describe the deep structures and the shape at depth of a granitic pluton. It mostly consists in surveying the area with detailed gravity measurements using a density of coverage of about 1 point per km^2. It also benefits of structural measurements recording the last movements of magmas while it was partly crystallized. Both sets of data are required to understand perfectly the mode of magma emplacement. The deepest zones inferred from gravity data inversion, that also show vertical lineations are interpreted as the magma root zones. They are controlled by the regional deformation field (Fig. 9). Granitic massifs intrusive during a shear regime are about 5 ± 2 km thick and present only one feeding zone, sometimes two in larger massifs, extending down to a maximum of about 6-12 km. In contrast, those granites intrusive during extensional regime show a thin, about 2-3 km, main unit with subhonzontal magmatic foliation planes and horizontal lineations, intruded by variously evolved facies in which magmatic structures are subvertical. When correlating chemical evolution of the magma to its position relative to the root zone, it appears that the rate of magma outcoming and the regional deformation rate have influence on the position of the mineralization. Therefore, we suggest that integrated studies are a requisite to most studies on granite emplacement and later chemical evolution. Such a joint study seems necessary to understand what has been the structural evolution of the magma during emplacement. It therefore has importance in determining the mechanical response of the pluton as a whole during later phases of tectonic activities and chemical alteration.

REFERENCES

[1] AJAKAIYE, D.E., HALL, D.R. and MILLAR, T.W., Interpretation of aeromagnetic data across the central crystalline shield area of Nigeria. Geophys. J. R. Astron. Soc. London, 83 (1985) 563-571.

[2] AMICE, M., and BOUCHEZ, J.L., Susceptibilité magnétique et zonation du batholithe granitique de Cabeza de Araya (Extremadura, Espagne). C.R. Acad. Sci. Paris, 308, 2, (1989),1171-1178.

[3] ARANGUREN, A., TUBIA, J.M., VIGNERESSE, J.L. and BOUCHEZ, J.L., Settlement of the granitic massif of Guitiriz, Spain. EOS Trans. AGU, 73 (1992) 275.

[4] ARCHANJO, C.J., OLIVIER, P. and BOUCHEZ, J.L., Plutons granitiques du Serido (Nordeste du Bresil): écoulement magmatique parallèle à la chaine relevé par leur anisotropie magnétique. Bull. Soc. Géol. Fr., 163 (1992) 509-520.

[5] AUDRAIN, J., AMICE, M., VIGNERESSE, J.L. and BOUCHEZ, J.L., Gravimetrie et geometrie tridimensionelle du pluton granitique de Cabeza de Araya (Extremadure, Espagne). C.R. Acad. Sci. Paris., 309 (1989a) 1757-1764.

[6] AUDRAIN, J., VIGNERESSE, J.L., CUNEY, M. AND FRIEDRICH, M., Modèle gravimétrique et mise en place du complexe granitique hyperalumineux de Saint Sylvestre (Massif Central français). C.R. Acad. Sci. Paris., 309, 2 (1989b) 1907-1914.

[7] BEAMISH, D., A deep geoelectric survey of the Carnmenellis granite. Geophys. J. Int., 102, 679-693 (1990).

[8] BLANCHARD, P., GAGNY, C. and LAURENT, J., Le mécanisme de décantation et ses implications géologiques: differenciation continue et litage (layering) magmatiques. C. R. Acad. Sci. Paris, 287, D (1978) 775-778.

[9] BORRADAILE, G.J., Magnetic susceptibility, petrofabrics and strain. Tectonophysics, 156 (1988) 1-20.

[10] BOTT, M.H.P., A geophysical study of the granite problem. Geol. Soc. London Quart., 112, 45-67 (1955).

[11] BOTT, M.H.P., and SIMPSON, S.P., Gravity investigations of subsurface shape and mass distibutions of granite batholiths. Geol. Soc. Am. Bull., 78 (1967) 859-878.

[12] BOUCHEZ, J.L., GLEIZES, G., DJOUADI, T. and ROCHETTE, P., Microstructure and magnetic susceptibility applied to emplacement kinematics of granites: the example of the Foix pluton (French Pyrenees). Tectonophysics, 184 (1990) 157-171.

[13] BOUCHEZ, J.L., GUILLET, P. and CHEVALIER, F., Structures d'écoulement liées à la mise en place du granite de Guérande (Loire-Atlantique, France). Bull. Soc. Géol. Fr., 7, 23 (1981) 387-399.

[14] BOURGEOIS, B., MATHIEU, F. and VALLA, P., La détection de gisements conducteurs profonds par la méthode électromagnétique de surface "Melis". Bull. Soc. Géol. Fr., 161, (1992) 31-49.

[15] BRISBIN, W.C., and GREEN, A.G., Gravity model of the Aulneau batholith, northwestern Ontario. Can. J. Earth Sci., 17 (1980) 968-977.

[16] BRUN, J.P., GAPAIS, D., COGNE, J.P., LEDRU, P. and VIGNERESSE, J.L., The Flamanville granite (NW France): An unequivocal example of an expanding pluton. Geol. J., 25 (1990) 271-286.

[17] BRUN J.P. AND PONS, J., Strain patterns of pluton emplacement in a crust undergoing non coaxial deformation. J. Struct. Geol., 3 (1981)219-229.

[18] CORDELL, L., HENDERSON, R.G., Iterative three dimensional solution of gravity anomaly using a digital computer. Geophysics, 33 (1968) 596-601.

[19] COURRIOUX, G., Exemple de mise en place d'un leucogranite pendant le fonctionnement d'une zone de cisaillement: le granite de Puentedeume (Galice, Espagne). Bull. Soc. Géol. Fr. 25 (1982) 301-307.

[20] CUNEY, M., Controles magmatiques et structuraux de la métallogenèse uranifere tardi-hercynienne: exemple du district de la Crouzille (Haute Vienne). Chron. Rech. Min., 499 (1990) 9-17.

[21] CUNEY, M., FRIEDRICH, M., BLUMENFELD, P., BOURGUIGNON, A., BOIRON, M.C., VIGNERESSE, J.L. and POTY, B., Metallogenesis in the French part of the Variscan orogen. Part I: U preconcentrations in the pre-Variscan formations - a comparison with Sn, W and Au. Tectonophysics, 177 (1990) 39-57.

[22] FAURE, M., BONNEAU, M. and PONS, J., Ductile deformation and syntectonic granite emplacement during the late Miocene extension of the Aegea (Greece). Bull. Soc. Géol. Fr. 162 (1991) 3-11.

[23] GLEIZES, G., NEDELEC, A., BOUCHEZ, J.L., AUTRAN, A. and ROCHETTE, P., Magnetic susceptibility of the Mont-Louis Andorra ilmenite-type granite (Pyrenees): a new tool for the petrographic characterization and regional mapping of zoned granite plutons. J. Geophys. Res., 98, 4317-4331 (1993).

[24] GREEN, A.G., and. MAIR, J.R., Subhorizontal fractures in a granitic pluton: Their detection and implications for radioactive waste disposal. Geophysics, 48 (1983) 1428-1449.

[25] GUILLET, P., BOUCHEZ, J.L. and VIGNERESSE, J.L., Le complexe granitique de Plouaret: mise en évidence structurale et gravimétrique de diapirs emboités. Bull. Soc. Géol. Fr., 8 (1985) 503-513.

[26] GUILLET, P., BOUCHEZ, J.L. and WAGNER, J.J., Anisotropy of magnetic susceptibility and magmatic structures in the Guerande granite massif (France). Tectonics, 2 (1983) 419-429.

[27] GUINEBERTEAU, B., BOUCHEZ, J.L. and VIGNERESSE, J.L., The Mortagne granite pluton (France) emplaced by pull-apart along a shear zone: stuctural and gravimetric arguments and regional implication. Geol. Soc. Am. Bull ., 99 (1987) 763-770.

[28] HAJNAL, Z., STAUFFER, M.R., KING, M.S., WALLIS, P.F., WANG, H.F. and JONES, L.E.A., Seismic characteristics of a Precambrian pluton and its adjacent rocks. Geophysics, 48 (1983) 569-581.

[29] HANMER, S.K., VIGNERESSE, J.L., Mise en place de diapirs syntectoniques dans la chaine hercynienne: exemple des massifs leucogranitiques de Locronan et de Pontivy. Bull. Soc. Géol. Fr., 22 (1980) 193-202.
[30[HODGE, D.S., ABBEY, D.A., HARBIN, M.A., PATTERSON, J.L., RING, M.J. and SWEENY, J.F., Gravity studes of subsurface mass distributions of granites in Maine and New Hampshire. Am. J. Sci., 282 (1982) 1289-1324.
[31] HOLLISTER, L.S., CRAWFORD, M.L., Melt-enhanced deformation: a major tectonic process. Geology, 14 (1986) 558-561.
[32] HROUDA, F., Magnetic anisotropy of rocks and its application in geology and geophysics. Geophys. Surveys, 5, (1982) 37-82.
[33] HUTTON, D.H.W., DEMPSTER, T.J., BROWN, P.E. and DECKER, S.D., A new mechanism of granite emplacement: intrusion in active extensional shear zones. Nature, 343 (1990) 452-455.
[34] ISHIHARA, S., The magnetite series and ilmenite series granitic rocks. J. Petrol., 25 (1977) 956-983.
[35] JURDY, D.M., PHINNEY, R.A., Seismic imaging of the Elberton granite Inner Piedmont Georgia, using COCORP southern Appalachian data. J. Geophys. Res., 88 (1983) 5863-5873,.
[36] LESPINASSE, M., PÊCHER, A., Microfracturing and regional stress field: a study of the preferred orientations of fluid inclusions planes in a granite from the Massif Central France. J. Struct. Geol., 8 (1986) 169-180.
[37] MATTHEWS, D.H., Can we see granites on reflection profiles? Annales Geophysicae, 5B (1986) 353-356.
[38] MEISSNER, R., BORTFELD, R.K., DEKORP Atlas, Springer Verlag, Heidelberg, 182 p. (1990).
[39] MILLER, H.G., TUACH, J., Gravity and magnetic signatures of the Auckley granite suite, southeastern Newfoundland: implications for magma emplacement. Can. J. Earth Sci., 26 (1989) 2697-2709.
[40] MOLLIER, B., BOUCHEZ, J.L., Structuration magmatique du complexe granitique de Brame-St Sylvestre-St Goussaud (Limousin, Massif Central français). C. R. Acad. Sci. Paris, 294, 2 (1982) 1329-1333.
[41] NABETANI, S., KANO, H., NARITAMI, K., TAKAGI, A., SUZUKI, M. and FUJIMOTO, Y., Gravimetric investigations on granitic plutons in the Kitakami Mountains, NE Japan. Butsuri Tanko. Geophys. Explor., 25, 4 (1976) 9-26.
[42] OERTEL, G., Der Pluton von Loch Doon in Sudscotland. Geoteckt. Forsh., 11 (1955) 1-83.
[43] PATERSON, S.R., TOBISH, O.T., Rates of processes in magmatic arcs: implications for the timing nature of pluton emplacement and wall rock deformation. J. Struct. Geol., 14 (1992) 291-300.
[44] PATERSON, S.C., VERNON, R.H. and TOBISCH, O.T., A review of criteria for the identification of magmatic and tectonic foliations in granitoids. J. Struct. Geol., 11 (1989) 349-363.
[45] PITCHER, W.S., Granites and yet more granites forty years on. Geol. Rund.,76 (1987) 51-79.
[46] PONS, J., Relations entre la structure et la petrofrabrique des roches eruptives de la bordure meridionale du massif granitique du Querigut (Ariege, France). CR. Acad. Sci. Paris, 271, D (1970) 1665-1668.
[47] PRATT, T.L., COSTAIN, J.K., CORUTH, C., GLOVER, L. and ROBINSON, E.S., Geophysical evidence for an allotochnous Appalachian granitoid beneath the basement surface of the coastal plain near Lumberton North Carolina. Geol. Soc. Am. Bull., 96 (1985) 1070-1076.
[48] RICHTER, C., Particle motion and the modelling of strain response in magnetic fabrics: Geophys. J. Int., 110 (1992) 451-464.
[49] ROCHETTE, P., JACKSON, M. and AUBOURG, C., Rock magnetism and the interpretation of anisotropy of magnetic susceptibility, Rev. Geophys., 30 (1992) 209-226.
[50] SCHWARZ, E.J., Magnetic expressions of intrusions including magnetic aureoles.

Tectonophysics, 192 (1992) 191-200.
[51] TIKOFF, B., TEYSSIER, C., Crustal scale en échelon "P-shear" tensional bridges: A possible solution to the batholithic room problem. Geology, 20 (1992) 927-930.
[52] VAN DER VOO, R., KLOOTWIJK, C.T., Paleomagnetic reconnaissance study of the Flamanville granite with special reference to the anisotropy of its susceptibility. Geol. Mijnb., 51 (1972) 609-617.
[53] VASSEUR, G., DUPIS, A., GALLART, J.G. and ROBIN, G., Données géophysiques sur la structure du massif leucogranitique du Eimousin. Bull. Soc. Géol. France, 8 (1990) 3-11.
[54] VIGNERESSE, J.L. Damped and constrained least squares method with application to gravity interpretation. J. Geophys. 45 (1978) 17-28.
[55] VIGNERESSE, J.L., Enracinement des granites armoricains estimé d'après la gravimétrie. Bull. Soc. Geol. Min. Bretagne, 15C, (1983) 1-15.
[56] VIGNERESSE, J.L., Formes et volumes des plutons granitiques. Bull. Soc. Géol. Fr., 8 (1988) 897-906.
[57] VIGNERESSE, J.L., Use and misuse of geophysical data to determine the shape at depth of granitic intusions. Geol. J., 25 (1990) 248-260.
[58] VIGNERESSE, J.L., CANNAT, M., Mesure des paramètres physiques dans le sondage d'Echassières (vitesse sismique, porosité, densité). Mem. Geol. Prof. France 1, Géol. Fr., 2-3 (1987) 145-148.
[59] WEBSTER, S.S., SCHEIBNER, E., Introduction to magnetic properties of New England granitoids. Explor. Geophys., 15 (1984) 67-73.

NATURAL GEOLOGICAL FACTORS AFFECTING THE ENVIRONMENT IN THE AREAS OF SANDSTONE TYPE URANIUM DEPOSITS WORKED BY UNDERGROUND LEACHING

I.G. MEL'NIK, V.I. VETROV, A.A. KAZAKOV
All-Russian Research Institute of Chemical Technology,
Moscow, Russian Federation

Abstract

One of the most important manifestations of the sandstone type deposits according to the IAEA statement is "...their general association with channelled sedimentary structures and redox barriers." The most peculiar features of such a type of deposits are:

1. the localization in loose, practically non-lithified sandy-gravelly sediments;
2. the relation with the formations composed by rhythmically-alternating horizons of permeable (the filtration coefficient from 1-10 m/day to 20 m/day) and well-graded sandstones - gritstones with water-confining clayey horizons;
3. considerable natural inundation of ore-bearing horizons not only by the oreformation period but at the present time, too;
4. deeply (50-500 m) deposited ore-bearing aquifers, effecting natural heads and even spontaneous flow;
5. Uranium being presented as easily soluble compounds — oxides, phosphates, carbonates in loose, finely dispergated forms, generally uniformly distributed throughout great thickness.

The above factors make it possible to apply the method of underground leaching by bore holes when working and primary treating most of the deposits of the sandstone type. The working and processing of the uranium ores deposits by the underground leaching (as well as by other methods) have a multifarious and variable technological impact on the geological medium and neighbouring surface hydrosphere and atmosphere. The natural factors determining the natural ecological conditions are generally the following:

- the geological-structural position (structural type) of the deposit:
- the mineralogical-geochemical ore properties of the deposit;
- the hydrogeological and hydrodynamic properties of the ore-bearing and adjacent water-bearing horizons;
- landscape-geographic and economic-infrastructural conditions of the deposit.

Already since the sandstone type deposits formation, some natural contamination with radionuclides and other elements takes place, affecting the ore-bearing aquifers, the encroachment lines of which could spread under the influence of the working solutions when the underground leaching technique is employed. The main technogenic factors contaminating the environment which should be ecologically assessed are the following:

- the working system (quarry, mine, combined, underground leaching, hydraulic mining) determining the rock mass hoisted up, the character of the underground cavity space and the dumps on the surface;
- size of the working systems (area, depth, section of the stages);
- the methods employed for draining or flooding of the deposits;
- the methods of the rock mass transportation and the rock dumps formation;
- the infrastructure of the mining facility (dressing plant, transport communications, drainage system, water source, dwellings, etc.)

In fact, the contamination extent of the deposits is generally determined not on the scale of a single natural or technogenic factor but by the character of their cumulative effect dependant on such a selection of engineering and technological means which would be profitable, environmentally safe and adoptable for inexpensive and simple schemes of soil recultivation. Among the natural factors of the sandstone type uranium deposits affecting the environment when worked by the underground leaching technique, the most important are the following: the deposit underground water condition, the lithological-facies and hydrodynamical factors, ore-bearing structures.

1. DEPOSITS UNDERGROUND WATERS CONDITION

The most hydrogeological structures enclosing the sandstone type deposits are characteristic of active water exchange and large fresh water reserves. Their native technogenic contamination has a negative impact on the water resources balance.

The most dangerous natural contamination of the ore-enclosing horizons waters takes place in the process of the exogenetic — epigenetic ore formation of large zones of stratal oxidation as well as the formation of an active redox barrier. Generally the redox processes pertaining to the early stages continue up to the present time, actively sustaining the hydro-geochemical conditions in various parts of the zonality, where three zones could be singled out: that of stratal oxidation, of non-oxidized and mineralized rocks with various hydrogeological and hydrogeochemical conditions.

In the stratal oxidation zones waters, the concentrations of practically all macro- and microcomponents are below the maximum permissible ones. Only the concentrations of highly toxic selenium are considerably high, reaching a few hundredths micrograms per litre, averaging, for instance. in the Karakum Province 37 mkg/l, thus exceeding the maximum permissible concentrations (MPC) by several or even tens and hundreds of times, with the selenium contaminated width extending at least for 10 km.

In the stratal waters of the mineralization zone the concentrations of most micro- and macroelements are about the same as in the waters of the stratal oxidation. The exception would be the concentrations of radium and other radionuclides, 2-5 times exceeding the MPC, making even the fresh waters of the mineralization useless for drinking and technical purposes.

And, at last, the stratal waters of the non-oxidized barren rocks are pure enough and can be used for drinking and other purposes. The concentrations of all macro- and microelements (especially of the toxic - beryllium, selenium, arsenic, cadmium, as well as of heavy metals - copper, mercury, chromium, nickel, zinc) are tens fold lower than the MPC values. The radium concentrations are by 1-2 orders and those of uranium by 3-4 orders lower than the MPC values. The waters purity in this zone is explained by the redoxiding and neutralizing effect of the geochemical barrier serving as a natural filter, efficiently cleaning the subterranean waters from the toxic elements.

Thus, the natural geochemical conditions in the zones of stratal oxidation and the adjacent mineralization zone would be unfavourable in the ore-enclosing horizons, considering their water made unusable for drinking for the presence of selenium, radionuclides and other toxic elements, within a 10 km wide band and over from the ore zone against the subterranean water flux vector. Taking into account the large areas (tens and hundreds of sq. m of the stratal oxidation zones in some regions — the Kizil Kum, the Chu-Sarysai depression, etc.), the water-bearing horizons there are useless as water sources throughout vast territories (tens of thousands of sq. km) due to contamination with toxic matter.

2. LITHOLOGICAL-FACIES AND HYDRODYNAMIC FACTORS

The naturally contaminated areas at the sandstone type deposits coincide with the paths of ore-bearing currents and contours of the ore bodies.

The morphology of the contaminating solutions paths is determined by the internal structure of the ore-enclosing bed, and mainly by the lithological-facies composition of the sandy water-bearing horizons and water-resisting clay marls, forming this bed. Their long continuations determine the simple stratal forms of contamination. Any hydraulic windows, open faults or thin lenticular

water-resisting layers make the ore-bearing solutions leak into the adjacent non-ore horizons and form there some small ore generating centres, resulting in native contamination of the waters.

The stratal waters in the sandstone type deposits, considering the native contamination protection degree, are classified as follows:

- Naturally unprotected waters — the ones confined to the ore-enclosing horizons, the limits of which contain both naturally contaminated and pure waters that could potentially get contaminated during the process of ore formation, regeneration or while being treated by the underground leaching method;

- weakly naturally protected — to these belong the oreless aquifers hydraulically linked with ore-forming structures and lithological ducts. These horizons bear the potential be locally contaminated;

- protected waters — these are the waters of aquifers isolated at the top and the bottom from the ore-bearing ones with thick (over 5 m) and steadfast water-resistant layers without any lithological windows nor faults.

The easiest passages for the ore-forming solutions, mapped by the natural contamination sources, of course would be as permeable for the productive solutions, if the deposit is being worked by the underground leaching method.

One can draw a conclusion that the natural contamination centres actually predetermine (map) the areas of probable spreading of technogenic contaminating reagents. Therefore any mapping of the native contamination areas will assists the forecasting of the technogenic solutions run-out dynamics. It follows that the geological survey and exploration data can be useful for the purposes of environmental mapping.

3. ORE-ENCLOSING STRUCTURES OF SANDSTONE TYPE DEPOSITS

According to the structure, size, impact on the ore process scale and the native environment conditions, we have singled out the following types of ore-enclosing structures (Figs 1 and 2):

1) Open type small erosio-tectonic troughs (valleys);

2) Semi-open type small erosio-tectonic troughs;

3) Large semi-open syneclises with multistaged mineralization;

4) Large semi-open graben-synclinoria with mineralization in basal levels;

5) Buried erosio-tectonic troughs.

3.1. OPEN TYPE EROSIO-TECTONIC TROUGHS

They represent shallow (30-100 m) cuttings into the crystalline basement of shields or folding regions. The valleys are up to 3-4 km wide extending from tens to a few hundred kilometres. The ore-controlling body there is the thin layer of flooded alluvial and lacustrine marsh deposits of paleoriverbeds, undergone surface oxidation. The ore bodies are generally confined to the interlayers of peats or sandstones enriched by the vegetal remnants. The form is lenticular, the thickness 1-10 m, the width - a few hundred metres, the length — a few kilometres.

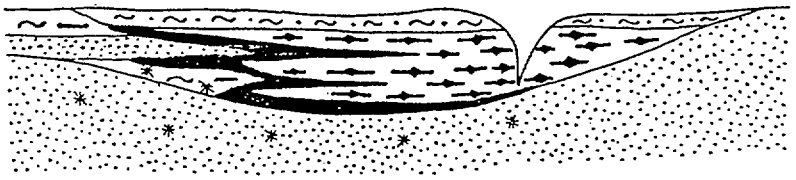

FIG. 1. Ore-bearing structures of sandstone type deposits (schematic): Small open erosio-tectonic troughs.

The ore-bearing areas (together with the anomalous contents) comprise ca. 30% and more of the troughs area, being unevenly distributed throughout the section, containing rather high concentrations of radionuclides.

The absence of water-resisting layers around the ore-bearing bed can make its waters contact the surface currents and water intakes in the crystalline basement. In such a case the working of the deposit by the underground leaching method would endanger the environment.

3.2. SEMI-OPEN TYPE SMALL EROSIO-TECTONIC TROUGHS

They do not differ from the above in size. They are filled with unicomposed alluvial water-bearing rather steadfast sandy-gravelly deposits, 5-10 m thick, overlapped with an argillo-aleurolite bed, which the water-bearing horizon from the surface currents.

The ore deposits formation is related to the development of the stratal oxidation zones, which often develop from two borts and together with the ore deposits take up practically all the space of

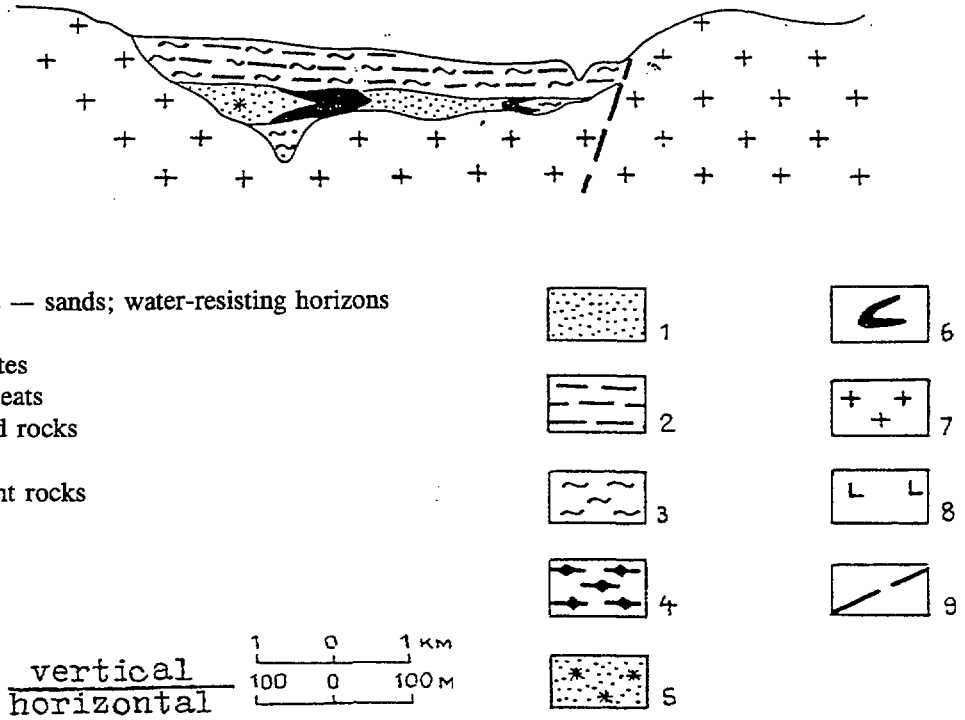

FIG. 2. Ore-bearing structures of sandstone type deposits (schematic): Small semi-open erosio-tectonic troughs.

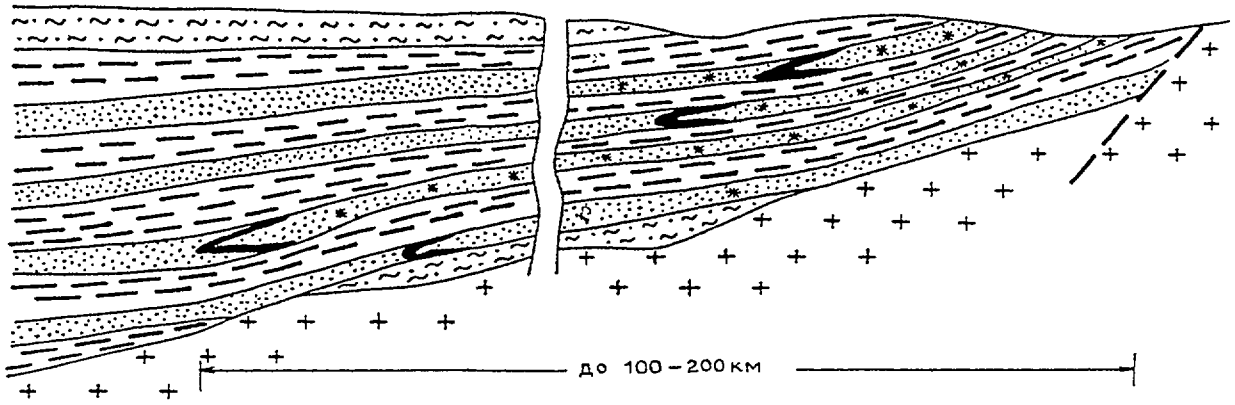

FIG. 3a. Ore-bearing structures of sandstone type deposits (schematic): Large semi-open syneclises, sub-type a.

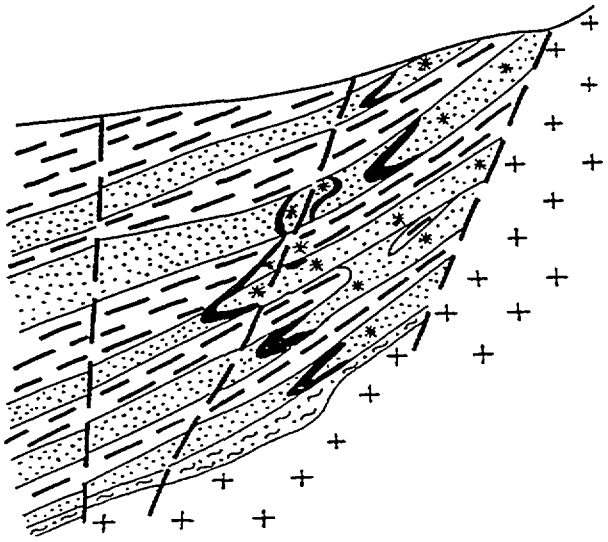

FIG. 3b. Ore-bearing structures of sandstone type deposits (schematic): Large semi-open syneclises, sub-type b.

the water-bearing horizon, filled up with fresh waters and contaminated with radionuclides. The water supply can be organized from the intakes situated in the crystalline basement and the borts of troughs.

Thus, this type of structures, rather well protecting the ore-bearing horizon from the surface factors, still bear the danger, like in the above type case, of disturbed dynamics of the water intakes, situated in the borts or the basement, due to a possible seaping of native contaminated waters and toxic solutions being pumped in or drained.

The details of the ecologic situation in this type of structures are not clear, though the general geological information testifies on the environment being endangered by such working by the underground leaching method.

3.3. LARGE SEMI-OPEN SYNECLISES

They are presented by extensive platformic brachy-troughs ranging from ten thousands to a few hundred thousands of square kilometres in the plane. They are filled with a thick (500-1000 m) complicatedly built stratum of continental-marine deposits, comprising alternating in section permeable

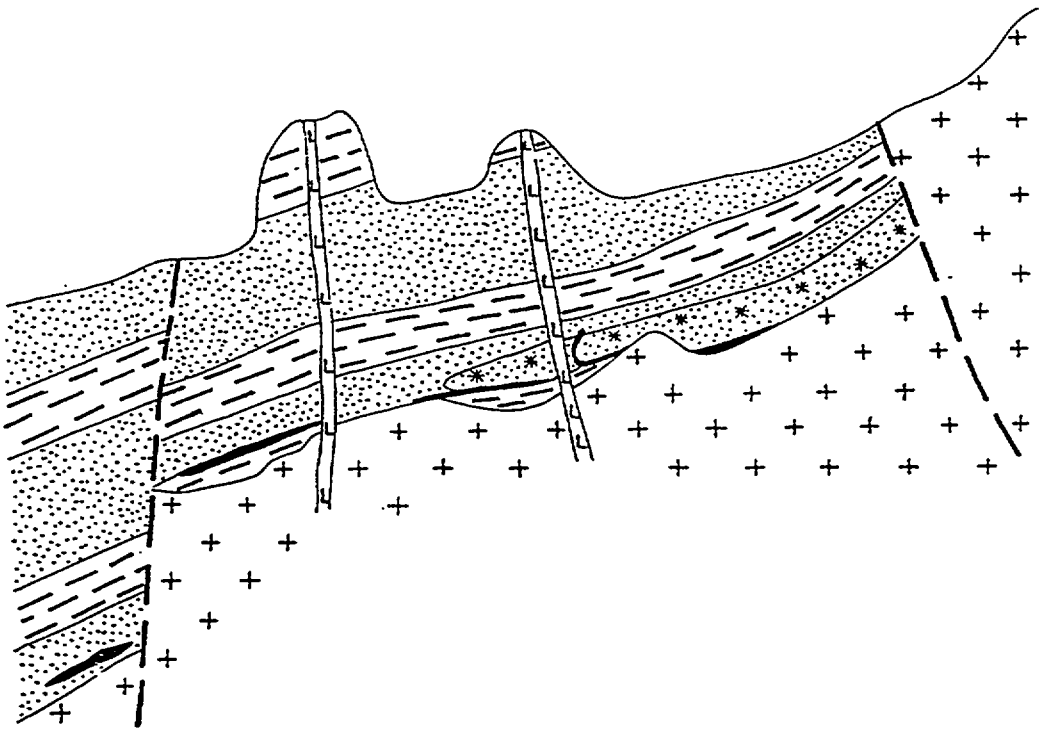

FIG. 4. Ore-bearing structures of sandstone type deposits (schematic): Large semi-open graben-synclinoria.

water-bearing sandy horizons and steadfast clay-marly water-resisting horizons. The water-bearing horizons possess large reserves of fresh and weakly mineralized waters. The ore deposits of such structures are located in their marginal parts, proximal to the sites of infiltration and heads in the water-bearing horizons. Several or all water-bearing horizons loften more than 10) are ore-bearing. According to the specific location or structural-lithological controlling there are two subtypes of ore-bearing semi-open syneclises to be singled out.

The first sub-type have deposits located both in the marginal and central parts of the troughs from 5-10 up to 100-200 km removed from the borts, being quite removed from each other spatially. The ore presence is manifested at various levels of the section throughout all water-bearing horizons.

The ore bodies are a few metres up to 20-30 m thick, 0.5-1.0 km wide, extending for tens of kilometres, and accounting for the entire ore-bearing band, controlled by a single zone of stratal oxidation — for hundreds of kilometres. Accounting by the width of the ore bodies containing radionuclides and the adjacent contaminated part of the oxidation zone (10 km wide), the contamination area in one single ore-bearing horizon will reach from several tens to one thousand of square kilometres, still comprising 0.1-1.0% of the total area of a water-bearing horizon.

Thus, when working a deposit by the underground leaching method, the environmental problems in the above sub-type structures will be governed by the following factors:

- disconnection of the deposits throughout space;
- large aureole of natural contamination with underground waters.

This will determine the main task of uranium mining — to confine the technogenic contamination aureole within the limits of the native contamination, and if it is not possible - to make

efforts directed to minimal spreading of the technogenic contamination beyond the limits of the native one. The result could be the sharply cut down danger to the fresh underground waters of ore-bearing artesian basins.

The other sub-type of ore-controlling syneclises (Fig. 3b), being similar in size and orebearing ability with the first one, due to some more complicated lithologic-facies and structural conditions (facies altering of the composition, presence of complicating positive brachy-elements, faults, etc.), is characteristic of a relative coincidence (telescoping) of ore deposits from horizon to horizon with their insignificant removal (1-7 km) from the borts of the troughs. Accordingly, the band width of the native contamination with radionuclides, scandium, rhenium, selenium in the ore deposits and the adjacent zone of stratal oxidation will reach 1-7 km, which would require the subtraction of the fresh waters of this band from the drinking water balance.

Often the leakage of ore-forming solutions, the depositing of ores and natural contamination of adjacent horizons can be observed in this band through the lithological windows and structural channels.

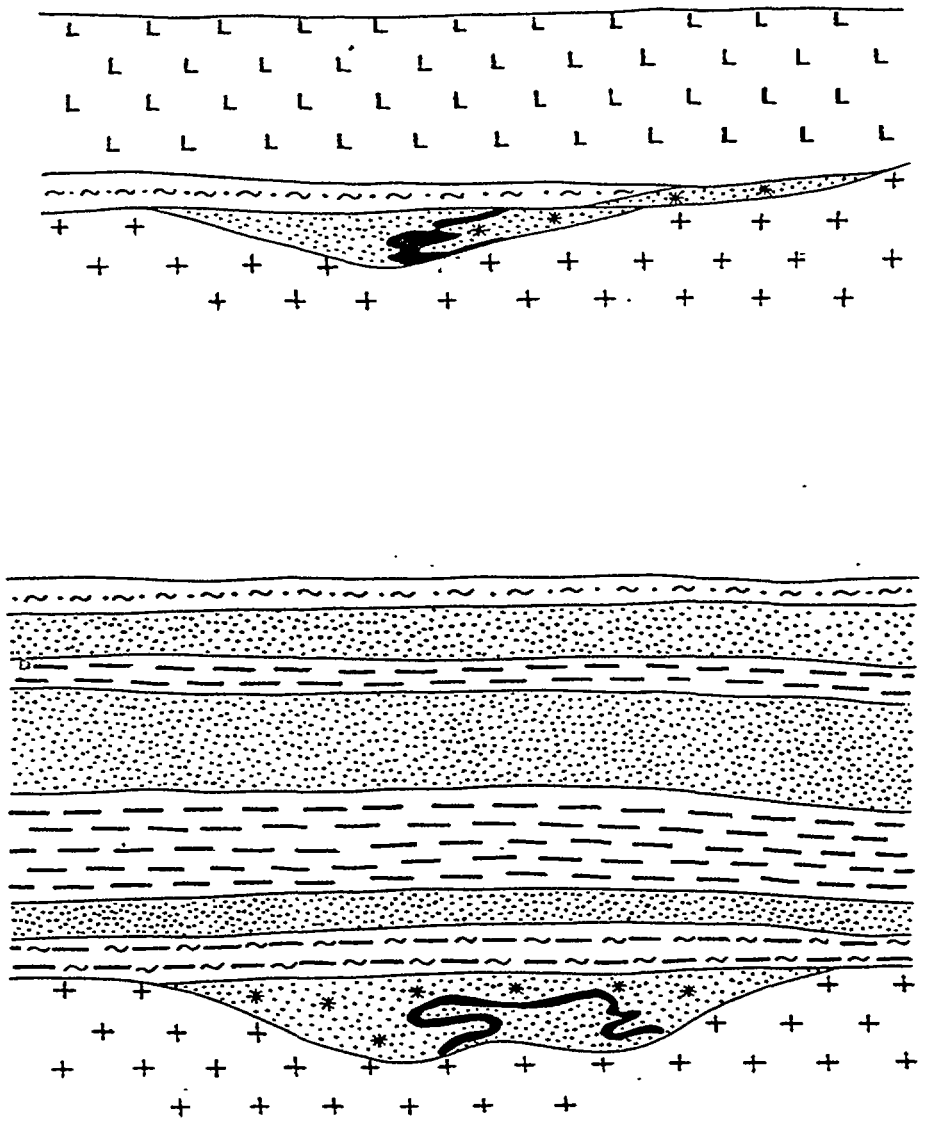

FIG. 5. Ore-bearing structures of sandstone type deposits (schematic): Buried erosio-tectonic troughs.

The negative environmental factors present in the above subtype of ore-bearing structures are the following:

- telescoping of the various horizons deposits, presenting environmental and technogenic strain during the working;
- native contamination of the most accessible parts of artesian basins, used for supplying of water in the bort adjacent areas in proximity to surface;
- troughs in a crystalline frame, where water intake should be eliminated due to possible leaking of the technogenic solutions.

Similarly to the foregoing subtype, one should take into account the zone of native contamination, which must not be used for the water intake, the decision be made prior to the beginning of the working of the deposit.

3.4. LARGE GRABEN-SYNECLINES

Large graben-syneclines (sized over 5 000km^2) present fault-attached troughs, filled with rhythmically formed beds of continental-marine deposits 1 000 m thick, intermitted with sandy water-bearing horizons.

The ore sills are located on the upraised structure limb in the basal water-bearing horizon, well isolated from the superjacent oreless water-bearing layers by a steadfast thick (over 50 m) water-resistant horizon, and by a lensing water-resistant horizon — from the crystalline basement. The ore deposition depth is 200 - 700 m. The ore deposits form a large oval ore field sized up to 1 000 km^2 with the aureole of non-payable ores and radioactivity anomalies. The young stratal oxidation zone is noted to regenerate the ore deposits, increasing the native contamination of the water-bearing horizon with radionuclides.

There is no natural leakage of ore-forming solutions into superjacent aquifers. There have been only slight anomalies observed in the proximity of some large faults, implying possible leaks of the technological solutions through these structures into the superjacent aquifers.

3.5. BURIED EROSIO-TECTONIC TROUGHS (PALEOVELLEYS)

They belong to the Mesozoic structures, overlapped with sedimentary (ya) or volcanogenic (yb) strata with the water-resistant horizons in the basement during the postore-formation period.

The deposits in this structure type are reliably isolated by the water-resistant horizons from the superjacent aquifers and water currents of the day surface. The ore bodies and stratal oxidation zones take up to 10-30% of the ore-bearing horizon area, where radionuclides, molybdenum, scandium and selenium are contained in the quantities exceeding the maximum permissible concentration values. The deposits working in this type of structure is considered environmentally safe.

Thus, the various types of ore-bearing structures considerably differ in their size, construction and distribution of the native contamination of aquifers. The smaller structures are relatively more naturally contaminated than the large ones.

4. LANDSCAPE-GEOGRAPHIC AND ECONOMIC SITUATION OF DEPOSITS

The effect of this factor is determined by the value of land taken for the construction of sites, roads, water supply lines, adsorption columns, etc.

It is natural that in poorly populated plain deserts or semi-desert the expenditures for the above purposes would be relatively low and the environmental impact weaker as compared with chernozem, forestly densely populated areas, where the environment would be endangered not only by the underground leaching working but by the industrial and agricultural activities too.

The environmental impact of the above factor should be evaluated for each single region specifically.

5. GENERAL CONCLUSIONS

1. Most structures enclosing the sandstone type deposits generally possess large reserves of freshwater, which could be sources of potable and communal water supply. The knowledge on the relationships concerning the location and degree of native contamination is vital when evaluating the environment conditions of orebearing structures, balancing the drinking-communal water-supply and conducting the deposits working by the underground leaching method.

2. The native conditions of ore-bearing aquifers are not favourable for the potable water intake within the limits of ore deposits and the oxidated rocks zone (at least up to 10 km and more removed from the ore zone against the vector of the underground water currents movement) due to the specific process of ore formation in the sandstone type deposits. The concentrations of radionuclides, selenium, iron, manganese and other elements in the waters there would exceed the maximum permissible concentrations 10- 100 times.

3. The native contamination morphology and the protection of adjacent horizons is determined by the internal structure of the ore-bearing strata, the stability of aquifers and water-resisting horizons, the presence of tectonic windows and faults.

4. The degree of native contamination directly relates to the type and extent of the ore-bearing structures with native contamination. In large syneclises and graben synclinora, the contaminated aquifers areas reach extensions of thousands of square kilometers, though in relation to the very structures they do not exceed 0.1-1.0%. In small erosio-tectonic valleys, the native contamination exceeds 30% of the ore-bearing horizons space.

5. The setting-up of the underground leaching fields according to the data on the naturally contaminated ore-bearing horizons would considerably decrease the ecological danger to water resources of aquifers undergoing technogenic contamination .

LIST OF PARTICIPANTS

Åkerblom, G.	Swedish Radiation Protection Institute, S-171 16 Stockholm, Sweden
Andjelov, M.	Institute of Geology, Geotechnics and Geophysics, Dimičeva 14, SLO-61000 Ljubljana, Slovenia
Armour-Brown, A.	Consultant, 1 Lyndewode Road, Cambridge CB1 2HL, United Kingdom
Ball, T.K.	British Geological Survey, Keyworth, Nottingham NG12 5GG, United Kingdom
Balla, Z.	Hungarian Geological Survey, Stefa'nia 14, H-1142 Budapest, Hungary
Barisic, D.	Ruder Boškovič Institute, Bijenička c. 88, Zagreb, Croatia
Barnet, I.	Czech Geological Survey, Malostranské nám. 19, CZ-11821 Prague 1, Czech Republic
Barthel, F.H.	Bundesanstalt für Geowissenschaften und Rohstoffe, Stilleweg 2, P.O. Box 510153, D-30631 Hannover 51, Germany
Bartosek, J.	ENVI-2000, Vaculilcova 1a, CZ-63800 Brno, Czech Republic
Baxter, M.S.	IAEA - Marine Environment Laboratory B.P. 800, MC-98012 Monaco Cedex, Monaco
Beguž, T.	Rudnik Žirovski Vrh, Todraž 1, SLO-64 224 Gorenja Vas, Slovenia
Bourgeois, C.	Commissariat à l'Energie Atomique (C.E.A.), Centre Valduc, Service S.P.R. F-21120 Is-sur-Tille, France
Cox, J.R.	EXPLORANIUM G.S. Ltd., 95 Healy Road, Unit 7, Bolton, Ontario, Canada L7E 5A2

Darnley, A.G.	Geological Survey of Canada, 601 Booth Street, Ottawa, Ontario, Canada K1A 0E8
Fernández Amigot, J.A.	ENUSA, Santiago Rusiñol 12, E-28040 Madrid, Spain
Gamba, M.A.	Comisión Nacional de Energía Atómica, Avenida del Libertador 8250, (1429) Buenos Aires, Argentina
Grasty, R.L.	Geological Survey of Canada, 601 Booth Street, Ottawa, Ontario, Canada K1A 0E8
Hogg, S.	UDL, 47 Jefferson Avenue, Toronto, Ontario, Canada M6K 1Y3
Hovgaard, J.	Ministry of the Interior, Emergency Management Agency, Datavej 16, DK-3460 Birkerød, Denmark
Jurza, P.	GMS a.s. Prague, Pristam 24, CZ-12004 Prague 1, Czech Republic
Kazakov, A.A.	Ministry of the Russian Federation for Atomic Energy, Staromonetny per. 26, 109180 Moscow, Russian Federation
Koczynski, A.	Central Laboratory for Radiological Protection, Ul. Konwaliowa 7, PL-03-194 Warsaw, Poland
Lindgren, P.J.S.	Geological Survey of Sweden, P.O. Box 670, S-751 28 Uppsala, Sweden
Logar, Z.	Rudnik Žirovski Vrh, Todraž 1, SLO-64 224 Gorenja Vas, Slovenia
Lovenhofer, P.	PICODAS Group Inc., Vinohradska 131, Prague 3, Czech Republic
Maleik, M.L.	Nuclear Materials Authority, Maadi, P.O. Box 530, Cairo, Egypt

Matolin, M.	Charles University, Faculty of Science, Albertov 6, CZ-128 43 Prague 2, Czech Republic
Mellander, H.O.	Swedish Radiation Protection Institute, S-171 16 Stockholm, Sweden
Multala, J.T.	Geological Survey of Finland, Betonimiehenkuja 4, FIN-02150 Espoo, Finland
Ochiai, Y.	Power Reactor and Nuclear Fuel, Development Corporation, Chubu Works, 953-31, Sonodo, Jyourinnji, Izumi-cho, Toki City, Gifu-ken, Japan
Otton, J.K.	US Geological Survey, P.O. Box 25046, M.S. 939, Denver Federal Center, Denver, Colorado 80225, United States of America
Papadopoulos, N.N.	National Centre for Scientific Research, DEMOKRITOS, Aghia Paraskevi, P.O. Box 60228, GR-15310 Athens, Greece
Prohic, E.	Faculty of Natural Science, University of Zagreb, Zvonimirova 8, 41000 Zagreb, Croatia
Roux, J.X.L.	Cogéma 2, Rue Paul Dautier, BP 4, F-78141 Velizy Cedex, France
Rybach, L.	Institute of Geophysics, Swiss Federal Institute of Technology, ETH-Hönggerberg, CH-8093 Zurich, Switzerland
Sanderson, D.C.W.	Scottish Universities Research & Reactor Centre (SURRC), East Kilbride, Glasgow G75 0QU, United Kingdom
Schwarz, G.F.	Institute of Geophysics, Swiss Federal Institute of Technology, ETH-Hönggerberg, CH-8093 Zurich, Switzerland
Seiberl, W.A.	Geologische Bundesanstalt (Geological Survey of Austria), Rasumofskygasse 23, A-1030 Vienna, Austria

Shiloni, Y.	Geological Survey of Israel, 30 Malkhe Israel Str., Jerusalem 95501, Israel
Shirav, M.	Geological Survey of Israel, 30 Malkhe Israel Str., Jerusalem 95501, Israel
Sideris, G.N.	Institute of Geology and Mineral Exploration, 70 Messoghion St., GR-115 27 Athens, Greece
Strzelecki, R.S.	Polish Geological Institute, Ul. Rakowiecka 4, PL-00-975 Warsaw, Poland
Tauchid, M.	International Atomic Energy Agency
Torres, L.M. de M.	Instituto Geológico e Mineiro, Rua Diogo do Couto, No. 1 3°, P-1100 Lisbon, Portugal
Vigneresse, J.L.	CREGU, Centre de Recherches sur la Géologie des Matères Premières Minérales et Energétiques, 3, Rue du Bois de la Champelle, BP 23 F-54501 Vandoevre-lès-Nancy Cedex, France

QUESTIONNAIRE ON IAEA-TECDOCs

It would greatly assist the International Atomic Energy Agency in its analysis of the effectiveness of its Technical Document programme if you could kindly answer the following questions and return the form to the address shown below. Your co-operation is greatly appreciated.

Title: **Application of uranium exploration data and techniques in environmental studies**
Number: **IAEA-TECDOC-827**

1. How did you obtain this TECDOC?

[ ] From the IAEA:
  [ ] At own request
  [ ] Without request
  [ ] As participant at an IAEA meeting
[ ] From a professional colleague
[ ] From library

2. How do you rate the content of the TECDOC?

[ ] Useful, includes information not found elsewhere
[ ] Useful as a survey of the subject area
[ ] Useful for reference
[ ] Useful because of its international character
[ ] Useful for training or study purposes
[ ] Not very useful. If not, why not?

3. How do you become aware of the TECDOCs available from the IAEA?

[ ] From references in:
  [ ] IAEA publications
  [ ] Other publications
[ ] From IAEA meetings
[ ] From IAEA newsletters
[ ] By other means (please specify)
[ ] If you find it difficult to obtain information on TECDOCs please tick this box

4. Do you make use of IAEA-TECDOCs?

[ ] Frequently
[ ] Occasionally
[ ] Rarely

5. Please state the institute (or country) in which you are working:

Please return to:
R.F. Kelleher
Head, Publishing Section
International Atomic Energy Agency
P.O. Box 100
Wagramerstrasse 5
A-1400 Vienna, Austria